**U.S. Army
Corps of Engineers**

New England District
Concord, Massachusetts

**U.S. Environmental
Protection Agency**

Region I
Boston, Massachusetts

MODELING FRAMEWORK DESIGN

Modeling Study of PCB Contamination in the Housatonic River

DCN: GE-100500-AADX

October 2000

Environmental Remediation Contract
General Electric (GE)/Housatonic River Project
Pittsfield, Massachusetts

Contract No. DACW33-00-D-0006

Task Order No. 0003

WESTON

MANAGERS   DESIGNERS/CONSULTANTS

MODELING FRAMEWORK DESIGN

Modeling Study of PCB Contamination in the Housatonic River

October 2000

Prepared by

R.B. Beach[1], P.M. Craig[2], R. DiNitto[3], A.S. Donigian[4], G. Lawrence[5], R.A. McGrath[1], R.A. Park[6], A. Stoddard[7], S.C. Svirsky[8], W.D. Tate[9], and C.M. Wallen[10]

[1] Roy F. Weston, Inc., West Chester, PA 19380
[2] Dynamic Solutions, LLC, Knoxville, TN 37932
[3] Sleeman, Hanley & DiNitto, Boston, MA 02138
[4] AQUA TERRA Consultants, Mountain View, CA 94043
[5] EVS Environment, North Vancouver, B.C. Canada V7P 2R4
[6] Eco Modeling, Diamondhead, MS 39525
[7] A. Stoddard & Associates, Hamilton, VA 20158
[8] U.S. EPA, Region 1, Boston, MA 02114
[9] U.S. EPA, Office of Water/Office of Science & Technology, Washington, DC 20460
[10] ZZ Consulting, LLC, Jefferson City, TN 37932

TABLE OF CONTENTS

Section **Page**

Section **Page**

TABLE OF CONTENTS
(Continued)

TABLE OF CONTENTS
(Continued)

Section   **Page**

LIST OF FIGURES

Title   **Page**

LIST OF FIGURES
(Continued)

Title   **Page**

LIST OF TABLES

Title **Page**

LIST OF ACRONYMS

ACO	Administrative Consent Order
ADCP	Acoustic Doppler Current Profiler
Ah	aryl hydrocarbon
ARM	Agricultural Runoff Management
AWT	Advanced Waste Treatment
BAFs	bioaccumulation factors
BBL	Blasland, Bouck and Lee, Inc.
BMPs	Best Management Practices
BNR	Biological Nutrient Removal
BOD	Biochemical Oxygen Demand
BSAFs	biota-sediment accumulation factors
CMS	Corrective Measures Study
CSOs	Combined Sewer Overflows
CTDEP	Connecticut Department of Environmental Protection
DEM	digital elevation model
DMR	Discharge Monitoring Report
DNAPL	dense nonaqueous phase liquids
DO	dissolved oxygen
DOC	dissolved organic carbon
DOJ	Department of Justice
DOM	dissolved organic matter
EFDC	Environmental Fluid Dynamics Code
EPA	U.S. Environmental Protection Agency
FWS	U.S. Fish & Wildlife Service
GE	General Electric
GIS	geographic information system
GSTARS	Generalized Stream Tube Model For Alluvial River Simulation
HSA	Hydrologic Study Area
HSP	Hydrologic Simulation Program
HSPF	Hydrological Simulation Program—FORTRAN
MADEP	Massachusetts Department of Environmental Protection
NAWQA	National Water-Quality Assessment Program
NITR	nitrogen
NO_2	nitrite

NO_3	nitrate
NOAA	National Oceanic and Atmospheric Administration
NPDES	National Pollutant Discharge Elimination System
NPS	nonpoint sources
NWS	National Weather Service
PAHs	polycyclic aromatic hydrocarbons
PCBs	polychlorinated biphenyls
PES	Particle Entrainment Simulator
PET	potential evapotranspiration
POC	particulate organic carbon
POM	particulate organic matter
POTW	Publicly Owned Treatment Works
PSA	Primary Study Area
QSPRs	Quantitative Structure-Property Relationships
R/FP	Riverine/Flood Plain
RCRA	Resource Conservation and Recovery Act
RFI	RCRA Facility Investigation
SCOX	side channels, backwaters, isolated meanders, or oxbows
SCS	Soil Conservation Service
SOD	Sediment Oxygen Demand
STORET	STORage and RETrieval
TEFs	Toxic Equivalency Factors
TKN	Total Kjeldahl Nitrogen
TMDL	total maximum daily load
TSS	total suspended solids
UBOD or BODU	Ultimate Biochemical Oxygen Demands
USACE	U.S. Army Corps of Engineers
USDA	U.S. Department of Agriculture
USGS	U.S. Geological Survey
WLA	Waste Load Allocation
WMS	Watershed Model System
WP	Woods Pond
WQS	Water Quality Standard
WWTP	wastewater treatment plant

EXECUTIVE SUMMARY

ES.1 PURPOSE AND OBJECTIVES OF THE MODELING FRAMEWORK DESIGN

Evaluation of the risks posed to human health and the environment from contaminated sediments often requires the application of coupled watershed/hydrodynamic/water quality models and contaminant fate and bioaccumulation models to address the full range of migration pathways of chemicals released to the environment. The use of a fully integrated modeling framework is needed to produce a scientifically defensible application of models to support regulatory decisionmaking.

The proposed modeling study was developed to (1) represent the full range of physical, chemical, and biological processes of concern for PCB fate, transport, and bioaccumulation in the Housatonic River watershed, and (2) address each of the following site-specific study objectives:

- Quantify future spatial and temporal distribution of PCBs (both dissolved and particulate forms) within the water column and bed sediment.

- Quantify the historical and relative contributions of various sources of PCBs on ambient water quality and bed sediment.

- Quantify the historical and relevant contribution of various PCB sources to bioaccumulation in targeted species.

- Estimate the time required for PCB-laden sediment to be effectively sequestered by the deposition of "clean" sediment (i.e., natural recovery).

- Estimate the time required for PCB concentrations in fish tissue to be reduced to levels that no longer pose either a human health or ecological risk based on various remediation and restoration scenarios, including allowing for natural recovery.

- Quantify the relative risk(s) of extreme storm event(s) contributing to the resuspension of sequestered sediment and the redistribution of PCB-laden sediment within the area of study.

ES.2 MODELING STUDY OVERVIEW

Historical releases of certain classes of organic and inorganic chemicals into waterbodies have left a legacy of aquatic sediment enriched with these contaminants. In some sediments these contaminants have accumulated to levels that may pose an unacceptable human health and ecological risk. Of particular concern is the historical release to waterbodies of compounds known as polychlorinated biphenyls (PCBs), given that they are toxic, persistent, and bioaccumulate in the food chain.

PCBs historically were released to the Housatonic River (see Figure 1-1) from the General Electric (GE) facility in Pittsfield, MA. Over a period of decades, these compounds have accumulated in the river's bed sediment and impoundments in Massachusetts and Connecticut. High-flow events have transported PCB-laden sediment onto the adjacent floodplain. Data collected from 1982 to the present have documented the magnitude and extent of the PCB contamination of the sediments and floodplain soils adjacent to the Housatonic River downstream of the GE facility. The extent of the PCB contamination was estimated in previous investigations to fall within the 10-year floodplain of the Housatonic River.

In addition, PCBs in fish tissue have accumulated to levels that pose a risk to human health. A recent U.S. Geological Survey (USGS) report notes that PCB concentrations in Housatonic River streambed sediments and fish tissue constitute some of the highest PCB levels of all of the National Water-Quality Assessment Program (NAWQA) study sites nationwide. In 1982, the Massachusetts Department of Environmental Protection (MADEP) issued a consumption advisory for fish in the Housatonic River from Dalton, MA, to the Connecticut border. Previously Connecticut had issued a fish consumption advisory for sections of the Housatonic River in Connecticut as a result of PCB contamination. In 1999, MADEP issued a consumption advisory for ducks collected from the river from Pittsfield to Rising Pond in Great Barrington, MA. Concerns expressed by local residents regarding possible health effects resulting from exposure to PCB contamination are being investigated by the Massachusetts Department of Public Health.

The geographic focus of the modeling study is from the confluence to Woods Pond Dam because historical data indicate that this area contains the principal mass of PCBs.

ES.3   REGULATORY FRAMEWORK

In September 1998, after years of scientific investigations and regulatory actions, a comprehensive agreement was reached between GE and various governmental entities, including EPA, MADEP, the U.S. Department of Justice, the Connecticut Department of Environmental Protection, and the City of Pittsfield. The agreement provides for the investigation and cleanup of the Housatonic River and associated areas. The agreement has been documented in a Consent Decree between all parties that was lodged with the Federal Court in October 1999.

Under the terms of the Consent Decree, EPA is conducting the following investigations:

- Human health risk assessment.

- Ecological risk assessment.

- Detailed modeling study of hydrodynamics, sediment transport, and PCB fate and bioaccumulation in the Housatonic River below the confluence of the East and West Branches and the encompassing watershed.

The Consent Decree also includes specific language that requires the risk assessments and components of the modeling studies to be submitted for formal Peer Review to help guide the effort and ensure consistency with EPA policy and guidance. This report, the proposed Modeling Framework Design, is the first component of the modeling study to be submitted for Peer Review.

ES.4   CONCEPTUAL MODEL OF THE HOUSATONIC RIVER

A conceptual model of the Primary Study Area (PSA) of the river was developed to summarize the significant physical, chemical, and biological processes that may affect the transport and fate of PCBs. The conceptual model combines an evaluation of the available data relevant to the study area with a determination of which processes are significant for inclusion in the modeling effort, which processes should be excluded, and which processes require further evaluation.

The Housatonic River in the PSA is a mature, highly meandering river system with four distinct hydraulic regimes that affect sediment and PCB transport and fate. PCBs have been detected across the entire study area out to the 10-year floodplain boundary, with the highest

1 concentrations detected in river sediments, along the riverbanks, and into adjacent floodplains.

2 Woods Pond Dam, which defines the downstream boundary of the PSA, is the first impoundment

3 downstream from the GE facility. The dam has created a backwater effect, resulting in

4 significant deposition of sediments and PCBs in the pond and backwater areas immediately

5 upstream. Extensive sampling of a wide variety of biota indicates that most of the biological

6 components of the system are also contaminated with PCBs.

7 Data collected since 1998 have indicated that the bulk of sediment transport and presumably of

8 PCBs through the system occurs primarily as a result of storm events rather than base flow in the

9 river. It appears that both bedload and suspended sediment loads contribute to much of the

10 sediment and PCB transport. The data further show that sequestering of PCBs is not occurring to

11 any appreciable extent. Data from Woods Pond show that the highest PCB concentrations occur

12 at or near the sediment surface. Evaluation of relative PCB concentrations in water and

13 sediments indicates that partitioning is not in equilibrium over large portions of the study area,

14 possibly as a result of free-phase PCBs in the system.

15 **ES.5   MODELING FRAMEWORK**

16 Modeling studies are based upon four fundamental principles: (1) conservation of momentum,

17 (2) conservation of mass and energy, (3) thermodynamics, and (4) ecological interactions and

18 processes.

19 An environmental modeling framework for a contaminant such as PCBs is designed to represent

20 the most important physical transport processes, pollutant loads, and physical, chemical, and

21 biological processes representing the fate of the chemical of concern, while maintaining mass

22 balance. This type of modeling study is designed to describe how releases of a chemical are

23 transported and become distributed throughout the watershed in the river, sediment bed,

24 floodplain, and aquatic and terrestrial animals and plants. The key components of an

25 environmental modeling framework are quantitative descriptions of (a) inputs of the contaminant

26 and other related constituents; (b) water motion from physical transport; and (c) kinetic transfers

27 of the contaminant and other related constituents between the water column, sediment bed,

28 floodplain, and biota.

1 To conduct a modeling study of the environmental impact of remedial scenarios in comparison to

2 the baseline or "no action" alternative, the modeling framework must first be systematically

3 tested (i.e., calibrated and validated) to ensure that the modeling framework is scientifically

4 credible. During the model calibration process, values of the parameters and coefficients of the

5 model, assigned from either site-specific data or the literature, are adjusted until the comparison

6 of model results to observed data satisfies the established criteria. Model results are then

7 validated by comparison to a second, independent set of data collected for a different time

8 period. The "goodness of fit" of the model and observed data used for validation are evaluated

9 using the criteria established for how well the model results agree with the observed data.

10 Substantial additional detail on model calibration and validation procedures and acceptance

11 criteria are provided in the Modeling Study QAPP (Beach et al., 2000).

12 In the calibration and validation of an environmental model, the fundamental test of any

13 modeling study is to demonstrate that a "mass balance" has been achieved for each key

14 constituent being modeled. For this investigation, the primary constituents included in the

15 assessment of mass balance are water, solids, and PCBs. The principle behind achieving a mass

16 balance is to ensure that all inputs, outputs, and internal gains and losses have been properly

17 accounted for by the descriptions of water motion and the kinetic pathways of solids and PCBs.

18 Satisfaction of the mass balance principle requires an accurate representation of the relevant

19 physical, chemical, biological, and geologic processes within the model framework that will be

20 used for this investigation.

21 The ability of any model to precisely answer questions and/or predict future conditions over a

22 period of decades must be carefully considered. Consequently, in the final analysis, a "weight of

23 evidence" approach will be taken, including all available information and tools in addition to the

24 model output.

25 The modeling framework was specifically developed to address each objective of the Housatonic

26 River PCB fate and transport modeling study described above and the requirements identified in

27 the development of the conceptual model. A modeling framework is needed because no single

28 model is capable of representing all the physical, chemical, and biological processes pertinent to

29 this investigation over the wide range of spatial and temporal scales that exist at the site.

1   The basic modeling framework for this study proposes the use of HSPF as the watershed

2   component, EFDC as the hydrodynamic and sediment transport component, and AQUATOX as

3   the PCB fate and bioaccumulation component.

4   **ES.6   HSPF–WATERSHED HYDROLOGY AND NONPOINT SOURCE LOADS**
5   **MODEL COMPONENT**

6   For the past 20 years, the Hydrological Simulation Program-FORTRAN (HSPF) has been the

7   state-of-the art model available for developing watershed-based simulations of hydrology and

8   water quality processes. HSPF has been widely accepted by experts in environmental modeling

9   and has been used for hundreds of complex applications, including the development of a

10   hydrologic model of the Housatonic River watershed for the State of Connecticut. HSPF has

11   been selected by EPA Office of Science & Technology as the watershed model component of the

12   BASINS model framework.

13   The watershed model encompasses the largest spatial extent of the system. The physical domain

14   of the watershed model includes 282 square miles of the drainage basin of the Housatonic River

15   from the headwaters to Great Barrington, MA. The watershed model is designed to account for

16   the hydrologic balance of the drainage basin between precipitation, infiltration, and streamflow

17   runoff.

18   The principal use of HSPF is to establish external boundary conditions for input to the

19   hydrodynamic and sediment transport model (EFDC) and the PCB fate and bioaccumulation

20   model (AQUATOX).

21   **ES.7   EFDC–HYDRODYNAMICS AND SEDIMENT TRANSPORT MODEL**
22   **COMPONENT**

23   The Environmental Fluid Dynamics Code (EFDC) is a public domain model developed with

24   funding from the Commonwealth of Virginia and the U.S. EPA. EFDC is a three-dimensional

25   (3D), state-of-the-art computational physics model that incorporates submodels for

26   hydrodynamics, sediment transport, contaminants, eutrophication, and water quality within a

27   single source code. EFDC has been selected by the EPA Office of Science & Technology to

1 provide the key hydrodynamic, sediment transport, contaminant, and eutrophication model

2 components for the EPA.

3 The spatial area represented in the EFDC model includes the PSA of the Housatonic River

4 extending 10.7 miles from the confluence of the East and West Branches of the river in Pittsfield

5 to Woods Pond Dam. The physical domain includes the river channel, the sediment bed, the 10-

6 year floodplain, Woods Pond, and the backwater areas of the Woods Pond impoundment.

7 The principal use of EFDC in the model framework is to provide AQUATOX with streamflow,

8 water volume, cross-sectional area, and inorganic solids loadings. Because the spatial and time

9 scales of the EFDC model are much more detailed than the coarse space and time scales used in

10 AQUATOX, the model results generated by EFDC will be integrated over a 24-hour time scale

11 and summed over the multiple EFDC grid cells that correspond to each larger AQUATOX reach.

12 **ES.8   AQUATOX–PCB FATE AND BIOACCUMULATION MODEL COMPONENT**

13 The AQUATOX model is a general ecological fate model that represents the combined

14 environmental fate and effects of energy, nutrients, organic matter, and contaminants through

15 several trophic levels of an aquatic ecosystem. AQUATOX has been applied to streams, ponds,

16 lakes, and reservoirs with representations of trophic food webs that include attached and

17 planktonic algae, macrophytes, invertebrates, and pelagic and bottom-feeding fish. AQUATOX

18 has been selected by the EPA Office of Science & Technology for wide dissemination to

19 encourage its use by EPA regional offices, state agencies, and universities in aquatic modeling

20 analyses.

21 The geographic area to be represented by the AQUATOX model extends from the confluence to

22 the Woods Pond Dam. The physical domain includes the river channel, the sediment bed,

23 Woods Pond, and the backwater areas of the Woods Pond impoundment. To represent the

24 pathways of PCBs and water quality constituents within the biota of the aquatic food web over

25 monthly, seasonal, and decadal time scales, a coarse spatial resolution of the physical domain

26 and a low-frequency daily time scale is considered appropriate for the PCB fate and

27 bioaccumulation model.

1   AQUATOX incorporates nutrients, organic matter, cohesive and noncohesive inorganic

2   suspended solids, dissolved oxygen, water column algae, attached algae, macrophytes,

3   zooplankton, invertebrates, pelagic fish, and bottom-feeding fish. PCBs, represented as

4   homologs and selected congeners, will be accounted for by partitioning of PCBs into dissolved

5   and particulate components in the water column and sediment bed. The AQUATOX model will

6   simulate the transfer of PCBs released into the river from water and solids throughout the food

7   web via adsorption, ingestion, and other ecological processes. The complex pathways and

8   interactions of PCBs and other components of the aquatic ecosystem provide the mechanisms for

9   tracking the distribution and transformation of PCBs throughout the water column, sediment bed,

10   and food web of the river.

1. INTRODUCTION

1.1 OVERVIEW

Historical releases of certain classes of organic and inorganic chemicals into waterbodies have left a legacy of aquatic sediment enriched with these contaminants. In some sediments these contaminants have accumulated to levels that may pose an unacceptable human health and ecological risk. Of particular concern is the historical release to waterbodies of compounds known as polychlorinated biphenyls (PCBs), given that they are toxic, persistent, and bioaccumulate in the food chain.

PCBs historically were released to the Housatonic River (see Figure 1-1) from the General Electric (GE) facility in Pittsfield, MA. Over a period of decades, these compounds have accumulated in the river's bed sediment and impoundments in Massachusetts and Connecticut. High-flow events have transported PCB-laden sediment onto the adjacent floodplain. Data collected from 1982 to the present have documented the magnitude and extent of the PCB contamination of the sediments and floodplain soils adjacent to the Housatonic River downstream of the GE facility. The extent of the PCB contamination was estimated in previous investigations to fall within the 10-year floodplain of the Housatonic River.

In addition, PCBs in fish tissue have accumulated to levels that pose a risk to human health (EPA, 1998a). A recent U.S. Geological Survey (USGS) report (Garabedian et al., 1998) notes that PCB concentrations in streambed sediments and fish tissue in the Housatonic are some of the highest of all their National Water-Quality Assessment Program (NAWQA) study sites across the country. In 1982, the Massachusetts Department of Environmental Protection (MADEP) issued a consumption advisory for fish in the Housatonic River from Dalton, MA, to the Connecticut border. Previously Connecticut had issued a fish consumption advisory for sections of the Housatonic River in Connecticut as a result of PCB contamination. In 1999, MADEP issued a consumption advisory for ducks collected from the river from Pittsfield to Rising Pond in Great Barrington, MA. Concerns expressed by local residents regarding possible health effects resulting from exposure to PCB contamination are being investigated by the Massachusetts Department of Public Health.

1   In September 1998, after years of scientific investigations and regulatory actions, a

2   comprehensive agreement was reached between GE and various governmental entities, including

3   EPA, MADEP, the U.S. Department of Justice (DOJ), Connecticut Department of Environmental

4   Protection, and the City of Pittsfield. The agreement provides for the investigation and cleanup

5   of the Housatonic River and associated areas. The agreement has been documented in a Consent

6   Decree between all parties that was lodged with the Federal Court in October 1999. Under the

7   terms of the Consent Decree, EPA is conducting the human health and ecological risk

8   assessments, as well as the detailed modeling study of PCB transport and fate for the Housatonic

9   River below the confluence of the East and West Branches ("Rest of River") and the surrounding

10 watershed.

11 The Consent Decree also includes specific language that requires the risk assessments and

12 components of the modeling studies to be submitted for formal Peer Review to help guide the

13 effort and ensure consistency with EPA policy and guidance. This report, the proposed

14 Modeling Framework Design, is the first component of the modeling study to be submitted for

15 Peer Review.

16 **1.2 PURPOSE AND OBJECTIVES OF THE HOUSATONIC RIVER MODELING**
17 **STUDY**

18 Evaluation of the risks posed to human health and the environment from contaminated sediments

19 often requires the application of coupled watershed/hydrodynamic/water quality models and

20 contaminant fate and bioaccumulation models to address the full range of migration pathways of

21 chemicals released to the environment. The use of a fully integrated modeling framework is

22 needed to produce a scientifically defensible application of models to support regulatory

23 decisionmaking.

24 The proposed modeling study design was developed to (1) represent the full range of physical,

25 chemical, and biological processes of concern for PCB fate, transport, and bioaccumulation in

26 the Housatonic River watershed, and (2) address each of the following site-specific study

27 objectives:

28 ▪   Quantify future spatial and temporal distribution of PCBs (both dissolved and
29   particulate forms) within the water column and bed sediment.

NY

MA

CT

Long Island Sound

Scale In Miles

4   0   4   8

Coltsville
City of Pittsfield
Dalton
East Branch
Housatonic River
West Branch
Housatonic River
Woods Pond
Rising Pond
Great Barrington
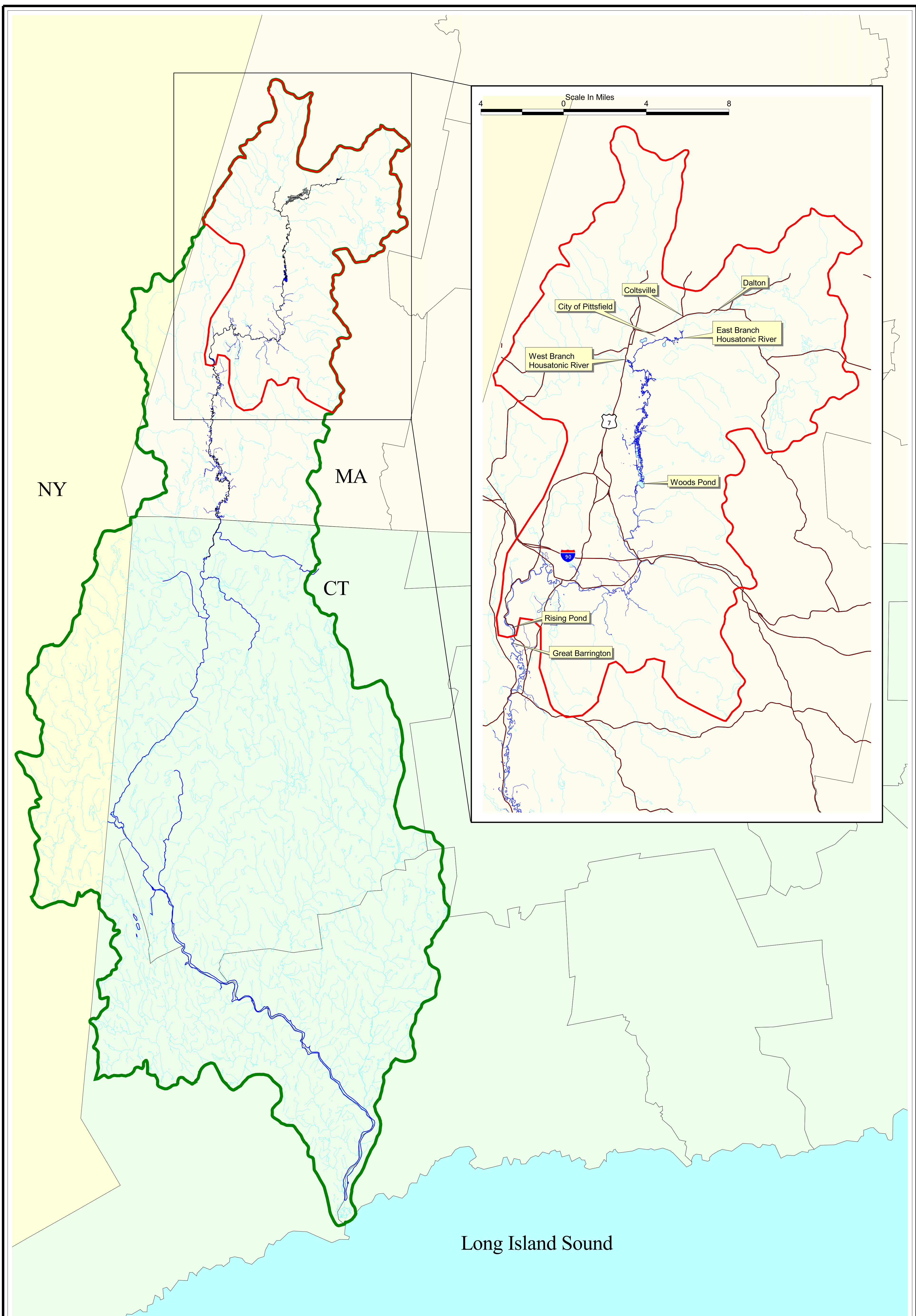
LEGEND:

Surface Hydrology
Housatonic Watershed Boundary
Watershed Area Above Great Barrington

N

Scale in Miles

6   0   6   12

Housatonic River Project
Pittsfield, Massachusetts

FIGURE 1-1
HOUSATONIC RIVER
WATERSHED

o:\gepitt\aprs\overview.apr | layout-figure1-1 | o:\gepitt\epsfiles\portrait24x36\in\figure1-1.eps | 10:44 AM, 10/5/2000

1   • Quantify the historical and relative contributions of various sources of PCBs on
2   ambient water quality and bed sediment.

3   • Quantify the historical and relevant contribution of various PCB sources to
4   bioaccumulation in targeted species.

5   • Estimate the time required for PCB-laden sediment to be effectively sequestered by
6   the deposition of "clean" sediment (i.e., natural recovery).

7   • Estimate the time required for PCB concentrations in fish tissue to be reduced to
8   levels that no longer pose either a human health or ecological risk based on various
9   remediation and restoration scenarios, including allowing for natural recovery.

10 • Quantify the relative risk(s) of extreme storm event(s) contributing to the
11   resuspension of sequestered sediment and the redistribution of PCB-laden sediment
12   within the area of study.

1.3 BROADER MODELING STUDY OBJECTIVES

14 In addition to meeting the site-specific objectives, the modeling study must be designed to

15 achieve even more basic objectives inherent to the successful execution of any modeling effort.

16 These broader objectives are discussed below.

1.3.1 Achieving Mass Balance

18 The fundamental test of any complex modeling study is to demonstrate that a "mass balance" has

19 been achieved for each of the key constituents being modeled. For this investigation, the

20 primary constituents being modeled are water, solids, and PCBs. The principle behind achieving

21 a mass balance is to ensure that all inputs, outputs, and internal source/sink terms have been

22 properly accounted for. This requires an accurate representation of the relevant physical,

23 chemical, biological, and geologic processes within the models that will be used for this

24 investigation.

1.3.1.1 Water Mass Balance

26 The modeling study must achieve an overall water mass balance that reproduces the historical

27 distribution of observed flows within the Housatonic River. This is an important component of

28 the analysis given the role hydrodynamics play in the physical transport of solids and PCBs. To

29 impose an appropriate external forcing function on the hydrodynamic model, a calibrated and

1 validated hydrologic model must be developed. The hydrologic model must account for

2 tributary flows into the region covered by the hydrodynamic model as well as movement of

3 water through the main river channel at the boundaries of the hydrodynamic model.

4 The hydrologic model must establish these external boundary conditions to the hydrodynamic

5 model under both historical conditions and projected future conditions. The hydrodynamic

6 model, in turn, uses the external boundary conditions to simulate the distribution of flows within

7 the system and resulting internal forces acting on the sediment bed. To represent future

8 conditions, an implicit assumption is made that historical conditions (e.g., spatial and temporal

9 distribution of flow and solids) are representative of future conditions. A validated hydrologic

10 model provides the technical basis for developing probability-based, future boundary conditions

11 to the hydrodynamic model.

12 ### *1.3.1.2 Solids Mass Balance*

13 Because of the preference for PCBs to adsorb to sediment, achieving mass balance of solids is

14 very important to the success of the model in accurately representing the conditions in the system

15 being modeled. A change in the solids mass balance will ultimately affect the overall PCB mass

16 balance. The purpose of the solids mass balance is to ensure that both short- and long-term

17 transport of solids can be reproduced within the model validation process.

18 ### *1.3.1.3 PCB Mass Balance*

19 The PCB mass balance is the primary objective of this study. Numerous complex fate and

20 transport processes influence the distribution of PCBs within the river and the floodplain. The

21 PCB mass balance will define what processes are controlling the ultimate distribution and fate of

22 PCBs within the study area.

23 Definition of the PCB mass balance requires accurate source characterization and representation

24 of the distribution of PCBs in the conceptual model for the site.

1.3.2 Ability to Provide an Estimation of Future Conditions

The primary objective that will be pursued after achieving acceptable mass balance in the models is the ability to answer questions regarding the future spatial and temporal distribution of PCBs in the various media under different potential remedial scenarios.

It should be emphasized that the ability of any model to accurately answer questions and/or predict future conditions that span a period of decades must be carefully considered. Consequently, in the final analysis a "weight of evidence" approach will be taken, including all available information and tools in addition to the model output.

1.3.3 Evaluation of Uncertainty

Any modeling study presumes that the fundamental questions to be answered with the assistance of models are known a priori. This is an appropriate assumption given that a scientifically valid modeling framework cannot be defined otherwise. Since the modeling framework provides the mathematical representation of the science underlying the study, it is necessary that the models applied within the framework are appropriate for the purpose of answering these questions. In other words, the models must incorporate algorithms that are credible representations of real-world processes.

Because natural systems inherently have complex, random, and nonlinear processes that cannot be accounted for in any model, it should be clearly emphasized that any model formulation strives for a compromise between physical reality and practicality of use. This is particularly true of numerous physical, chemical, and biological processes occurring within this system. In many cases, no empirical or predictive methods exist that would allow a model to reproduce the consequences of these processes.

However, one cannot simply dismiss these processes as only introducing marginal or second-order error terms into the solids and PCB mass balance equations because no empirical relationships exist to predict their distribution and occurrence. Therefore, as stated above, model output will be augmented using a "weight of evidence" approach with other nondeterministic methods to reduce the degree of uncertainty associated with these processes. In addition, effort

1   will be made to identify other areas of uncertainty such as changes in channel dimensions,

2   entrainment of slumped bank sediments, dissolution and transport of dense nonaqueous phase

3   liquids (DNAPL), population fluctuations, and sporadic macrophyte die-back.

2. BACKGROUND

This section provides a discussion of the historical discharge of PCBs and the regulatory history of the site, and a description of the physical setting of the Housatonic River watershed. The following two sections draw heavily on existing information and recent reports prepared as part of the Housatonic River investigation; many sections are taken from the Source Characterization Report (WESTON, 1998a) and the Supplemental Investigation Work Plan (WESTON, 2000a).

2.1 SITE HISTORY AND REGULATORY BACKGROUND

2.1.1 Site History

The following section on site history was extracted from the Supplemental Investigation Work Plan prepared by Roy F. Weston, Inc. (WESTON, 2000a):

The Housatonic River is located in the center of a rural area of western Massachusetts where farming was the main occupation from colonial settlement through the late 1800s. As with most rivers, the onset of the industrial revolution in the late 1800s brought manufacturing to the banks of the Housatonic River. The manufacture of paper and textiles began in Pittsfield and the area to the south during the late 19th century. The city's manufacturing base grew to include machinery and electrical transformers during the early 20th century, when industries such as the Stanley Electric Company and the Berkshire Gas Company and its predecessors occupied portions of the property near the intersection of East Street and Merrill Road. GE began its operations in its present location in 1903. Three manufacturing divisions have operated at the GE facility (Transformer, Ordnance, and Plastics).

The GE plant in Pittsfield has historically been the major handler of PCBs in western Massachusetts, and is the only known source of PCB wastes discovered in the Housatonic River sediments and floodplain between Pittsfield and Lenox. Although GE performed many functions at the Pittsfield facility throughout the years, the activities of the Transformer Division were the likely primary source of PCB contamination. Briefly, GE's Transformer Division's activities included the construction and repair of electrical transformers using dielectric fluids, some of which contained PCBs (primarily mixtures referred to as Aroclors 1254 and 1260). GE manufactured and serviced electrical transformers containing PCBs at this facility from approximately 1932 through 1977.

According to GE's reports, from 1932 through 1977 releases of PCBs reached the wastewater and storm systems associated with the facility and were subsequently conveyed to the East Branch of the Housatonic River and to Silver Lake (Supplemental Phase II/RCRA Facility Investigation Report for Housatonic River and Silver Lake,

Volume I, by BBL, January 1996). In or around 1968, a 1,000-gallon PCB storage tank located in Building 68 of the GE facility collapsed, releasing liquid Aroclor 1260 onto the riverbank soil and into the Housatonic River. Based on visual observation, Aroclor-contaminated soils and sediments were excavated by GE and eventually landfilled; however, significant contamination remains as a result of this release.

During the 1940s, efforts to straighten the Pittsfield reach of the Housatonic River by the City of Pittsfield and the U.S. Army Corps of Engineers (USACE) resulted in 11 former oxbows being isolated from the river channel. These areas were filled with materials that were later discovered to contain PCBs and other hazardous substances.

Areas of the 254-acre GE manufacturing facility; the Housatonic River, riverbanks, and associated floodplains from Pittsfield, MA, to Rising Pond Dam (approximately 30 miles); former river oxbows that have been filled; neighboring commercial properties; Allendale School; Silver Lake; and other properties or areas have become contaminated as a result of GE's facility operations.

Surface water runoff from sources, flooding of sources by the Housatonic River, migration of nonaqueous phase liquids, direct discharge of PCB fluids from the Building 68 tank implosion, and groundwater discharge from the sources to the Housatonic River have been interpreted as the cause of the sediment contamination in the Housatonic River. Migration and redistribution of sediments contaminated with Aroclor 1254 and 1260 and other hazardous materials within the Housatonic River have further resulted in contamination detected in the floodplain downstream from the site.

Numerous studies conducted since 1988 have documented PCB contamination of soils within the floodplain of the Housatonic River downstream of the GE plant and former oxbows. Most of the floodplain soil PCB contamination (exceeding 1 ppm total PCBs) detected historically falls within the approximate extent of the river's 5-year floodplain. PCBs have also been detected in sediments beyond the Massachusetts/Connecticut state line, located approximately 46 miles below the facility. PCB contamination downstream is believed to result from the redistribution by flooding of PCB wastes released from wastewater discharge, flooding of source areas by the Housatonic River, migration of nonaqueous phase liquids, and direct discharge of PCB fluids from the Building 68 tank implosion and groundwater discharge from the sources to the Housatonic River have been interpreted as the cause of the sediment contamination in the Housatonic River. In some cases, the contaminated soil is located on residential properties and within 200 ft of the residences on these properties. Other contaminated areas include parts of the Audubon Society's Canoe Meadow Wildlife Sanctuary and the Housatonic River Valley State Wildlife Management Area. The Housatonic River was closed to all but catch and release fishing from Dalton, MA, to the Connecticut border by the MADEP in 1982 as a result of PCB contamination in the river sediments and fish tissues, and sections of the river in Connecticut were posted earlier due to PCB contamination. In addition, MADEP issued a consumption advisory for ducks taken from the river between Pittsfield and Rising Pond in 1999. Concerns expressed by local residents regarding possible health effects resulting from exposure to PCB contamination are being investigated by the Massachusetts Department of Public Health.

1	Analyses of sediment samples collected upstream of the GE site reveal trace or non-detectable concentrations of Aroclor 1254 or 1260. Beginning at the confluence of
2	
3	Unkamet Brook and the Housatonic River, either Aroclor 1254, or 1260, or both, as well
4	as other hazardous substances, have been detected in samples collected at the GE facility,
5	and from within the banks and floodplain of the Housatonic River. The highest
6	concentrations of Aroclor 1254 and 1260 have been detected near the GE facility in the
7	vicinity of the site, downstream of the former Building 68 PCB spill. Previous
8	investigations suggest that the majority of the PCB-contaminated sediment and floodplain
9	soil is found above Woods Pond.

1   Analyses of sediment samples collected upstream of the GE site reveal trace or non-
2   detectable concentrations of Aroclor 1254 or 1260. Beginning at the confluence of
3   Unkamet Brook and the Housatonic River, either Aroclor 1254, or 1260, or both, as well
4   as other hazardous substances, have been detected in samples collected at the GE facility,
5   and from within the banks and floodplain of the Housatonic River. The highest
6   concentrations of Aroclor 1254 and 1260 have been detected near the GE facility in the
7   vicinity of the site, downstream of the former Building 68 PCB spill. Previous
8   investigations suggest that the majority of the PCB-contaminated sediment and floodplain
9   soil is found above Woods Pond.

10   The Housatonic River flowed through the City of Pittsfield in its natural state until the
11   1940s when the river was channelized within the City of Pittsfield, isolating several
12   oxbows. In addition, the Massachusetts Department of Public Works undertook flood
13   control work based on reports by the USACE. Work within the site area included the
14   East Branch within the City of Pittsfield, and the riverbanks above and below Woods
15   Pond. The river's course is relatively unaffected (with the exception of the dams
16   discussed below) in areas south of the city.

17   The many dams that are part of the historical development of the Housatonic River may
18   have potentially affected the downstream distribution of PCBs and other contaminants
19   from the GE facility. Multiple dams were constructed on the Housatonic River as
20   industrial development created a demand for water power, water supplies, and
21   hydroelectric power. There are a total of 13 dams on the river in Massachusetts and 5
22   dams on the river in Connecticut. Between the confluence of the East and West Branches
23   of the Housatonic River and the Connecticut state line, there are six dams: one at Woods
24   Pond in Lee, MA; two other small dams in Lee, MA; two small dams in Stockbridge and
25   the Village of Housatonic; and one at Rising Pond near Great Barrington.

26   **2.1.2 Site Regulatory Background**

27 The GE Housatonic River site has been subject to regulatory investigations dating back to the

28 late 1970s. These investigations were consolidated under two regulatory mechanisms: an

29 Administrative Consent Order (ACO) with the Massachusetts Department of Environmental

30 Protection (MADEP) and a Corrective Action Permit with the U.S. Environmental Protection

31 Agency (EPA) under the Hazardous and Solid Waste Amendments to the Resource Conservation

32 and Recovery Act (RCRA).

33 In 1991, EPA issued a RCRA Corrective Action Permit to the GE facility. Following an appeal

34 and subsequent modification, the permit was reissued in 1994. The permit included the 254-acre

35 facility, Silver Lake, the Housatonic River and its floodplains and adjacent wetlands, and all

36 sediments contaminated by PCBs migrating from the GE facility.

1   In addition to the permit, the ACO between GE and MADEP became effective in 1990 and

2   included those areas defined in the permit as well as three additional study areas: Newell Street

3   Area I, the Former Housatonic River Oxbows, and the Allendale School Property. Under the

4   ACO, GE has performed several investigations and short-term cleanups.

5   In September 1998, representatives of EPA, MADEP, U.S. Department of Justice (DOJ),

6   Connecticut Department of Environmental Protection (CTDEP), the City of Pittsfield, GE, and

7   others reached a comprehensive agreement relating to the GE facility and the Housatonic River.

8   This agreement provides for the investigation and cleanup of the Housatonic River and

9   associated areas. In addition, the agreement provides for the cleanup and economic

10 redevelopment of the GE facility, environmental restoration of the Housatonic River,

11 compensation for natural resource damages, and government recovery of past and future

12 response costs.

13 Under the scope of the agreement, EPA will conduct additional characterization sampling to

14 determine the nature and extent of contamination, as well as to support the conduct of human

15 health and ecological risk assessments, and surface water modeling.

16 The agreement includes the following actions for the "Rest of River," the river below the

17 confluence of the East and West Branches.

18   ▪   EPA/MADEP to conduct additional sampling, human health and ecological risk
19   assessments, and modeling, and will submit both risk assessments and modeling for
20   Peer Review.

21   ▪   GE to compile all data into a RCRA Facility Investigation (RFI) report and a
22   Corrective Measures Study (CMS).

23   ▪   The governments intend to submit drafts of major technical documents to the Citizens
24   Coordinating Council for review and discussion.

25   ▪   At the conclusion of the studies, EPA will issue a Statement of Basis and modify the
26   RCRA permit.

27   ▪   GE agrees to perform cleanup unless it invokes dispute resolution:

28   -   Review process can include both internal EPA and federal court review.

1   -   During dispute resolution, all work not subject to the dispute continues, and EPA
2   can proceed with designing disputed aspects of cleanup.

3   ▪   GE to perform cleanup as determined after dispute resolution.

4   This agreement was codified in a Consent Decree (00-0388, 00-0389, 00-0390) lodged in U.S.

5   District Court, Massachusetts, Western Division, in October 1999.

6   ## 2.2   PHYSICAL SETTING AND BACKGROUND

7   The Housatonic River is located in the center of a rural area of western Massachusetts in

8   Berkshire County. The river and its tributaries lie in an alluvial plain with the Berkshire Hills to

9   the east and the Taconic Range to the west. Elevations of the drainage basin range from sea

10 level at the river mouth in Connecticut to 2,600 ft above sea level at Brodie Mountain,

11 Massachusetts. The elevation of the riverbed at the GE facility in Pittsfield is 972 ft (msl) and at

12 the Massachusetts-Connecticut border the elevation is approximately 650 ft (msl).

13 The river flows approximately 150 miles from near Pittsfield, MA, to Long Island Sound and

14 drains an area of approximately 1,950 square miles in Massachusetts, New York, and

15 Connecticut. Within Massachusetts, the river drops approximately 600 ft and drains an area of

16 about 500 square miles. Studies have focused on the 52-mile section of the river from Dalton,

17 MA, to the Massachusetts-Connecticut border (see Figure 1-1). The topography near the GE

18 facility (located on the East Branch north of the confluence with the West Branch) is generally

19 flat with little or no relief. Bordering areas slope mildly toward the Taconic Range to the north

20 and west. The facility is adjacent to an area of flat and swampy land to the south and east that

21 borders highlands rising sharply to Tully and Day Mountains.

22 The section of the river in Massachusetts is located in the Humid Temperate Domain, Warm

23 Continental Mountains, Adirondack–New England Mixed Forest–Coniferous Forest–Tundra

24 ecoregion. This province is composed of subdued glaciated mountains and maturely dissected

25 plateaus of mountainous topography. Many glacially broadened valleys have glacial outwash

26 deposits and contain numerous swamps and lakes. The forests within this ecoregion are

27 characterized by sugar maple, yellow birch, beech, and a mixture of hemlock within valleys.

28 Low mountain slopes contain spruce, fir, maple, beech, and birch.

1   Land use in the area around the GE facility is primarily commercial and residential. The GE

2   facility is mainly surrounded by residential areas: Brattle Brook Park, residential neighborhoods,

3   and several schools are located within a 1-mile radius of the facility. Rainfall and melting snow

4   are the main water sources that feed the Housatonic River systems. The average annual

5   precipitation in this river basin is approximately 46 inches per year. Approximately 24 inches

6   per year leave the basin as runoff through the Housatonic River, another 20 inches per year

7   escape to the atmosphere by evaporation and transpiration, while the remaining 2 inches per year

8   infiltrate into the ground.

9   The three tributaries feeding the Housatonic River in the area of the GE facility are Barton

10   Brook, Brattle Brook, and Unkamet Brook. The watershed of these tributaries and the East

11   Branch of the Housatonic River is considered a well-drained area with 0.13 to 0.17 million

12   gallons per day per square mile flowing as runoff. Groundwater also discharges into the river in

13   the area of the GE facility, contributing to the river flow.

14   The flood potential of the Housatonic River Basin has been documented in various studies by the

15   United States Department of Agriculture (USDA) Soil Conservation Service (SCS), the USGS,

16   and USACE. A mapping study was performed by GE between the USGS gaging station in

17   Coltsville and the Connecticut state line. This study shows the extent of 10-year floodplains

18   found by interpolating data from a FEMA report and using data from HEC-2 modeling. The 10-

19   year floodplain is quite narrow adjacent to the GE facility. Downstream of the facility within the

20   Pittsfield City limits, the floodplain widens and includes numerous residential and commercial

21   areas.

22   The watershed study area for the modeling effort encompasses the entire Housatonic River

23   watershed, beginning at the headwaters, down to the USGS gage in Great Barrington, MA,

24   draining an area of approximately 282 square miles. In addition to the overall watershed area,

25   the section of the river from the confluence of the East and West Branches to the Woods Pond

26   Dam (see Figure 1-1) and the associated 10-year floodplain forms the domain of the detailed

27   river modeling study described herein.

28   The current modeling effort will include the river reaches downstream to Woods Pond because

29   of the higher concentration of PCBs in the sediments in the main channel and PCBs accumulated

1   in Woods Pond, the first large depositional area downstream of the GE facility. The following

2   reaches have been defined from Dalton to Woods Pond (Figure 2-1): (1) Dalton to Unkamet

3   Brook; (2) Unkamet Brook to Newell Street Bridge; (3) Newell Street Bridge to Lyman Street

4   Bridge; (4) Lyman Street Bridge to Confluence of the West and East Branches; (5) Confluence

5   to Woods Pond; and (6) Woods Pond. The physical characteristics of each reach provide some

6   insight into the likely physical transport processes that are occurring within them.   Data

7   presented in this brief discussion are taken from Table 2.3-1 and Table 2.3-2 in *Volume I, Final*

8   *Supplemental Investigation Work Plan for the Lower Housatonic River* (WESTON, 2000a).

9   **Reach 1: Dalton to Unkamet Brook.** In the upper section of the Housatonic River from
10 Hubbard Street in Dalton (the location of the USGS Coltsville gage) to the confluence with
11 Unkamet Brook, the channel slope (29.4-42.2 ft/mile) is relatively steep with the riverbed
12 elevation dropping 121 ft over this 2.8-mile section. In this section of the study area, the
13 river alternates between an E-W and N-S orientation and has a narrow floodplain as a result
14 of a portion of the river being previously channelized. The width of the river averages
15 approximately 15 meters with typical water depths varying from 1 to 2 ft. In this steep
16 section of the river, flow is moderate with sediment bed properties characterized as having a
17 depositional area near Unkamet Brook with cobble, gravel, and boulders as the dominant
18 substrate in the upper portions of this reach.

19 **Reach 2: Unkamet Brook to Newell Street Bridge.** In this reach of the East Branch of the
20 Housatonic River, the channel slope (4.8 ft/mile) is considerably more gradual than Reach 1
21 with the riverbed elevation dropping 10 ft over this 2.0-mile section. The river, characterized
22 by both meanders and a channelized section, is oriented roughly NE-SW with a wider
23 floodplain than in Reach 1. The width of the river in this reach typically averages 15 meters
24 with average water depths ranging from 0.2 to 5.0 ft. In this section of the river, flow is slow
25 to moderate with bed features characterized by terrace, channel, and aggrading bar deposits.

26 **Reach 3: Newell Street Bridge to Lyman Street Bridge.** In this urbanized reach of the
27 East Branch of the Housatonic River, the channel slope (6.9 ft/mile) is slightly steeper than
28 Reach 2 with the riverbed elevation dropping 3 ft over this 0.5-mile section. The channelized
29 river is oriented roughly NE-SW with a negligible floodplain. The width of the river in this
30 reach is about 12 to 20 meters with average water depths ranging from 1 to 3.5 ft. In this
31 reach, flow is slow to moderate with sediment bed properties characterized by cobbles,
32 gravel, and coarse sands with very little silt and clay.

33 **Reach 4: Lyman Street Bridge to Confluence of West and East Branches.** In this
34 channelized reach, the channel slope (4.7 ft/mile) is slightly less steep than Reach 3, with the
35 riverbed elevation dropping 7 ft over this 1.4-mile reach. The channelized river is oriented
36 roughly NNE-SSW with a small floodplain near the confluence with the West Branch. The
37 width of the river in this reach is about 12 to 20 meters with average water depths ranging
38 from 0.2 to 4 ft. In this reach, flow is slow to fast with sediment bed properties characterized
39 by cobbles, gravel, and coarse sands with very little silt and clay.

Reach 4a from Pomeroy Avenue Bridge to the confluence with the West Branch is downstream of the channelized reach.

Reach 5: Confluence to Woods Pond. From the confluence of the West and East Branches to the headwaters of Woods Pond, the channel slope (1.6 ft/mile) is very gradual over this 8.0-mile reach with the riverbed elevation dropping 13 ft to the confluence of Woods Pond. Reach 5 is characterized as having two different flow regimes; one that is essentially free-flowing (*Reaches 5a and 5b*) and the other where flows are subject to the backwater influences (*Reach 5c*) caused by Woods Pond Dam. These subreaches are shown on Plate No. 1.

Reach 5a downstream of the confluence with the West Branch to the Wastewater Treatment Plant (WWTP) and *Reach 5b* downstream from the WWTP to Roaring Brook are characterized by a free-flowing river, oriented roughly NNW-SSE, with a wide floodplain and numerous meanders and remnant oxbows and riverbanks that are generally scoured and eroded. The width of the meandering river in the free-flowing section is about 15 to 36 meters with depths up to 10 ft. Reflecting the generally slow velocity characteristics of this flat reach, the sediment bed consists of coarse to fine sands with approximately 10% silts and clay.

Reach 5c downstream of the confluence with Roaring Brook is the section of Reach 5 where flows are influenced by a backwater effect from the Woods Pond Dam; the river, oriented approximately N-S, is characterized by a broad wetland floodplain (~800- to 3,000-ft width) on the west bank with numerous backwater areas, channels, and meanders. The inundated remnant floodplain is easily visible in this section of the river as broad and shallow backwater "embayments" with stands of emergent vegetation, macrophytes, and surface algal mats. On the east bank of the river the narrow floodplain is confined by the steep slopes of October Mountain. The width of the river channel ranges from about 18 to 48 meters with depths of 4 to 8 ft. Under high-flow conditions, the numerous backwater areas are hydraulically connected to flow in the main river channel; under low-flow conditions, however, the backwater areas appear to be largely isolated from the influence of flows in the main river channel. The depositional sediment bed is characterized predominantly by fine sands and silts.

Reach 6: Woods Pond. Woods Pond is a broad, shallow, 60-acre impoundment of the Housatonic River formed by construction of the Woods Pond Dam in the early 1900s; the adjacent upstream deep channel (*Reach 6a*) and backwater areas (*Reach 6b*) account for an additional 62 acres. These subreaches are shown on Plate No. 1. The remnant river channel on the eastern and southern shores of Woods Pond is considerably deeper (maximum depth ~16 ft) than the shallower depths (~1 to 3 ft) of the remnant floodplain to the west and north that are characterized by stands of emergent macrophytes and dense surface algal mats. A deep "hole" of approximately 16 ft depth, is located in the southeastern area of the remnant stream channel (*Reach 6c*). The "hole" is further characterized by a thick deposit (~16 ft) of soft silty-clay sediments that has accumulated over the past 100 years since construction of the Woods Pond Dam. In the shallow remnant floodplain areas of Woods Pond (*Reach 6d*), the sediments are silt and clay with a high organic content. Although the broad, shallow

MA

NY

CT

Long Island Sound

Scale In Miles
2   0   2   4

USGS Gaging Station
Coltsville

General Electric Facility

Reach 5
Confluence East and West Branches
To Woods Pond
(See Plate 1 For More Detail)

5a

5b

5c

Reach 6
Woods Pond

Reach 7
Woods Pond Dam
To Rising Pond

Reach 8
Rising Pond

USGS Gaging Station
Great Barrington

Reach 9
Rising Pond Dam
To Long Island Sound
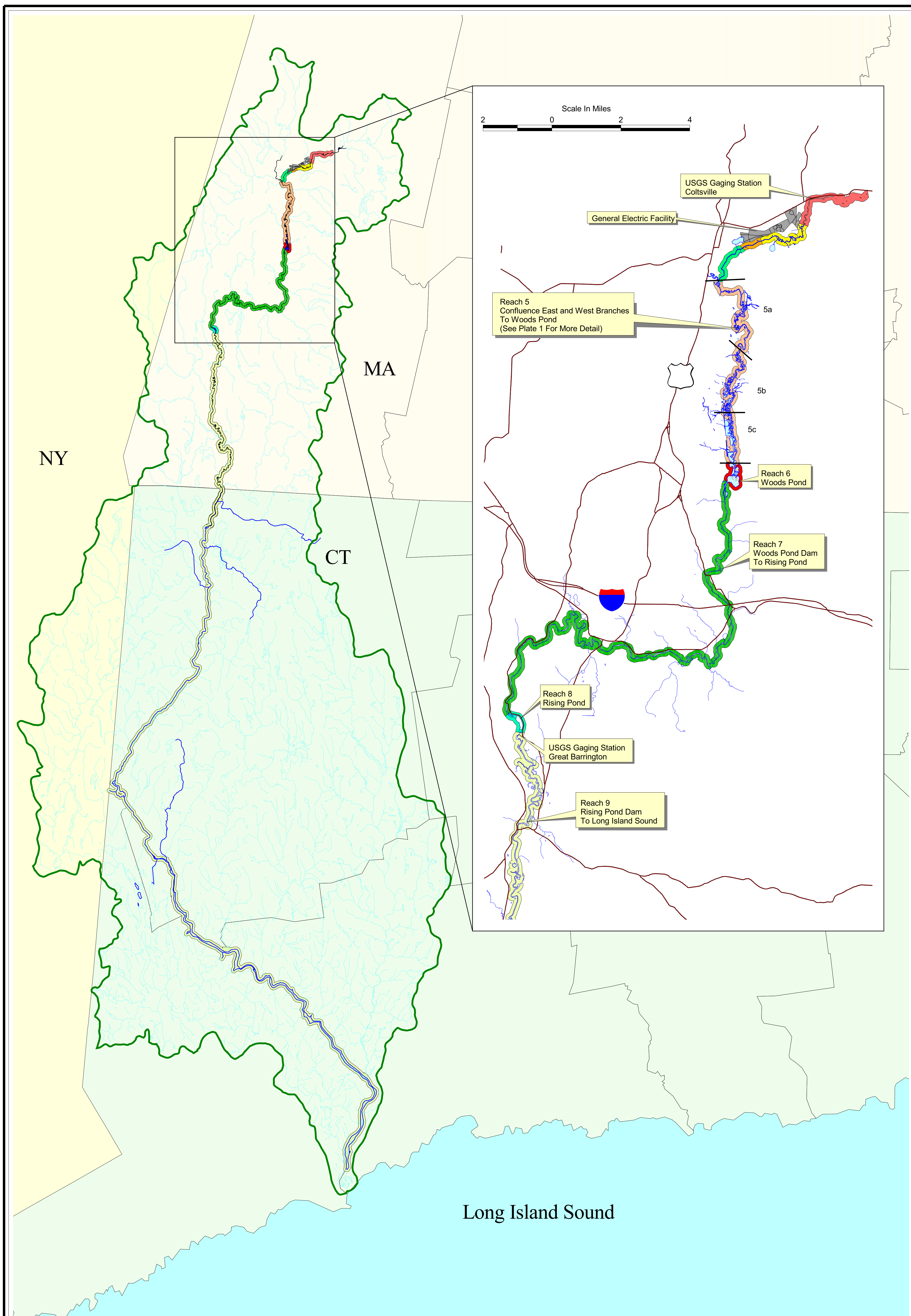
LEGEND:

⋀⋁ Surface Hydrology

▭ Housatonic Watershed Boundary

Housatonic River Subreaches:

Reach 1
Reach 2
Reach 3
Reach 4
Reach 5
Reach 6
Reach 7
Reach 8
Reach 9

N

Scale in Miles
6   0   6   12

Housatonic River Project
Pittsfield, Massachusetts

FIGURE 2-1
HOUSATONIC RIVER REACHES
1 TO 9

| o:\gepitt\aprs\overview.apr | Layout-watershed-overview | o:\gepitt\epsfiles\portrait24x36\in\watershed-overview.eps | 10:38 AM, 10/5/2000 |

1   areas of Woods Pond are well-mixed, the "deep hole" exhibits some thermal stability and
2   dissolved oxygen stratification during the summer.

3   Reaches 7, 8, and 9 include the river sections from Woods Pond to Rising Pond, Rising Pond,

4   and downstream of Rising Pond, respectively. These reaches include five dams below the

5   Woods Pond Dam and five dams in Connecticut. Although the modeling activity does not

6   incorporate these reaches, they are included in the "Rest of River" defined in the Consent Decree

7   (October 1999) and extend through Connecticut. These lower reaches may be the focus of later

8   modeling studies.

3. DATA EVALUATION AND THE CONCEPTUAL MODEL

3.1   INTRODUCTION

The first step in conducting the modeling study of the Housatonic River was to develop a conceptual model of the river system.   The conceptual model presents a series of working hypotheses regarding which hydrologic, hydrodynamic, sediment and PCB transport, fate, and biotic processes are significant within the area of study for the modeling efforts. This conceptual model is based on fundamental scientific principles and processes, generally applicable laws and constants, and an analysis of available site-specific data.   A modeling study is not a linear process, but represents a dynamic and iterative process often requiring the modeling team to "learn" from the model results and data as they become available.   Assumptions made early in the process may be modified as the effort progresses (Figure 3-1).

Within a system such as the Housatonic River, there are many chemical, physical, and biological processes to be considered and evaluated in developing a conceptual model.   This evaluation will aid in determining which processes should be included explicitly in the model. This section of the report presents the "global" list of processes that have been considered for this modeling effort, the data required and used in determining which

Figure 3-1 The Role of the Conceptual Model In a Generalized Model Application Process

processes are likely to be significant, and an overall conceptual model of the portion of the Housatonic River being studied and modeled. Additional data collection activities, as discussed in this section, will result in site-specific data beyond that presented in this document and will generate additional specific model inputs. Any new information will be incorporated into the

1   conceptual model and modeling study as appropriate and will be further discussed in the model

2   calibration and validation reports.

3   This modeling study refers to two areas of interest. The hydrologic study area (HSA) includes

4   the entire Housatonic River watershed above the Great Barrington USGS gaging station. The

5   HSA will be used primarily for the hydrologic model components. The focused area of interest

6   includes the watershed from the confluence of the East and West Branches of the Housatonic

7   River (approximately 2 miles downstream of the GE facility) to Woods Pond Dam,

8   approximately 10.7 miles downstream of the confluence. This area is hereafter referred to as the

9   Primary Study Area (PSA) (see Plate No. 1), the area of the Housatonic River and floodplain in

10 which the majority of PCB contamination is located, based upon the review of previously

11 collected data.

3.1.1   Model Parsimony

13 The identification of a physical, chemical, or biological process in an ecological system does not

14 necessarily require the explicit incorporation of that process in the mathematical model. Models

15 vary in the complexity employed in representing the fate of chemicals; they also vary in terms of

16 the basic model formulations employed (e.g., mass transfer rate models versus concentration or

17 fugacity gradient models). Modeling must strike a compromise between maximizing the

18 incorporation of practical (empirical) and theoretical knowledge with minimizing the uncertainty

19 associated with increased model complexity and limiting parameters that are difficult to specify

20 accurately. The optimal model is known as a parsimonious model.

21 Parsimony may be defined as the state of optimal model efficiency, in which unexplained

22 variance is reduced using the fewest number of variables. Figure 3-2 shows schematically how a

23 parsimonious model attempts to minimize uncertainty. Models that include too few processes or

24 parameters may be under-specified and not describe sufficiently the mechanisms that affect

25 chemical fate. On the other hand, models that include too many processes are over-specified,

26 particularly if the data used to parameterize the model have high uncertainty. Seeking model

27 parsimony is somewhat analogous to specifying an optimal multiple regression equation to fit a

28 set of data points. Adding an additional variable in a regression equation will always "improve"

Optimal Model
(Parsimonious)

Improved
Model
(Reduced
Uncertainty)

Under specified
(Important
Process Ignored)

Over specified
(Too much detail, too
many parameters,
uncertainty outweighs
explanatory power)

Increased
Model Complexity
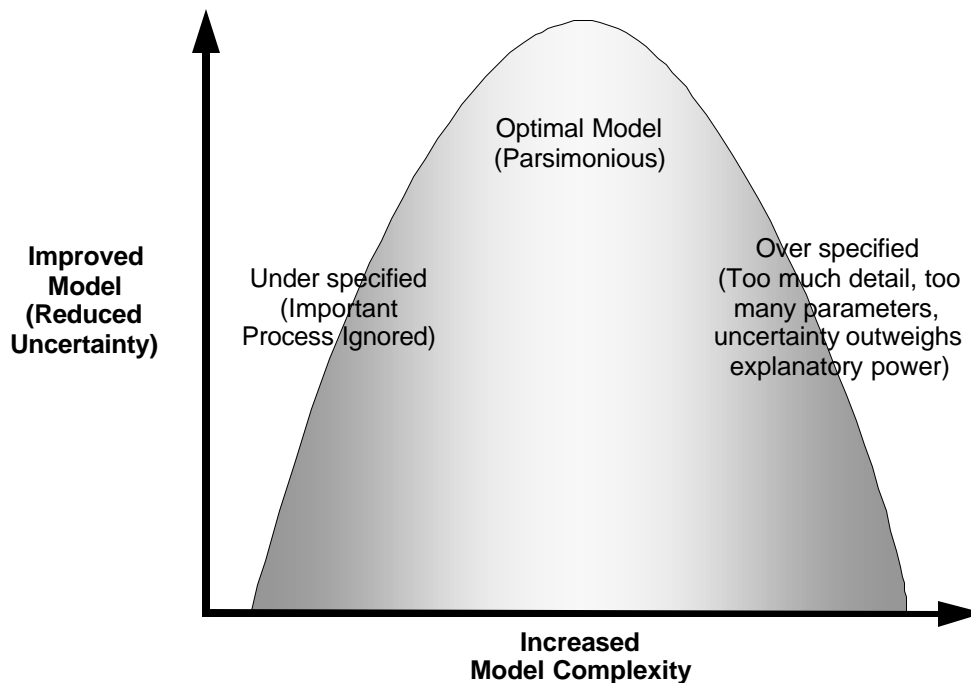
1
2 **Figure 3-2 Idealized Relationship Between Model Complexity and Model**
3 **Predictiveness**

4 the fit of the model to the data, in the sense that the R-squared value will always increase.

5 However, at some point, arbitrarily increasing the number of variables, without considering their

6 causality, will result in a less predictive model. A similar approach will be applied in the

7 development of the mathematical models for the Housatonic River. Processes that are known or

8 believed to exist in nature may be excluded from the model formulation if the benefit of

9 explaining some of the variability in nature is outweighed by the uncertainty resulting from a

10 more complex model.

11 **3.1.2   Combining Theory and Empirical Data**

12 A wide body of knowledge is available on hydrodynamic and sediment transport modeling and

13 the environmental fate of PCBs. This knowledge has been derived from theoretical concepts,

14 laboratory experiments, and empirical data from other contaminated sites. However, since every

1   site is unique, collection of site-specific field data is necessary to "ground truth" the conditions

2   and processes predicted using theory.

3   Both field data and the theoretical aspects of modeling are important; neither approach is

4   adequate in isolation. The use of field data and theoretical formulations each has advantages and

5   disadvantages.

6   The main advantage of field data is that numerous physical, chemical, and biological processes

7   can be integrated in a single field measurement, and processes that are unique to the site may be

8   accounted for directly by empirical measurement. The disadvantage of field data is that it is not

9   logistically possible to sample all the variations in space and time. Disequilibrium in

10 environmental systems and natural variation limits the degree to which field sampling can be

11 applied to make predictions about how chemicals such as PCBs behave in the environment.

12 Empirical observations cannot always be used to make predictions of how environmental

13 conditions will change.

14 Theoretical formulations have an advantage in that they provide a mechanistic explanation for

15 physical, chemical, and biological processes and chemical fate. The main disadvantage of theory

16 is that it may not always match field observations, particularly when using synoptic

17 measurements.

18 The goal of the modeling framework is to optimize the use of both types of information during

19 model implementation. Theoretical concepts will be used to identify processes that may be

20 important in nature and to account for processes in the model framework that cannot easily be

21 defined with field data. Evaluation of field data can also assist in determining whether some

22 processes are important in the system being modeled.

23 **3.1.3 Tiered Approach**

24 The model framework will incorporate a tiered design, where revisions to the conceptual model

25 and, if necessary, to the model code will be made as more information becomes available.

26 However, the objective is not to excessively calibrate the models to fit historical data. There is

27 an important distinction to be drawn between "goodness of fit" and model predictivity. If a

1 model is forced to fit observed data without an understanding of the model processes, the model

2 may actually become less predictive, particularly if environmental conditions change over time.

3 The available literature and theory may be used to establish constraints to model calibration,

4 such that the model is not arbitrarily adjusted to fit the data, at the expense of common sense or

5 known fate processes.

6 **3.1.4 Procedure for Including or Removing a Process**

7 To maintain clarity and transparency of the thought process followed during the development of

8 the conceptual model and subsequently through model implementation, a comprehensive list of

9 processes that could be pertinent to the modeling study of the Housatonic River was developed.

10 This list of processes is provided in Table 3-1, and the processes are discussed throughout this

11 chapter. As part of the discussion, the specific process is described and then evaluated for

12 inclusion, exclusion, or further consideration in the modeling study. The criteria used in this

13 evaluation are:

14 ▪ The physical, chemical, or biological importance of the process relative to the
15   physical/biological domain and PCB fate, transport, and bioaccumulation in the
16   Housatonic River and the spatial and temporal scale defined in the modeling study
17   objectives.

18 ▪ The sensitivity of model(s) to the process (with the goals of either maintaining mass
19   balance, or accurately representing PCB fate through the system).

20 ▪ The need to explicitly maintain information for the purpose of enhancing model
21   calibration/validation capability, or for the purpose of achieving a modeling study
22   objective (e.g., an endpoint of interest for the evaluation of ecological or human
23   health risk).

24 ▪ The availability of data (either site-specific or in the literature) for use in constraining
25   the process.

26 This evaluation of processes will be iterative in nature as are the other components of the

27 conceptual model; that is, as more information is available and/or implementation of the

28 modeling study of the Housatonic River system progresses, the status of any given process may

29 be reevaluated against the criteria listed above.

Table 3-1

Global List of Processes for Evaluation/Inclusion in Modeling Efforts

Model Area	Primary Process	Mechanism	Processes Affecting Transport Mechanism
Water Balance	Hydrology	Base Flow Storm Flows	• Precipitation (rainfall, snow) • Evaporation • Transpiration • Infiltration • Base flow • Soil storage • Surface runoff • Depression storage • Interflow • Groundwater flow and discharge • Tributary loading
	Hydrodynamics	Water Flow in Streams/Rivers/Ponds/Lakes	• Water velocities • Spatial velocity distribution • Flow resistance/shear stress • Vertical stratification • Thermal balance/heat exchange • Hydraulic structures
Solids Mass Balance	Sediment Transport	Suspended Load – consists of both cohesive and noncohesive sediments	• Upstream and tributary loading • Resuspension • Mass erosion • Mass wasting/bank slumping • Localized scour around structures • Scouring around natural debris in streams • Deposition/burial • Bed armoring • Flocculation
		Bedload – consists of noncohesive sediments only	• Upstream and tributary loading • Deposition/burial • Bioturbation • Bed armoring
		Particle Mixing	• Bioturbation • Anthropogenic sources

Table 3-1

Global List of Processes for Evalution/Inclusion in Modeling Efforts (Continued)

Model Area	Primary Process	Mechanism	Processes Affecting Transport Mechanism
PCB Mass Balance	PCB Transport and Fate	Water Transport	• Diffusion • Advection • Sorption/desorption (partitioning) • Volatilization • Dechlorination (biodegradation/photolysis) • Wind • Bioturbation • Atmospheric sources
		Sediment Transport	• Upstream and tributary loading • Sorption/desorption • Resuspension • Deposition/burial
		Atmospheric Transport	• Airborne transport • Wind effects
Biota	Partitioning at Base of Food Web	Chemical Partitioning	• PCB complexation with organic carbon in water • Polarity differences and partitioning among types of organic carbon • Riverine disequilibria • Sediment PCB biotransformation
	Uptake	Direct Contact	• Uptake kinetics in phytoplankton, periphyton, and macrophytes • Dermal contact (absorption, adsorption) • Respiration
		Dietary Uptake	• Benthic feeding strategies/preferences • Fish feeding strategies/preferences • Fish migratory behavior (effect on feeding)
	Assimilation	PCB Transfer Within Biota (e.g., fish)	• Gastrointestinal transfer • Internal PCB transfer • Lipid partitioning and reproduction • Equilibrium partitioning and fugacity • Biomagnification
	Elimination	PCB Loss	• Metabolism • Depuration • Growth dilution • Toxicity feedback loops
	Biota Transport	Physical Movement or Disturbance	• Fish migration • Benthic drift • Storms and scour

3.1.5 Global Process List

The global list of processes is organized relative to the goals of achieving mass balance for water, solids, and PCBs as discussed in Section 1.3.1, and also in relation to the five key groups of processes under discussion: Hydrology, Hydrodynamics, Sediment Transport, PCB Transport and Fate, and Biota. Further discussion regarding each of these processes and the relative importance of the processes in the conceptual model of the Housatonic River is included in Section 3.3.

3.2 DATA REQUIREMENTS AND EVALUATION

The development of a conceptual model requires the evaluation of the available data on contaminant distribution, the significant processes associated with contaminant behavior in the system, and the hydrologic and hydrodynamic processes of the system being modeled. Table 3-2 provides a general summary of the types of data used as part of this investigation and the time periods over which data were collected. These tables are not intended to be exhaustive, but rather to provide an overall picture of available historical and current data. Appendix F includes a complete listing of data available for the river above Canaan, CT, and for meteorological data stations being evaluated in the modeling efforts. The references and sources used to develop the information in Table 3-2 are listed in Appendix F. They include published reports by GE and their consultants, USGS data, and the EPA Housatonic River Project Database.

A key consideration in the use of available data is whether these data are representative of the processes of concern at the site being modeled and whether the data meet the applicable data quality objectives. Beyond formulation of a conceptual model of the site, some of these data will be used directly in the models as state variables, and in model calibration and validation as discussed later in this document and more fully in the Modeling Study QAPP (Beach et al., 2000).

A summary of the types of data needed and how these data will be used for modeling the Housatonic River is presented below. This is not intended to be an exhaustive discussion of all data needed to run the model; rather it is a summary of key data elements, their availability, and their expected uses for evaluating the process under discussion.

Table 3-2 Timeline Summary of Housatonic River Data Studies above Great Barrington, MA, 1979-99

	General Location	Sample Type	REF / SOURCE	Timeline 1979–2000
Flow	Great Barrington, MA	Flow	USGS[1]	(data line 1979–1997)
	Coltsville, MA	Flow	USGS[2]	(data line 1979–2000)
Stage/ Temp	Woods Pond Dam	St-30min / T-30min	GE/QEA / GE/QEA	(1996)
	Woods Pond Headwaters	St-30min / T-30min	GE/QEA / GE/QEA	(1996)
	Rising Pond Dam	St-30min / T-30min	GE/QEA / GE/QEA	(1996)
	PSA Stations	SW/Events	Weston/USEPA	(1998)
Biota	GE - MA/CT border	Comp.	Stewart	(1980, 1982)
	Burlington Hatchery	Indiv.	ANS	(1986, 1988)
	Woods Pond Dam	Indiv.	BBL[1]	(1990, 1993)
	Rising Pond Dam	Indiv. / F,WB,Comp. / F,WB,Comp.	BBL[1] / USEPA / GE	(1990; 1997; 1997)
	GE Plant Site	Comp.	BBL[1]	(1996–1997)
	Upper E. Br. - Dalton	F,WB,Comp.	USEPA	(1997)
	Three Mile Pond	F,WB,Comp.	USEPA	(1997)
	Goodrich Pond	F,WB,Comp. / F,WB	USEPA / GE	(1997)
	W. Br. Confluence - WWTP	F,WB,Comp. / F,WB,Comp.	USEPA / GE	(1997)
	WWTP - Woods Pond Headwaters	F,WB,Comp. / F,WB,Comp.	USEPA / GE	(1997–1999)
	Woods Pond and Backwaters	F,WB,Comp. / F,WB,Comp.	USEPA / GE	(1997–1999)
Sed.	Coltsville, MA	PSD / TSS / TSS	USGS/CAES / GE,BBL[2] / USEPA	(1979–1980; 1989–1990; 1995–1998)
	Pittsfield, MA (PSA Stations)	PSD / PSD,TSS / PSD,TSS	USGS/CAES / GE/BBL[2] / Weston/USEPA	(1979–1980; 1990; 1995–1998)
	Great Barrington, MA	PSD,BD / TSS / PSD,TSS / TSS / TSS / PSD,TSS	LMS / LMS / Stewart / GE/BBL[2] / USGS/CTDEP / USGS[1]	(1990–1992; 1980; 1982; 1983–1991; 1994; 1979–1980)

Explanation of Sample Types

Flow - Discharge measurement	WB - Whole Body sample of biota	GSvsC - Grain Size vs PCB Concentration	T&UNH$_3$ - Total and Un-ionized Ammonia concentrations
St-30min - Stage taken at 30-minute increments	TSS - Total Suspended Solids concentration	BOD$_5$ - Biological Oxygen Demand 5 day	NO$_3$ - Nitrate concentration in water-column sample
T-30min - Temperature taken at 30-minute increments	PSD - Particle Size Distribution of sediment sample	WC - Water Column sample	Oil&Grease - Oil and Grease concentration
Comp. - Composite sample of biota	BD - Bulk Density (net weight) of sediment samples	Hazardous - Various Hazardous Constituents other than PCBs	Tmp - Temperature measurement taken at daily increments
Indiv. - Individual sample of biota	CS - Core Sediment sample	DO - Dissolved Oxygen concentration	Nutr - Nutrients
F - Fillet sample of biota	SS - Surficial Sediment sample	GrbS - Grab Sample	

Years across top: 1979 | 1980 | 1981 | 1982 | 1983 | 1984 | 1985 | 1986 | 1987 | 1988 | 1989 | 1990 | 1991 | 1992 | 1993 | 1994 | 1995 | 1996 | 1997 | 1998 | 1999 | 2000 (each subdivided Jan/May/Aug/Dec)

Category	General Location	Sample Type	REF / SOURCE
PCBs	Coltsville, MA	CS	Stewart
		CS,GrbS	USGS/CAES
		WC	GE/BBL[2]
		WC	USEPA
	Pittsfield, MA	CS	Stewart
		CS,GrbS	USGS/CAES
		CS,GrbS	GE/BBL[2]
		WC	GE/BBL[2]
		WC	Weston/USEPA
	Great Barrington, MA	CS,WC	Stewart
		CS,GrbS	USGS/CAES
		WC	LMS
		CS,GrbS	LMS
		WC	USGS/CTDEP
		CS	GE/BBL[2]
		WC	GE/BBL[2]
TOC	Coltsville, MA	CS,GrbS	USGS/CAES
		CS,GrbS	USEPA
	Pittsfield, MA	CS,GrbS	GE/BBL[2]
		WC,CS	Weston/USEPA
		CS,GrbS	USGS/CAES
	Great Barrington, MA	CS,GrbS	LMS
		SS,CS	USGS/CAES
Other	Pittsfield, MA	Hazardous	GE/BBL[2]
		DO, pH	BBL[2]
		T&UNH$_3$,NO$_3$	BBL[2]
		Oil&Grease	BBL[2]
	(PSA Stations)	Nutr,BOD$_5$	Weston/USEPA
	Great Barrington, MA	Tmp,DO	USGS[1]
		Hazardous	GE/BBL[2]

Notes:

USGS[1] - U.S. Geological Survey: Surface-water station on the Housatonic River near Great Barrington, MA (01197500).

USGS[2] - U.S. Geological Survey: Surface-water station on the Housatonic River at Coltsville, MA (01197000).

BBL[1] - Blasland, Bouck and Lee: General Electric Company 1999. Preliminary Draft of Biota Database Summary. Prepared for discussion purposes only.

BBL[2] - Blasland, Bouck and Lee: General Electric Company 1996. Supplemental Phase II/RCRA Facility Investigation Report for Housatonic River and Silver Lake. Vol. II.: with Figures and Tables. Prepared by Blasland, Bouck and Lee.

QEA - Quantitative Environmental Analysis: Quantitative Environmental Analysis. 1998. Technical Memorandum - Spring 1997 High Flow Monitoring & Summer 1997 Bathymetric Sediment Bed Mapping Survey. Prepared to present data collected by BB&L and HydroQual.

Stewart - Stewart Laboratories, Inc. 1982. Housatonic River Study 1980 and 1982 Investigations. Prepared for General Electric Company.

ANS - Academy of Natural Sciences: General Electric Company 1999. Preliminary Draft of Biota Database Summary. Prepared for discussion purposes only.

USEPA - U.S. Environmental Protection Agency: General Electric Company 1999. Preliminary Draft of 1998 Biota Database Summary. Prepared for discussion purposes only.

GE - General Electric Company: General Electric Company 1999. Preliminary Draft of 1998 Biota Database Summary. Prepared for discussion purposes only.

LMS - Lawler, Matusky and Skelly Engineers: General Electric Company. 1994. Housatonic River Connecticut Cooperative Agreement B Task IV.B: PCB Fate and Transport Model: Additional Monitoring and Model Verification. Prepared by Lawler, Matusky and Skelly Engineers.

Weston - Roy F. Weston, Inc.: Roy F. Weston, Inc. 1999. Microsoft Access Database Data Mart. Preliminary summary of available data.

USGS/CAES - CAES, CDEP, and USGS: Frink, C.R., K.P. Kulp, C.G. Fredette. 1981. PCBs in Housatonic River Sediments: Determination, Distribution and Transport. Draft. Prepared by CAES, CDEP, and USGS.

USGS/CTDEP - USGS and CT Department of Environmental Protection: Kulp, K.P. 1991. Concentration and Transport of Polychlorinated Biphenyls in the Housatonic River Between Great Barrington, Massachusetts, and Kent, Connecticut, 1984-1988, 1991. Prepared by USGS and CT Department of Environmental Protection.

USGS – U.S. Geological Survey: General Electric Company 1999. Preliminary Draft of 1998 Sediment Database Summary. Prepared for discussion purposes only.

Explanation of Sample Types

Flow - Discharge measurement	WB - Whole Body sample of biota	GSvsC - Grain Size vs PCB Concentration	T&UNH$_3$ - Total and Un-ionized Ammonia concentrations
St-30min - Stage taken at 30 minute increments	TSS - Total Suspended Solids concentration	BOD$_5$ - Biological Oxygen Demand 5 day	NO$_3$ - Nitrate concentration in water-column sample
T-30min - Temperature taken at 30 minute increments	PSD - Particle Size Distribution of sediment sample	WC - Water Column sample	Oil&Grease - Oil and Grease concentration
Comp. - Composite sample of biota	BD - Bulk Density (net weight) of sediment samples	Hazardous - Various Hazardous Constituents other than PCBs	Tmp - Temperature measurement taken at daily increments
Indiv. - Individual sample of biota	CS - Core Sediment sample	DO - Dissolved Oxygen concentration	Nutr - Nutrients
F - Fillet sample of biota	SS - Surficial Sediment sample	GrbS - Grab Sample	

MK01|O:\20123001.096\MFD_Tbl32.xls   10/13/00

1   The following generalized areas are discussed below in terms of data requirements:[1]

2   ▪ Watershed hydrology
3   ▪ Hydrodynamics
4   ▪ Sediment
5   ▪ PCBs
6   ▪ Biota
7

8   ### 3.2.1 Hydrology

9   The hydrology of the Housatonic River basin has a direct and controlling influence on
10   hydrodynamics and sediment transport within the study area, and in determining the spatial and
11   temporal distribution of PCBs within the system. Given the persistent nature of PCBs, it is
12   necessary to include an evaluation of the long-term processes that control their fate in a riverine
13   system. Therefore, there is a need for long-term hydrologic data to support the modeling study.
14   The Hydrologic Study Area (HSA) encompasses the entire 282 square mile watershed above the
15   U.S. Geological Survey (USGS) gage at Great Barrington, MA.

16   Of specific interest in this study is the determination of a historical water balance, which is a
17   mass balance that accounts for all water inflow, storage, and outflow terms. Balance between
18   these terms is needed to adequately represent the hydrology within the study area. Of particular
19   importance is how the physical characteristics of the study area exert a controlling influence on
20   the distribution of outflows from the tributaries within the Housatonic River basin.   The
21   distribution of rainfall events, land cover, slope, physical aspects, soils, man-made alterations to
22   the landscape, and underlying geology all directly influence the allocation of total outflows
23   between evaporation, evapotranspiration, surface runoff, interflow (near-surface flows), and
24   groundwater flow.   The eventual intersection and routing of surface and subsurface flows
25   through a network of interconnected channels exerts a periodic forcing function that affects
26   sediment transport capacity and the advection of dissolved/particulate PCBs.

27   To properly represent the distribution of flows that impact sediment transport and PCB fate and
28   transport in the principal area of study, over the long-term, the following data are required:

---

[1]The data presented in this section, either in tabular form or in figures and charts, are given in the units in which the
data were measured or collected and reported. Both metric and U.S. equivalent units are used.

Meteorological

Meteorological data include:

- Precipitation.
- Evapotranspiration.
- Evaporation.
- Maximum/minimum temperature.
- Dewpoint temperature.
- Wind speed.
- Solar radiation.
- Cloud cover.

These data are available for a period extending beyond the 20-year historical period of interest for validation for this modeling study. Data sources that are available include National Oceanic and Atmospheric Administration (NOAA) cooperative sites in the Pittsfield region, including the Pittsfield Airport station. Additional meteorological data are available from a GE-operated station located at the Pittsfield, MA, facility, and other regional meteorological stations.

Physiographical

Physiographical data include:

- Topography.
- Watershed and sub-watershed boundaries.
- Soil delineation and hydrologic/erosion properties.
- Land cover type and distribution.

These data are readily available or derived from historical data collected specifically for this region, particularly by federal agencies. Topography data in the form of a digital elevation model (DEM) are available in electronic form for the entire study area. Additional 1:24000-scale digital terrain maps are also available from the USGS for the entire watershed. These data will be used principally to derive key hydrologic attributes such as the distribution of slopes within each of the tributary areas (i.e., a hypsometric curve). These data will also be used to determine the watershed and sub-watershed boundaries throughout the region of study, to estimate the average distance that overland flow travels before it intercepts either a wet or dry channel, and to assign tributary areas to individual channel or reach segments.

1 USDA soil survey data are available for all of Berkshire County. These data identify the

2 distribution of soil types and their underlying properties, e.g., permeability, soil layer depths,

3 bulk density, and soil erodibility characteristics. In addition, 1:100000-scale soil maps are also

4 available from the USDA STATSGO database. Because hydrologic investigations typically

5 employ a lumped parameter approach in the absence of spatially detailed data, the principal

6 source of soils data will be the STATSGO database. These data will be combined with available

7 land use/cover data from USGS GIRAS database to derive hydrologic response units (i.e., areas

8 that will be treated as having similar hydrologic response characteristics) for all tributary areas

9 within the watershed.

10 **Hydrography and Channel Network Characteristics**

11 Hydrographical data and network characteristics include:

12 - Channel lengths and slopes.
13 - Channel cross-sectional geometry.
14 - Bed substrate composition (grain size distribution).
15 - Hydraulic structures.
16
17 The channel network configuration (e.g., lengths and slopes) data are largely derived from

18 detailed topographic data for the study area and 1:100000-scale DEM data available from USGS.

19 An autodelineation tool developed by the USDA was used to generate the network and the

20 individual channel lengths and slopes. Extensive (200+) and detailed cross-sectional

21 measurements for the principal study area are available in the 2-mile stretch of the East Branch

22 along and below the GE facility. Additional cross-sectional measurements have been collected

23 below the confluence, including data provided by GE from a 1997 bathymetric survey (QEA,

24 1998b). To provide the capability to properly route flows through the entire study area and to

25 eventually conduct a detailed hydrodynamic investigation, a detailed survey of channel geometry

26 throughout the remainder of the system down to the Woods Pond Region, and including selected

27 tributaries, was conducted. This survey included 204 cross sections of the channel morphology;

28 the data are currently under review.

29 Bed substrate composition data are available from numerous sources, including historical data

30 collected in the early 1980s (Stewart Laboratories, 1982) and more recent sediment core and

1   surficial sediment data that were collected by EPA throughout the principal area of study. In

2   addition, GE provided qualitative bed sediment classifications from a 1997 bed mapping survey

3   that included 124 channel transects from Pittsfield, MA, to Bulls Bridge, CT (QEA, 1998b).

4   Although grain size data can be used for multiple purposes, their principal use when evaluating

5   hydrology is to establish bed roughness characteristics throughout the region of study.

6   The presence of hydraulic structures such as dams on the Housatonic River is of particular

7   importance given their direct impact on the distribution of flows within the system. In addition,

8   these structures produce artificial impoundments that can function as highly effective sediment

9   traps. Over long periods of time, these structures can have a significant impact on the transport

10 of sediment and PCBs within the system. Data on the location of dams within the Housatonic

11 River basin are readily available from several sources including Phase I inspection reports from

12 the National Dam Inspection Program conducted by the U.S. Army Corps of Engineers

13 (USACE), and information summarized by GE. An electronic database of dams within the

14 region is also available from USACE. This database includes physical descriptions that can also

15 be used to assist with establishing stage-discharge relationships. For the Woods Pond Dam,

16 engineering drawings are available from GE. However, information on the operations of these

17 dams, both permitted and otherwise, is not readily available.

18 ### 3.2.2 Hydrodynamics

19 The transport of cohesive and noncohesive sediment is governed principally by the

20 hydrodynamics of the system. Of particular interest is determining how the distribution of flows

21 (and their associated velocities) influence sediment and PCB transport at various locations within

22 the Housatonic River.   These flows and their resulting velocities exert an internal forcing

23 function that must be accounted for to obtain an accurate sediment and PCB mass balance for the

24 system.

25 In bounded shear flows, a vertical velocity distribution produces shear stresses both within the

26 water column and between the water column and the underlying bed. The magnitude of the

27 shear stress imposed on the bed and the bed composition govern whether net sediment deposition

28 or erosion is occurring or is likely to occur. Under certain hydrodynamic conditions, neither net

29 sediment deposition or erosion may be occurring. The influence of hydrodynamics on advective

transport of PCBs must also be evaluated for all relevant size fractions. A mass balance on the PCBs can be obtained only by the accurate representation of sediment erosion and depositional processes throughout the entire system. Hydrodynamics also control the rate at which dissolved PCBs are transported.

The following types of data are necessary to represent the hydrodynamics of this system:

- Upstream and tributary flows.
- Velocity distribution.
- Bed substrate and vegetation composition.
- Channel bathymetry, slope, and shoreline configurations.

A substantial period of record of observed flows within the PSA is available from the USGS Coltsville and Great Barrington stations. Historical flows are often used to calibrate a hydrologic model or as a boundary condition to a hydrodynamic model. For this study, the hydrologic model must reproduce historical and future hydrologic conditions so that a proper boundary condition can be established to represent the hydrodynamics of the system. The observed flow measurements will be used to both calibrate and validate the hydrologic model and to ensure that a proper boundary condition is established for the hydrodynamic model.

Observed velocity measurements are required to determine whether internal forces are properly represented within a system. While observed velocities, like observed flow, are used primarily for calibrating and validating models, these data have other uses as well. One issue is whether significant, fine-scale hydrodynamic processes are occurring as a result of the physical complexity of the Housatonic River system. The succession of meanders within the PSA results in frequent changes in the principal direction of flow and the loss of momentum due to the interaction of the flow with the channel sidewalls and large woody debris.

These data will also be used to determine whether lateral velocity distributions must be represented in a hydrodynamic model in order to accurately simulate sediment transport. If velocity in the channel is treated as being uniform across the channel, then the resulting sediment transport capacity will also be treated as uniform. This may not be suitable for the Housatonic River.

1 At present, there are insufficient site-specific velocity data to verify that a hydrodynamic model

2 of the river is properly constructed. Additional lateral velocity measurements are being

3 collected periodically using hand-held current meters at wet weather monitoring locations as well

4 as measurements made using an Acoustic Doppler Current Profiler (ADCP). The ADCP is being

5 used to collect high resolution, 3-dimensional velocity data at up to five different river stages.

6 This data collection effort will provide a distribution of velocities characteristic of those

7 occurring during dry and wet weather periods.

8 Bed substrate data are necessary to specify spatially varying bed roughness characteristics that

9 cause resistance to flow. The presence of submerged aquatic vegetation is important because

10 dense submerged vegetation can exert a significant resistance to flow. Historical and current

11 grain size and core sample data are available throughout the primary study area and will be used

12 to represent characteristic bed roughness heights (a hydrodynamic calibration parameter). These

13 data will be augmented by information on the presence or absence of aquatic vegetation noted in

14 ongoing surveys; for example, TechLaw (1999).

15 Channel bathymetry and shoreline data are needed to specify a realistic physical representation

16 of the system. These data are used to specify representative cross-sectional boundaries,

17 elevations of adjoining floodplain regions, and the slope of the channel. This information is

18 particularly critical for the Woods Pond area, where flow circulation may be complex. Detailed

19 shoreline and bathymetric data are readily available for the PSA, and additional data, as

20 discussed in the hydrology section, are being collected.

21 Historical bathymetric data for Woods Pond, circa 1980, are not available. However, estimates

22 of the historical bathymetry in Woods Pond can be made from deposition rates derived from

23 cesium-137, lead-210, and beryllium-7 dated sediment cores. These estimates will be used to

24 establish initial conditions for bathymetry in the hydrodynamic model for the start of the model

25 simulation period in 1980. More recent bathymetric data from 1998 are available and will be

26 used for model calibration.

3.2.3 Sediment Transport

Development of a comprehensive sediment mass balance for the region under study is an important element of this investigation. The sediment mass balance should include all sediment loads derived from surficial erosion processes, internal sources of sediment (i.e., those derived from in-channel resuspension and deposition) in watershed tributary areas, and internal sources of sediment originating from within the PSA (i.e., between the confluence and the Woods Pond Dam). A key element in achieving mass balance is to properly account for two major classes of sediment, noncohesive and cohesive. Each has a distinctively different transport behavior that prohibits treating all sediment particles as a single size class. The cohesive sediment fraction is defined as those particles less than 63 μm diameter. Under certain conditions, cohesive sediments can form flocs in fresh water. The settling velocity of flocs of cohesive particles is several orders of magnitude greater than that of individual clay-size particles (Tetra Tech, 2000e). The noncohesive size fraction of solids includes particles greater than 63 μm.

Developing a sediment mass balance requires the following types of data:

- Grain size distribution.
- Specific weight.
- Bed bulk density (by depth).
- Erosion potential (by depth).
- Bedload transport rates.

Detailed grain size distribution, bulk density, and specific weight data are available for the period 1980 to 1982 (Stewart Laboratories, 1982). These data include samples from the PSA. Additional data were collected to more fully characterize Woods Pond and the main channel above Woods Pond. These data will provide additional information on bulk density and specific weight. Recently collected core data, providing grain size distribution by depth, are also available for numerous locations in the study area. Grain size distribution is especially critical because it is key information that can be incorporated into a sediment transport model and can also be used to qualitatively and quantitatively characterize dominant transport processes for any specific region of interest.

Another use of grain size data will be to determine the extent to which bed armoring or shielding is likely to be occurring in specific parts of the system. Bed armoring is defined as the process

1   by which coarser particles effectively shield smaller or finer grain-size particles from being

2   eroded from the bed, in effect reducing the shear stress imposed on the fine grain particles.

3   An investigation is underway to better understand how the void ratio in bed solids changes over

4   time within the PSA (i.e., time since deposition). This information is important when developing

5   a sediment transport model that must account for erosion of bed sediment under different shear

6   stress conditions. Bulk density is significant when estimating the rate of solids flux from the

7   sediment bed to the overlying water column.

8   Simulating the rate of erosion from the sediment bed requires site-specific data, specifically data

9   that indicate how the rate of erosion varies with depth under various shear stress conditions.

10   Historically, limited data were available on the erosion potential of the Housatonic River

11   sediment bed. Moreover, the Particle Entrainment Simulator (PES) device employed to derive

12   these data is limited to a small stress range that is not necessarily representative of the full range

13   of conditions encountered. To address this data gap, sediment bed cores from the river were

14   subjected to extensive hydraulic testing with a Sedflume (McNeil et al., 1996) with concurrent

15   PES tests. The Sedflume allows measurements to be made that reveal the variation in erosion

16   potential with depth. It can also impose shear stress conditions an order of magnitude greater

17   than the PES.

18   Data from the Sedflume tests and PES will be used to develop algorithms describing initiation of

19   resuspension rates for Housatonic River sediments. Algorithms will relate observed critical

20   shear stresses for initiation of resuspension as a function of the measured sediment bulk

21   densities. These data will also be used to develop bulk density profiles for sediments that are

22   well consolidated and algorithms to predict bulk density profiles of consolidating sediments as a

23   function of time after deposition.

24   ### 3.2.4   PCB Transport and Fate

25   Substantial amounts of historical water quality data have been collected over the past 20 years

26   for the study area. These data include PCB (as totals, Aroclors, congeners, and homologs), total

27   suspended solids, polycyclic aromatic hydrocarbons (PAHs), inorganics, dioxins/furans,

28   pesticides, nutrients and conventional water quality parameters. Additional water sample types

1 include dissolved and particulate fractions in the water column (e.g., total organic carbon [TOC],

2 PCBs). Samples were collected at numerous locations throughout the study area including the

3 region between Center Pond in Dalton (above the PSA) and Woods Pond Dam (Figure 3-3).

4 Surficial and core samples have been collected to characterize bed sediment throughout the study

5 area, providing a historical picture of the change in PCB concentration with depth. Historical

6 PCB core data include those from Stewart Laboratories (1982) and Blasland, Bouck and Lee,

7 Inc. (BBL) (1996). Additional surficial and core samples of sediment and floodplain soils have

8 been collected by EPA from the confluence to Woods Pond Dam. These soil and sediment

9 samples have been analyzed for PCBs (totals and Aroclors), PCBs (congeners and homologs

10 [approximately 10% of the samples]), and for TOC and grain size. Maps that graphically depict

11 the sampling locations and magnitude of PCBs detected are available at the EPA GE/ Housatonic

12 River web site (http://www.epa.gov/region01/ge/thesite/restofriver-maps.html).

13 To gain an understanding of the approximate time at which PCB-laden sediments were

14 deposited, existing isotope markers, such as cesium-137 (Cs-137), have been analyzed to

15 indicate the approximate depth that corresponds to a particular time. In the case of Cs-137, the

16 depth at which Cs-137 concentrations reach zero is considered to coincide with the period just

17 before nuclear weapons testing. Other markers such as lead-210 (Pb-210) have been used for

18 more recent periods; decreases in lead coincide with substantial reductions in atmospheric Pb

19 emissions in the 1970s. These data may be used to calibrate and validate sediment transport and

20 PCB fate models that simulate long-term sediment resuspension, deposition, and transport. Total

21 accumulated depth of sediment from sediment cores from various depositional environments can

22 be compared to those simulated by a spatially distributed sediment transport model.

23 In addition to water quality data, an extensive data set of fish tissue residue concentrations

24 (whole body, composite, and fillet analyzed for PCBs) is available for various periods of the last

25 20 years. Of particular interest for this investigation are limited fish tissue samples (Stewart

26 Laboratories, 1982) collected at various locations between Center Pond (Dalton, MA) and

27 Woods Pond in 1980 and 1982, and more extensive fillet, whole body, and composite data for

28 the same area from 1992 to the present, with the most spatially and temporally rich data sets

29 available for the area from the confluence to Woods Pond.

3.2.5 Biota

Site-specific data are needed to understand a number of key biological processes within the Housatonic River system to complete the development of the conceptual model. Overall, the data required to understand these processes can be considered at three levels of organization:

- Broad biological organization (e.g., trophic status, feeding preferences, migration).

- Specific biological data (e.g., growth rates, residue tissue concentrations, lipid contents of organisms).

- Abiotic media data (e.g., organic carbon in sediment and water column, light extinction, temperature, detritus settling rates, etc.).

The subsections below describe the most pertinent data requirements for the model framework design. While all three levels of organization must be considered in the actual model implementation phase, the processes at the "broad organization" level are the most important for developing the conceptual model; therefore, the following subsections emphasize these broad scale processes.

3.2.5.1 Food Web Structure

Site-specific data defining the resident organism types and the pathways by which PCBs may move through the system are required to develop the conceptual model. Specifically, an understanding of the detritus, algae, macrophytes, invertebrates, and fish resident in the river is necessary to model the transfer of PCBs through the aquatic community.

Because in many cases historical data are not available, specific components of the community are being sampled, as detailed in the Supplemental Investigation Work Plan (WESTON, 2000a). These efforts will expand on historical studies of the aquatic food web. Information is being developed on algae, macrophytes, detritus, and benthic macroinvertebrates in the study area and at reference locations. Fish communities in the study area have also been studied historically and as part of this project. Available data are summarized in Woodlot (1999), WESTON (2000a), Stewart Laboratories (1982), Barry and Machowski (1993), and U.S. Fish & Wildlife Service (FWS) (1999).

RM 41
SW000015
ST000002
SW000016
RM 40
ST000003
SW000014
SW000012 RM 8   RM 9
RM
SW000011
SW000010
SW000009
RM 6
SW000008
ST000004
SW000007
ST000005 RM 5
SW000006
RM 06
RM 4
ST000006
RM 3
RM 2
SW000005
RM 1
SW000017
RM 0
ST000007 SW000004
RM 29
ST000008
RM 28
RM 27
RM 26
SW000003
RM 25
ST000009
SW000002
SW000001
RM 24
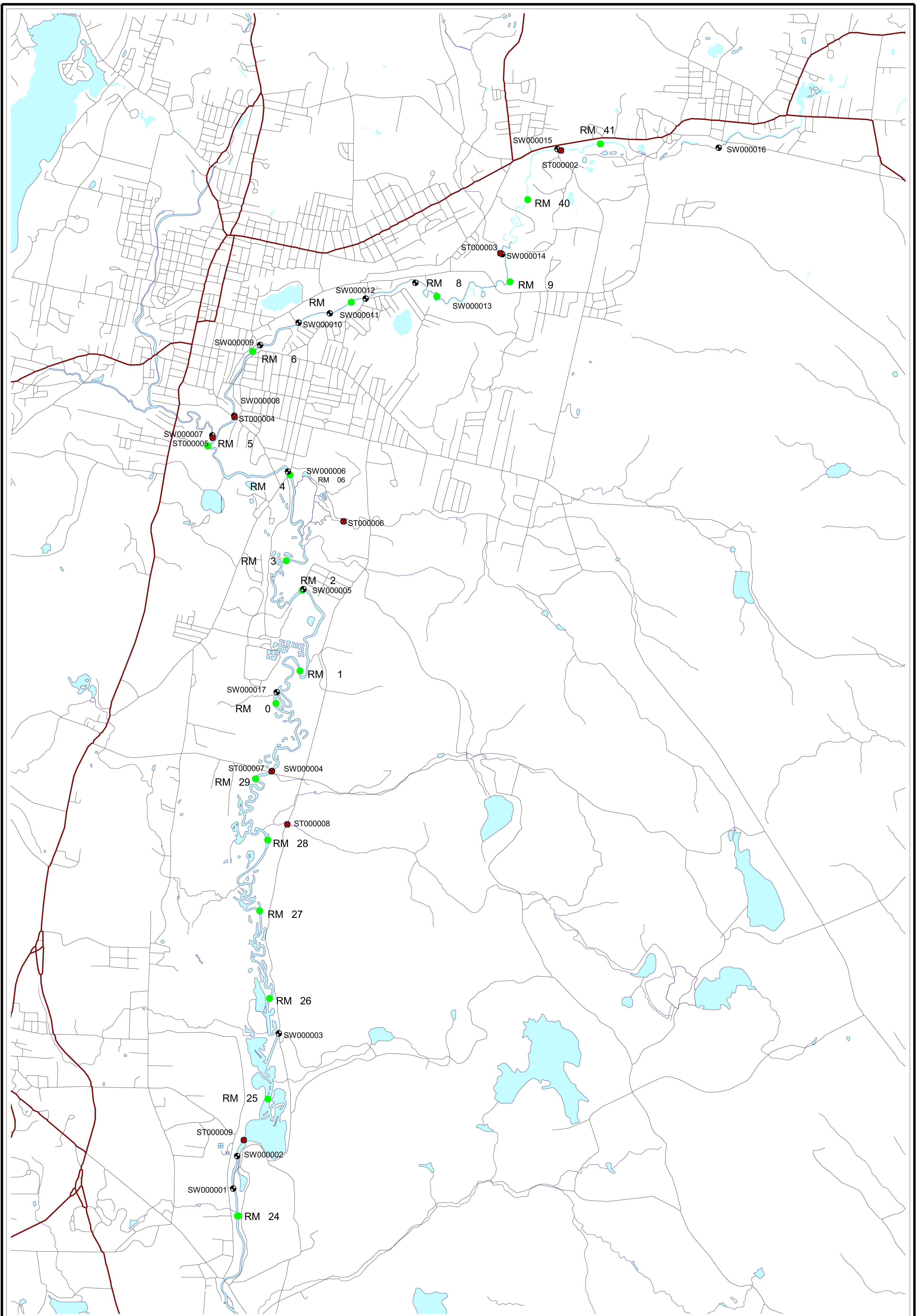
LEGEND:
- Surface Water Sample Locations
- Storm Water Sample Locations
- Housatonic River   iles
- Hydrology
- Roads

N

Scale in Feet
2000   0   2000   4000   6000

Housatonic River Project
Pittsfield, Massachusetts

Figure 3-3
STORM AND SURFACE WATER
SAMPLING LOCATION MAP

3.2.5.2   Relative Abundances

The abundances and/or biomass of organisms are important in two main respects. First, the abundance data may be considered in selecting candidate organisms (i.e., surrogate species) for formulating the conceptual model. Second, the abundance of animals may be considered in the actual parameterization of the model (e.g., assignment of prey preferences in the model based on information on availability of prey species). Biomass estimates provide the most useful information for this purpose. In some cases, species may be selected for the conceptual model even if they are not the most abundant. Selection will be based upon their representativeness of feeding niches or trophic levels, sensitivity to potential effects from PCBs, as well as the amount and quality of data available on the given species for model calibration purposes.

Benthic community structure data will be processed to obtain relative abundance information for the observed species. Specific data have also been collected to provide standing crop estimates for primary producers and detritus. Macrophytes, periphyton, plankton/detritus, and filamentous algae have been sampled in habitats where generally high biomass occurs. Data on temporal trends will not be collected due to logistical limitations.

Fish and invertebrates in the Housatonic River have been enumerated and are reported in Woodlot (1999), WESTON (2000a), Patrick (1999), Stewart Laboratories (1982), FWS (1999), and Barry and Machowski (1993). Further fish community data are being generated from an ongoing study conducted specifically to obtain estimates of fish biomass.

Preliminary review of the site-specific data available for the Housatonic River for abundance/biomass of fish and invertebrates is provided in Section 3.3.5.1.

3.2.5.3   Feeding Preferences

Because of the lipophilic nature of PCBs, their biological fate is strongly influenced by dietary uptake processes. For this reason, a detailed understanding of the dietary preferences of each organism represented in the food web is important. Feeding preferences may be determined based on site-specific data, consideration of the available prey and knowledge of organism life

1   history, and dietary preference data assembled from literature sources or from other sites, such as

2   the Hudson River and Sudbury River.

3   Feeding preferences of fish and invertebrates will be based primarily on the scientific literature.

4   Exponent (1998) described fish diets for species in the Upper Hudson River, and this information

5   is applicable to some species found in the Housatonic River. An analysis of fish diet and benthic

6   communities for the Sudbury River is found in Johnson and Dropkin (1995).   Feeding

7   preferences for other fish in the Housatonic River can be found in Wydoski and Whitney (1979).

8   Preliminary review of feeding preference data for adjacent rivers suggests that some species may

9   be highly opportunistic; therefore, application of feeding preference data from nearby watersheds

10   will require careful consideration of the available prey (i.e., similarity of habitats and prey

11   assemblages between watersheds) as well as seasonality of prey preferences and abundances.

12   ### 3.2.5.4   *Habitat and Fish Migration Patterns*

13   The Housatonic River is, to some extent, physically compartmentalized (i.e., with dams and

14   other obstructions). However, within the PSA between the confluence and Woods Pond, there

15   are few significant impediments to fish passage. Therefore, it is useful to understand the extent

16   to which organisms (particularly fish) will move throughout the system. This understanding is

17   required to determine which geographical areas are connected to a given fish species via the

18   dietary intake pathway. Furthermore, the presence of different habitat types (e.g., backwater

19   pools) requires the examination of how certain fish species may preferentially use specific

20   habitats. Data on food web structure and relative abundance of fish can be used for this section

21   as well. Further discussion of the importance of fish migration is included in Section 3.3.5.2,

22   under the headings of *Fish Feeding Strategies* and *Biotic Transport*.

23   ### 3.2.5.5   *Life History Processes*

24   An understanding of the biological processes that occur at the individual level are important for

25   both conceptual model development and model implementation. Relevant data include organism

26   growth rates, respiration rates, excretion or elimination rates, and feeding rates. These data are

27   derived primarily from the scientific literature. In addition, there are processes that are also

28   important at the population level, including carrying capacity, biomass drift, and spawning

1 behavior. These data will be collected from a review of the scientific literature in conjunction
2 with the evaluation of aquatic habitat and hydrodynamic data available for the system.

3 ### 3.2.5.6 Organic Carbon Pools

4 Because PCBs partition strongly to organic carbon, understanding of the amount and type of
5 organic carbon is important in the development of the food web model. An understanding of the
6 organic carbon pools present in the river is necessary to the development of the model, both in
7 terms of the amount and type of organic carbon in each biotic compartment and how these may
8 change over time due to processes such as phytoplankton blooms or reproductive/seasonal
9 changes in fish lipids.

10 ### 3.2.5.7 Chemical Concentrations

11 Knowledge of the chemical concentrations within each major environmental compartment serves
12 two main objectives. First, examination of the chemical concentrations in various organisms can
13 provide insights into the bioaccumulation processes that are taking place. For example, higher
14 PCB concentrations at the top of the food web would confirm that biomagnification through
15 trophic transfer is an important process. Alternatively, reductions in concentrations of specific
16 PCB congeners (e.g., PCB 77) may indicate that selective metabolism of PCB congeners is
17 occurring. Chemical concentrations in various biotic compartments are important for the
18 calibration and validation of the model. Ideally, tissue residue data are available at numerous
19 trophic levels, such that each major physical trophic transfer process can be validated in the
20 model.

21 Data are available that define the nature and extent of PCB concentrations in sediments
22 (summarized in Section 3.3.4). Biota samples that will be analyzed for tissue residue
23 concentrations are being collected in accordance with the work plan, and historical data are also
24 available. Samples of primary producers and detritus collected for standing crop estimates will
25 also be analyzed for chemical concentrations of PCBs, dioxins, and furans (WESTON, 2000a).
26 Stewart Laboratories (1982) has historical data on PCB concentrations in aquatic plants. Benthic
27 invertebrates, crayfish, and numerous fish species have been analyzed for tissue residue
28 concentration (WESTON, 2000a). Historical fish data are available for selected species (Coles,

1   1999; Stewart Laboratories, 1982). GE has collected young-of-the-year bass, perch, and bluegill

2   for tissue residue analysis for PCBs on a biannual basis since 1994 (BBL, 1996).

3   ### *3.2.5.8   Chemical Properties*

4   Knowledge of chemical fate and transport properties is essential to describe the biological fate of

5   PCBs, since partitioning is constrained by these chemical properties.   These properties are

6   generally derived from the literature (e.g., octanol-water partition coefficients, vapor pressures,

7   solubilities).   However, some environmental parameters can incorporate site-specific data, such

8   as the microbial degradation rate in sediments.

9   ### *3.2.5.9   Physical Processes and Conditions*

10 A number of physical processes are linked to biological fate.   Although not critical for

11 developing the conceptual model, they are necessary for providing the environmental description

12 to run the model.   These processes include light extinction rates, temperatures, decomposition

13 rates, and nutrient dynamics.   These data are derived from a combination of site-specific

14 measurements and literature studies.   Both historical and current data are available, including

15 water quality parameters such as nutrient concentrations, dissolved oxygen, pH, and temperature

16 (WESTON, 2000a).

17 ## 3.3   CONCEPTUAL MODEL

18 This conceptual model of the significant processes that affect sediment and PCB transport within

19 the Housatonic River is based upon historical data sources as well as data collected since 1998

20 by EPA (WESTON, 2000a).   As noted above, the area of the Housatonic River selected for

21 detailed modeling is referred to in this document as the Primary Study Area or PSA. The PSA

22 encompasses 10.7 miles of the Housatonic River from the confluence of the East and West

23 Branches (some 2 miles downstream of the GE facility in Pittsfield) to the dam at Woods Pond,

24 along with the associated 10-year floodplains bordering the river.   This stretch of river has been

25 designated Reaches 5 and 6 for the purpose of the project.

1   This section summarizes the processes currently considered potentially significant and therefore
2   necessary to include in the modeling study as well as those that have been excluded from further
3   consideration, and presents an evaluation of site-specific data or related information that led to
4   the selection of these processes. This section also includes a discussion of those processes whose
5   importance is still undetermined pending further data collection and/or model calibration and
6   validation.

7   ### 3.3.1 Hydrology

8   The hydrology and water balance of the Housatonic River watershed provides the foundation for
9   the movement of water, sediment, and associated contaminants throughout the system. The
10   Hydrologic Study Area (HSA) was selected as the basis for modeling the components of the
11   water balance, including the rate and volume of flow to and through the river, particularly for
12   generating the boundary conditions for the Primary Study Area (PSA). The HSA for the purpose
13   of this model encompasses the entire 282 square-mile watershed above the USGS gage in Great
14   Barrington, MA. This area completely encloses the Primary Study Area that is the subject of the
15   detailed modeling efforts.

16   The primary hydrologic transport mechanisms within the HSA are storm events and the
17   subsequent runoff into the river. Base flow, although important for inclusion in the modeling
18   effort, is not expected to play a major role in sediment and PCB transport. The precipitation and
19   storm events monitored over the course of this study have shown that the river responds rapidly
20   to most rainfall events with a rise in stage height within hours of the precipitation. This response
21   indicates that the river receives a significant amount of its flow from rainfall via surface runoff.
22   The various processes contributing to the surface runoff and increased flow in the river are:

23   ▪ Precipitation
24   ▪ Evaporation
25   ▪ Transpiration
26   ▪ Infiltration
27   ▪ Soil storage
28   ▪ Depression storage
29   ▪ Interflow
30   ▪ Groundwater flow and discharge
31   ▪ Tributary loading
32

1   Some of these processes, specifically those that contribute to surface water runoff and storm flow

2   along the river, have a greater impact than others.

3   The following sections present the relevant parameters and data evaluated to describe the

4   watershed and river hydrology for the model.

3.3.1.1   *Drainage Basin Characteristics*

6   Drainage basin characteristics, in and of themselves, are not processes related to the model.

7   However, they define how the processes are modeled and, therefore, an understanding of these

8   characteristics is necessary for the conceptual model.

9   The USGS Coltsville gage, located within the HSA, upstream of the GE facility provides for

10   HSA submodel calibration and upstream control. Table 3-3 presents the drainage areas for the

11   major subareas and points of interest within the HSA.

12   In addition to the drainage area, another important parameter is the length of the drainage

13   area/flow paths. The drainage basin subareas within the HSA and the corresponding channels

14   need to be defined during the modeling process. Table 3-4 presents how the Housatonic River

15   has been subdivided into river reaches and their corresponding river miles, both for the HSA and

16   the PSA.

17   Definition of the slope of the subbasin areas and of the channel is also necessary for

18   understanding and constructing a hydrologic model. For the HSA, Figure 3-4 shows the

19   hydraulic slopes from Center Pond, in the headwaters, to the Massachusetts-Connecticut border,

20   approximately 20 miles past the Great Barrington gage. The river reaches above Pittsfield and

21   the GE facility are generally much steeper than the rest of the river, especially compared to the

22   PSA from the confluence to Woods Pond.

Table 3-3
Summary of Drainage Areas Within the Hydrologic Study Area (HSA)

Point Description	Drainage Area (sq mi)
USGS Gaging Stations (see Figure 1-1)	
Coltsville	57.6
Great Barrington	282.0
Housatonic River Main Stem (see Plate 1)	
East Branch at Confluence	70.45
West Branch at Confluence	58.85
Confluence	129.30
New Lenox Road	143.80
Woods Pond	162.65
Tributaries (see Plate 1)	
Roaring Brook	5.49
Sackett Brook	9.55
Yokun Brook	5.26

Table 3-4
Summary of Reach Lengths and River Miles Within the HSA

Point Description	Housatonic River Miles	Study Area Lengths (mi)	Sub-Domain Reach Lengths (mi)	Sub-Domain Reach ID
Hubbard Ave Bridge	140.6			
Coltsville Gage	140.5			
Unkamet Brook	139.1			
Newell Street Bridge	137.1			
GE Bldg 68 (closest RM)	136.7			
Elm Street Bridge	136.1			
1st Pomeroy Ave Bridge	135.4			
Confluence	135.1	0.0		
2nd Pomeroy Ave Bridge	134.2	0.9	4.9	Reach 5a
Holmes Road Bridge	134.0	1.1		
Sackett Brook	133.5	1.6		
Wastewater Treatment Plant	130.2	4.9	2.1	Reach 5b
New Lenox Rd	129.1	6.0		
Roaring Brook	128.1	7.0	3.6	Reach 5c
Woods Pond	124.6	10.5		
Woods Pond Dam	124.4	10.7	0.3	Reach 6
Great Barrington	100.7			

Note: River mile designations start at the mouth of the Housatonic River in Connecticut and continue upstream to the headwaters in Massachusetts.
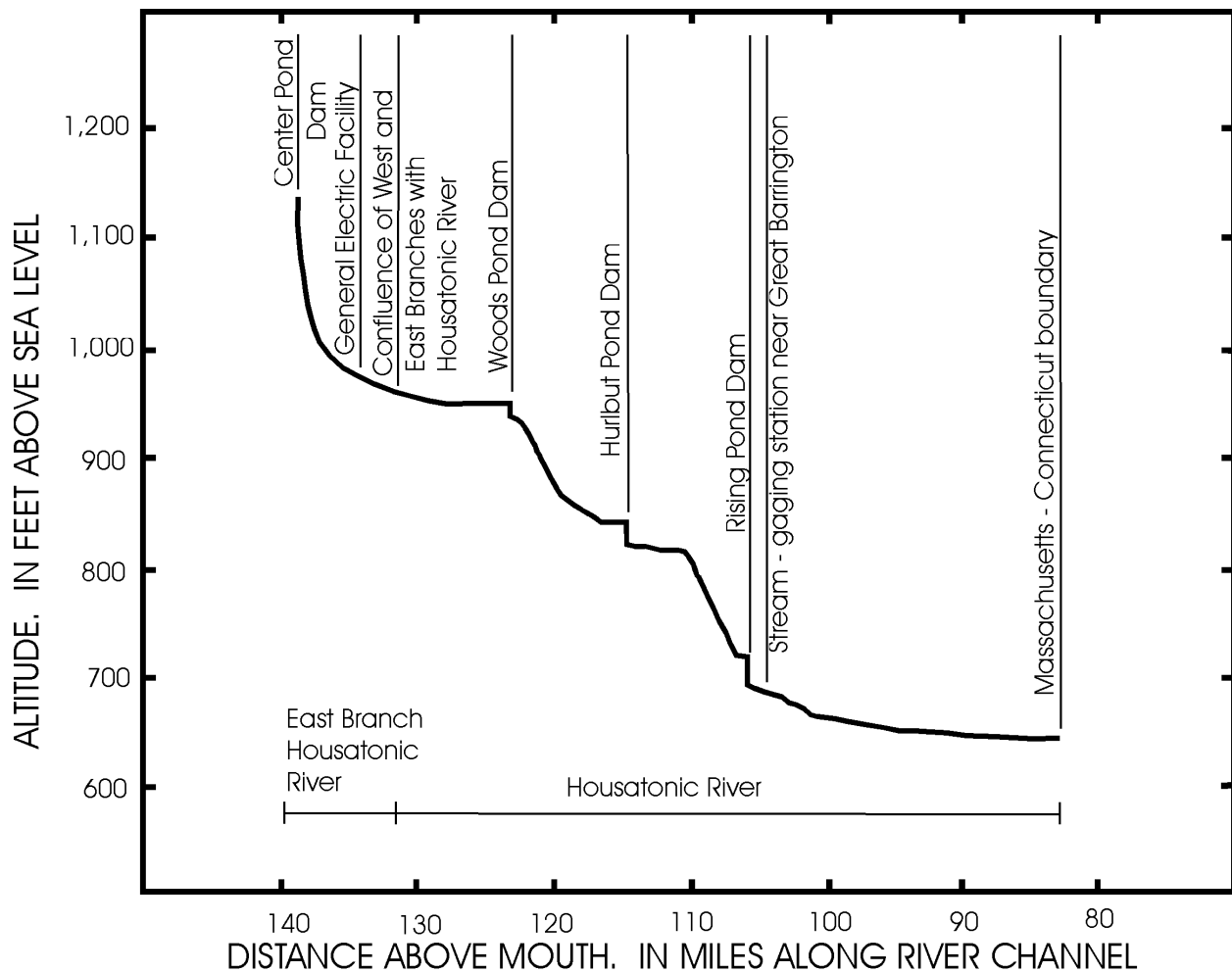
Figure 3-4 Hydraulic Profile of the Housatonic River, Headwaters to the Massachusetts/Connecticut Border (After Gay and Frimpter, 1985)

3.3.1.2   Land Use and Cover in Drainage Basin

The current land use distribution within the watershed upstream of the Great Barrington gage (Table 3-5) will be used for establishing infiltration, soil storage, depression storage, and evaporation characteristics within the HSA to calculate surface runoff. This region is undergoing a slow change from predominantly Forest and Agricultural lands to Forest and Urban lands. It is anticipated that this transition will continue.

Table 3-5

Current Watershed Land Use Above Great Barrington

Description	Percentage
Urban	15
Agriculture	10.8
Forest, Deciduous	39.1
Forest, Evergreen	28.2
Forest, Mixed	1.1
Lakes/Reservoirs	1.8
Wetlands	4

The watershed of the HSA is located in the Humid Temperate Domain, Warm Continental Mountains, Adirondack New England Mixed Forest Coniferous Forest Tundra ecoregion. This province is composed of subdued glaciated mountains and maturely dissected plateaus of mountainous topography. Many glacially broadened valleys have glacial outwash deposits and contain numerous swamps and lakes. The forests within this ecoregion are characterized by sugar maple, yellow birch, and beech, with a mixture of hemlock within valleys. Low mountain slopes contain spruce, fir, maple, beech, and birch.

Because of the importance of surface water runoff to the river system, precipitation, evaporation, infiltration, and soil storage are required processes for inclusion in the model.

3.3.1.3   Climate, Rainfall, and Flow Data

The water balance of the HSA defines the overall water flows that affect sediment and PCB transport. A review of the available data on meteorological, physiographic, and hydrologic parameters of the HSA provided a preliminary assessment of the water balance and the relative importance of base flow, surface water runoff, and storm flows.

The water balance for the HSA indicates that an average of 43.5 inches of precipitation falls on the HSA annually, with 47% lost due to evaporation and transpiration, and an estimated 23 inches per year exiting the basin as runoff. Data from the two USGS gages and the eight gages established for this study show that there is a rapid response in river stage heights and flow to

1   rainfall. This suggests that storm events and associated runoff and flow are important processes
2   within the HSA and PSA.

3   The storm events shown in Table 3-6 were monitored in detail during 1999 to determine the
4   effect of storms on the HSA and the PSA. Sampling for a variety of parameters was conducted
5   during these events at eight monitoring stations (Figure 3-3) along the Housatonic River.

6   These data indicate that storm events appear to have a greater effect on the river in the upper half
7   of the PSA, as indicated by the increased stage heights and increased suspended sediment loads.
8   One of the storm events that were monitored in 1999 is shown in Figure 3-5, where the stage
9   heights for three locations along the river (at Pomeroy Avenue, New Lenox Road, and Woods
10   Pond) are plotted, along with the associated total suspended solids (TSS) load, on a hydrograph.
11   The suspended sediment load, as measured by total suspended solids (TSS) at these stations
12   during this storm event, shows the effect that the storm had on moving an increased volume of
13   sediment downstream.

14   As can be observed in the figure, the TSS response to storm flows is more pronounced in the
15   upstream stations (Pomeroy and New Lenox), than at Woods Pond. The TSS usually peaks prior
16   to peak flow and then begins to decrease due to the decreasing flow acceleration rate.

17   A summary of historical flows, developed from the USGS gages located within the HSA, is
18   presented in Table 3-7. The average daily flows per unit area for both USGS gages (Coltsville
19   and Great Barrington) are identical. This similarity indicates that the watershed is fairly
20   homogeneous with respect to the bulk runoff characteristics. The watershed is highly responsive
21   to rainfall, depending on antecedent moisture conditions, rainfall totals, and rainfall intensities.
22   Therefore, all processes referred to in Table 3-1 for developing the hydrology of the HSA are
23   relevant and will be included in the modeling study.

Table 3-6

Storm Event Summary

Storm Event	Dates	Total Precipitation* (in.)	Flow**			Stage**			Notes
			Min (cfs)	Max (cfs)	Storm Increase (1,000 cf)	Min (ft)	Max (ft)	Difference (ft)	
1	19-21 May 1999	2.23	36	1,410	131,577	0.81	3.77	2.96	Full sampling protocol
2	14-15 June 1999	0.14	21	25	55	0.62	0.67	0.05	Full sampling protocol
3	17-18 June 1999	0.11	20	25	138	0.60	0.68	0.08	Full sampling protocol
4	29-30 June 1999	1.93	41	157	1,453	0.86	1.51	0.65	Staff gages at primary locations
5	2 July 1999	0.33	31	55	880	0.75	0.97	0.22	Full sampling protocol
6	6-8 July 1999	0.66	34	92	4,835	0.79	1.21	0.42	TSS at primary locations, staff gages at all locations
7	14-16 Aug 1999	2.91	12	118	5,094	0.43	1.34	0.91	Full sampling protocol
8	26 Aug 1999	0.46	15	19	102	0.51	0.58	0.07	Staff gages at all locations
9	15-19 Sept 1999	4.42	15	660	66,205	0.51	2.68	2.17	Full sampling protocol
10	30 Sept - 1 Oct 1999	1.11	21	107	7,234	0.61	1.29	0.68	Full sampling protocol

*Measured at Pittsfield Airport.

**All readings taken from USGS station at Coltsville, MA.

 All values are associated with the entire storm event.
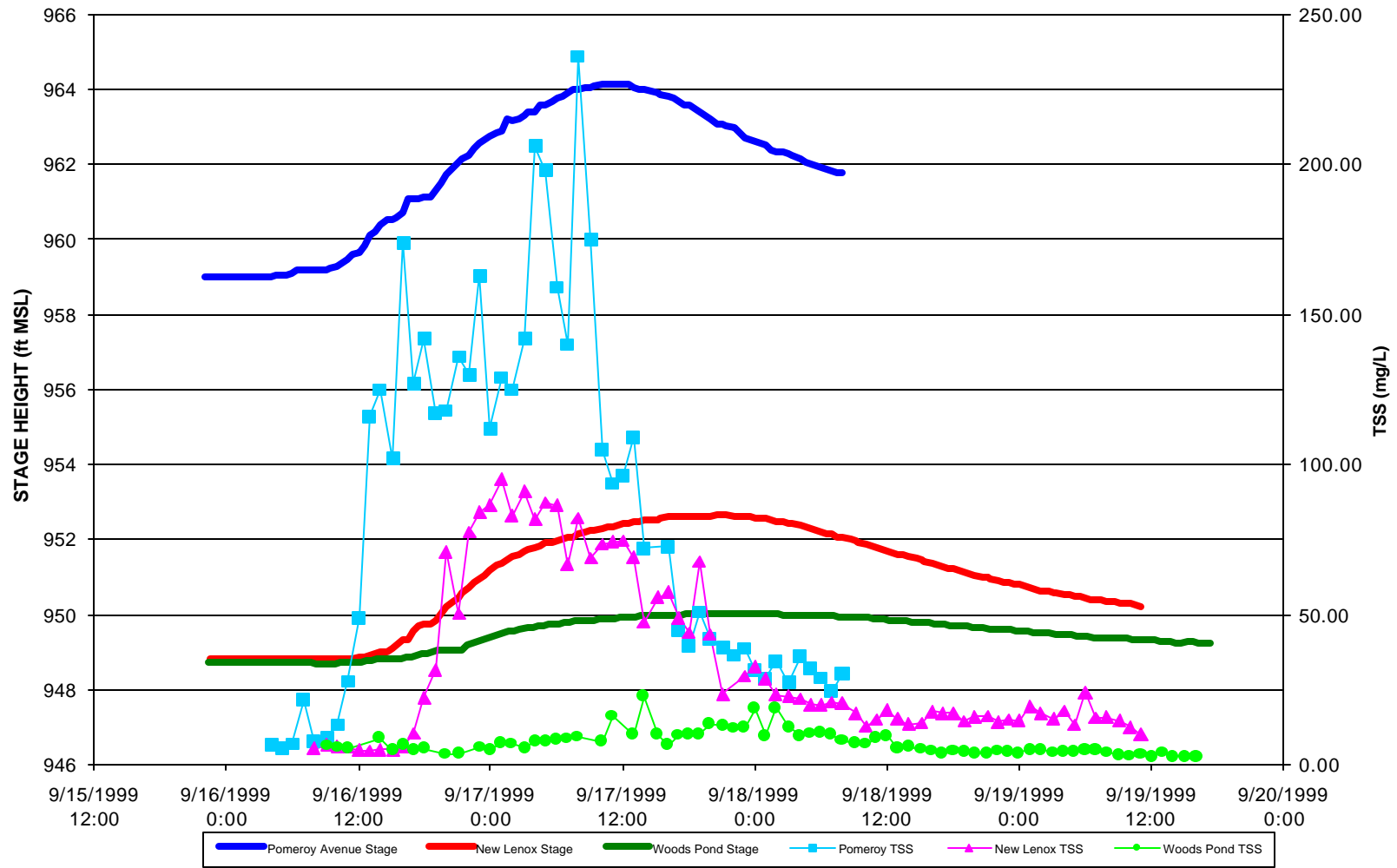
Figure 3-5 Stage Heights and TSS for September 1999 Storm Event

Table 3-7

Summary of Historical Flows for the USGS Gages

		USGS Gage at Coltsville Station 1197000	USGS Gage at Great Barrington Station 1197500
Period of Record		1937-97	1914-1997
Years of Daily Data		61	84
Flood Events (cfs)	Return period		
	100-yr	3,790	10,603
	50-yr	3,276	9,137
	25-yr	2,791	7,786
	10-yr	2,186	6,142
Peak Flows and Years in Current Record			
		4,350 – 1949	11,101 – 1949
		3,110 – 1938	11,000 – 1938
		2,860 – 1987	9,940 – 1984
Average Daily Flow (cfs)		107.2	525.8
Average Daily Flow/sq. mi.		1.86	1.86

3.3.2 Hydrodynamics

3.3.2.1 General Characteristics

The Housatonic River hydraulics/hydrodynamic modeling will focus on the PSA, from the confluence to Woods Pond Dam. The existing data have been reviewed to develop an understanding of the important characteristics and processes of the hydraulics and hydrodynamics of the Housatonic River (also referred to as the hydraulic regime), especially as they impact sediment and PCB transport. The processes, mechanisms, and factors currently considered to be important and that will be included in this modeling study are:

- Upstream and tributary flow rates.
- Water velocities.
- Flow resistance/shear stresses.
- Spatial velocity distributions.
- Vertical stratification.
- Channel slopes.
- Hydraulic structures.

The hydraulic regime cannot be interpreted in isolation from either the basin hydrology or the resulting geomorphology. The observed channel forms are the result of the long-term fluvial and sedimentary processes, which in turn are driven by the hydrology, hydrodynamics, bed material, sediment loading characteristics, and man-made structures (bridges and dams). Therefore, an analysis of the hydraulics and hydrodynamics of the PSA begins with an evaluation of the channel morphology.

Four physical and topographic hydraulic regimes have been identified within the PSA, based on the geomorphology of the area and river characteristics described below. These four regimes are:

1. Confluence to Wastewater Treatment Plant (WWTP) (Reach 5a).
2. WWTP Discharge to Roaring Brook (Reach 5b).
3. Roaring Brook to Woods Pond and associated backwaters (Reach 5c).
4. Woods Pond (Reach 6).

These four regimes correspond to the river reach designations, which are shown in Figure 2-1.

1   The geomorphological and riverine characteristics that were evaluated in defining the regimes
2   include:

3   ▪ Observed flow differences.
4   ▪ Width of the channel.
5   ▪ Comparison of bank and thalweg elevations.
6   ▪ Slopes.
7   ▪ Change in wetland habitats.
8
9   The slope of the riverbed, in contrast to the slope of the riverbanks of the river within the PSA,

10 illustrates some of the variation between these hydraulic regimes. Figure 3-6 illustrates the

11 slopes of the riverbed and banks (derived from the channel morphology data, WESTON, 2000a)

12 in the PSA. Although the riverbed decreases in elevation throughout the course of the river, the

13 riverbanks begin to decrease in slope at about river mile 130, coincident with the WWTP and at

14 the breakpoint between Reaches 5a and 5b.
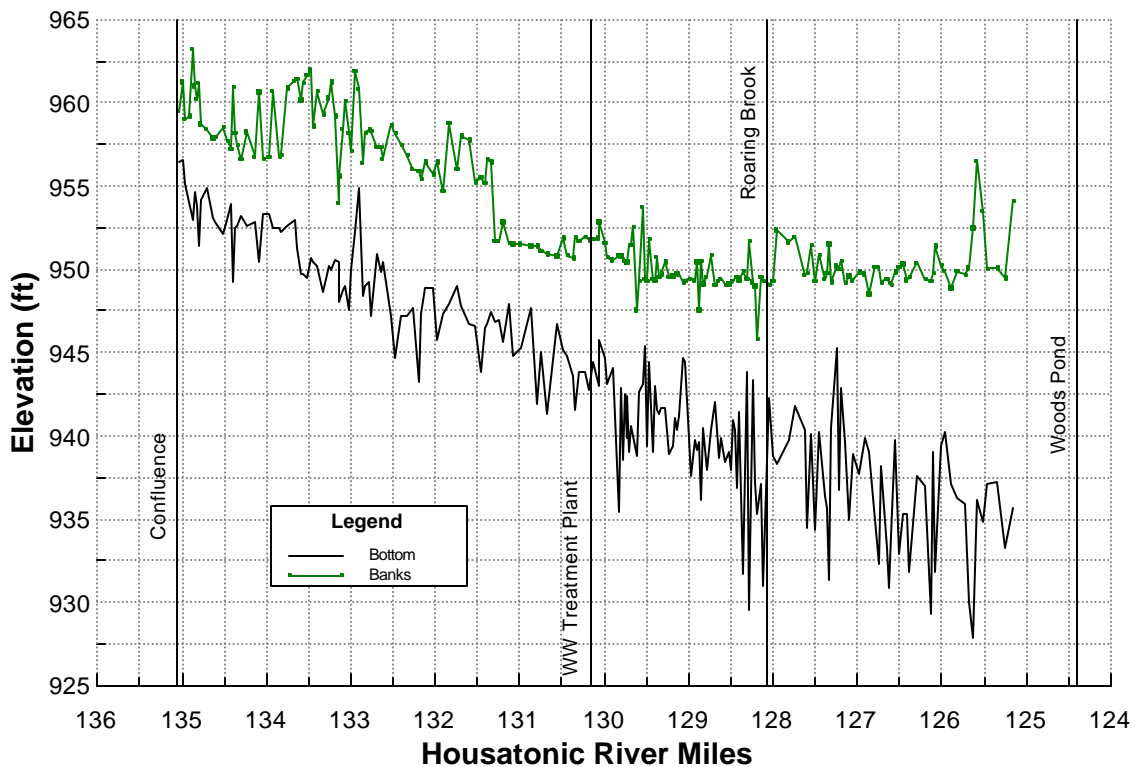
15

16   **Figure 3-6 Primary Study Area Bottom and Top of Bank Profiles**

17 Three of the four hydraulic regimes are defined within the riverine portion of the PSA and reflect

18 general changes in the energy gradient, as the river transitions from higher to lower gradients.

1   The first two regimes consist of free-flowing segments of the river (Reaches 5a and 5b),

2   followed by the backwater transition zone (Reach 5c). The three regimes are characterized by

3   differing channel depths, flows, and channel slopes. Generally, the channel segments transition

4   from shallower to deeper average depths, and higher to lower average shear stresses. The free-

5   flowing channel extends from the confluence to Roaring Brook, although riverbank elevation

6   changes are seen within this hydraulic regime, as mentioned above. In addition, due to both the

7   topography and the effects of the Woods Pond Dam, the floodplain in Reach 5c is substantially

8   greater in extent than would be the case if the dam were not present. The fourth hydraulic

9   regime, Reach 6, comprises Woods Pond and reflects a very low velocity and low energy

10   gradient section. This is the most downstream section of the PSA.

11   ### *3.3.2.2   Topography and Geomorphology of the Basin and Study Area*

12   **Topography**

13   The topography of the PSA is relatively flat, with a gentle slope from the confluence to Woods

14   Pond. Steep elevations, associated with October Mountain, occur immediately adjacent to the

15   eastern edge of the PSA from approximately New Lenox Road to Woods Pond. This steep

16   elevation to the east has prevented the development of a large floodplain on that side of the river.

17   From the confluence to New Lenox Road, the river drops in elevation from approximately 961 ft

18   msl to 951 ft, with a relatively narrow river channel and floodplain. The width of the 10-year

19   floodplain averages approximately 800 ft in this area, occasionally extending to 1,000 ft.

20   Just beyond New Lenox Road and just before where Roaring Brook enters the main channel, the

21   overall width of the channel and associated floodplain widens considerably. Although October

22   Mountain prevents substantial floodplain development to the east, broad floodplains have

23   developed on the western side of the PSA, extending up to 3,000 ft from the river channel. A

24   railroad right-of-way and associated berm within the floodplains and along the western side of

25   the PSA creates a partial barrier to floodwaters.

26   A site-specific digital elevation model (DEM) was developed for the PSA to facilitate the

27   construction of a topographic model for the modeling study. The DEM was developed from

1   topography established by GE in 1997 based upon aerial stereo photographs taken in 1990. The

2   DEM was then compared with surveyed cross sections of the PSA conducted by the U.S. Army

3   Corps of Engineers under the current Work Plan (WESTON, 2000a). The accuracy of the DEM

4   was determined to be within the typical error range (+/- the contour interval) for a USGS

5   topographic map, and therefore the DEM has been adopted as the basis for the modeling study.

6   As part of the Supplemental Investigation conducted by EPA (WESTON, 2000a), over 200

7   channel morphological cross sections in the PSA and in selected tributaries were surveyed to

8   support both the hydrodynamics and the hydrological studies. These data have been used to

9   develop detailed channel maps and to supplement the topographic data from the DEM. Figure

10   3-7 is a contour map of one small portion of the river within the PSA. This map shows the

11   channel morphology and surrounding terrain as developed from the DEM and associated channel

12   cross sections. The lines shown in the figure represent the XY locations of the contour/channel

13   morphology data used to generate the DEM.

14   The Housatonic River displays various features that are clear indications of how the river and

15   associated floodplains were formed. For example, the floodplain exists as a separate and distinct

16   landform from the river channel itself. These features were created through various fluvial

17   processes including river water erosion, sediment transport and deposition, and the effects of

18   flooding events. For this study, the PSA has been separated into five terrains and Woods Pond.

19   The five terrains are:

20   ▪ River channel.
21   ▪ Riverbank.
22   ▪ Floodplain (both distal and proximate).
23   ▪ River bars, terraces, or benches.
24   ▪ Side channels, backwaters, isolated meanders, or oxbows (SCOX).
25
26   The floodplain has been operationally defined at this site as the 10-year floodplain indicated in

27   the Supplemental Investigation Work Plan (WESTON, 2000a).

28   **Channel Morphology, Meandering Patterns, and History**

29   The morphology of a river channel is a function of the discharge and the materials that compose

30   the channel. As the mean discharge of a river increases downstream, channel width, channel

depth, and mean current velocity increase. Rivers with sediment loads composed of high percentages of silts and clays tend to produce narrow, relatively deep channels with trapezoidal-shaped cross sections. This morphology minimizes surface area and allows effective transport of the suspended load (Bloom, 1978). Experiments by Schumm (1960a, 1960b) demonstrated that the depth-width ratio (F) of the channel is inversely related to the percentage of fine-grained sediments in the bank such that as the suspended clay/silt load increases in proportion to the bedload, F decreases, and the channel tends to become narrow and deep. As a result, more of the energy of the river is expended against the banks, resulting in an increase in the sinuousity of the channel. Furthermore, experiments by Schumm and Khan (1972) that attempted to produce meandering channels in flume experiments by varying slope, discharge, and sediment loads produced a meandering channel only after 3% by weight of clay (kaolinite) was added to the original poorly sorted sand alluvium.

The occurrence of meanders is related to the flow of the channel, dimensions of the channel, erodibility of the stream bank, and proportion of suspended load versus bedload. The increased sinuosity and formation of meanders results in an increase in the length of the channel and thereby decreases the slope of the channel.

Within the PSA, from the confluence to the vicinity of WWTP (Reach 5a), the river can be described as a sinuous channel with some meanders present. Between the WWTP and Woods Pond (Reaches 5b and 5c), the river becomes a highly meandering channel with adjacent oxbows frequently present. The increase in meandering frequency below the WWTP is consistent with the decrease in gradient (refer to Figure 3-6) and an increase in the percentage of silt/clay sediments (Figure 3-8) below the WWTP. Likewise, the trapezoidal-shape profile is the dominant channel shape indicated in the majority of more than 200 main channel cross sections in the study area.

The current evaluation of the history of meandering patterns indicates that this process is important to sediment and PCB transport, as it represents erosional processes that may release PCB-contaminated sediments into the river from channel sidewalls and former floodplains. This process will be further evaluated for its inclusion in the detailed modeling effort.
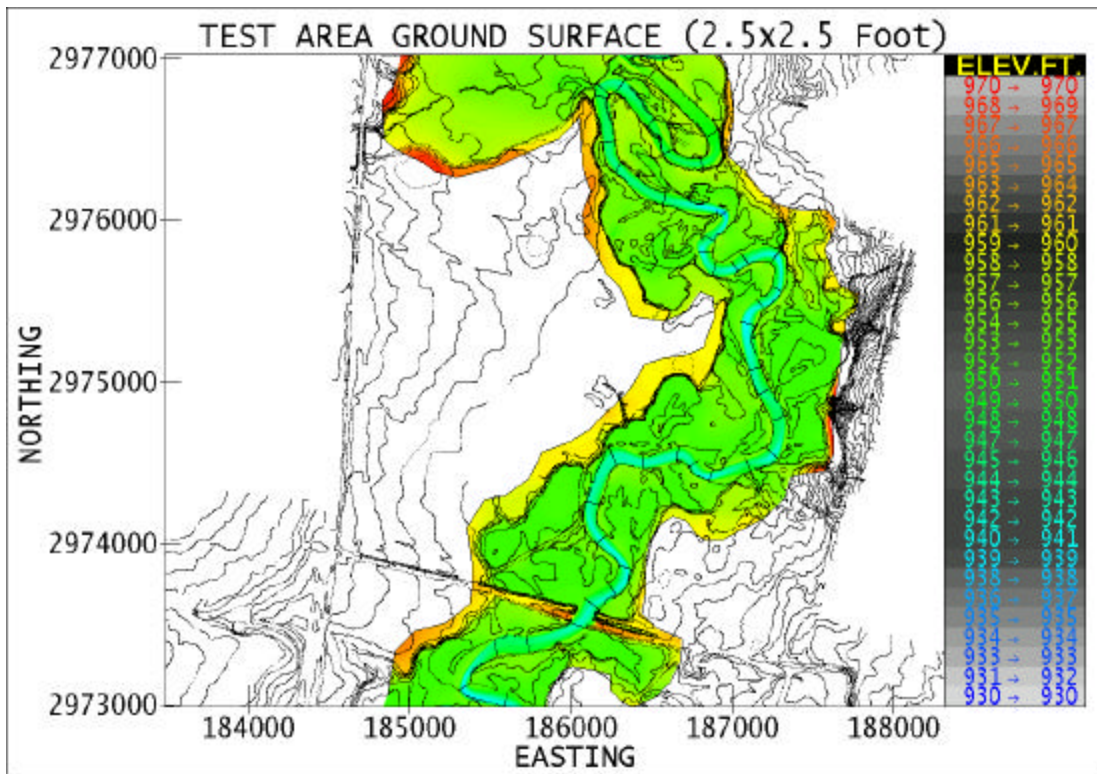
Figure 3-7 Topographic Map of One Area of the PSA
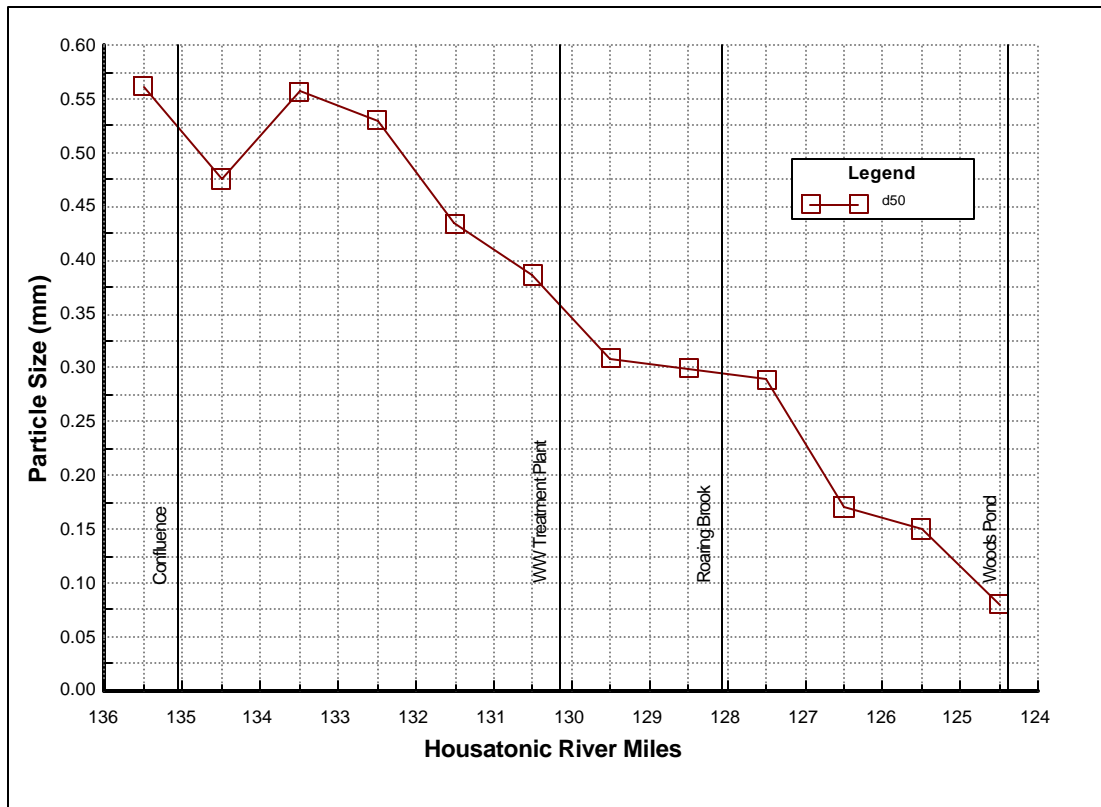
Figure 3-8 Median Grain Size (d50) for Sediments by River Mile

1 ### *3.3.2.3   Channel/Floodplain Water Velocities*

2 As highlighted during the discussion of data requirements, the determination of water velocities

3 in the river and floodplain is fundamental and relevant to all of the hydraulic and hydrodynamic

4 processes, but most particularly in determining shear stress and the resultant effects. From site-

5 specific data, velocities were computed throughout the PSA and range from 0.2 fps to > 4 fps,

6 depending on flow and cross-sectional area, but were typically higher in the upstream portions of

7 the river. Figure 3-9 (cross section just upstream of the New Lenox Road Bridge) shows an

8 example of how the hydraulic calculations for a cross section are computed.

9
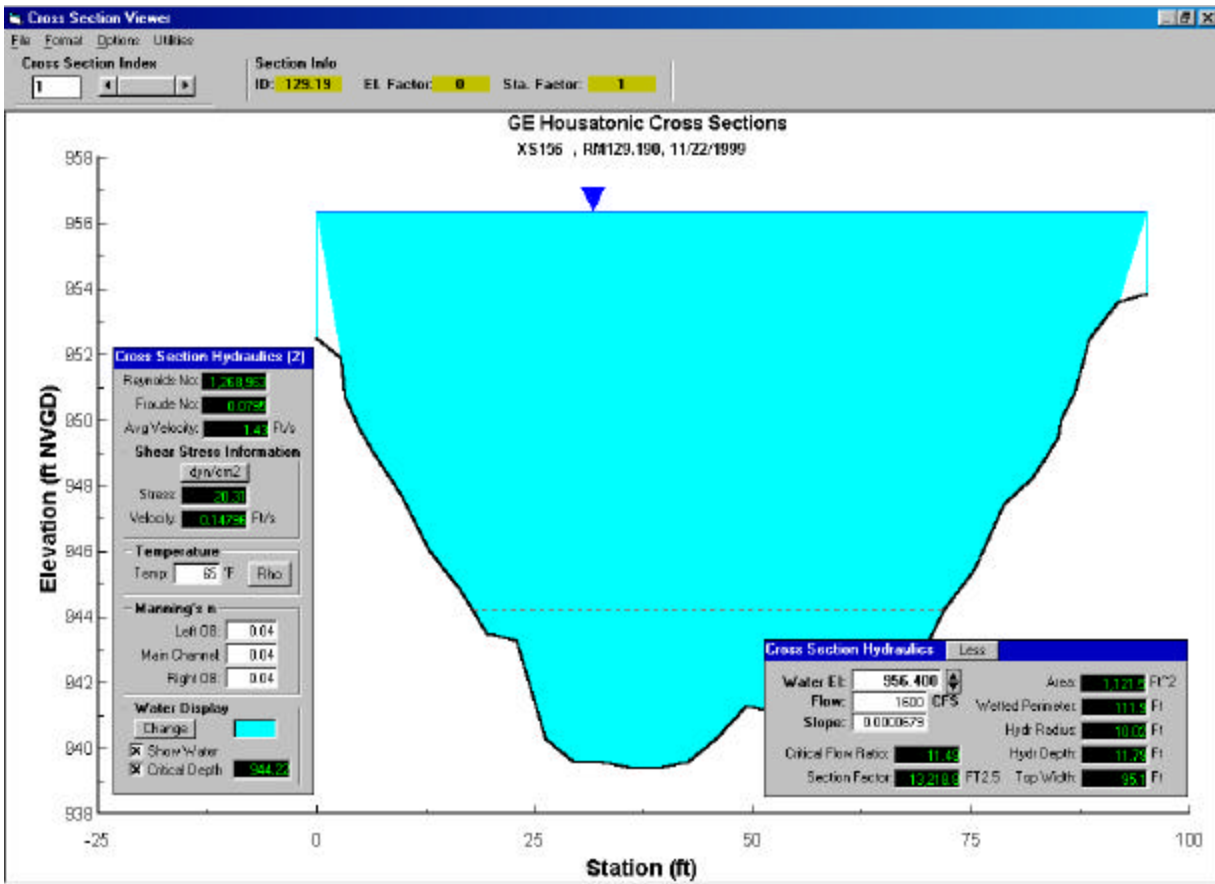
10 **Figure 3-9 Cross Section of Housatonic River Upstream of the New Lenox Road**
11   **Bridge**

12 The additional data being collected on observed river velocities within the PSA will provide

13 high-resolution three-dimensional velocity data that will be used in determining whether varying

14 current speeds and flow directions are properly represented in the model.

3.3.2.4 *Channel/Floodplain Energy Losses*

Channel flow resistance is a function of channel bed material, channel morphology, vegetation, and deadfalls. Several general hydraulic models have been developed for the Housatonic River, with sections encompassing the PSA. One study (BBL, 1992) provided a range of Manning's n of 0.015 in Woods Pond and its backwaters, to 0.05 in the upper reaches in the main channel. The lower value for Manning's n in the lower reaches reflects the smoother bottom surfaces associated with the more fine-grained bed material. The higher numbers reflect the coarser bed material (i.e., gravels and cobbles) in the upper reaches. Given the substantial differences in *n* demonstrated in the previous studies, it is obvious that the definition of channel energy loss is important for this modeling study. Data generated from the study on the shear stress of sediments within the PSA will allow better determination of the values used in the model and the sediments to which they are applied.

The values for Manning's n in the floodplain ranged from 0.043 to 0.15 (BBL, 1992). These numbers reflect the amount and nature of the vegetation, as well as natural and man-made obstructions such as buildings, parking lots, and agricultural use, that were assumed. These general ranges and patterns of resistance terms will be used as a starting point for the hydraulic and hydrodynamic studies.

Vegetation covers most of the PSA, especially the floodplains. To account for flow resistance, the entire PSA has been delineated and mapped into 14 distinct wetland types:

- Lacustrine, Open Water
- Palustrine, Aquatic Bottom/Unconsolidated Bottom
- Palustrine, Emergent
- Palustrine, Forested
- Palustrine, Forested/Emergent
- Palustrine, Forested/Scrub-Shrub
- Palustrine, Scrub-Shrub
- Palustrine, Scrub-Shrub/Emergent
- Palustrine, Unconsolidated Bottom
- Riverine, Aquatic Bottom
- Riverine, Open Water
- Sand
- Uplands
- Wet Meadow

1   Each of these wetland types is distinct and is defined by a unique combination of the three
2   criteria that determine the character of a wetland—vegetation, hydrology, and soil type. In turn,
3   these wetlands affect the flow of water during flooding events, changing water velocity and
4   direction, as well as acting as an effective sediment trap. The effect of these wetland types on
5   sediment transport, as noted below, is an important process for consideration in the modeling
6   study.

7   Sediment deposition on vegetation after flooding events has been observed throughout the PSA
8   from the riverbank outward onto the adjacent floodplains. Where present, a thick herbaceous
9   understory within these habitats has produced an effective trap for sediments carried by
10   floodwaters that overtop the riverbanks. Forested wetlands adjacent to the river appear to have
11   the most dense understory and thus the greatest sediment trapping ability. Scrub-shrub habitats
12   are less effective. Emergent wetlands, when directly adjacent to the main river channel, also
13   appear to be very effective in trapping suspended sediments, but when located near side
14   channels, former meanders, and oxbows, the trapping efficiency of these emergent wetlands
15   seems less effective due to reduction in understory vegetation.

16   The effectiveness of vegetation in trapping sediment is also seasonal. Vegetation has its greatest
17   trapping efficiency in summer when the foliage is at a maximum (size and density); is less
18   effective in spring and fall, and is at the lowest trapping efficiency in the winter months.
19   Duration and frequency of flooding events can also affect the ability of the understory to create
20   an effective sediment trap. Prolonged or repeated flooding may cause the vegetation to lay flat,
21   thus allowing additional suspended loads to migrate farther into the floodplains. Similarly,
22   vegetation may be killed if inundated for prolonged periods.

23   The energy loss in the channel and from vegetation in the floodplains (during flooding events) is
24   a determining factor for water surface elevations, energy gradients, and response under differing
25   driving inflows. Thus flow resistance/energy loss must be included in the modeling study.
26   Dams and other hydraulic structures, such as bridges, also have an important impact on the
27   system, producing energy losses, and must be included in the model.

3.3.2.5   Thermal Effects on the System

Vertical Stratification

Vertical water-quality profiling was conducted in Woods Pond to determine if stratification of the water column was occurring to an extent that 3-D modeling would be required. Figures 3-10 and 3-11 represent plots of the measured parameters by depth at two of the sampling locations in late summer.

These vertical profiles indicate that stratification within Woods Pond, and specifically within the "deep hole," may be occurring at approximately 5 ft below the water surface. Isothermal profiles in November were typical of winter conditions, with stratification observed in summer months, indicative of a spring turnover. Within the river channel itself, just upstream of Woods Pond, the vertical stratification is less evident, with a slight break occurring at approximately 10 ft below the water surface. Turbidity and specific conductance show virtually no change with depth.

Because eutrophication and dissolved oxygen depletion processes in Woods Pond will be represented as a two-layer system with the upper layer (epilimnion) separated from the lower layer (hypolimnion), the hydrodynamic model must be developed to account for vertical stratification of the water column.

The temperature dynamics of Woods Pond will be modeled through heat/temperature modeling. Important inputs to the thermal balance are Housatonic River inflow, inflow temperatures, Woods Pond bathymetry, and meteorological conditions.
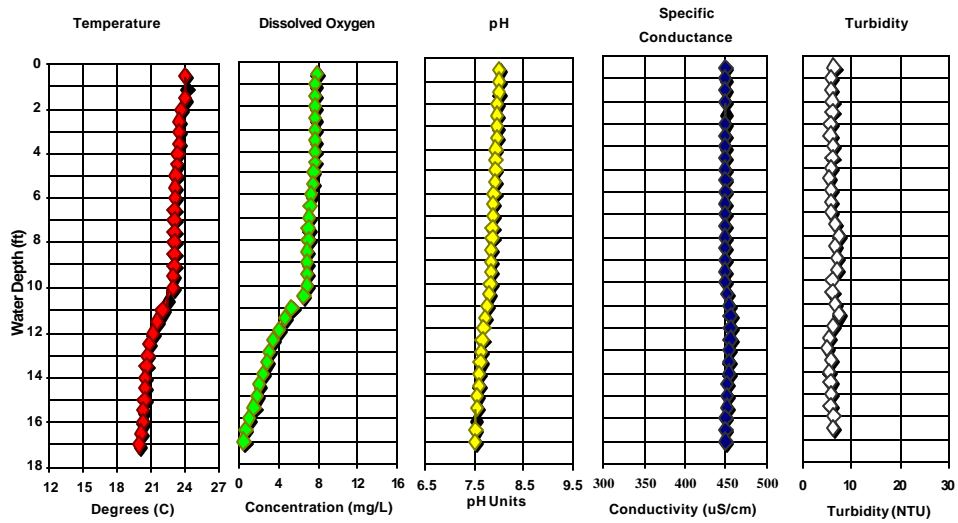
Figure 3-10 Vertical Profiles of Water Quality Data Upstream of Woods Pond
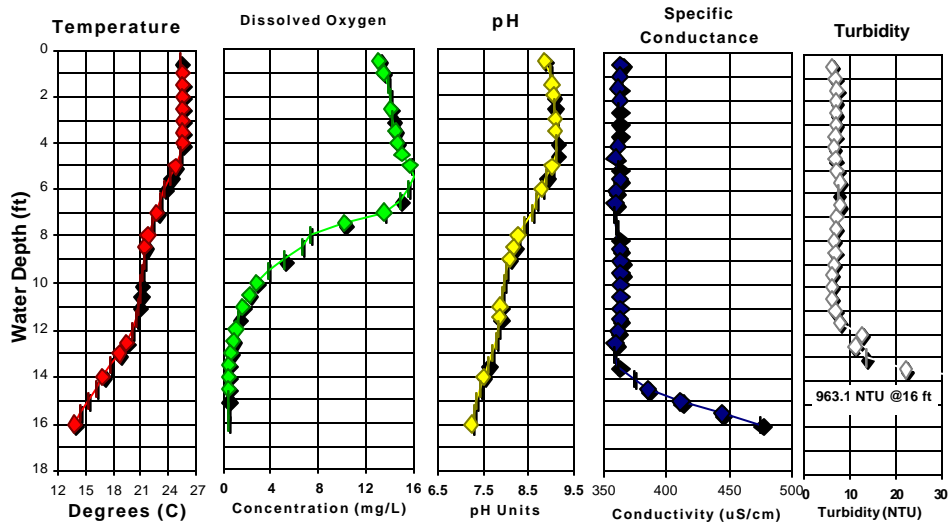
Figure 3-11 Vertical Profiles of Water Quality Data at the Deep Hole of Woods Pond

3.3.3 Sediment Transport

3.3.3.1 Summary of Transport Processes

Sediment transport within the PSA is dominated by two important mechanisms: suspended sediment transport and bedload transport. Different processes affect these mechanisms, and those that are considered for inclusion in the modeling study are listed below:

- Suspended Load:
    - Upstream and tributary loading
    - Resuspension
    - Mass erosion
    - Mass wasting/bank slumping
    - Localized scouring around structures and debris
    - Deposition and burial
    - Bed armoring
    - Flocculation

- Bedload:
    - Upstream and tributary loading
    - Deposition/burial
    - Bed armoring
    - Bioturbation

The importance of suspended load transport within the PSA was evident in the increased volumes of suspended solids observed during the storm event monitoring conducted in 1999. Storms resulted in an increased load of sediment via resuspension of sediments, erosion of the channel, and runoff-induced erosion of soils in the watershed, with subsequent transport in the tributaries and the river, highlighting the importance of suspended solids in the transport of PCBs in the system. The observed trapping of sediment on vegetation within the wetlands was evidence of the effective transport of suspended solids into the floodplain during storm events.

Movement of bedload is also an important transport mechanism, especially within the first two hydraulic regimes (Reaches 5a and 5b) where coarser sediments predominate (see sediment characteristics below).

Tributary contributions to the suspended load are considered important, whereas tributary contributions to the bedload are currently considered to be insignificant. However, the data are

1   still being evaluated for tributary bedload inputs and, if found to be significant, this process will

2   be reevaluated for inclusion.

3   Bioturbation can affect sediments and PCB dynamics in several ways, depending on the actual

4   biological process. For example, sediment plumes have been observed from carp feeding. This

5   activity can impact bulk density, particle mixing, and resuspension/transport. In another

6   example, infaunal invertebrate activity can also cause sediment mixing and decreased bulk

7   density. These processes will be retained to further evaluate their impact on suspended load and,

8   to a lesser extent, on bedload. An evaluation of the effect of bioturbation, including delineation

9   of the spatial extent and depth where bioturbation may occur, is being conducted. This study

10 will aid in determining whether bioturbation is sufficiently important for any of the potentially

11 impacted processes listed above.

12 Anthropogenic sources, such as boat prop wash and wake effects, can also have similar impacts,

13 although these are much less important than bioturbation, due to the ban on gasoline engines

14 throughout much of the PSA. These sources will not be included in the modeling study.

15 ### *3.3.3.2   Erosional and Depositional Processes*

16 Within the PSA, an understanding of both erosional and depositional processes is crucial in

17 determining the movement of sediment and ultimately of PCBs through the system and must be

18 included in the model. Erosional processes consist of resuspension/scouring, bank slumping

19 along channel sidewalls, scouring of the channel near man-made structures such as bridges,

20 scouring of the channel near downed trees/woody debris, and mass erosion of cohesive solids.

21 A visual inspection along the river within the PSA was conducted to evaluate the extent to which

22 scouring is occurring. This inspection indicated that erosion along the river is widespread and

23 therefore is an important process. This information, combined with variable water velocity

24 measurements, site-specific shear stress, and sediment grain size distributions along the channel

25 bed, will be used to calculate the magnitude of resuspension within the system.

26 Man-made structures, particularly bridges, were also observed to create localized scouring.

27 However, because of the limited number of these structures within the PSA, it may not be

necessary to include this process in the modeling study, but it is still being evaluated for its overall importance.

Natural debris within the river can create both depositional and erosional features. However, because of the spatial and temporal variability of the debris and resulting effects, scouring due to natural debris will not specifically be included within the modeling study.

Within the PSA, depositional processes are equally as important as erosional processes. The visual inspection conducted of channel scouring also identified numerous bars and depositional features along the river, primarily in the first two upstream hydraulic regimes.

The floodplain is a major area of sediment deposition within the PSA. The primary process responsible for this deposition is vegetation resistance mentioned previously. Erosion of the floodplain can occur under extreme high flow events and from bank slumping.

Settling velocities drive the rate of solids settling and thus deposition for each class of solids. For larger noncohesive particles, settling velocities can be reasonably computed using Stokes Law. However, for smaller silts and cohesive solids, it is better to use measured settling velocities rather than theoretical velocities. For these smaller solid classes, many factors influence settling, including concentration, floc formation, organic content, and specific weight. Because of these factors, settling velocities and associated factors, such as flocculation, are being further studied.

3.3.3.3   Sediment Characteristics

Grain size analysis was conducted on sediment samples collected from the PSA to determine the relative percentages of the three grain-size classes to be used in the modeling study:

- $> 250\,\mu m$
- $250\text{-}63\,\mu m$
- $< 63\,\mu m$

These ranges were selected for the modeling study to allow evaluation of bedload and to distinguish cohesive from noncohesive sediments; the division between the two classifications is $63\,\mu m$.

1 Figure 3-12 shows the percentage of each of the three grain size classes observed in recent
2 sampling within the channel bed (top 6 inches) from the confluence to Woods Pond. The coarser
3 grain size materials (> 250 µm) dominate (50 to 60%) the sediments in the uppermost hydraulic
4 regime (Reach 5a). The intermediate size class (63 to 250 µm) is the dominant grain size in most
5 of the next two hydraulic regimes, ultimately being replaced by the smallest size class in Woods
6 Pond and associated backwaters.

7
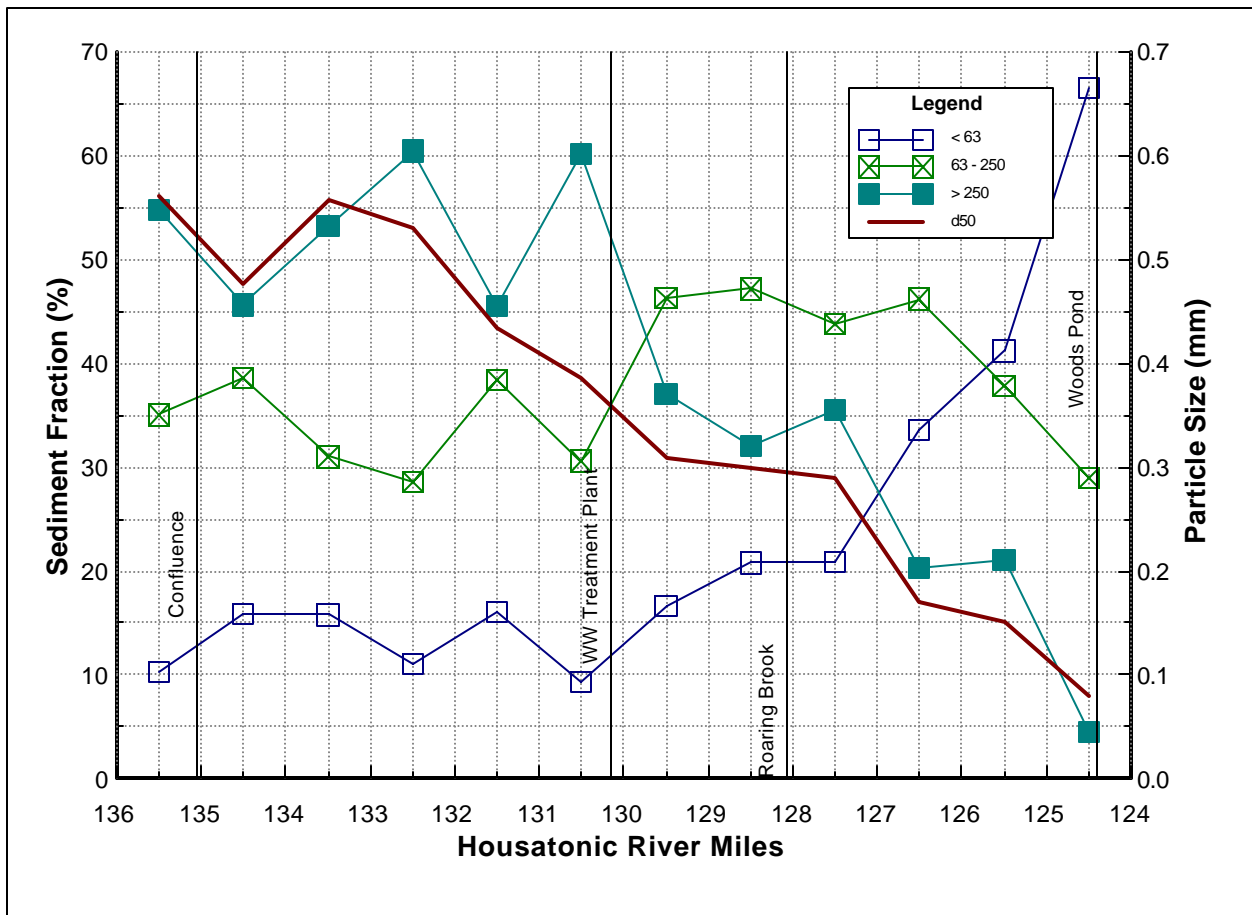
Figure 3-12 Summary of Sediment Grain Size Composition and Median Grain Size (d50) by River Mile

10 The need to include processes such as bedload transport and resuspension in the modeling study
11 is reinforced by the dramatic changes observed in dominant grain size along the length of the
12 PSA.

1   *3.3.3.4*   *Channel/Floodplain Interactions*

2   Water flow between the river channel and the floodplain occurs during storms and associated

3   flooding events. As noted above, the heavy vegetative cover along the edge of the river results

4   in decreased flow velocity and, consequently, increased sediment deposition. Using the amount

5   of vegetative cover, the floodplain can be divided into proximate (near the riverbank) and distal

6   (the larger portion of the floodplain away from the river) components. The proximate

7   floodplains will typically have a width measured in tens of feet up to 150 ft. This variation in the

8   width of the proximate floodplain can be seen in topographic maps of the study area where small

9   levees are evident within the proximal areas.

10   Transport from the floodplain to the river is less likely, but can occur during especially large

11   flooding events, when the flow across the floodplain begins to entrain previously deposited

12   material. The vegetative cover across the floodplain will likely minimize this process.

13   Remobilization of floodplain soils/sediments can also occur when the river channel changes

14   course and cuts back into the floodplain. This process has been observed over time within the

15   PSA as discussed in Section 3.3.2.2.

16   **3.3.4   PCB Transport and Fate**

17   *3.3.4.1*   *Summary of Processes*

18   Chemical, physical, and biological factors and processes control the transport and fate of PCBs

19   in any aquatic environment. Within a given river system, any number of these factors or

20   processes may be active with varying degrees of significance. A preliminary evaluation of

21   available data for the Housatonic River System was conducted to understand what factors and

22   processes control or contribute to the fate and transport of PCBs. This evaluation included

23   analyses of soil, sediment, and water samples for PCBs and other chemical parameters. This

24   evaluation has determined that the principal transport and fate processes for PCBs to be included

25   in the modeling study are as follows:

- Partitioning of PCBs to:
  - Organic carbon
  - Sediments
- Non-partitioning of PCBs (free-phase NAPL)
- Diffusion to the water column
- Bedload transport
- Advection (groundwater/surface water)
- Bioturbation

The following subsections describe the evaluation of the available data and a discussion of the likely mechanisms for PCB transport and fate. To obtain a thorough understanding of the nature and extent of PCBs within the PSA, one must examine the data as a three-dimensional distribution, rather than solely as summary metrics. A series of maps have been produced depicting the distribution of PCBs in soils and sediments in the PSA in three-dimensions. This series of maps is available on-line at http://www.epa.gov/region01/ge/thesite/restofriver-maps.html.

3.3.4.2   Distribution of PCBs In Soils and Sediments

An understanding of the distribution of PCBs within sediments and soils is needed:

- To determine the various processes at work within the river system.

- To establish the initial conditions for the model.

- To understand the transport pathways among the various processes at work within the PSA.

The evaluation of PCB distribution in soils and sediments of the PSA was conducted separately for each of the five geomorphological terrains defined in Section 3.3.2.2 and for Woods Pond. Each of these areas was compared in terms of summary metrics such as mean and maximum concentrations measured, number of samples with detected versus nondetected PCBs, and number of locations with at least one PCB result above detection limits. Because of the need to ensure consistency of data in a comparative evaluation of this type, only data collected by EPA since 1998 (WESTON, 2000a) and validated following EPA Region 1 procedures discussed in the project QAPP (WESTON, 1998) were considered. This resulted in an available data set containing approximately 5,000 samples collected within the PSA that were analyzed for PCBs

1 (total, Aroclors). Approximately 10% of the soil and sediment samples were also analyzed for

2 PCBs (congeners, homologs), but these results are not yet available for evaluation.

Distribution of PCBs by Terrain

4 Samples were collected from the surface (0-6 inches) to depths that varied from 1 ft to over 4 ft.

5 The frequency distribution of PCBs detected, by ranges of concentration, across each of the

6 geomorphological terrains upstream of Woods Pond, is shown in Figures 3-13 and 3-14.

7 Figure 3-13 presents a plot by terrain of the percentage of samples (as individual sample results)

8 with PCBs within given concentration ranges (e.g., 26.7% of all samples collected from the

9 floodplains had PCBs at concentrations between 10 and 50 mg/kg). Figure 3-14, using the same

10 data, shows a frequency distribution of the highest concentration detected in any sample from a

11 given location, whether at the surface or from depth.

12 As shown in these two figures, PCBs are found in soils and sediments throughout all five of the

13 terrains within the PSA upstream of Woods Pond. PCBs were detected in 77% of all the samples

14 collected, with the highest frequency of "detects" occurring in bars/terraces (98.5% of samples)

15 and in riverbank samples (86.8%). Table 3-8 provides a statistical summary of the data used for

16 this evaluation.

17 When the data are evaluated by location (Figure 3-14), PCBs were detected at 82% of the

18 locations sampled. This percentage is higher than in the sample-by-sample comparison, due to

19 each location having been sampled at various depths. All of the bars and terraces sampled, and

20 90% of the riverbanks, had PCBs at one or more depths.

21 For the entire PSA upstream of Woods Pond, more than 15% of the locations sampled contained

22 PCBs above a concentration of 50 mg/kg in at least one sample collected from that location. The

23 bar and terrace terrain had the highest percentage of locations with concentrations of PCBs above

24 50 mg/kg. This same terrain also contains the highest number of samples or locations with PCBs

25 above 10 mg/kg, followed by riverbank samples and locations, and then river channel sediments,

26 side channels and oxbow sediments (SCOX), and floodplain soils.
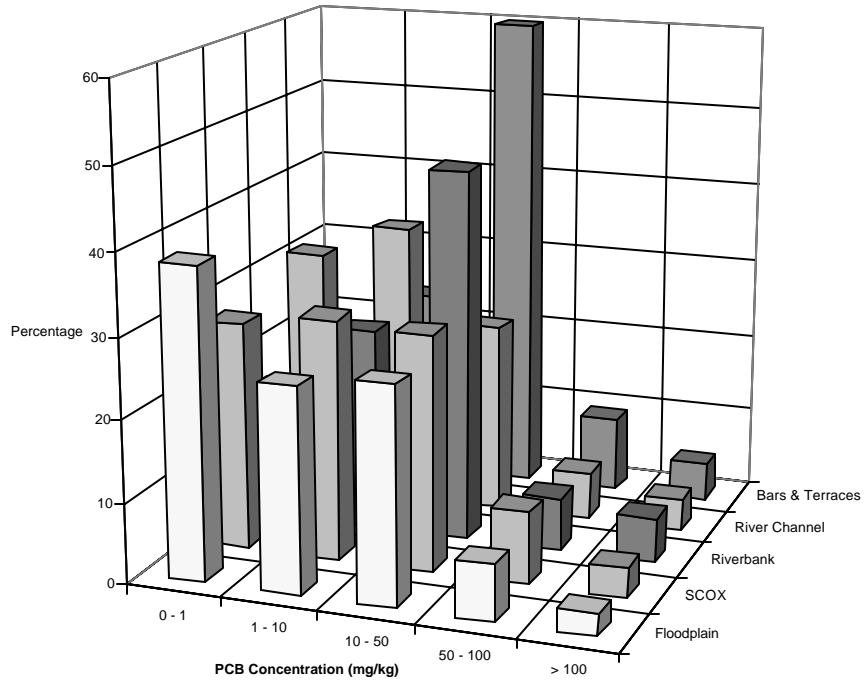
Figure 3-13 Distribution of PCB Concentrations by Sample by Terrain Type
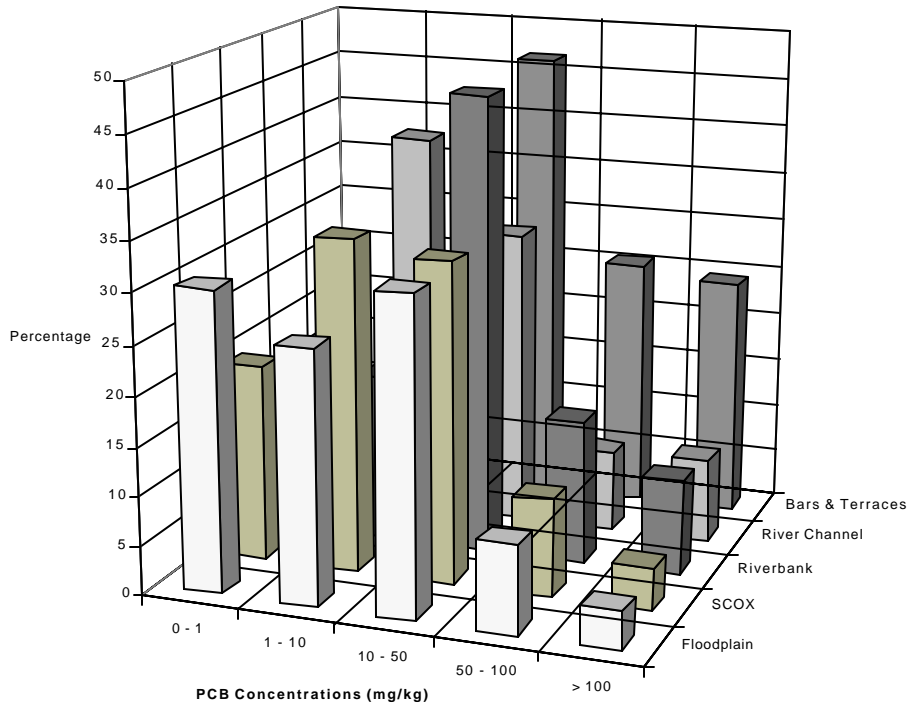
Figure 3-14 Distribution of PCB Concentrations by Location by Terrain Type

Table 3-8

Statistical Summary of PCB Data Collected Upstream of Woods Pond

	Floodplain	Side Channels and Oxbows	Riverbanks	River Channel	Bars and Terraces
Number of samples	1,937	623	91	1,727	585
Number of "detects"	1,325	480	79	1,361	576
% of detections in samples	68.4%	77.1%	86.8%	78.8%	98.5%
Mean (mg/kg)	17.5	20.4	23.4	18.2	28.5
Median (mg/kg)	3.5	6.4	11.9	4.5	14.5
Standard deviation	42.5	33.2	34.4	42.3	46.8
Maximum (mg/kg)	907	290	171	614	605
% of samples > 10 mg/kg	36.3%	41.9%	58.2%	33.5%	73.9%
% of samples > 50 mg/kg	9.6%	12.7%	12.1%	9.8%	13.9%
Number of locations	1244	474	41	586	90
Locations with "detects"	924	396	37	547	90
% of detections in locations	74.3%	83.5%	90.2%	93.3%	100%
% of locations > 10 mg/kg	44.2%	46.4%	70.7%	47.3%	96.7%
% of locations with at least 1 sample > 50 mg/kg	12.5%	14.1%	24.4%	17.1%	50%

Distribution by Depth

PCBs were detected in sediment and soil samples collected at depth as well as in samples collected from the surface. For each of the five geomorphological terrains, the mean PCB concentration was calculated for each 6-inch interval below the ground surface from which samples were collected. The number of samples collected by depth within each terrain and the mean PCB concentrations are presented in Table 3-9.

Table 3-9

Summary of Samples and Mean PCB Concentration by Depth and Terrain

Depths	Floodplain		Side Channels and Oxbows		Riverbanks		River Channel		Bars and Terraces	
	n	Mean PCB (mg/kg)	n	Mean PCB (mg/kg)	n	Mean PCB (mg/kg)	n	Mean PCB (mg/kg)	n	Mean PCB (mg/kg)
0.0-0.5	1282	17.2	505	22.6	42	18.8	897	18.7	99	22.3
0.5-1.0	268	12.4	48	14.9	29	28.9	172	19.1	95	23.9
1.0-1.5	202	23.8	31	8.5	20	13.8	387	19.1	93	30.1
1.5-2.0			6	NA			119	13.7	87	23.5
2.0-2.5	183	20.5	14	18.4	20	36.8	108	15.0	83	30.9
2.5-3.0			2	NA			13	NA	58	31.6
3.0-3.5	1	NA	2	NA			7	NA	43	51.1
3.5-4.0			2	NA			4	NA	19	27.8
4.0-4.5			2	NA			4	NA	6	NA
4.5-5.0			2	NA			3	NA	1	NA
5.0-5.5			2	NA			4	NA	1	NA
5.5-6.0			2	NA			4	NA		
6.0-6.5			2	NA			3	NA		
6.5-7.0			2	NA			2	NA		

4
5   Note – blank cells indicate that no sample was collected from that depth interval. NA indicates that the
      sample size was too small to calculate an informative mean PCB concentration.

6

7   Each terrain was sampled at 6-inch intervals to varying depths. The 1.5 to 2.0-ft interval in the

8   floodplain and riverbanks was not sampled, thereby increasing the depth at which PCB

9   concentrations could be determined. Woods Pond is the exception, where samples were taken at

10   greater depths and in greater quantity, and is discussed in more detail below.

11   Mean PCB concentrations were calculated for each interval down to 2.5 ft for each terrain and to

12   4.0 ft for bars and terraces. Means are not presented for deeper intervals due to the small sample

13   numbers (typically < 10).

1   While every attempt was made to sample at 6-inch intervals, some samples may not reflect an
2   exact 6-inch interval because of the data quality objectives or physical sampling restrictions.
3   The sample collection methods are described in the Supplemental Investigation Work Plan
4   (WESTON, 2000a).

5   Evaluation of mean PCB concentrations from all of the terrains collectively shows little variation
6   by depth. This result suggests little if any sequestering is occurring within the PSA, as no
7   significant increases of PCBs with depth were evident. The one exception is within bar and
8   terrace samples, where a slight increase in PCB concentration appears to occur at depth. The
9   statistical significance of this observation is not known at this time.

10   **Distribution by River Mile**

11   PCB concentrations in sediments were evaluated by river mile for samples collected from the
12   river channel within the PSA and from bars and terraces from river mile 135 to 129. Figure 3-15
13   shows the mean PCB concentrations in river sediments at 1-mile intervals from the confluence to
14   Woods Pond.

15   PCB concentrations in river sediments decrease from the confluence to Roaring Brook, and
16   begin to increase again at approximately river mile 127.5 on through to Woods Pond. When
17   only the river channel samples are evaluated (excluding the bar and terrace samples), this pattern
18   is even more evident. These observations suggest that the river from the confluence to Roaring
19   Brook, i.e., the first two hydraulic regimes of the PSA (Reaches 5a and 5b), is net erosional,
20   consistent with increased energy gradients in this area. The higher PCB concentrations in the
21   upstream portions of the PSA are also consistent with the historical release of PCBs upstream
22   from the confluence. From Roaring Brook to the Woods Pond Dam (Reach 5c), the patterns in
23   the data suggest a net depositional environment, which is consistent with the slower flows and
24   lower energy in this portion of the PSA.

25   The higher mean PCB concentrations detected from the confluence (RM 135.1) to the WWTP
26   discharge (RM 130.2), Reach 5a, correspond to the same section of the river where the dominant
27   sediment grain size is coarse sands and gravels. Immediately downstream, in Reach 5b, where
28   the lowest mean PCB concentrations were detected, the dominant grain size changes from coarse
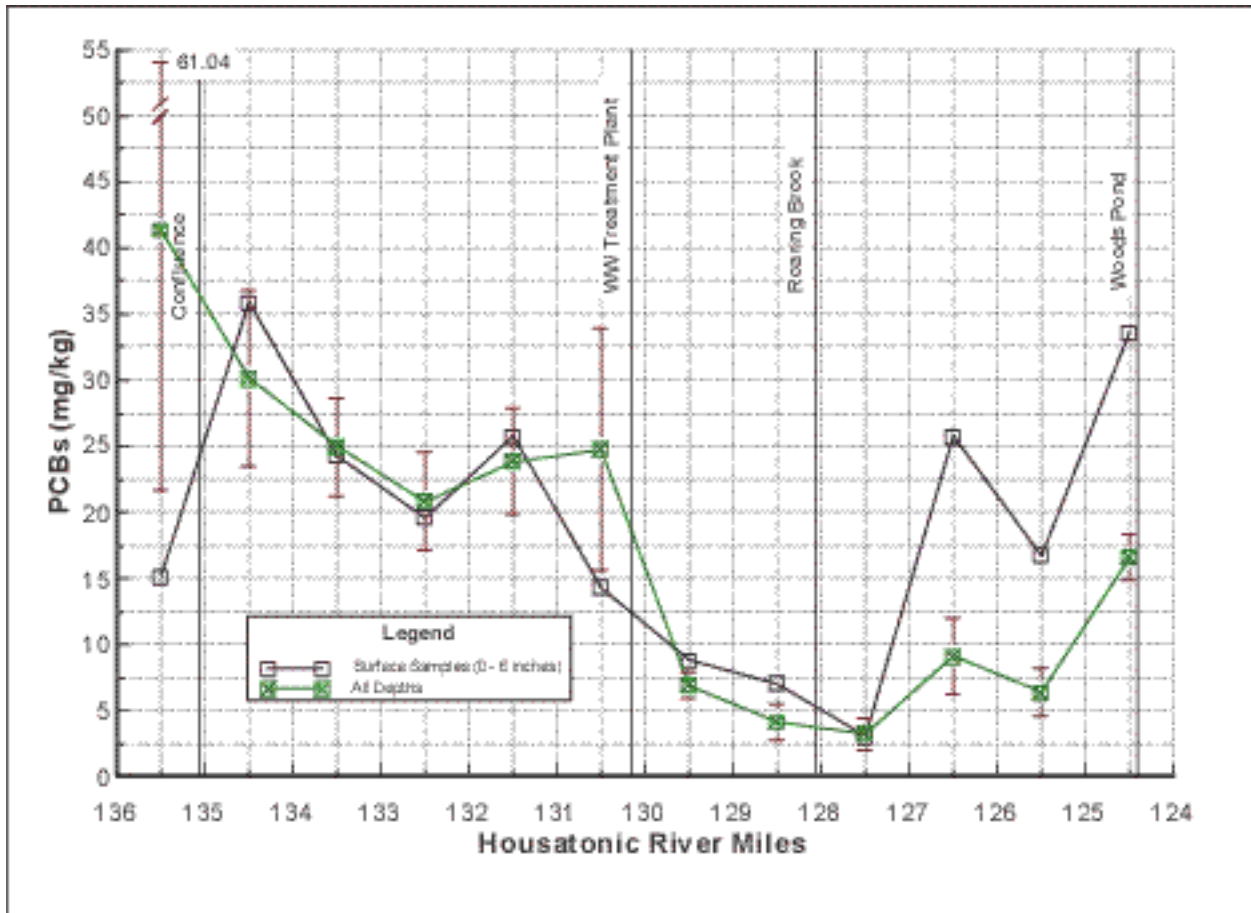
**Figure 3-15 Mean PCB Concentrations in Housatonic River
Sediments Within the PSA**

sand and gravels to fine sands and silts. From just south of Roaring Brook at river mile 127.5 to
Woods Pond 124.4 (Reaches 5c and 6), the mean PCB concentration increases, corresponding to
the change from the fine sands and silts to predominantly silts and clays.

Within Woods Pond, 555 sediment samples at varying depths from 63 sampling locations were
collected for PCB analysis. The distribution of PCBs in the sediment and along the banks
indicates that PCBs are present across the entire lateral extent of Woods Pond. PCBs were
detected in 87% of the locations sampled, with 32% of the locations containing at least one
sample with a PCB concentration above 50 mg/kg (Table 3-10).

The highest concentrations of PCBs (> 50 mg/kg) are consistently detected along the main
channel of the river where it enters the pond, and along a fairly straight pathway to the outlet of

Table 3-10

Statistical Summary of Sediment Data from Woods Pond

Statistics	Results
Number of samples	555
No. of samples with "detects"	287
Percent of "detects"	51.7%
Mean concentration, mg/kg	19.4
Median, mg/kg	0.6
Standard deviation	55.8
Maximum concentration, mg/kg	668
% of samples above 10 mg/kg	23.6%
Percent of samples above 50 mg/kg	11.5%
Number of locations	63
No. of locations with "detects"	55
Percent of locations with "detects"	87.3%
% of locations above 10 mg/kg	60.3%
Percent of locations above 50 mg/kg	31.8%

the pond. Many of the samples (49 out of 63) with concentrations of PCBs greater than 50 mg/kg were collected at or near the sediment surface. In addition, high concentrations of PCBs (> 50 mg/kg) were observed along the slope of the deep hole adjacent to the area where elevated PCB concentrations have been detected along the main channel.

As noted above, the highest concentrations of PCBs are typically observed at or near the sediment surface. PCB concentrations at depth vary laterally across the pond; however, concentrations of PCBs typically fall below 1 mg/kg at between 3 and 4 ft below the sediment surface (Table 3-11). However, PCBs above 1 mg/kg at depths greater than 4 ft have been detected in the southeast quadrant of Woods Pond, in and adjacent to the deep hole.

Wind may affect sediment PCB distribution in Woods Pond via wind-driven transport of floating solids and plant material suspended in the water. This process is suggested by the elevated shoreline sediment PCB concentrations in areas that are not adjacent to submerged sediments with similarly elevated PCB concentrations.

Table 3-11

Mean PCB Concentration by Depth in Woods Pond Sediment Samples

Depths	Mean PCB Concentrations (mg/kg)	n
0 – 0.5	46.38	85
0.5 – 1.0	38.15	47
1.0 – 1.5	20.69	51
1.5 – 2.0	19.41	29
2.0 – 2.5	6.19	24
2.5 – 3.0	9.46	19
3.0 – 3.5	4.36	21
3.5 – 4.0	0.75	13
4.0 – 4.5	0.71	13
4.5 – 5.0	0.48	12
5.0 – 5.5	0.58	10
5.5 – 6.0	14.95	9
6.0 – 6.5	0.26	10
6.5 – 7.0	0.38	8

Summary of PCB Distribution

PCBs are widely distributed in soils and sediments throughout the entire PSA from the confluence to Woods Pond, and across portions of the 10-year floodplain. PCBs have been detected both in surficial sediments and at depths within the sediment up to several feet. The distribution of PCBs by depth indicates that sequestering of PCB-contaminated sediments by more recently deposited cleaner sediments may only be occurring in limited areas in the PSA. Within Woods Pond, the PCB-contaminated sediments are distributed as expected based on likely depositional patterns resulting from decreasing flow velocities. The highest concentrations of PCBs (> 50 ppm) are typically observed in surficial deposits along the line of flow into the pond and where the channel re-emerges at the southwest end of the pond. Concentrations generally decrease with depth in the sediment, with the highest concentrations observed at or near the surface, strongly indicating that sequestering of PCBs has not occurred.

1   The majority of PCB contamination is clearly associated with the main river channel, in
2   particular the bed sediment and associated bars and terraces, and proximate floodplain deposits.
3   However, the presence of PCBs in more distal areas of the 10-year floodplain indicates that
4   transport of PCB-laden sediments has occurred through flooding events. The patterns of PCB
5   distribution in the PSA are consistent with the historical releases upstream of the confluence.

6   In general, PCB concentrations are highest in soils and sediments in the upstream portions of the
7   PSA, decreasing slightly downstream to the Roaring Brook tributary; from that point
8   concentrations in the sediments begin to increase downstream to Woods Pond. This pattern is
9   related to the slower water velocities in this area due to the influence of the Woods Pond Dam.

10 This pattern of PCB distributions illustrates the importance of several processes within the PSA.
11 The transport of PCBs via bedload and suspended solids is an important process that will be
12 included in the modeling study. Resuspension of sediments from the channel bed, banks, and
13 proximal floodplain will also be included in the model, as numerous scours and erosional
14 features have been observed along the entire length of the PSA. As discussed in preceding
15 sections, tributary loading of PCB-containing sediments is excluded as an important process
16 because there is no indication in the data of PCB sources in the tributary watersheds, although it
17 should be noted that contributions are likely from the West Branch. Bed armoring may be
18 important within the upstream portions of the PSA where coarse sands and gravels predominate;
19 this process will be evaluated further. Because of the elevated concentrations of PCBs in the
20 coarser sediments in the upstream portion of the PSA, the explanation of PCB distribution in the
21 upstream reaches of the PSA is complex and is discussed further in Section 3.3.4.3.

22 Effects of wind-driven transport in Woods Pond have been noted and this process will be
23 evaluated further for inclusion in the model. Other processes, such as volatilization and
24 bioturbation, are still being evaluated. Known physical properties of PCBs indicate that
25 volatilization may be an important process to be included in the model, especially for lower
26 chlorinated homologs; volatilization of C_5 homologs is predicted to be about 2.5 times as rapid
27 as volatilization of C_6 homologs and 20 times as rapid as volatilization of C_7 homologs. Life
28 history information for common Housatonic River invertebrates and direct observations of carp
29 feeding and spawning suggest that bioturbation also is important.

1   *3.3.4.3   Organic Carbon and Relationship with PCBs and Grain Size*

2   Approximately 1,200 soil and sediment samples collected from the PSA were analyzed for TOC

3   and grain size distribution in addition to PCB concentrations. Virtually all of the sediment

4   samples were analyzed for TOC, but only 10% of floodplain soils were evaluated due to greater

5   homogeneity in soil type. An additional 66 samples (from two depths: 0 to 0.5 and 1.0 to 1.5 ft

6   below the sediment surface) were fractionated into three grain size groups and subsequently

7   analyzed for PCBs and TOC. These data provide information on the relationship of PCBs to

8   organic carbon and sediment grain size.

9   **Organic Carbon Distribution**

10   TOC in sediments is shown by river mile in Figure 3-16. The mean concentration of TOC

11   remains fairly constant at about 0.8% from the confluence downstream to mile 129/128, where

12   sediment TOC content begins to rise rapidly. From mile 129/128 the mean TOC increases to

13   4.5% at Woods Pond. This increase in sediment organic carbon beginning at mile 129/128

14   corresponds to the break between Reach 5b and to Reach 5c, the same location where an increase

15   in both fine-grained sediments and PCB concentrations was observed.

16
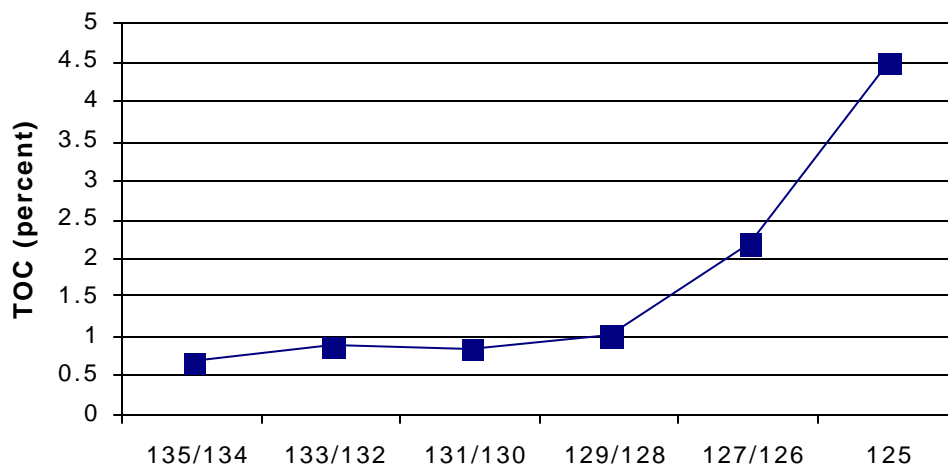
17   **Figure 3-16 Mean Sediment TOC Concentration by River Mile**

18   TOC-normalized PCB concentrations by river mile are shown in Figure 3-17. TOC-normalized

19   PCB concentrations decrease from the confluence downstream to Roaring Brook, then remain

20   relatively constant throughout Reach 5c. The elevated TOC-normalized PCB concentrations in

1 the upstream portion of the PSA (Reach 5a) correspond to that portion of the river where

2 absolute PCB concentrations are elevated and organic carbon concentrations are low, and where

3 the sediment is dominated by larger grain-size class. In downstream reaches of the river this

4 pattern reverses; TOC-normalized PCB concentrations are lower and the dominant grain size

5 class is the finer silts and clays. This evaluation suggests that sediment PCB concentrations in

6 the upstream portion of the PSA are not in equilibrium with sediment TOC, nor are the PCB

7 concentrations controlled by grain size. In the downstream portion of the river, sediment PCB

8 concentrations can be better explained by the conventional theories associated with adsorption to

9 organic carbon and fine-grained material.

10 **TOC/PCB/Grain Size Relationship**

11 To further evaluate the relationship between PCB, TOC, and grain size, correlation coefficients

12 were calculated by river mile for each possible pairing of these parameters. The results, shown

13 in Figure 3-18, indicate that the relationship between these three parameters increases

14 downstream in the PSA, particularly downstream of mile 129/128 at Roaring Brook. The

15 correlations in the upper reach are actually negative. The change in correlations at mile 129/128

16 understandably corresponds to the same pattern observed in the individual parameters discussed

17 above. However, the correlations that were observed for PCBs versus TOC, and PCBs versus %

18 fines are generally very weak. This lack of strong positive correlation suggests that PCB

19 distribution cannot be explained by partitioning to organic carbon or fine-grained sediments in

20 the upstream sediments of the PSA. The increasing correlation of PCBs with TOC and % fines

21 in the downstream reaches of the PSA may support the interpretation that PCBs are sorbed to

22 either organic carbon or fines in that area. However, even in these reaches, the correlation is still

23 poor ($r < 0.5$).

24 For the fractionated sediment samples (66 samples, 33 from each of two depths), PCB and TOC

25 concentrations have similar patterns of variation across the three grain size fractions
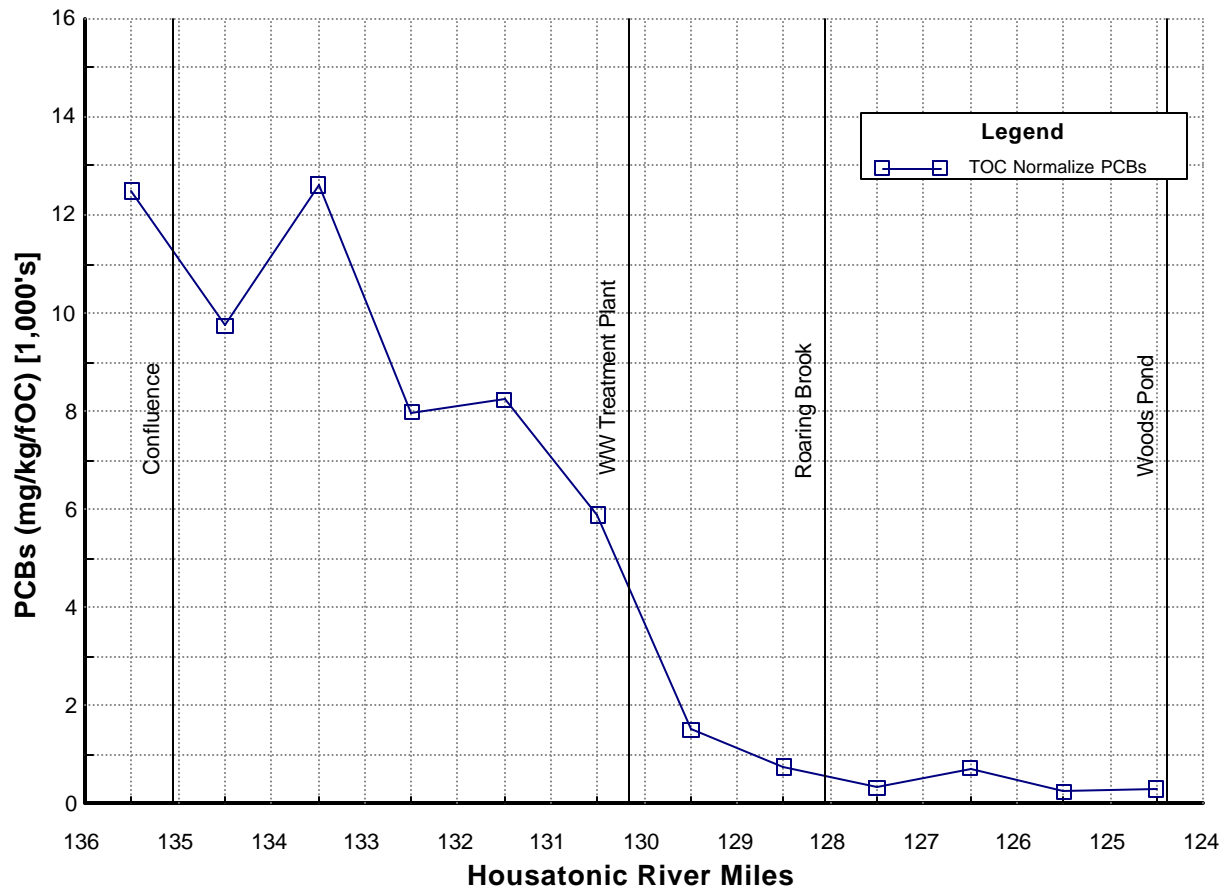
Figure 3-17 TOC-Normalized PCB Concentrations by River Mile
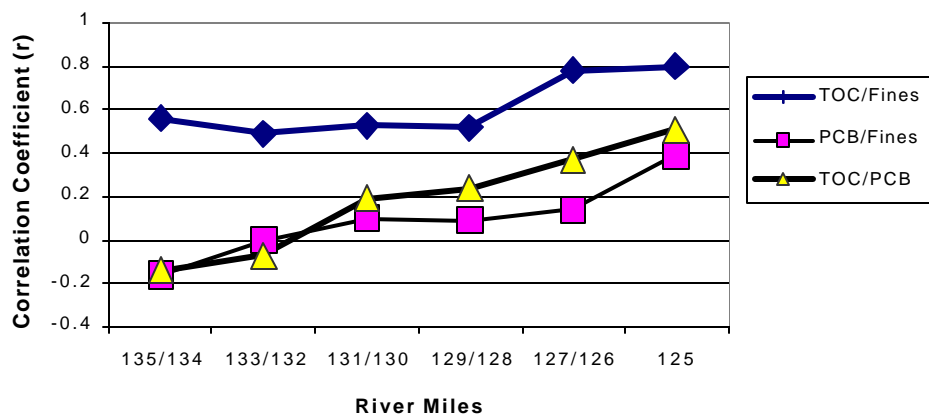
Figure 3-18 TOC/PCB/Grain Size Correlations by River Mile

1   (Figure 3-19) and, as would be expected, the highest concentrations of TOC and PCB are in the

2   fine fraction ($< 63\mu m$). However, when the total mass of PCBs is plotted by grain size fraction

3   (Figure 3-20), the greatest mass of PCBs (more than 80%) is associated with the coarser fractions

4   ($> 250\mu m$). This pattern of greater PCB mass in the coarse grain size classes is observed in both

5   the surficial samples as well as in the deeper sediments. This supports the previous observations

6   that suggest the majority of PCBs in the river system are not strongly associated with or sorbed

7   to either TOC or the smallest grain size class. The increasing correlation among these three

8   parameters with increasing distance from the confluence to Woods Pond may indicate that the

9   PCBs are achieving equilibrium with organic carbon and fine-grained sediments in the more

10 downstream areas of the PSA.

11 These data support the need to model bedload movement as an important process within the

12 PSA, and indicate that a third phase (in addition to a dissolved and/or sorbed phase) of PCBs,

13 either as a coating on individual grains or as aggregated particulate (or some other form), may

14 exist. Further evaluation of this issue is ongoing.

15 **Partition Coefficients**

16 Partition coefficients for PCBs in surface water and pore water within the Housatonic River have

17 been calculated for the samples with available data. Table 3-12 presents these calculations and

18 coefficients.

19 These data indicate that partitioning of PCBs in surface water appears to be within accepted

20 ranges (K_ds of 10^5 to 10^7 for surface water samples). However, for pore water samples, the K_ds

21 are much lower (10^2 to 10^3), which also supports the possibility of a third-phase PCB component

22 present in the river channel sediments. The determination of the presence and nature of this free-

23 phase material is critical to understanding PCB transport and to defining the processes and

24 associated formulations of the modeling study. However, the explanation may be beyond current

25 theory and analytical technique, posing challenges in deriving a mechanistic process to represent

26 this phenomenon in the modeling study.
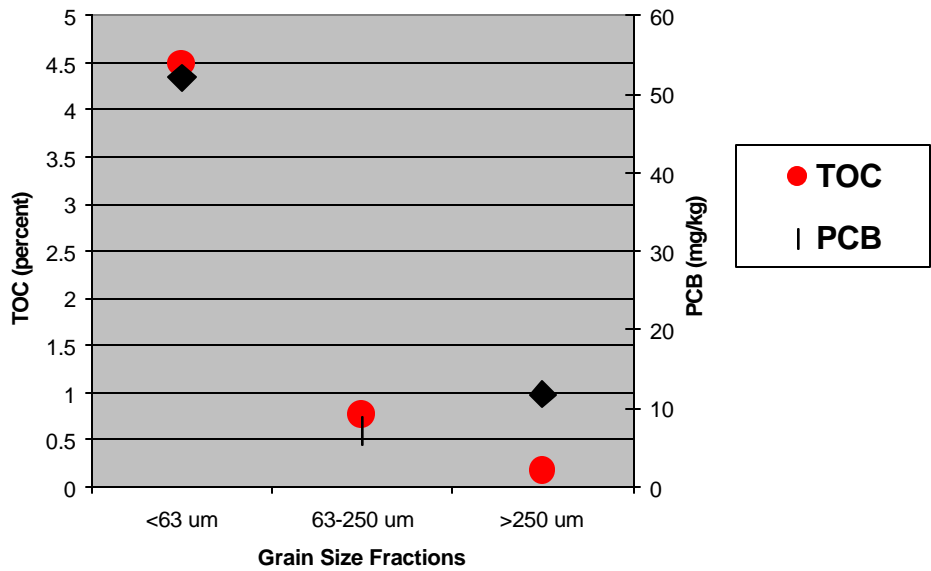
Figure 3-19 TOC/PCB Relationships by Grain Size
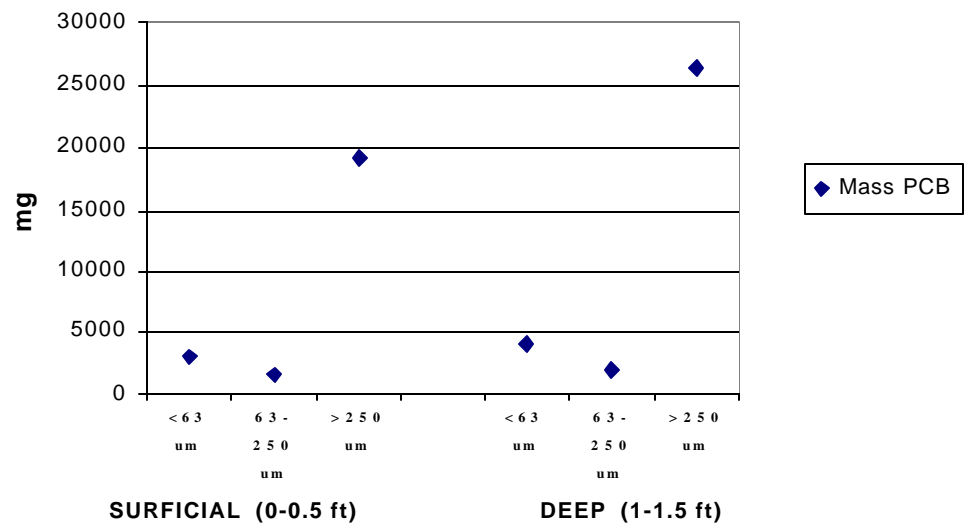
Figure 3-20 PCB Mass by Grain Size

Table 3-12

Partition Coefficients from Samples within the Housatonic PSA

Sample	River Miles	tPCB	dPCB	pPCB	TSS	PCB/kgp	Kd SW	Kd PW
H5-SW000001-0-8D17	124	0.018	0.017	0.001	1.8	555.56	3.27E+04	
SE000771	126							7.5E+02
H3-SE001024	126							1.76E+02
H3-SE000772	126							6.1E+02
H3-SE001025	127							8.2E+02
H3-SE001026	128							4.0E+02
H3-SE001027	129							7.18E+02
H3-SE001048	130							1.67E+03
H3-SE000773	131							7.5E+03
H3-SW000017-0-8N23	131	0.034	0.015	0.019	1.3	14615.38	9.74E+05	
H3-SE001049	131							2.37E+03
H3-SE001050	132							3.81E+03
H3-SE000774	133							3.7E+03
HW-SE000775	135							3.0E+03
H2-SW000009-0-8N24	136	0.051	0.034	0.017	2.8	6071.43	1.79E+05	
H2-SW000008-0-8N24	136	0.060	0.016	0.044	3.4	12941.18	8.09E+05	
H1-SW000010-0-8N24	137	0.800	0.014	0.786	2.3	341739.13	2.44E+07	
H0-SW000014-0-8C27	139	0.470	0.028	0.442	11.7	37777.78	1.35E+06	
H0-SW000014-0-9G31	139	0.360	0.072	0.288	7.8	36923.08	5.13E+05	
H0-SW000014-0-9S29	139	2.900	0.083	2.817	3.1	908709.68	1.09E+07	
H0-SW000014-0-9Y27	139	0.220	0.064	0.156	4.1	38048.78	5.95E+05	

Notes:

tPCB = total PCB (μg/L).
dPCB = dissolved PCB (μg/L).
pPCB = particulate PCB (μg/L).
TSS = total suspended solids (mg/L).
PCB/kgp = PCB concentration on suspended sediments (μg/kg).
Kd SW = PCB partition coefficient in water column.
Kd PW = PCB partition coefficient in sediment.

3.3.4.4 PCBs in Surface Waters/Stormwater

PCB fate and transport within the water column is controlled by substantially the same chemical, physical, and biological factors that control PCB fate and transport in sediments. The evaluation of available data indicates that the important processes for consideration within surface waters of the PSA are:

- Diffusion
- Advection
- Sorption/desorption
- Dechlorination

Surface water in the Housatonic River transports any PCBs entering the system from upstream sources. In addition, the river will transport and redistribute resuspended PCBs, based upon the site and river conditions. During higher flows, the principal source of PCBs in the water column is from resuspended sediments, from both upstream and within the PSA. During lower flow conditions, PCB-contaminated sediments act as the primary source of PCBs through the processes of diffusion and groundwater advection through PCB-contaminated sediment and associated pore water.

Surface water sampling was conducted on 15 occasions between August 1998 and September 1999 at 17 locations, both within the PSA (seven locations) as well as above and below the PSA (Figure 3-3). Samples were analyzed for PCBs (total and dissolved), suspended solids (total and dissolved), and organic carbon (total and dissolved), as well as for other parameters (e.g., BOD and nutrients).

PCBs were detected in all surface water sampling locations within the PSA. Plots of two sampling events for PCBs by station location are shown in Figures 3-21 and 3-22. These plots also show the total suspended solids concentrations at each sampling location.

Concentrations of PCBs in surface water were generally less than 0.2 µg/L; however, more than half of the samples contained PCBs above the chronic ambient water quality criterion (cAWQC) for protection of aquatic life of 0.014 µg/L. The maximum detected PCB concentration was at a location upstream of the PSA, at Unkamet Brook, located within the northern boundary of the

Key

	Detected	Nondetected
PCB	●	○
Dissolved PCB	■	□
TSS	▲	△

Total PCB (ug/L)

Total Suspended Solids (mg/L)

	Crane Paper Co.	Hubbard Ave. Bridge	Unkamet Brook	Newell Street Bridge	Newell Street Parking	Lyman Street Bridge	Elm Street Bridge	Pomeroy Ave. Bridge	West Branch	Holmes Road Bridge	Joseph Drive	WWTP	New Lenox Road	Woods Pond Hdwtr	Woods Pond	Lenoxdale Bridge
PCB	0.013	0.013	0.209	0.013	0.054	0.071	0.045	0.015	0.012	0.03	0.039		0.04	0.055	0.5	
Dissolved PCB											0.26					
TSS	3.5	2.6	6.2	2.9	3.5	5.7	5	8.2	2.4	0.8	1.6		2.2	2.7	5	

00P-1980-1

Figure 3-21 PCB and TSS Concentrations at Surface Water Sampling Locations, 3 August 1998
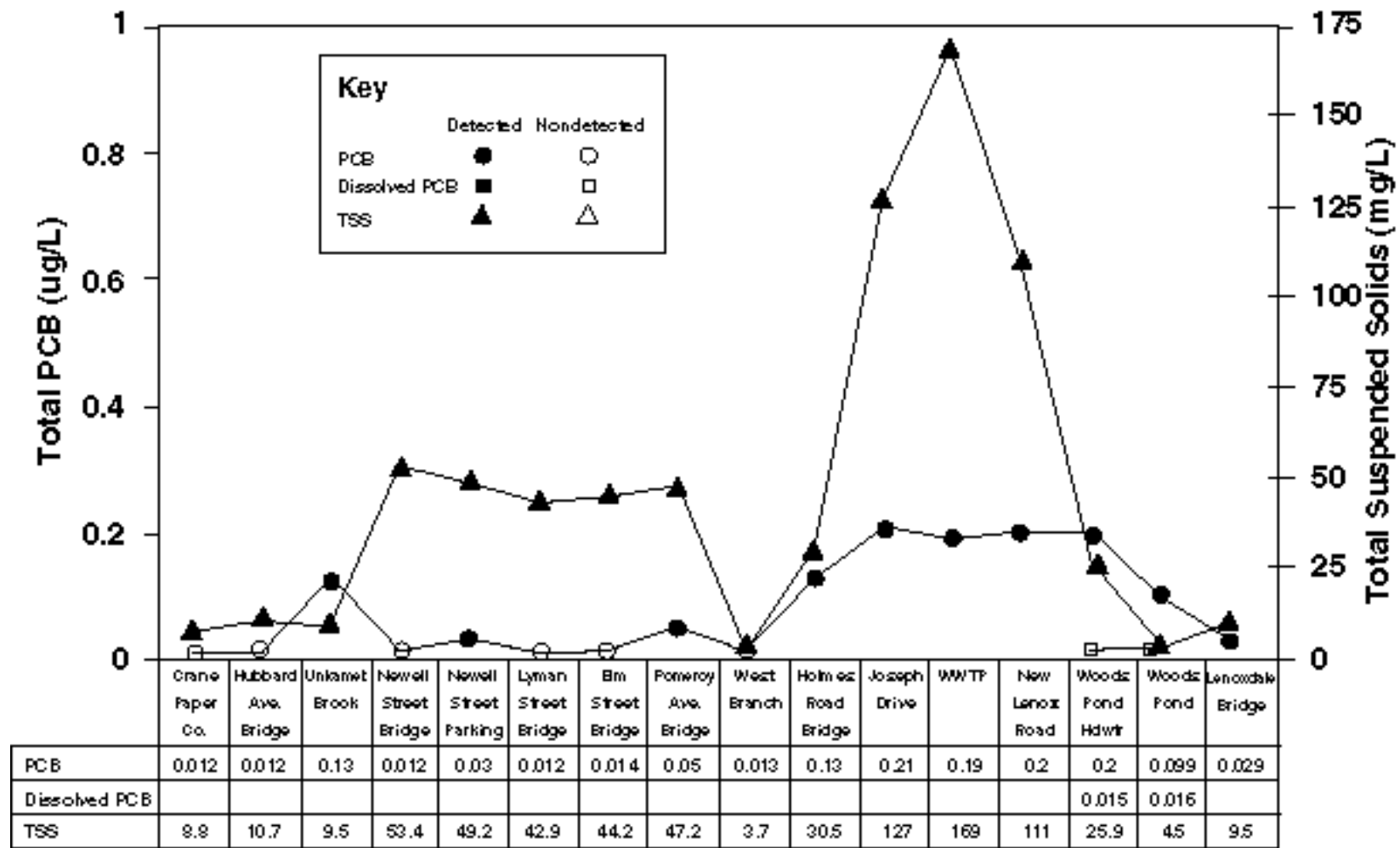
Figure 3-22 PCB and TSS Concentrations at Surface Water Sampling Locations, 22 March 1999

	Crane Paper Co.	Hubbard Ave. Bridge	Unkamet Brook	Newell Street Bridge	Newell Street Parking	Lyman Street Bridge	Elm Street Bridge	Pomeroy Ave. Bridge	West Branch	Holmes Road Bridge	Joseph Drive	WWTP	New Lenox Road	Woods Pond Hdwr	Woods Pond	Lenoxdale Bridge
PCB	0.012	0.012	0.13	0.012	0.03	0.012	0.014	0.05	0.013	0.13	0.21	0.19	0.2	0.2	0.099	0.029
Dissolved PCB														0.015	0.016	
TSS	9.8	10.7	9.5	53.4	49.2	42.9	44.2	47.2	3.7	30.5	127	169	111	25.9	4.5	9.5

00P-1980-2

1   GE facility and flowing through the site of a former landfill, an area identified in the Consent
2   Decree for future remediation.

3   TSS concentrations were generally less than 10 mg/L, except when influenced by high-flow
4   conditions resulting from storm/precipitation events. This is evident in the second of the two
5   figures (Figure 3-22), where the TSS concentration increased by an order of magnitude.
6   Correspondingly, the PCB concentrations increased within the PSA, suggesting either
7   resuspension of sediment from the channel bed or erosion of the channel sidewalls.

8   As noted in Section 3.3.1.3 (Climate, Rainfall, and Flow Data), 10 storm events were monitored
9   during 1999. Seven of these events were monitored for PCBs and TSS to determine the effect
10   storms and associated rainfall and runoff would have on suspended loads, PCB concentrations,
11   and resuspension of bed and channel sidewall materials. TSS was monitored hourly throughout
12   the storm events, whereas PCBs were analyzed at selected intervals.

13   A plot of the data for one of these storm events (August 1999) is presented in Figure 3-23. This
14   plot is for data collected from the river at New Lenox Road, at the approximate midpoint of the
15   PSA. As shown in the figure, TSS is closely correlated with stage height.
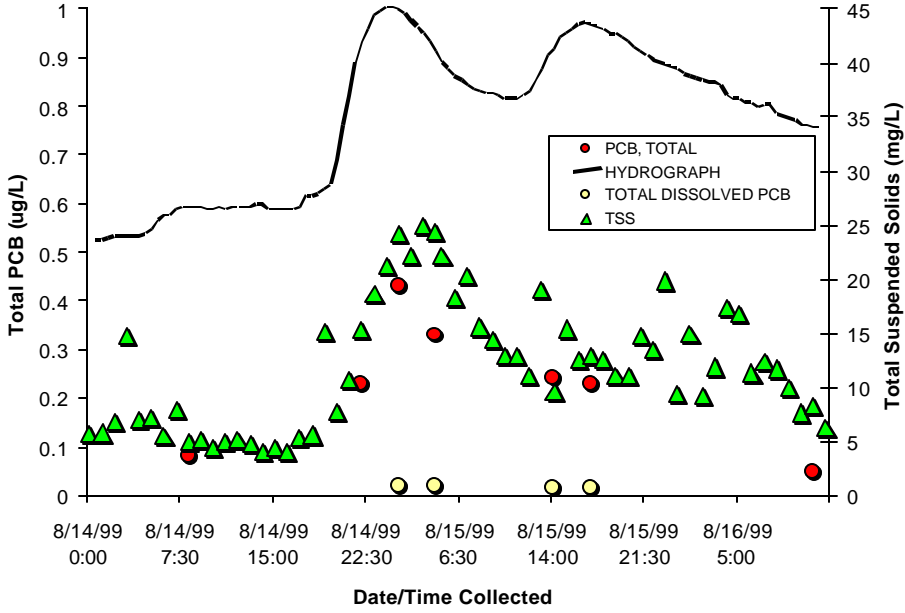
16
17   **Figure 3-23 Storm Event Data, August 1999**

1 Similarly, PCBs detected in samples during the same event increased correspondingly with TSS
2 and stage height. For this storm event, four samples were analyzed for dissolved PCBs; none
3 were detected, indicating that the elevated PCBs are associated with the particulate fraction.
4 This pattern of increased total PCBs with an increase in TSS is observed throughout most of the
5 storm events. This pattern was typical for all storm events sampled.

6 The generally low concentrations of PCBs detected in water samples during nonstorm events
7 (base flow) and the increased concentrations during storm events indicate that PCBs are being
8 mobilized with the suspended load as a result of high flows associated with storm events.
9 Increased TSS loads during storm events demonstrate that erosion and resuspension of bed
10 sediments and channel sidewall material is occurring. These are important processes that will be
11 included in the model.

12 These storm data show that PCBs are primarily associated with the particulates as opposed to
13 being dissolved in the water column, indicating the importance of the sorption/desorption
14 partitioning process for the model. Of the storm events monitored during 1999, the majority of
15 the suspended load consisted of silts and clays, except for material collected during the largest
16 storm event monitored, where up to 71% of the suspended load consisted of noncohesive
17 materials. It is believed that the increased coarser material observed in this larger storm event
18 represents capture of bedload sediments.   Further evaluation of these data and the
19 interrelationships of the sediment grain size/PCB/TOC data are being conducted.

20 ### 3.3.4.5   PCB Congeners and Homologs

21 All surface water samples, all samples collected at primary storm water locations, and
22 approximately 10% of all soil and sediment samples from within the PSA were analyzed for
23 PCB congeners and homologs. The laboratory analysis has been completed, but the data are
24 undergoing validation and evaluation at this time, and therefore are not discussed here.   Of
25 particular importance will be whether dechlorination is occurring and should be included in the
26 model. As these data are thoroughly evaluated, any relevant processes will be revisited and
27 discussed in the model calibration report.

3.3.5 Biota

This section provides a synthesis of the data and theory used to develop the conceptual model for the aquatic biological components of the Housatonic River. The domain for the model, the PSA, ranges from the confluence of the East and West Branches of the Housatonic River to Woods Pond. The floodplain biota are not a part of the modeling study; therefore, that aspect of the ecosystem is not described here. Section 3.3.5.1 provides a description of the key biological compartments in the river; these compartments are used to provide a simplified representation of the complex aquatic food web (Figure 3-24). Site-specific data are presented to demonstrate how the compartments shown in Figure 3-24 apply to the Housatonic River (e.g., species distributions and abundance/biomass across the study area). Section 3.3.5.2 provides a discussion of the biological processes that may govern PCB fate in aquatic biota, and site-specific data are used to determine which processes are important for quantitative consideration in the PCB fate modeling in biota.

3.3.5.1 Description of Housatonic Aquatic Food Web

Nutrients and other chemicals (such as PCBs) are in a constant state of flux within freshwater systems, creating a dynamic interaction among the various compartments of the ecosystem. The fate of PCBs in the environment is strongly influenced by the structure of the food web and bioaccumulation processes that control the circulation of energy and materials within an ecosystem. There are two broad categories within the food web: the grazing web, which begins with green plants, algae, or photosynthesizing plankton; and the detrital web, which begins with organic debris. In the grazing web, materials typically pass from plants to herbivores to carnivores. In the detrital web, materials pass from plant and animal matter to decomposers (bacteria and fungi), then to detritivores, and finally to carnivores. Both plankton and detritus may occupy important positions in the base of the Housatonic River food web, influencing the extent to which PCBs and related chemicals bioaccumulate in the upper trophic level biota.

The following section provides a brief characterization of the ecology of the study area that will influence species composition and the associated food web and specific biotic components found in the aquatic system.
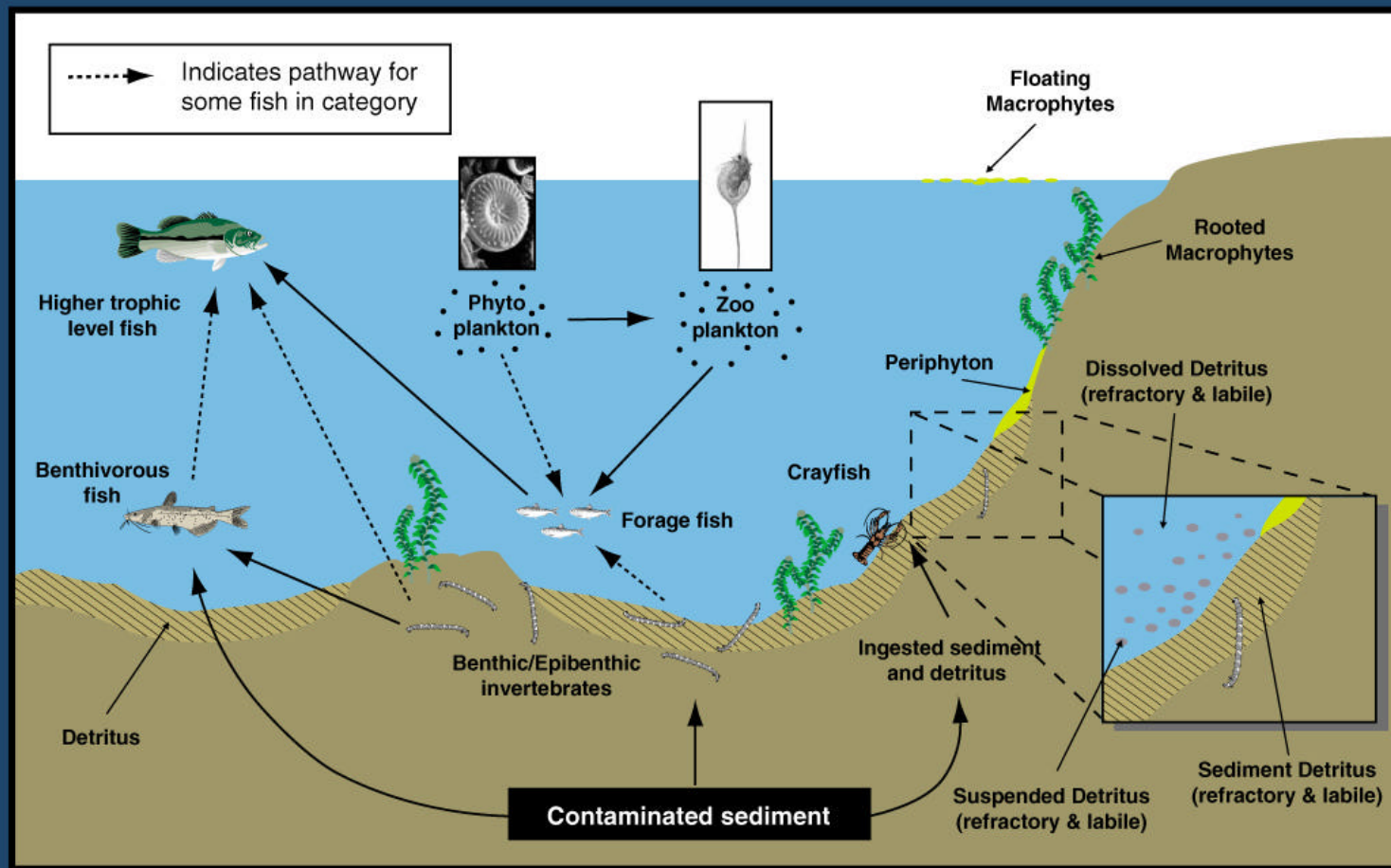
Figure 3-24 Conceptual Model of Housatonic River Aquatic Community

General Habitat Description

Several habitat types are common in the PSA, including floodplain forests, shrub swamps, emergent marsh, and low gradient stream (TechLaw, 1999). The composition of the habitat types in and adjacent to the river gradually changes moving downstream. Generally the extent of floodplain wetland increases, as does the amount of open water and emergent marsh. The characteristics of the river change as well. The low-gradient stream community upstream of the wastewater treatment plant (WWTP) (Reach 5a) is shallower, has faster current, a significant amount of large woody debris, coarser bed materials (i.e., more sands and gravels), more riffles, and fewer pools. These features provide habitat for a similar fish community as found downstream, although the occurrence of particular species and the abundance of others differ. White suckers and fallfish are more common here than downstream, and largemouth bass, pumpkinseed, and bluegill sunfish are less common. In addition, the occasional smallmouth bass and salmonid are found in this section of the river, but not downstream. There are similar patterns in invertebrates, macrophytes, and algae communities; the same species occur, but in different densities.

Downstream of the WWTP (Reach 5b), average flows decrease, and the dominant morphological characteristics of the river change as well. The frequency of large, deep pools and runs increases, riffle habitat decreases, and the dominant bed material becomes finer. Macrophyte abundance increases in shallower portions of the streambed and provides more cover for juvenile fish than found upstream. The abundance of yellow perch and sunfish increases, and fallfish and white suckers decrease. There is a shift in the invertebrate community as well; species that prefer finer sediment and slower flows (e.g., chironomids) become more common, and filter-feeding caddisflies are less common. Similar to areas upstream, large woody debris is still common and influences river morphology and fish habitat by helping to create scour pools, and providing cover for both predators (i.e., largemouth bass) and prey (i.e., centrarchids and cyprinids).

In Reach 5c of the PSA, the riparian zone widens. The topography is primarily flat, and in conjunction with the effect of the Woods Pond Dam, results in large areas of open water and emergent marsh. Floodplain forests dominate the western portion of this reach.

1   Woods Pond (Reach 6) is the downstream end of the PSA and functions as a sedimentation basin

2   (HEC, 1996; Stewart Laboratories, 1982). It has a maximum depth of 16 ft but is mostly 1 to 3 ft

3   deep. Shallow areas of the pond contain dense macrophyte beds and algal mats, which are most

4   common in the late summer. Canada waterweed (*Elodea canadensis*), a water milfoil

5   (*Myriophyllum spicatum*), and curly pondweed (*Potamogeton crispus*) are the most common

6   macrophytes. Overhanging vegetation, woody debris, rock piles, and submerged macrophytes

7   continue to provide structural diversity to the river habitat. Because of the lower flow velocities,

8   the dominant sediments are primarily silts, with a high percentage of organic matter. Common

9   fish in this reach include yellow perch, sunfish, largemouth bass, brown bullhead, common carp,

10   and goldfish.

11   The following section describes the major biotic compartments found in the aquatic system:

12   algae, macrophytes, invertebrates, fish, and detritus.

13   **Algae**

14   Algae are autotrophic, single-celled organisms that can be found in either the water column

15   (phytoplankton) or on bottom substrates such as sediments and rock (periphyton). As primary

16   producers, algae contribute a significant portion of the energy flow through the food web. Algae

17   are classified into the following taxonomic orders: Chlorophyta (green algae); Chrysophyta,

18   (diatoms and yellow-green algae); Cyanophyta (blue-green algae or cyanobacteria);

19   Euglenophyta; and Cryptophyta. Within each of these taxonomic groups, there are algae that

20   represent either phytoplankton or periphyton. The primary consumers of green algae, blue-green

21   algae, and diatoms are zooplankton and planktivorous fish.

22   Blue-green algae are primary producers that have the ability to fix nitrogen from the atmosphere

23   into ammonia, which is then incorporated into amino acids. Nitrogen fixation can represent a

24   significant amount of nitrogen input to an ecosystem. Blue-green algae contain gas vesicles that

25   allow the cells to float and clump together, creating a scum on the water surface and providing a

26   food source for fish, zooplankton, and waterfowl. Blue-green algae can reduce efficiency in

27   predator-prey food chains because the filamentous nature of the algae precludes effective grazing

28   by filter-feeding zooplankton, and at high densities, blue-green algae are directly toxic to

1 zooplankton, fish, and mammals, and have been shown to suppress zooplankton populations.
2 Blue-green algae generally dominate in the late summer or when eutrophication increases algal
3 biomass and phosphorus content. When green algae and diatoms are more prevalent, a low-light
4 and low-CO_2 environment is created and blue-green algae thrive (Welch, 1992).

5 Green algae are found mostly in freshwater ecosystems; 90% of species are found in freshwater
6 systems and 10% in marine systems (Lee, 1989). This group of algae is large and diverse, and
7 many species have a cosmopolitan distribution; few species are endemic to a single area. They
8 contribute to grazing food chains as well as detritus food webs, and form an important basis of
9 aquatic systems.

10 Diatoms represent another group of algae and comprise a significant portion of the freshwater
11 flora. They may occur as plankton or periphyton. Diatoms have silicified cell walls, and both
12 unicellular and colonial forms are common. Similar to other algae, many planktonic diatoms
13 have regular annual fluctuations in growth that can be attributed to environmental conditions
14 such as light, temperature, and nutrients. Both planktonic and periphyton forms provide a high-
15 energy food source for herbivores, functioning as an essential base to the food web.

16 Periphyton in aquatic habitats is generally dominated by diatom species. However, when
17 inorganic nutrients are high, filamentous green algae can occur in swifter rivers, or blue-green
18 algae in more stagnant waters (Welch, 1992).

19 Figure 3-25 presents the chlorophyll-a concentrations in surface water for a sampling location
20 just above Woods Pond. Chlorophyll-a can be used as an index of primary production in the
21 water column to which algae is a major contributor. The figure illustrates the strong seasonal
22 trend in chlorophyll-a. In both 1998 and 1999, the maximum concentrations were in late
23 summer (August) during the period of major algal mat coverage; minimum concentrations were
24 observed during the winter months. The marked seasonality suggests that consideration of
25 temporal aspects of algae production is important in the Housatonic River. Temporal variations
26 may be attributed to changes in light, temperature, and nutrients.
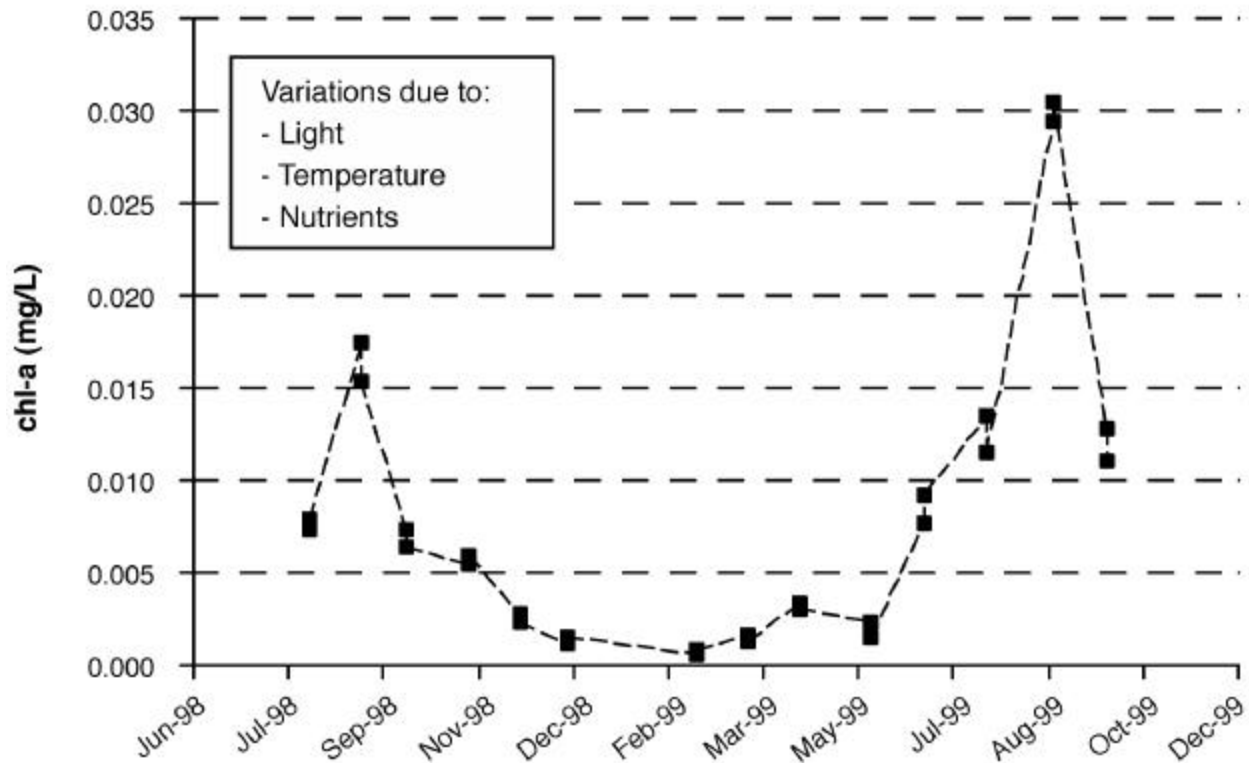
**Figure 3-25 Chlorophyll-a Concentrations in Surface Water
Above Woods Pond Dam (Station H4-SW000002)**

Figure 3-26 presents the average chlorophyll-a concentrations for the same time period, but includes stations located throughout the PSA. From the graph, it is apparent that the summer peaks in primary production are associated with the downstream portions of the study area (i.e., Reach 5c and Woods Pond). The faster-flowing upper reaches of the river exhibit relatively low seasonal variability. This suggests that consideration of temporal variation in primary production increases in importance moving downstream toward Woods Pond. This pattern is reinforced by data presented in Figure 3-27, which shows the geographical pattern in chlorophyll-a during the August 1999 sampling event. Primary production was relatively constant between the confluence of the East and West Branches and Reach 5b of the Housatonic, but increased rapidly in Reach 5c and Woods Pond.

Macrophytes

Submerged aquatic vegetation or macrophytes are an important food web component in many aquatic ecosystems. Macrophytes represent the highest level of organization of plants in aquatic
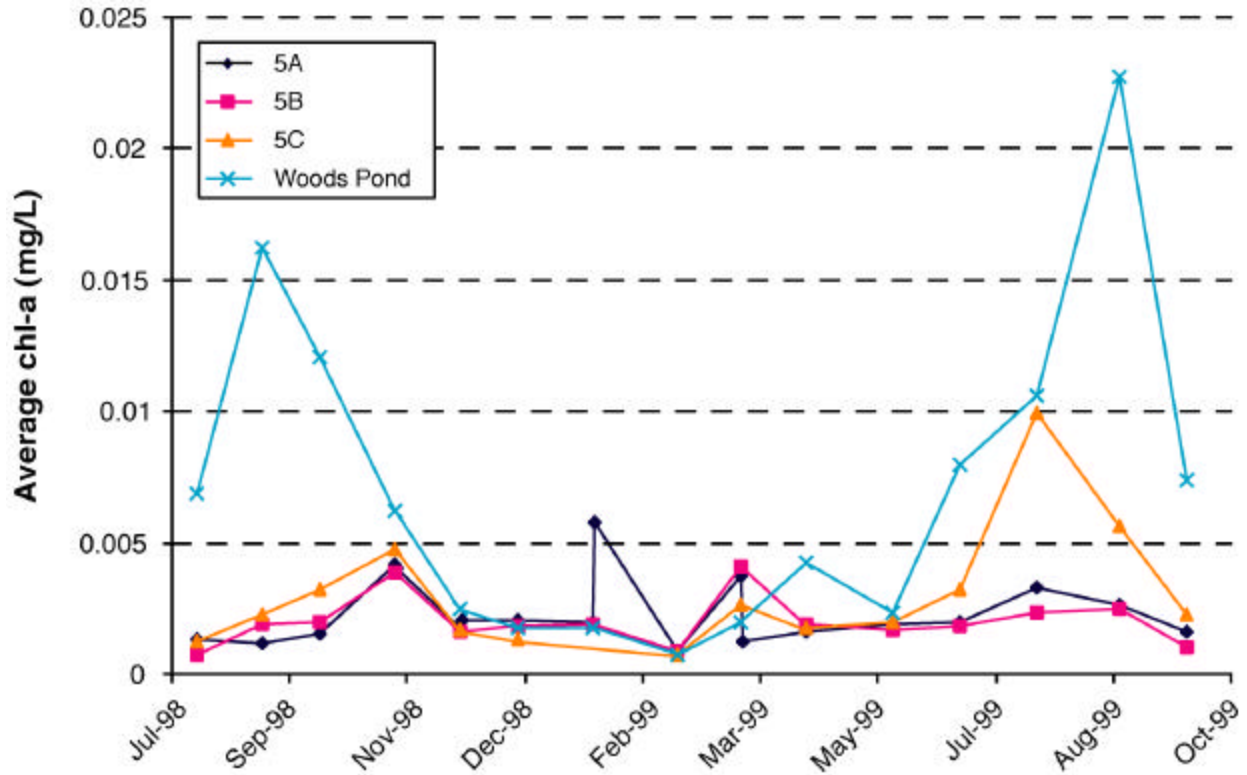
Figure 3-26 Average Chlorophyll-a Concentrations in Surface Water by Reach
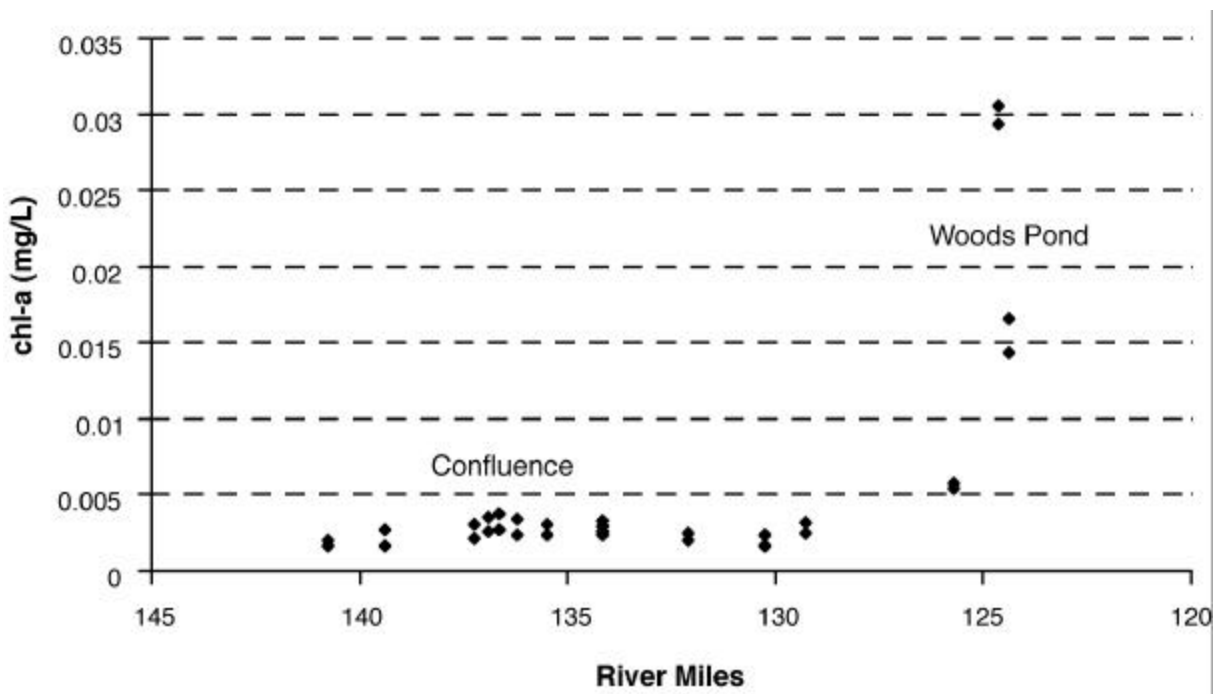
Figure 3-27 Chlorophyll-a Concentrations in Surface Water by River Mile During August 1999 Sampling

1 environments, are usually rooted, and have rigid cell walls. Submerged macrophytes are
2 common in slow-moving or stagnant reaches of rivers. The roles that macrophytes play in
3 aquatic systems include a food source; substrate for invertebrates, algae, and other biota; and
4 cover for fish, reptiles, and amphibians. Macrophytes are widely distributed in the PSA but may
5 not contribute significantly to primary productivity in the upper portion of the study area due to
6 unfavorable habitat conditions. This is being evaluated in the estimation of biomass currently
7 being performed. Macrophytes and filamentous algae can accumulate contaminants from the
8 aquatic environment and potentially transfer those contaminants to organisms that feed on them
9 (Gobas et al., 1991).

10 Macrophytes observed in the river included curly pondweed, common waterweed, European
11 water milfoil, lesser duckweed, greater duckweed, hornwort, and yellow water-lily (WESTON,
12 2000a). Shoreline portions of low-gradient stream communities contain false nutsedge (*Cyperus*
13 *strigosus*), smooth creeping love-grass (*Eragrostis hypnoides*), tufted love-grass (*Eragrostis*
14 *pectinacea*), false pimpernel (*Lindernia dubia*), ditch stonecrop (*Penthorum sedoides*), and
15 water-pepper (*Persicaria hydropiper*) (TechLaw, 1999). Slow, shallow stretches of the river are
16 dominated by Canada waterweed (*Elodea canadensis*), water milfoil (*Myriophyllum* cf.
17 *spicatum*), curly pondweed (*Potamogeton crispus*), prickly hornwort (*Ceratophyllum*
18 *echinatum*), ribbonleaf pondweed (*Potamogeton epihydrus*), and flatstem pondweed
19 (*P. zosteriformis*).

20 **Invertebrates**

21 Invertebrates in aquatic systems are diverse and fill a variety of trophic niches such as grazers,
22 detrital feeders, and predators. Aquatic invertebrates process and use energy entering aquatic
23 systems from either periphyton production or from allochthonous sources (i.e., leaves, needles,
24 and other particulate matter from the terrestrial ecosystem). The composition of freshwater
25 benthic communities depends in part on the sediment grain size. Data from two studies of the
26 benthic communities of the Housatonic River are discussed: Chadwick & Associates (1994)
27 examined the benthic communities associated with coarse-grained sediments or sediments found
28 in the fast-flowing sections of the river; the EPA data (WESTON, 2000a) represent samples
29 collected in soft sediments. These two data sets can be evaluated to gain a greater understanding

1 of the range of benthic invertebrates found throughout the river. Table 3-13 identifies the taxa of
2 the most common benthic organisms that were identified.

3 Insects often dominate freshwater macroinvertebrate communities. They composed 50% of the
4 invertebrates found in coarse-grained sediments throughout the study area (Chadwick &
5 Associates, 1994). The highest density of organisms was represented by dipterans (Chadwick &
6 Associates, 1994); however, the sampling methods used emphasized hard-bottom habitats.
7 When soft-bottom sampling techniques were applied (WESTON, 2000a), different results were
8 obtained, as expected. Specifically, in sediment grabs, dipterans were a small percentage of
9 invertebrate biomass throughout the PSA. The majority of invertebrate biomass in samples from
10 Reaches 5a and 5b was attributable to bivalves and gastropods. In Reaches 5c and Woods
11 Ponds, bivalves and gastropods were also major contributors to invertebrate biomass; however,
12 dragonfly larvae (Odonata), leeches, and other insects also contributed substantially to biomass.

13 The feeding strategies of macroinvertebrates, based on conventional categories, include large-
14 particle detritivores (shredders), small-particle detritivores (collectors and selectors), grazers
15 (periphyton scrapers), and predators. For the conceptual model, four main categories of
16 invertebrates were defined on the basis of their life history (benthic versus water column feeding
17 strategy). Life history characteristics have been demonstrated to be important for representing
18 PCB bioaccumulation in some systems (Morrison et al., 1996). The four groups are:

19   ▪ Filter/Gatherer—Benthic organism that gathers fine suspended matter from the water
20   column or collects detritus from the sediment surface.

21   ▪ Shredder/Grazer—Benthic organism that shreds or chews large particulate detritus or
22   live plants, or scrapes plants and algae from rocks and surfaces of debris.

23   ▪ Predator—Benthic organism that consumes live prey.

24   ▪ Zooplankton—Microscopic animals in the water column that may be herbivorous or
25   predatory.

Table 3-13

Classification of Key Taxa in the Housatonic River Aquatic Ecosystem

Phylum	Class	Order	Common Name
Annelida	Oligochaeta		Segmented worms
Arthropoda	Insecta	Collembola	Springtails
Arthropoda	Insecta	Coleoptera	Beetles
Arthropoda	Insecta	Diptera	True flies
Arthropoda	Insecta	Ephemeroptera	Mayflies
Arthropoda	Insecta	Hemiptera	True bugs
Arthropoda	Insecta	Lepidoptera	Aquatic moths
Arthropoda	Insecta	Odonata	Dragonflies
Arthropoda	Insecta	Plecoptera	Stoneflies
Arthropoda	Insecta	Trichoptera	Caddisflies
Arthropoda	Malacostraca	Amphipoda	Sideswimmers
Arthropoda	Malacostraca	Decapoda	Crayfish
Mollusca	Gastropoda		Snails
Mollusca	Pelecypoda		Clams
Nematoda			Non-segmented worms
Platyhelminthes	Turbellaria		Flatworms

4   Sources: Exponent, 1998; ITIS; 2000.

1　Table 3-14 lists typical species found in the Housatonic River classified into the four categories

2　described above. However, different species in the same taxonomic group often have different

3　feeding methods, and exceptions to these categorizations can be found.

4　**Table 3-14**

5

6　**Examples of Invertebrate Species for Each Category**

Filter/Gatherers	Shredders/Grazers	Predators	Zooplankton
Net-spinning caddisflies	Case-building caddisflies	Dragonflies	Cladocerans
Sow bugs	Some beetles	Some leeches	Copepods
Chironomids	Snails	A few stoneflies	Rotifers
Clams	True flies	Some beetles	
Snails		Some midges	
Mayflies		Alder flies	
Some stone flies		Some caddisflies	
Blackflies			

7　Source: Wetzel, 1983.

8

9　Several groups of detritivorous insects were observed in coarse-grained sediment, including

10　springtails, beetles, and fly larvae. Dipterans had the highest density of any invertebrate, and

11　average densities ranged from 950 to 3,800 individuals per square meter (Chadwick &

12　Associates, 1994). However, as noted above, the high densities of dipterans observed in the

13　Chadwick study did not translate into high biomass estimates for this group in the soft bottom

14　sampling (WESTON, 2000a).

15　In the water column, zooplankton are often the primary consumers of phytoplankton in deep

16　slow-moving rivers where the principal energy pathway is through a predator-prey-oriented food

17　web (Welch, 1992). Zooplankton are microscopic animals that graze upon phytoplankton. They

18　can be herbivorous or predatory, and feed by filtering the water as they move. They are

19　composed primarily of populations of rotifers, cladocerans, and copepods. Zooplankton, in turn,

20　provide a food source for planktivorous fish and predatory invertebrates.

1   Data collected by EPA include benthic community samples collected from 13 fine-grained
2   sediment stations, four of which are reference locations. Figure 3-28 presents the average
3   biomass of the three benthic invertebrate categories measured by EPA (WESTON, 2000a) at the
4   nine stations located within the PSA. The data are organized by study reach (5a, 5b, 5c, Woods
5   Pond) as well as by major taxa, though it should be recognized that the design and scope of this
6   study dictate that comparisons between reaches should be made with caution. Invertebrate
7   biomass is highest in the Woods Pond reach. Invertebrates classified as filterer/gatherers are the
8   most abundant category in Reaches 5b and 5c and Woods Pond. Biomass of predatory
9   invertebrates, while lower than the other consumer groups in all reaches, contributed more
10 significantly to total biomass in the lower reaches of the PSA (i.e., Reach 5c and Woods Pond)
11 relative to the upstream reaches. An important caveat in the interpretation of the data presented
12 in Figure 3-28 is that the sampling methods were targeted toward soft-bottom environments. For
13 reaches that are not dominated by a soft-bottom substrate (e.g., Reach 5a), the benthic
14 community data may therefore not be representative of the reach as a whole. The entire benthic
15 data set, including historical studies, will be reviewed in more detail during model
16 implementation.

17 **Fish**

18 Fish species are the main component of the upper trophic levels and can be classified according
19 to their functional feeding group: predators, foragers (insectivorous and planktivorous), and
20 bottom feeders (benthivores). Predators consume other fish but are also somewhat opportunistic,
21 and might also consume insects, benthic invertebrates, and/or zooplankton. Early life stages of
22 piscivorous fish also have diets more comparable to a forage fish, and switch to larger prey with
23 age. Foragers have opportunistic feeding habits, consuming primarily insects and plankton; they
24 are also a food source for predators. Bottom feeders consume primarily benthic invertebrates,
25 including insects. Some fish can be classified under more than one category, depending on a
26 particular life stage. It is common for juveniles and adults of the same species to have different
27 dietary niches. Many juveniles consume plankton, switching to insects and/or fish as they
28 mature and become adults.
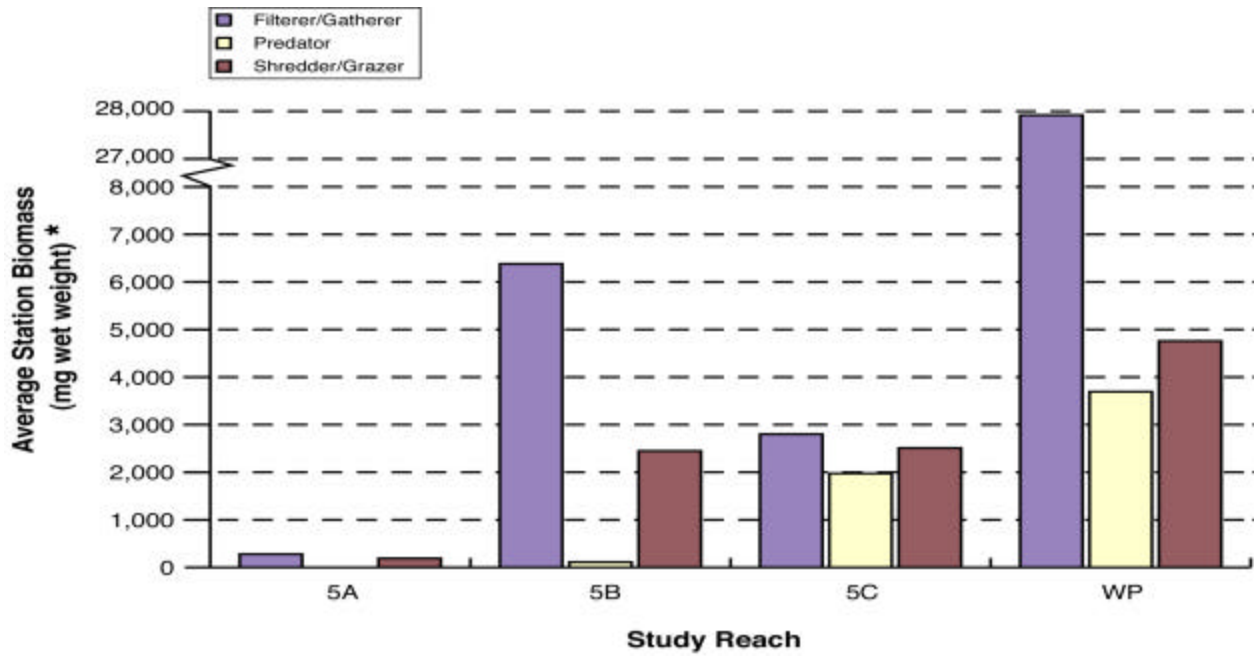
*Total Biomass per 12 petite Ponar replicate grabs (total area sampled = 0.278 m^2)

**Figure 3-28 Benthic Invertebrate Biomass by Reach Designation
Within the PSA (WESTON, 2000a)**

1   Twenty-three fish species were found in the PSA (Woodlot, 1998). Fish species that are
2   common to the Housatonic River (expected in each survey of suitable habitat) are listed by
3   feeding strategy in Table 3-15.

4   **Table 3-15**
5
6   **Housatonic River Common Fish Species**

Bottom	Forage	Predators
White sucker *Catastomus commersoni*	Golden shiner *Notemigonus crysoleucas*	Yellow perch *Perca flavescens*
Goldfish *Carassius auratus*	Bluegill *Lepomis macrochirus*	Largemouth bass *Micropterus salmoides*
Common carp *Cyprinus carpio*	Pumpkinseed *Lepomis gibbosus*	Fallfish *Semotilus corporalis*
Brown bullhead *Ameiurus nebulosus*	Dace and Shiners Cyprinidae	Brown trout *Salmo trutta*
	Rock bass *Ambloplites rupestris*	Chain pickerel *Esox niger*
	Black crappie *Pomoxis nigromaculatus*	Northern pike *Esox lucius*
	Spottail shiner *Notropis hudsonius*	Smallmouth bass *Micropterus dolomieu*
	Longnose dace *Rhinichthys cataractae*	
	Blacknose dace *Rhinichthys atratulus*	

7   Source: Woodlot, 1998.
8
9   Woodlot (1998) presents a summary of fish sampling conducted in September-October 1998
10   within the PSA. Fish species abundance (number of individuals) for this sampling period is
11   shown in Figure 3-29, broken down by sampling reach and fish type (bottom fish, forage fish,
12   and predators). These data illustrate the spatial patterns consistent with the general river habitat
13   features described above. Specifically, the faster-flowing portions of the PSA (Reach 5a) have a
14   lower diversity of bottom and forage fish relative to the backwater and stillwater areas found
15   closer to Woods Pond. White suckers were observed in high numbers throughout Reach 5, but
16   are less abundant in Woods Pond. In Woods Pond, other bottom feeders such as goldfish and

1   brown bullhead are more numerous. The most numerous predatory species over most of the PSA
2   were yellow perch and largemouth bass. Higher numbers of sunfish (bluegill, pumpkinseed) and
3   shiners were observed in the middle and southern reaches of the PSA utilizing the feeding niches
4   in the complex habitats found there.   These data are being supplemented by a fish species
5   biomass study that is underway, which will provide more information about the fish communities
6   specific to each reach.

* Bluegill and pumpkinseed combined in sunfish category for Woods Pond; spot tail shiners, longnose dace,
and blacknose dace were combined in shiners and dace category for Woods Pond
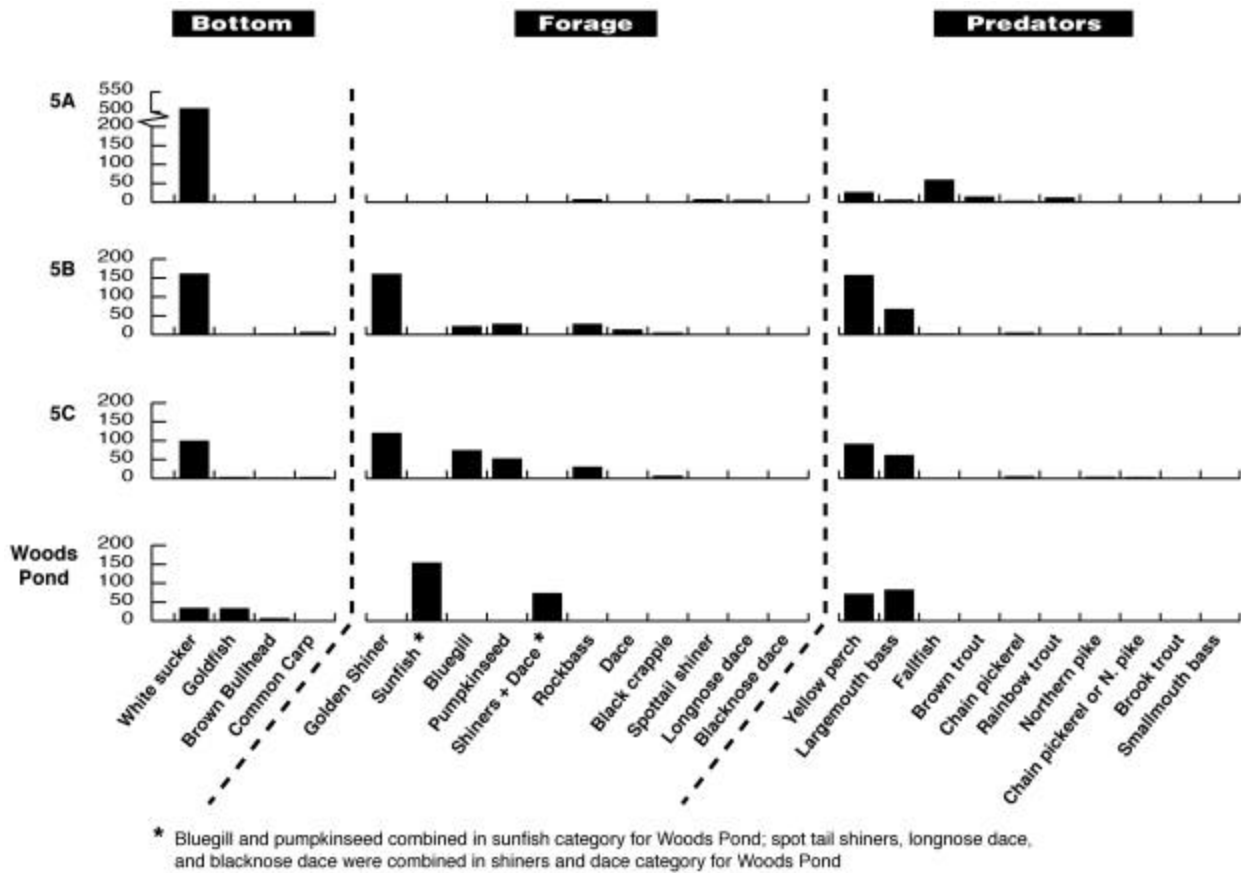
**Figure 3-29 Fish Species Abundance Estimates (Number of Individuals) in Four
Reaches of the Housatonic River (Sept.-Oct., 1998)**

10   Through biomagnification processes, fish are expected to have the highest concentrations of
11   PCBs of any of the taxa in an aquatic system (excluding the semi-aquatic piscivorous species
12   such as otter and heron). Concentrations of PCBs in fish tissue vary between different species of
13   fish due to differences in feeding habits. Fish species that consume organisms at lower levels of
14   the food chain, i.e., planktivores, will tend to have lower levels of PCB accumulation compared
15   to large predatory species.

1 To evaluate whether PCB concentrations in various species, trophic levels, and age classes of

2 fish are consistent with what would be expected based on the conceptual model and literature on

3 PCB partitioning, a preliminary analysis was conducted using PCB concentrations observed in

4 fish collected in Woods Pond. Table 3-16 presents a summary of total PCB concentrations in

5 fish from Woods Pond, with fish organized by feeding niche (bottom, forage, predatory) and size

6 class (i.e., 5 to 15 cm, 15 to 30 cm, and 30+ cm size classes for largemouth bass). PCB

7 concentrations are expressed both on a wet weight basis and on a lipid-normalized basis.

8 Evaluation of the data in Table 3-16 indicates several general patterns:

9 ▪ Concentrations of PCBs are lowest in forage fish. On a wet weight basis, the five
10   forage fish classes have the lowest mean PCB concentrations, whereas on a lipid-
11   normalized basis, forage fish exhibited the three lowest normalized PCB
12   concentrations (shiners, juvenile, and adult pumpkinseed). This is consistent with
13   what would be expected based on the conceptual model for an aquatic system.
14   Forage fish are lower on the food chain relative to predators and therefore have less
15   potential for biomagnification. Furthermore, they have less contact with
16   contaminated bottom sediments and associated pore water, relative to bottom fish.

17 ▪ PCB concentrations are higher in bottom fish (brown bullhead, goldfish). This is
18   consistent with what would be predicted considering their exposure (i.e., direct
19   contact with bottom sediments and pore water). Although these fish are not high on
20   the food chain relative to other fish species, their feeding habits and exposure to
21   sediments may explain their higher concentrations. This is consistent with results
22   observed in other freshwater systems, in which hydrophobic organic chemicals are
23   elevated in bottom feeders. For example, in The Fraser River of British Columbia,
24   demersal mountain whitefish (*Prosopium williamsoni*) have accumulated high
25   concentrations of hydrophobic contaminants, such as polychlorinated dioxins and
26   furans (Gobas et al., 1998).

27 ▪ PCB concentrations are elevated in predators (yellow perch, largemouth bass) relative
28   to most other species. This is consistent with the theory of biomagnification, which
29   would predict higher PCB concentrations in predatory fish via trophic transfer. The
30   largemouth bass concentrations also increase with fish size class. This is consistent
31   with other sites (e.g., Zaranko et al., 1997), which documented age-dependent
32   bioaccumulation of PCBs in predatory fish.

33 Therefore, preliminary review of site-specific PCB data appears to support the conceptual model

34 description of the fish community and the importance of separating fish species and feeding

35 strategy in the modeling study.

Table 3-16

Mean Total PCB Concentrations (Whole Body) in Fish Collected in Woods Pond

Category	Species Name	n	Size Class (cm)	Min. Length (cm)	Max. Length (cm)	Mean Total PCB (mg/kg wet)	Mean Total PCB (mg/kg lipid)	Maximum Total PCB (mg/kg wet)	Maximum Total PCB (mg/kg lipid)
Bottom Fish									
	Brown bullhead	26	all	23	31	62.9	6,828	126.8	90,370
	Goldfish	23	all	28	37	188.4	1,650	447.8	4,717
Forage Fish									
	Pumpkinseed (J)	6	< 15	8	15	32.7	1,205	66.1	2,134
	Pumpkinseed (A)	25	> 15	16	20	46.7	1,052	108.3	3,674
	Golden shiner	5	all	6.1	14	22.5	724	26.4	942
	Yellow perch (J)	7	< 20	9	20	37.8	1,793	73.5	5,139
	Largemouth bass (J)	9	< 15	7	14	31.6	1,728	99.8	3,577
Predators									
	Yellow perch (A)	23	> 20	21	29	114.7	2,507	204.7	6,903
	Largemouth bass (A)	7	15-30	18	28	49.1	1,882	126	2,999
	Largemouth bass (A)	15	> 30	31	40	146.4	3,569	388.8	7,624

1 **Detritus**

2 Detritus is nonliving organic matter that may provide a substantial energy base for the aquatic
3 food web. In general, detritus can be characterized as either dissolved organic matter (DOM) or
4 particulate organic matter (POM). The direct and dietary uptake of PCBs by aquatic organisms
5 may be controlled in part by dissolved and particulate organic detritus. Therefore, an
6 understanding of the relative contributions of the dissolved, suspended, and sedimentary detritus
7 is important in quantifying the contribution of detritus to PCB concentrations in aquatic
8 organisms.

9 Three detritus pools are being considered:

10   ▪ Dissolved detritus.
11   ▪ Suspended detritus.
12   ▪ Sedimentary detritus.
13
14 The relative contributions of these detritus pools may be important for modeling PCBs in the
15 Housatonic River. The theoretical and empirical basis for discriminating among these pools in
16 discussed in more detail in Section 3.3.5.2.

17 In general, three processes affect detritus entering an aquatic system and allow for nutrient
18 cycling in the system: leaching of soluble compounds, microbial degradation, and consumption
19 by heterotrophs. Leaching of soluble materials usually occurs fairly rapidly, ranging from
20 minutes to weeks. The leached dissolved material is readily available to microbial heterotrophs
21 for uptake and mineralization. Microbial activity, primarily by fungi and bacteria, continues to
22 degrade the detritus via enzyme activity. Leaching and degradation can occur simultaneously.
23 For example, enzyme activity could release dissolved organic carbon, which could then be lost to
24 leaching or directly taken up by microbes. Sugars and some proteins are often taken up by
25 microbes, but cellulose, waxes, and certain phenolic compounds are less degradable. Organic
26 matter with high content of phenolic polymers and complexes is classified as refractory organic
27 matter and will decay at a much slower rate than labile detritus.

28 Detritivores will take up nonliving organic material and the associated microbial community and
29 provide a prey resource for higher trophic levels. Assimilation of organic material by

1   detritivorous invertebrates results in a food source that is available to higher trophic groups such
2   as fish. The combined assemblage of plankton and detritus forms the base of the freshwater
3   aquatic food web, serving as an essential energy and contaminant source to the higher trophic
4   level organisms (WESTON, 2000a).

5   **The Aquatic Biological Conceptual Model**

6   Conceptual models describe how a stressor might affect the components of an ecosystem (EPA,
7   1992). Figure 3-24 shows all of the major biological compartments of the Housatonic River,
8   with arrows indicating the trophic transfer pathways that are considered relevant for PCBs in this
9   system. In the sediments, the base of the aquatic food web consists of detritus and sediments that
10   may be ingested by benthic and epibenthic invertebrates (including sediment infauna, emerging
11   insects, and macroinvertebrates such as bivalves and crayfish) and some benthivorous fish. In
12   the water column, the base of the aquatic food web consists of phytoplankton, which is
13   consumed by zooplankton that in turn serves as a food source for forage fish. The top of the
14   food chain is composed of higher trophic level fish (e.g., largemouth bass) that consume lower
15   trophic level fish and other prey organisms.

16   Because of the potential importance of the detritus pool in PCB partitioning, Figure 3-24 shows
17   the three subcompartments of this organic carbon pool (dissolved, sedimentary, and suspended).
18   Aquatic macrophytes (floating and rooted) may not be a significant component of the aquatic
19   food chain, but are important in the detritus cycle and represent a significant biomass for
20   accumulation of PCBs; therefore, they are represented in the general conceptual model.

21   *3.3.5.2   Evaluation of Biological PCB Fate Processes*

22   Modeling of PCB fate within aquatic biota requires quantifying the biological linkages shown in
23   Figure 3-24. Several early bioaccumulation models used the concept of a food chain multiplier,
24   which is now considered excessively simplistic (Campfens and Mackay, 1997). Food-web
25   modeling is considered necessary except for screening level studies (Abbott et al., 1995). The
26   best way to accurately assess bioaccumulation is to use more complex models, provided the data
27   needs of the models can be met and there is sufficient time to implement such a model (Pelka,

1 1998). Food web models "provide a means for validation because they mechanistically describe

2 the bioaccumulation process and ascribe causality to observed relationships between biota and

3 sediment or water" (Connolly and Glaser, 1998). This approach requires that the basic

4 governing processes of PCB biological fate be adequately identified and described in the selected

5 model formulation.

6 This section provides a discussion of the important fate processes that may affect the movement

7 of PCBs through the biotic components of the Housatonic River. These processes have been

8 identified based on literature review and evaluation of similarly contaminated river systems. At

9 this stage in the development of the conceptual model, the key objective is to identify the

10 potentially relevant processes, with consideration of the need to select an appropriate biological

11 fate model. Therefore, at the end of each section, an evaluation of the importance of each

12 process is made. Furthermore, for some processes, there are multiple ways of representing the

13 process in mathematical models; therefore, this section provides insights into the way the

14 processes should be handled in the model formulation.

15 The biological fate processes are organized under the following outline; these categorizations are

16 somewhat arbitrary and there is overlap in the groupings (e.g., gill ventilation/respiration

17 comprises a means of both uptake and elimination). However, this organization is designed to

18 provide a structure for discussing individual processes.

19 A. Partitioning at the Base of the Food Web
20 ▪ PCB Complexation with Organic Carbon in Water
21 ▪ Polarity Differences and Partitioning Among Types of Organic Carbon
22 ▪ Riverine Disequilibria
23 ▪ Sediment PCB Biotransformation
24
25 B. Uptake
26 ▪ Uptake Kinetics in Phytoplankton, Periphyton, and Macrophytes
27 ▪ Dermal Contact (Absorption, Adsorption)
28 ▪ Respiration
29 ▪ Benthic Feeding Strategies/Preferences
30 ▪ Fish Feeding Strategies/Preferences
31 ▪ Fish Migratory Behavior
32

1   C. Assimilation
2   ▪   Gastrointestinal Transfer
3   ▪   Internal PCB Transfer
4   ▪   Lipid Partitioning and Reproduction
5   ▪   Equilibrium Partitioning and Fugacity
6   ▪   Biomagnification
7
8   D. Elimination
9   ▪   Metabolism
10   ▪   Depuration
11   ▪   Growth Dilution
12   ▪   Toxicity Feedback Loops
13
14   E. Biotic Transport
15   ▪   Fish Migration
16   ▪   Benthic Drift
17   ▪   Storms and Scour
18
19   **Partitioning at the Base of the Food Web**

20   ***PCB Complexation with Organic Carbon in Water***

21   Dissolved and particulate organic matter are very important in controlling both the direct and

22   dietary uptake of PCBs, and this process will be included in the model. The bioavailability of

23   PCBs in the water column represents an important consideration for modeling biological fate.

24   Conceptually, the differences between PCBs in the water column that are: 1) truly dissolved; 2)

25   complexed with colloidal and dissolved organic carbon; or 3) associated with particulates, can be

26   determined. This distinction differs from that used operationally to discriminate between

27   "dissolved" and "particulate" organic carbon concentrations (i.e., use of a set filter mesh size,

28   such as 0.45 microns). For example, in a study using algal exudate and PCB-180 with log K_{OW} of

29   7.36, 98% of the "dissolved" concentration was as a DOC complex and only 2% was

30   bioavailable (i.e., freely dissolved) (Koelmans and Heugens, 1998).

31   Discriminating between all three phases of organic carbon is desirable because bioavailability is

32   much greater for truly dissolved concentrations of PCBs relative to PCBs associated with

33   colloidal and dissolved organic carbon (DOC) (Hwang et al., 1998). Bioavailability is reduced in

34   the latter phase because organic carbon-associated contaminants are sequestered and therefore

35   much less available for uptake by organisms (Stange and Swackhamer, 1994; Gilek et al., 1996).

1   However, older data and modeling efforts conducted historically at other sites failed to
2   distinguish between PCBs that were truly dissolved and those that were associated with organic
3   carbon. For example:

4   ▪ PCB water concentrations for Lake Ontario, reported by Oliver and Niimi (1988) and
5   used by many subsequent researchers, included both dissolved and OC-associated
6   PCBs.

7   ▪ In their steady-state model of PCBs in the Great Lakes, Thomann and Mueller (1983)
8   defined "dissolved" as that which passed a 0.45-micron filter.

9   ▪ In their Hudson River PCB model, Thomann et al., (1991) again used this operational
10   definition of dissolved PCBs (0.45-micron filter).

11 In contrast, recent PCB modeling efforts (Gobas, 1993; Morrison et al., 1996; EPA, 2000a,
12 2000b, 2000c) have attempted to better define the bioavailability (e.g., by extrapolating from
13 operational concentrations to truly dissolved concentrations) using equations that incorporate the
14 dissolved and particulate organic carbon concentrations measured in the field.

15 *Polarity Differences and Partitioning Among Types of Organic Carbon*

16 PCBs in the Housatonic River may be present in several forms (i.e., truly dissolved, associated
17 with dissolved organic matter, associated with particulate organic matter, or in another as yet to
18 be defined phase discussed earlier). The association of PCBs with dissolved and particulate
19 organic matter is referred to as sorption and is a process by which the dissolved and particulate
20 matter acts as an organic solvent for the PCBs.

21 The tendency of a specific PCB congener to associate with organic matter is determined by its
22 aqueous solubility and the nature of the organic matter. Highly chlorinated congeners, with
23 relatively low aqueous solubilities, will have a strong tendency to be associated with organic
24 matter. PCBs will have a higher affinity for nonpolar organic matter due to their nonpolar
25 nature. The distribution of the PCB congeners between the aqueous and organic phases is
26 described using a partition coefficient (K_d), which is simply the ratio of the organic phase
27 concentration to the aqueous phase concentration. A partition coefficient commonly measured in
28 the laboratory is the ratio of a compound's concentration in octanol and water (K_{ow}).

1   Organic matter is not homogeneous. There is a wide variety of different sources of organic

2   matter to the river including primary production within the river and the deposition of terrestrial

3   organic matter. In addition to differences due to sources, organic matter within the river will

4   change over time due to geochemical and biological weathering processes. The variability in the

5   nature of organic matter will affect the affinity of PCBs for specific pools of organic matter.

6   The greatest differences in PCB sorption will be seen between particulate and dissolved organic

7   matter. In general, dissolved organic material will be more polar than particulate organic matter

8   and therefore have a lower affinity for PCBs. A review of the literature in combination with site-

9   specific data will be used to identify the most appropriate partition coefficients to describe the

10   partitioning of PCBs with the dissolved and particulate organic matter in the Housatonic River.

11   More subtle differences in polarity can occur within the pools or particulate and dissolved

12   organic matter. However, because these differences are expected to be less important and

13   because of the difficulty in obtaining measurements of the relative polarity of field-collected

14   organic material, these intra-pool differences will not be explicitly considered in the model

15   formulation.

16   ### *Riverine Disequilibria*

17   Although the simplest theoretical construct for PCB partitioning (i.e., equilibrium partitioning)

18   would predict thermodynamic equilibrium among environmental compartments, in reality

19   chemical concentrations in sediment and overlying water can be in considerable disequilibrium

20   in rivers. This disequilibrium may result from temporal changes in chemical loadings, e.g.,

21   physical transport of dissolved or suspended PCBs during storm events, as well as rates of

22   exchange between sediments and water that are slow relative to the water flow rates.

23   Furthermore, the rates of exchange between sediments and water are slow relative to those

24   between water and organisms. As a result of this disequilibrium, it is important to consider

25   water-column and sediment pathways separately in model formulations. Evidence from similar

26   river systems, such as the Hudson River, indicates that fish may accumulate PCBs from both

27   water-column and sediment pathways, and at different rates, and that these broad

28   "compartments" are generally not in equilibrium with each other. A challenge for modeling

1   uptake processes in these flowing river systems is that some animals exhibit life histories that

2   include both sediment and overlying water exposures.

3   Disequilibria between fish and their surroundings can result from insufficient exposure time or

4   organism growth, metabolic biotransformation, dietary exposure, and nonlinear relationships for

5   very large and/or superhydrophobic compounds (Bertelsen et al., 1998). Although it is important

6   to have a knowledge of thermodynamic partitioning because it is an indication of the condition

7   toward which systems tend (Bertelsen et al., 1998), it is often impossible to determine steady-

8   state potential due to changes in bioavailability and physiology (Landrum, 1998). PCBs may not

9   be at steady state even in large systems such as Lake Ontario that have been polluted over a long

10   period of time (Cook and Burkhard, 1998).

11   These observations suggest the importance of decoupling the benthic and pelagic exposure

12   pathways in PCB food web models; therefore, this decoupling will be incorporated in the

13   modeling study. Recent developments in modeling have resulted in the improved ability to

14   differentiate between pelagic and benthic contributions to organism exposures. Whereas some

15   earlier models tightly coupled the active layer of sediment and the overlying water column,

16   newer models allow for differential modeling of sediment-water coupling and explicit modeling

17   of pore waters. To this end, it is beneficial if all animals can be characterized by the fraction of

18   their exposure attributed to the water column versus pore waters (e.g., carp and diurnally

19   migrating *Chaoborus* may be assigned a greater exposure to pore waters than tube-dwelling

20   oligochaetes). Biodiffusion may also be modeled explicitly for particles and pore waters in the

21   active layer.

22   ***Sediment PCB Biotransformation***

23   Some PCB congeners can be dechlorinated by either aerobic or anaerobic bacteria (Butcher

24   et al., 1997). Only the more chlorinated congeners are dechlorinated anaerobically, and only the

25   less chlorinated congeners are degraded aerobically (Jafvert and Rogers, 1990). Some

26   methanogenic bacteria, which are anaerobic, dechlorinate PCBs at the *meta* and *para* positions,

27   enhancing Cl_1, Cl_2, and Cl_3 *ortho*-substituted PCBs, and counteracting selective enrichment of

28   some congeners (Bright et al., 1995).

1   Although disputed by some, Sokol et al., (1998b) found that removal is a function of PCB

2   concentration and that dechlorination is effective only above a threshold concentration. *Ortho*

3   dechlorination was not observed; however, anaerobic transformation of highly chlorinated

4   congeners into lower chlorinated congeners in a variable environment makes them subject to

5   later aerobic microbial degradation, which can oxidatively mineralize lower-Cl congeners to

6   carbon dioxide and water (Gerstenberger et al., 1997; Sokol et al., 1998b). In one study,

7   anaerobic dechlorination decreased total Cl by 36%; however, more than 33% of *meta* and *para*

8   Cl remained after 39 months of anaerobic incubation (Sokol et al., 1998a). In another study,

9   highly chlorinated congeners declined between 1988 and 1993 in an Ontario stream due to

10 dechlorination by anaerobic bacteria (Zaranko et al., 1997). Anaerobic dechlorination has been

11 coupled with aerobic biodegradation as a mechanism for bioremediation of PCBs (Abramowicz,

12 1994).

13 Aside from volatilization and biotransformation by microbes and higher organisms, PCBs are

14 remarkably stable.   They are affected by neither hydrolysis nor oxidation.   Atmospheric

15 photodegradation has been shown to break down Cl_2 homologs, but higher chlorinated

16 compounds are very resistant to this degradation pathway (Neely, 1983).

17 For the purposes of this modeling study design, microbial degradation of PCBs is evaluated in

18 conjunction with physical transport and fate processes. Therefore, this process will not be

19 included explicitly in the model. However, biotransformation by fish is separately evaluated

20 later in this section. Note that algae lack enzymes for dechlorinating PCBs (Hill and Napolitano,

21 1997), and no metabolism of PCBs has been reported for algae.

22 **Uptake**

23 *Uptake Kinetics in Phytoplankton, Periphyton, and Macrophytes*

24 The uptake of chlorinated hydrocarbons by phytoplankton, aquatic macrophytes, and filamentous

25 algae is rapid and follows first-order kinetics (Zaranko et al., 1997). PCBs bioaccumulate into

26 algae through partitioning to cell lipids and organic carbon pools. Rates of PCB depuration by

1   algae and macrophytes are slower and limited by lack of metabolism (Manhanty, 1986; Zaranko

2   et al., 1997.)

3   Some PCB bioaccumulation models (Gobas et al., 1995) assume that bioaccumulation of PCBs

4   in phytoplankton is represented by an equilibrium partitioning of PCB with the freely dissolved

5   chemical in the ambient water. This assumption was made because the half-lifetimes of PCBs in

6   water exceed those in plankton, resulting in rapid changes in plankton concentrations for a given

7   change in water concentration. It is noted, however, that rapid increases in biomass during

8   plankton blooms may invalidate this assumption because an increase in the plant weight or

9   volume has a diluting effect on the chemical concentrations in the algae.

10   In contrast to the simplified partitioning of the Gobas models for plankton (Gobas, 1993; Gobas

11   et al., 1995), some food-web models have incorporated more detail in terms of the partitioning to

12   organic carbon pools and the uptake-depuration kinetics. The combination of lipid content,

13   surface area, and growth rate results in species differences in bioaccumulation among algae

14   (Wood et al., 1997). Bioaccumulation of PCBs in algae is dependent on solubility,

15   hydrophobicity, and molecular configuration of the congener; growth rate, surface area, and type

16   of algae; and content and type of lipid in the algae (Stange and Swackhamer, 1994).

17   PCBs partition to lipids in algae, but the relationship is not a simple one. In phytoplankton,

18   lipids can range from 3 to 30% by weight (Swackhamer and Skoglund, 1991), and different lipid

19   types exhibit different partitioning properties. Polar phospholipids occur on the surface. PCBs

20   preferentially partition to internal neutral lipids, but those are usually a minor fraction of the total

21   lipids, and they vary depending on growth conditions and species (Stange and Swackhamer,

22   1994). Algal lipids have a much stronger affinity for PCBs than does octanol, so that the algal

23   $BAF_{lipid} > K_{ow}$ (Stange and Swackhamer, 1994; Koelmans et al., 1995; Sijm et al., 1998). Also,

24   the pattern of bioaccumulation in algae varies among PCB congeners (Stange and Swackhamer,

25   1994).

26   Uptake in algae is much more rapid than in macrophytes, but even algae may be in

27   disequilibrium during rapid growth, as Swackhamer and Skoglund (1991) have shown. For this

28   reason, in environments where algae and macrophytes form significant and time-variable food

29   sources for other organisms, such as the Housatonic River, it is useful to model uptake into these

1   organisms as disequilibrium processes. Such complexity may be warranted in the Housatonic

2   River due to the potentially large biomass (e.g., macrophytes in Woods Pond) or the potential

3   importance of these biota in the food web (e.g., algae). Gobas et al. (1991) conducted uptake and

4   elimination experiments with PCBs and other chemicals in macrophytes using the common

5   aquatic weed *Myriophyllum spicatum,* and developed a kinetic model that fit the observed data

6   well.

7   In summary, information on PCB kinetics in algae and macrophytes and consideration of the

8   temporal variations in primary production in the PSA (i.e., summer algal mats and plankton

9   blooms) indicate that a time-dependent model formulation for aquatic flora is warranted.

10   ***Dermal Contact***

11   There is some conflicting information in the literature on the significance of dermal contact with

12   PCBs in fish. According to Shaw and Connell (1984), absorption of PCBs through the fish

13   epidermis is not a significant transport pathway. Gobas (1993) also states that chemical

14   absorption via the skin is usually insignificant. Therefore, absorption of PCBs through body

15   surfaces is generally not considered in food-web models of PCBs.

16   However, dermal uptake may be significant for benthic feeders such as bullhead, catfish, and

17   carp, which forage in sediments for aquatic organisms (Leadley et al., 1998). Juvenile spot fed

18   copepods in contaminated sediment accumulated 4.83 times more PCBs than fish fed in clean

19   sediment, although exposure occurred through both skin and gills (DiPinto and Coull, 1997).

20   With the exception of algae and macrophytes, sorption to the body has been disregarded in most

21   models. However, some of the available models include fractional exposure to water column

22   and pore waters, which allows modeling of significant gill exposure of benthic fish. In this way,

23   potentially increased PCB exposures to carp, bullhead, and other active benthic feeders are

24   accounted for in the model. Direct sorption to invertebrate chitin or fish epidermis is not

25   considered, but the exposure to the pore water in contact with the sediment is explicitly

26   considered. The latter is a more important pathway for transport of PCBs into fish and

27   invertebrate tissues.

1   The need for incorporating a direct body sorption pathway in the model is not being pursued in
2   the current modeling study, but may be revisited if the data or the calibration exercise suggest
3   that there is a basis to do so.

4   In summary, the modeling study will likely exclude adsorption to fish and invertebrate body
5   surface and absorption through the fish epidermis, but will retain exposure to pore water as a
6   potential significant biological fate process.

Respiration

8   Respiratory uptake represents the dominant PCB uptake mechanism directly from the water
9   column (i.e., dissolved PCBs). There are a number of characteristics of fish that control their
10   ability to bioaccumulate PCBs via this process, including ventilation volume, gill surface area,
11   epithelium layer of gill, and aqueous stagnant layer of gill (Shaw and Connell, 1984; Kadlec and
12   Bush, 1994; LeBlanc and Brownawell, 1994). Gill exposure is a function of respiration rate,
13   decreasing in larger fish (Thomann and Mueller, 1987).

14   Several mass transfer models have been developed to represent the respiratory uptake of PCBs
15   by biota directly from water (Connolly, 1991; Connolly et al., 1992). In these models,
16   contaminant mass transfer at the gill is determined from an uptake rate constant for respiration.
17   In implementing the mass balance model, the respiration uptake rate constant is derived
18   considering the respiration rate, as determined by the bioenergetics of the fish; the concentration
19   of oxygen in the water; and the ratio of chemical:oxygen mass transfer rates (QEA, 1999). In
20   practice, the latter ratio is determined or estimated using experimental data. Other model types
21   (e.g., Gobas, 1993), describe gill respiration in terms of a net flux of chemical into an organism,
22   with first order rate constants used to describe uptake from water via the gills and elimination via
23   the gills to the water. In these models, the gill uptake rate constant is a function of the gill uptake
24   efficiency (see discussion below), gill ventilation rate, and the volume of the fish. Models for
25   the chemical elimination of PCBs from gill to water are closely related to the chemical uptake
26   rate constants.

27   Some authors (McKim et al., 1985; Gobas, 1993) report that gill uptake efficiency varies with
28   chlorination of PCBs. As the chlorination increases, so does the K_{ow}. Congeners with log K_{ow}

1 between 4.5 and 6.5 exhibit comparable chemical transfer efficiencies, but gill "uptake

2 efficiency" decreases at higher K_{ow}. This phenomenon may be due to slower diffusion rates for

3 the larger PCB molecules. Some authors have suggested that steric hindrance of larger

4 molecules makes it more difficult for PCBs to pass through the phospholipid bi-layer of the fish

5 (Opperhuizen, 1986; Barron, 1990). Accordingly, diffusion through the aqueous layers on either

6 side of the gill may limit the diffusion of PCBs with higher K_{ow}. Other authors have suggested

7 that the observed decrease in gill uptake efficiency at higher K_{ow} is a result of increased binding

8 of the chemicals with DOC and/or experimental errors associated with the difficult water

9 concentration measurements (Gobas, 1993; Gobas and Mackay, 1987) and not to an actual

10 decrease in gill uptake efficiency.

11 For organisms exposed to PCBs over a long period, uptake and depuration via the gill is thought

12 to be biphasic. This is likely the result of organisms having both readily accessible and deeper

13 absorptive sites for lipophilic contaminants (QEA, 1999). (For further discussion, see the

14 subsection entitled "Internal PCB Transfer.")

15 Studies in the literature present conflicting evidence on the relative importance of

16 bioconcentration through the gills. Shaw and Connell (1984) found that gill uptake of PCBs can

17 be a dominant uptake process. Caged fish fed clean food have also been demonstrated to

18 accumulate PCBs from the water column (Kadlec and Bush, 1994). Other studies suggest that

19 gill ventilation is a less important process than dietary intake. Studies conducted in the Hudson

20 River indicate that the degree of importance of the water column pathway varies depending of

21 the trophic status of the fish. Forage fish have been found to be more sensitive to water column

22 concentrations, whereas benthic feeding fish are less sensitive to water column concentrations

23 (TAMS et al., 2000). However, in the latter analysis, the importance of dietary differences, i.e.,

24 differences in the consumption of water column-associated versus sediment-associated prey,

25 must be acknowledged. The importance of gill uptake also varies depending on the PCB

26 congener in question; gill uptake tends to be more important for lower chlorinated PCBs, while

27 dietary accumulation is the driving mechanism for moderate to highly chlorinated PCBs.

28 In summary, while gill ventilation may not be the dominant PCB biological fate process in most

29 species or for most PCB congeners, it is clear that it represents a highly important process, and is

1   a necessary component of any valid PCB food web model. Accordingly, the modeling study will

2   incorporate gill ventilation/respiration. Respiration in animals will be modeled as a function of

3   temperature-sensitive basal respiration plus specific dynamic action, which is related to food

4   assimilation. Withdrawal efficiency of contaminants will likely follow the studies of McKim

5   et al. (1985) with a piecewise fit to his data.

6   **Dietary Uptake**

7   **Benthic Feeding Strategies/Preferences**

8   Feeding strategy and prey digestibility are important factors controlling the magnitude of

9   bioaccumulation in benthos (Morrison et al., 1996). Simple equilibrium partitioning does not

10   adequately distinguish between different feeding strategies among benthic invertebrates such as

11   filter feeding and detritus composition, which can result in interspecies differences in

12   bioaccumulation and biomagnification. For example, in the application of AQUATOX to the

13   Lake Ontario food web (Park, 1999), benthic amphipods could be represented as feeding on

14   labile detritus from freshly sedimented phytoplankton rather than on aged detritus or

15   "phytoplankton," resulting in improved model performance for this component of the food chain.

16   In some cases, disequilibrium between sediment and overlying water can increase the importance

17   of differences in feeding strategies. The equilibrium partitioning model assumes that sediment,

18   pore water, and organisms are in thermodynamic equilibrium. However, disequilibria between

19   sediment and water may result in large differences between pore water and overlying water

20   concentrations. Depending on the species, the overlying water may represent a more relevant

21   exposure route. For example, *Hyalella* have been demonstrated to be more sensitive to

22   contaminant concentrations in the water column than to pore water or sediment concentrations

23   (Wang et al., 1999).

24   Much attention has been given to the role of pore water in the uptake of PCBs by benthos.

25   However, contaminants dissolved in pore water are not necessarily the most bioavailable because

26   many animal burrows are lined, and the composition of the water in burrows is equivalent to that

27   of the overlying water (Forbes et al., 1998). Campfens and Mackay (1997) found that predicted

28   PCB concentrations in benthos exceeded those measured for high K_{OW} congeners, possibly due

1   to assumptions regarding the respiration of pore water. Uptake of very hydrophobic compounds

2   from sediment was observed to be one to five times greater than that predicted by equilibrium

3   partitioning from pore water (Loonen et al., 1997).

4   Bioaccumulation of lighter homologs may reflect direct uptake from water (Bright et al., 1995).

5   The exposure of filter feeders to the overlying water is quite different from that of deposit

6   feeders. For example, the pumping rate of mussels is 100 times greater than that of a deposit-

7   feeding clam; however, this is offset somewhat by decreased efficiency of uptake at higher

8   pumping rates (Björk and Gilek, 1999).

9   Because of the rapid organism-water exchange in small, lower trophic level organisms, food-web

10   accumulation of PCBs in these animals has received less attention in the literature relative to

11   fish. Nevertheless, recent modeling efforts (Morrison et al., 1996) have attempted to evaluate the

12   dietary preferences of benthos and their influence on bioconcentration and biomagnification.

13   Some field studies have indicated considerable variation in the magnitude of invertebrate biota-

14   sediment accumulation factors (BSAFs), which would indicate that consideration of feeding

15   preferences is important. For example, one study (Markwell et al., 1989, as cited in Morrison

16   et al., 1996) documented an average BSAF in oligochaetes of 11.0. However, empirical data

17   from the Hudson River (TAMS et al., 2000) indicate that differential bioaccumulation of PCBs

18   among invertebrates with different feeding strategies is not always important. In the Hudson

19   River study, the mean BSAF of all species was approximately 1.0, which is consistent with the

20   values of 1 to 2 that would be predicted on the basis of equilibrium partitioning. Furthermore,

21   the mean BSAF for each major taxon (amphipod, bivalve, chironomid, gastropod, isopod,

22   odonata, oligochaete) did not exceed 2, and 60% of the BSAFs for invertebrates fell between 0.4

23   and 1.5 (TAMS et al., 2000). There are limited data on site-specific BSAFs for the Housatonic

24   River, although additional data are currently being generated as part of the Work Plan

25   (WESTON, 2000a).

26   There are limited site-specific data available at this time to assess the importance of different

27   feeding strategies and/or the potential for biomagnification for benthos in the Housatonic.

28   However, benthic invertebrate samples have been screened by feeding strategy and submitted for

29   PCB tissue residue analysis; these data may provide a more definitive answer to these questions.

1   Historical data are available from the Connecticut portion of the river below the PSA (West

2   Cornwall) about 20 km downstream of the Massachusetts/Connecticut border (Figure 3-30,

3   Patrick, 1999). The total PCB concentration (based on sums of congeners) is presented for three

4   taxa, including a filter-feeding caddisfly (Hydropsychidae), a predatory dobsonfly (Corydalidae)

5   and a predatory stonefly (Perlidae). The upper graph in Figure 3-30 shows that although

6   differences in PCB concentrations are evident (i.e., dobsonfly > caddisfly > stonefly), there do

7   not appear to be major differences among feeding strategies. This is more evident in the lower

8   graph, which shows that when predators are merged, historical data (1978 to 1998) do not

9   suggest consistent or large differences between PCB concentrations in filter feeders and

10 predators.

11 Patrick (1999) provides lipid data only for the 1998 data; lipid content was lower in the caddisfly

12 sample (0.4%) relative to the stonefly and dobsonfly samples (1.2 and 6.2% lipid, respectively).

13 Adjusting for lipid content results in higher lipid-normalized PCB concentrations in the filter-

14 feeding caddisfly relative to the two predatory taxa (i.e., approximately five- to sixfold in the

15 1998 sampling round). It is not known whether the differences in lipid contents were as

16 pronounced in previous years.

17 In summary, it is currently unclear whether differences in feeding preferences of invertebrates

18 should be explicitly considered in the bioaccumulation model. However, pending review of the

19 site-specific data, the modeling study will retain the consideration of differences in benthic

20 feeding preferences of invertebrates, in a similar fashion to fish. This decision will be

21 reevaluated as additional Housatonic River data become available. The model should also have

22 the capacity to discriminate between pore water and overlying water exposure pathways, and

23 allow for specification of specific types of organic carbon in food.

24 *Fish Feeding Strategies/Preferences*

25 Bioaccumulation of PCBs via dietary uptake pathways has been demonstrated to be a very

26 important process. For many fish species, consumption of contaminated prey items represents

27 the dominant source of PCB uptake, especially for PCBs with log K_{ow} above approximately 6.

28 Thomann and Connolly (1984) demonstrated that for Lake Michigan lake trout, the vast majority

29 of PCB accumulation was attributable to food chain transfer. The rate at which chemicals are
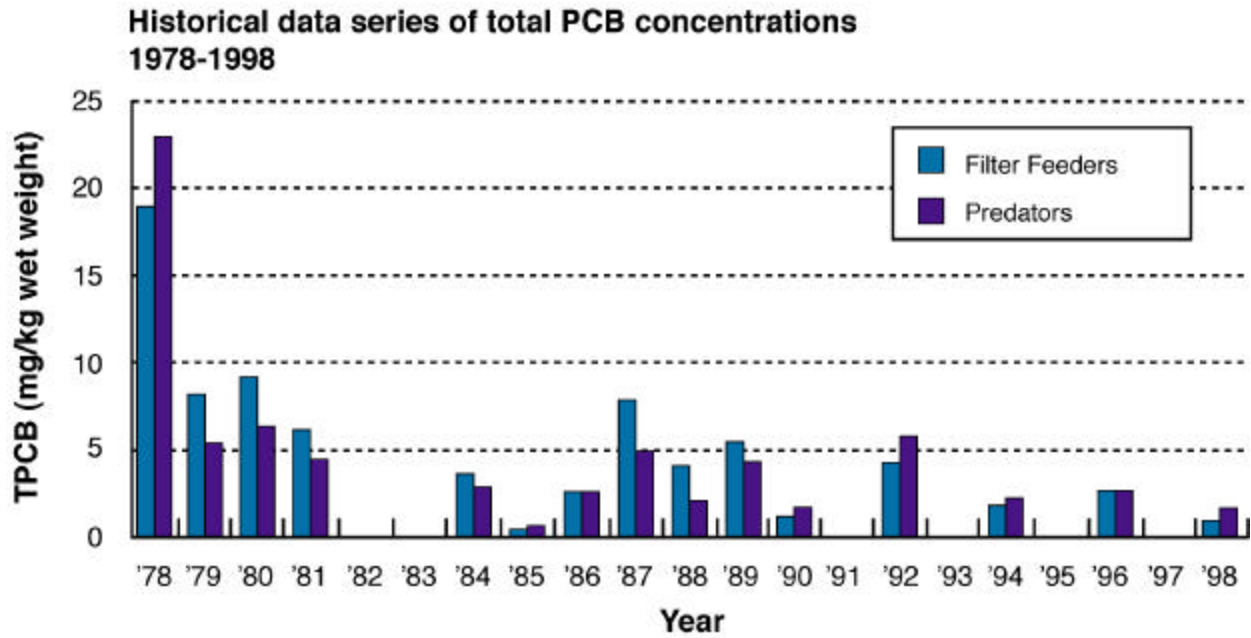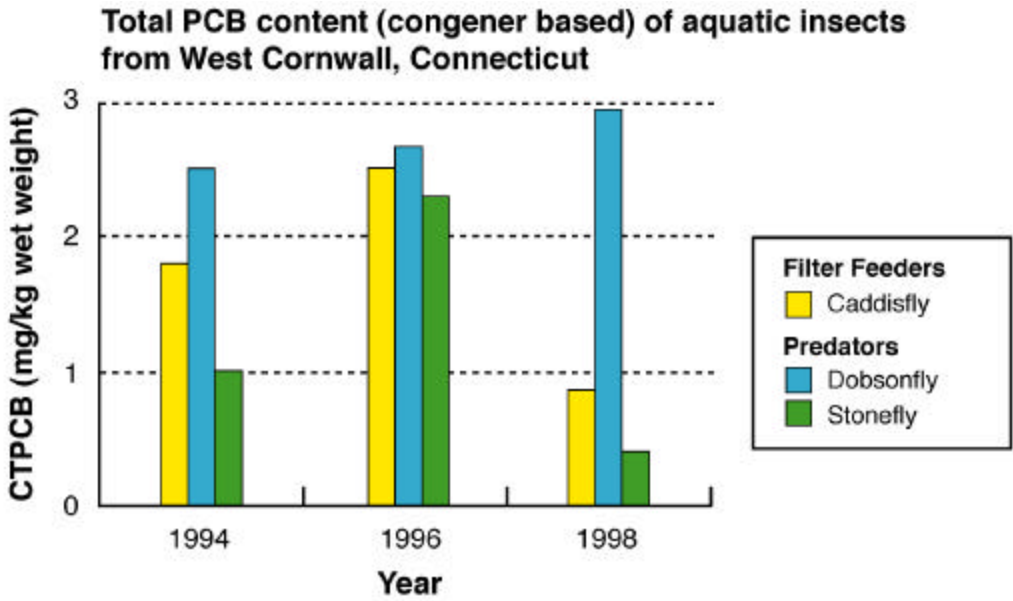
Figure 3-30 PCB Concentrations in Benthic Invertebrates

1 absorbed by organisms via the gastrointestinal tract is the combined process of the food ingestion
2 rate and the net transfer of PCB across the intestinal wall.

3 Because of the importance of food as an exposure pathway to fish and other organisms, feeding
4 strategy of these animals is a key component of PCB modeling. In essence, the chemical
5 concentration in the predator is highly related to that in its prey. To this end, the lipid content
6 and labile organic carbon content of the dietary items are important, as are the chemical
7 concentrations within the prey items. Dietary preferences do not remain constant over the
8 lifetime of an animal, or even across seasons. Dietary preferences can also change as a result of
9 changes in the abundance and density of prey; trophic feedback loops are also possible, with
10 opportunistic prey-switching.

11 In the modeling study, variations in feeding preferences will be desirable to provide flexibility
12 for including opportunistic feeding and prey switching. However, although prey switching is
13 known to occur in nature, the trade-offs between model complexity and uncertainty must be
14 evaluated further during model calibration.

15 ***Fish Migratory Behavior***

16 Migratory behavior of fish can be important in determining their exposure. For example,
17 minnows migrate during early spring and fall; PCB concentrations in minnows in an Ontario
18 stream varied seasonally, with the lowest concentration in October (Zaranko et al., 1997).
19 Similarly, migration of striped bass in the Hudson River estuary is substantial and contributes to
20 the observed variability in PCBs (Thomann and Farley, 1998). In contrast, largemouth bass are
21 known to be highly territorial and tend to stay in their home areas (Parker and Hasler, 1959).

22 Preliminary model runs will be used to determine whether migration of fish between river
23 reaches is of sufficient importance to warrant its inclusion in the model. The modeling study
24 should provide the capability of simulating this process, in conjunction with the opportunistic
25 feeding and prey switching. However, the benefit of incorporating this degree of complexity in
26 the model is questionable at this time without site-specific model calibration.

1 **Assimilation**

2 *Gastrointestinal Transfer*

3 In mass transfer models, PCB mass transfer at the gut wall is determined by the amount of food
4 consumed and the PCB assimilation efficiency (QEA, 1999). Assimilation efficiency refers to
5 the fraction of ingested contaminant that is transferred across the gut wall and into the animal.
6 Assimilation efficiency in these models also appears to be closely linked to the dietary
7 assimilation of lipids (Van Veld, 1990). Based on studies by Connolly et al., (1992) and
8 Parkerton (1993), PCB congeners with log K_{ow} below 6.75 generally have assimilation
9 efficiencies in the range of 0.75 and 0.85, with substantial declines in efficiency for log K_{ow} of 7
10 and higher (QEA, 1999). Food consumption rates may be derived using bioenergetic equations.

11 An alternative representation of PCB dynamics at the gut interface is based on the theory that
12 uptake of PCBs via the gastrointestinal tract occurs via diffusion (Gobas et al., 1993a, 1993b).
13 As food is digested, the total mass of the food and the lipid content decreases. The decreasing
14 pool of lipid creates a matrix less able to absorb the PCB molecules and consequently, the PCB
15 fugacity in the intestine increases. If the PCB fugacity in the gut is higher than that in the fish, a
16 net flux of PCB will occur across the epithelial layer into the fish. This diffusive mechanism is
17 the basis of one theory of gastrointestinal magnification and can define the mechanism of
18 biomagnification.

19 There are two major implications of this theory for PCB fate modeling. First, it implies that
20 organisms feeding on less digestible food (such as sediment organic matter) will likely exhibit
21 less gastrointestinal magnification. This is due to the development of a smaller fugacity gradient
22 across the gut epithelium. Second, if diffusion of PCB molecules occurs across the
23 gastrointestinal wall, then fecal egestion becomes an important PCB elimination mechanism
24 when an organism is feeding while in a depuration cycle, i.e., when the organism switches to a
25 less contaminated food source.

26 In the modeling study, it will be assumed that gut efficiency equals assimilation efficiency for
27 food, similar to the Connolly models. Combined with the bioenergetics portion of the model,
28 this encompasses the process of biomagnification.

1 ***Internal PCB Transfer***

2 The pharmacokinetics of PCBs within the body may be considered in PCB fate modeling.
3 However, the importance of modeling internal PCB dynamics varies, depending on the overall
4 model formulation selected. Multiple-compartment models for organisms such as fish may be
5 used to represent the mass transfer of PCBs. For example, QEA (1999) presents a two-
6 compartment model for PCB mass transfer in fish. This process was included to account for the
7 differences between mass transfer rates to and from blood, considered to be a compartment with
8 relatively rapid exchange, and "deeper" storage compartments with relatively slow exchange.
9 Division of fish into these compartments is consistent with evidence of biphasic elimination of
10 PCBs from fish.

11 In the mass-transfer models developed by Connolly and others, there is insufficient information
12 to describe all of the necessary rate constants and partition coefficients for the full multi-
13 compartmental model. Therefore, the "resistance" to chemical flux caused by relatively slow
14 chemical kinetics between lipids in "deep storage" compartments and blood is represented in a
15 more simplified manner. First, the gill elimination rate is computed under the assumption that
16 there is rapid equilibration between lipid and blood; then this rate is multiplied by a resistance
17 factor (fraction) that accounts for the slow transfer of PCBs from lipids to blood (QEA, 1999).

18 Because the mass transport models developed by Connolly and others are sensitive to
19 elimination rate constants, division of the body into compartments with different elimination
20 properties is necessary. For models that consider gastrointestinal elimination as a significant fate
21 process, consideration of biphasic elimination is less important. In summary, the importance of
22 internal PCB dynamics depends on the structure of the model chosen.

23 ***Lipid Partitioning and Reproduction***

24 Because lipids play a fundamental role in PCB partitioning behavior in aquatic systems, temporal
25 changes in lipid contents can affect PCB fate in food webs. Lipid contents in organisms can be
26 highly variable within and between years. Furthermore, reproduction also results in seasonal
27 changes in lipid content and PCB body burdens.

1   The amount of lipid is quite variable among species and even in the same species over the course
2   of a year or lifetime. Lipid concentrations in fish have been documented to range from 2 to 28%
3   (Sijm and van der Linde, 1995; Zaranko et al., 1997; Gerstenberger et al., 1997). Fathead
4   minnows have been observed to have post-spawning reductions in lipid content of as much as
5   72% in males and 46% in females due to breeding activities, including cleaning and defense of
6   nests, as well as egg laying (Suedel et al., 1997).

7   From a modeling perspective, the effects of lipid are very important. Therefore, they are
8   considered in nearly all model formulations, though the detailed formulations may vary. For
9   example, lipid stores affect the bioenergetics-based models by affecting the rates of gill
10   ventilation. The concentration-based models are also affected, by altering the fugacity gradient
11   both between fish and water, and between the gastrointestinal tract and fish tissue.

12   In summary, there are numerous ways of incorporating lipid content changes in food-web
13   models. The adequacy of the model is more a function of the models' ability to adequately
14   simulate the time-dynamics of changes in lipid content. Modeling seasonally varying lipid
15   content will be a goal in the development of the modeling study, but may not be explicitly
16   incorporated, pending initial model runs.

17   *Equilibrium Partitioning and Fugacity*

18   Due to their lipophilicity, PCBs tend to accumulate in the lipid portions of organisms. Although
19   some organic carbon/lipid pools have greater ability to sorb PCBs than others, lipid content is a
20   significant driving factor in the biological fate of PCBs. The simplest thermodynamic-based
21   fugacity models assume chemical equilibrium, with PCBs distributed among environmental
22   compartments relative to their fugacity.

23   Fugacity is a term used to describe the escaping tendency of hydrophobic organic contaminants;
24   it is a function of the chemical concentration and the fugacity capacity (i.e., binding affinity) of
25   the media for sorbing PCBs. The simplest equilibrium partitioning models assume that chemical
26   concentrations in benthic invertebrates, sediment, and pore water seek thermodynamic
27   equilibrium, i.e., equal fugacity. Equilibrium partitioning has been commonly used to describe
28   the bioaccumulation of PCBs in sediment-based benthic communities. Using field data from the

1 Great Lakes, Bierman (1990) determined that sediment-associated invertebrates including

2 oligochaetes, chironomids, and amphipods reflected PCB concentrations consistent with

3 equilibrium partitioning.

4 The tendency of PCBs to partition in accordance with their basic chemical properties (e.g.,

5 octanol-water partition coefficient, organic carbon-water coefficient, Henry's Law constant,

6 vapor pressure) is advantageous in that it allows for modeling of not only PCB mixtures, but also

7 PCB congeners. Accumulation patterns in plankton and fish from sediment are largely

8 determined by degree of chlorination. Maximum bioaccumulation occurs for Cl_5, Cl_6, and Cl_7

9 congeners; Cl_3 and Cl_4 congeners are depleted due to low lipophilicity; Cl_8 congeners are

10 depleted due to size or steric effects (Willman et al., 1997; Oliver and Niimi, 1988; Campfens

11 and Mackay, 1997; DiPinto and Coull, 1997).

12 Within homolog groups, congeners with less *ortho*-substitution have greater K_{OW} values and are

13 accumulated up the food chain to a greater extent than other congeners in their homolog group.

14 Changes in distributions of congeners mainly are caused by transfers among biotic compartments

15 (Campfens and Mackay, 1997). There is no enrichment of mono- and non-*ortho*-substituted

16 congeners with an increase in trophic level. However, many coplanar congeners, especially the

17 more toxic PCB 77, may potentially be depleted with increasing trophic level (Campfens and

18 Mackay, 1997).

19 Although chemicals such as PCBs exhibit a natural tendency to achieve thermodynamic

20 equilibrium, biological, chemical, and environmental processes can prevent such equilibrium

21 from being achieved (Morrison et al., 1996). When maintained over extended periods of time,

22 kinetically controlled but stable concentration may be achieved. In other instances, rapid

23 environmental changes may result in varying concentrations. The latter is often the case for river

24 systems, where time-dependent models are best used as prediction tools (TAMS et al., 2000;

25 QEA, 1999).

26 In such river systems, organisms are exposed to both sediments and water in disequilibrium, and

27 are subject to relatively rapid changes in exposure concentration, physiology (i.e., lipid content)

28 and/or food web structure. For example, phytoplankton biomass may double or triple in one day

29 and periphyton turnover may be so rapid that some PCBs will not reach equilibrium (Hill and

1   Napolitano, 1997).   Equilibrium partitioning may be used to set constraints on PCB

2   concentrations, but full equilibrium is unlikely to be achieved.

3   Some food web models have developed bioaccumulation factors to represent the partitioning

4   between PCB concentrations in biota and those in water and sediment. Bioaccumulation factors

5   (BAFs) represent the ratio of the concentration of PCBs in organisms to those dissolved in the

6   water column. Biota-sediment accumulation factors (BSAFs) represent the ratio between the

7   concentration of PCBs in organisms to those found within sediment. Commonly, BAFs and

8   BSAFs are normalized to lipid or organic carbon content to reflect the preferential association of

9   PCBs with organic matter.

10   There are a number of disadvantages to the use of BAFs and BSAFs in PCB food-web modeling.

11   First, the values are empirically derived and therefore have a limited mechanistic basis. Second,

12   the exposure of organisms cannot always be neatly divided into overlying water routes and

13   sediment routes, particularly for epifauna. Third, the BAF and BSAF approaches assume a

14   steady state. This assumption has been shown to be invalid for dynamic systems like the

15   Housatonic River, for the reasons described above. For these reasons, a simplified modeling

16   approach based upon empirically derived partition coefficients is not recommended to describe

17   the biological fate of the Housatonic River.

18   Therefore, it is a goal for the modeling study to consider the differential partitioning of PCBs to

19   biological compartments with varying affinity to PCBs. As such, the model should compute

20   partition coefficients for use as constraints in the competitive uptake of contaminants among

21   various compartments. As stated above, there are a number of non-equilibrium processes that

22   prevent environmental systems such as the Housatonic River from reaching thermodynamic

23   equilibrium; therefore, the partition coefficients should be used only in constraining parameters

24   in the model.

25   ***Biomagnification***

26   Many studies have shown that aquatic organisms are capable of bioaccumulating PCBs above

27   concentrations that would be predicted on the basis of direct partitioning between water,

28   sediment, and tissues (Zaranko et al., 1997).   Therefore, biomagnification through trophic

1   transfer is a relevant "disequilibrium" process that results in the concentration of PCBs in
2   predator tissue being greater than that in food items.

3   The consequence of biomagnification in aquatic systems is that higher trophic levels accumulate
4   greater concentrations of PCBs relative to lower trophic levels, even after species are
5   standardized by physical parameters such as lipid content. For example, in a freshwater creek in
6   Ontario, Canada, fish and leeches occupying the top of the food web accumulated more PCBs
7   than organisms occupying lower trophic positions, e.g., crayfish, oligochaetes, and chironomids
8   (Zaranko et al., 1997). In a German rural lake, the PCB concentration of pike muscle tissue
9   (normalized to lipid content) was found to be 1.3 to 4.0 times the concentration that of roach
10   muscle tissue, clearly indicating a biomagnification of PCBs from prey to predator (Looser,
11   1998). The bioenergetics-based biomagnification processes described above can also account for
12   fish with high respiration rates that uptake PCBs rapidly in spite of being relatively low in the
13   food web.

14   The site-specific data presented in Table 3-16 suggests that biomagnification of PCBs in fish
15   may be occurring in the Housatonic River. This is indicated by the lipid-normalized PCB
16   concentrations in higher trophic level fish (largemouth bass, yellow perch) that exceed those in
17   forage fish species.

18   There are both empirical and theoretical grounds that indicate that biomagnification can also be a
19   relevant process for benthic invertebrates, although this process is less critical in invertebrates
20   than in fish (Morrison et al., 1996; Gobas, 1993).

21   The process by which biomagnification occurs in fish remains controversial. One hypothesis is
22   that the digestion of food in the gastrointestinal tract results in a reduction in fugacity capacity of
23   the prey items, causing a corresponding "fugacity pump" from the gut to the tissues of the
24   organism as discussed earlier. This hypothesis has been validated in laboratory experiments
25   (e.g., Gobas et al., 1993a, 1993b) using laboratory fish, which clearly demonstrate an increase in
26   chemical fugacity with distance along the gastrointestinal tract. There is not, however, universal
27   support for gastrointestinal pumping as an explanation for biomagnification.

1   Another theory is derived from the science of bioenergetics, assuming that PCBs travel with food
2   as they pass the gastrointestinal wall. The theory considers that if all assimilated food was
3   allocated to fish growth, then the biomass of the fish would increase proportionate to the feeding
4   rate, and the contaminant concentration would remain unchanged. However, in reality, as a fish
5   feeds, only a fraction of assimilated food may be assigned to growth; much of it is respired. If
6   the contaminant is reasonably conservative, it is "left behind" in the fish tissues while the food is
7   in part converted to energy. The greater the fraction of respiration as a percentage of the food
8   energy, the greater the tendency of the fish to accumulate PCB molecules internally.

9   The major distinction between these two schools of thought regarding PCB gut dynamics is in
10 the mode of transport across the gut wall. The "fugacity pump" theory assumes that the PCB
11 transport occurs primarily by diffusion across the gut lining, whereas the bioenergetics approach
12 assumes that PCB molecules are transported with the food as it is assimilated. Both models have
13 been successfully applied to describe bioaccumulation and biomagnification in aquatic food
14 webs. The former model places increased importance on the fecal egestion pathway as an
15 elimination process, whereas the latter requires a more detailed understanding of fish
16 bioenergetics and respiration. Further discussion on this topic is provided below in the context
17 of modeling depuration of PCBs in fish.

18 Biomagnification will be incorporated in the approach recommended for the modeling study,
19 considering both bioenergetics and contaminant transport. A fully implemented bioenergetics
20 approach with respiration as an explicit loss term yields credible biomagnification results in what
21 might be viewed as the reverse of growth dilution—a process that cascades down the food chain
22 and is an integral part of the well-accepted trophic transfer efficiency.

23 **Elimination**

24 *Metabolism*

25 PCBs are metabolized by fish and other macroorganisms, but generally at a very slow rate. The
26 metabolic transformation rate is often assumed to be zero, because although its true value is
27 unknown, it is generally recognized to be small compared to other elimination rates in fish, and

1 hence ignored (Gobas, 1993; Gobas et al., 1995). In this context, metabolic transformation is

2 viewed as producing only a small increase in the elimination rate. Biotransformation has the

3 greatest effect on hydrophobic compounds where excretion approaches zero; limited

4 accumulation of lower-chlorinated homologs may be due in part to biotransformation (Endicott

5 and Cook, 1994).

6 Although metabolism is not a dominant process for PCB mixtures, there is some evidence of

7 metabolism of individual congeners in recent literature. Fish are known to metabolize certain

8 congeners: 101, 105, 107, 110, 138, and 170 (Hill and Napolitano, 1997), many of which are

9 toxic. Few fish show enzyme induction that would suggest lower-Cl congeners are metabolized

10 (Gerstenberger et al., 1997). In fact, this may account for the bioaccumulation of lower-Cl

11 congeners in salmonids (Bright et al., 1995). Many coplanar congeners, especially the more

12 toxic PCB 77, are depleted with increasing trophic level; PCB 77 is almost certainly metabolized

13 (Campfens and Mackay, 1997).

14 Site-specific information is available that can provide insight regarding the importance of PCB

15 biotransformation in fish. Figure 3-31 shows the homolog profile for detected PCB congeners in

16 six representative fish species from Woods Pond. The graph shows that the homolog fingerprint

17 is very similar among fish species. If substantial biotransformation was occurring within fish,

18 we would expect to see differences in homolog profile moving up the food chain (i.e., a different

19 profile for higher trophic level fish such as largemouth bass). The data presented in Figure 3-31

20 does not exclude the possibility of a biotransformation that affects all fish species equally,

21 however.

22 Figure 3-32 presents a comparison of observed concentrations of specific PCB congeners in fish

23 species from Woods Pond that have been identified as being metabolized in fish (Hill and

24 Napolitano, 1997; Campfens and Mackay, 1997). The graph also shows the total PCB

25 concentration, such that the relative contribution of each congener may be put into perspective.

26 PCB 77 concentrations have been multiplied by 1,000 to make the graph legible. Figure 3-32

27 indicates that there are no pronounced differences between fish species with respect to the

28 concentrations of these individual congeners. The concentrations of each congener vary in
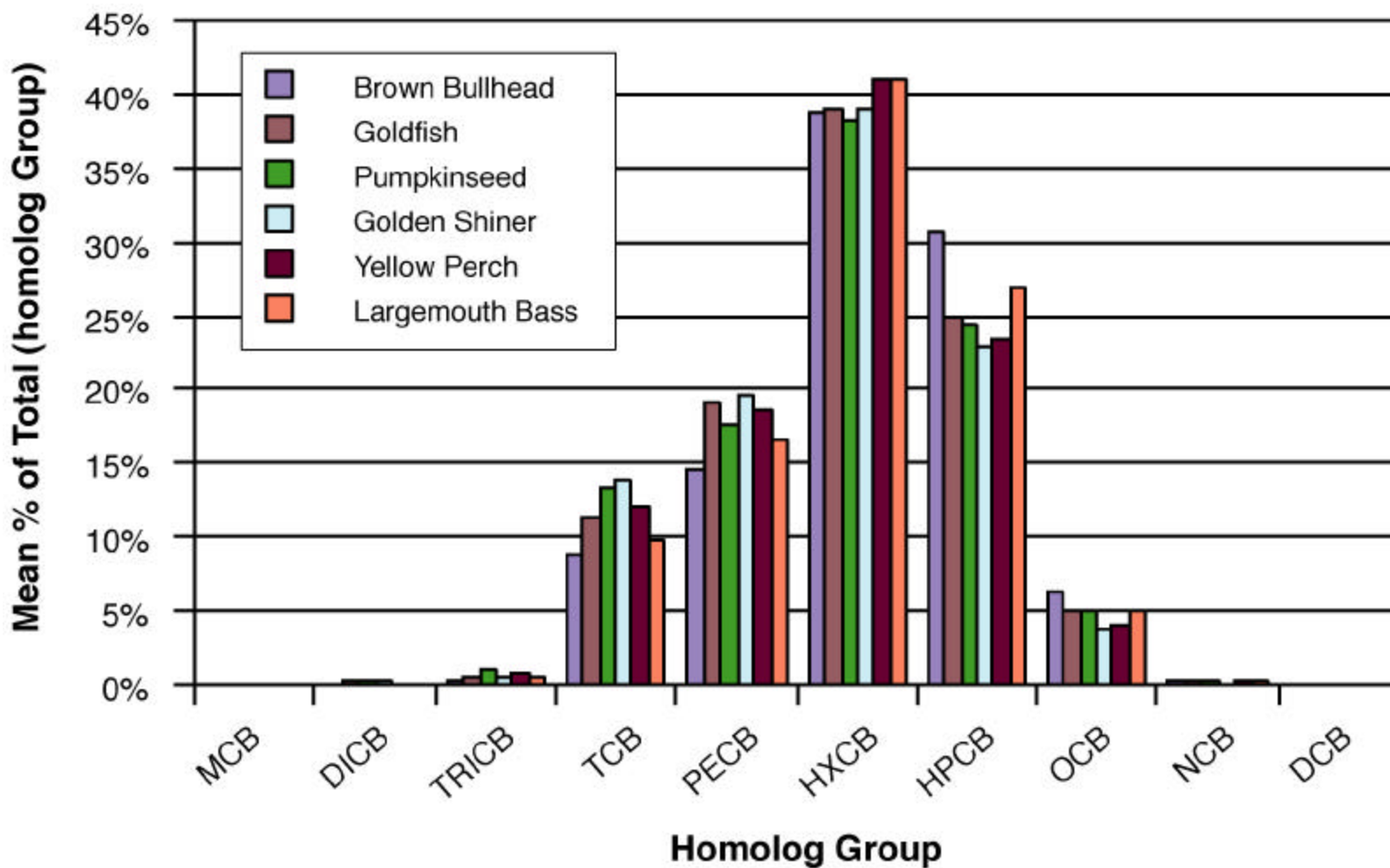
Figure 3-31 Species-Specific-Homolog Profiles for Woods Pond Fish
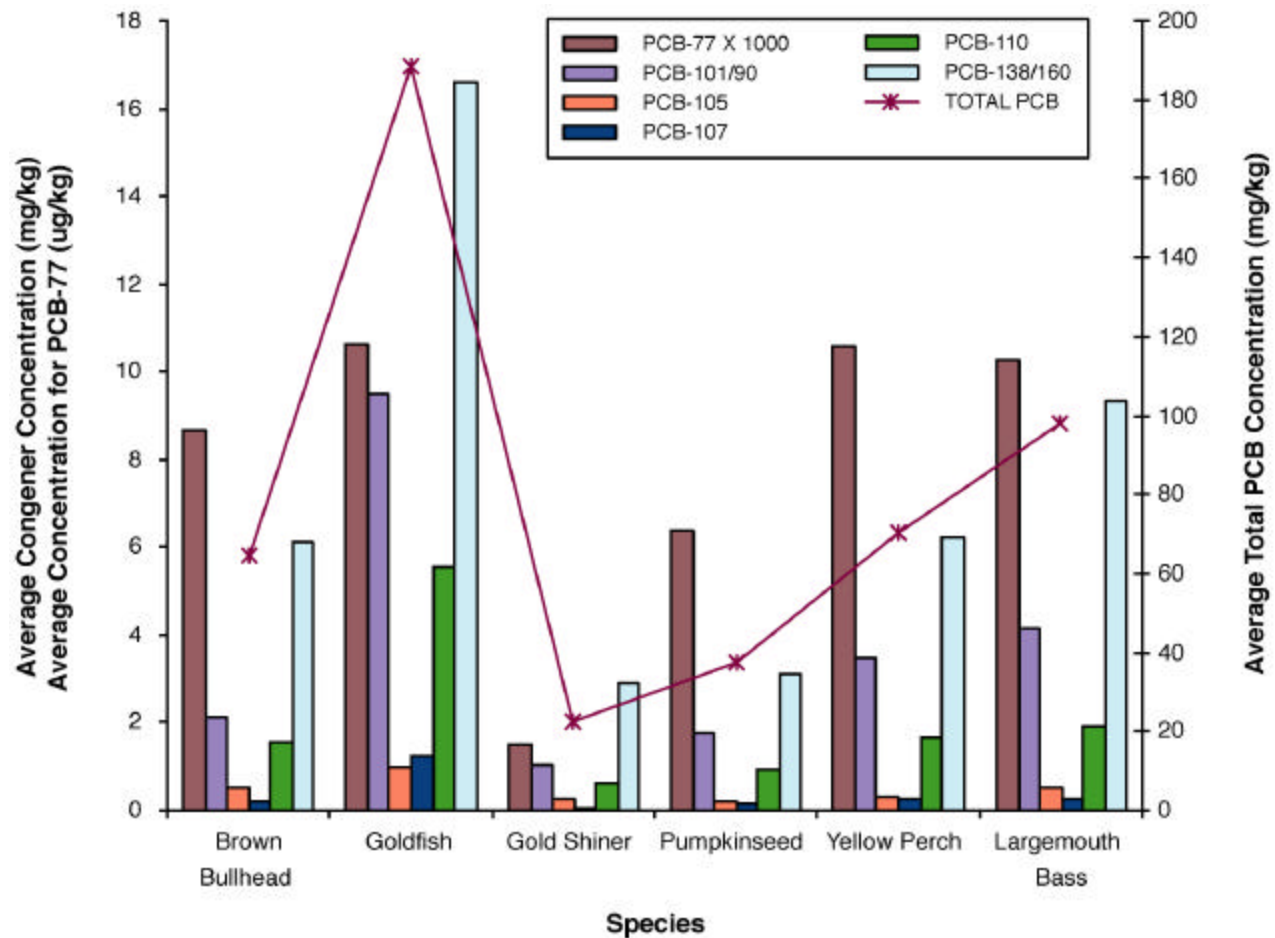
Figure 3-32 Species-Specific Concentrations of Total PCBs and Selected PCB Congeners in Woods Pond Fish

1   approximate proportion to the total PCB concentration. Therefore, there is little evidence to

2   suggest that PCB biotransformation is occurring within these fish from Woods Pond.

3   In summary, dechlorination of PCBs can occur, but it is usually mediated by bacterial action in

4   sediments. Based on preliminary review of the field data, metabolism does not appear to occur to

5   a substantial degree within fish collected from Woods Pond. As part of the model development,

6   further analyses will be undertaken to evaluate whether selective dechlorination of PCBs occurs

7   across the food web. For the purposes of food-web modeling, PCBs have typically been

8   assumed to biodegrade at a negligible rate, or alternatively biodegradation is included with other

9   loss rates. Although recent literature suggests that some metabolism of specific PCB congeners

10   is possible, the site-specific data do not appear to support this. Nevertheless, the model should

11   include the capacity to simulate the biodegradation of PCB congeners in fish pending more

12   thorough data review.

13   Detailed evaluation of the congener/homolog profiles between species in the PSA will be

14   undertaken in conjunction with the food-web modeling, to assess whether there are changes in

15   profiles that cannot be explained by differential uptake. While this process is unlikely to

16   substantially affect the overall biological fate of total PCBs or homologs, the process may be

17   relevant to specific congeners such as PCB 77, which are important because of their toxicity.

18   ***Depuration***

19   Depuration can be an important pathway for elimination of PCBs in fish. Depuration in juvenile

20   trout exhibits a curvilinear relationship with log K_{ow}, apparently decreasing beyond log $K_{ow} = 7$,

21   perhaps because equilibrium is not attained among compartments in the fish (Fisk et al., 1998).

22   Lipid content and size of the organism are important for determining the elimination rate

23   constant. Much lower depuration rates (and hence longer half-lives) occur in larger and/or fatter

24   fish. For example, the half-life of a Cl_4 PCB in a 0.1-g guppy was 43 days, compared to 5.6

25   years in a 900-g rainbow trout (Sijm and van der Linde, 1995). Elimination may occur across

26   the skin as well as through the gills, increasing in small fish with large surface-area-to-volume

27   ratios (Sijm and van der Linde, 1995).

1   There appear to be conflicting views regarding the importance of gut elimination in the

2   biological fate of PCBs. Isolating the magnitude of individual loss mechanisms is difficult and

3   instead of looking at individual loss mechanisms separately, many modelers have opted to ignore

4   this level of complexity in favor of presenting a single elimination rate constant. Connolly et al.,

5   (1992) suggest that elimination of moderately hydrophobic contaminants across the gut and

6   subsequent fecal egestion is of limited importance relative to overall elimination rate. Instead,

7   these models treat assimilation of PCBs from the gastrointestinal tract as an important process,

8   but essentially consider egested PCBs as chemicals not assimilated by the organism, as opposed

9   to elimination of PCBs previously sorbed to internal tissues of the animal. Therefore, some

10   models assume that the gill is the major site of depuration and that the mass-transfer across the

11   gills is equivalent to the whole-body loss rate (QEA, 1999).

12   Other models consider gastrointestinal elimination to be a separate and potentially important loss

13   mechanism for fish. In these models (Gobas, 1993; Gobas et al., 1995), uptake of chemical via

14   the diet is dependent on ingestion rate, dietary uptake efficiency, gastrointestinal elimination, and

15   the fecal egestion rate. Gobas et al. (1989, 1993a, 1993b, 1999) has investigated the potential

16   role of intestinal elimination in the depuration of PCBs, and concludes that intestinal elimination

17   becomes an important loss mechanism for PCBs with log K_{ow} greater than 6.5. Gobas et al.

18   (1989) compiled log elimination rate constant data for selected halogenated aromatic

19   hydrocarbons in the guppy. Using knowledge of gill kinetics, Gobas separates the elimination

20   rate constants for guppies into gill elimination and fecal elimination. The plots thus divided

21   suggest that fecal elimination becomes the predominant loss mechanism for persistent

22   halogenated compounds having log K_{ow} greater than 6.5. In another paper, Gobas et al. (1993a,

23   1993b) derived transport parameters from experimental data. Gill elimination and metabolic

24   losses become small in this model, compared to fecal elimination for chemicals with large log

25   K_{ow}.

26   Although there are different paradigms for modeling the depuration of PCBs from fish, both of

27   the basic approaches described above have been successfully applied to field data. The modeling

28   study will represent fecal loss by egestion with associated unassimilated contaminant, and

29   therefore depuration will be considered to occur primarily through the gills.

1   ***Growth Dilution***

2   Growth can have a considerable effect on concentrations in fish, particularly for higher-
3   chlorinated PCBs. Growth of the fish essentially acts to "dilute" concentrations of PCBs and
4   may therefore be considered as a "loss" mechanism. In strict terms, growth dilution is not a loss
5   rate, but simply reflects that chemical concentrations are reduced as the organism incorporates
6   "clean" tissue. A number of equations have been developed to describe fish growth rates, which
7   are dependent on seasonal feeding effects, fish size/volume, and water temperature. The
8   importance of this growth effect is such that it is incorporated into both mass-balance and
9   concentration gradient models of PCB fate in biota.

10   The importance of growth dilution is also beginning to be recognized in phytoplankton. During
11   rapid growth periods, concentrations in plankton may be lower than what would be predicted
12   using equilibrium partitioning from water. This may be an important process in the Housatonic
13   River during algae blooms.

14   In summary, the effects of growth on PCB concentrations in organisms should be accounted for
15   in the modeling study, incorporating organism growth and biomass as well as contaminant
16   burdens; therefore "growth dilution" should be implicit for all organisms. This capability should
17   include phytoplankton, which should be modeled in disequilibrium throughout the growing
18   season.

19   ***Toxicity Feedback Loops***

20   Few PCB congeners exhibit acute toxicity (Bright et al., 1995), but exposure may result in
21   chronic effects, adversely affecting survival, growth, and reproduction (Suedel et al., 1997).
22   Because of congener-specific toxicities, total body burden of PCBs is inadequate for predicting
23   effects (Schweitzer et al., 1997). Acute toxicity is demonstrated by non-*ortho*-substituted planar
24   congeners similar to dioxins; these dioxin-like congeners also exhibit chronic toxicity (Bergen et
25   al., 1996), including wasting disease (Suedel et al., 1997).

26   In contrast, *ortho*-substituted congeners have a low affinity for the aryl hydrocarbon (*Ah*)
27   receptor and may exhibit low toxicity, and perhaps insignificant sublethal effects (Suedel et al.,

1997). However, exposure to some di-*ortho* congeners (including 138, 153, 180, and 194) produce adverse effects (carcinogenicity, neurotoxicity, and endocrine disruption) (Kannan, et al., 1998).

In a study with an estuarine minnow, reduced feeding and reduction in growth occurred in fish fed medium and high doses of PCBs. The bioaccumulation of congeners was proportional to that observed in fish collected in the field, except for PCB 77, which may have been metabolized (Gutjahr-Gobell et al., 1999). In another study, fecundity was reduced in association with the reduction in growth; egg production was reduced by 77% at the highest dose (part of which was due to 58% mortality) (Black et al., 1998a). This relationship was not found in the field, suggesting differences in exposure routes (Black et al., 1998b).

In theory, changes in populations resulting from toxic effects of PCBs could result in modifications to the food web, since prey-switching could occur as one species (either invertebrate or prey fish) is reduced in relative and/or total abundance. Although site-specific PCB toxicity data have been collected, it would be very difficult to accurately predict how these toxic effects would cascade through the ecosystem in terms of biomass and/or PCB concentrations. Therefore, toxicity feedback loops will not be considered in the modeling study.

Biotic Transport

Movement of biota throughout the Housatonic River system is an important biological fate process:

- Migration of fish will affect their exposure to food items with differing PCB concentrations. Although some fish (e.g., largemouth bass) are territorial, other fish may be relatively mobile and be exposed to a wide range of sediment and water PCB concentrations. The modeling study will initially emphasize fish species with high site fidelity. During the model implementation stage, detailed evaluation of site data will determine whether it is necessary to simulate movement between modeled river reaches for more mobile species.

- Benthic drift (i.e., downstream baseline drift) is an important fate process that will be retained in the modeling study. Some models also have the capability of simulating contaminant-induced drift. However, because of the uncertainties in this latter process, it will be excluded from the modeling study.

1   ■   Storm events and scour will be retained as potentially significant biological fate
2   processes. Major storm events can result in the scour of substantial biomass of
3   periphyton, and even macrophytes.

3.4   SUMMARY AND CONCLUSIONS

5   In Section 3.1, Introduction, Table 3-1 presents the global list of processes considered for

6   inclusion in the modeling study. Each of these processes is discussed in this section and, based

7   on the level of understanding of each process, the available site-specific data, and the goal of

8   achieving model parsimony, each process is designated as necessary for inclusion in the model,

9   excluded from the model, or requiring further evaluation before a decision could be reached.

10   Table 3-17 repeats the list of individual processes listed in Table 3-1 and indicates the current

11   disposition of each with respect to the modeling study.

12

Table 3-17

Processes To Be Included, Excluded, or Further Evaluated for Model

Model Area	Primary Process	Mechanism	Processes Affecting Transport Mechanism	Included	Excluded	Further Evaluation
Water Balance	Hydrology	Base Flow Storm Flows	• Precipitation (rainfall, snow)	X		
			• Evaporation	X		
			• Transpiration	X		
			• Infiltration	X		
			• Base flow	X		
			• Soil storage	X		
			• Surface runoff	X		
			• Depression storage	X		
			• Interflow	X		
			• Groundwater flow and discharge	X		
			• Tributary loading	X		
	Hydrodynamics	Water Flow in Streams/Rivers/ Ponds/Lakes	• Water velocities	X		
			• Spatial velocity distribution	X		
			• Flow resistance/shear stress	X		
			• Vertical stratification	X		
			• Thermal balance/heat exchange	X		
			• Hydraulic structures	X		
Solids Mass Balance	Sediment Transport	Suspended Load – consists of both cohesive and noncohesive sediments	• Upstream and tributary loading	X		
			• Resuspension	X		
			• Mass erosion	X		
			• Mass wasting/bank slumping	X		
			• Localized scour around structures			X
			• Scouring around natural debris in streams		X	
			• Deposition/burial	X		
			• Bed armoring			X
			• Flocculation			X
		Bedload – consists of noncohesive sediments only	• Upstream and tributary loading			X
			• Deposition/burial			
			• Bioturbation			X
			• Bed armoring			X
		Particle Mixing	• Bioturbation			X
			• Anthropogenic sources		X	

Table 3-17

**Processes To Be Included, Excluded, or Further Evaluated for Model
(Continued)**

Model Area	Primary Process	Mechanism	Processes Affecting Transport Mechanism	Included	Excluded	Further Evaluation
PCB Mass Balance	PCB Transport and Fate	Water Transport	• Diffusion	X		
			• Advection	X		
			• Sorption/desorption (partitioning)	X		
			• Volatilization			X
			• Dechlorination (biodegradation/photolysis)			X
			• Wind			X
			• Bioturbation			X
			• Atmospheric sources		X	
		Sediment Transport	• Upstream and tributary loading		X	
			• Sorption/desorption	X		
			• Resuspension	X		
			• Deposition/burial	X		
		Atmospheric Transport	• Airborne transport		X	
			• Wind effects			X
Biota	Partitioning at Base of Food Web	Chemical Partitioning	• PCB complexation with organic carbon in water	X		
			• Polarity differences and partitioning among types of organic carbon		X	
			• Riverine disequilibria	X		
			• Sediment PCB biotransformation		X	
	Uptake	Direct Contact	• Uptake kinetics in phytoplankton, periphyton, and macrophytes	X		
			• Dermal contact (absorption, adsorption)		X	
			• Respiration	X		
		Dietary Uptake	• Benthic feeding strategies/preferences			X
			• Fish feeding strategies/preferences			X
			• Fish migratory behavior (effect on feeding)			X
	Assimilation	PCB Transfer Within Biota (e.g., fish)	• Gastrointestinal transfer	X		
			• Internal PCB transfer			X
			• Lipid partitioning and reproduction	X		
			• Equilibrium partitioning and fugacity	X		
			• Biomagnification	X		

Table 3-17

**Processes To Be Included, Excluded, or Further Evaluated for Model
(Continued)**

Model Area	Primary Process	Mechanism	Processes Affecting Transport Mechanism	Included	Excluded	Further Evaluation
Biota (continued)	Elimination	PCB Loss	• Metabolism	X		
			• Depuration	X		
			• Growth dilution	X		
			• Toxicity feedback loops		X	
	Biota Transport	Physical Movement or Disturbance	• Fish migration			X
			• Benthic drift	X		
			• Storms and scour	X		

1

4. MODELING FRAMEWORK AND APPROACH

The modeling framework was specifically developed to address each of the objectives of the Housatonic PCB fate and transport modeling effort as described in Section 1.2 and the requirements identified in the development of the conceptual model. In this section, the modeling framework and its significant components are described, including a summary of each of the models selected to represent the Housatonic watershed system, the physical domain of each model, and the manner in which the models will be linked to each other for hydrodynamic, sediment transport, and PCB fate and transport simulations.

4.1 THE MODELING FRAMEWORK

The Supplemental Investigation (WESTON, 2000a) is being performed to gather information for use in determining if remediation of areas contaminated with PCBs in the Lower River is necessary, and if so, where and to what extent. Addressing this complex question and other technical issues requires developing an appropriate modeling framework to serve as one of the primary technical tools for decisionmaking. Such a framework must be able to address both historical and future conditions and questions involving various remediation scenarios, including no action.

Furthermore, a modeling framework is needed because no single model is capable of representing all the physical, chemical, and biological processes that apply to this investigation over the wide range of spatial and temporal scales existing at the site, as illustrated in the previous discussion of the conceptual model for the site.

Figure 4-1 illustrates the basic modeling framework for this investigation, including the specific modeling codes and the purpose for which the code will be used. Within this framework, the watershed model, HSPF, encompasses the largest spatial extent of the system, the Hydrologic Study Area. The principal use of HSPF is to establish external boundary conditions for the models being applied within the Primary Study Area (PSA). The PSA is further modeled by the hydrodynamic/sediment transport model, EFDC, and the PCB bioaccumulation model,

1 AQUATOX. Thus, the EFDC and AQUATOX models are effectively nested within the larger

2 spatial domain of the HSPF model.
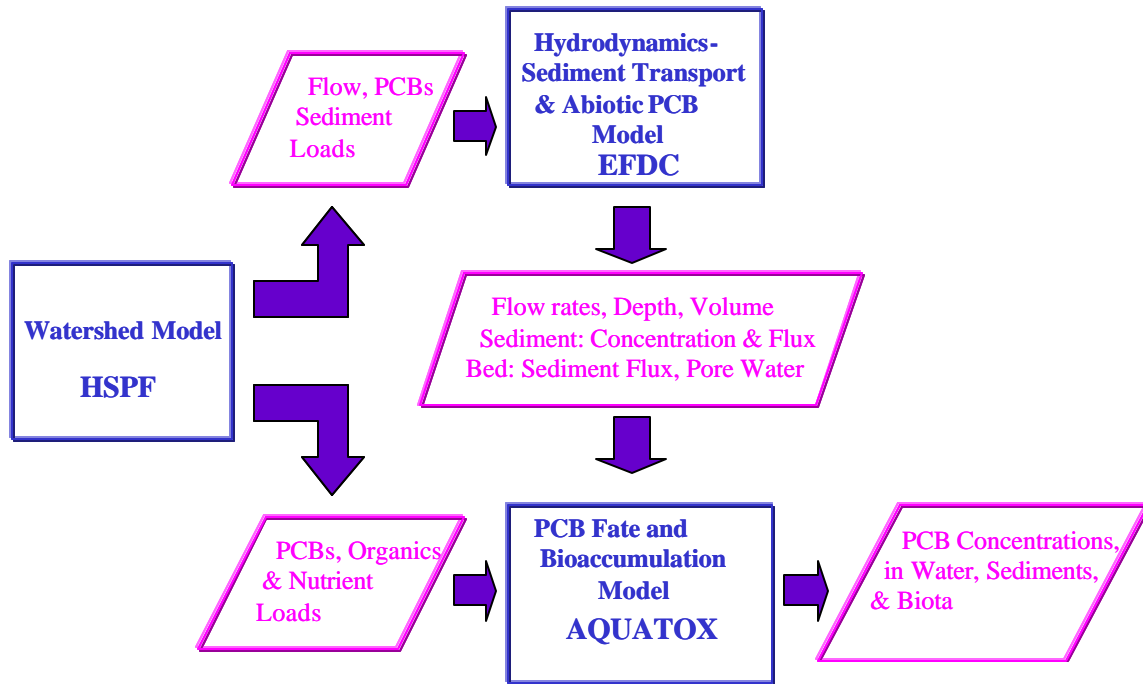
3
4 **Figure 4-1 Housatonic River PCB Modeling Framework**

5
6 Logically, the exchange of model outputs as inputs to other models will be aggregated in space

7 and time in a manner consistent with the spatial and temporal scales simulated by each respective

8 model. Thus, the outputs from the watershed model (HSPF) will serve as inputs to the

9 hydrodynamic/sediment transport model (EFDC), and the PCB bioaccumulation model

10 (AQUATOX). For example, surface and subsurface flows, solids, and PCB loading rates

11 simulated by the watershed model will be used to define loading inputs at specific locations

12 within the physical domains defined by EFDC and AQUATOX. Mass fluxes of water and solids

13 (deposition and resuspension, as separate fluxes) simulated by EFDC will subsequently be post-

14 processed as input to AQUATOX at a coarser spatial and temporal resolution, consistent with the

15 coarser segmentation scheme required by this model. A separate abiotic PCB fate and transport

16 component is included in EFDC. The abiotic PCB component is included in EFDC to evaluate

17 the consequences of the spatial and temporal aggregating scheme outlined in this conceptual

1   framework, and to serve as the mechanism to transport PCBs into the floodplain. Model linkage

2   issues are discussed in detail in Section 4.4.

3   The spatial domain, model time step, and the characteristics of each model are further identified

4   in Table 4-1. The "spatial domain" column in Table 4-1 defines the physical portion of the

5   watershed/river system represented by each model (greater detail, including the scale at which

6   the models are being applied, is provided in Section 4.3); the "time step" column shows the time

7   step of the internal model process calculations. The "constituents" column identifies the key

8   output variables calculated by each model, which are either inputs to the other models, outputs

9   that are compared with field observations as part of the calibration effort, and/or the critical

10 model predictions (e.g., PCB concentrations).

11 Figure 4-2 shows the Housatonic River watershed upstream of the U.S. Geological Survey

12 (USGS) gaging station (ID # 01197500) at Great Barrington, MA, an area of about 282 square

13 miles. Figure 4-2 also shows the mainstem of the Housatonic River, the major tributaries,

14 subbasin drainage areas, and the PSA represented by the 10-year floodplain (shaded area)

15 between the confluence of the East and West Branch and Woods Pond. An expanded view of the

16 area between Dalton and Woods Pond, including the PSA, is shown in Figure 4-3.

17   **Table 4-1**

18
19   **Housatonic River PCB Modeling System Components**

Model	System Component	Spatial Domain	Time Step	Constituents
HSPF	Watershed Hydrology and NPS Loads	Watershed area headwaters to Great Barrington, 282 square miles	Hourly	Flow, solids, PCBs, and nutrient loads
EFDC	Hydrodynamics, Sediment, and Abiotic PCB Transport	Confluence of East and West Branches to Woods Pond Dam	Variable, minutes	Flow, stage, abiotic PCBs and solids (cohesive and noncohesive)
AQUATOX	PCB Fate and Bioaccumulation	Confluence of East and West Branches to Woods Pond Dam	Variable; daily output	PCBs, DO, organic matter, nutrients, solids, detritus, aquatic biota

20
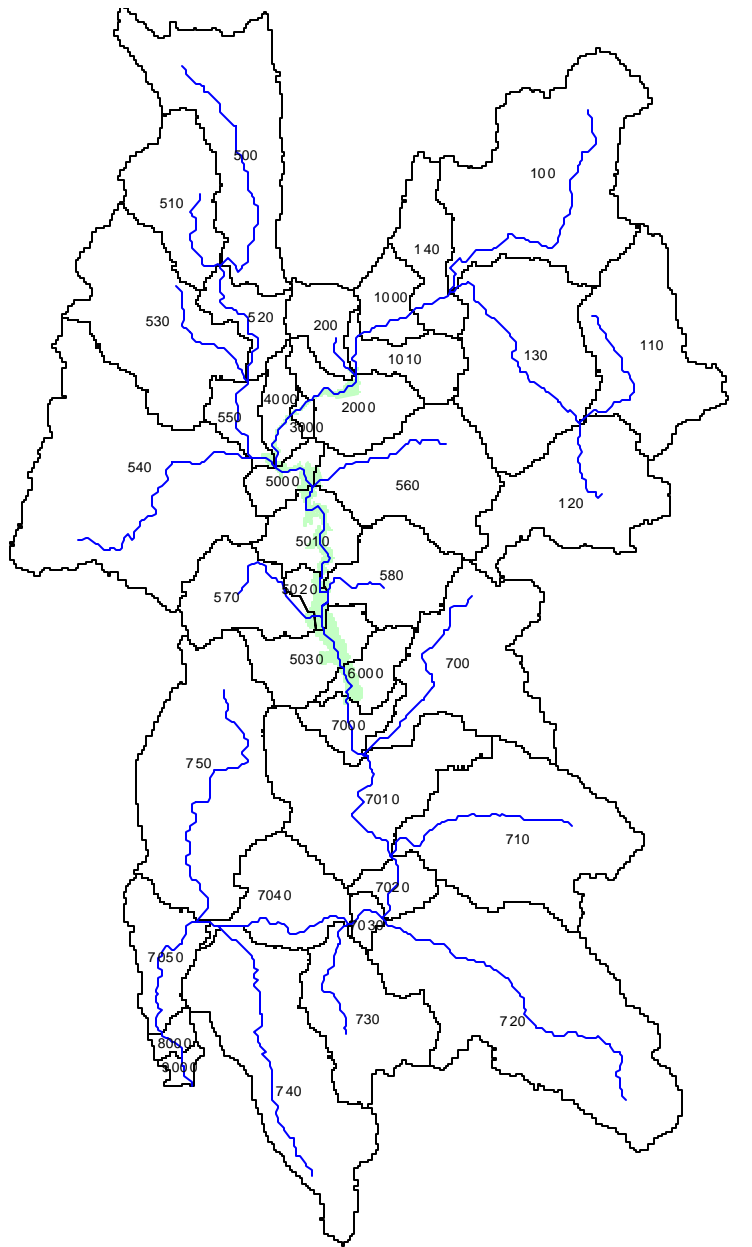
Figure 4-2 Housatonic River Watershed Segmentation
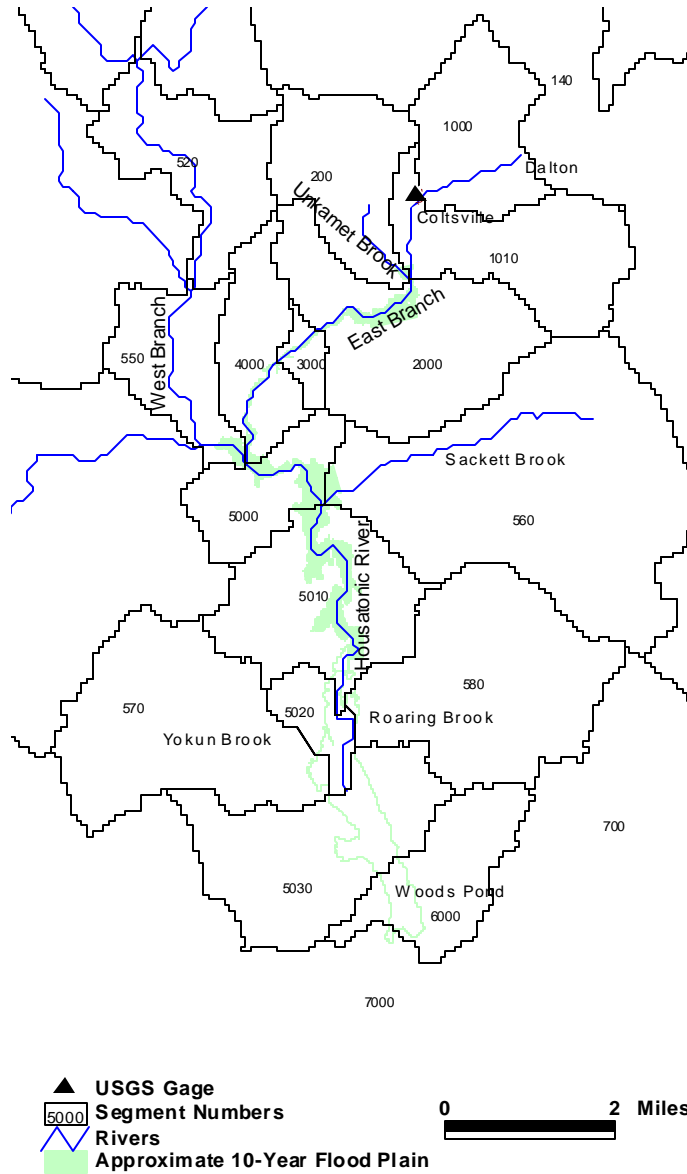
Figure 4-3 Watershed Model Segmentation Within the Primary Study Area

4.2　SUMMARY OF COMPONENT MODELS

The three component models are briefly described in this section, with an expanded discussion and additional source references for each model provided in the appendices (see Appendices B, C, and D).

4.2.1　HSPF

4.2.1.1　Overview

The Hydrological Simulation Program-FORTRAN, known as HSPF, is a mathematical model developed under EPA sponsorship to simulate hydrologic and water quality processes in natural and man-made water systems. It is an analytical tool that has application in the planning, design, and operation of water resource systems. The model enables the use of probabilistic analysis in the fields of hydrology and water quality management. HSPF uses such information as the time history of rainfall, temperature, evaporation, and parameters related to land use patterns, soil characteristics, and agricultural practices to simulate the processes that occur in a watershed.

Runoff flow rate, sediment loads, nutrients, pesticides, contaminants, and other water quality constituent concentrations can be predicted. The model uses these results and stream channel information to simulate instream processes. From this information, HSPF produces a history of water quantity and quality at any point in the watershed.

HSPF is one of the most comprehensive and flexible models of watershed hydrology and water quality currently available. It is one of very few models that can simulate either continuous, dynamic event, or steady-state behavior of both hydrologic/hydraulic and water quality processes in a watershed, with an integrated linkage of surface, soil, and stream processes. The model is also unusual in its ability to represent the hydrologic regimes of a wide variety of streams and rivers with reasonable accuracy. It has been applied to such diverse climatic regimes as the tropical rain forests of the Caribbean, the arid conditions of Saudi Arabia and the southwestern United States, the humid conditions of Europe and the eastern United States, and snow-covered regions of eastern Canada.

1 **Historical Development**

2   HSPF was first released publicly in 1980, as Release No. 5 (Johanson et al., 1980), by the EPA

3   Water Quality Modeling Center (now the Center for Exposure Assessment Modeling).

4   Throughout the 1980s and early 1990s, HSPF underwent a series of enhancements, culminating

5   in the release of Version No. 11 in 1997 (Bicknell et al., 1997). HSPF Version No. 12 (Bicknell

6   et al., 2000) is scheduled for final release in late 2000 with additional software and water quality

7   model algorithm enhancements funded by a variety of federal, state, and regional agencies.

8   Since 1981, the USGS has supported HSPF development work and has been developing software

9   tools to facilitate watershed modeling by providing interactive capabilities for model input

10 development, data storage and data analysis, and model output analysis including hydrologic

11 calibration assistance. The most recent major product of these efforts is the GenScn GUI

12 interface to HSPF (Kittle et al., 1998) designed to perform these interactive capabilities; GenScn

13 and HSPF Version No. 12 will be applied in this study.

14 Since its initial release in 1980, HSPF applications have been worldwide and number in the

15 hundreds; more than 50 current active applications continue around the world, with the greatest

16 concentration in North America. Numerous studies have been completed or are continuing in the

17 Pacific Northwest, the Washington, DC, metropolitan area, and the Chesapeake Bay region.

18 Today the model serves as the focus for cooperation and integration of watershed modeling and

19 model support efforts between EPA and USGS. HSPF was recently selected as the key

20 watershed modeling component for the EPA BASINS system (Lahlou et al., 1998), a tool for

21 supporting development of total maximum daily loads (TMDLs) required under Section 303(d)

22 of the Clean Water Act. In addition, HSPF is currently being incorporated into the USACE

23 Watershed Model System (WMS) (Deliman et al., 1999). Over the years, these development

24 activities, model enhancements, and model applications have continued to improve the model's

25 capabilities and preserve its status as a state-of-the-art tool for watershed analysis.

1   **Overview of HSPF Capabilities and Components**

2   HSPF contains three application modules and five utility modules. The three application
3   modules simulate the hydrologic/hydraulic and water quality components of the watershed. The
4   utility modules are used to manipulate and analyze time-series data. Table 4-2 summarizes the
5   constituents and capabilities of the HSPF application modules.

6   The three application modules within HSPF, and their primary functions, are as follows:

7   (1) PERLND—Simulates runoff and water quality constituents from pervious land areas
8   in the watershed.

9   (2) IMPLND—Simulates impervious land area runoff and water quality.

10   (3) RCHRES—Simulates the movement of runoff water and its associated water quality
11   constituents in stream channels and mixed reservoirs.

12   A variety of storage zones are used to represent the processes that occur on the land surface and
13   in the soil horizons. Snow accumulation and melt are also included in the PERLND module so
14   that the complete range of physical processes affecting the generation of water and associated
15   water quality constituents can be represented. Some of the many capabilities available in the
16   PERLND module include the simulation of:

17   ▪ Water budget and runoff components.
18   ▪ Snow accumulation and melt.
19   ▪ Sediment production and removal.
20   ▪ Accumulation and washoff of user-defined nonpoint pollutants.
21   ▪ Nitrogen and phosphorus fate and runoff.
22   ▪ Pesticide fate and runoff.
23   ▪ Movement of a tracer chemical.
24
25   IMPLND is used for impervious land surfaces, primarily for urban land categories, where little
26   or no infiltration occurs. However, some land processes do occur, and water, solids, and various
27   pollutants are removed from the land surface by moving laterally downslope to a pervious area,
28   stream channel, or reservoir. IMPLND includes most of the pollutant washoff capabilities of the
29   commonly used urban runoff models, such as the STORM, SWMM, and NPS models.

30   RCHRES is used to route runoff and water quality constituents simulated by PERLND and
31   IMPLND through stream channel networks and reservoirs. The module simulates the processes

Table 4-2

HSPF Application Modules and Capabilities

PERLND	IMPLND	RCHRES
Snow	Snow	Hydraulics
Water	Water	Conservative Constituents
Sediment	Solids	Temperature
Soil temperature	Water Quality*	Sediment
Water Quality*		Nonconservative Constituents
Pesticide		BOD/DO
Nitrogen		Nitrogen
Phosphorus		Phosphorus
Tracer		Carbon/pH
		Plankton

*Up to 10 user-specified water quality parameters.

1   that occur in a series of open or closed channel reaches or a completely mixed lake. Flow is

2   modeled as unidirectional. A number of processes and parameters can be modeled, including:

3   ▪ Hydraulic behavior.

4   ▪ Heat balance processes that determine water temperature.

5   ▪ Inorganic sediment deposition, scour, and transport by particle size.

6   ▪ Chemical partitioning, hydrolysis, volatilization, oxidation, biodegradation, and
7   generalized first-order (e.g., radionuclides) decay, parent chemical/metabolite
8   transformations.

9   ▪ DO and BOD balances.

10   ▪ Inorganic nitrogen and phosphorus balances.

11   ▪ Plankton populations.

12   ▪ pH, carbon dioxide, total inorganic carbon, and alkalinity.

13   *4.2.1.2*   *HSPF Data Requirements*

14   Data requirements for HSPF are extensive, in both spatial and temporal detail, especially for a

15   watershed of the size and complexity of the Housatonic. Table 4-3 lists the typical data

16   requirements for running an HSPF application on a river such as the Housatonic. Fortunately,

17   for this study an extensive database exists to support such an application. As noted in Section 3,

18   historical data collected by GE, EPA, USGS, and various state agencies, supplemented by the

19   ongoing data collection efforts of these same groups, provides a sound basis for the watershed

20   modeling effort.

21   **Precipitation and Meteorologic Data**

22   Precipitation is the primary driving force in any watershed modeling effort, followed in

23   importance by evaporation and air temperature; the remaining meteorologic data (listed in Table

24   4-3) are required for modeling snow accumulation and melt processes, and water temperature. In

25   Appendix F, Table F-8 shows the available precipitation and meteorologic data within and

26   neighboring the Housatonic River watershed. Long-term hourly precipitation data required to

27   drive the watershed modeling effort is limited to the National Weather Service (NWS) station at

1

Table 4-3

Data Requirements For Typical HSPF Model Applications

1.	**Precipitation and meteorologic data (for simulation period)**
	a. Hourly Precipitation
	b. Daily pan evaporation
	c. Daily maximum and minimum air temperature
	d. Total daily wind movement
	e. Total daily solar radiation
	f. Daily dewpoint temperature
	g. Average daily cloud cover
2.	**Watershed land use/land cover characteristics**
	a. Topographic map/data of watershed and subwatersheds
	b. Land use/cropping delineation and acreages
	c. Soils delineation and characteristics
3.	**Hydrography and channel characterization**
	a. Channel lengths and slopes
	b. Channel cross sections and geometry
	c. Channel bed composition
	d. Diversions, point sources, channelization segments, etc.
	e. Tributary area (and land use distribution) for each channel reach
4.	**Monitoring program observations**
	a. Flow rates during all monitored storm events
	b. Flow volume/rate totals for storm/daily, monthly, annual
	c. Sediment concentrations and mass losses in runoff
	d. Chemical concentrations and mass losses in runoff
	e. Soil concentrations of chemical/nutrient forms, if available
	f. Estimated/actual chemical concentrations in precipitation
	g. Particle size distributions (sand, silt, clay fractions) of soils and eroded sediments
5.	**Other useful information**
	a. Description/quantification of any other contaminant sources (e.g., point sources) or other relevant information (e.g., ponds, dams, marshes)
	b. Technical reports or articles that analyze and/or summarize the monitoring data
	c. Soils characterization information for estimating model parameters

2

1   Lanesborough, MA (in model segment #500, shown in Figure 3-2) in the northern portion of the

2   watershed, and the NWS stations at Littleville Lake, MA (about 20 miles east) and Copake, NY

3   (about 20 miles southwest). In addition, since 1994, GE has collected 15-minute and hourly data

4   at its Pittsfield facility; these GE data will be used extensively for the most recent time period

5   because it is the closest location to the PSA.

6   There are a number of currently active NWS stations with long-term daily precipitation data

7   surrounding the watershed, e.g. Great Barrington Airport, West Otis, Chesterfield, and Berlin

8   (see Table F-8). The standard practice in watershed modeling is to use the available hourly data

9   to distribute (or disaggregate) the daily records to derive estimated hourly records (and

10   distribution during the day) at these stations. Thus, the hourly data at Lanesborough and the GE

11   facility, supplemented by the Littleville Lake and Copake stations (as needed), will be used to

12   distribute these daily records into hourly values for use in neighboring portions of the watershed.

13   Pan evaporation data are used in watershed modeling to estimate total potential

14   evapotranspiration (PET), which includes both direct evaporation and plant transpiration

15   processes. Typically a "pan coefficient" is applied to the observed pan evaporation data, either

16   on an annual or monthly basis, to estimate PET; pan coefficients have been tabulated and

17   mapped for the conterminous U.S. by the National Weather Service (NWS, 1982a; 1982b). For

18   the Housatonic River watershed, the closest pan evaporation data are recorded at the Albany and

19   Hartford airports, which are approximately 30 miles northwest and southeast, respectively, from

20   the watershed (see Figure 1-1). Pan evaporation does not demonstrate much spatial variability,

21   and it is common practice to use pan evaporation data from such distances for watershed

22   modeling. The Albany and Hartford data will be supplemented and compared with recent pan

23   evaporation data collected by GE at its Pittsfield, MA, facility starting from 1999.

24   Daily maximum and minimum air temperature readings are collected at many of the same NWS

25   stations that collect daily precipitation; thus many of these same stations are listed in appendix

26   Table F-8 for air temperature. The hourly temperature data collected at the GE facility will be

27   used for the time period starting in 1994 with the daily data used for the earlier time periods.

28   The daily values are distributed to hourly by imposing a standard sinusoidal variation during the

29   day. Since hourly values are available at the GE facility, the standard sinusoidal distribution will

1   be checked with the GE data and adjusted as needed. In addition, air temperature values are

2   adjusted as a function of elevation differences between the gage site and the model segment.

3   For the remaining meteorologic data, i.e., solar radiation, wind, dewpoint temperature, and cloud

4   cover, observations at either Albany or Hartford will be used and supplemented with the

5   available GE Pittsfield data. Periods of missing data are typical of all meteorologic data; the

6   additional stations listed in Appendix F will be used to supplement those mentioned above and

7   fill in any missing periods.

8   **Watershed Land Use/Land Cover Characteristics**

9   The watershed land use and land cover data were discussed in Section 4.3.1 as part of the

10   watershed segmentation and characterization of the physical domain of the watershed model.

11   Based on the DEM data and procedures described in that section, Appendix D provides lists of

12   the segment areas, land uses and associated areas within each segment, and slopes for each

13   model segment. In addition, major soil types and characteristics, such as texture, erodibility,

14   bulk density, available water capacity, and hydraulic conductivity, can be identified and

15   tabulated for each model segment as a basis for parameterization.

16   **Hydrography and Channel Characterization**

17   Section 4.3.1 describes the model domains and identifies the procedures used to estimate the

18   major channel characteristics within each model segment; Appendix D lists the estimated

19   channel lengths, slopes, and elevation changes within each reach. This information will be

20   supplemented with cross-section data collected by EPA and GE, USGS rating curves (i.e., stage

21   versus discharge curves) for their gages within the watershed, the GE 1997 bathymetric survey

22   and bed sediment mapping data (QEA, 1998a, 1998b), and additional cross-section data needed

23   for the EFDC grid development. Within the channel module of HSPF, each stream reach is

24   represented by a hydraulic function table, called an FTABLE, that defines the flow rate, surface

25   area, and volume as a function of the water depth. Since HSPF uses a much simpler

26   representation of channel processes than EFDC, the data required for EFDC (discussed in

27   Section 4.6.2) are entirely adequate for the channel simulation data needs within HSPF. The data

28   currently developed and listed in Appendix D are considered "preliminary" because the reach

1   boundaries will be modified to coincide with specific EFDC grid cells and AQUATOX segments

2   when the spatial representation for both models is finalized.

3   **HSPF Data Requirements**

4   The HSPF watershed model calibration will rely on available data at the USGS Coltsville and

5   Great Barrington gages, supplemented with the synoptic and stormwater monitoring data

6   collection, both past and current, performed by Roy F. Weston, Inc., as part of the SIWP, and by

7   GE.   Observed data are required for all the constituents simulated by HSPF in this effort,

8   including flow, sediment, water temperature, DO, BOD, TOC, nutrients, and PCBs.

9   The hydrology calibration will focus primarily on the available continuous flow data at the two

10   USGS gages, and will perform consistency checks with synoptic flow measurements available

11   for selected tributaries and other monitoring sites within the PSA. Although Table 3-1 shows the

12   recent sediment and water quality data covering a period of years since 1994 and 1995, the data

13   are not continuous.   Consequently the watershed water quality calibration will rely on

14   comparisons of observed and simulated concentrations at selected sites and selected points in

15   time, covering a limited number of both storm and nonstorm periods.   The ongoing SIWP

16   stormwater sampling is designed to supplement the available historical data.   However, these

17   comparisons will be made within the overall mass balance approach and framework discussed in

18   Section 1.3 to ensure that a reasonable mass balance for flow, solids, and PCBs is represented

19   within the watershed model. Further discussion of the details of calibration and validation of

20   HSPF is presented in Section 4.5 of the Modeling Study QAPP (Beach et al., 2000).

21   **Initial Conditions**

22   Evaluation of initial conditions is less critical for the HSPF watershed model than for the EFDC

23   and AQUATOX models because the watershed is a self-contained, well-defined system not

24   impacted by external forces at its spatial boundaries (i.e., drainage basin). The driving forces are

25   meteorologic conditions, represented by the time series of precipitation, evaporation, and other

26   climate inputs, along with any anthropogenic inputs (e.g., point-source loads) and impacts. To

27   avoid any short-term effects of initial starting values of state variables (e.g., soil moisture

1 conditions), the model is usually run for many years, and starting conditions are then readjusted

2 to reflect state variable conditions at comparable times during subsequent years of the model run.

3 For example, if the model run starts on 1 October, soil moisture conditions at the beginning of

4 October for subsequent years will be evaluated as a basis for readjusting the starting moisture

5 conditions of the run. Climate conditions prior to the model run will also be checked to assess

6 whether further adjustments are needed. In most cases, starting values will only impact model

7 simulations for a short time period (e.g., a few weeks to a few months), and often simulations are

8 begun 6 months to a year before the period of interest to avoid any potential impacts of the

9 starting condition values.

10 **4.2.2 EFDC**

11 *4.2.2.1 Overview*

12 The Environmental Fluid Dynamics Code (EFDC), a public domain model sponsored by the

13 Commonwealth of Virginia and EPA, is a 3-D computational physics model that incorporates

14 modules for hydrodynamics, sediment transport, contaminants, and eutrophication/water quality

15 within a single source code (Hamrick, 1992a; 1992b). Figures 4-4 and 4-5 present schematic

16 diagrams of the conceptual linkage in EFDC between the hydrodynamic, sediment transport, and

17 contaminant submodels that will be applied in the Housatonic River study.

18 EFDC uses a finite difference spatial grid scheme to represent the physical domain of a

19 waterbody as a fully 3-D domain; lateral or vertical averaging is used to represent a waterbody in

20 either one-dimensional (1-D) or two-dimensional (2-D) domains. The physical domain is

21 represented in the vertical domain using a stretched ("sigma") coordinate scheme and in the

22 horizontal domain the waterbody is represented with either (a) cartesian; (b) boundary fitted,

23 curvilinear-orthogonal grid schemes, or c) some combination of the two.

24 EFDC can be executed in two modes: (1) fully coupled mode with simultaneous computation of

25 hydrodynamics, sediment and contaminant transport and fate, or (2) hydrodynamic transport-
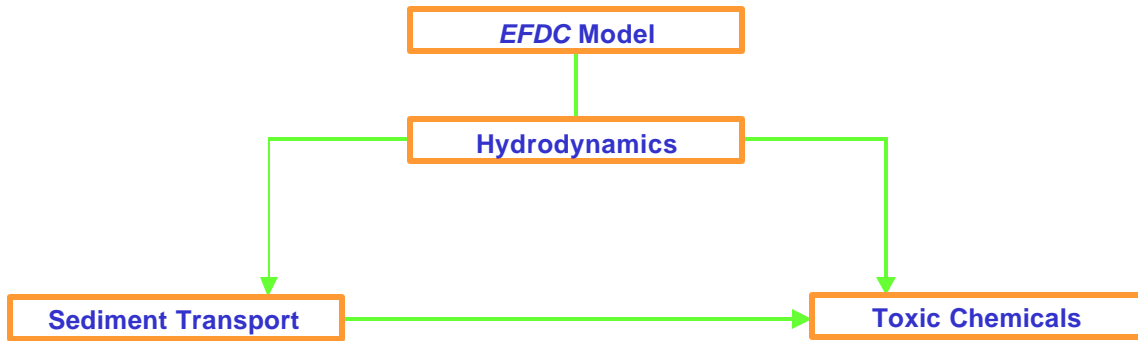
Primary Sub-Models of the EFDC Model
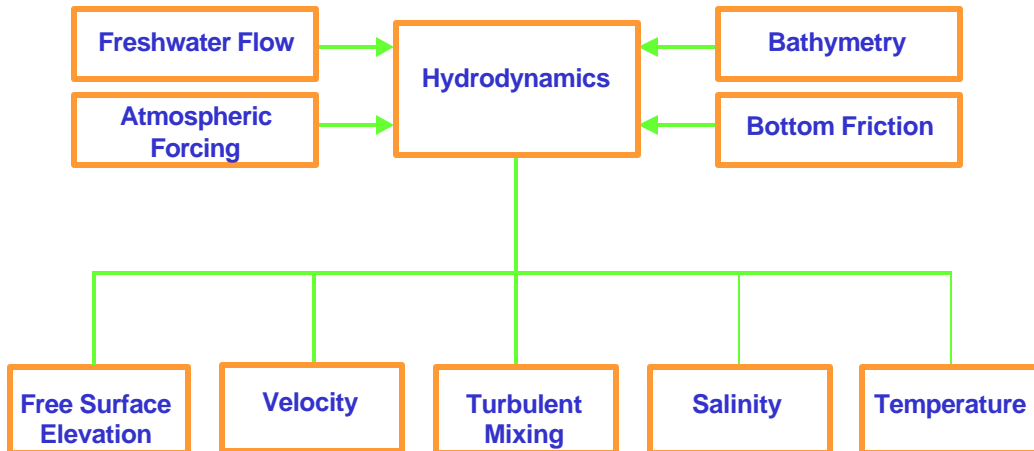
Structure of the EFDC Hydrodynamic Model

Figure 4-4 Structure and Modules of the EFDC
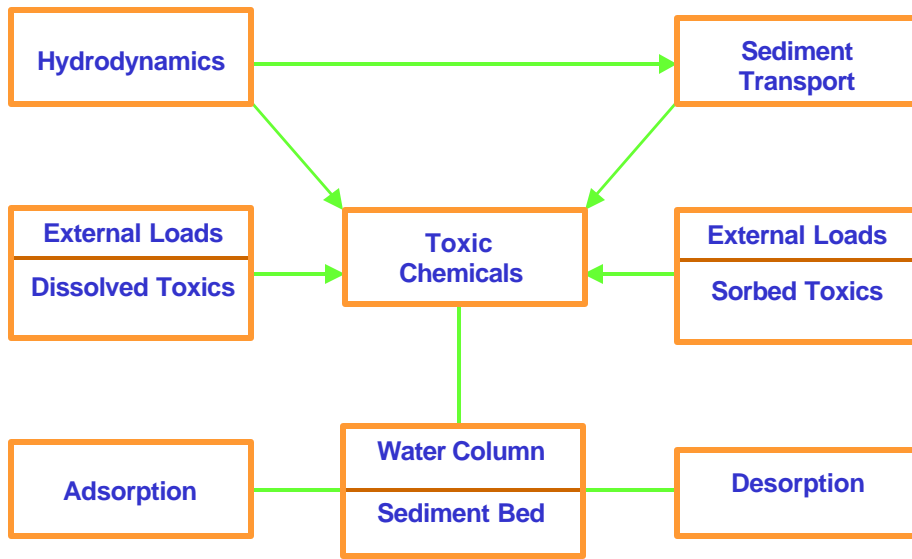
Model Structure of the EFDC Sediment Transport Model
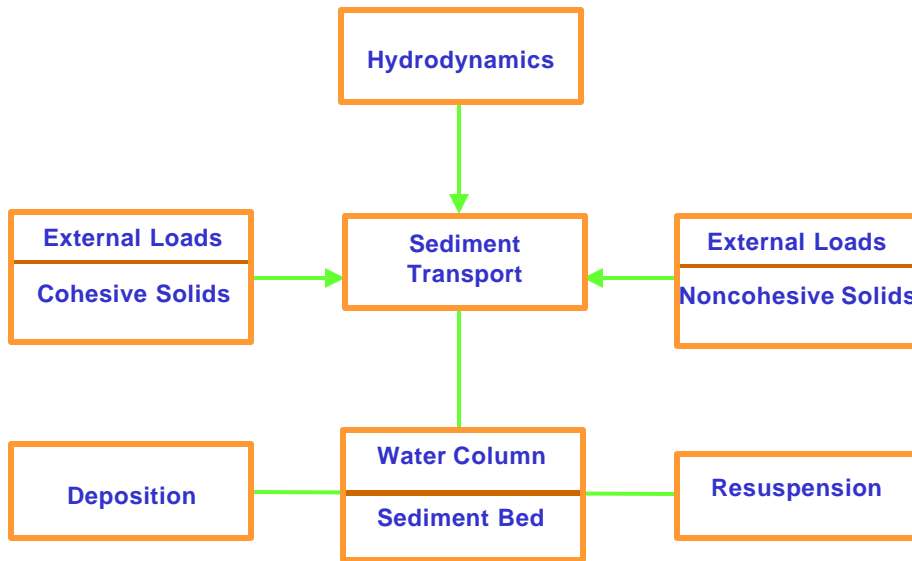
Structure of the EFDC Toxic Model for Abiotic PCBs

**Figure 4-5 Structure of EFDC Sediment Transport Model
and Toxic Model for Abiotic PCBs**

1   only mode with the distribution of sediments and chemical constituents simulated by using saved

2   hydrodynamic data as an external input file to drive the constituent transport and fate submodels.

3   The computational techniques used in EFDC have been shown to be very efficient (Hamrick and

4   Wu, 1997) in benchmark tests of internal processing speed where EFDC executed about a factor

5   of two faster (Wu et al., 1997c) than the well-known ECOM3D model (Blumberg and Mellor,

6   1987).

7   EFDC has been extensively tested and applied for many modeling studies of hydrodynamics,

8   sediment transport, contaminants, and eutrophication in complex marine (e.g., Chesapeake Bay,

9   Hamrick, 1994a) and freshwater (e.g., Florida Everglades, Hamrick, 1994b) ecosystems.

10 EFDC has been applied in estuarine cohesive sediment transport simulations (Yang, 1996; Tetra

11 Tech, 1999c) and coastal noncohesive sediment transport (Zarillo and Surak, 1995). The model

12 is currently being applied to investigate cohesive sediment transport in Lake Okeechobee, FL

13 (Hamrick, 1996b). EFDC has been applied for simulations of solids and metals transport and

14 fate in the Blackstone River (Tetra Tech, 1999a) and solids, metals, and organic contaminants

15 transport and fate in the Duwamish Waterway-Elliott Bay in Puget Sound (Tetra Tech, 1998).

16 An overview of the key processes of the hydrodynamic, sediment transport, and contaminant

17 submodels of EFDC is presented below. The features of EFDC used for the Housatonic River

18 study are described in Appendix C.1. The theory and formulations incorporated in the sediment

19 transport model (Tetra Tech, 2000d) are described in Appendix C.3. Complete descriptions of

20 the options available in EFDC are presented in the user's manual (Hamrick, 1996a). Technical

21 details of the theory and model formulations for the hydrodynamic model are found in Hamrick

22 (1992a). The model formulations in EFDC for the toxic contaminant submodel are detailed in

23 Tetra Tech (1999e).

24 **Hydrodynamics**

25 The hydrodynamic component of EFDC simulates the 3-D equations of motion based on

26 conservation of mass and momentum to compute velocity and turbulent mixing in the horizontal

27 and vertical domains.   The physics of the EFDC model, as well as many features of the

1 computational schemes, are functionally equivalent to the well-known Blumberg and Mellor

2 (1987) model of hydrodynamics. Designed for application to marine or freshwater systems,

3 EFDC solves the 3-D vertically hydrostatic, free surface, turbulent averaged, coupled barotropic,

4 and baroclinic equations of motion for a variable density field. Dynamically coupled transport

5 equations for turbulent kinetic energy and turbulent length scale, solved using two turbulence

6 parameter transport equations, are based on Galperin's et al. (1988) modification of the Mellor

7 and Yamada (1982) level 2.5 turbulence closure scheme. These formulations are used to

8 simulate eddy viscosity and diffusivity in the vertical direction. The bottom stress formulation

9 for friction, describing the rate of momentum loss at the sediment bed-water interface, is

10 represented using a turbulent boundary layer formulation via a quadratic function of near-bottom

11 velocity.

12 Salinity and water temperature are solved as an integral part of the hydrodynamic model with

13 heat transport simulated using the atmospheric heat exchange model developed by Rosati and

14 Miyakoda (1988) at the NOAA Geophysical Fluid Dynamics Laboratory. Enhancements to

15 EFDC have been designed to allow for specification of (a) wetting and drying of shallow areas

16 using a mass-conserving scheme for applications for wetlands, tidal flats, or floodplains and (b)

17 discharge control structures such as weirs, dam spillways, and culverts. For the simulation of

18 flow in heavily vegetated areas, such as wetlands or riverine floodplains, EFDC uses a

19 formulation developed for the Florida Everglades (Hamrick, 1994b) to represent vegetation

20 friction resistance.

21 The dominant physical factors that will influence hydrodynamic transport in the Housatonic

22 River are changes in topographic elevation of the riverbed (i.e., channel slope), bottom friction

23 from the sediment bed, the extreme sinuosity of numerous meanders within a wide floodplain,

24 and the presence of backwaters and a broad impoundment created by the Woods Pond Dam.

25 The computational burden for an EFDC riverine application to an area of the scope and nature of

26 the Housatonic River is anticipated to be quite large. Work is being conducted to investigate

27 code enhancements and model constructs to improve model computational efficiency. Areas

28 being investigated are parallel processing, coding optimizations/streamlining, variable

1 timestepping schemes, and stepped hydrodynamics. Changes to the code will undergo thorough

2 third-party review and testing and will become part of the calibration report.

Sediment Transport

4 The sediment transport module of EFDC allows for specification of multiple size classes to

5 describe both cohesive and noncohesive solids. The transport of solids suspended in the water

6 column is based on the same advection and diffusion scheme that is used for heat transport (i.e.,

7 water temperature) and salinity in the hydrodynamic model. The transport of solids in the

8 sediment bed (bedload) by sliding, rolling, or saltation on, or near, the bed is based on near-

9 bottom velocity and the particle size and density characteristics. The transport of solids in the

10 river is thus governed by the external supply of solids washed from the watershed and the

11 internal supply of solids from the sediment bed.

12 Solid particles in natural waters, described using characteristic size fractions as (a) cohesive silts

13 and clays (less than 63 microns) and (b) coarser noncohesive materials (63 to 250 microns, and

14 greater than 250 microns), settle out of the water column as a result of gravitational force.

15 Depending on the force of the ambient flow conditions, particles can also be eroded from the

16 sediment bed and resuspended into the water column. At low solids concentrations, the settling

17 velocity for noncohesive solids is primarily dependent on the discrete particle size. Under high

18 solids concentrations, the settling velocity of noncohesive materials can be reduced by hindered

19 settling conditions near the riverbed (van Rijn, 1984; Cao et al., 1996).

20 At the water column-sediment interface, the net vertical flux of noncohesive solids is controlled

21 primarily by the shear stress of near-bottom flow and the particle size and density of the

22 noncohesive materials in the surficial sediments. Under equilibrium conditions for flow and

23 solids loading, the water column equilibrium concentration of noncohesive solids can be

24 functionally described using particle size and density, bed stress, and vertical turbulent

25 diffusivity (Garcia and Parker, 1991; Smith and MacLean, 1977; Van Rijn, 1984). Under

26 nonequilibrium conditions, the net flux of noncohesive sediment between the bed and the water

27 column is dependent on the near-bed settling velocity and the gradient between the equilibrium

28 and actual near-bed concentration.

1   The settling behavior of cohesive particles is quite complex since individual cohesive particles

2   may flocculate into larger clumps of material that have very different settling characteristics than

3   the individual particles that make up the floc. As an alternative to computationally intensive

4   "first principle" models that are under development for describing settling of cohesive particles,

5   the settling velocity of flocs has been parameterized into empirical functional relationships

6   (Ariathurai and Krone, 1976; Hwang and Mehta, 1989; Ziegler and Nisbet, 1994; Shrestha and

7   Orlob, 1996) in terms of fundamental particle size, cohesive solids concentration, and shear

8   characteristics of the turbulent flow regime.

9   Net deposition of cohesive materials between the water column and sediment bed is related to

10   the flow-induced bed surface stress and the properties of the cohesive material. As bed stress

11   decreases in relation to a critical shear stress for deposition of cohesive particles, the probability

12   of particle deposition tends to increase. Resuspension of cohesive solids from the bed into the

13   water column occurs by (a) mass and (b) surface erosion modes. Mass erosion occurs rapidly

14   when the flow-induced bed shear stress exceeds the depth-dependent shear strength of the

15   sediment bed. Surface erosion, in contrast, occurs slowly when the bed stress is less than the bed

16   shear strength near the surface but greater than a critical resuspension stress dependent on the

17   shear strength and density of the bed.

18   The sediment bed may be represented in EFDC with either a single-surface sediment layer or

19   multiple sediment layers. The multiple-layer sediment bed is represented by a user-specified

20   maximum number of layers having time-varying thicknesses and porosity or void ratio. The

21   void ratios of the multiple layers are either (a) specified as input by the user or (b) determined

22   internally by an empirical relationship or dynamic bed-consolidation model. Vertical transport

23   of sediment and sorbed contaminants (such as PCBs) between bed layers is implicitly

24   represented by sediment particle displacement in response to layer thickness variations

25   dynamically determined by the bed consolidation formulation. The multiple-layer bed enables a

26   relationship of time-since-deposition as a function of the depth in the sediment bed to be

27   established. Changes in the water column-sediment bed interface elevation can also be

28   incorporated as an option in the hydrodynamic model to provide bathymetric feedback to the

29   continuity equation.

Contaminants

With many contaminants (such as PCBs) exhibiting preferential partitioning onto solids, the chemical submodel of EFDC is designed to be coupled with the sediment transport submodel, with the contaminants represented as abiotic constituents. The chemical submodel enables the mass balance simulation of contaminants in both the water (dissolved) and sediment (particulate) phases of the water column and the sediment bed. Water-sediment phase interactions are represented by either equilibrium partitioning or nonlinear sorption processes. With the sediment bed described by multiple layers, sediment bed water volume and dissolved contaminant mass balances allow contaminants to be transported back into the water column by sediment resuspension, pore water expulsion due to bed consolidation, and pore water diffusion.

4.2.2.2   EFDC Data Requirements

The modules of the EFDC model that will be used for the Housatonic River study include the hydrodynamic, sediment transport, and abiotic PCB transport and fate submodels.

The hydrodynamic model requires physical information to describe grid cell geometry, inflows and outflows of water, bottom friction and elevations of the water surface and the riverbed, and other physical forcings (e.g., hydraulic control structures) that influence the transport of water in a riverine environment. The sediment transport model requires data to describe the spatially and temporally varying cohesive and noncohesive sediment distributions in the riverbed and the water column.

The sediment transport model requires specification of the cohesive and noncohesive sediment characteristics of solids loading from point and nonpoint sources to the river. Information is also needed to parameterize the depositional and erosional characteristics of cohesive and noncohesive sediments to simulate the vertical transport of solids between the water column and the riverbed.

The abiotic PCB model requires data to describe the spatially and temporally varying distributions of PCBs in the riverbed and the water column. The abiotic PCB model, representing both dissolved and sorbed contaminants, requires data to define the transfer of PCBs

1   between the dissolved and particulate phases via equilibrium partitioning, and transfer between

2   the water and atmosphere via volatilization if implemented.

3   **Hydrodynamic Model**

4   EFDC requires the following physical input data for the hydrodynamic simulation:

5   <u>**Horizontal Grid Specification**</u>

6   ▪ **Grid Cell Geometry**—Water surface elevation, riverbed and floodplain elevations,
7   and initial conditions of water depth, volume, length, and width are specified for each
8   EFDC grid cell in the physical domain of the Housatonic River study area. Physical
9   data will be obtained from cross-section surveys of (a) numerous transects taken
10   along the Housatonic River in the vicinity of Pittsfield, MA, upstream of the
11   confluence, (b) transects taken to characterize topography and channel depths for the
12   meanders, backwaters, floodplain, and Woods Pond, and (c) the data provided by GE
13   from its 1997 monitoring and bathymetric/bed sediment survey (QEA, 1998a, 1998b).

14   Bathymetric data are needed to define the spatial variation of water column depth in Woods

15   Pond and the backwater areas upstream of Woods Pond. Very detailed bathymetric data for

16   Woods Pond and the backwater areas are available from a survey conducted for this study in

17   December 1998. The survey data from December 1998 will be used to characterize the spatial

18   distribution of depth in Woods Pond and the backwater areas for the EFDC simulation of

19   "contemporary" conditions circa 1998-1999. Comparable detailed bathymetric data for Woods

20   Pond and the backwaters are not available for the representation of historical conditions circa

21   early 1980s.

22   The net sediment accumulation rate in Woods Pond has been estimated based on sediment core

23   measurements of cesium-137, lead-210, and beryllium-7. Using detailed bathymetry data and

24   sediment thickness measured in 1998 in combination with estimates of the net sediment

25   accumulation rate extrapolated over a period of ~20 years, estimates of the bottom depths of

26   Woods Pond will be developed to represent bathymetry for the simulation of historical

27   conditions circa early 1980s. For the simulation of projected PCB distributions under various

28   remediation alternatives, the 1998 bathymetric data set will be used to define the initial

29   conditions of bottom depth of Woods Pond and the backwater areas. Over the decadal time scale

30   that will be used for remediation scenarios, the bottom depths of Woods Pond and the backwater

1   areas will progressively change as a simulated response to continued net sediment accumulation

2   in the pond.

3   ■ **Grid Cell Connectivity**—The horizontal connectivity of each EFDC grid cell is
4   defined by identification of one of the following types of cells represented in the
5   physical domain: water cell; "wetting and drying" cell; land cell adjacent to water
6   cell; or dry land cell. Grid cell types will be identified by overlaying the EFDC
7   discretization grid scheme with GIS files to define EFDC grid cells types as 10-year
8   floodplain, the main river channel, the backwater areas, and Woods Pond.

9   **Initialization Data**

10   ■ **Initial Conditions**—The initial spatial distributions of water surface elevations and
11   chlorides must be defined to start the simulation. Data to define initial surface water
12   elevations will be obtained from stage height versus streamflow rating curves
13   developed for various reaches of the river. Data to define the initial salt distribution
14   will be obtained from available water quality monitoring records to characterize
15   chloride distributions in the Housatonic River.

16   **Forcing Functions and Boundary Conditions**

17   ■ **Forcing Functions and Boundary Conditions**—Time series (uniform or non-
18   uniform) are defined to describe the temporal variability of: (a) meteorologic and
19   climatologic data (incident solar radiation, air temperature, precipitation,
20   evapotranspiration, winds); (b) water surface elevation; (c) freshwater inflows and
21   outflows; and (d) concentration of chlorides. The same time series of meteorological
22   and climatological data sets that are used as input to the HSPF watershed model will
23   also be used as input to EFDC to simulate water temperature. Time series of
24   freshwater inflow and chlorides will be provided by linking the output from the
25   coarse HSPF transport reaches as input to the finer spatial resolution of EFDC grid
26   cells. HSPF will provide water inflow to EFDC as time series of surface runoff and
27   subsurface inflows based on simulation results generated for each coarse HSPF
28   transport reach. Both surface and subsurface inflow data will be normalized by the
29   length scale of the long HSPF reaches for input as a unit inflow rate ($m^3 s^{-1} m^{-1}$) to the
30   much shorter length of the EFDC grid cells.

31   **Physical Processes**

32   ■ **Vegetation Resistance**—The frictional influence of vegetation will be represented by
33   parameterization of empirical relationships describing natural flow in heavily
34   vegetated waterways (Hamrick, 1994b). This feature will be used to characterize
35   overland flow within grid cells defined for the 10-year floodplain. Existing wetland
36   delineation, vegetation surveys, and aerial photographs of the floodplain will be used
37   to estimate appropriate vegetative parameter values assigned to floodplain grid cells
38   to distinguish between differing vegetation types.

39   ■ **Soil Moisture Model**—A simple soil moisture model, typically used for wetland
40   simulations (Hamrick, 1994b), can be used to describe the temporal and spatial

variation of soil moisture within an active zone below each "wetting and drying" grid cell. The effective porosity of the soil layer and a maximum infiltration rate are the key parameters needed to describe the amount of water that can be stored within the soil layer. This feature may be needed to represent the water balance within the "wetting and drying" grid cells of the 10-year floodplain.

- **Hydraulic Control Structures**—Flow between upstream and downstream pairs of grid cells can be controlled by hydraulic structures such as dams, weirs, or spillways and pumping stations. This feature of EFDC will be used in the Housatonic River model to define streamflow over the Woods Pond Dam at the downstream boundary of the physical domain. A rating curve for the dam will be developed to describe streamflow over the Woods Pond Dam spillway as a function of the water surface elevation (stage height) at the dam using the specifications that were established at the time of construction of the dam.

Sediment Transport Model

EFDC requires the following input information for sediment transport simulations. Solids will be defined in the Housatonic River model using three particle size classes to represent cohesive (< 63 microns) and two classes of noncohesive (63-250 microns; > 250 microns) solids.

- **Water Column Initial Conditions**—Initial concentrations for each cohesive and noncohesive solids class are assigned to each model grid cell. This information will be obtained from particle size distributions and water column TSS monitoring samples. Grain size distribution data will be used to estimate the fraction of total solids that is assigned to the cohesive and noncohesive size classes along the length of the river.

- **Sediment Bed Conditions**—The riverbed will be characterized by multiple sediment layers consisting of a surficial "active" layer and one or more "deep" sediment layers. The vertical thickness, bulk density, and solids class distributions for each riverbed layer for each horizontal grid cell is required for each size class of particles. This information will be determined from sediment core data taken at numerous station locations in the river. EFDC will internally compute the corresponding void ratios and bulk densities.

In situ field data are being collected for this project to characterize bulk density, water content, mean particle size, organic carbon content, critical shear stresses, and erosion rates for a number of locations along the Housatonic River. Since a first-principles model is not available to describe solids deposition and resuspension, a number of empirical models have been developed to represent these processes. Empirical model parameter values determined from field data are thus essential to develop a credible model of cohesive and noncohesive solids transport in the Housatonic River.

Depth-dependent erosion rates and critical shear stress measurements needed for input to EFDC will be obtained using a device called a Sedflume initially developed and tested by McNeil et al. (1996), and a Particle Entrainment Simulator (PES) (Tsai and Lick, 1986). In contrast to data obtained from field measurements of the resuspension potential measured using "shaker" (PES) tests where shear stresses are limited to less than 10 dynes cm^{-2}, the experimental approach of McNeil et al. is designed to provide a characterization of depth-dependent erosion rates and critical stresses for sediment cores ~2 meters thick over a wide range of bottom shear stresses (~1-100 dynes cm^{-2}) that are characteristic of ambient conditions in rivers and lakes. The results of the Sedflume experiments and the PES tests will be used to define the depth-dependent critical stresses that result in resuspension of discrete particles and mass erosion of bottom sediments.

- **Solids Loads**—Time series of inflowing suspended solids loads and concentrations corresponding to point and nonpoint source inflows from surface runoff, tributaries, and wastewater treatment dischargers are required to define external inputs of cohesive and noncohesive solids. The time series of total suspended solids loading that is generated by HSPF will be split to represent the proportion of total solids loading assigned to the cohesive and noncohesive size classes for input to EFDC. Observed grain size distribution data obtained from TSS samples with corresponding streamflow measurements taken from the mainstem of the Housatonic River and selected tributaries will be used to estimate flow-dependent fractional splits of TSS as cohesive and noncohesive solids.

- **Noncohesive Sediment Processes**—Representative particle diameter, density, specific volume, specific gravity, and a reference settling velocity will be assigned to the noncohesive solids class. User-specified critical shear stress, derived from experiments performed on site sediments, will control particle deposition and resuspension processes. EFDC internally computes an equilibrium concentration of noncohesive sediment for simulation of a net flux of particle deposition and resuspension that accounts for hindered settling under high solid concentrations near the riverbed. A constant bed porosity is assigned that is also used to represent the porosity of noncohesive solids being deposited in the riverbed.

   In the riverbed, a maximum concentration (as mass per total volume) of noncohesive solids is assigned for the bed consolidation model. Riverbed armoring by noncohesive solids can be represented in the model using formulations described by Garcia and Parker (1991), van Rijn (1984), and Smith and MacLean (1977). It is expected that the van Rijn formulation will be used if armoring is included in the model. For the single class of noncohesive solids that will be represented, EFDC restricts the thickness of the surface bed equal to the dimensional reference height defined by the user as a multiple of the grain size diameter assigned to noncohesive solids.

- **Cohesive Sediment Processes**—Representative solids density, specific volume and specific gravity, and a reference settling velocity will be assigned to the cohesive size class of solids. A user-specified, or selected, relationship between settling velocity,

1 cohesive solids concentration, and ambient shear or turbulent intensity is used in
2 EFDC to describe the net flux of deposition and resuspension. A user-specified, or
3 selected, relationship between shear strength, surface erosion rates, and surface
4 erosion critical stresses and bed bulk density is used to simulate resuspension
5 processes. User-specified critical boundary stresses are defined for deposition and
6 resuspension. Surface erosion is represented with user-specified data to describe the
7 reference rate for surface erosion and the boundary stress above which surface
8 erosion occurs. Bulk sediment properties, erosion rates, and critical boundary stresses
9 will be obtained from the site-specific field measurements. For the empirical bed
10 consolidation model, the ultimate void ratio and the consolidation time scale must be
11 specified. For the dynamic bed consolidation model, functional relationships between
12 bed compressibility, hydraulic conductivity, and void ratio must be provided as input
13 to the model. Maximum and minimum fluid mud concentrations of cohesive solids
14 are assigned for the bed representation. The void ratio of cohesive solids deposited to
15 the bed is assigned as is a minimum bed void ratio for cohesive solids.

16 **Abiotic PCBs Transport and Fate Model**

17 PCBs will be modeled in EFDC as total PCBs. The transport and fate of PCBs in EFDC will be

18 represented only by abiotic processes. Dissolved and particulate phases of PCBs will be

19 transported via advection and turbulent mixing. PCB fate will be described by equilibrium

20 partitioning for sorption and desorption between contaminants and solids, settling and

21 resuspension of sorbed PCBs, potentially volatilization between the water surface and the

22 atmosphere, and kinetic degradation. Biotic processes that influence the distribution and fate of

23 PCBs will be represented in AQUATOX with mass loading of PCBs provided by HSPF and

24 mass fluxes of water and solids provided by EFDC as external loads. EFDC requires the

25 following input data for PCB transport and fate simulations:

26 ▪ **Water Column Initial Conditions**—Initial total PCB concentrations in the water
27 column will be assigned to each model grid cell. Partition coefficients assigned to the
28 noncohesive and cohesive solids classes will be used internally in the model to
29 compute the dissolved and solid phases of PCBs.

30 ▪ **Sediment Bed Initial Conditions**—The riverbed will be characterized by multiple
31 sediment layers consisting of a surficial "active" layer and one or more "deep"
32 sediment layers. Total PCB concentration for each riverbed layer and each horizontal
33 grid cell is required. This information will be determined from depth-dependent PCB
34 measurements taken from sediment core data. EFDC will internally compute the
35 corresponding dissolved and particulate phases of PCBs from partition coefficients.

1   ■ **PCB Loads**—Time series of PCB loading rates corresponding to point and nonpoint
2   source inputs from surface runoff, groundwater-influenced flux, tributaries, municipal
3   and industrial wastewater treatment dischargers, and atmospheric deposition (wet and
4   dry) are required to define external inputs of the PCBs to EFDC. The time series of
5   surface runoff of PCB loads generated for each coarse HSPF transport reach will be
6   used with estimates of the dissolved and particulate fractional splits to define the
7   input data needed for the finer resolution EFDC grid cells. The time series of
8   subsurface discharge rates simulated in HSPF for assignment to each EFDC grid cell
9   will be coupled with estimates of the pore water PCB concentrations to generate the
10   loading rates of dissolved PCBs from subsurface inflows to the river. For the long-
11   term simulation projections of remediation scenarios, spatial and temporal
12   distributions of pore water PCB concentrations will be defined to reflect each
13   remediation scenario.

14   ■ **Abiotic Processes**—Equilibrium partitioning coefficients will be assigned for the two
15   noncohesive and cohesive solids classes. Separate data sets describing equilibrium
16   partition coefficients must be specified for the water column and the riverbed. First
17   order degradation rates will be assigned for both the water column and sediment bed.

18 The evaluation of site-specific data for PCB concentrations, sediment grain size, and sediment

19 organic carbon content raises the possibility of another mode of transport for the PCBs beyond

20 the traditional PCB sorption process as a function of solids and/or organic carbon. This

21 evaluation is ongoing, and when complete, the results may require the reassessment of the

22 approach for modeling abiotic PCBs (see Figure 3-1).

23 **4.2.3 AQUATOX**

24 *4.2.3.1   Overview*

25 The AQUATOX model represents the combined environmental fate of conventional pollutants,

26 such as nutrients, and contaminants in aquatic ecosystems. It has been used in modeling streams,

27 ponds, lakes, and reservoirs. It incorporates several trophic levels, including attached and

28 planktonic algae and submerged aquatic vegetation, zoobenthos and zooplankton, and

Phosphate	Ammonia	Nitrate and Nitrate	Carbon Dioxide	Oxygen

Filamentous Algae and Duckweed	Phytoplankton	Periphyton	Rooted Macrophyte
Toxicant	Toxicant	Toxicant	Toxicant

Zoobenthos Gatherer/Filterer midges, sphaerids, oligochaetes	Zoobenthos Grazer/Shredder mayflies, snails	Herbivorous Zooplankton cladocerans	Predatory Invertebrate dragonflies, crayfish
Toxicant	Toxicant	Toxicant	Toxicant

Bottom Fish carp/goldfish brown bullhead, white suckers	Forage Fish shiner, pumpkinseed	Piscivore yellow perch	Multi-Aged Piscivore bass
Toxicant	Toxicant	Toxicant	Toxicant

Dissolved Organic Matter	Dissolved Organic Toxicants (up to 20)	Suspended Detritus
Toxicant		Toxicant

Sediment Detritus	Suspended and Sedimented Cohesive Inorganics	Dissolved and Colloidal Pore Water Toxicants	Suspended and Sedimented Noncohesive Inorganics	Noncohesive Inorganic Bedload
Toxicant	Toxicant		Toxicant	Toxicant

00M-0320 USEPA GE.ppt

Figure 4-6 Compartments (State Variables) in AQUATOX

forage, bottom-feeding, and game fish; it also represents associated organic contaminants (Figure 4-6). Relevant previous applications include validation with data on the fate and effects of pesticides in Minnesota and Israeli pond mesocosms (Park, 2000), verification with PCB data from East Fork Poplar Creek, Tennessee (Park, unpub.), and validations with PCB data from Lake Ontario and pesticide data from Coralville Reservoir, Iowa (EPA, 2000c).

AQUATOX represents the aquatic ecosystem (Figure 4-7) by simulating the changing concentrations (in g/m^3 or g/m^2) of organisms, nutrients, chemicals, and sediments in a unit volume of water or area of sediment. As such, it differs from population models, which represent the changes in numbers of individuals. As O'Neill et al. (1986) stated, ecosystem models and population models are complementary; one cannot take the place of the other. Population models excel at modeling individual species at risk and modeling fishing pressure and other age/size-specific aspects. However, recycling of nutrients, the fate of organic chemicals (Figure 4-8), and other interdependencies in the aquatic ecosystem are important aspects of a system such as the Housatonic River that AQUATOX represents, and that cannot be addressed by a population model.
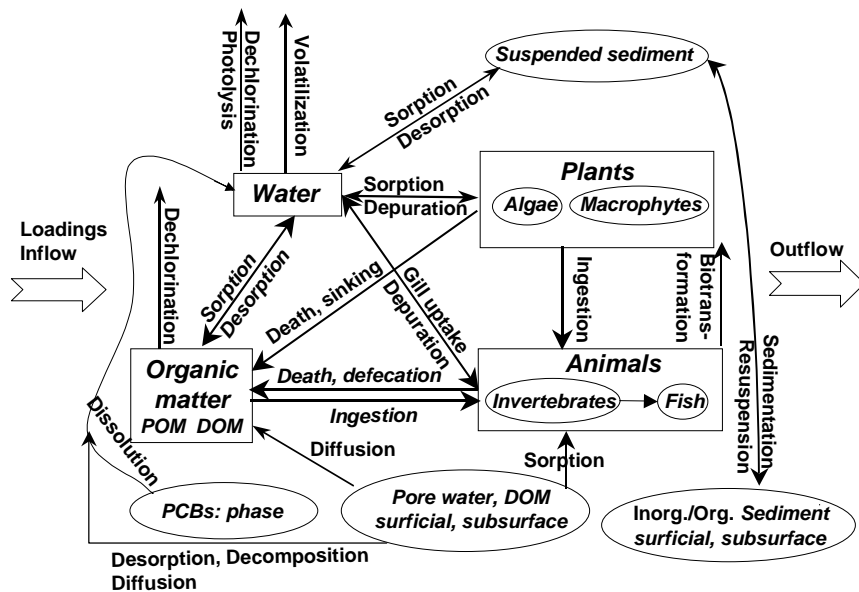
Figure 4-7 Fate and Bioaccumulation of PCBs
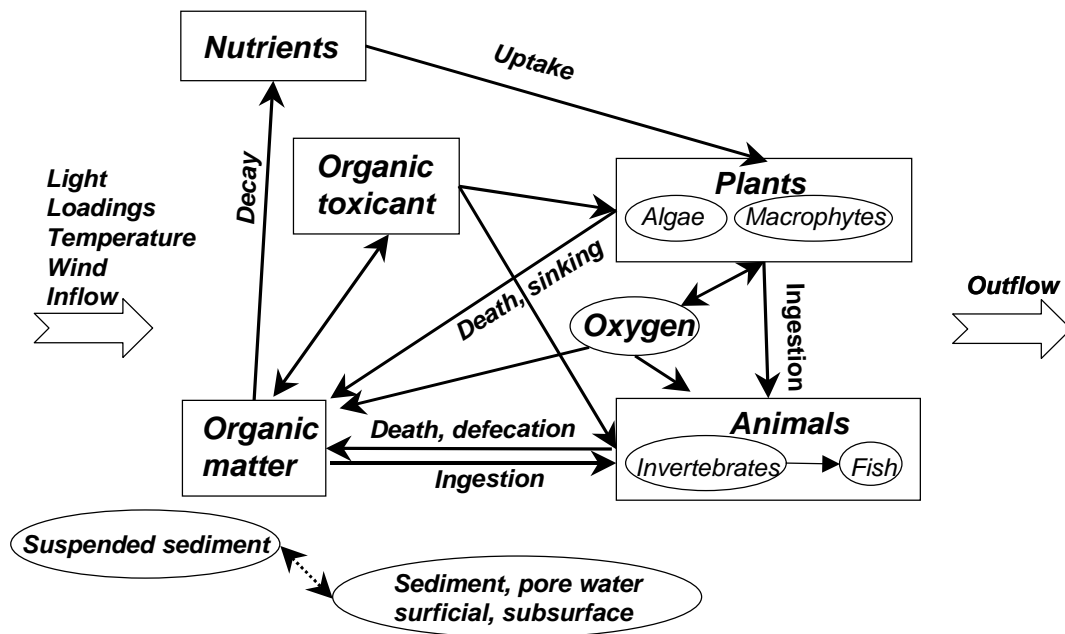
Figure 4-8 Processes Linking Ecosystem Components in AQUATOX

1   The model is written in object-oriented Pascal using the Delphi programming system for

2   Windows™. An object is a unit of computer code that can be duplicated; its characteristics and

3   methods also can be inherited by higher-level objects. This modularity is the basis for the

4   flexibility of the model, including the ability to add and delete state variables interactively and to

5   replicate the segment structure, providing the spatially distributed functionality required for this

6   project.

7   The model has been optimized to address the specifics of PCB transfer in a riverine system.

8   AQUATOX represents linked segments, including subreaches, backwater areas, and the

9   epilimnion and hypolimnion in Woods Pond. Advection, diffusion, and migration link the

10 segments.   Two size classes can be represented for each fish species, and one species

11 (largemouth bass) is represented by up to 15 age classes to better evaluate age-dependent

12 bioaccumulation. As many as 20 chemicals or chemical groups, including PCB homologs or

13 selected congeners, can be represented simultaneously. Up to 10 sediment layers and associated

14 pore water can be simulated; the model is linked to the sediment transport module of the EFDC

15 model. Animals can be parameterized to reflect their proportionate exposures to contaminants in

16 pore waters and in the water column. Bioturbation is modeled as affecting the thickness of the

17 active layer and biodiffusion.

18 The fate portion of the model is applicable specifically to organic contaminants such as PCBs.

19 This portion includes kinetic partitioning among organisms, suspended and sedimented detritus,

20 suspended and sedimented inorganic sediments, and water; volatilization; photolysis;

21 biotransformation; and microbial degradation.

22 **Temporal Resolution**

23 Usually the reporting time step in AQUATOX is one day, but numerical instability is avoided by

24 allowing the step size of the integration to vary to achieve a predetermined accuracy in the

25 solution. This is a numerical approach, and the step size is not directly related to the temporal

26 scale of the ecosystem simulation. AQUATOX uses a very efficient fourth- and fifth-order

27 Runge-Kutta integration routine with adaptive step size to solve the differential equations (Press

28 et al., 1986). The routine uses the fifth-order solution to determine the error associated with the

1   fourth-order solution; it decreases the step size when rapid changes occur and increases the step

2   size when there are slow changes, such as in winter. However, the step size is constrained to a

3   maximum of 1 day so that daily contaminant loadings are always detected.

PCB Degradation and Loss

5   Biodegradation of contaminants such as PCBs is modeled as a maximum observed degradation

6   rate (Km) modified for pH, temperature, and dissolved oxygen factors. Enhanced degradation

7   under anaerobic conditions and elevated temperatures is explicitly modeled. Anaerobic Km

8   values will be calculated for specific congeners, and hence proportionately for homologs that

9   contain those congeners, using experimental data with microorganisms from Woods Pond

10   obtained by Bedard and colleagues (Bedard and May, 1996; Van Dort et al., 1997; Wu et al.

11   1996, 1997a, 1997b). Bedard and May (1996) concluded that Aroclor 1260 accounted for at

12   least 95% of the PCBs in Woods Pond—Aroclor 1254 accounting for no more than 5%—and

13   that the congener distribution is the result of Processes N and P.

14   With 50 years of dechlorination, as Van Dort et al. (1997) assumed, and following the major

15   routes of dechlorination postulated by Bedard and May (1996), Kms and half-lives can be

16   computed for major components of Aroclor 1260. For example, based on the Bedard and May

17   (1996) data, the computed half-life of the Cl_7 homolog group in Woods Pond is 129 years, with

18   congeners 2345-2'4'5' being 168 years and 2345-2'3'4' being 92 years. It is beyond the sensitivity

19   required for this application to model the N and P processes separately, so the rates will be based

20   on the mean annual temperature, and seasonal temperature adjustments will be taken,

21   recognizing that the overall optimal temperature of 30°C for PCB microbial dechlorination is

22   higher than the maximum summer temperature of 22°C (Wu et al., 1996). Other studies will be

23   used to estimate Km values for aerobic microbial degradation of lighter PCB homologs (for

24   example, see Abramowicz, 1994).

25   The loss of an organic chemical through volatilization is modeled as a function of the Henry's

26   Law constant for the compound, which is estimated using the HenryWin Ver. 3.02 program and

27   compared with published values when available (Brunner et al., 1990; Dunnivant et al., 1992)

28   and also corrected for ambient temperature. Volatilization also depends on the depth and flow

1 rate of the river and wind speed, particularly for standing water such as Woods Pond.

2 Volatilization can be a significant loss for the lighter PCB homologs. If appropriate, specific

3 homologs and congeners be modeled separately.

4 **PCB Sorption and Bioaccumulation**

5 Sorption kinetics of PCBs involves dissolved and particulate organic matter and resulting

6 bioavailability to biotic groups. Numerous studies have stressed the importance of

7 distinguishing between truly dissolved PCB concentrations and dissolved and colloidal organic

8 complexes because of differing bioavailability (for example, Landrum et al., 1985, 1987; Butcher

9 et al., 1998). AQUATOX computes bioaccumulation factors with both truly dissolved and

10 apparent dissolved chemicals to facilitate comparison with available data.

11 AQUATOX represents the kinetics of sorption and desorption, but the bioconcentration factors

12 for biota (Figure 4-9) and steady-state partition coefficients for detritus are computed to indicate

13 the maximum concentrations for direct uptake from a given dissolved level.

14 Computations are sped up by scaling and apportioning uptake relative to the maxima, thus

15 avoiding numerical instabilities with competing rapid sorption processes. The partition

16 coefficients, uptake rate constants, and depuration rate constants in AQUATOX will be

17 calibrated using field observations on concentrations in sediments, water, and organisms,

18 keeping in mind that a true steady-state is unlikely to occur in the river.

19 Exposure to PCBs is a function of diet, gill uptake, and direct sorption. The latter process is

20 considered important for algae and macrophytes as discussed in the conceptual model. The

21 sigmoidal curve for algal uptake in AQUATOX is being modified to account for steric effects in

22 highly chlorinated homologs. AQUATOX allows the user to designate the proportions of

23 overlying water and pore water that a given category of animal respires, and to account for

24 exposure and nonlinear uptake through filtration activities. Prey preferences can be important

25 for determining dietary exposures; the model weights available prey by specific predator

26 preferences (using published values for the given fish species from rivers in the Northeast); this
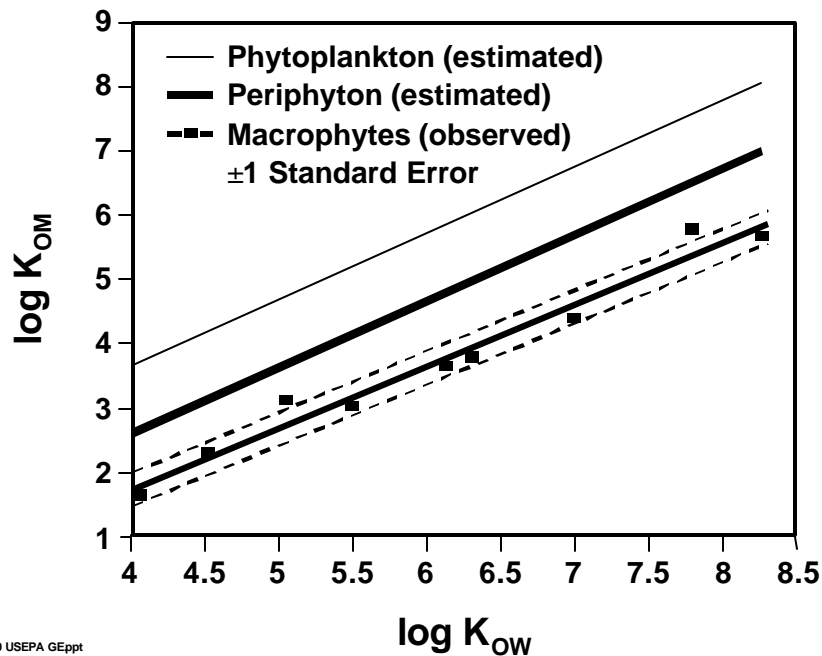
Figure 4-9 Steady-State Partition Coefficients in Plants

construct accounts for the reality of opportunistic and seasonally variable feeding. The gut absorption efficiency in AQUATOX is a function of the assimilation efficiency of the contaminated food, based on recently published observations (NIEHS, 1999) and similar to the approach taken in a bioaccumulation model for PCBs in the Upper Hudson River (QEA, 1999).

The model divides elimination into excretion and biotransformation. Loss of PCBs from algae by excretion and lysis is modeled explicitly. AQUATOX can be parameterized to represent degradation pathways in invertebrates and fish, including biotransformation from one congener to another. It is generally accepted that the *para* chlorines in the lower chlorinated congeners are readily hydroxylated and that biotransformation decreases with the degree of chlorination (Safe, 1980; Endicott and Cook, 1994). However, capacity for biotransformation varies by species; Gerstenberger et al. (1997) state that few fish exhibit P450 IIB1- and IIB2-type enzyme induction responsible for metabolizing lower chlorinated congeners (see also Bright et al., 1995). Given the ambiguity in the literature and the lack of definitive species-specific studies, site-specific data are being collected, and some degree of calibration will likely be necessary.

Modeling Endpoints

The model predicts concentrations of nutrients and dissolved and particulate detritus, biomass of various functional and taxonomic groups of organisms, concentrations of contaminants such as PCBs in the dissolved phase, and concentrations and bioconcentration factors associated with the detrital and biotic compartments. It also simulates control conditions, such as a no action alternative and a remediation alternative, in side-by-side runs. The output can be exported in database format suitable for post-processing.

4.2.3.2   AQUATOX Data Requirements

AQUATOX is designed to be run with varying quantities and qualities of data, depending on availability and purpose. In this modeling study, more than sufficient data are available for the calibration of most parameters. However, the historical Aroclor or total PCB tissue and sediment data from the 1980s are marginally adequate (and congener data are lacking) for validation, so more recent data for homologs and selected congeners will be used to validate the latter years of long-term simulations. The comparability of the analytical techniques used in generating the older PCB data with those used in more recent analyses is being evaluated to determine if older data can or need to be "adjusted" to account for any differences if they are used in this modeling study, analogous to the "tri+" approach that was necessary in the Hudson River modeling effort (Butcher et al., 1997).

As described in detail in Section 4.4.2, most of the estimated loadings and physical characteristics will come from HSPF and EFDC.

Physical Characteristics

For each segment, EFDC will provide to AQUATOX time-varying volume, surface area, mean depth, maximum depth, and cross-sectional area. Vertical diffusivity will be simulated and provided by EFDC for the epilimnion and hypolimnion of the deep hole of Woods Pond.

1   **Ecosystem Loadings and Driving Variables**

2   HSPF will provide time-varying loadings of NO_x, NH_4, PO_4, dissolved organic matter, and

3   dissolved oxygen (mg/L) for each river segment to AQUATOX. EFDC will provide time-

4   varying loadings of particulate organic matter, sand, silt, and clay (mg/L), inflow (m^3/d), and

5   water temperature (EC) for each segment. Data obtained at the site will be used for time-varying

6   solar radiation (Langleys/d), wind (m/s), and pH. The solar radiation will be corrected for

7   seasonal riparian shading for each reach; wind will be important only for Woods Pond and will

8   be corrected for height above water and shoreline sheltering.

9   **Contaminant Loadings**

10   HSPF will provide time-varying point-source and nonpoint-source loadings of PCBs (g/d or

11   µg/L in inflow water) to AQUATOX.

12   **Observations on Ecosystem Components**

13   Data that have been or are being collected for the Supplemental Investigation for the AQUATOX

14   river segments include biomass estimates for periphyton and macrophytes (g/m^2), phytoplankton

15   (g/m^3), and invertebrates by functional or taxonomic group (g/m^2 or g/m^3), and fish by species

16   (g/m^3), with measurement of length, weight, and for some species lipid content and age. Data

17   also have been collected on concentrations of dissolved and particulate organic matter.

18   **Observations on PCBs**

19   Data have been or are being collected on concentrations of total PCBs and PCB congeners and

20   homologs in the dissolved phase (µg/L), in sediment (µg/kg), associated with periphyton,

21   phytoplankton, and macrophytes (µg/kg), in invertebrates (µg/kg), and in fish by species and size

22   (µg/kg).

Chemical Parameters

Observed or estimated physicochemical and degradation parameter values are available for PCB homologs and selected congeners (see Table A-1 for examples). These include molecular weight, solubility, vapor pressure, Henry's Law constant, and octanol-water partition coefficients. Congener-specific microbial anaerobic degradation rates from Woods Pond will be used. Biotransformation rates are available for some congeners, and congener profiles in organisms are being generated specifically at the site. Henry's Law constants will be based on experimental values when available (e.g., Dunnivant and Elzerman, 1988; Dunnivant et al., 1988) and otherwise estimated using the Brunner procedure (Brunner et al., 1990).

Initial and Boundary Conditions

Calibration data from surface samples and cores (BBL, 1996; WESTON, 2000a) will be used to establish initial conditions for homologs and selected congeners in surficial and subsurface sediments. Body burdens in organisms will be set to 0, and the model will be run with average conditions and loadings for individual segments for several years to "spin up" simulated body burdens prior to the first observed fish data from the calibration period (Smith and Coles, 1997). Then time-varying concentrations in all compartments will be simulated for the period of 1995-2000 and compared to available data, both published and current.

Validation data from surface samples and cores (Stewart Laboratories, 1982) will be used to establish initial conditions for total PCBs in surficial and subsurface sediments. For purposes of the long-term validation, the proportions of homologs and selected congeners will be assumed to be those of the fresh Aroclors 1254 and 1260, with 1260 predominating (for example, see Bedard and May, 1996). Similar to the calibration, a steady-state spin-up period will be used to simulate bioaccumulation in fish prior to the first observed fish data in the validation period (Stewart Laboratories, 1982). Then homologs and selected congeners will be simulated from 1979 through 2000. Comparisons of predicted homologs and congeners will be made with more recent biotic and sediment data, and results will be converted to total PCBs and Aroclors to facilitate comparisons with older fish and sediment data.

1 The two upstream segments, the East and West Branches just above their confluence, will be
2 used to define boundary conditions. They are short, low travel-time subreaches, so they will be
3 simulated separately and linked to the downstream segments using the "cascade" advection
4 scheme. Upstream loadings of total PCBs, provided by HSPF, will be split into homologs and
5 key congeners according to observed ratios.

6 ## 4.3   PHYSICAL DOMAINS OF COMPONENT MODELS

7 Each component model is applied to a particular physical portion of the Housatonic River
8 watershed system, and at a spatial scale appropriate to the processes being simulated. In some
9 cases, the physical domains overlap, to accommodate data and calibration issues. In other cases,
10 the domains are coincident, but the spatial scales are different because of the differing physical,
11 chemical, and biological processes of interest, the sensitivity of the calculations, and the
12 computational efficiency of each model. In this section, the physical domains and spatial scales
13 of each model are presented, starting with HSPF for the watershed hydrologic study area (HSA),
14 followed by EFDC and AQUATOX for the PSA.

15 ### 4.3.1   HSPF Housatonic Watershed Domain

16 As noted above, the physical domain of the HSPF model for this study is the entire watershed
17 that drains to the gage at Great Barrington, MA, an area of approximately 282 square miles. This
18 downstream boundary was selected because of the long-term flow record available (more than 80
19 years) for calibration. The watershed area at this point encompasses the entire PSA of the
20 Housatonic River downstream from the GE facility at Pittsfield, the area in which historical data
21 suggest that the majority of PCB-contaminated sediment and floodplain soil is located.

22 Whenever HSPF, or any watershed model, is applied to an area of this size, the entire study area
23 must undergo a process referred to as "segmentation." The purpose of watershed segmentation
24 is to divide the study area into individual land and channel segments, or pieces, that are assumed
25 to demonstrate relatively homogenous hydrologic/hydraulic and water quality behavior. This
26 segmentation then provides the basis for assigning similar or identical parameter values or
27 functions to where they can be applied logically to all portions of a land area or channel length
28 contained within a segment. Since HSPF and most watershed models differentiate between land

1 and channel portions of a watershed, and each is modeled separately, each undergoes a

2 segmentation process to produce separate land and channel segments that are linked together to

3 represent the entire watershed area. The initial watershed and channel segmentation of the

4 Housatonic River watershed are discussed separately below. The initial segmentation is shown

5 in Figure 4-2.

6 ### 4.3.1.1   Watershed Segmentation

7 Watershed segmentation is based on individual characteristics of the watershed, including

8 topography, drainage patterns, land use distribution, meteorologic variability, and soil

9 conditions. The process is essentially an iterative procedure of overlaying these data layers and

10 identifying portions of the watershed with similar groupings of these characteristics. Over the

11 past decade, the advent of geographic information systems (GIS) and associated software tools,

12 combined with advances in computing power, have produced automated capabilities that can

13 efficiently perform the data-overlay process.

14 For the Housatonic River watershed, the topographic and drainage pattern analysis for subbasin

15 delineation was performed using the tool AVSWAT (Di Luzio et al., 1998), which produces map

16 layers of subbasins and river segments using a digital elevation model (DEM) grid as input.

17 AVSWAT automatically defines subbasins based upon a user-specified threshold number of grid

18 cells, but it also allows the user to specify locations as subbasin outlets. For this application the

19 DEM from the BASINS system (Lahlou et al., 1998), with a resolution of 100 meters, was used

20 to define 39 separate subbasins within the Housatonic River watershed down to Great

21 Barrington, MA. These subbasins range in size from 0.4 to 23.8 mi^2, and include stream reaches

22 that range in length from 0.6 miles to 8.8 miles. The land and channel segmentation will require

23 further refinement to produce a reasonable representation of the watershed consistent with the

24 EFDC grid and the AQUATOX segments. The guidelines followed and issues encountered in

25 producing the segmentation shown in Figure 4-4 are outlined below:

26   1. Two of the model segments were defined with outlets at the USGS gaging stations at
27   Coltsville and Great Barrington to facilitate hydrologic calibration to the available flow
28   data at these sites.

2. The threshold level of aggregation of grid cells with AVSWAT was adjusted to define channel locations that extended throughout most of each subbasin so that the drainage pattern within each segment would be adequately represented.

3. The segment division that corresponds to the 10-year floodplain between Dalton and Woods Pond was designed to correspond to the river segments defined in the Supplemental Investigation Work Plan (WESTON, 2000a); thus, WESTON river Reach 1 corresponds to HSPF reach No. 1000, WESTON Reach 2 corresponds to HSPF reach No. 2000, etc. Also, model segments that drain to these reaches were numbered consistently so that segments with numbers in the 100s contribute to WESTON Reach 1, segments labeled in the 200s contribute to WESTON Reach 2, etc.

4. Although the SI Work Plan defined a single reach from the confluence of the East Branch and West Branch to Woods Pond, a finer segmentation was imposed in this region to provide better spatial definition for this reach for both the hydrology calibration and the linkage with AQUATOX (discussed below).

5. In areas with very flat slopes and/or incised channels, the watershed-scale DEM resolution was not sufficient to accurately define the channel location, such as between the confluence of the East Branch and West Branch and Woods Pond, and downstream of Coltsville. In these cases, the USGS maps and the EPA RF3 stream coverages were used to properly define the channel locations.

AVSWAT also generates tables of attributes with each map layer. The subbasins were overlayed with the land use data to determine the area of each land use contributing to each river segment. This analysis was performed using the land use coverage from BASINS along with the ArcView GeoProcessing Tool. The BASINS land use data layer (circa 1980-84) includes 17 different land use categories, which were combined, using the AVSWAT tool, into seven groups for simulation.

The seven AVSWAT land use groupings provide the basis for selecting categories for simulation within each subbasin with HSPF. Since the focus of the HSPF component in this study is on sediment, PCB, and nutrient loadings, we will simulate only four of the seven land use categories: urban, forest, agriculture, and wetlands. Appendix E includes tables with the land use areas for each of the seven AVSWAT categories for each subbasin. The overall land use distribution for the entire watershed area at Great Barrington is as follows:

Urban	15.0 %
Agriculture	10.8 %
Forest, Deciduous	39.1 %
Forest, Evergreen	28.2 %

1	Forest, Mixed	1.1 %
2	Lakes/Reservoirs	1.8 %
3	Wetlands	4.0 %

4

5   Appendix E also includes subbasin areas, elevations, and slopes all derived from the DEM data

6   using the AVSWAT tool.

7   Although the land use coverage available for the site was generated in the early 1980s, the

8   predominant rural/agricultural nature of the entire watershed has not significantly changed since

9   that time. However, further evaluation of the urbanization of the watershed is being performed

10   and any changes identified in specific model segments will be incorporated into the land use

11   coverage.

12   ### *4.3.1.2   Channel Segmentation*

13   Segmentation of the channel was also performed with the AVSWAT tool because it uses DEM

14   data to determine drainage divides and stream locations for the mainstem and all tributaries. In

15   this approach, a single HSPF stream or channel reach within each subbasin was included as

16   shown in Figure 4-2. Since detailed hydrodynamics and sediment transport will be performed by

17   EFDC, and detailed PCB simulations will be performed by AQUATOX, the stream simulation in

18   HSPF is performed primarily to allow calibration at the primary sampling locations along the

19   river. Appendix E shows stream channel attribute data, including the subbasin in which the

20   channel resides, the downstream subbasin, reach length, elevation drop across its length, and

21   slope. This information summarizes the initial physical characterization of the channel system;

22   however, the DEM resolution may be too coarse to generate accurate information; the generated

23   channel data will be evaluated against the detailed cross-section data collected for the mainstem

24   to define the EFDC grid (discussed below) and revised if necessary.

25   ### 4.3.2   EFDC Housatonic River and Floodplain Domain

26   ### *4.3.2.1   Introduction*

27   As discussed above, the EFDC model will be used to simulate hydrodynamics, solids transport,

28   and abiotic PCB fate and transport in the Housatonic River, and will simulate overbank transport

1　of water and solids into the associated floodplain. Using available shoreline, channel cross-

2　section, bathymetry, and floodplain elevation data, the physical domain of the Housatonic River

3　will be spatially discretized into a computational scheme as a (a) boundary fitted, orthogonal,

4　curvilinear, (b) cartesian, or (c) nested or hybrid grid consisting of a fine-scale grid representing

5　the main channel and a coarse-scale grid representing the floodplain region.

6　Specification of an appropriate grid scheme is critical to properly representing the external and

7　internal forces occurring and their influence on the transport of both sediment and PCBs in a

8　river with characteristics such as those of the Housatonic. A grid representing the physical

9　domain of the study area provides the computational framework by which resulting forces are

10　translated throughout the system in terms of both magnitude and direction. The physical

11　complexity of this system presents challenges, where neither a cartesian nor a curvilinear-

12　orthogonal grid is easily fitted to the shoreline boundary.

13　The complexity of this system requires a strategy to determine the grid scheme that will result in

14　a scientifically credible, yet computationally feasible model. The strategy must provide a

15　framework for evaluating the compromise between depicting the physical realities of the river

16　and floodplain system and computational feasibility. This section presents the proposed strategy

17　and rationale for determining an optimal grid configuration.

18　A key consideration in defining an optimal grid configuration is the need to aggregate outputs

19　from a fine grid used for the hydrodynamic and sediment transport to the coarse grid used by the

20　PCB fate and bioaccumulation model. Consequently, the strategy must include a means of

21　determining whether artificial biases are introduced into the modeling analysis as a result of

22　using different grid configurations and/or as a result of the process of spatial and temporal

23　aggregation between different models.

24　There are two distinct physical domains that need to be modeled in this system. The first

25　physical domain is the main river channel and associated 10-year floodplain between the USGS

26　station at Coltsville to the upstream influence of the backwaters of the Woods Pond Dam. The

27　domain of this model will be referred to as the Riverine/Flood Plain (R/FP) Model. The second

28　physical domain is the Woods Pond impoundment and its backwaters, which will be referred to

29　as the Woods Pond (WP) Model. Because of their differing characteristics and needs, the two

physical domains will be represented in EFDC using two separate coupled grid schemes. The downstream boundary of the R/FP Model will be set at a location defined by the farthest upstream influence of the backwater resulting from the Woods Pond Dam. Downstream boundary time-series results of the R/FP Model (stage height, flow, solids loading, abiotic PCB loading) will be coupled as the upstream boundary for the WP Model. Each model domain will thus have its own grid scheme to represent the major differences in the two physical domains. An additional benefit realized by this approach is a better coupling with the AQUATOX segmentation.

Unlike the difficulties that are discussed below for the numerical grid representation of the main river channel of the R/FP Model, spatial discretization of the Woods Pond and backwater region represents a situation more typical of the traditional applications of a curvilinear or cartesian grid for open-water systems such as lakes, estuaries, or coastal waters. Fitting either a curvilinear or cartesian grid scheme to the WP Model does not require the same level of testing as described below for the R/FP model. For the WP Model, a 3-D cartesian grid using variable horizontal cell sizes (e.g., 5 to 20 m) and three to seven vertical layers as a "sigma" coordinate system is proposed for Woods Pond and its backwater areas. The vertical resolution envisioned in Woods Pond is intended to address such issues as thermal stratification that occurs in the deeper regions of Woods Pond during summer.

The remainder of this section presents a discussion of the strategy proposed to address computational issues associated with the spatial discretization of the complex physical domain of the main river channel and floodplain for the R/FP Model necessary to realistically depict the processes within the Housatonic River PSA.

4.3.2.2   Technical Strategy for Developing an Optimal Grid Scheme for the R/FP Model

The strategy that will be used to determine the optimal grid configuration achieves a balance beween the representativeness and computational feasibility involves of a representative section of the river referred to as the "test reach." Figure 4-10 shows the test reach and its location just upstream of New Lenox Road. For the test reach, a series of coarse to highly refined cartesian grids and a range of nested grids will be evaluated.
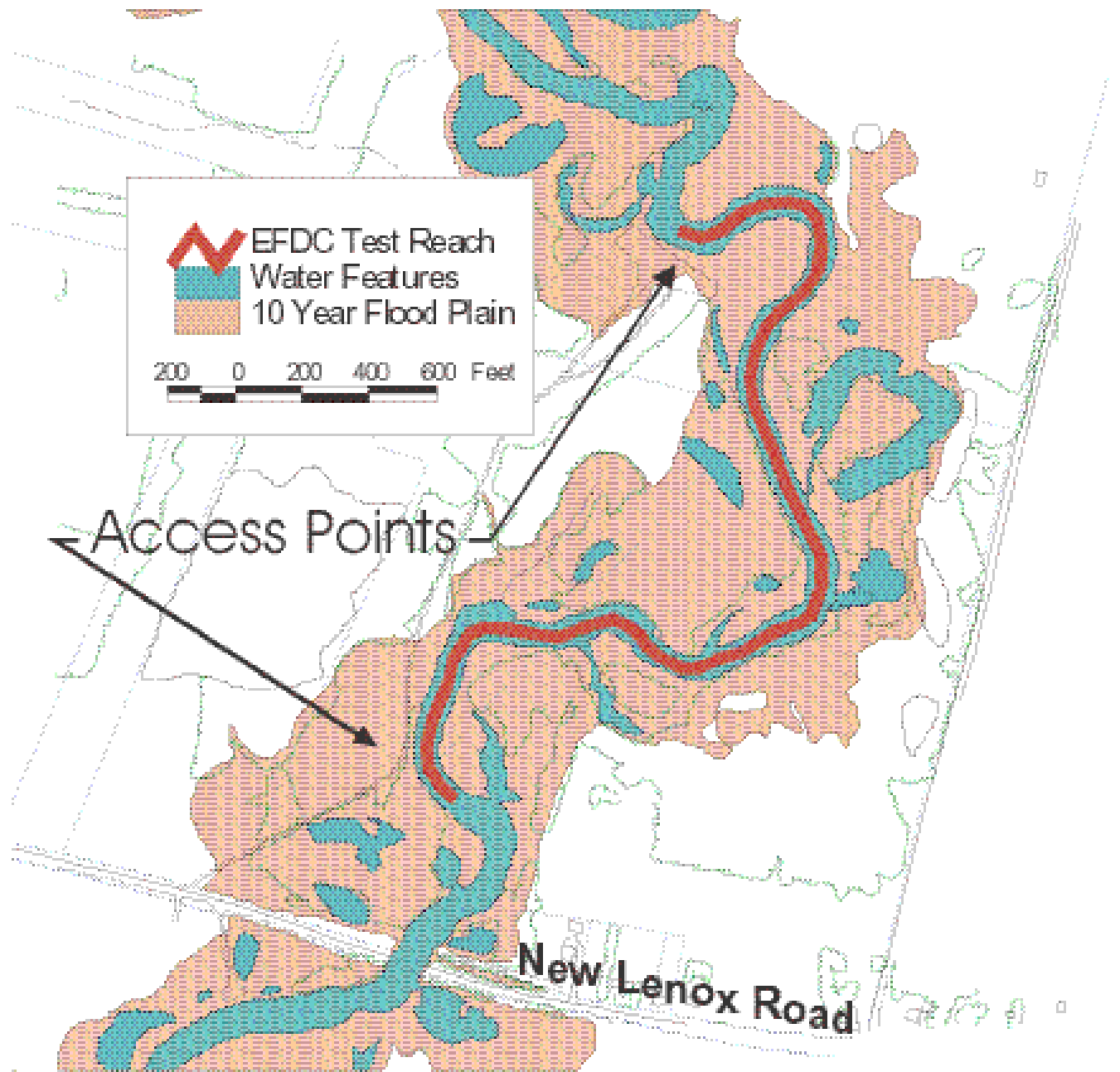
Figure 4-10 EFDC Test Reach Location

1   Testing will be performed to find the most appropriate grid scheme and spatial scale for the R/FP

2   Model to address the concerns discussed above.

3   Results from the evaluation of alternative methods will be compared to detailed site-specific

4   field measurements of flow, velocity, stage height, and TSS (total, cohesive and noncohesive

5   size fractions).   Through an iterative process, the resolution of each test case will be

6   progressively coarsened through subsequent simulations to evaluate the effects associated with

7   the loss of information accompanying the loss of spatial resolution. Once significant errors or

8   differences occur between simulations, the prior cell size will be identified as the "appropriate"

9   discretization for that scheme. The ease of application and computational requirements for each

10   of type of grid scheme will be evaluated and a final grid scheme and discretization will be

11   selected for the entire study area.

12   Technical issues that will be evaluated using the test cases include examining the potential

13   resolution of (1) "staircase" transport in reaches where the sinuous channel is not oriented with

14   the N-S and E-W alignment of the faces of the cartesian cells; (2) lateral transport and

15   resuspension and deposition of solids in reaches characterized by highly sinuous meanders; and

16   (3) interaction of flow between the river channel and the floodplain during bankfull flows in the

17   various test case scenarios.

18   *Staircase Transport*—The presence of meanders is characteristic of natural rivers and represents

19   the most stable channel configuration. The PSA of the Housatonic River exhibits this pattern of

20   complex sinuosity. One option identified above is superimposing a cartesian grid scheme on the

21   system and attempting to preserve the natural sinuosity of system by identifying "active" cells

22   that are reasonably aligned with the main channel. There are difficulties in precisely mapping a

23   cartesian grid to a naturally meandering system. As shown in Figure 4-11, this usually results in

24   "staircase" transport where flows are periodically routed through alternating N-S to E-W to N-S

25   cells.   The extent to which abrupt changes in the direction of flows introduce errors into the

26   momentum terms of the hydrodynamic solution needs to be carefully evaluated in the test cases.

1
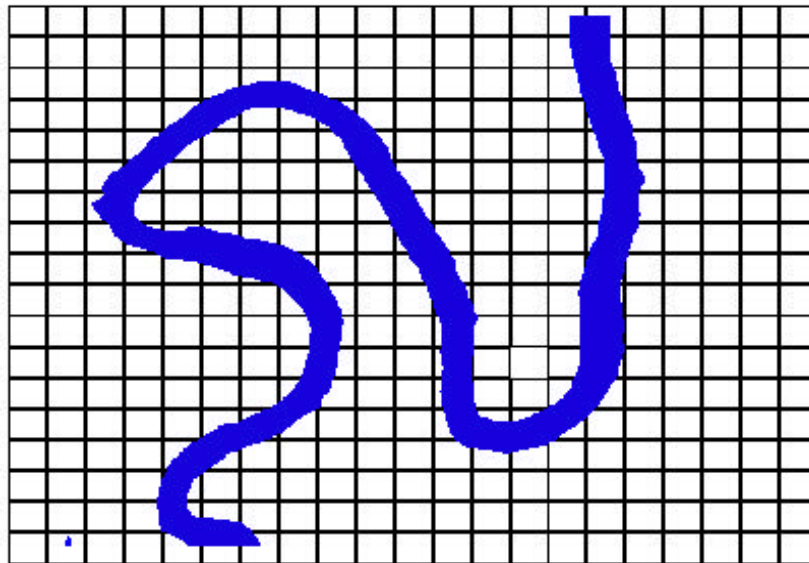
Figure 4-11 Sample Cartesian Grid

As an alternative, a boundary-following curvilinear grid may be developed to provide the most accurate simulation of fine-scale hydrodynamic processes and act as a benchmark to compare results from the cartesian grid test cases.

Lateral Transport in Meanders—Physical transport processes within meandering rivers are inherently complex, with erosion occurring as expected along the exterior or outer bank and deposition occurring on the interior or inner bank. In any channel meander, the velocities in the downstream direction of flow are dependent on the path length, with slower velocities occurring at the inner bank and faster velocities occurring at the outer bank. The differences in lateral velocity distribution across a channel directly influence the sediment transport capacity within the channel. Therefore, the significance of this lateral gradient must be evaluated in establishing an optimal grid scheme. Using a single lateral cell in any grid to represent a portion of the main channel is equivalent to treating sediment transport as being uniform across the channel, in effect eliminating this process. If the lateral variation in solids transport is not considered, then the model could potentially generate a systematic error in the solids balance (and hence PCB mass balance). An additional concern arises in those instances where net solids deposition or erosion is occurring, as would be expected on the inner and outer sides of the meander, respectively. The model would treat the entire cell as being in either net depositional or erosional, which may or

1   may not be a realistic representation of the overall solids and PCB mass balances.   The

2   implementation of the proposed strategy using different scales of spatial resolution and exploring

3   different boundary-fitted and cartesian grid schemes will test the significance of representing

4   portions of the main channel as a single cell in comparison to representing the river channel with

5   multiple lateral grid cells.

6   ***Interaction of Flow Between Channel and Floodplain***—Because the floodplain within the PSA

7   is known to contain elevated levels of PCBs (up to 800 ppm detected), the interaction of out-of-

8   bank flow between the river channel and the floodplain must be represented in the model to

9   achieve mass balance and to accurately represent the distribution of solids and PCBs between the

10   channel and floodplain, particularly under high-flow conditions. For this study, the extent of the

11   10-year floodplain will be represented in the physical domain of the model as a 2-D network of

12   "wetting and drying" grid cells.

13   The spatial resolution necessary to represent out-of-bank flows onto the floodplain must be

14   evaluated within the scale of the 10-year floodplain to preserve the observed conditions, yet ease

15   the computational load. For example, a uniform 20-m x 20-m cartesian grid superimposed on

16   the 10-year floodplain would require on the order of approximately 13,000+ "wetting and

17   drying" cells within the PSA. Such a scheme raises concerns about computational feasibility.

18   On the other hand, there is a concern that if too coarse a cell size is used to represent the main

19   channel, then a significant loss of physical process information could result. This issue has been

20   addressed successfully in the Florida Everglades using a nested-grid approach (Hamrick, 1994b).

21   A nested-grid approach in which the floodplain is represented by a coarse cartesian grid scale

22   and the river channel defined by a "nested" curvilinear grid as a subgrid scale model will also be

23   evaluated for the Housatonic River. In the nested grid, the subgrid interacts with the larger scale

24   "host" cells via exchange flow at the boundaries of the coarse floodplain grid cells (Hamrick and

25   Moustafa, 1999a, 1999b; Moustafa and Hamrick, 2000). If it can be demonstrated that a dual

26   grid strategy can provide a reasonable simulation for coupling channel flow with the floodplain

27   under flood conditions, by comparison to the results generated from a uniform cartesian grid

28   resolution model as well as observed data, then significant computational efficiencies can be

1   realized in applying a nested-grid scheme for the physical domain of the Housatonic River

2   floodplain for the EFDC model.

4.3.3   AQUATOX Domain

4   The AQUATOX model will be used to simulate the fate and bioaccumulation of PCBs and, if

5   necessary, other toxic organic contaminants in the PSA. This aquatic ecosystem model will be

6   applied to the main channel, Woods Pond, and the backwater areas of Woods Pond. Overbank

7   conditions during flood stage will not be simulated because floodplain processes are not included

8   in AQUATOX. The following segments, including subreaches of the Housatonic River and

9   subdivisions of Woods Pond, will be simulated in AQUATOX with linkages to HSPF and EFDC

10   described in detail in Subsection 4.4:

11   **Reach 4a: Pomeroy Avenue Bridge to Confluence**. This segment provides the upstream

12   East Branch boundary conditions for simulating both the ecosystem components and the

13   organic contaminants. This segment begins approximately 2 miles downstream from the GE

14   facility and provides the external loadings from the East Branch for the simulations.

15   Segment 4a is also downstream of the channelized reach and represents the beginning of the

16   natural river channel.

17   **Reach 4b: West Branch Housatonic River.**   This segment forms the other upstream

18   boundary condition, on the West Branch. There is appreciable flow and adequate aquatic

19   habitat in the West Branch or impoundments upstream. In addition, during the course of the

20   Supplemental Investigation, PCBs were detected in the West Branch; further investigation is

21   ongoing.

22   **Reach 5a: Confluence of West and East Branches to Wastewater Treatment Plant.**

23   Shallow, meandering, free-flowing, and with little human alteration, this subreach represents

24   the first depositional area for finer grained sediments (up to 10% silt and clay) and PCBs.

25   Snags (larger woody debris) and bars are common features.

26   **Reach 5b: Wastewater Treatment Plant Discharge to Roaring Brook.** This subreach

27   receives effluent from the Pittsfield Wastewater Treatment Plant. It is a dynamic, graded

1 stream with numerous active meanders and backwater areas. Macrophytes become more

2 abundant in the shallow channel, and abundant algae and zoobenthos reflect the enriched

3 habitat.

4 **Reach 5c: Roaring Brook to Woods Pond.**   In contrast to Reach 5b, this subreach is

5 characterized by a slower-moving river that occupies a more stable channel due to the

6 influence of the Woods Pond Dam. The banks of the river are more heavily wooded in

7 stretches, and the channel has many deep runs and pools (7 ft or more in depth). Organic

8 content of the sediments is greater than upstream, and the fauna is diverse.

9 **Reach 6a: Deep Channel Immediately Upstream from Woods Pond**.   The channel

10 deepens as it reaches the inundated floodplain just upstream of Woods Pond proper. The low

11 floodplain broadens, with a marked increase in macrophytes and algae during the growing

12 season.

13 **Reach 6b: Backwater Areas Immediately Upstream from Woods Pond.** Extensive, very

14 shallow areas of inundated floodplain occur just upstream of Woods Pond. These are prime

15 macrophyte and zoobenthos habitat, and also provide habitat for assemblage of biota that

16 prefer shallow, still water. Although somewhat isolated from the flow of the river, these

17 backwaters do receive sediments and associated contaminants during high-flow conditions,

18 as demonstrated by the PCB concentrations observed in sediment. The backwater areas will

19 be modeled as a single composite segment accounting for the total surface area and volume.

20 **Reach 6c: Deep Hole in Woods Pond.** The eastern portion of Woods Pond was the pre-

21 impoundment meander of the river, currently inundated, and has a maximum depth of 16 ft in

22 thickness. It is also an area of sediment deposition of up to 16 ft. It is stratified during the

23 growing season and will be modeled as two segments—epilimnion and hypolimnion. It

24 supports a typical eutrophic pelagic ecosystem.

25 **Reach 6d: Shallow Portion of Woods Pond.** The western segment of Woods Pond,

26 although in line with the upstream river channel, is a very shallow (1 to 2 ft deep), inundated

27 pre-impoundment floodplain. It is similar to Reach 6c in that it supports a typical eutrophic

28 pelagic system as demonstrated by the predominant cover of dense macrophytes and

1   filamentous algae. This shallow area has between 3 to 6 ft of sediment accumulation as

2   measured by the refusal depth of hammer-driven probes.

4.4   MODEL LINKAGE

4.4.1   Introduction

5   The integrated modeling framework described in Section 4.1 was developed because no single

6   model is capable of representing all the relevant physical, biogeochemical, and biological

7   processes that operate over a wide range of time and space scales to influence the distribution of

8   PCBs in the water column, sediments, and biota of the Housatonic River. The design of a

9   methodology for linkage of inputs and outputs among the models requires consideration of both

10   spatial and temporal issues, since all three models simulate different processes at different time

11   and space scales. The physical domains of each model and the resulting transfer of information

12   (i.e., model results) must be closely integrated to allow for the efficient operation and effective

13   representation of the Housatonic River watershed system.

4.4.1.1   Overview of Model Linkage

15   Figure 4-12 illustrates an overview of the linkage of the outputs from the watershed model

16   (HSPF) as water inflows and constituent loads from nonpoint sources (drainage basin runoff) and

17   point sources (tributaries and wastewater dischargers), to the hydrodynamic and sediment

18   transport model (EFDC), and the PCB fate and bioaccumulation model (AQUATOX). Figure

19   4-12 also shows an overview of the linkage of the output from EFDC as inputs of water inflows,

20   reach geometry, and solids loads to AQUATOX. HSPF will provide AQUATOX with water

21   temperature and point and nonpoint source loads for inorganic phosphorus (as P), nitrate+nitrite

22   (as N), ammonia (as N), dissolved oxygen, water temperature, BOD, organic matter, and PCBs.

23   HSPF will provide EFDC with point and nonpoint source inpus for steamflow, water

24   temperature, and loads for total suspended solids and total PCBs. EFDC will provide

25   AQUATOX with streamflow, reach geometry (volume, surface area, cross-sectional area), and

26   loads of inorganic solids.
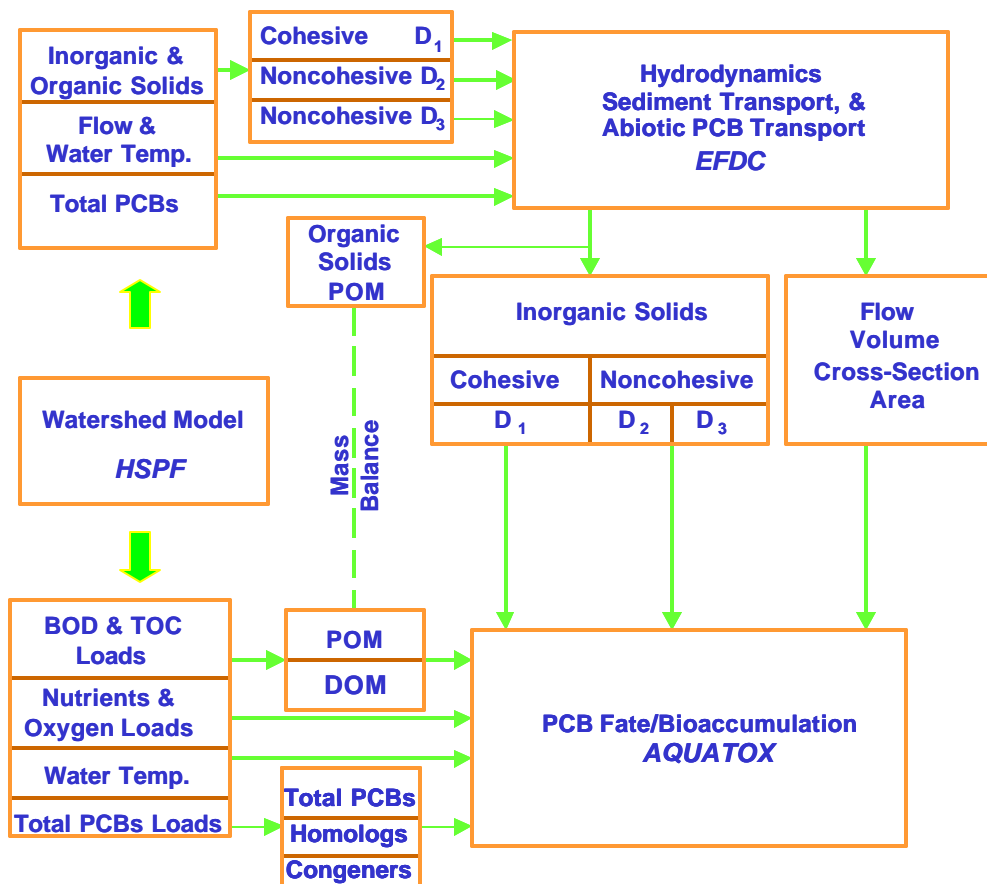
**Figure 4-12 Overview of Model Linkage and Data Transfers within
the Modeling Framework for HSPF, EFDC, and AQUATOX**

Using streamflow, water temperature, solids, and PCB loading data provided by HSPF, EFDC
will simulate water temperature, velocity, stage height, and streamflow in the hydrodynamic
model; cohesive and noncohesive size classes of solids in the sediment transport model; and
PCBs in the abiotic PCB transport and fate model. Using streamflow, reach geometry, and
inorganic solids loading data provided by EFDC, AQUATOX will account for inorganic solids
in the water column and simulate evolution of the sediment bed based on erosion and deposition
fluxes of solids provided by EFDC. Using water temperature and the loading data provided
directly by HSPF, AQUATOX will simulate organic matter, dissolved oxygen, inorganic
nutrients, and trophic levels of biota that include algae, macrophytes, benthic invertebrates, and
fish. AQUATOX will simulate homologs and selected congeners of PCBs in the water column
and sediment bed and bioaccumulation in the biota.

4.4.1.2   *Spatial Scales*

As shown in Figure 4-12, the framework for the three models reflects a "nested" model approach with each model defined by a physical domain and relevant spatial and temporal scales. Within the physical domain of AQUATOX, the river is represented by a series of coarse-scale, single-layer, cascading reaches for the mainstem of the river, and a coarse-scale network of interconnected, two-layer reaches for the backwater areas of the river and Woods Pond. Within the physical domain of HSPF, the spatial scale of the mainstem of the Housatonic River is designed to overlay identically with the spatial scale of the reaches specified for AQUATOX. The procedure for linkage of pollutant loads from HSPF to AQUATOX is straightforward because all the nonpoint source loads and point source loads generated within an HSPF reach of the Housatonic River will be input at the upstream boundary of the corresponding AQUATOX reach.

The hydrodynamic and sediment transport model (EFDC) represents the finest resolution of spatial scale of the model framework. As discussed above, it is represented by two coupled models: (1) river/floodplain (R/FP) and (2) Woods Pond and backwaters (WP).

The procedure for the linkage of streamflow, reach geometry, and solids loads from EFDC to AQUATOX is less straightforward since the mass fluxes (i.e., [flow] x [concentration]) of water and solids simulated within each EFDC grid cell of the river channel and Woods Pond must be summed horizontally and vertically over the boundaries of each AQUATOX R/FP reach and WP segment. The horizontal flux of water and solids is summed for each grid cell across the upstream boundary to define the upstream input to each AQUATOX R/FP reach and WP segment. The export (or import) of fluxes of water volume, solids, and PCBs between the river channel and floodplain will be tracked by summing the fluxes over each grid cell along the floodplain/channel boundary.

Because the domain of AQUATOX does not include the floodplain, fluxes of water volume and solids to/from the floodplain must be computed and tracked to maintain the mass balance of water and solids provided from EFDC to the AQUATOX R/FP reaches and WP segments. In the WP model, the vertical fluxes of water volume and solids deposition and solids resuspension

1   are summed over the array of grid cells corresponding to each AQUATOX segment to define the

2   total vertical flux for input to AQUATOX.

4.4.1.3   Time Scales

4   Using high-frequency meteorology and upstream streamflow as input data, HSPF generates

5   streamflow, water temperature, and constituent loads on a time scale of hours. Hourly time

6   series of streamflow, water temperature, and solids loading data provided by HSPF as input to

7   EFDC are linearly interpolated in EFDC to match the very high frequency time step (~minutes)

8   needed for the hydrodynamic model. The output results of EFDC are written to external files for

9   post-processing at a high-frequency interval (e.g., 1 to 2 hrs) designed to capture the

10   hydrodynamic and sediment transport processes associated with the runoff hydrograph of storm

11   events. In contrast to both HSPF and EFDC, AQUATOX is designed to represent the behavior

12   of physical, chemical, and biological processes operating on a low-frequency time scale. With a

13   daily time scale used to define inputs of streamflow and pollutant loads and resulting ecological

14   processes, AQUATOX can resolve changes that are detectable over a monthly to seasonal time

15   scale. To link output data sets from HSPF and EFDC as input time series to AQUATOX, the

16   high-frequency results from HSPF and EFDC are numerically integrated over a 24-hour period

17   to generate daily time series for input to AQUATOX.

4.4.1.4   Relationship of Modeling Framework Design and Modeling Study QAPP

19   The following section (4.4.2) presents a detailed description of the methodology used to

20   construct the data linkages for the model framework, HSPF, EFDC, and AQUATOX. The

21   Modeling Study QAPP (Beach et al., 2000) presents a detailed description of QA/QC procedures

22   proposed to ensure that the linkages between HSPF, EFDC, and AQUATOX are performed

23   correctly. The driving principle in designing QA/QC procedures for testing the model linkages

24   is the requirement to maintain a mass balance of water, solids, nutrients, and PCB loads provided

25   to AQUATOX by HSPF and EFDC.

4.4.2 Linkage Methodologies

The details of the methodologies adopted for linkage of the three models are described in this section. The discussion accompanying the variables listed below is intended to provide the necessary information for evaluating the adequacy of the methodology proposed for linking HSPF and EFDC output as input to AQUATOX, and is intended to address the following issues:

- What point and nonpoint source loads are generated by HSPF?
- How are HSPF loads linked to AQUATOX?
- How are HSPF loads linked to EFDC?
- How are EFDC fluxes linked to AQUATOX?
- What I/O transformations are used?
- What field data are used to support I/O transformations?

The discussion is organized by related groups of state variables as follows:

- Streamflow, water temperature, and reach geometry
- Inorganic nutrients and dissolved oxygen
- Solids, BOD, and organic matter
- PCBs

4.4.2.1 *Streamflow, Water Temperature, and Reach Geometry*

Figure 4-13 illustrates the linkage of nonpoint and point source inputs of flow generated by HSPF with EFDC and AQUATOX. This section describes the methodology that will be used to link streamflow, water temperature, and reach geometry data provided by HSPF and EFDC and the transformation of these data necessary to maintain a correct water balance and heat balance, and reach volume, depth, cross-sectional area, and surface area for input to AQUATOX.

HSPF

Driven by time-series input of precipitation and upstream boundary inflows, the HSPF watershed model generates high-frequency streamflow based on hydrologic processes describing surface runoff and subsurface inflow as nonpoint source inputs and flow routing in the tributaries as point source inflows. A one-dimensional transport model is used in HSPF for in-stream routing of flow in the mainstem of the Housatonic River and its tributary reaches. Based on climatology

```
┌─────────────────────────┐        ┌─────────────────────────┐
│         Flow            │───────▶│          EFDC           │
│                         │        ├─────────────────────────┤
│   Water Temperature     │        │     Hydrodynamics       │
└─────────────────────────┘        └─────────────────────────┘
            ▲
            │
┌─────────────────────────┐
│          HSPF           │
├────────────────┬────────┤
│ Non Point      │ Point  │
│ Source         │ Source │
├────────┬───────┼────────┤
│Subsurf.│Surface│Tributary
│        │       │ Reach  │
└────────┴───────┴────────┘
```
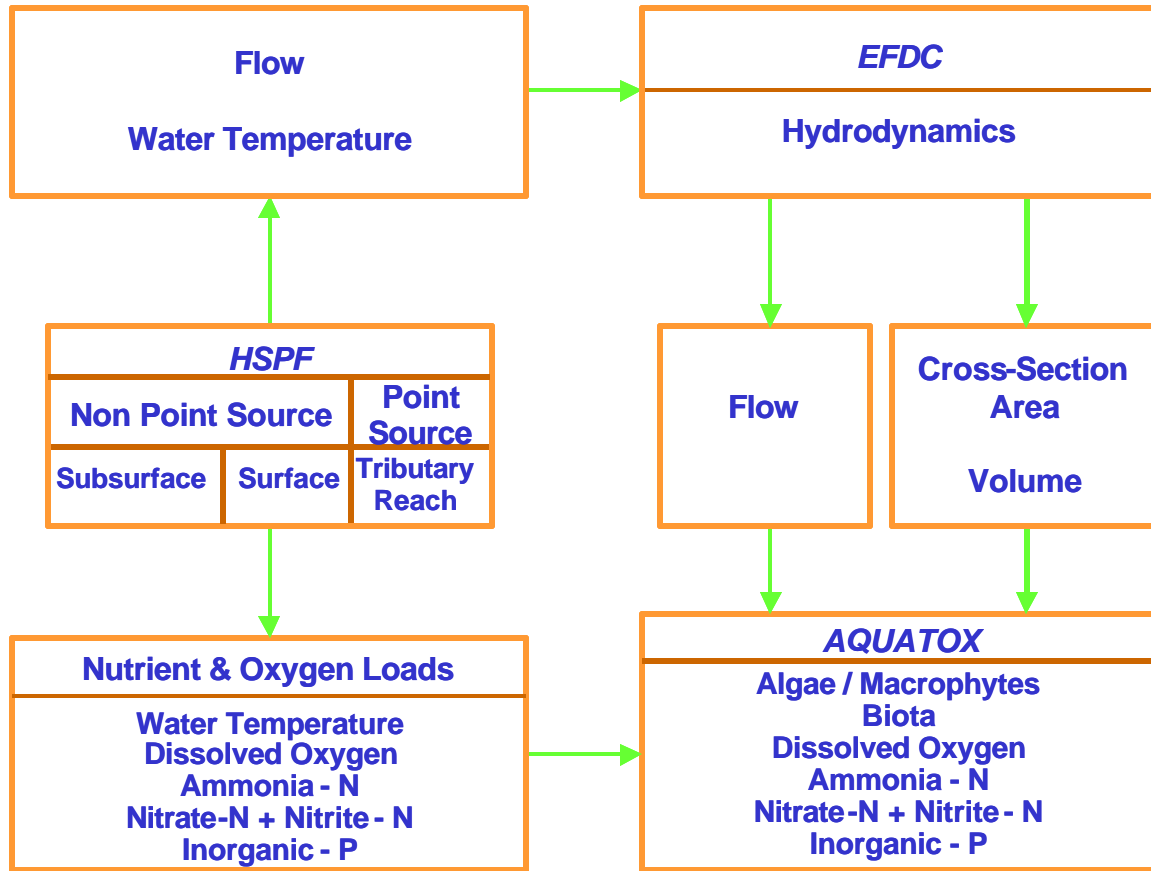
Figure 4-13 Model Linkage Within the Modeling Framework for Flow, Reach Geometry, Water Temperature, Inorganic Nutrients, and Dissolved Oxygen

and meteorologic time series data, a one-dimensional heat balance model is used in HSPF to simulate water temperature in the mainstem and tributary reaches of the watershed model.

HSPF-EFDC

Surface and subsurface inflows generated by HSPF as nonpoint runoff are distributed to each EFDC grid cell in proportion to the length of the grid cell and the length of the HSPF mainstem reach. Point source inputs of flow and water temperature contributed by tributary inflows and wastewater discharges are input to specific EFDC grid cells corresponding to the spatial location of the tributary or wastewater discharge.   Hourly time series of streamflow and water temperature data provided by HSPF for input to EFDC are linearly interpolated in EFDC to match the high-frequency time step (~minutes) needed for the hydrodynamic model. For both

1 nonpoint and point sources, flow and water temperature are specified for input to EFDC grid

2 cells as time series data sets to define boundary inflows as follows:

3   Boundary inflow of water……………………………………………………..$(m^3 \; sec^{-1})$
4   Water temperature……………………………………………………………(^oC)

5 **EFDC-AQUATOX**

6 Driven by the boundary inflows of water provided by the watershed model, the hydrodynamic

7 model simulates water temperature, stage height, velocity, and streamflow in the coupled R/FP

8 and WP models. Streamflow is summed over the EFDC grid cells across the upstream boundary

9 and the channel/floodplain boundary of each matching AQUATOX R/FP reach and each WP

10 segment. In the WP model, mean horizontal and vertical dispersion coefficients are computed

11 for the set of EFDC grid cells to define: (a) mixing across horizontal interfaces; and (b) mixing

12 between the epilimnion and hypolimnion of each two-layer AQUATOX segment. Time series of

13 upstream streamflow, floodplain/channel flow (to/from), and vertical and horizontal mixing

14 coefficients are numerically integrated over a 24-hour period for input to AQUATOX as daily

15 time series.

16 Grid cell volumes and surface areas are spatially summed over the horizontal array of EFDC grid

17 cells that correspond to each AQUATOX reach in the R/FP model and each AQUATOX

18 segment in the WP model. Time series of spatially summed cell volumes and surface areas are

19 numerically integrated over a 24-hour period for input to AQUATOX as daily time series to

20 define reach geometry. Using the low-frequency daily time series of volume and surface area

21 and assuming the reach/segment computational volume is defined as a rectangular box, the mean

22 depth and mean cross-sectional area are computed from the following ratios:

23   Reach Depth = Reach Volume/Reach Surface Area……………………………….Eq. (4-1)
24   Reach Cross-Section Area = Reach Volume/Reach Length………………………Eq. (4-2)

25 EFDC provides AQUATOX with the following reach geometry and transport parameters as daily

26 time series:

27   Volume……………………………………………………………………………..(m^3)
28   Cross-sectional area at upstream-downstream interfaces……………………………..(m^2)

1   Surface area (horizontal)……………………………………………………………(m^2)
2   Horizontal flow at upstream boundary…………………………………………..(m^3 day^{-1})
3   Horizontal flow to/from channel/floodplain………………………………………..(m^3 day^{-1})
4   Horizontal dispersion rate for WP interfaces…………………………………(m^2 day^{-1})
5   Vertical dispersion rate for WP eplimnion-hypolimnion…………………………..(m^2 day^{-1})
6

7   *4.4.2.2   Inorganic Nutrients and Dissolved Oxygen*

8   Figure 4-13 also illustrates the linkage of nonpoint and point source loads of nutrients and

9   dissolved oxygen generated by HSPF as input to AQUATOX.   This section describes the

10   methodology that will be used to link nutrients and dissolved oxygen provided by HSPF to

11   AQUATOX.   There is no linkage between HSPF and EFDC for inorganic nutrients and

12   dissolved oxygen.

13   HSPF

14   HSPF generates inorganic nutrients and dissolved oxygen with the simulated loads calibrated to

15   observed water quality data collected in the tributaries and at mainstem stations of the

16   Housatonic River.   Inorganic nutrient loads generated by HSPF account for nitrogen as

17   ammonia-N, nitrite-N plus nitrate-N, and phosphorus as orthophosphate-P. The organic forms of

18   nitrogen and phosphorus are represented as the nutrient equivalents (nitrogen: dry weight;

19   phosphorus: dry weight) of particulate organic matter (as dry weight). HSPF generates nonpoint

20   source loads of nutrients and dissolved oxygen delivered to the edge of a stream as subsurface

21   inputs and surface runoff over the incremental drainage area between tributary reaches. Surface

22   runoff loads of dissolved oxygen are based on 100% saturation. Subsurface inputs of oxygen are

23   based on mean monthly concentrations observed in groundwater.

24   A one-dimensional water quality model is used in HSPF for instream advective routing with

25   kinetic sources and sinks of nutrients and oxygen simulated in the mainstem and tributary

26   reaches. Kinetic processes for dissolved oxygen include atmospheric reaeration, decomposition

27   of BOD and total organic carbon, nitrification, and sediment oxygen demand. A eutrophication

28   model defines the interactions of algae and nutrients. Using the results of the in-stream model,

29   point source loads of nutrients and dissolved oxygen are simulated at the confluence of the

30   mainstem of the Housatonic River with the tributary reaches.

1   **HSPF-AQUATOX**

2   Point source loads of inorganic nutrients and dissolved oxygen, contributed by tributary inflows

3   and wastewater dischargers, are input at the upstream boundary of each AQUATOX reach.

4   Nonpoint source loads, generated from the surface and subsurface runoff components of HSPF,

5   are aggregated over each HSPF reach and input at the upstream boundary of each AQUATOX

6   reach. The sum of point and nonpoint source loads of dissolved oxygen and nutrients generated

7   by HSPF are numerically integrated for input as the upstream boundary to AQUATOX as time

8   series of daily loads as follows:

9   Dissolved oxygen……………………………………………………………(g day^{-1})
10   Ammonia-N…………………………………………………………………..(g day^{-1})
11   Nitrite-N + Nitrate-N………………………………………………………(g day^{-1})
12   Orthophosphate-P…………………………………………………………(g day^{-1})

13 ### *4.4.2.3   Solids, BOD, and Organic Matter*

14 Figure 4-14 illustrates the linkage of nonpoint and point source loads of solids, BOD, and

15 organic carbon generated by HSPF as input to EFDC and AQUATOX. Suspended solids are

16 provided by HSPF to EFDC while organic carbon and BOD are provided by HSPF to

17 AQUATOX. This section describes the methodology that will be used to link suspended solids,

18 bedload solids, BOD and organic carbon provided by HSPF and EFDC, and the transformation

19 of these loads to inorganic solids and organic matter needed to maintain a correct mass balance

20 for input to AQUATOX.

21 ### *HSPF*

22 HSPF generates TSS, BOD, and TOC with the simulated loads calibrated to observed TSS,

23 BOD, and TOC data collected in the tributaries and at mainstem stations of the Housatonic

24 River. TSS loads generated by HSPF account for both organic and inorganic components of

25 suspended solids. BOD and TOC loads generated by HSPF account for both dissolved and

26 particulate forms of organic carbon. HSPF generates nonpoint source loads delivered to the edge

27 of a stream as subsurface inputs of BOD and surface runoff of TSS and BOD over the

28 incremental drainage area between tributary reaches. Using cohesive and noncohesive size
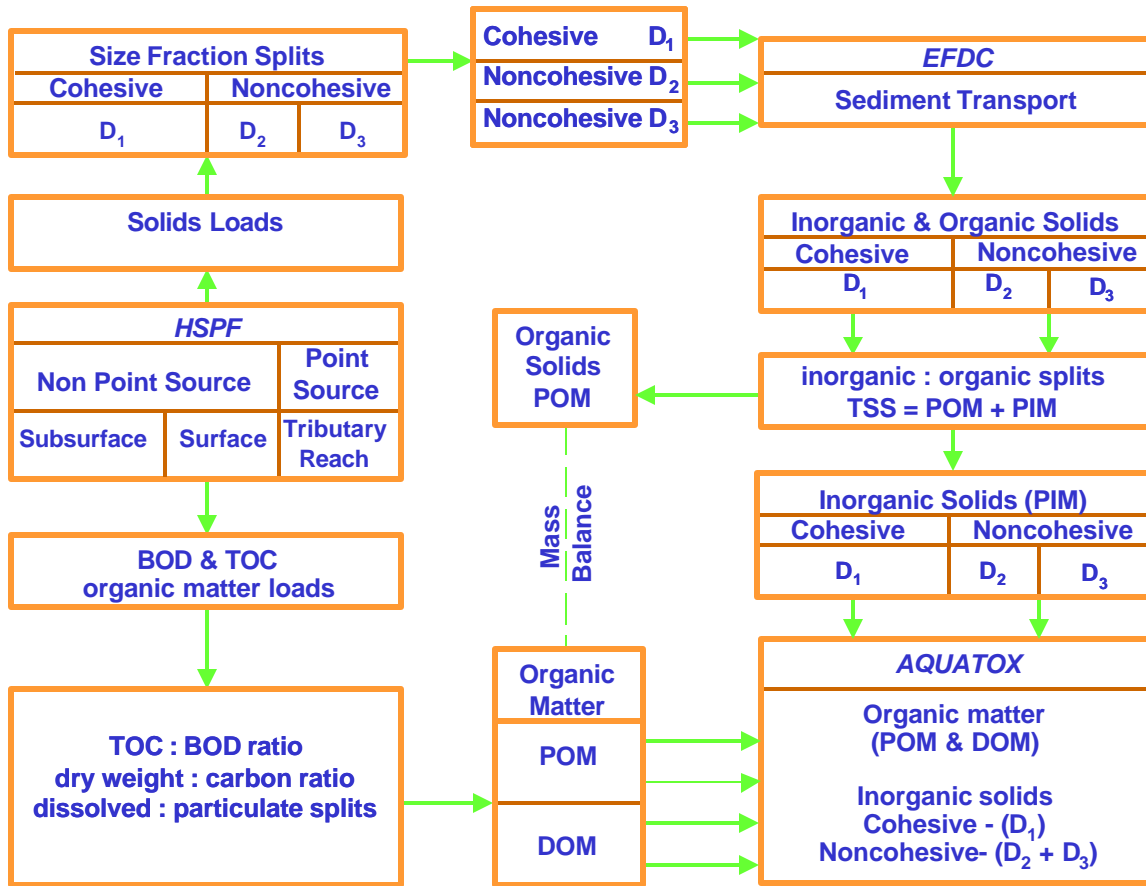
**Figure 4-14 Model Linkage Within the
Modeling Framework for TSS, BOD, and Organic Matter**

fraction splits for TSS and TOC:BOD ratios to transform nonpoint source loads of TSS and BOD

for input to tributary reaches, HSPF generates point source loads of cohesive (silts and clays) and

noncohesive (sands) solids, BOD, and TOC at the confluence of the mainstem of the Housatonic

River with the tributary reaches. A one-dimensional water quality model is used for instream

advective routing with kinetic sources and sinks simulated in the mainstem and tributary reaches.

HSPF-EFDC

In EFDC, inorganic solids are represented as suspended solids and bedload solids using three

size classes: (1) cohesive (< 63 microns); (2) fine to medium noncohesive (63 to 250 microns);

and (3) coarse noncohesive (>250 microns). Using site-specific grain size distribution data to

define spatial and seasonally varying size fraction splits for TSS, nonpoint source surface runoff

1   loads of TSS from HSPF are split to provide input time series to EFDC as three classes of

2   cohesive and noncohesive solids. Nonpoint source loads of TSS generated by HSPF are

3   distributed to each EFDC grid cell in proportion to the length of the grid cell and the length of

4   the HSPF mainstem reach. Point source loads of TSS contributed by tributary inflows and

5   wastewater discharges are input to specific EFDC grid cells to correspond to the spatial location

6   of the tributary or wastewater discharge inflows. Hourly time series of suspended solids loading

7   data provided by HSPF for input to EFDC are linearly interpolated in EFDC to match the high-

8   frequency time step (< hour) needed for the hydrodynamic and sediment transport model. For

9   both nonpoint and point sources, TSS loads are input to EFDC grid cells as time series data sets

10   of boundary inflows (cubic meters per second) and TSS concentrations (mg/L) for the three size

11   classes of solids.

12   Suspended solids are input to EFDC at a grid cell as hourly time series of boundary inflows and

13   suspended solids concentration as follows:

14   Boundary inflow……………………………………………………………(m^3 sec^{-1})
15   TSS#1 (cohesive, <63 microns)……………………………………………….(mg/L)
16   TSS#2 (noncohesive, 63-250 microns)………………………………………..(mg/L)
17   TSS#3 (noncohesive, >250 microns)………………………………………….(mg/L)

18   **EFDC-AQUATOX**

19   EFDC generates a fine grid distribution of cohesive and noncohesive solids driven by the

20   simulation of suspended load and bedload processes. Cohesive and noncohesive solids mass

21   fluxes ([flow] x [concentration]) are summed over the EFDC grid cells across the upstream

22   boundary and the channel/floodplain boundary of the matching AQUATOX reach. Deposition

23   and resuspension mass fluxes ([velocity] x [concentration]) for solids are summed over the

24   EFDC grid cells that correspond to each AQUATOX reach. The upstream mass flux of solids,

25   floodplain/channel solids flux (to/from), deposition flux, and resuspension flux of solids are

26   numerically integrated over a 24-hour period for input to AQUATOX as daily time series.

27   TSS represented in both HSPF and EFDC include both particulate organic (POM) and particulate

28   inorganic (PIM) components of matter. Since POM is provided to AQUATOX from HSPF via

29   transformations of BOD and TOC, the organic matter fraction of TSS (i.e., POM) represented in

1   EFDC must be excluded from the linkage to AQUATOX. As shown in Figure 4-14 with a

2   dashed line, the mass flux of POM subtracted from the TSS flux simulated in EFDC must

3   balance the mass load of POM provided by HSPF to AQUATOX. Site-specific field data are

4   used to define spatial and seasonal splits for the organic fraction of TSS as the ratio of TOC:TSS

5   and the ratio of dry weight:carbon (DW:C) to estimate the POM accounted for as TSS in EFDC

6   (see Eq. 4-3). To maintain a correct mass balance of inorganic (PIM) and organic (POM) matter

7   provided by HSPF and EFDC to AQUATOX, the organic matter component (POM) (see Eq.

8   4-5) must be subtracted as shown in Eq. 4-6 from the cohesive and noncohesive solids fluxes

9   (Eq. 4-4) provided by EFDC to AQUATOX:

10   TSS   =   POM + PIM……………………………………………………………….Eq. (4-3)
11   PIM   =   noncohesive (sands) + cohesive (silts and clays)………………………..Eq. (4-4)
12   POM =   TSS * (TOC:TSS) * (DW:C)……………………………………………Eq. (4-5)
13   PIM   =   TSS - POM = TSS * [1 - (TOC:TSS) * (DW:C)]……………………Eq. (4-6)

14   The inorganic matter (PIM) component of suspended solids generated in EFDC is provided as a

15   time series to AQUATOX as horizontal fluxes of cohesive and noncohesive inorganic solids at

16   the upstream boundary, the channel/floodplain boundary, and vertical fluxes at the bed-water

17   interface representing deposition and resuspension. Using seasonal and spatially varying

18   estimates of TOC:TSS in the water column of the Housatonic River and tributaries, horizontal

19   fluxes of inorganic solids across the upstream and river/floodplain boundaries for the cohesive

20   and two noncohesive size classes are determined using Eq. 4-6. Solids deposition fluxes

21   provided to AQUATOX are also transformed using seasonal and spatially varying water column

22   estimates of TOC:TSS. Solids resuspension fluxes provided from EFDC to AQUATOX are

23   transformed using seasonally and spatially varying sediment bed estimates of TOC:TSS.

24   Horizontal fluxes at the upstream boundary and the channel/floodplain boundary and vertical

25   fluxes of deposition and resuspension are provided to AQUATOX as time series data sets for

26   cohesive and noncohesive solids with units of grams per day.

27   In the river channel, backwater areas of the river, and Woods Pond, net sediment accumulation is

28   accounted for by external watershed loading of inorganic solids and particulate organic matter

29   and internally produced biogenic organic matter. In contrast to EFDC, in which internal

30   biological production of organic matter is not represented in the sediment transport model,

1   AQUATOX does account for internal biological production of particulate organic matter and

2   subsequent net deposition between the water column and the sediment bed. Deposition and

3   resuspension processes of POM are parameterized in AQUATOX by assuming that the behavior

4   of cohesive solids subject to deposition and resuspension in EFDC can be used to infer

5   equivalent deposition and resuspension velocities for POM that would also be subject to the

6   same physical processes as cohesive solids. Deposition and resuspension fluxes simulated in

7   EFDC for the cohesive size class of solids are aggregated over the grid cells corresponding to

8   each AQUATOX reach to compute equivalent velocities to simulate deposition and resuspension

9   fluxes of POM in AQUATOX as:

10   TSS#1 (cohesive, deposition velocity)………………………………………….(m day^{-1})
11   TSS#1 (cohesive, resuspension velocity)………………………………………….(m day^{-1})

12 EFDC provides AQUATOX with the total solids sum of suspended and bedload particulate

13 inorganic solids (PIM) (computed from Eq. 4-4) as daily time series to define upstream boundary

14 conditions (BC) input data as:

15   Solids PIM#1 BC (cohesive, <63 microns)…………………………………………(g day^{-1})
16   Solids PIM#2 BC (noncohesive, 63-250 microns)………………………………….(g day^{-1})
17   Solids PIM#3 BC (noncohesive, >250 microns)……………………………………(g day^{-1})

18 EFDC provides AQUATOX with suspended loads of particulate inorganic solids (PIM)

19 (computed from Eq. 4-6) as daily time series to define the export/import (E/I) of solids to/from

20 the river channel and floodplain (R/FP) as:

21   Suspended PIM#1 R/FP E/I (cohesive, <63 microns)………………………………(g day^{-1})
22   Suspended PIM#2 R/FP E/I (noncohesive, 63-250 microns)………………………..(g day^{-1})
23   Suspended PIM#3 R/FP E/I (noncohesive, >250 microns)…………………………(g day^{-1})

24 Because the physical domain of AQUATOX does not include the floodplain, the total PCB load

25 provided by HSPF to AQUATOX must be adjusted internally within AQUATOX to account for

26 the mass flux export(loss)/import(gain) of PCBs sorbed onto solids between the river channel

27 and floodplain. The mass flux of solids exchanged between the river channel and the floodplain

28 provided by EFDC is coupled with the internally generated concentration of sorbed and

29 dissolved PCBs simulated in AQUATOX to specify the mass flux exchange of sorbed PCBs

1   from the river channel to the floodplain. For floodplain resuspension, which is considered a very

2   rare occurrence, a zero flux condition of PCBs resuspended from the floodplain to the river is

3   assumed.

4   EFDC provides AQUATOX with the mass fluxes of suspended particulate inorganic solids

5   (PIM) (computed from Eq. 4-6) as daily time series to define deposition and resuspension of

6   solids as:

7   Suspended PIM#1 Deposition (cohesive, <63 microns)………………………………(g day^{-1})
8   Suspended PIM#2 Deposition (noncohesive, 63-250 microns)………………………..(g day^{-1})
9   Suspended PIM#3 Deposition (noncohesive, >250 microns)…………………………(g day^{-1})

10   Suspended PIM#1 Resuspension (cohesive, <63 microns)……………………………(g day^{-1})
11   Suspended PIM#2 Resuspension (noncohesive, 63-250 microns)……………………..(g day^{-1})
12   Suspended PIM#3 Resuspension (noncohesive, >250 microns)………………………(g day^{-1})

13   **HSPF-AQUATOX**

14   Using site-specific data to characterize spatial and seasonally varying ratios for TOC:BOD and

15   dissolved (DOC:TOC) and particulate (POC:TOC) fractions of TOC, nonpoint source subsurface

16   and surface runoff loads of BOD are transformed to provide time series input to AQUATOX as

17   dissolved (DOC) and particulate (POC) organic carbon. The dissolved and particulate

18   components of TOC are further split with a dry weight to carbon (DW:C) conversion of organic

19   carbon to organic matter (as dry weight) for input to AQUATOX. The arithmetic definitions and

20   procedures for linkage of HSPF output as input to AQUATOX are given by the following set of

21   equations:

22   BOD   = dissolved BOD + particulate BOD…………………………………Eq. (4-7)
23   TOC   = DOC + POC…………………………………………………..Eq. (4-8)

24   Subsurface and surface runoff BOD loads generated by HSPF are transformed to TOC as

25   follows:

26   TOC   = BOD * (TOC:BOD)…………………………………………….Eq. (4-9)

1   Using a DW:C ratio, TOC generated by HSPF in the tributaries, and the subsurface and surface

2   runoff load of BOD transformed to TOC using Eq. 4-9 is split into dissolved and particulate

3   fractions of organic matter (as dry weight) as follows:

4   DOM   = TOC * (DOC:TOC) * (DW:C)……………………………………Eq. (4-10)
5   POM   = TOC * (POC:TOC) * (DW:C)……………………………………Eq. (4-11)

6   Nonpoint and point source loads of organic matter accounted for by subsurface and surface

7   runoff, tributary inflows, and wastewater discharges are input at the upstream boundary of each

8   AQUATOX reach. Using Eq. 4-9 through Eq. 4-11, HSPF provides AQUATOX with the sum

9   of point and nonpoint source loads of dissolved (DOM) and particulate (POM) organic matter as

10   daily time series to define the following upstream boundary loads :

11   DOM……………………………………………………………………………………($g\ day^{-1}$)
12   POM…………………………………………………………………………………..($g\ day^{-1}$)

4.4.2.4   PCBs

14   Figure 4-15 illustrates the linkage of loads of total PCBs generated by HSPF as input to EFDC

15   and AQUATOX. Total PCBs are provided by HSPF to EFDC while total PCBs provided by

16   HSPF are split as homologs and selected congeners for input to AQUATOX as described below.

17   EFDC will simulate total PCBs as an abiotic constituent with the primary process being

18   adsorption and desorption of total PCBs with solids. AQUATOX will simulate abiotic processes

19   for PCBs (e.g., adsorption and desorption), biotransformation, and bioaccumulation of PCBs

20   within the Housatonic River system. EFDC will track the mass balance of the deposition of

21   sorbed PCBs onto the floodplain. In addition, on a much finer spatial scale of resolution than that

22   for the coarse spatial scale used in AQUATOX, the simulation of total PCBs in EFDC will allow

23   for the high-resolution spatial distribution of PCBs.

24   The following sections describe the methodology that will be used to link total PCB

25   concentrations provided by HSPF to EFDC and by HSPF to AQUATOX. These sections also

26   describe the transformation of total PCB loads to homologs and selected congeners as needed to

27   maintain a correct mass balance for input of PCBs to AQUATOX.
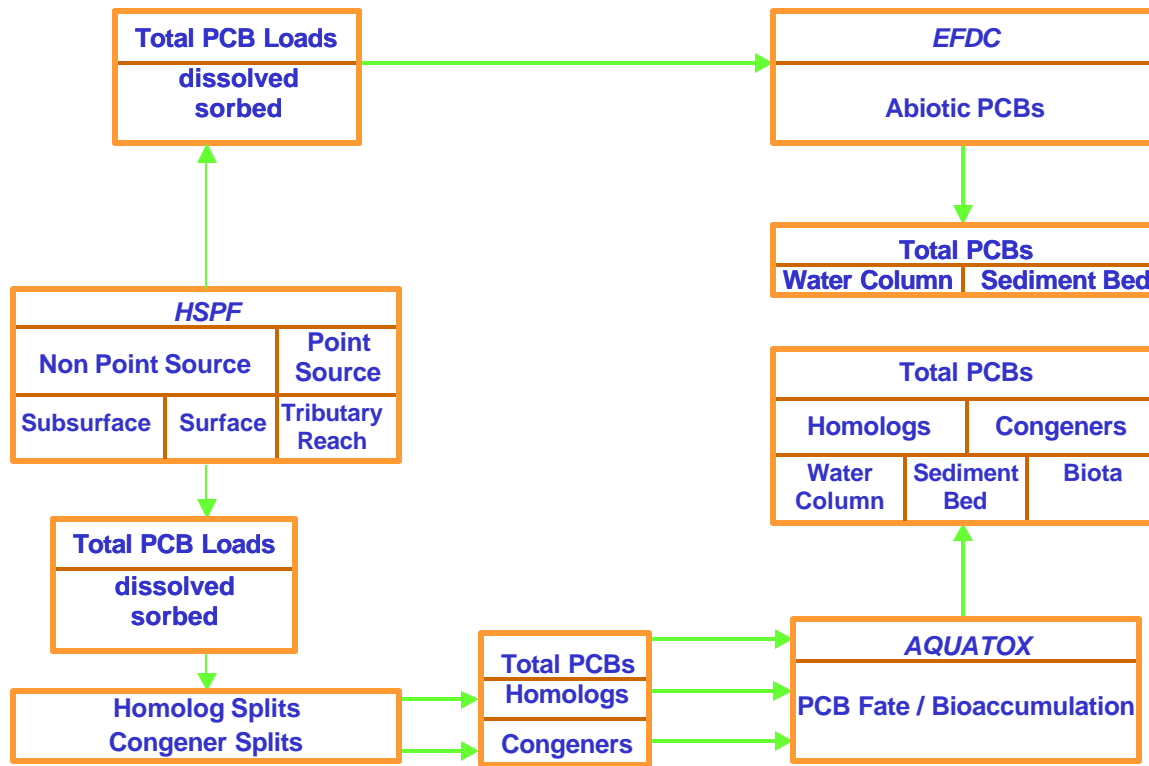
**Figure 4-15 Model Linkage Within the
Modeling Framework for PCBs**

HSPF

HSPF generates total PCB loading from surface runoff of dissolved and sorbed PCBs and subsurface inflow of dissolved PCBs over the drainage area of each HSPF catchment subbasin, and from instream tributary reaches or boundary conditions, with total PCBs split into three components: (1) dissolved PCBs, (2) PCBs sorbed on cohesive solids, and (3) PCBs sorbed on noncohesive solids. Dissolved and sorbed components of PCBs are simulated internally in HSPF for advective routing using partition coefficients for noncohesive and cohesive solids within tributary reaches. Simulated PCB loads are calibrated to observed total PCB data in tributaries and the mainstem stations of the Housatonic River. Total PCBs generated by HSPF are considered to account for both the dissolved and sorbed components.

1 HSPF-EFDC

2 Loadings of PCBs from tributary inflows are input to specific EFDC grid cells corresponding to

3 the spatial locations of the source inflows. Hourly time series of PCB loading data provided by

4 HSPF for input to EFDC are linearly interpolated in EFDC to match the high-frequency time

5 step (~minutes) needed for the hydrodynamic model. Total PCBs are input to EFDC at a grid

6 cell as hourly time series of boundary inflows and concentration as follows:

7   Boundary inflow……………………………………………………………………$(m^3 \ sec^{-1})$
8   Total PCBs…………………………………………………………………………..(µg/L)

9 The PCB transport and abiotic fate submodel in EFDC generates a fine grid distribution of total

10 PCBs for the water column and the sediment bed, including the distribution of sorbed PCBs in

11 the floodplain that results from overbank flow. Total PCBs are partitioned in the model as

12 dissolved and sorbed fractions. PCB partition coefficients assigned to cohesive and noncohesive

13 size classes of solids are used in EFDC to account for the abiotic fate of total PCBs. Observed

14 total PCBs measurements in the water column and sediment bed are compared to simulated total

15 PCBs for calibration and validation of the abiotic PCB transport and fate model of EFDC.

16 HSPF-AQUATOX

17 Loadings of total PCBs from tributary inflows are input at the upstream boundary of an

18 AQUATOX reach. The watershed model (HSPF) simulates loading of total abiotic PCBs as

19 dissolved and sorbed forms of PCBs.

20 AQUATOX simulates the bioaccumulation of three forms of PCBs: (1) total PCBs; (2) PCB

21 homologs; and (3) selected congeners. The total PCB loads simulated in HSPF, adjusted to

22 account for the sorbed PCB exchange between the river channel and floodplain, must be

23 transformed to define multiple homolog and selected congener loads of PCBs for input to

24 AQUATOX. Using splits of total PCBs to define multiple homologs and selected congeners,

25 total PCB loads are defined for input to AQUATOX using three forms of PCBs as: (1) total

26 PCBs; (2) homologs; and (3) selected congeners of PCBs as follows:

1   Total PCBs………………………………………………………………(g day^{-1})
2   PCB homologs………………………………………………..…………(g day^{-1})
3   Selected PCB congener(s)…………………………………………………(g day^{-1})

4 PCB partition coefficients assigned to dissolved and particulate organic matter are used in

5 AQUATOX to account for fate and bioaccumulation of total PCBs, multiple homologs, and

6 selected congeners of PCBs. Observed PCB measurements in the water column (dissolved and

7 sorbed), sediment bed, and biota are compared to simulated PCBs in these three compartments

8 for calibration and validation of the PCB bioaccumulation model of AQUATOX.

5. MODEL CALIBRATION AND VALIDATION PROCEDURES

5.1   OVERVIEW

All model applications typically include three primary phases or steps: database development, system characterization, and calibration and validation. Section 3 described the general data availability and the conceptual model for the PSA. The data requirements specific to each model were described in Section 4.2, and Section 4.3 presented a discussion of the physical domains that characterize the systems represented by each model. This section provides an overview of the calibration and validation procedures for each model. More detail on the procedures that will be followed during model calibration and validation is provided in the Modeling Study QAPP (Beach et al., 2000).

Model calibration and validation are a necessary and critical step in any model application. Calibration is an iterative procedure of parameter evaluation and refinement, comparing simulated and observed values of interest. Model validation is in reality an extension of the calibration process. The purpose of validation is to ensure that the calibrated model properly represents all the variables and conditions that can affect model results. Model credibility is based on the ability of a single set of parameters to represent the entire range of observed data.

While there are several approaches to calibrating/validating a model, perhaps the most effective procedure is to use only a portion of the available record of observed values for calibration; once the final parameter values are developed through calibration, simulation is performed for the remaining period of observed values, and goodness of fit between recorded and simulated values is reassessed. This type of split-data set calibration/validation procedure will be followed for the Housatonic River modeling.

The final check of the modeling results will be performed using a "weight of evidence" approach, evaluating the results obtained from the model together with an objective analysis of the data and other related studies, including those summarized in Section 6. This is a key component of the overall conceptual modeling approach described in Section 3.

1 **5.2   HSPF CALIBRATION AND VALIDATION PROCEDURES**

2 The application of HSPF to the Housatonic River watershed will follow the standard model

3 application procedures as described in the HSPF Application Guide (Donigian et al., 1984), in

4 numerous watershed studies over the past 15 years (see Bibliography for HSPF [Donigian,

5 1999]), and recently in the HSPF application to the Chesapeake Bay Watershed (Donigian et al.,

6 1994).   Model application procedures for HSPF include database development, watershed

7 segmentation, (discussed in the previous sections) and hydrology, sediment, and water quality

8 calibration and validation.

9 **5.2.1 Model Calibration**

10 Model calibration is required for parameters that cannot be deterministically evaluated from

11 topographic, climatic, edaphic, or physical/chemical characteristics.   The majority of HSPF

12 parameters are not in this category.   Calibration will be based on several years of simulation (at

13 least 3 to 5 years) in order to evaluate parameters under a variety of climatic, soil moisture, and

14 water quality conditions.   The areal variability of meteorologic data series, especially

15 precipitation and air temperature, may introduce some as yet unknown level of uncertainty in the

16 simulation; this will be evaluated explicitly during the calibration process.   Years with heavy

17 precipitation are often better simulated because of the relative uniformity of large events over a

18 watershed.   In contrast, low annual runoff may be caused by a single or a series of small events

19 that did not have a uniform areal coverage.   Parameters calibrated on a dry period of record may

20 not adequately represent the processes occurring during the wet periods.   Also, the effects of

21 initial conditions of soil moisture and pollutant accumulation can extend for several months

22 beyond the period of record in which the data were collected, resulting in biased parameter

23 values calibrated on short simulation periods.   Calibration should result in parameter values that

24 produce the best overall agreement between simulated and observed values throughout the

25 calibration period.

26 When modeling land surface processes, hydrologic calibration (runoff and streamflow) must

27 precede sediment and water quality calibration because runoff is the transport mechanism by

28 which nonpoint loadings occur.   Likewise, adjustments to the instream hydraulics simulation

1 must be completed before instream sediment and water quality transport and processes are

2 calibrated.

5.2.2 Model Validation

4 Model performance and validation will be evaluated through graphical, quantitative, qualitative,

5 and statistical measures.

6 For flow simulations where continuous records are available, all these techniques will be used

7 during both the calibration and validation phases. Comparisons of simulated and observed

8 values will be performed for daily, monthly, and annual values, in addition to flow-frequency

9 duration assessments. Statistical procedures will include correlation and model-fit efficiency

10 coefficients.

11 For sediment and water quality constituents, model performance will be based primarily on

12 visual and graphical presentations because the frequency of observed data is often inadequate for

13 accurate statistical measures. However, alternative model performance assessment techniques

14 consistent with the population of observed data available for model testing are discussed and

15 described in the Modeling Study QAPP (Beach et al., 2000).

5.3 EFDC CALIBRATION AND VALIDATION PROCEDURES

17 EFDC will be used to model the Housatonic River's hydrodynamics, sediment transport, and

18 abiotic PCB transport. The calibration/validation of EFDC will be dependent on the final HSPF

19 model. EFDC will obtain boundary conditions from HSPF for water quantity and timing (i.e.,

20 flow rates), sediment loads, and tributary PCB loadings.

21 It is important to conduct the modeling in sequential steps for both the calibration and validation

22 periods. A logical and sequential process must be followed that first resolves the

23 hydrodynamics, then the sediment transport, and finally the abiotic PCB parameters. The steps

24 of the calibration/validation process, and the parameters upon which the focus will be placed at

25 each step are shown in Table 5-1. A fundamental principle underlying the calibration/validation

26 process is the need to maintain mass balance for every constituent. This will be evaluated early

27 in each step of the process to ensure that there are no unaccounted-for gains or losses.

1 Additional calibration/validation efforts will be necessary for the Woods Pond submodel as this

2 may include implementation of a 3-D component of EFDC to capture the Woods Pond

3 dynamics. The additional focus will be on the vertical profiles of temperature, dissolved oxygen,

4 and pH.

5 **Table 5-1**

6

7 **EFDC Model Calibration/Validation Steps**

Step	Parameters of Focus
Initial Condition Development	Bathymetry, sediment distribution, PCB distribution, roughness conditions
Inflow Development	HSPF-linked results to each upstream condition, point tributary, and local runoff/distributed inflows/loadings
Hydraulic Head/Stage Comparisons	Comparison of New Lenox and Woods Pond elevations and timing
Velocity Comparisons	Comparisons to manual velocity measurements and ADCP velocities
Sediment Transport	Comparisons of total loads, areal distribution of depositional/erosional areas, and Woods Pond deposition rates
Abiotic PCBs	Comparisons of water column fluxes/concentrations, distribution of high/low-concentration areas

8

9 ### 5.3.1   Model Calibration

10 EFDC will be calibrated for hydrodynamics, sediment transport, and abiotic PCBs to the periods

11 that have the highest density and quality of data. The storm event data collected during 1999

12 meet these criteria and will be a fundamental basis for calibration. Ten storms were monitored

13 with seven of these events having the full protocol achieved for sampling and analysis. This data

14 set provides a good basis for developing short-term event calibrations. The steps outlined in

15 Table 5-1 will be followed for each storm event. However, the initial conditions may not be

16 changed from one storm event to the next, depending on a detailed evaluation of the data. The

17 final step of the calibration process will be a 2-year simulation from early 1999 to the present to

18 evaluate the intermediate time scale processes. An iterative approach may be necessary to apply

19 new parameterizations to prior periods to ensure consistency and achieve calibration tolerances

20 defined in the Modeling Study QAPP.

21 The calibration will include comparisons of averaged (time and space) model output to measured

22 data.   The measured data will be preprocessed to similar time and space scales that are

1 appropriate for the model scale. Depending on the nature of the event/period, model results may

2 be averaged into hourly, daily, yearly, or decadal time scales. Spatial scales may be points,

3 increments of river miles, or spatially averaged segments, depending on the nature of the

4 parameter. For example, the evaluation of the total sediment load passing New Lenox Road will

5 vary in scale from that used for determining wetland PCB distributions. Specific metrics that

6 will be used in calibration are provided in the Modeling Study QAPP (Beach et al., 2000).

7 ### 5.3.2 Model Validation

8 The validation starting point will be 1979-1980. Data collected by USGS and the Connecticut

9 Agricultural Experimental Station in 1979 and data collected by Stewart (Stewart Laboratories,

10 1982) during the 1980-1982 timeframe are being evaluated for usability. It is expected that one

11 or the other will be used to set the initial conditions of the model. The validation will include a

12 period of approximately 20 years, ending in 2000. The same process will be followed as that

13 used in calibrations, with only the date of initial conditions and duration of the simulation being

14 different. It is possible that the longer term simulation performed during the validation will

15 detect some divergence from the observed data and will require some model adjustments. Any

16 revision to a "calibrated" model during the validation step will necessarily require recalibration.

17 However, the parameters (or magnitude of change) that would be modified based upon the

18 results obtained during validation are not likely to have a noticeable effect on the calibration

19 results representing a shorter time period. Further discussion of the comparisons that will be

20 made to evaluate the validation effort are provided in the Modeling Study QAPP (Beach et al.,

21 2000). Ultimately, the model is expected to reasonably represent the entire range of observed

22 data, at which point it will be considered validated and ready for predictive simulations and

23 alternative analyses.

24 ## 5.4 AQUATOX CALIBRATION AND VALIDATION PROCEDURES

25 The philosophy of the application of AQUATOX, emphasizing generality and reality, is one that

26 has been used for the past 25 years by Park and colleagues (Park et al. 1974; Collins, 1980; Park

27 et al. 1981; Park and Collins, 1982). Because AQUATOX is to be applied to changing

28 conditions at the ecosystem level in the Housatonic River, it must be general, and it should be

1 realistic in its representation of both the ecosystem and the fate of PCBs in that system. Taken

2 together, these characteristics represent a measure of accuracy. The goal will be the simulation

3 of biotic and contaminant behavior with a robust set of parameters, some that are site-specific

4 and some that are independent of site conditions.   While precise matches between model

5 predictions and observed data are not expected, comparisons will be made to ensure that the

6 predictive capability of the model produces results that are reasonable when evaluated against

7 site-specific data.   This evaluation will be performed within the framework of ecological

8 variability through space and time, particularly at the scale needed to address the purposes of the

9 model in evaluating the response associated with remedial alternatives when compared with

10 baseline conditions.

11 There is a long history of development and testing of the aquatic ecosystem formulations that are

12 embodied in AQUATOX, and application to diverse aquatic systems continues. Literature on

13 the fate of PCBs on the toxicity of specific congeners, site-specific data, and independent data

14 sets derived from other contaminated sites (see Appendix D) provide an excellent basis for

15 parameterizing and testing the process-level chemodynamic formulations in AQUATOX.

16 Calibration will involve iterative parameterization and testing of river ecosystem and PCB fate

17 and bioaccumulation constructs. Validation or verification of the model implementation for the

18 Housatonic River will involve comparison with existing site data to ensure that the model results

19 represent the known trends in the fate and effects of PCBs. The model will then provide the

20 capability to forecast future behavior of PCBs in the Housatonic River, given changing

21 conditions under various remediation alternatives.

22 **5.4.1 River Ecosystem Calibration**

23 The PSA includes shallow and deep reaches and backwater areas of the Housatonic River, and

24 shallow and deep segments of Woods Pond. Proposed biotic state variables representing the

25 complex   food   web   include   periphyton,   phytoplankton,   macrophytes,   filamentous

26 algae/duckweed, invertebrates (cladocerans, mayflies, caddisflies, dragonflies, midges, worms,

27 and crayfish), and fish (minnows, goldfish and carp, brown bullhead, white suckers, sunfish,

28 yellow perch, and largemouth bass).

Because of extensive previous applications to impoundments, AQUATOX will represent the Woods Pond ecosystem with little additional calibration necessary. Application to the river ecosystem also will be relatively straightforward. AQUATOX has a large database of parameters representing many riverine invertebrates and fish; therefore, only minor adjustments for calibration are anticipated. In addition, the generality of the model in representing periphyton, macrophytes, various invertebrates, and fish in the river will be tested using available data from other streams and small rivers, in addition to data from the Housatonic. In particular, published data from East Poplar Creek and Walker Branch, Tennessee, and the Little Miami River, Ohio, will be used to further augment the river implementation. The goal is to represent the ecosystem and food web of the Housatonic River realistically so that dietary exposure and bioenergetics of the invertebrates and fish can be used to predict fate and bioaccumulation of PCBs. Biomagnification of hydrophobic compounds such as PCBs is sensitive to the number of trophic levels and to the structure of detritus-based and plant-based food webs, so it is important to represent the complexity of the Housatonic biota, given the available data and general principles of aquatic ecology.

5.4.2 PCB Calibration

The goal is to model PCB homologs and three or more selected congeners in sufficient detail so that the selective microbial degradation and volatilization of homologs and congeners can be predicted, as well as the selective bioaccumulation and biotransformation. The first step is to parameterize and, as necessary, modify fate and effects formulations to best represent PCBs in the Housatonic River. Process-level equations will be tested against experimental data available in the literature (see Appendix D). Simulations will be run using newly collected PCB data, particularly congener data, from the Housatonic River. Similarly, published (Hill and Napolitano, 1997) and unpublished congener data from East Fork Poplar Creek, Tennessee (which is similar to the Housatonic River in several respects) will be used to further refine the model. Sensitivity analyses will be run to determine which parameters have the most effect on the simulations. If the model is inappropriately sensitive to a parameter, then the formulation will be reconsidered and modified if necessary. Sensitive parameters will be noted for use in uncertainty analyses in later simulations.

1 The second phase of calibration will involve running the distributed version of AQUATOX in

2 tandem with the EFDC and HSPF models to test and modify the hydrodynamic and sediment

3 linkages and their applicability to modeling PCB transport, sedimentation, burial, bioturbation,

4 and resuspension.

5 ### 5.4.3 AQUATOX Validation

6 Validation will be performed using Housatonic data starting at the beginning of the period of

7 record until present; only a subset of these data will be used for calibration. Observed data for

8 the earlier years include total PCBs and Aroclors in sediments and fish. Given the limited

9 historical PCB data, particularly for biota, and absence of historical congener data at the site, the

10 validation process will be based on congener distributions in Aroclors 1254 and 1260 and the

11 congener patterns observed in the site-specific data. An effort is underway to evaluate the

12 analytical methodologies used in developing the various data sets during the period of record to

13 determine how best to adjust the data, if needed or possible, to provide comparability between

14 data sets.

15 Because of long half-lives of the more chlorinated PCBs in adult fish and slow degradation rates

16 in sediments, a long simulation period (1979 to 2000) will be used for validation. This period

17 includes the calibration period, but, with initiation 15 years earlier, will provide an independent

18 test with the high-quality data available from more recent studies.

19 There are several measures of model performance that can be used (Bartell et al., 1992; Schnoor,

20 1996). The difficulty is in comparing general model behavior over long periods—with rapid

21 fluctuations due to natural occurrences such as storm events and algal blooms, seasonal

22 fluctuations, and annual variability—to observed data from a few points in time with poorly

23 defined sample variability. Recognizing that the evaluation process is limited by the quantity

24 and quality of data, stringent measures of goodness of fit are inappropriate; therefore, a sequence

25 of tests will be used to evaluate the calibration and validation of the model. Further details are

26 provided in the Modeling Study QAPP (Beach et al., 2000).

1 **5.5 PROPOSED CALIBRATION AND VALIDATION PERIODS**

2 Based on the review to date, the recommendations for calibration and validation periods are

3 presented in Table 5-2.

4 **Table 5-2**

5
6 **Calibration and Validation Periods**

	Calibration	Validation
Streamflow	1991-2000	1979-2000
Water temperature	1991-2000	1979-2000
Sediment loads	1991-2000	1979-2000
Nonpoint loads (nutrients/BOD/organics)	1996-2000	1979-2000
Stage height	1999-2000	1979-2000
Velocity	1999-2000	suitable data not available
Suspended solids (water column)	1999-2000	1979-2000
Sediment bed solids	1999-2000	1979-2000
PCBs (water column/bed)	1999-2000	1979-2000
PCBs (fate and bioaccumulation)	1995-2000	1979-2000

7 Note: The validation period uses the longest period of time and is bounded by available data. This approach
8 allows use of the longest timeframe for which model performance can be evaluated. The resulting validated
9 model is more suitable for evaluating the model's predictive capability for simulating baseline conditions and
10 the long-term effects of potential remedial alternatives.

11 Two basic types of data will be used for model calibration. The first type is continuously

12 recorded data (i.e., flow records) and the second type is periodic/episodic data (i.e., all other

13 data). The HSPF model uses both the first and second types of data, but particularly relies upon

14 the continuous streamflow records for the hydrology calibration. The EFDC and the

15 AQUATOX models primarily use the second type of data for calibration/validation.

16 For the hydrologic data records, the most important factor in selecting a calibration and

17 validation period (assuming the data are available and representative) is the need to represent a

18 range of hydrologic conditions. Calibrating to a period of record that includes extremes such as

19 large storm events and long droughts would be ideal. The goal would then be to validate to

1 another period that has similar variability. The dates selected for the calibration/validation listed

2 above are expected to achieve this goal.

3 Due to the relatively limited availability of the episodic data throughout the long time period

4 required for this modeling effort (more than 50 years), it is preferable to use as much of the

5 available data as possible during validation. The use of the long-term period for validation will

6 allow the evaluation of trends expected over longer time periods in the modeling results that

7 cannot be adequately assessed using the shorter time periods in the calibration process. In order

8 to achieve the longest validation period for this modeling study, the validation period will extend

9 to present-day, incorporating the calibration period.

10 The dates listed in Table 5-2 represent data from reports prepared by numerous authors and

11 produced for various purposes. The 1998-2000 (WESTON, 2000a) data set is the only one that

12 was specifically collected for the purposes of the modeling presented in this document. Not

13 every data set will be useful for each modeling effort. For example, PCB fate calibration of

14 AQUATOX will use the 1995 Smith and Coles data (Smith and Coles, 1997), among others, but

15 these data (tissue residue concentrations) will not be useful for EFDC and HSPF. The Modeling

16 Study QAPP (Beach et al., 2000) provides a complete summary of the general application of

17 each data set.

18 **5.6   SENSITIVITY/UNCERTAINTY ANALYSES**

19 **5.6.1 Sensitivity/Uncertainty Analyses for EFDC and HSPF**

20 The computational demands of both EFDC and HSPF are such that formal probabilistic analyses

21 with numerous iterations of simulation runs are not readily feasible. Consequently, the approach

22 for these system components will be to perform sensitivity analyses on selected model

23 parameters and boundary conditions that are known to be critical based on past experience with

24 both models. The focus will be twofold: (1) evaluate the impacts of key calibration parameters

25 on both process representations and critical flux input from EFDC and HSPF to AQUATOX, and

26 (2) develop a basis for selecting an appropriate distribution of loadings and fluxes from

27 EFDC/HSPF for use in AQUATOX uncertainty analyses.

1 For HSPF, the analyses will focus on the representation of the transport and nonpoint load
2 generation processes in the model; evaluating the sensitivity of the PCB loads to variations in the
3 critical model parameters. These transport parameters will include those related to both runoff
4 generation (i.e., infiltration, soil moisture capacity, surface characteristics) and sediment erosion
5 (i.e., soil erodibility, vegetative cover). It is expected that, due to the nature of historical loading
6 of PCBs at this site, the source characterization will be one of the most uncertain aspects of the
7 PCB loading simulations, and therefore a focus of the sensitivity analyses. Alternative
8 approaches will be investigated for quantifying the PCB loads, ranging from the use of simulated
9 flows and observed PCB concentrations to direct modeling and calibration of PCBs as a function
10 of surface runoff and sediment loads. Each alternative approach will be subjected to sensitivity
11 analyses as part of the assessment.

12 For EFDC, the focus will be on the hydrodynamic and sediment transport parameters that control
13 the corresponding processes. The primary hydrodynamic parameters of concern are the bottom
14 roughness and the vegetation resistance to flow, and the spatial variation of these throughout the
15 model domain. The sediment transport parameters that will be included in the sensitivity
16 analysis include, but are not necessarily limited to, critical shear stress governing resuspension
17 and deposition, terms relating time-varying dry bed density to bed shear strength (during
18 cohesive bed consolidation), and effective settling velocities for both noncohesive and cohesive
19 sediment.

20 In addition to the evaluation of sensitivity within the component models, the sensitivity of the
21 model linkages will be evaluated in terms of the data transfers among the models. This will
22 include the associated assumptions of time and spatial aggregation involved in processing output
23 of one model for input to the other, and the impacts of these assumptions (as discussed
24 previously in Section 4.4) on the model predictions.

25 **5.6.2 Sensitivity/Uncertainty Analyses for AQUATOX**

26 Sensitivity analyses will be performed on critical biotic parameters such as maximum
27 consumption and natural mortality rates, which vary among experiments and representative
28 organisms. Also of interest are the relative effects of physicochemical characteristics such as
29 octanol-water partition coefficients and Henry's Law constants that cannot be measured easily;

1   and chemodynamic parameters such as microbial degradation, which may be subject to both

2   measurement errors and poorly determined environmental controls. These will be evaluated

3   during the calibration phase and they may influence the formulation and parameterization of the

4   model.

5   The effects of uncertain inputs and natural variability on the model predictions are important and

6   will be evaluated. Uncertainty analysis also will consider sources of uncertainty and variation

7   inherent in natural systems and with regard to contaminants (specifically PCBs). These include:

8   site characteristics such as water depth; environmental loadings such as water flow, temperature,

9   and light, which may have a stochastic (random) component; and the characterization of

10 pollutant loadings from runoff and point sources, which may vary stochastically from day to day.

11 The aggregate effect of these components on the simulation results will be examined.

12 Probabilistic modeling approaches may be used as tools for evaluating the implications of

13 uncertainty in the analyses. In this modeling study, AQUATOX provides this capability by

14 allowing the user to specify the types of distribution and key statistics for a wide selection of

15 input variables. Depending on the specific variable and the amount of available information, any

16 one of several distributions may be the most appropriate. A lognormal distribution is the default

17 for environmental and contaminant loadings; distributions for constant loadings can be sampled

18 daily, providing day-to-day variation; distributions for dynamic loadings, which will drive the

19 AQUATOX simulations, use multiplicative factors that can be sampled once each simulation

20 (Figure 5-1).

21 **Figure 5-1 Distribution Screen for Point-Source Loading of Toxicant in Water**
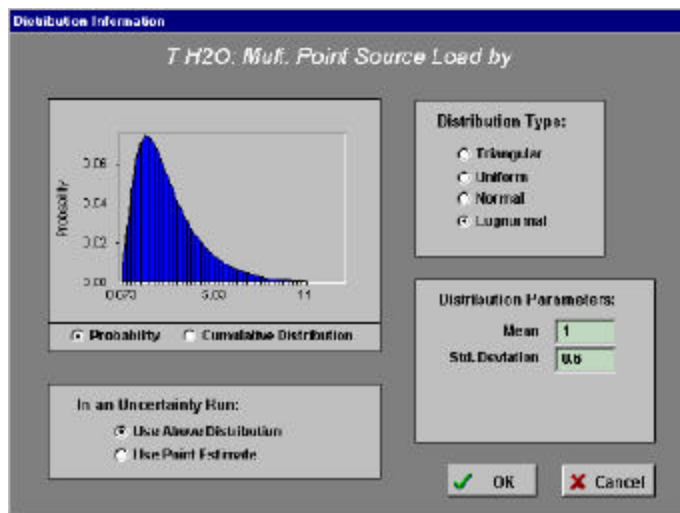
1   A sequence of increasingly defined distributions should be considered for most parameters. If

2   only two values are known and nothing more can be assumed, the two values may be used as

3   minimum and maximum values for a uniform distribution (Figure 5-2). If minimal information

4   is available but there is reason to accept a particular value as most likely, perhaps based on

5   calibration, then a triangular distribution may be most suitable (Figure 5-3); note that the

6   minimum and maximum values for the distribution are constraints that have zero probability of

7   occurrence. If additional data are available indicating both a central tendency and spread of

8   response, then a normal distribution (Figure 5-4) may be most appropriate. All distributions are

9   truncated at zero because negative values would have no meaning.

10 **Figure 5-2 Uniform Distribution for**
11 **Henry's Law Constant for**
12 **Esfenvalerate**
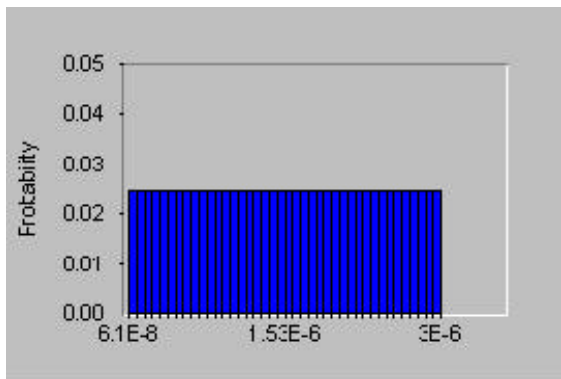
13 **Figure 5-3 Triangular Distribution for**
14 **Maximum Consumption Rate for**
15 **Bass**
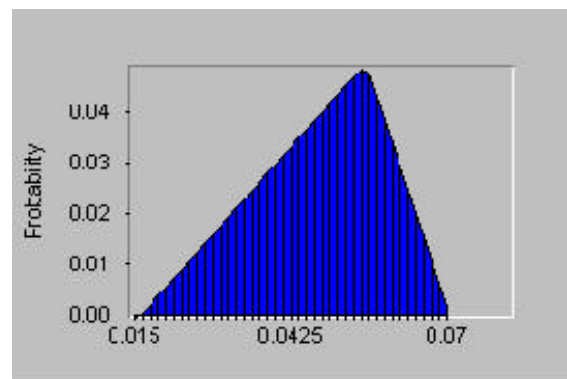
16

17   Efficient sampling from the distributions is obtained with the Latin hypercube method (McKay

18   et al., 1979; Palisade Corporation, 1991). This procedure is used by AQUATOX with algorithms

19   originally written in FORTRAN (Anonymous, 1988). Depending on how many iterations are

20   chosen for the analysis, each cumulative distribution is subdivided into that many equal

21   segments. Then a uniform random value is chosen *within* each segment and used in one of the

22   subsequent simulation runs (Figure 5-5). This method is particularly advantageous because all

23   regions of the distribution, including the tails, are sampled. The default is 20 iterations, meaning

24   that 20 simulations will be performed with sampled input values; this should be considered the

25   minimum number to provide any reliability. The optimal number can be determined

26   experimentally by noting the number required to obtain convergence of mean response values for

27   key state variables; i.e., at what point do additional iterations not result in significant changes in

1 the results? As many variables may be represented by distributions as desired, but the method
2 assumes that they are independently distributed. By varying one parameter at a time the
3 sensitivity of the model to individual parameters can be determined.

4 **Figure 5-4 Normal Distribution for Maximum Photosynthetic Rate for Diatoms**
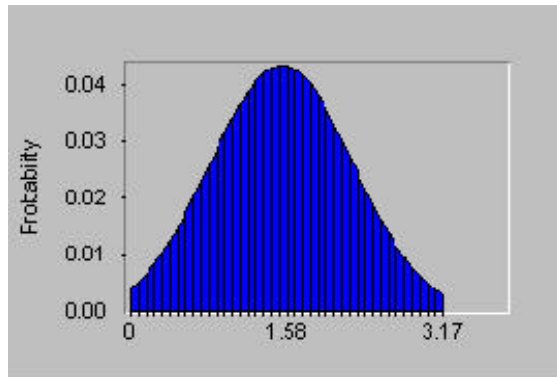
5

6 **Figure 5-5 Latin Hypercube Sampling of a Cumulative Distribution with a Mean of**
7 **25 and Standard Deviation of 8 Divided into 5 Intervals**

8
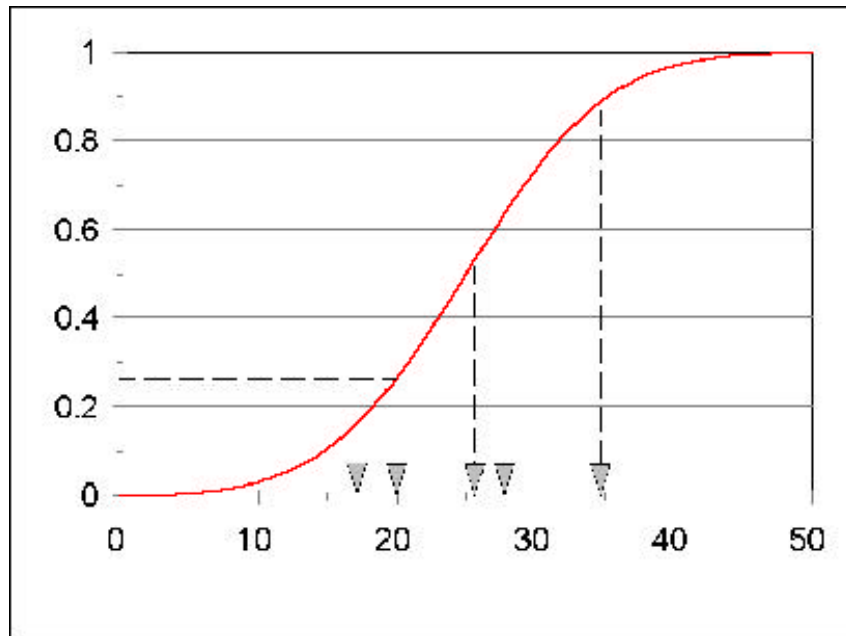
6. ADDITIONAL SUPPORTING ANALYSES

6.1   INTRODUCTION

As discussed throughout this document, there are numerous challenges posed in trying to predict the distribution of PCBs in various media over a period spanning decades. The physical complexity of the Housatonic River only increases the difficulties of making such predictions. Although the emphasis has been placed on the use of deterministic models to address the study objectives, it is prudent to employ alternative analyses that can be used to supplement the modeling analysis and which can be used to reinforce the interpretation of results. This section discusses the additional supporting analyses that will be employed as a "weight-of-evidence" approach to evaluate the extent to which the conclusions derived from the proposed modeling are supported by alternative assessment techniques. These techniques include the use of two alternative modeling tools and a geomorphological investigation. A brief discussion of the purpose and applicability of these tools is provided below.

6.2   APPLICATION OF THE GENERALIZED STREAM TUBE MODEL FOR ALLUVIAL RIVER SIMULATION (GSTARS)

As indicated above in Section 4 of this document, the computational grid scheme developed for this model was originally developed for applications in open water bodies, e.g., estuaries, lakes, and large river systems, where precise mapping of a grid to the shoreline boundary was not a critical factor in the ability to defensibly model the system. Such is not the case in the Housatonic River. The physical complexity of the system in terms of its meanders and relatively narrow width raises the question as to whether the grid scheme would introduce a bias into the numerical solution.

To determine whether such a bias exists, the investigation will use a widely applied riverine sediment transport model (Yang et al., 1998; Molinas and Yang, 1986). This model incorporates many features that make it an appropriate tool to evaluate the concerns raised above. Unlike

1 traditional 1-D models, GSTARS allows the specification of one or more stream tubes,[1] which

2 provides for a quasi 2-D solution for flow and sediment routing. The stream tube approach

3 allows for scour and deposition to be computed across the channel.

4 Unlike the grid schemes available for use with EFDC, GSTARS allows for the detailed

5 specification of the channel cross-section dimensions. Instead of a vertical rectangular cell that

6 cannot map to the complex boundaries of the channel cross-section, changes in flow with depth

7 can be closely simulated with GSTARS. Longitudinally, the lengths of discrete stream tube

8 sections are simply specified. Laterally, the river is specified using up to seven stream tubes

9 (typically three in the channel and one or two in the "floodplain" on each side) across the width

10 of the channel.

11 The principal sediment transport formulation within the GSTARS model is based on the unit

12 stream power approach developed by the model's author (Yang, 1976). The unit stream power

13 approach is based on the concept that changes in river channel geometry occur as a result of the

14 system striving to achieve a minimum rate of energy dissipation necessary to maintain a stable

15 channel form. More specifically, the author states "for subcritical flow in an alluvial channel, the

16 channel will adjust its velocity, slope, roughness and geometry in such a manner that a minimum

17 amount of unit stream power is used to transport a given sediment and water discharge." Unit

18 stream power is defined as the product of flow velocity and channel slope (VS).

19 The theory of minimum rate of energy dissipation (Yang and Song, 1979) holds that the ability

20 of the system to maintain a dynamic equilibrium condition is accomplished by adjusting

21 numerous physical variables (e.g., pattern, geometry, bed form, roughness, slope) until such time

22 as a minimum rate of energy dissipation is achieved. Numerous studies on the application of this

23 theory and the GSTARS model to simulate sediment transport in alluvial rivers have been

24 published in the technical literature (Lee et al., 1998; Lee et al., 1997; Song et al., 1995; Yang

25 et al., 1996). The model formulations are well developed for noncohesive sediment transport

26 investigations and should be useful to this investigation, given the prevalence of noncohesive

---

[1] A stream tube is defined as a portion of a river channel where hydraulic and sediment routing is computed separate from the remainder of the channel. A channel made up of multiple stream tubes provides a means of computing lateral variation in hydraulic and sediment routing.

1   sediment in the bed in the region above Woods Pond. The model also incorporates numerous

2   other well-known sediment transport formulations (Yang, 1998).

3   GSTARS incorporates an additional feature that is distinguishable from traditional models in that

4   it allows the user to simulate changes in channel width over time. The variation in mechanical

5   properties of the materials comprising an embankment makes it difficult to predict such changes

6   with accuracy, particularly for embankments made up of both noncohesive and cohesive

7   materials. While this is not a primary reason for using this model, validating this feature of the

8   model against observed field data may provide useful information relevant to this study.

9   **6.3   HEC-6 SCOUR AND DEPOSITION IN RIVERS AND RESERVOIRS**

10   The HEC-6 model (USACE, 1991) is a 1-D model specifically designed to simulate long-term

11   scour and deposition in rivers and reservoirs. Unlike GSTARS and EFDC, HEC-6 is limited to

12   examining changes in bed elevation that occur over extended periods of time. The model was

13   not intended to simulate specific storm events. In addition, the model is principally meant to be

14   applied under conditions of subcritical flows.

15   For reasons similar to those discussed above for GSTARS, HEC-6 does allow for a detailed

16   specification of the channel geometry. In addition, the user specifies both the lengths of the right

17   and left banks for a specific section. This allows the model to account, to some degree, for the

18   curvature of the channel when performing hydraulic and sediment routing. Since HEC-6 has

19   been widely applied for long-term sediment scour and deposition studies, comparison of long-

20   term results between HEC-6 and EFDC will be used to ensure that predictions between the

21   models are reasonably consistent where applicable (e.g., sediment scour and depositional areas

22   coincide).

23   **6.4   GEOMORPHOLOGICAL INVESTIGATION**

24   There are a number of references in this document to the inability of models to predict the

25   occurrence of numerous geomorphological processes. It has also been stated that these processes

26   are relevant to examining issues of sediment transport. In lieu of suitable modeling techniques,

27   some quantitative measure of the significance of these processes is clearly warranted.

1   It is widely accepted that changes in the pattern, profile, and dimension of a river channel go

2   hand-in-hand with changes in fluvial processes. This goes to the concept of "natural river

3   stability" in that a river evolves to a form that will result in a stable channel configuration.

4   Changes occurring within the tributary watershed to the river may or may not result in changes in

5   the physical characteristics of the channel. A stable channel can be described as one where its

6   features remain unchanged and the channel is neither aggrading or degrading (Rosgen, 1994a).

7   A number of historical changes have occurred within the Housatonic River basin that have

8   resulted in physical changes to the river. Numerous references to these physical changes in the

9   river have been cited in this document. The principal concern is whether these changes

10 constitute a departure from what would be normally be encountered in similar systems, or

11 whether they are representative of the influences of anthropogenic effects. A mechanism to

12 assess the degree of departure, if any, has been developed by Rosgen (1985, 1994a) and has been

13 widely applied. This method incorporates quantitative metrics that describe the pattern, profile,

14 and dimension of the river channel. Using these metrics, departures from a stable channel

15 configuration can be derived from comparisons with unimpacted systems residing within the

16 same physiographic region. A principal concern for this investigation is to determine whether

17 physical processes are occurring that are contributing to channel instability and whether those

18 processes are accelerated as a consequence of man-made influences. If circumstances were to

19 demonstrate that man-made influences are contributing to channel instability and thus increasing

20 the rate at which channel evolution is occurring, then this goes to the issue of the overall stability

21 of the river system and to the possibility that PCBs adsorbed to bank and floodplain sediments

22 will be reintroduced into the system.

23 Under this investigation, a geomorphologic characterization of the study area will be performed.

24 As part of this investigation, successive regions of the system will be classified according to the

25 techniques devised by Rosgen (1994b). The classification of each region of the river will be

26 compared to a river system within the same physiographic region that is reaching its potential,

27 i.e., is unimpacted. The extent of the departure from its potential will be used as a basis for

28 determining whether man-made influences are contributing to channel instability within the

29 system. In addition, control sections will be established in the meander region where toe pins

30 will be installed in channel banks to measure the rate of change in channel width over time. In

1   addition, detailed cross-sectional measurements will be made periodically to determine changes

2   in bed elevation and bed substrate.

7. REFERENCES

Abbott, J.D., S.W. Hinton, and D.L. Borton. 1995. Pilot Scale Validation of the RIVER/FISH Bioaccumulation Modeling Program for Nonpolar Hydrophobic Organic Compounds Using the Model Compounds 2,3,7,8-TCDD and 2,3,7,8-TCDF. *Environmental Toxicology and Chemistry*, 14(11):1999-2012.

Abramowicz, D.A. 1994. Aerobic PCB Degradation and Anaerobic PCB Dechlorination in the Environment. *Res. Microbiol.*, 145:42-46.

Anonymous. 1988. *Latin for* Unpublished FORTRAN computer code presumably developed at Oak Ridge National Laboratory.

Ariathurai, R. and R.B. Krone. 1976. Finite element model for cohesive sediment transport. *J. Hyd. Div. ASCE*, 102:323-338.

Barron, M. 1990. Bioconcentration. *Environ. Sci. Technol.*, 24: 1612-1618.

Bartell, S.M., R.H. Gardner, and R.V. O'Neill. 1992. *Ecological Risk Assessment.* Boca Raton: Lewis Publishers, 252 pp.

Barry, T. and E.A. Machowski. 1993. Assessment of a Riverine Population of Smallmouth Bass in the Housatonic River. State of Connecticut Department of Environmental Protection, Fisheries Division, Hartford, CT.

BBL (Blasland, Bouck and Lee, Inc.). 1996. Supplemental Phase II RCRA Facility Investigation Report for Housatonic River and Silver Lake. January 1996. Report, Study. 375 pp. (AR No. 02.02.2, Doc. No. 000019).

BBL, 1992. Addendum to MCP Interim Phase II Report / Current Assessment Summary for Housatonic River. Volume I of II. Prepared for General Electric Co. August 1992.

Beach, R.B, P.M. Craig, J.S. Clough, A.S. Donigian, R.A. Park, A. Stoddard, S.C. Svirsky, and C.M. Wallen. 2000. Modeling Study of PCB Contamination in the Housatonic River - Quality Assurance Project Plan. Prepared for U.S. EPA, Region I, Boston, MA. 76 p.

Bedard, D.L. and R.J. May. 1996. Characterization of the Polychlorinated Biphenyls in the Sediments of Woods Pond: Evidence for Microbial Dechlorination of Aroclor 1260 *in Situ. Environ. Sci. Technology*, 30:1:237-245.

Bedard, D.L., H.M. Van Dort, R.J. May, and L.A. Smullen. 1997. Enrichment of Microorganisms that Sequentially *meta, para*-Dechlorinate the Residue of Aroclor 1260 in Housatonic River Sediment. *Environ. Sci. Technol.* 31:3308-3313.

Bergen, B.J., W.G. Nelson, and R.J. Pruell. 1996. Comparison of nonplanar and coplanar PCB congener partitioning in seawater and bioaccumulation in blue mussels (*Mytilus edulis*). *Environ. Toxicol. Chem*, 15(9):1517-1523

Bertelsen, S.L., A.D. Hoffman, C.A. Gallinat, C.M. Elonen, and J.W. Nichols. 1998. Evaluation of Log K_{OW} and Tissue Lipid Content as Predictors of Chemical Partitioning to Fish Tissues. *Environmental Toxicology and Chemistry*, 17(8):1447-1455.

Bicknell, B.R., J.C. Imhoff, J.L. Kittle Jr., A.S. Donigian, Jr. and R.C. Johanson. 1997. Hydrological Simulation Program – FORTRAN. User's Manual for Release 11. EPA/600/R-97/080. U.S. EPA Environmental Research Laboratory, Athens, GA. 763 p.

Bicknell, B.R., J.C. Imhoff, J.L. Kittle Jr., T.H. Jobes, and A.S. Donigian, Jr. 2000. Hydrological Simulation Program - FORTRAN. User's Manual for Release 12. FINAL DRAFT. U.S. EPA Ecosystem Research Division, Athens, GA. & U. S. Geological Survey, Office of Surface Water, Reston, VA.

Bierman, V.J. Jr. 1990. Equilibrium partitioning and biomagnification of organic chemicals in benthic animals. *Environ. Sci. Technol.*, 24: 1407-1412.

Björk, M. and M. Gilek. 1999. Efficiencies of polychlorinated biphenyl assimilation from water and algal food by the blue mussel (*Mytilus edulis*). *Environ. Toxicol. Chem*, 17(7):1405-1414.

Black, D.E., R. Gutjahr-Gobell, R.J. Pruell, B. Bergen and A.E. McElroy. 1998a. Effects of a mixture of non-*ortho*- and mono-*ortho*-polychlorinated biphenyls on reproduction in *Fundulus heteroclitus* (Linnaeus). *Environ. Toxicol. Chem*, 17(7):1396-1404.

Black, D.E., R. Gutjahr-Gobell, R.J. Pruell, B. Bergen, L. Mills and A.E. McElroy. 1998b. Reproduction and polychlorinated biphenyls in *Fundulus heteroclitus* (Linnaeus) from New Bedford Harbor, Massachusetts, USA. *Environ. Toxicol. Chem*, 17(7):1405-1414.

Bloom, A.L. 1978. *Geomorphology.* Prentice Hall, Inc., Englewood Cliffs, NJ.

Blumberg, A.F., and G.L. Mellor, 1987. A description of a three-dimensional coastal ocean circulation model. In: Three-Dimensional Coastal Ocean Models, *Coastal and Estuarine Science,* Vol. 4. (Heaps, N. S., ed.) American Geophysical Union, pp. 1-19.

Bright, D.A., S.L. Grundy, and K.J. Reimer. 1995. Differential bioaccumulation of non-*ortho*-substituted and other PCB congeners in coastal arctic invertebrates and fish. *Environ. Sci. Technol.*, 29(10):2504-2512.

Brunner, S., E. Hornung, H. Santi, E. Wolff, O.G. Piringer, J. Altschuh, and R. Brüggemann. 1990. Henry's Law Constants for Polychlorinated Biphenyls: Experimental Determination and Structure-Property Relationships. *Environ. Sci. Technology*, 24:1751-1754.

Butcher, J.B., E.A. Garvey, and V.J. Bierman. 1998. Equilibrium Partitioning of PCB Congeners in the Water Column: Field Measurements from the Hudson River. *Chemosphere*, 36(15):3149-3166.

Butcher, S.P., T.D. Bauthier, and E.A. Garvey. 1997. Use of historical PCB aroclor measurements: Hudson River fish data. *Environ. Toxicol. Chem*, 16(8):1618-1623.

Campfens, J. and D. Mackay. 1997. Fugacity-Based Model of PCB Bioaccumulation in complex aquatic food webs. *Environ. Sci. Technol.*, 31(2):577-583.

Chadwick & Associates, Inc. 1994. Aquatic Ecology Assessment of the Housatonic River, Massachesetts, 1993. Prepared for General Electric Company, Pittsfield, Massachusetts.

Cao, Z., L. Wei, and J. Xie, 1996: Sediment-laden flow in open channels from two-phase flow viewpoint. *J. Hyd. Engrg.,* 121, 725-736.

Coles, J.F. 1999. Length-age relationships and PCB content of mature white suckers from the Connecticut and Housatonic River basins. *Northeastern Naturalist*, 6(3):263-275.

Collins C.D. 1980. Formulation and Validation of a Mathematical Model of Phytoplankton Growth. *Ecology*, 6:639-649.

Connolly. 1991. Application of a food chain model to polychlorinated biphenyl contamination of the lobster and winter flounder food chains in New Bedford Harbor. *Environ. Sci. Technol.*, 25: 760-770.

Connolly, J.P., T.F. Parkerton, J.D. Quadrini, S.T. Taylor, and A.J. Thuman. 1992. Development and application of a model of PCBs in the Green Bay, Lake Michigan walleye and brown trout and their food webs. Report for Large Lakes Research Station, U.S. Environmental Protection Agency, Grosse Ile, Michigan 48138 Cooperative Agreement CR-815396.

Connolly, J.P., and D. Glaser. 1998. Use of Food Web Models to Evaluate Bioaccumulation. *National Sediment Bioaccumulation Conference Proceedings*. U.S. Environmental Protection Agency Office of Water EPA 823-R-98-002, p.4-5-4-17.

Consent Decree. United States of America, State of Connecticut, and Commonwealth of Massachusetts, Plaintiffs v. General Electric Company, Defendant. October 1999.

Cook, P.M., and L.P. Burkhard. 1998. Development of Bioaccumulation Factors for Protection of Fish and Wildlife in the Great Lakes. *National Sediment Bioaccumulation Conference Proceedings*. U.S. Environmental Protection Agency Office of Water EPA 823-R-98-002, p. 3-19-3-27.

Deliman, P.N., W.J. Pack, and E.J. Nelson. 1999. Integration of the Hydrologic Simulation Program-FORTRAN (HSPF) Watershed Water Quality Model into the Watershed Modeling System (WMS). Technical Report W-99-2. U.S. Army Corps of Engineers, ERDC, Waterways Experiment Station, Vicksburg, MA. 58 p.

Di Luzio M., R. Srinivasan,. and J.G. Arnold. 1998. Watershed Oriented Non-Point Assessment Tool. In: Proceedings of the 7th International Conference "Computers in Agriculture". Orlando, Florida USA. October 26-30, 1998. American Society of Agricultural Engineers, St. Joseph, MO. pp.233-241

DiPinto, L.M. and B.C. Coull. 1997. trophic transfer of sediment-associated polychlorinated biphenyls from meiobenthos to bottom-feeding fish. *Environ. Toxicol. Chem*, 16(12):2568-2575.

Donigian, A.S. Jr. 1999. Bibliography for HSPF and Related References. AQUA TERRA Consultants, Inc. Mountain View, CA

Donigian, A.S. Jr. and H.H. Davis. 1978. User's Manual for Agricultural Runoff Management (ARM) Model. EPA-600/3-78-080. U.S. EPA Environmental Research Laboratory, Athens, GA.

Donigian, A.S. Jr. and N.H. Crawford. 1979. User's Manual for the Nonpoint Source (NPS) Model. Unpublished Report. U.S. EPA Environmental Research Laboratory, Athens, GA.

Donigian, A.S., Jr., J.C. Imhoff, B.R. Bicknell and J.L. Kittle, Jr. 1984. Application Guide for the Hydrological Simulation Program - FORTRAN EPA 600/3-84-066, Environmental Research Laboratory, U.S. EPA, Athens, GA. 30613.

Donigian, A.S. Jr., B.R. Bicknell, A.S. Patwardhan, L.C. Linker, C.H. Chang, and R. Reynolds. 1994. Chesapeake Bay Program - Watershed Model Application to Calculate Bay Nutrient Loadings: Final Findings and Recommendations (FINAL REPORT). Prepared for U.S. EPA Chesapeake Bay Program, Annapolis, Maryland. 283 p.

Dunnivant, F.M., and A.W. Elzerman. 1988. Aqueous Solubility and Henry's Law Constant Data for PCB Congeners for Evaluation of Quantitative Structure-Property Relationships (QSPRs). *Chemosphere* 17(3):525-541.

Dunnivant, F.M., J.T. Coates, and A.W. Elzerman. 1988. Experimentally Determined Henry's Law Constant for 17 Polychlorobiphenyl Congeners. *Environ. Sci. Technol.* 22:448-453.

Dunnivant, F.M., A.W. Elzerman, P.C. Jurs, and M.N. Hasan. 1992. Prediction of Aqueous Solubility and Henry's Law Constants for PCB Congeners Using Quantitative Structure-Property Relationships. *Environ. Sci. Technol.*, 26, 1567-1573.

Endicott, D.D. and P.M. Cook. 1994. Modeling the partitioning and bioaccumulation of TCDD and other hydrophobic organic chemicals in Lake Ontario. *Chemosphere*, 28(1):75-87.

EPA (U.S. Environmental Protection Agency). 2000a. *AQUATOX for Windows: A Modular Fate and Effects Model for Aquatic Ecosystems–Volume 1: User's Manual.* EPA-823-R-00-006.

EPA. 2000b. *AQUATOX for Windows: A Modular Fate and Effects Model for Aquatic Ecosystems–Volume 2: Technical Documentation.* EPA-823-R-00-007.

EPA. 2000c. *AQUATOX for Windows: A Modular Fate and Effects Model for Aquatic Ecosystems–Volume 3: Model Validation Reports.* EPA-823-R-00-008.

EPA. 1998. Potential Human Health Risks from Consuming Fish from Houstonic River in Massachusetts. Technical Memorandum dated 14 May 1998 from M. Ballew to B. Olson. U.S. EPA, Boston, MA. 15 p.

EPA. 1992. A framework for ecological risk assessment. EPA/630/R-93/001. U.S. Environmental Protection Agency, Risk Assessment Forum, Washington, DC.

Exponent. 1998. Macroinvertebrate Communities and Diets of Selected Fish Species in the Upper Hudson River, Spring 1998: Data Report. Prepared for General Electric Company, Albany, NY. Exponent, Bellevue, WA.

FWS (U.S. Fish and Wildlife Service). 1999. Age determination of Largemouth Bass (*Micropterus salmoides*) from the Housatonic River Watershed. Office of Fishery Assistance, U.S. Fish and Wildlife Service, Laconia, NH.

Fisk, A.T., R.J. Norstrom, C.D. Cymbalisty, and D.C.G. Muir. 1998. Dietary accumulation and depuration of hydrophobic organochlorines: bioaccumulation parameters and their relationship with octanol/water partition coefficient. *Environ. Toxicol. Chem*, 17(5):951-961.

Forbes, T.L., V.E. Forbes, A. Giessing, R. Hansen, and L.K. Kure. 1998. Relative role of pore water versus ingested sediment in bioavailability of organic contaminants in marine sediments. *Environ. Toxicol. Chem*, 17(12):2453-2462

Galperin, B., L.H. Kantha, S. Hassid, and A. Rosati. 1988. A quasi-equilibrium turbulent energy model for geophysical flows. *J. Atmos. Sci.*, 45, 55-62.

Garabedian, S.P., J.F. Coles, S.J. Grady, E.C.T. Trench, and M.J. Zimmerman. 1998. Water Quality in the Connecticut, Housatonic, and Thames River Basins, Connecticut, Massachusetts, New Hampshire, New York, and Vermont, 1992-95. U.S. Geological Survey Circular 1155. U.S. Geological Survey, Marlborough, MA. 32 p.

Garcia, M. and G. Parker. 1991. Entrainment of bed sediment into suspension. *J. Hyd. Engrg.,* 117, 414-435.

Gay, F.B. and M.H. Frimpter. 1985. Distribution of Polychlorinated Biphenyls in the Housatonic River and Adjacent Aquifer, Massachusetts. U.S. Geological Survey Water-Supply Paper No. 2266. U.S Geological Survey, Alexandria, VA. 26 p.

Gerstenberger, S.L., M.P. Gallinat, and J.A. Dellinger. 1997. polychlorinated biphenyl congeners and selected organochlorines in Lake Superior fish, USA. *Environ. Toxicol. Chem*, 19(11):2222-2228.

Gilek, M., M. Björk, D. Broman, N. Kautsky, and C. Näf. 1996. Enhanced accumulation of PCB congeners by Baltic Sea blue mussels, *Mytilus edulis*, with increased algae enrichment. *Environ. Toxicol. Chem*, 15(9):1597-1605.

Gobas, F.A.P.C. 1993. A model for predicting the bioaccumulation of hydrophobic organic chemicals in aquatic food webs: Application to Lake Ontario. *Ecological Modeling*, 69: 1-17.

Gobas, F.A.P.C. and D. Mackay. 1987. Dynamics of hydrophobic organic chemical bioconcentration in fish. *Environ. Toxicol. Chem.*, 6: 495-504.

Gobas, F.A.P.C., K.E. Clark, W.Y. Shiu, and D. Mackay. 1989. Bioconcentration of polybrominated benzenes and piphenyls and related superhydrophobic chemicals in fish: role of bioavailability and faecal elimination. *Environ. Toxicol. Chem*., 8: 231-247.

Gobas, F.A.P.C., E.J. McNeil, L. Lovett-Doust, and G.D. Haffner. 1991. Bioconcentration of chlorinated aromatic hydrocarbons in aquatic macrophytes. *Environ. Sci. Technol.*, 25(5): 924-929.

Gobas, F.A.P.C., X. Zhang, and R. Wells. 1993a. Gastrointestinal magnification: The mechanism of biomagnification and food chain accumulation of organic chemicals. *Environ. Sci. Technol.*, 27: 2855-2863.

Gobas, F.A.P.C, J.R. McCorquodale, and G.D. Haffner. 1993b. Intestinal absorption and biomagnification of organochlorines. *Environ. Toxicol. Chem.*, 12: 567-576.

Gobas, F.A.P.C., M.N. Z'Graggen, and X. Zhang. 1995. Time response of the Lake Ontario ecosystem to virtual elimination of PCBs. *Environ. Sci. Technol.*, 29:2038-2046.

Gobas, F.A.P.C., J.P. Pasternak, K. Lien, and R.K. Duncan. 1998. Development & Field-Validation of a multi-media exposure assessment model for waste load allocation in aquatic ecosystems: Application to TCDD and TCDF in the Fraser River Watershed. *Environ. Sci. Technol*., 32: 2442-2449.

Gutjahr-Gobell, R.E., D.E. Black, L.J. Mills, R.J. Pruell, B.K. Taplin, and S. Jayaraman. 1999. Feeding the mummichog (*Fundulus heteroclitus*) a diet spiked with non-*ortho*- and mono-*ortho*-substituted polychlorinated biphenyls: accumulation and effects. *Environ. Toxicol. Chem*, 18(4):699-707.

Hamrick, J.M. 1992a. A Three-Dimensional Environmental Fluid Dynamics Computer Code: Theoretical and Computational Aspects. The College of William and Mary, Virginia Institute of Marine Science, Special Report 317, 63 pp.

Hamrick, J.M. 1992b. Estuarine environmental impact assessment using a three-dimensional circulation and transport model. Estuarine and Coastal Modeling, Proceedings of the 2nd International Conference, M.L. Spaulding et al. (eds.), American Society of Civil Engineers, New York, 292-303.

Hamrick, J.M. 1994a. Linking hydrodynamic and and biogeochemical transport model for estuarine and coastal waters. Estuarine and Coastal Modeling, Proceedings of the 3rd International Conference, M. L. Spaulding, et al. (eds.), American Society of Civil Engineers, New York, 591-608.

Hamrick, J.M. 1994b. Application of the EFDC, environmental fluid dynamics computer code to SFWMD Water Conservation Area 2A. A report to South Florida Water Management District. JMH-SFWMD-94-01, J. M. Hamrick, Consulting Engineer, Williamsburg, VA, 126 pp.

Hamrick, J.M. 1996a. Users manual for the environmental fluid dynamic computer code. The College of William and Mary, Virginia Institute of Marine Science, Special Report, 328, 224 pp.

Hamrick, J.M. 1996b. Application of the EFDC hydrodynamic model to Lake Okeechobee. a report to South Florida Water Management District, JMH-SFWMD-96-2, John M. Hamrick, Consulting Engineer, Williamsburg, VA, 63 pp.

Hamrick, J.M. and M.Z. Moustafa. 1999a. Development of the Everglades Wetland Hydrodynamic Model, Part I Model Formulation. Water Resources Research (In Review).

Hamrick, J.M. and M.Z. Moustafa. 1999b. Development of the Everglades Wetland Hydrodynamic Model, Part II: Model Implementation. Water Resources Research (In Review).

Hamrick, J.M. and T.S. Wu. 1997. Computational design and optimization of the EFDC/HEM3D surface water hydrodynamic and eutrophication models. Next Generation Environmental Models and Computational Methods. G. Delich and M. F. Wheeler (eds.), Society of Industrial and Applied Mathematics, Philadelphia, 143-156.

HEC (Harrington Engineering and Construction, Inc.). 1996. Report on the Preliminary Investigation of Corrective Measures for Housatonic River and Silver Lake Sediment. Prepared for General Electric Company.

Hill, W.R. and G.E. Napolitano. 1997. PCB congener accumulation by periphyton, herbivores and omnivores. *Arch. Environ. Contam. Toxicol.*, 32:449-455.

Hwang, K.-N. and A.J. Mehta. 1989. Fine sediment erodibility in Lake Okeechobee. Coastal and Oeanographic Enginnering Dept., University of Florida, Report UFL/COEL-89/019, Gainesville, FL.

Hwang, B., J. Kwan-Soo, L. Young-Dae, and L. Wu-Seng. 1998. Importance of DOC in sediments for contaminant transport modeling. *Water Sci. Tech.*, 38(11): 193-199.

ITIS 2000. Integrated Taxonomic Information System. Agriculter and Agri-food Canada. http://res.agr.ca/it is/

Jafvert, C.T. and J.E. Rogers. 1990. Biological remediation of contaminated sediments, with special emphasis on the Great Lakes. Great Lakes National Program Office, EPA-600-991-001.

Johanson, R.C., J.C. Imhoff, and H.H. Davis. 1980. User's Manual for the Hydrologic Simulation Program - FORTRAN (HSPF). EPA-600/9-80-105. U.S. EPA Environmental Research Laboratory, Athens, GA.

Johnson, J.H. and D.S. Dropkin. 1995. An analysis of fish diet composition and the benthic invertebrate community of the Sudbury River, Massachusetts. National Biological Service.

Kadlec, M.J. and B. Bush. 1994. Bioconcentration of congener specific polychlorinated biphenyl (PCB) in rainbow trout (*Oncorynchus mykiss*) exposed to the water column of the General Motors Superfund site, Massena, NY. Presented at the Superfund XIV Conference, Hazardous Materials Research Institute. Washington, DC.

Kannan, K., H. Nakata, R. Stafford, G.R. Masson, S. Tanabe, and J.P. Giesy. 1998. *Environ. Sci. Technol.*, 32:1214-1221.

Kittle, J. L. Jr., A.M. Lumb, P.R. Hummel, P.B. Duda, and M.H. Gray. 1998. A Tool for the Generation and Analysis of Model Simulation Scenarios for Watersheds (GenScn). Water-Resources Investigation Report 98-4134. U.S. Geological Survey, Reston, VA. 152 p.

Koelmans, A.A. and E.H.W. Heugens. 1998. Binding constants of chlorobenzenes and polychlorobiphenyls for algal exudates. *Water Science Technology*, 37(3):67-73.

Koelmans, A.A., S.F.M. Anzion, and L. Lijklema. 1995. Dynamics of organic micropollutant biosorption to cyanobacteria and detritus. *Environ. Sci. Technol.*, 29(4):933-940.

Lahlou, M., L. Shoemaker, S. Choudhury, R. Elmer., A. Hu, H. Manguerra, and A. Parker. 1998. Better Assessment Science Integrating Point and Nonpoint Sources. BASINS, Version 2.0 User's Manual. EPA-823-B-98-006. U.S. EPA, Washington, D.C. 65 p.

Landrum, P.F., M.D. Reinhold, S.R. Nihart, and B.J. Eadie. 1985. Predicting the Bioavailability of Organic Xenobiotics to *Pontoporeia hoyi* in the Presence of Humic and Fulvic Materials and Natural Dissolved Organic Matter. *Environmental Toxicology and Chemistry*, 4:459-467.

Landrum, P.F., S.R. Nihart, B.J. Eadie, and L.R. Herche. 1987. Reduction in Bioavailability of Organic Contaminants to the Amphipod *Pontoporeia hoyi* by Dissolved Organic Matter of Sediment Interstitial Waters. *Environ. Toxicol. Chem.*, 6:11-20.

Landrum, P. 1998. Kinetic models for assessing bioaccumulation. National Sediment Bioaccumulation Conference Proceedings. U.S. Environmental Protection Agency Office of Water EPA 823-R-98-002, P. 1-47-1-50.

Larsson, P. 1987. Uptake of polychlorinated biphenyls by the macroalga *Cladophora glomerata. Bull. Environ. Contam. Toxicology* 38(1): 58-62.

LeBlanc, L. and B. Brownawell. 1994. Tests of bioaccumulation models for PCBs: a study of young-of-the-year bluefish in the Hudson River Estuary. Report to the 1993 Polgar Fellowship Program. Pp. VII-1 – VII-42.

Leadley, T.A., G. Balch, C.D. Metcalfe, R. Lazar, E. Mazak, J. Habowsky, and G.D. Haffner. 1998. Chemical accumulation and toxicological stress in three brown bullhead (*Ameiurus nebulosus*) populations of the Detroit River, Michigan, USA. *Environ. Toxicol. Chem.*, 17(9):1756-1766.

Lee, R.E. 1989. *Phycology*. Second edition. Cambridge University Press, New York, NY. 645 pp.

Lee, H.Y., H.M. Hsieh, J.C. Yang, and C.T. Yang. 1997. Quasi-Two Dimensional Simulation of Scour and Deposition in Alluvial Channels. Journal of the Hydraulics Division, American Society of Civil Engineers, Vol. 123, No. 7.

Lee, H.Y. et al. 1998. Numerical Simulations of Scour and Deposition in a Channel Network. In Proceedings of the First Federal Interagency Hydrologic Modeling Conference. Las Vegas, NV.

Loonen, H., D.C.G. Muir, J.R. Parsons and H.A.J. Govers. 1997. Bioaccumulation of polychlorinated dibenzo-*p*-dioxins in sediment by oligochaetes: Influence of exposure pathway and contact time. *Environ. Toxicol. Chem.*, 16(7):1518-1525.

Looser, R. 1998. Biomagnification of polychlorinated biphenyls (PCBs) in freshwater fish. Fresenius. *J. Anal. Chem.*, 360: 816-819.

Manhanty, H.K. 1986. Polychlorinated biphenyls: accumulation and effects upon plants. In J.S. Waid, Ed., PCBs and the Environment, Volume II. CRC, Boca Raton FL, USA, pp. 1-8.

Markwell, R.D., D.W. Connell, A.J. Gabric. 1989. *Water Ses.*, 13:1443.

McKay, M.D., W.J. Conover, and R.J. Beckman. 1979. A Comparison of Three Methods for Selecting Values of Input Variables in the Analysis of Output from a Computer Code. *Technometrics,* 211:239-245.

McKim, J.M., P.K. Schneider, and G. Veith. 1985. Absorption dynamics of organic chemical transport across trout gills as related to octanol-water partition coefficient. *Toxicol. Appl. Pharmacol.*, 77: 1-10.

McNeil, J., C. Taylor, and W. Lick. 1996. Measurements of Erosion of Undisturbed Bottom Sediments with Depth. *Journal of Hydraulic Engineering,* 122 (6): 316-324.

Mellor, G. L., and T. Yamada, 1982: Development of a turbulence closure model for geophysical fluid problems. *Rev. Geophys. Space Phys.,* 20, 851-875.

Molinas, A., and C.T. Yang, 1986. Computer Program User's Manual for GSTARS (Gneralized Stream Tube model for Alluvial River Simulation), U.S. Bureau of Reclamation, Denver, CO.

1   Morrison, H.A., F.A.P.C. Gobas, R. Lazar, and G.D. Haffner. 1996. Development and
2   verification of a bioaccumulation model for organic contaminants in benthic invertebrates.
3   *Environ. Sci. Technol.*, 30: 3377-3384.

4   Moustafa, M.Z. and J. M. Hamrick. 2000. Calibration of the Wetland Hydrodynamic Model to
5   the Everglades Nutrient Removal Project. *Water Quality and Ecosystem Modeling* (In
6   Review).

7   NWS (National Weather Service). 1982a. Evaporation Atlas for the Contiguous 48 United
8   States. NOAA Technical Report NWS 33. U. S. Department of Commerce, NOAA.
9   Washington, DC. 26 p.

10 NWS (National Weather Service). 1982b. Mean Monthly, Seasonal, and Annual Pan
11   Evaporation for the United States. NOAA Technical Report NWS 34. U. S. Department of
12   Commerce, NOAA. Washington, DC. 82 p.

13 Neely, W.B. 1983. Chapter 5 Reactivity and Environmental Persistence of PCB Isomers. In
14   Mackay, D., S. Paterson, S.J. Eisenreich, and M.S. Simmons (eds.), Physical Behavior of
15   PCBs in the Great Lakes, Ann Arbor Mich.: Ann Arbor Science, pp. 71-88.

16 NIEHS. 1999. *Research Brief 50: Bioavailability of Chlorinated Hydrocarbons in the Diet*.
17   NIEHS/EPA Superfund Research Program, 2 pp.

18 Oliver, B.G. and A.J. Niimi. 1988. Trophodynamic Analysis of Polychlorinated Biphenyl
19   Congeners and Other Chlorinated Hydrocarbons in the Lake Ontario Ecosystem. *Environ.*
20   *Sci. Technol.*, 22:388-397.

21 O'Neill, R.V., D.L. DeAngelis, J.B. Waide, and T.F.H. Allen. 1986. *A Hierarchical Concept of*
22   *the Ecosystem*. Princeton University Press, Princeton, N.J.

23 Opperhuizen, A. 1986. Aquatic Toxicology and Environmental Fate. ASTM STP 921. pp. 304-
24   315.

25 Palisade Corporation. 1991. *Risk Analysis and Simulation Add-In for Lotus 1-2-3.* Newfield New
26   York, 342 pp.

27 Park, R.A. 1998. *Validation of the AQUATOX Model with Mesocosm Data for Toxic Organic*
28   *Chemicals*. Contract 7W-4330-NALX, Washington, DC. U.S. Environmental Protection
29   Agency, 9 pp.

30 Park, R.A. 1999. Evaluation of AQUATOX for predicting bioaccumulation of PCBs in the Lake
31   Ontario Food Web. EPA Contract 68-C-0051, Work Assignment 4-13 under Subcontract
32   0051-ECOMOD-1 from The Cadmus Group, Inc. U.S. Environmental Protection Agency.
33   August 1999.

34 Park, R.A. 2000. Unpublished Results of AQUATOX Simulations.

Park, R.A., R.V. O'Neill, J.A. Bloomfield, H.H. Shugart, Jr., R.S. Booth, J.F. Koonce, M.S. Adams, L.S. Clesceri, E.M. Colon, E.H. Dettman, R.A. Goldstein, J.A. Hoopes, D.D. Huff, S. Katz, J.F. Kitchell, R.C. Kohberger, E.J. LaRow, D.C, McNaught, J.L. Peterson, D. Scavia, J.E. Titus, P.R. Weiler, J.W. Wilkinson, and C.S. Zahorcak. 1974. A Generalized Model for Simulating Lake Ecosystems. *Simulation*, 23(2):30-50. Reprinted in *Benchmark Papers in Ecology*.

Park, R.A., B.H. Indyke, and G.W. Heitzman. 1981. Predicting the Fate of Coal-Derived Pollutants in Aquatic Environments. Paper presented at Energy and Ecological Modeling symposium, Louisville, Kentucky, April 2023, 1981. Developments in Environmental Modeling 1. 7 pp.

Park, R.A., and C.D. Collins. 1982. Realism in Ecosystem Models. *Perspectives in Computing,* 2(2):18S27.

Parker, R.A., and A.D. Hasler. 1959. Movements of Some Displaced Centrarchids. *Copeia,* 1959(1):11-18. Cited in Bryant, H.E., and A. Houser. Population Estimates and Growth of Largemouth Bass in Beaver and Bull Shoals Reservoirs. In Hall, G.E., ed. 1971. *Reservoir Fisheries and Limnology*, Washington DC: American Fisheries Society, pp. 349-357.

Parkerton, T.F. 1993. Ph.D. Dissertation, Manhattan College, New York, 1993.

Patrick (Patrick Center for Environmental Research). 1999. PCB concentrations in fishes and benthic insects from the Housatonic River, Connecticut, in 1984 to 1998. Prepared for the General Electric Company. November 15, 1998).

Pelka, A. 1998. Bioaccumulation Models and Applications: Setting Sediment Cleanup Goals in the Great Lakes. *National Sediment Bioaccumulation Conference Proceedings*. U.S. Environmental Protection Agency Office of Water EPA 823-R-98-002, p. 5-9-5-30.

Press, W.H., B.P. Flannery, S.A. Teukolsky, and W.T. Vetterling. 1986. *Numerical Recipes: The Art of Scientific Computing*. Cambridge University Press, Cambridge, U.K. 818 pp.

QEA (Quantitative Environmental Analysis, LLC). 1998a. Technical memorandum to Andrew Silfer (GE) from C. Kirk Ziegler (QEA) re: "Erosion Properties of Cohesive Sediments in the Housatonic River", November 6, 1998. Montvale, NJ.

QEA. 1998b. Technical memorandum to Andrew Silfer (GE) from James Rhea and Kevin Russell (QEA) re: "High Flow Monitoring and Bathymetric/Sediment Bed Mapping Survey", November 6, 1998. Liverpool, NY.

QEA. 1999. PCBs in the Upper Hudson River. Prepared for General Electric, Albany NY. May 1999.

Rosati, A.K. and K. Miyakoda. 1988. A general circulation model for upper ocean simulation. *J. Phys. Ocean.*, 18, 1601-1626.

Rosgen, D.L. 1985. A Stream Classification System. In: Riparian Ecosystems and Their Management. First North American Riparian Conference, Rocky Mountain Forest and range Experiment Station, General Technical Report RM-120. Pp. 91-95.

Rosgen, D.L. 1994a. A Classification of Natural Rivers. *Catena*, 22:169-199.

Rosgen, D.L. 1994b. *Applied River Morphology*. Wildland Hydrology, Pagosa Springs, CO.

Safe, S. 1980. Metabolism, Uptake, Storage and Bioaccumulation of Halogenated Aromatic Pollutants. In: Kimbrough, R.D., ed., *Halogenated Biphenyls, Terphenyls, Naphthalenes, Dibenzodioxins and Related Products.* Amsterdam: Elsevier Science Publishers, pp. 81-107.

Schnoor, J.E. 1996. *Environmental Modeling: Fate and Transport of Pollutants in Water, Air, and Soil.* New York: John Wiley & Sons, Inc., 682 pp.

Schumm, S.A. 1960a. The effect of sediment type on the shape and stratification of some modern fluvial deposits. *Am. Jour. Sci.*, 258:117-84.

Schumm, S.A. 1960b. Shape of alluvial channels in relation to sediment type: U.S. Geol. Survey Prof. Paper 352 -B, pp. 17-30.

Schumm, S.A. and H.R. Khan. 1972. Experimental study of channel patterns. *Geol. Soc. of America*, 83:1755-70.

Schweitzer, L.E., J.E. Hose, I.H. Suffet, and S.M. Bay. 1997. Differential toxicity of three polychlorinated biphenyl congeners in developing sea urchin embryos. *Environ. Toxicol. Chem.*, 16(7):1510-1514.

Shaw, G.R. and D.W. Connell. 1984. Factors controlling bioaccumulation of PCBs. In: PCBs and the Environment, Volume 1. National Technical Information Service, pp. 501-516.

Shrestha, P.A., and G.T. Orlob. 1996: Multiphase distribution of cohesive sediments and heavy metals in estuarine systems. *J. Environ. Engrg.*, 122:730-740.

Sijm, D.T.H.M. and A. ven der Linde. 1995. Size-dependent bioconcentration kinetics of hydrophobic organic chemicals in fish based on diffusive mass transfer of allometric relationships. *Environ. Sci. Technol.*, 29(11):2769-2777.

Sijm, D.T.H.M., K.W. Broersen, D.F. de Roode, and P. Mayer. 1998. Bioconcentration kinetics of hydrophobic chemicals in different densities of *Chlorella pyrenoidosa*. *Environ. Toxicol. Chem.*, 17(9):1695-1704.

Smith, S.B. and J.F. Coles. 1997. Endocrine Biomarkers, Organochlorine Pesticides, and Congener Specific Polychlorinated Biphenyls (PCBs) in Largemouth Bass (Micropterus salmoides) from Woods Pond, Housatonic River, Massachusetts, September 1994 and May 1995. U.S. Geological Survey, Reston, VA. 14 p.

Smith, J.D. and S.R. McLean. 1977. Spatially averaged flow over a wavy surface. *J. Geophysical Res.*, 82, 1735-1746.

Sokol, R.C., C.M. Bethoney, and G-Y. Rhee. 1998a. Effect of Aroclor 1248 concentration on the rate and extent of polychlorinated biphenyl dechlorination. *Environ. Toxicol. Chem.*, 17(10):1922-1926.

Sokol, R.C., C.M. Bethoney, and G-Y. Rhee. 1998b. Reductive dechlorination of preexisting sediment polychlorinated biphenyls with long-term laboratory incubation. *Environ. Toxicol. Chem.*, 17(6):982-987.

Song, C.C.S., Y. Zheng, and C.T. Yang. 1995. Modeling of River Morphologic Changes, International Journal of Sediment Research 10(2).

Stange, K. and D.L. Swackhamer. 1994. Factors affecting phytoplankton species-specific differences in accumulation of 40 polychlorinated biphenyls (PCBs). *Environ. Toxicol. Chem.*, 13(11):1849-1860.

Stewart Laboratories, Inc. 1982. Housatonic River Study 1980 and 1982. Volumes I and II.

Suedel, B.C., T.M. Dillon and W.H. Benson. 1997. Subchronic effects of five di-*ortho* PCB congeners on survival, growth and reporduction in the fathead minnow *Pimephales promelas. Environ. Toxicol. Chem.*, 16(7):1526-1532.

Swackhamer, D.L. and R.S. Skoglund. 1991. The Role of Phytoplankton in the Partitioning of Hydrophobic Organic Contaminants in Water. In Baker, R.A. (ed.), *Organic Substances and Sediments in Water Vol. 2 C Processes and Analytical*, Lewis: Chelsea, MI, pp. 91-105.

TAMS (TAMS Consultants, Inc), Limno-Tech, Inc., Menzie-Cura & Associates, Inc., and Tetra Tech, Inc. 2000. Phase 2 Report – Review Copy. Further Site Characterization and Analysis – Volume 2D – Revised Baseline Modeling Report – Hudson River PCBs Reassessment RI/FS. Prepared for U.S. Environmental Protection Agency, Region 2 and U.S. Army Corps of Engineers, Kansas City District. January 2000.

Techlaw, Inc. 1999. General Electric II, Pittsfield, Massachusetts: Final Preliminary Ecological Characterization, Newell Street to Woods Pond. Volumes I and II. Prepared for U.S. EPA, Boston, MA.

Tetra Tech, Inc., 1998: Calibration and verification of the Elliott Bay and Duwamish River hydrodynamic model. Prepared for the King County, Washington, Dept. of Natural Resources. Tetra Tech, Inc., Fairfax, VA.

Tetra Tech, Inc. 1999a. Pilot scale application of existing water quality models to derive NPDES permits based on sediment quality. Prepared for the U.S. Environmental Protection Agency. Tetra Tech, Inc., Fairfax, VA.

Tetra Tech, Inc. 1999b. Hydrodynamic and thermal model of the cooling water discharge from the Pentagon heating and refrigeration plant into the Potomac River. Prepared for DMJM/3DI, Inc. Tetra Tech, Inc., Fairfax, VA.

Tetra Tech, Inc. 1999c. Hydrodynamic, sediment transport and water quality model of Morro Bay, California. Prepared for the Morro Bay National Estuary Program. Tetra Tech, Inc., Fairfax, VA.

Tetra Tech, Inc. 1999d. A hydrodynamic, and water quality model of the Christina River Basin. Prepared for U.S. EPA Region 3. Tetra Tech, Inc., Fairfax, VA.

Tetra Tech, Inc. 1999e. A theoretical description of toxic contaminant transport formulations used in the EFDC model. Tech. Memo TT-EFDC-99-2, Tetra Tech, Inc., Fairfax, VA.

Tetra Tech. 2000a. Hydrodynamic and Water Quality Model of Christina River Basin, Final Report. For U.S. EPA Region 3, Philadelphia, PA. By Tetra Tech, Inc., Fairfax, VA. May 31, 2000.

Tetra Tech. 2000b. Low-flow Water Quality Modeling Analysis in Support of TMDL Development for Poteau River and Fourche Maline Creek in the Poteau River Watershed, Oklahoma. 2000. U.S. EPA Region 6 and Oklahoma Department of Environmental Quality. March 2000. (Wister Lake)

Tetra Tech. 2000c. Low-flow Water Quality Modeling Analysis in Support of TMDL Development for Ballard Creek, Baron Fork, Flint Creek, Illinois River, Tahlequah Creek and West Brook in the Illinois River Watershed, Oklahoma. 2000. U.S. EPA Region 6 and Oklahoma Department of Environmental Quality. March 2000. (Tenkiller Lake)

Tetra Tech. 2000d. EFDC Technical Memorandum: Theoretical and Computational Aspects of Sediment Transport in the EFDC Model. Prepared for U.S. Environmental Protection Agency, Office of Science & Technology, Washington, DC.

Tetra Tech Inc. 2000e. A theoretical description of sediment transport formulations used in the EFDC model. Tech. Memo TT-EFDC-99-1, Tetra Tech, Inc., Fairfax, VA.

Thomann, R.V. and J.A. Mueller. 1983. Steady-state modeling of toxic chemicals-Theory and application to PCBs in the Great Lakes and Saginaw Bay, Mackay et al. (eds.), *Physical Behavior of PCBs in the Great Lakes*, Ann Arbor Science, Ann Arbor, MI, 442 pp.

Thomann, R.V. and J.P. Connolly. 1984. Model of PCB in Lake Michigan lake trout food chain. *Environ. Sci. Technol.*, 18: 65-71.

Thomann, R.V. and J.A. Mueller. 1987. *Principles of Surface Water Quality Modeling and Control.* Harper & Row, New York, NY. 644 pp.

Thomann, R.V. and K.J. Farley. 1998. Bioaccumulation Modeling of PCBs in the Hudson Estuary: A Review and Update. *National Sediment Bioaccumulation Conference*

Proceedings. U.S. Environmental Protection Agency Office of Water EPA 823-R-98-002, p. 4-19-4-22.

Thomann, R.V., J.A. Mueller, R.P. Winfield and Chi-Rong Huang. 1991. Model of fate and accumulation of PCB homologues in Hudson estuary. *Journal of Environmental Engineering*, 117(2):161-178.

Tsai, C.H. and. W. Lick. 1986. A portable device for measuring sediment resuspension. *Jour. Great Lakes Res.*, 12(4):314-321

U.S. Army Corps of Engineers, 1991. HEC-6: Scour and Deposition in Rivers and Reservoirs Model. Hydrologic Engineering Center, Davis, CA.

Van Dort, H.M., L.A. Smullen, R.J. May, and D.L. Bedard. 1997. Priming Microbial *meta*-Dechlorination of Polychlorinated Biphenyls That Have Persisted in Housatonic River Sediments for Decades. *Environ. Sci. Technology*, 31:11:3300-3307.

Van Rijn, L.C. 1984. Sediment transport, Part II: Suspended load transport. *J. Hyd. Engr.,* 110, 1613-1641.

VanVeld, P.A. 1990. Absorption and metabolism of dietary xenobiotics by the intestines of fish. *Rev. Aquat. Sci.*, 2:185-203.

Wang, F.W., P.M. Chapman, and D. Herbert. 1999. A critique of testing sediment biological effects with *Hyalella azteca*. Environ. Toxicol. Chem. (In review). Presented at Society of Environ. Toxicol. Chem 20th Annual Congress. April 1999.

Welch, E.B. 1992. *Ecological effects of wastewater: applied limnology and pollutant effects.* Second edition. Chapman and Hall, New York, NY. 425 pp.

WESTON (Roy F. Weston, Inc.). 2000a. Supplemental Investigation Work Plan, Technical Support Services, General Electric (GE) Housatonic River Project, Pittsfield, Massachusetts. FINAL Report. Vol. I - Text and Figures & Vol. II - Appendices. Prepared by R.F. Weston, Inc. West Chester, PA. Prepared for U. S. Army Corps of Engineers, New England District, Concord, MA.

WESTON (Roy. F. Weston, Inc.). 2000b. *Final Quality Assurance Project Plan, General Electric (GE) Housatonic River Project, Pittsfield, Massachusetts.* Prepared for U.S. Environmental Protection Agency. Prepared by Roy F. Weston, Inc., West Chester, PA.

WESTON (Roy F. Weston, Inc.). 1998b. *Source Area Characterization Report*. Prepared by U.S. Army Corps of Engineers. Prepared by Roy F. Weston, Inc., West Chester, PA.

Wetzel. 1983. *Limnology*. Sanders College Publishing, Fort Worth TX.

Willman, E.J., J.B. Manchester-Neesvig, and D.E. Armstrong. 1997. Influence of *ortho*-substitution on patterns of PCB accumulation in sediment, plankton, and fish in a freshwater estuary. *Environ. Sci. Technol.*, 31(12):3712-3718.

Wood, L.W., P.O. Keefe, and B. Bush. 1997. Similarity analysis of PAH and PCB bioaccumulation patterns in sediment-exposed *Chironomus tentans* larvae. *Environ. Toxicol. Chem.*, 16(2):283-292.

Woodlot, 1998. 1998 Fish Characterization Data for the Housatonic River. Unpublished manuscript.

Woodlot. 1999. Technical Memorandum. Fish Biomass Estimate - Housatonic River, Massachusetts. Memo sent by K. Karwacky to J. Lortie, December 29, 1999.

Woodlot (Woodlot Alternatives Inc.). 2000. General Electric/Housatonic River Superfund site fish captures - data sheets. Woodlot Alternatives Inc., Topsham, ME.

Wu, Q. and J. Wiegel. 1997. Two Anaerobic Polychlorinated Biphenyl-Dehalogenating Enrichments That Exhibit Different *para*-Dechlorination Specificities. *Applied and Environmental Microbiology*, 63:12:4826-4832.

Wu, Q., D.L. Bedard, and J. Wiegel. 1996. Influence of INCUBATION Temperature on the Microbial Reductive Dechlorination of 2,3,4,6-Tetrachlorobiphenyl in Two Freshwater Sediments. *Applied and Environ. Microbiology*, 62:11:4174-4179.

Wu, Q., D.L. Bedard, and J. Wiegel. 1997a. Effect of Incubation Temperature on the Route of Microbial Reductive Dechlorination of 2,3,4,6-Tetrachlorobiphenyl in Polychlorinated Biphenyl (PCB)-Contaminated and PCB-Free Freshwater Sediments. *Applied and Environmental Microbiology*, 63:7:2836-2843.

Wu, Q., D.L. Bedard, and J. Wiegel. 1997b. Temperature Determines the Pattern of Anaerobic Microbial Dechlorination of Aroclor 1260 Primed by 2,3,4,6-Tetrachlorobiphenyl in Woods Pond Sediment. *Applied and Environmental Microbiology*, 63:12:4818-4825.

Wu, T.S., J.M. Hamrick, S.C. McCutcheon, and R.B. Ambrose. 1997c. Benchmarking the EFDC/HEM3D surface water hydrodynamic and eutrophication models. Next Generation Environmental Models and Computational Methods, G. Delic and M.F. Wheeler, (eds.), Society of Industrial and Applied Mathematics, Philadelphia.

Wydoski, R.S. and R.R. Whitney. 1979. *Inland Fishes of Washington.* University of Washington Press, Seattle and London. 220 pp.

Yang, C.T., 1976. Minimum Unit Stream Power and Fluvial Hydraulics. Journal of the Hydraulics Division, American Society of Civil Engineers, 102(7).

Yang, C.T., and C.C.S. Song. 1979. Theory of Minimum Rate of Energy Dissipation. Journal of the Hydraulics Division, American Society of Civil Engineers, 105(7).

Yang, C.T., T. Mark, and S. Francisco. 1998. Generalized Stream Tube Model for Alluvial River Simulation, Version 2.0. U.S. Bureau of Reclamation, Denver, CO.

1 Yang, C. T., A. Molinas, and B. Wu. 1996. Sediment Transport in the Yellow River. Journal of
2   the Hydraulics Division, American Society of Civil Engineers, Vol. 122, No. 5.

3 Yang, Z., 1996. Variational inverse methods for transport problems. Ph.D. dissertation, the
4   College of William and Mary, Williamsburg, VA, 150 pp.

5 Zaranko, D.T., R.W. Griffiths, and N.K. Kaushik. 1997. Biomagnification of Polychlorinated
6   Biphenyls Through a Riverine Food Web. *Environ. Toxicol.Chem.*, 16(7):1463-1471.

7 Zarillo, G. A., and C.R. Surak, 1995. Evaluation of submerged reef performance at Vero Beach,
8   Florida, using a numerical modeling scheme. a report to Indian River County Florida.
9   Florida Institute of Technology, 56 pp.

10 Ziegler, C.K., and B.S. Nisbet. 1994. Fine-grained sediment transport in Pawtuxet River, Rhode
11   Island. *J. Hyd. Engrg.*, 120, 561-576.

12 Ziegler, C.K., and B.S. Nisbet. 1995. Long-Term Simulation of Fine-Grained Sediment
13   Transport in Large Reservoir. *Journal of Hydraulic Engineering*, November: 773-781.

14

APPENDIX A

PCB ENVIRONMENTAL FATE AND EFFECTS

TABLE OF CONTENTS

Section	Page

LIST OF TABLES

Title	Page

LIST OF FIGURES

Title	Page

APPENDIX A

PCB ENVIRONMENTAL FATE AND EFFECTS

Because PCBs are the compounds of greatest concern in the area of the Housatonic River under study, they will be the focus of this discussion. However, it is possible that other chemicals, such as dioxins/furans, will warrant evaluation as well; the modeling concepts discussed below are equally applicable to all hydrophobic, and in particular, bioaccumulative contaminants.

PCB CLASSIFICATION AND PHYSICAL/CHEMICAL PROPERTIES

Polychlorinated biphenyls (PCBs) are synthetic organochlorine chemicals of 12 carbon atoms, with chlorine atoms substituted for hydrogen atoms in any of the 10 numbered positions, as shown in (**Figure 1**). The positions can be referred to by name, with four *ortho* positions, four *meta* positions, and two *para* positions. Positions occupied by chlorine atoms can be indicated, for example as 2,4' or by the nonstandard but more convenient notation 2/4, which indicates the bilateral structure more readily. The latter convention will be used in this appendix.
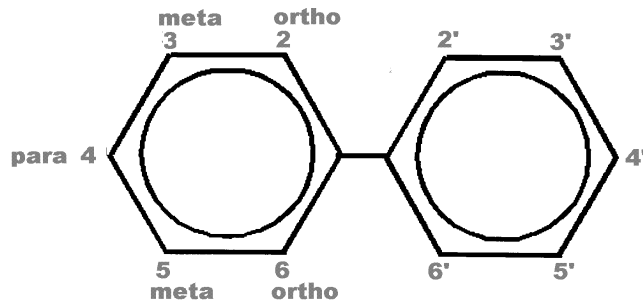
Figure 1   Structure and Nomenclature of PCBs

PCBs can be classified into level-of-chlorination homolog groups, which are groups of PCB congeners having the same number of chlorine substitutions. Level of chlorination affects various physicochemical properties of the PCB molecule such as the octanol/water partition coefficient (K_{ow}), solubility, vapor pressure, and Henry's Law constant, which in turn affect processes such as volatilization, and loss from water, sediments, and floodplain soils. Similarly, level of chlorination also controls (in part) biologically mediated processes such as biotransformation, uptake, and accumulation (Schweitzer et al., 1997). Although there is still a range of variation within a homolog group, in general PCB congeners with similar levels of chlorination tend to share similarities with regard to these properties and processes. K_{ow}, in particular, generally increases with increasing level of chlorination and is a major controlling variable affecting the lipophilic behavior of PCBs, with increased chlorine substitution usually resulting in a higher K_{ow} and consequent elevated affinity for lipids. The relationship between certain physical constants and PCB homolog group is shown for a number of PCB congeners in Table 1.

Table 1

Examples of Structure and Physical/Chemical Properties of PCBs

Homolog	IUPAC No.	Structure	Aroclor 1254 wt. %	Aroclor 1260 wt. %	Toxicity TEF	Molecular Weight g/mol	Solubility g/m³	V Press Pa	Henry's Law X 10^4 atm m³/mol	log K_{OW}
Mono CBP			0	0		189	7.2	2.3		4.47
	1	2							7.38	4.601
	2	3							4.88	4.421
	3	4							4.88	4.401
Di CBP			0.244	0.16		223	2.2	0.6		5.19
	4	2/2							5.35	5.023
	8	2/4	0.094						3.53	5.301
	15	4/4	0.15	0.16					2.34	5.335
Tri CBP			0.643	0.275		257	0.67	0.2		5.62
	5	26/2							3.88	5.481
	17	24/2	0.19	0.05					2.56	5.761
	18	25/2	0.13	0.11		257.5			1.69	5.551
	27	26/3							2.56	5.447
	29	245/		0.02					1.69	5.743
	31	25/4	0.24	0.05	*				1.69	5.677
	28	24/4	0.083	0.045					1.69	5.691
Tetra CBP			16.02	0.482		292	0.23	0.06		6.54
	47	24/24	0.17	0.11					1.23	6.291
	52	25/25	6.2	0.24					1.23	6.091
	49	24/25	1.1	0.06					1.23	6.221
	44	23/25	2.6	0.048					1.23	5.811
	74	245/4	0.92	0.03					0.81	6.671
	70	25/34	3.9	0.054					0.81	6.231
	66	24/34	1.3	0.05	*				0.81	5.452
	77	34/34	0.022	0.006	0.0005				0.28	6.523
Penta CBP			53.3	9.939		326	0.072	0.015		6.73
	95	236/25	11	4	*				0.89	6.137
	101	245/25	10	3.5					0.59	7.071
	99	245/24	3.5	0.12					0.59	7.211
	97	245/23	3	0.079					0.59	6.671
	87	234/25	4.8	0.39					0.59	6.371
	105	234/34	3.3	0.12	0.0001				0.59	6.657
	110	236/34	10	1.3	*				0.59	6.532
	114	2345/4			0.0005				0.39	6.657
	118	245/34	7.7	0.43	0.0001				0.39	7.121
	123	345/24	0.81		0.0001				0.39	6.747
	126	345/34	0.003		0.1				0.26	6.897
Hexa CBP			26.19	40.84		361	0.021	0.005		7.16
	151	2356/25	0.99	4.2					0.42	6.647
	149	2346/25	4.9	11					0.42	7.281
	153	245/245	5.1	11					0.28	7.751
	132	234/236	2.8	2.9					0.42	6.587
	137	2345/24	0.46	0.14					0.28	>7.711
	138	234/245	7.7	9.3	*				0.28	7.441
	158	2346/34	1.1	0.85					0.28	7.027
	128	234/234	1.7	0.49					0.28	6.961
	156	2345/34	1	0.45	0.0005				0.19	7.187
	157	234/345		0.14	0.0005				0.19	7.187
	167	245/345	0.21	0.21	0.00001				0.19	7.277
	169	345/345	0.23	0.16	0.01				0.12	7.427
Hepta CBP			3.09	38.27		395	0.006	(0.0015)		7.28
	187	2356/245	0.39	7.2					0.20	7.177
	183	2346/245	0.31	3.3					0.20	7.207
	174	2345/236	0.49	6.2					0.20	7.117
	177	235/2346	0.29	3.2					0.20	7.087
	180	2345/245	0.97	13	0.00001				0.13	7.367
	170	2345/234	0.64	5.2	0.0001				0.13	7.277
	189	2345/345		0.17	0.0001				0.09	7.717
Octa CBP			0.731	10.2		430	0.002	(0.0005)		7.88
	201	2346/2356	0.68	2.9					0.15	7.627
	203	23456/245	0.051	3.1					0.10	7.657
	195	23456/234		1.3					0.10	7.567
	194	2345/2345		2.9	*				0.06	8.683
Nona CBP			0	0.72		464	0.0007	(0.00015)		9.14
	207	23456/2346		0.05					0.07	7.747
	206	23456/2345		0.67					0.05	9.143
Deca CBP			0	0.05		499	0.0002	(0.00004)		9.6
	209	23456/23456		0.05					0.03	9.603
Sum			100.218	100.936						

MW, solubility, and v. pressure from Mackay et al., 1983; K_{OW} from Eisler and Belisle, 1996;* = non-Ah toxicity,
TEF = toxic equivalencies from Eisler and Belisle, 1996; Gerstenberger et al., 1997; and Kannan et al., 1998; structure from
Eisler and Belisle, 1996; Newman et al., 1998; parentheses indicate speculative values; Henry's Law, Brunner et al., 1990 est.

The pattern of chlorine substitution affects toxicity (Schweitzer et al., 1997) and also influences metabolism (biotransformation to other congeners) and thus bioaccumulation (Bright et al., 1995). The more toxic PCBs are the coplanar congeners that have zero or one Cl in the *ortho* position (Campfens and Mackay, 1997). The availability of adjacent unsubstituted carbons in *meta* and *para* positions facilitates metabolic transformation (Bright et al., 1995) and detoxification and excretion (Gutjahr-Gobell et al., 1999).

The Monsanto Company historically produced nine mixtures of PCBs known as Aroclors 1221, 1232, 1016, 1242, 1248, 1254, 1260, 1262, and 1268; the last two digits represent the percent Cl by mass, except for 1016, which has 41% Cl by mass (Newman et al., 1998). PCBs present in the Housatonic River appear to be predominantly Aroclor 1260, although Aroclors 1254 and 1242 were discharged as well (WESTON, 2000). Only approximately 75% of the 209 possible congeners were actually produced in the synthesis of the commercial Aroclor mixtures. Congener-specific analysis is important because of effects that have been linked to specific congeners (Gerstenberger et al., 1997; Van den Berg et al., 1998).

It is not feasible to model all congeners in this modeling effort because of the computational load. DiPinto and Coull (1997) found that in bioaccumulation studies classifying congeners according to K_{OW} was more useful than classifying them according to degree of chlorination; K_{OW} is a function of both the number and positioning of Cl on the PCB molecule. This methodology is also limiting because it can mask patterns of biotransformation. Therefore, a compromise is to model homologs, much as Thomann et al. (1991) did for the Hudson River, and to separately model some of the more toxic congeners (e.g., PCBs 77, 126, and 169).

CHEMICAL AND MICROBIAL DEGRADATION AND LOSS

Some congeners are dechlorinated selectively by either aerobic or anaerobic bacteria (Butcher et al., 1997). Only the heavier congeners are dechlorinated anaerobically, and only the lighter congeners are degraded aerobically (Jafvert and Rogers, 1990). Some methanogenic bacteria, which are anaerobic, dechlorinate PCBs at *meta* and *para* positions, enhancing Cl_1, Cl_2, and Cl_3 *ortho*-substituted PCBs, and counteracting selective enrichment of some congeners (Bright et al., 1995).

The rate of anaerobic dechlorination depends primarily on *meta* and *para* removal (Brown et al., 1984; Bedard and Quensen, 1995; Quensen et al., 1998; Sokol et al., 1998b). Different geographic sites exhibit different characteristic specificities for PCB dechlorination; at least seven distinct microbial dechlorination activities have been identified in Woods Pond (Wu et al., 1997a). Process P is restricted to removal of *para* chlorines with at least one adjacent chlorine; primarily homologs Cl_4 through Cl_7 are affected, with a large increase in congener 25/25, as has been noted in Woods Pond (Bedard and May, 1996).

This process has a temperature optimum at 20°C (Wu et al., 1996) and a range of 12 to 34°C (Wu et al., 1997b). Process N is restricted to removal of *meta* chlorines with at least one adjacent chlorine; nearly all Cl_6 and Cl_7 and many Cl_5 homologs in Aroclor 1260 are subject to this process, resulting in a large increase in congener 24/24, as noted in Woods Pond (Bedard and May, 1996). This process has a range of 8 to 30°C (Wu et al., 1997b). Van Dort and Bedard (1991) found *ortho* dechlorination of a congener; however, this process does not appear to be important in the field.

This process has a temperature optimum at 15 and 27 °C and a range of 8 to 30°C (Wu et al., 1996); it dominates at 15 °C (Wu et al., 1997b).

Bedard et al. (1997) stimulated a new unflanked *para* dechlorination activity, which they called Process LP; this process works in concert with Process N to further dechlorinate PCBs. Process LP has a temperature range of 18 to 30°C (Wu et al., 1997b). Overall, dechlorination of Aroclor 1260 occurs above 8°C, with optimal removal between 20 and 27°C (Wu and Wiegel, 1997). Temperatures in the top 45 cm of sediments in Woods Pond are 1 to 4 °C in winter, 8 to 12 °C in spring and fall, and 15 to 22 °C in summer (Wu et al., 1999).

Although disputed by some, Sokol et al. (1998b) found that removal is a function of PCB concentration and that dechlorination is effective only above a threshold concentration. Anaerobic transformation of highly chlorinated congeners into lower chlorinated congeners in a variable environment makes them subject to later aerobic microbial degradation, which can oxidatively mineralize lower Cl congeners, especially homologs Cl_1 and Cl_2, to carbon dioxide and water (Bedard et al., 1987; Bedard and Quensen, 1995; Gerstenberger et al., 1997; Sokol et al., 1998b). In one study, anaerobic dechlorination decreased total Cl by 36%; however, more than 33% of *meta* and *para* Cl remained after 39 months of anaerobic incubation (Sokol et al., 1998a). In another study, highly chlorinated congeners declined between 1988 and 1993 in an Ontario stream due to dechlorination by anaerobic bacteria (Zaranko et al., 1997). Anaerobic dechlorination has been coupled with aerobic biodegradation as a mechanism for bioremediation of PCBs (Abramowicz, 1994).

Volatilization can provide an important pathway for loss of PCBs. The lower chlorinated homologs in particular are subject to volatilization, as indicated by their higher vapor pressures and lower Henry's Law constants summarized in Table 1 (the Henry's Law constants currently are being estimated using HenryWin Ver. 3.02 with verification from the experimental literature). This can result in both a loss and source of the lighter homologs—a source because upon volatilization the atmosphere is enriched with these homologs, which are then subject to atmospheric deposition. PCBs, especially those that have been dechlorinated to Cl_1, Cl_2, and Cl_3, are very susceptible to volatilization upon drying; a maximum of 1.7% of PCBs were emitted per day in one experiment (Bushart et al., 1998). Another experiment, using very thin sediment layers, found even larger loss rates (Chiarenzelli et al., 1996).

Aside from volatilization and biotransformation by microbes and higher organisms, PCBs are remarkably stable. They are affected by neither hydrolysis nor oxidation. Atmospheric photodegradation has been shown to break down Cl_2 homologs, but higher chlorinated compounds are very resistant to this degradation pathway (Neely, 1983). In contrast, experiments with high-intensity UV lamps showed significant dechlorination of Cl_3 through Cl_7 congeners and accumulation of Cl_2 through Cl_4 congeners in soil; however, direct sunlight exposure gave no detectable response (IT Corp., 1999).

SORPTION AND DESORPTION TO ORGANIC MATTER AND BIOAVAILABILITY

Dissolved and particulate organic detritus are very important in controlling both the direct and dietary uptake of PCBs. Association of PCBs with colloidal and dissolved organic matter (DOM) reduces bioavailability; such contaminants are unavailable for uptake by organisms (Landrum et al., 1985, 1987; Stange and Swackhamer, 1994; Gilek et al. 1996; Butcher et al., 1998). Therefore, it is imperative that DOM and DOM complexation with PCBs be modeled correctly. Not all organic material is equal in sorptive affinity (Brannon et al., 1998).

Hydrophobic chemicals partition in nonpolar organic matter (Abbott et al., 1995). Humic acids exhibit high polarity. In one study, natural humic acids from a Finnish lake with extensive marshes were spiked with Cl_4-PCB, but a resulting PCB-humic acid complex could not be demonstrated (Maaret et al., 1992). In another study, Freidig et al. (1998) used artificially prepared Aldrich humic acid to determine a humic-acid DOC partition coefficient:

$$\log K_{DOC} = 0.67 \cdot \log K_{OW} + 1.46$$

This is, in turn, compared to the relationship reported by Koelmans and Heugens (1998) for partitioning to algal exudate:

$$\log K_{DOC} = 1.0 \cdot \log K_{OW} - 0.055$$

This strong association was found to limit availability to the living algae (Koelmans and Heugens, 1998). Nonpolar lipids in algae occur in the cell contents, and it is likely that they constitute part of the exudate, which may be both excreted and lysed material.

Association of PCBs with particulate organic matter (POM) also removes the PCBs from being available for direct uptake, but makes them available to the detrital food web, which is an important pathway in rivers such as the Housatonic. Again, there appears to be a dichotomy in partitioning, but in this case the literature suggests that it is the opposite of the pattern exhibited by DOM, in that labile POM does not take up PCBs as rapidly as refractory POM. Algal cell membranes contain polar lipids, and it is likely that this polarity is retained in the early stages of decomposition. The coefficient of partitioning of PCBs to particulate organic carbon (K_{POC}), does not remain the same upon aging, death, and decomposition, probably because of polarity changes. In an experiment using fresh and aged algal detritus, there was a 100% increase in K_{POC} with aging (Koelmans et al., 1995). K_{POC} increased as the C/N ratio increased, indicating that the material was becoming more refractory. In another study, K_{POC} doubled between day 2 and day 34, probably due to deeper penetration and lower polarity (Cornelissen et al., 1997).

Bioavailability depends on the type of dissolved and particulate organic matter in the system. Binding capacity of PCBs with POC is greater than that observed with DOC in Great Lakes waters (Gilek et al., 1996) (Stange and Swackhamer, 1994). In a study using Baltic Sea water, less than 7% of the PCBs were associated with DOC; most were associated with algae (Björk and Gilek, 1999).

In contrast, in a study using algal exudate and PCB 180 with log K_{OW} of 7.36, 98% of the dissolved concentration was as a DOC complex and only 2% was bioavailable (Koelmans and Heugens, 1998).

Unfortunately, older data and modeling efforts failed to distinguish between PCBs that were truly dissolved and those that were complexed with DOM. For example, the PCB water concentrations for Lake Ontario, reported by Oliver and Niimi (1988) and used by many subsequent researchers, included both dissolved and DOC-complexed PCBs (a fact that they recognized). In their steady-state model of PCBs in the Great Lakes, Thomann and Mueller (1983) defined "dissolved" as that which is not particulate (passing a 0.45-micron filter). In their Hudson River PCB model, Thomann et al. (1991) again used this operational definition of dissolved PCBs.

The structure of a PCB congener and its origin are also important in determining the fate in the detrital system. In deeper bodies of water, POM is often released as fecal pellets and sinks rapidly to the bottom sediments (Baker et al. 1991). Cl_2 to Cl_4 homologs may be present in higher concentrations in fecal material, but they are also released quickly (Baker et al., 1991). Planar PCBs bind strongly to POM and are less bioavailable (van Bavel et al. 1996). Highly chlorinated homologs sorb strongly to POM and are not assimilated easily by detritus feeders (Boese et al., 1995).

BIOACCUMULATION AND BIOTRANSFORMATION

General Principles

Several early bioaccumulation models used the concept of a food-chain multiplier, which is now considered excessively simplistic (Campfens and Mackay, 1997). Food-web modeling is now considered necessary except for screening level studies (Abbott et al., 1995). The best way to assess bioaccumulation accurately is to use more complex models, but only if the data needs of the models can be met and there is sufficient time (Pelka, 1998). "Food web models provide a means for validation because they mechanistically describe the bioaccumulation process and ascribe causality to observed relationships between biota and sediment or water" (Connolly and Glaser, 1998).

Often there is an absence of equilibrium, especially in fish, due to insufficient exposure time or organism growth, metabolic biotransformation, dietary exposure, and nonlinear relationships for very large and/or superhydrophobic compounds (Bertelsen et al., 1998). Although it is important to have a knowledge of equilibrium partitioning because it is an indication of the condition toward which systems tend (Bertelsen et al.,1998), it is often impossible to determine steady-state potential due to changes in bioavailability and physiology (Landrum, 1998). PCBs may not be at steady state even in large systems such as Lake Ontario that have been polluted over a long period of time. In fact, PCBs in Lake Ontario exhibit a 25-fold disequilibrium (Cook and Burkhard, 1998). The challenge is to obtain sufficient data for a kinetic model (Gobas et al., 1995).

Accumulation from sediment in plankton and fish is largely determined by degree of chlorination, which affects both surface sorption and partitioning. Maximum bioaccumulation occurs for Cl_5, Cl_6, and Cl_7 congeners; Cl_3 and Cl_4 congeners are depleted due to low lipophilicity; Cl_8 congeners are depleted due to size or steric effects (Willman et al., 1997). Plankton and fish are enriched in high-K_{OW} congeners and depleted in low-K_{OW} congeners; there is a systematic enrichment of Cl_5, Cl_6, and

Cl_7 congeners and depletion in Cl_3 congeners with increasing trophic level (Oliver & Niimi, 1988; Campfens and Mackay, 1997; DiPinto and Coull, 1997).

Within homolog groups, congeners with less *ortho*-substitution have greater K_{OW} values and are accumulated up the food chain at a greater rate than other congeners in their homolog group. Changes in distributions of congeners mainly are caused by transfers among biotic compartments (Campfens and Mackay, 1997). There is no enrichment of mono- and non-*ortho*-substituted congeners with an increase in trophic level. However, many coplanar congeners, especially the more toxic PCB 77, are depleted with increasing trophic level; PCB 77 is almost certainly metabolized (Campfens and Mackay, 1997).

Algae (Periphyton and Phytoplankton)

Bioaccumulation of PCBs in algae is dependent on solubility, hydrophobicity and molecular configuration of the congener, and growth rate, surface area and type, and content and type of lipid in the algae (Stange and Swackhamer, 1994). Phytoplankton biomass may double or triple in 1 day and periphyton turnover may be so rapid that some PCBs will not reach equilibrium (Hill and Napolitano, 1997); therefore, one should use the term "bioaccumulation factor" (BAF) for plants as well as animals rather than "bioconcentration factor," which implies equilibrium (Stange and Swackhamer, 1994).

PCBs partition to lipids in algae, but the relationship is not a simple one. In phytoplankton, lipids can range from 3 to 30% by weight (Swackhamer and Skoglund, 1991). However, not all lipids are the same. Polar phospholipids occur on the surface. PCBs preferentially partition to internal neutral lipids, but those are usually a minor fraction of the total lipids, and they vary depending on growth conditions and species (Stange and Swackhamer, 1994). Algal lipids have a much stronger affinity for PCBs than does octanol, so that the algal $BAF_{lipid} > K_{OW}$ (Stange and Swackhamer, 1994; Koelmans et al., 1995; Sijm et al., 1998).

There is probably a two-step bioaccumulation mechanism for PCBs to algae, with rapid surface sorption of 40 to 90% within 24 hours and then a small, steady increase with transfer to interior lipids for the duration of the exposure (Swackhamer and Skoglund, 1991). Uptake increases with increase in the surface area of algae (Wang et al., 1997). Therefore, the smaller the organism the larger the uptake rate constant (Sijm et al., 1998). However, in small phytoplankton, such as the nannoplankton that dominate the Great Lakes, although a high surface-to-volume ratio can increase sorption, high growth rates can limit PCB concentrations (Swackhamer and Skoglund, 1991). The combination of lipid content, surface area, and growth rate results in species differences in BAF among algae (Wood et al., 1997).

The pattern of bioaccumulation to algae varies among PCB homologs: Cl_2-Cl_5 have favorable steric factors but low BAFs; Cl_5-Cl_7 have favorable BAFs, some have favorable steric factors and high BAFs, others have low steric factors and low BAFs; Cl_7 - Cl_{10} have high K_{OW}s, but poor steric factors, so low BAFs (Stange and Swackhamer, 1994). Highly chlorinated congeners are associated with cell membranes (phospholipids) (Stange and Swackhamer, 1994). There is no direct relationship between BAF and K_{OW} for log $K_{OW} > 7$ (Swackhamer and Skoglund, 1991).

Desorption is significantly slower than sorption (Swackhamer and Skoglund, 1991). Depuration from algae is very slow (Zaranko et al., 1997). Elimination is not just a function of physicochemical properties, but is assumed to be dependent on exudation (Koelmans and Heugens, 1998; Sijm et al., 1998). It has been noted that sorption to algal exudates decreases bioavailability and, in many studies, has resulted in underestimation of uptake rate constants and BAFs (Sijm et al., 1998). Algae lack enzymes for dechlorinating PCBs (Hill and Napolitano, 1997), and no metabolism of PCBs has been reported for algae.

Macrophytes

Gobas et al. (1991) conducted uptake and elimination experiments with PCBs and other chemicals using the common aquatic weed *Myriophyllum spicatum,* and developed a kinetic model that fit the observed data well.

Invertebrates (Zoobenthos and Zooplankton)

Invertebrates are a critical link in both detrital and phytoplankton food webs. Higher molecular weight and more hydrophobic compounds are incorporated into sediments and are recycled by the zoobenthos (Baker et al., 1991). Lower weight, lower hydrophobicity compounds tend to be dissolved (Wood et al,. 1997), and their uptake is enhanced in filter feeders through sorption to phytoplankton (Gilek et al., 1996).

The partitioning between sediment carbon and lipids in zoobenthos is referred to as the biota sediment accumulation factor (BSAF, cf. Boese et al., 1995):

$$BSAF = \frac{tissue\ conc/tissue\ lipid}{sed\ conc/sed\ TOC}$$

Uptake of PCBs by benthic organisms is rapid (Zaranko et al., 1997). Ingestion rates in deposit feeders can be greater than 100 times body weight/day (Forbes et al., 1998), and they feed selectively on fine organic matter, which tends to have higher PCB concentrations (Boese et al., 1995, 1996). *Diporeia*, a common freshwater amphipod, feeds on particles from 20 to 63 microns in size (Wood et al., 1997); tubificids, which often dominate more polluted habitats, feed selectively on sediments with high organic matter; chironomids (common midge larvae) are grazers of algae and gatherers of detritus (Zaranko et al., 1997).

Much attention has been given to the role of pore water in the uptake of PCBs by benthos. However, "it may be unwise to uncritically assume that pore-water contaminant is the most bioavailable." Many animal burrows are lined, and the composition of the water in burrows is equivalent to that of the overlying water (Forbes et al., 1998). Campfens and Mackay (1997) found that predicted PCB concentrations in benthos exceeded those measured for high-K_{OW} congeners, possibly due to assumptions regarding the respiration of pore water. Uptake of very hydrophobic compounds from sediment was observed to be one to five times greater than that predicted by equilibrium partitioning

from pore water (Loonen et al., 1997)—clearly the important pathway of exposure is through the ingested detritus.

Bioaccumulation of lighter homologs may reflect direct uptake from water (Bright et al., 1995). The exposure of filter feeders to the overlying water is quite different from that of deposit feeders. The pumping rate of mussels is 100 times greater than that of a deposit-feeding clam; however, this is offset somewhat by decreased efficiency of uptake at higher pumping rates (Björk and Gilek, 1999).

Optimum bioaccumulation in invertebrates occurs with homologs Cl_5 to Cl_7; homologs $< Cl_5$ have reduced partition values, and those $> Cl_7$ have an unfavorable steric (size) effect (Wood et al., 1997). A parabolic relationship was observed between *Mytilus* log BAF and log K_{OW} (Gilek et al., 1996). Bioavailability declines with increasing hydrophobicity in Cl_7-Cl_{10} homologs, and there is a negative relationship for BSAF and log K_{OW} (Maruya and Lee, 1998). In *Macoma nasuta* there was an observed reduction in uptake with increasing K_{OW}, possibly due to reduced desorption rates from sediment, increasing steric hindrance, and reduced translocation to lipid pools (Boese et al., 1997). As a result, many experiments with highly chlorinated congeners do not reach steady state; for example, uptake of Cl_8 did not reach steady state in *M. nasuta* in 30 days (Boese et al., 1995). *M. nasuta* uptake efficiency for Cl_{10} was 0% (Kannan et al., 1998).

The longevity of homologs in sediments reflects in part the uptake or lack of uptake by invertebrates. For example, in one study, CL_9 predominated in sediments (Kannan et al., 1998). In an experiment by Boese et al. (1995) with deposit feeders, Cl_3 through Cl_6 declined significantly in spiked sediments over 30 days.

The quantitative relationships of dietary uptake have been quantified by several authors. In one modeling study, gut absorption efficiency was computed by an empirical relationship with a maximum of 0.43 (Campfens and Mackay, 1997). Data on uptake by small fish published by Gobas et al. (1993) suggest a mean of 0.63, with no trend in efficiency between log K_{OW} 4.5 and 7.5 (although that was not their conclusion). Nichols et al. (1998) demonstrated that uptake is more efficient in larger fish, with a mean of about 0.90. Invertebrates generally exhibit lower efficiencies; Landrum and Robbins (1990) showed that values ranged from 0.42 to 0.24 for chemicals with log K_{OW}s from 4.4 to 6.7. Assimilation efficiencies of PCB congeners from algae were determined for *Mytilus edulis*: 0.1 to 0.5 for PCB 31, 0.1 to 0.7 for PCB 49, and 0.2 to 0.7 for PCB 153 (log K_{OW} = 7.751). PCB 153 assimilation efficiency was measured as 0.69 for zebra mussels; the formation of pseudofeces (rejected food) in the presence of high algal concentrations could have caused underestimation of the *M. edulis* assimilation efficiencies (Björk and Gilek, 1999).

M. edulis gill assimilation efficiencies from water were 0.1-0.2 for PCB 31, 0.1-0.4 for PCB 49, and 0.3-0.6 for PCB 153 (Björk and Gilek, 1999). *Macoma nasuta*, a deposit feeder, had an uptake efficiency of 0.82 (Björk and Gilek, 1999). Gill assimilation efficiencies decline with an increased ventilation rate because of diffusional dead space and decreased contact time between gills and water (Björk and Gilek, 1999).

No relationship was found between depuration and K_{OW} (Boese et al., 1997). For reasons that are not understood, PCBs accumulated from water are retained longer than those obtained from food (Wang, 1998). Biotransformation of Cl_3 is rapid in *M. nasuta* (Boese et al., 1995). Chironomid

larvae retained 97.8% of Aroclor 1242 after 7 days (Wang, 1998). Generally, non-*ortho*-substituted congeners are stable in invertebrates (Bright et al., 1995). Coplanar PCBs biomagnify and achieve steady state in *Mytilus* faster than nonplanar PCBs (Bergen et al., 1996). More detailed structural activity relationships can be elucidated (for example, Wood et al. [1997]), but they are very specific and are beyond the scope of this application.

Fish

Bioaccumulation of PCBs in fish is of concern because of risks to fish, wildlife, and humans. Hydrophobic contaminants such as PCBs accumulate in fish with both increasing age, size, and position in the food web. Stow and Carpenter (1994) found that age is a better predictor of PCBs than size in Lake Michigan salmon.

There are several published K_{OW}-BCF models; in all, the intercept terms are negative because limited accumulation in tissues other than lipid reduces concentrations expressed on a whole-fish basis (Bertelsen et al., 1998). Unlike algae, there is no theoretical basis for a K_{OW}-lipid coefficient for fish other than 1.0. In a study by Bertelsen et al. (1998), 90% of variance in the data was accounted for by the combined model of log K_{OW} and total lipid:

$$\log \ (K_{tw} - \textit{Waterfrac}) \ = \ 0.74 \cdot \log K_{OW} \ + \ 1.00 \cdot \log \textit{Lipidfrac} \ + \ 0.72$$

where:

K_{tw}	=	tissue-water partition coefficient;
Waterfrac	=	water content (fraction); and
Lipidfrac	=	lipid fraction.

Lipid fraction is quite variable among species and even in the same species over the course of a year or lifetime. Lipid concentrations in fish have been documented to range from 2 to 27.6% (Sijm and van der Linde, 1995; Zaranko et al., 1997; Gerstenberger et al., 1997). Fathead minnows have been observed to have post-spawning reductions in lipid content of as much as 72% in males and 46% in females due to breeding activities, including cleaning and defense of nests as well as egg laying (Suedel et al., 1997).

Uptake kinetics are important for representing the short-term exposures associated with storm events and accidental spills. There are two pathways for direct uptake: through the gills and through the skin. Bioconcentration has been modeled over the last decade as diffusion through aqueous and lipid layers (Gobas and Mackay, 1987; Barber et al., 1988; Erickson and McKim, 1990; Sijm and van der Linde, 1995). The uptake rate constant k_1 increases with K_{OW} up to log K_{OW} 3, is constant between log K_{OW} 3 and 6, then decreases with log $K_{OW} > 6$ (McKim et al., 1985); resistance changes from lipid to aqueous at log $K_{OW} \approx 3$ (Sijm and van der Linde, 1995). PCBs with 4 or fewer Cl atoms are most readily sorbed through the gills (Gerstenberger et al., 1997). Gill exposure is a function of respiration rate, decreasing in larger fish (Thomann and Mueller, 1987).

Dermal uptake can be significant for benthic feeders such as bullhead, which forage in sediments for aquatic organisms (Leadley et al., 1998). Juvenile spot fed copepods in contaminated sediment accumulated 4.83 times more PCBs as fish fed in clean sediment; exposure was through both skin and gills (DiPinto and Coull, 1997).

Dietary uptake may vary with molecular weight of the chemical, size of the predator, and the nature of the food. The literature differs on the importance of the K_{OW}. In pike fed spiked rainbow trout there was no dependency of dietary uptake efficiency on K_{OW}, but uptake efficiency did vary with molecular weight. Uptake efficiency was observed to be greatest at a molecular weight of ~450, which may be due to the structure of the membrane proteins; mediated uptake of pollutants associated with proteins has been suggested (Burreau et al., 1997). Gobas et al. (1988) found that uptake efficiency was constant up to log $K_{OW} = 7$ (discussed above with regard to invertebrates). In brook trout (150 g mean weight) net gut uptake efficiencies were >80%, compared to juvenile (5 to 9 g) rainbow trout and whitefish, with 43-58% and 66-76% uptake efficiencies, respectively. If changes occur with growth then this suggests that a single PCB uptake coefficient optimized for subadults would overestimate for juveniles (Nichols et al., 1988). Dietary composition can affect the uptake of PCBs, as shown by experiments with channel catfish (NIEHS, 1999).

Both depuration and, for some congeners, biotransformation can be important pathways for elimination of PCBs in fish. Depuration in juvenile trout exhibits a curvilinear relationship with log K_{OW}, apparently decreasing beyond log $K_{OW} = 7$, perhaps because equilibrium is not attained among compartments in the fish (Fisk et al., 1998). Lipid content and size are important for determining the elimination rate constant. Much lower depuration rates (and hence higher half-lives) occur in larger and/or fatter fish; for example, the half-life of a Cl_4 PCB in a 0.1-g guppy is 43 days, compared to 5.6 years in a 900-g rainbow trout (Sijm and van der Linde, 1995). Elimination may occur across the skin as well as through the gills, increasing in small fish with large surface area-to-volume ratios (Sijm and van der Linde, 1995).

Metabolic transformation increases the elimination rate. Biotransformation has the greatest effect on hydrophobic compounds where excretion approaches zero; limited accumulation of lower chlorine homologs may be due in part to biotransformation (Endicott and Cook, 1994). Fish are known to metabolize certain congeners, namely PCBs 101, 105, 107, 110, 138, and 170 (Hill and Napolitano, 1997); primarily these are planar congeners, which are toxic. Few fish show enzyme induction that would suggest lower Cl congeners are metabolized (Gerstenberger et al., 1997). In fact, this may account for the bioaccumulation of lighter Cl congeners in salmonids (Bright et al., 1995).

Migratory behavior of fish can be important in determining their exposure. For example, minnows migrate during early spring and fall; PCB concentrations in minnows in an Ontario stream varied seasonally with the lowest concentration in October (Zaranko et al., 1997). Likewise, migration of striped bass in the Hudson estuary is significant and contributes to the observed variability in PCBs (Thomann and Farley, 1998). In contrast, largemouth bass are known to be territorial and tend to stay in their home areas (Parker and Hasler, 1959).

Birds

PCB concentrations in mallards have been reported to be highly correlated with exposure (Cobb et al., 1997) and exposure of mallards and wood ducks to PCBs has been documented in the Housatonic River. Studies on tree swallows, which feed on emergent insects, have shown that total PCB values in eggs and nestlings may attain near-steady-state and that enrichment of Ah-active congeners occurs while other congeners are dechlorinated (Froese et al., 1998). Planar PCB congeners (77 and 126) are very toxic to hatching chicken embryos (Hoffman et al., 1998). Young of all bird species in the Green Bay, Wisconsin, area accumulated the toxic congeners PCBs 77, 105, 126, and 169 (Ankley et al., 1993).

A relatively simple two-compartment model representing the partitioning between fat and blood plasma in gulls was shown to describe the concentration dynamics (Clark et al., 1988).

Mammals

Piscivorous mammals are exposed to high levels of pollutants due to feeding at the top of aquatic food webs (Bremle et al., 1997). Variation in the rate of bioaccumulation of different congeners may be due to steric factors that affect the binding energy of a substrate (Bright et al., 1995). In general, higher-chlorinated PCBs have higher BAFs than lower-chlorinated PCBs. Congeners lacking Cl in the *meta* and *para* positions exhibit low BAFs; in many mammals these are hydroxylated and excreted (Bright et al., 1995; van Bavel et al., 1996).

Reduction in birth rate and weights have been observed in several studies of mink fed PCB-contaminated food (Russell et al., 1997; Halbrook et al., 1999). A preferential enrichment of dioxin-like congeners PCBs 126 and 169 occurs from fish to otters; these toxic compounds are retained in the liver (Leonards et al., 1997). PCB 77, another toxic congener, appears to be metabolized in otters (Leonards et al., 1997). A model developed by Traas et al. (in press) simulates bioaccumulation and toxicity of dioxin-like congeners in otters. Sample and Suter (1999) used @RISK to model the effects of PCBs on otter, mink, heron, and osprey in Poplar Creek and Clinch River, Tennessee.

TOXICITY

Although the toxicity of PCBs was briefly mentioned in the previous section on bioaccumulation, a more detailed discussion is provided below. Few PCB congeners exhibit acute toxicity (Bright et al., 1995), but exposure may result in chronic effects, adversely affecting survival, growth, and reproduction (Suedel et al., 1997). Because of congener-specific toxicities, total body burden of PCBs is inadequate for predicting effects (Schweitzer et al., 1997). Acute toxicity is demonstrated by non-*ortho*-substituted planar congeners similar to dioxins; these dioxin-like congeners also exhibit chronic toxicity (Bergen et al., 1996), including wasting disease (Suedel et al., 1997). The non-*ortho*-substituted PCBs assume a planar configuration and have a high affinity for the dioxin (Ah) receptor (Bright et al., 1995; Campfens and Mackay, 1997). The planar congeners PCBs 77, 126, and 169 have been demonstrated to date to be the most toxic congeners in fish and mammals (Campfens and Mackay, 1997). Dioxin-like compounds have additive toxicity (Suedel et al., 1997; Elonen et al., 1998). It is common to express the toxicities as toxic equivalency factors (TEFs)

relative to the toxic potency of 2,3,7,8, tetradibenzodioxin (for example, Kannan et al., 1998; Traas et al., in press). The mammalian, fish and bird TEFs are summarized in Table 2.

In contrast, *ortho*-substituted congeners have a low affinity for the Ah receptor and may exhibit low toxicity—even insignificant sublethal effects (Suedel et al., 1997). However, exposure to some di-*ortho* congeners (including PCBs 138, 153, 180, and 194) produce adverse effects (carcinogenicity, neurotoxicity, and endocrine disruption) (Kannan et al., 1998). Other congeners that are not dioxin-like include PCBs 28+31, 47+48, 66+95 (pairs that are analytically indistinguishable) and PCBs 110, which have also been shown to be toxic in lab animals (Gerstenberger et al., 1997).

Information concerning toxicity of PCB metabolites is scarce; in general, metabolites of PCBs are considered to be less toxic than their parent compounds. However, it has been demonstrated that hydroxylated metabolites of PCB 77 bind competitively and are retained persistently in blood (Klasson-Wehler et al., 1998).

In a study with an estuarine minnow, reduced feeding and reduction in growth occurred in fish fed medium and high doses of PCBs. The bioaccumulation of congeners was proportional to that observed in fish collected in the field, except for PCB 77, which may have been metabolized (Gutjahr-Gobell et al., 1999). In another study, fecundity was reduced in association with the reduction in growth; egg production was reduced by 77% at the highest dose (part of which was due to 58% mortality) (Black et al., 1998a). This relationship was not found in the field, suggesting differences in exposure routes (Black et al., 1998b). In addition, it has been shown that Aroclor 1260 can alter sex ratios in trout at environmental concentrations (Matta et al., 1998).

Table 2

World Health Organization Toxic Equivalency Factors
(van den Berg et al., 1998)

Congener	Human/Mammals	Fish	Birds
2,3,7,8-TetraCDD	1	1	1
1,2,3,7,8-PentaCDD	1	1	1[b]
1,2,3,4,7,8-HexaCDD	0.1[a]	0.5	0.05[b]
1,2,3,6,7,8-HexaCDD	0.1[a]	0.01	0.01[b]
1,2,3,7,8,9-HexaCDD	0.1[a]	0.01[c]	0.1[b]
1,2,3,4,6,7,8-HeptaCDD	0.01	0.001	<0.001[b]
OctaCDD	0.0001[a]	<0.0001	0.0001
2,3,7,8-TetraCDF	0.1	0.05	1[b]
1,2,3,7,8-PentaCDF	0.05	0.05	0.1[b]
2,3,4,7,8-PentaCDF	0.5	0.5	1[b]
1,2,3,4,7,8-HexaCDF	0.1	0.1	0.1[b,d]
1,2,3,6,7,8-HexaCDF	0.1	0.1[d]	0.1[b,d]
1,2,3,7,8,9-HexaCDF	0.1[a]	0.1[c,d]	0.1[d]
2,3,4, 6,7,8-HexaCDF	0.1[a]	0.1[d,e]	0.1[d]
1,2,3,4,6,7,8-HeptaCDF	0.01[e]	0.01[e]	0.01[e]
1,2,3,4,7,8,9-HeptaCDF	0.01[e]	0.01[c,e]	0.01[e]
OctaCDF	0.0001[a]	<0.0001[c,e]	0.0001[e]
3,4,4',5-TetraCB(81)	0.0001[a,c,d,e]	0.0005	0.1[c]
3,3',4,4'-TetraCB(77)	0.0001	0.0001	0.05
3,3',4,4',5-PentaCB(126)	0.1	0.005	0.1
3,3',4,4',5,5'-HexaCB (169)	0.01	0.00005	0.001
2,3,3',4,4'-PentaCB(105)	0.0001	<0.000005	0.0001
2,3,4,4',5-PentaCB (114)	0.0005[a,d,e,f]	<0.000005[e]	0.0001[g]
2,3',4,4',5-PentaCB(118)	0.0001	<0.000005	0.00001
2',3,4,4',5-PentaCB(123)	0.0001[a,d,f]	<0.000005[e]	0.00001[g]
2,3,3',4,4',5-HexaCB (156)	0.0005[d,e]	<0.000005	0.0001
2,3,3',4,4',5'-HexaCB (157)	0.0005[d,e,f]	<0.000005[d,e]	0.0001
2,3',4,4',5,5'-HexaCB (167)	0.00001[a,f]	<0.000005[c]	0.00001[g]
2,3,3',4,4',5,5'-HeptaCB (189)	0.0001[a,d]	<0.000005	0.00001[g]

Abbreviations: CDD, chlorinated dihenzodioxins; CDF, chlorinated denzofurans; CR chlorinated biphenyls;
     QSAR, quantitative structure-activity relationship.

[a] Limited data set.

[b] In vivo CYP1A induction after in ovo exposure.

[c] In vitra CYP1A induction.

[d] QSAR modeling prediction from CYP1A induction (monkey, pig, chicken, or fish).

[e] Structural similarity.

[f] No new data from 1993 review.

[g] QSAR modeling prediction from class-specific TEFs.

REFERENCES

Abbott, J.D., S.W. Hinton, and D.L. Borton. 1995. Pilot Scale Validation of the RIVER/FISH Bioaccumulation Modeling Program for Nonpolar Hydrophobic Organic Compounds Using the Model Compounds 2,3,7,8-TCDD and 2,3,7,8-TCDF. *Environmental Toxicology and Chemistry*, 14(11):1999-2012.

Ankley, G.T., G.J. Niimi, K.B. Lodge, H.J. Harris, D.L. Beaver, D.E. Tillett, T.R. Schwartz, J.P. Giesy, P.D. Jones, and C. Hagley. 1993. Uptake of Planar Polychlorinated Biphenyls and 2,3,7,8-substituted Polychlorinated Dibenzofurans and Dibenzo-*p*-dioxins by Birds Nesting in the Lower Fox River and Green Bay, Wisconsin, USA. *Archives of Environmental Contamination and Toxicology*, 24:332-344.

Baker, J.E., S.J. Eisenreich, and B.J. Eadie. 1991. Sediment Trap Fluxes and Benthic Recycling of Organic Carbon, Polycyclic Aromatic Hydrocarbons, and Polychlorobiphenyl Congeners in Lake Superior. *Environmental Science & Technology*, 25(3):500-508.

Barber, M.G., L.A. Suarez, and R.R. Lassiter. 1988. Modeling Bioconcentration of Nonpolar Organic Pollutants by Fish. *Environ. Toxicol. Chem.*, 7:545-558.

Bedard, D.L. and R.J. May. 1996. Characterization of the Polychlorinated Biphenyls in the Sediments of Woods Pond: Evidence for Microbial Dechlorination of Aroclor 1260 *in Situ*. *Environ. Sci. Technology*, 30:1:237-245.

Bedard, D.L., H.M. Van Dort, R.J. May, and L.A. Smullen. 1997. Enrichment of Microorganisms that Sequentially *meta, para*-Dechlorinate the Residue of Aroclor 1260 in Housatonic River Sediment. *Environ. Sci. Technol.* 31:3308-3313.

Bedard, D.L., R.E. Wagner, M.J. Brennan, M.L. Haberl, and J.F. Brown, Jr. 1987. Extensive Degradation of Aroclors and Environmentally Transformed Polychlorinated Biphenyls by *Alcaligenes eutrophus* H850. *Applied Environ. Microbiology*, 53:1094-1102.

Bedard, D.L. and J.F. Quensen III. 1995. Microbial Reductive Dechlorination of Polychlorinated Biphenyls, *in* L.Y. Young and C.E. Cerniglia, Eds., *Microbial Transformation and Degradation of Toxic Organic Chemicals*, New York: Wiley-Liss, pp. 127-216.

Bergen, B.J., W.G. Nelson, and R.J. Pruell. 1996. Comparison of nonplanar and coplanar PCB congener partitioning in seawater and bioaccumulation in blue mussels (*Mytilus edulis*). Environ. Toxicol. Chem, 15(9):1517-1523.

Bertelsen, S.L., A.D. Hoffman, C.A. Gallinat, C.M. Elonen, and J.W. Nichols. 1998. Evaluation of Log K_{OW} and Tissue Lipid Content as Predictors of Chemical Partitioning to Fish Tissues. *Environmental Toxicology and Chemistry*, 17(8):1447-1455.

Björk, M. and M. Gilek. 1999. Efficiencies of polychlorinated biphenyl assimilation from water and algal food by the blue mussel (*Mytilus edulis*). Environ. Toxicol. Chem, 17(7):1405-1414.

Black, D.E., R. Gutjahr-Gobell, R.J. Pruell, B. Bergen and A.E. McElroy. 1998a. Effects of a mixture of non-*ortho*- and mono-*ortho*-polychlorinated biphenyls on reproduction in *Fundulus heteroclitus* (Linnaeus). Environ. Toxicol. Chem, 17(7):1396-1404.

Black, D.E., R. Gutjahr-Gobell, R.J. Pruell, B. Bergen, L. Mills and A.E. McElroy. 1998b. Reproduction and polychlorinated biphenyls in *Fundulus heteroclitus* (Linnaeus) from New Bedford Harbor, Massachusetts, USA. Environ. Toxicol. Chem, 17(7):1405-1414.

Boese, B.L., H. Lee II, and S. Echols. 1997. Evaluation of a First-Order Model for the Prediction of the Bioaccumulation of PCBs and DDT from Sediment into the Marine Deposit-Feeding Clam *Macoma nasuta*. *Environmental Toxicology and Chemistry*, 16(7):1545-1553.

Boese, B.L., H. Lee II, D.T. Specht, J. Pelletier, and R. Randall. 1996. Evaluation of PCB and Hexachlorobenzene Biota-Sediment Accumulation Factors Based on Ingested Sediment in a Deposit-Feeding Clam. *Environmental Toxicology and Chemistry*, 15(9):1584-1589.

Boese, B.L., M. Winsor, H. Lee II, S. Echols, J Pelletier, and R. Randall. 1995. PCB Congeners and Hexachlorobenzene Biota Sediment Accumulation Factor for *Macoma nasuta* Exposed to Sediments with Different Total Organic Carbon Contents. *Environmental Toxicology and Chemistry*, 14(2):303-310.

Bremle, G., P. Larsson, and J.O. Helldin. 1997. Polychlorinated Biphenyls in a Terrestrial Predator, the Pine Marten (*Martes martes* L.). *Environmental Toxicology and Chemistry*, 16(9):1779-1784.

Bright, D.A., S.L. Grundy, and K.J. Reimer. 1995. Differential bioaccumulation of non-*ortho*-substituted and other PCB congeners in coastal arctic invertebrates and fish. Environ. Sci. Technol., 29(10):2504-2512.

Brown, J.F., Jr., R.E. Wagner D.L. Bedard, M.J. Brennan, J.C. Carnahan, R.J. May, and T.J. Tofflemire. 1984. PCB Transformations in Upper Hudson Sedimets. *Northeast Environmental Science*, 3:167-179.

Brunner, S., E. Hornung, H. Santi, E. Wolff, O.G. Piringer, J. Altschuh, and R. Brüggemann. 1990. Henry's Law Constants for Polychlorinated Biphenyls: Experimental Determination and Structure-Property Relationships. *Environ. Sci. Technology*, 24:1751-1754.

Burreau, S., J. Axelman, D. Broman, and E. Jakobsson. 1997. Dietary Uptake in Pike (*Esox lucius*) of Some Polychlorinated Biphenyls, Polychlorinated Naphthalenes and Polybrominated Diphenyl Ethers Administered in Natural Diet. *Environmental Toxicology and Chemistry*, 16(12):2508-2513.

Bushart, S.P., B. Bush, E.L. Barnard, and Amelie Bott. 1998. Volatilization of Extensively Dechlorinated Polychlorinated Biphenyls from Historically Contaminated Sediments. *Environmental Toxicology and Chemistry*, 17(10):1927-1933.

Butcher, J.B., T.D. Bauthier, and E.A. Garvey. 1997. Use of historical PCB Aroclor measurements:

Hudson River fish data. Environ. Toxicol. Chem, 16(8):1618-1623.

Butcher, J.B., E.A. Garvey, and V.J. Bierman, Jr. 1998. Equilibrium Partitioning of PCB Congeners in the Water Column: Field Measurements from the Hudson River. *Chemosphere*, 36(15):3149-3166.

Campfens, J. and D. Mackay. 1997. Fugacity-Based Model of PCB Bioaccumulation in complex aquatic food webs. *Environ. Sci. Technol.*, 31(2):577-583.

Chiarenzelli, J., R. Scrudato, G. Arnold, M. Wunderlich, and D. Rafferty. 1996. Volatilization of Polychlorinated Biphenyls During Drying at Ambient Conditions. *Chemosphere*, 33:899-911.

Clark, T., K. Clark, S. Paterson, D. Mackay, and R.J. Norstrom. Wildlife Monitoring, Modeling, and Fugacity. *Environ. Sci. Technol.*, 22(2):120-127.

Cobb, G.P., P.D. Wood, and M. Quinn. 1997. Polychlorinated Biphenyls in Eggs and Chorioallantoic Membranes of American Alligators (*Alligator mississippiensis*)From Coastal South Carolina. *Environmental Toxicology and Chemistry*, 16(7):1456-1462.

Connolly, J.P., and D. Glaser. 1998. Use of Food Web Models to Evaluate Bioaccumulation. *National Sediment Bioaccumulation Conference Proceedings*. U.S. Environmental Protection Agency Office of Water EPA 823-R-98-002, p.4-5-4-17.

Cook, P.M., and L.P. Burkhard. 1998. Development of Bioaccumulation Factors for Protection of Fish and Wildlife in the Great Lakes. *National Sediment Bioaccumulation Conference Proceedings*. U.S. Environmental Protection Agency Office of Water EPA 823-R-98-002, p. 3-19-3-27.

Cornelissen, G., P.C.M. van Noort, and H.A.J. Govers. 1997. Desorption kinetics of chlorbenzenes, polycyclic aromatic hydrocarbons, and polychlorinated biphenyls: Sediment extraction with tenex and effects of contact time and solute hydrophobicity. Environ. Toxicol. Chem, 16(7):1351-1357.

DiPinto, L.M. and B.C. Coull. 1997. Trophic transfer of sediment-associated polychlorinated biphenyls from meiobenthos to bottom-feeding fish. Environ. Toxicol. Chem, 16(12):2568-2575.

Eisler, R., and A.A. Belisle. 1996. Planar PCB Hazards to Fish, Wildlife, and Invertebrates: A Synoptic Review. Biological Report 31, National Biological Service, U.S. Department of the Interior: Washington DC, 75pp.

Elonen, G.E., R.L. Spehar, G.W., Holcombe, R.D. Johnson, J.D. Fernandez, R.J. Erickson, J.E. Tietge, and P.M. Cook. 1998. Comparative Toxicity of 2,3,7,8-Tetrachlorodibenzo-*p*-Dioxin to Seven Freshwater Fish Species During Early Life-Stage Development. *Environmental Toxicology and Chemistry*, 18(3):472-483.

Endicott, D.D., and P.M. Cook. 1994. Modeling the partitioning and bioaccumulation of TCDD and other hydrophobic organic chemicals in Lake Ontario. Chemosphere, 28(1):75-87.

Erickson, R.J., and J.M. McKim. 1990. A Model for Exchange of Organic Chemicals at Fish Gills. *Aquatic Toxicology*, 18:175-198.

Fisk, A.T., R.J. Norstrom, C.D. Cymbalisty, and D.C.G. Muir. 1998. Dietary accumulation and depuration of hydrophobic organochlorines: bioaccumulation parameters and their relationship with octanol/water partition coefficient. Environ. Toxicol. Chem, 17(5):951-961.

Forbes, T.L., V.E. Forbes, A. Giessing, R. Hansen, and L.K. Kure. 1998. Relative role of pore water versus ingested sediment in bioavailability of organic contaminants in marine sediments. Environ. Toxicol. Chem, 17(12):2453-2462

Freidig, A.P., E.A. Garciano, and F.J.M. Busser. 1998. estimating impact of humic acid on bioavailability and bioaccumulation of hydrophobic chemicals in guppies using kinetic solid-phase extraction. Environ. Toxicol. Chem, 147(6):998-1004.

Froese, K.L., D.A. Verbrugge, G.T. Ankley, G.J. Niimi, C.P. Larsen, and J.P. Giesy. 1998. Bioaccumulation of Polychlorinated Biphenyls From Sediments to Aquatic Insects and Tree Swallow Eggs and Nestlings in Saginaw Bay, Michigan, USA. *Environmental Toxicology and Chemistry*, 18(3):484-492.

Gerstenberger, S.L., M.P. Gallinat, and J.A. Dellinger. 1997. polychlorinated biphenyl congeners and selected organochlorines in Lake Superior fish, USA. Environ. Toxicol. Chem, 19(11):2222-2228.

Gilek, M., M. Björk, D. Broman, N. Kautsky, and C. Näf. 1996. Enhanced accumulation of PCB congeners by Baltic Sea blue mussels, *Mytilus edulis*, with increased algae enrichment. Environ. Toxicol. Chem, 15(9):1597-1605.

Gobas, F.A.P.C., and D. Mackay. 1987. Dynamics of Hydrophobic Organic Chemical Bioconcentration in Fish. *Environ. Toxicol. Chem.*, 6:495-504.

Gobas, F.A.P.C., E.J. McNeil, L. Lovett-Doust and G.D. Haffner. 1991. Bioconcentration of chlorinated aromatic hydrocarbons in aquatic macrophytes. Environ. Sci. Technol. 25(5): 924-929.

Gobas, F.A.P.C., D.C.G. Muir, and D. Mackay. 1988. Dynamics of Dietary Bioaccumulation and Faecal Elimination of Hydrophobic Organic Chemicals in Fish. *Chemosphere*, 17:943-962.

Gobas, F.A.P.C., X. Zhang, and R. Wells. 1993. Gastrointestinal magnification: the mechanism of biomagnification and food chain accumulation of organic chemicals. Environ. Sci. Technol. 27: 2855-2863.

Gobas, F.A.P.C., M.N. Z'Graggen, and X. Zhang. 1995. Time response of the Lake Ontario ecosystem to virtual elimination of PCBs. Environ. Sci. Technol. 29:2038-2046.

Gutjahr-Gobell, R.E., D.E. Black, L.J. Mills, R.J. Pruell, B.K. Taplin, and S. Jayaraman. 1999. Feeding the mummichog (*Fundulus heteroclitus*) a diet spiked with non-*ortho*- and mono-*ortho*-substituted polychlorinated biphenyls: accumulation and effects. Environ. Toxicol. Chem, 18(4):699-707.

Halbrook, R.S., R.J. Aulerich, S.J. Bursian, and L. Lewis. 1999. Ecological Risk Assessment in a Large River-Reservoir: 8. Experimental Study of the Effects of Polychlorinated Biphenyls on Reproductive Success in Mink. *Environmental Toxicology and Chemistry*, 18(4):649-654.

Hill, W.R., and G.E. Napolitano. 1997. PCB congener accumulation by periphyton, herbivores and omnivores. Arch. Environ. Contam. Toxicol. 32:449-455.

Hoffman, D.J., M.J. Melancon, P.N. Klein, J.D. Eisemann, and J.W. Spann. 1998. Comparative Developmental Toxicity of Planar Polychlorinated Biphenyl Congeners in Chickens, American Kestrels, and Common Terns. *Environmental Toxicology and Chemistry*, 17(4):747-757.

IT Corp. 1999. *Bench-scale Testing of Photolysis, Chemical Oxidation and Biodegradation of PCB Contaminated Soils and Photolysis of TCDD Contaminated Soils*. Cooperative Agreement CR816817-020-0, Risk Reduction Engineering Laboratory; Cincinnati: U.S. Environmental Protection Agency.

Jafvert, C.T., and J.E. Rogers. 1990. Biological remediation of contaminated sediments, with special emphasis on the Great Lakes. Great Lakes National Program Office, EPA-600-991-001.

Kannan, K., H. Nakata, R. Stafford, G.R. Masson, S. Tanabe, and J.P. Giesy. 1998. Environ. Sci. Technol., 32:1214-1221.

Klasson-Wehler, E., Å. Bergman, M. Athanniadou, J.P. Ludwig, H.J. Auman, K. Kannan, M. Van Den Berg, A.J. Murk, L.A. Feyk, and J.P. Giesy. 1998. Hydroxylated and Methylsulfonyl Polychlorinated Biphenyl Metabolites in Albatrosses from Midway Atoll, North Pacific Ocean. *Environmental Toxicology and Chemistry*, 17(8):1620-1625.

Koelmans, A.A., and E.H.W. Heugens. 1998. Binding constants of chlorobenzenes and polychlorobiphenyls for algal exudates. Water Science Technology, 37(3):67-73.

Koelmans, A.A., S.F.M. Anzion, and L. Lijklema. 1995. Dynamics of organic micropollutant biosorption to cyanobacteria and detritus. Environ. Sci. Technol. 29(4):933-940.

Landrum, P. 1998. Kinetic models for assessing bioaccumulation. National Sediment Bioaccumulation Conference Proceedings. U.S. Environmental Protection Agency Office of Water EPA 823-R-98-002, P. 1-47-1-50.

Landrum, P., S.R. Nihart, B.J. Eadie, and L.R. Herche. 1987. Reduction in Availability of Organic

Contaminants to the Amphipod *Pontoporeia hoyi* by Dissolved Organic Matter of Sediment Interstitial Waters. *Environ. Toxicol. Chem.*, 6:11-20.

Landrum, P.F., M.D. Reinhold, S.R. Nihart, and B.J. Eadie. 1985. Predicting the Bioavailability of Organic Xenobiotics to *Pontoporeia hoyi* in the Presence of Humic and Fulvic Materials and Natural Dissolved Organic Matter. *Environmental Toxicology and Chemistry*, 4:459-467.

Landrum, P.F., J. A. Robbins. 1990. Bioavailability of Sediment-Associated Contaminants to Benthis Invertebrates. In R. Baudo, J.P. Giesy, and H. Muntau (eds) *Sediments: Chemistry and Toxicity of In-Place Pollutants*, Ann Arbor: Lewis Publishers, pp. 237-263.

Leadley, T.A., G. Balch, C.D. Metcalfe, R. Lazar, E. Mazak, J. Habowsky, and G.D. Haffner. 1998. Chemical accumulation and toxicological stress in three brown bullhead (*Ameiurus nebulosus*) populations of the Detroit River, Michigan, USA. Environ. Toxicol. Chem. 17(9):1756-1766.

Leonards, P.E.G., Y. Zierikzee, U.A.T. Brinkman, W.P. Cofino, N.M. van Straalen, and B. van Hattum. 1997. The Selective Dietary Accumulation of Planar Polychlorinated Biphenyls in the Otter (*Lutra lutra*). *Environmental Toxicology and Chemistry*, 16(9):1807-1815.

Loonen, H., D.C.G. Muir, J.R. Parsons and H.A.J. Govers. 1997. Bioaccumulation of polychlorinated dibenzo-*p*-dioxins in sediment by oligochaetes: Influence of exposure pathway and contact time. Environ. Toxicol. Chem. 16(7):1518-1525.

Maaret, K., K, Leif, and H. Bjarne. 1992. Studies on the Partition Behavior of Three Organic Hydrophobic Pollutants in Natural Humic Water. *Chemosphere*, 24(7):919-925.

Mackay, D., W.Y. Shiu, J. Billington, and G.L. Huang. 1983. Chapter 4 Physical Chemical Properties of Polychlorinated Biphenyls. In D. Mackay, S. Paterson, S.J., Eisenreich, and M.S. Simmons (eds.) *Physical Behavior of PCBs in the Great Lakes*. Ann Arbor, Mich.: Ann Arbor Science, pp. 59-69.

Maruya, K.A., and R.F. Lee. 1998. Biota-Sediment Accumulation and Trophic Transfer Factors for Extremely Hydrophobic Polychlorinated Biphenyls. *Environmental Toxicology and Chemistry*, 17(12):2463-2469.

Matta, M.B., C. Cairncross and R.M. Kocan. 1998. Possible effects of polychlorinated biphenyls on sex determination in rainbow trout. Environ. Toxicol. Chem. 17(1):26-29.

McKim, J.M., P.K. Schneider, and G. Veith. 1985. Absorption dynamics of organic chemical transport across trout gills as related to octanol-water partition coefficient. Toxicol. Appl. Pharmacol. 77: 1-10.

Neely, W.B. 1983. Chapter 5 Reactivity and Environmental Persistence of PCB Isomers. In Mackay, D., S. Paterson, S.J. Eisenreich, and M.S. Simmons (eds.), Physical Behavior of PCBs in the Great Lakes, Ann Arbor Mich.: Ann Arbor Science, pp. 71-88.

Newman, J.W., J.S. Becker, G. Blondina, and R.S. Tjeerdema. 1998. Quantitation of Aroclors Using Congener-Specific Results. *Environmental Toxicology and Chemistry*, 17(11):2159-2167.

Nichols, J. W., K. M. Jensen, J. E. Tietge, and R. D. Johnson. 1998. Physiologically Based Toxicokinetic Model for Maternal Transfer of 2,3,7,,8-Tetrachlorodibenzo-*p*-Dioxin in Brook Trout (*Salvelinus fontinalis*). *Environmental Toxicology and Chemistry*, 17(12):2422-2434.

NIEHS. 1999. *Research Brief 50: Bioavailability of Chlorinated Hydrocarbons in the Diet*. NIEHS/EPA Superfund Research Program, 2 pp.

Oliver, B.G. and A.J. Niimi. 1988. Trophodynamic Analysis of Polychlorinated Biphenyl Congeners and Other Chlorinated Hydrocarbons in the Lake Ontario Ecosystem. Environ. Sci. Technol. 22:388-397.

Parker, R.A., and A.D. Hasler. 1959. Movements of Some Displaced Centrarchids. *Copeia,* 1959(1):11-18. Cited in Bryant, H.E., and A. Houser. Population Estimates and Growth of Largemouth Bass in Beaver and Bull Shoals Reservoirs. In Hall, G.E., ed. 1971. *Reservoir Fisheries and Limnology*, Washington DC: American Fisheries Society, pp. 349-357.

Pelka, A. 1998. Bioaccumulation Models and Applications: Setting Sediment Cleanup Goals in the Great Lakes. *National Sediment Bioaccumulation Conference Proceedings*. U.S. Environmental Protection Agency Office of Water EPA 823-R-98-002, p. 5-9-5-30.

Quensen, J.F., M.A. Mousa, S.A. Boyd, T. Sanderson, K.L. Froese, and J.P. Giesey. 1998. Reduction of Aryl Hydrocarbon Receptor-Mediated Activity of Polychlorinated Biphenyl Mixtures Due to Anaerobic Microbial Dechlorination. *Environmental Toxicology and Chemistry*, 17(5):806-813.

Russell, R.W., K.A. Gillan, and G.D. Haffner. 1997. Polychlorinated Biphenyls and Chlorinated Pesticides in Southern Ontario, Canada, Green Frogs. *Environmental Toxicology and Chemistry*, 16(11):2258-2263.

Sample, B.E., and G.W. Suter II. 1999. Ecological Risk Assessment in a Large River-Reservoir: 4. Piscivorous Wildlife. *Environmental Toxicology and Chemistry*, 18(4):610-620.

Schweitzer, L.E., J.E. Hose, I.H. Suffet and S.M. Bay. 1997. Differential toxicity of three polychlorinated biphenyl congeners in developing sea urchin embryos. Environ. Toxicol. Chem. 16(7):1510-1514.

Sijm, D.T.H.M. and A. van der Linde. 1995. Size-dependent bioconcentration kinetics of hydrophobic organic chemicals in fish based on diffusive mass transfer of allometric relationships. Environ. Sci. Technol. 29(11):2769-2777.

Sijm, D.T.H.M., K.W. Broersen, D.F. de Roode, and P. Mayer. 1998. Bioconcentration kinetics of hydrophobic chemicals in different densities of *Chlorella pyrenoidosa*. Environ. Toxicol. Chem. 17(9):1695-1704.

Sokol, R.C., C.M. Bethoney, and G-Y. Rhee. 1998a. Effect of Aroclor 1248 concentration on the rate and extent of polychlorinated biphenyl dechlorination. Environ. Toxicol. Chem. 17(10):1922-1926.

Sokol, R.C., C.M. Bethoney, and G-Y. Rhee. 1998b. Reductive dechlorination of preexisting sediment polychlorinated biphenyls with long-term laboratory incubation. Environ. Toxicol. Chem. 17(6):982-987.

Stange, K. and D.L. Swackhamer. 1994. Factors affecting phytoplankton species-specific differences in accumulation of 40 polychlorinated biphenyls (PCBs). Environ. Toxicol. Chem. 13(11):1849-1860.

Stow, C.A., and S.R. Carpenter. 1994. PCB Accumulation in Lake Michigan Coho and Chinook Salmon: Individual-Based Models Using Allometric Relationships. *Environmental Science & Technology*, 28:1543-1549.

Suedel, B.C., T.M. Dillon and W.H. Benson. 1997. Subchronic effects of five di-*ortho* PCB congeners on survival, growth and reporduction in the fathead minnow *Pimephales promelas*. Environ. Toxicol. Chem. 16(7):1526-1532.

Swackhamer, D.L., and R.S. Skoglund. 1991. The Role of Phytoplankton in the Partitioning of Hydrophobic Organic Contaminants in Water. In Baker, R.A., ed., *Organic Substances and Sediments in Water Vol. 2 C Processes and Analytical*, Lewis: Chelsea MI, pp. 91-105.

Thomann, R.V., and K.J. Farley. 1998. Bioaccumulation Modeling of PCBs in the Hudson Estuary: A Review and Update. *National Sediment Bioaccumulation Conference Proceedings*. U.S. Environmental Protection Agency Office of Water EPA 823-R-98-002, p. 4-19-4-22.

Thomann, R.V. and J.A. Mueller. 1983. Steady-state modeling of toxic chemicals-Theory and application to PCBs in the Great Lakes and Saginaw Bay, Mackay et al., eds. *Physical Behavior of PCBs in the Great lakes*, Ann Arbor Science, Ann Arbor, MI, 442. pp

Thomann, R.V. and J.A. Mueller. 1987. *Principles of Surface Water Quality Modeling and Control.* Harper & row, New York, NY. 644 pp.

Thomann, R.V., J.A. Mueller, R.P. Winfield and Chi-Rong Huang. 1991. Model of fate and accumulation of PCB homologues in Hudson estuary. Journal of Environmental Engineering 117(2):161-178.

Traas, T.P., R. Luttik, O. Klepper, P.E.G. Leonards, J.E.M. Beurskens M.D, Smit, and A.G.M. van Hattum. In Press. Modeling Time-Trends of PCBs on Otters and Associated Quality Objectives for PCB in Sediments.

van Bavel, B., P. Andersson, H. Wingfors, J. Åhgren, P-A Bergqvist, L. Norrgren, C. Rappe, and M. Tysklind. 1996. Multivariate Modeling of PCB Bioaccumulation in Three-spined Stickleback (*Gasterosteus aculeatus*). *Environmental Toxicology and Chemistry*, 15(6):947-954.

Van den Berg, M. L. Birnbaum, A.T.C. Bosveld, and 20 other co-authors. 1998. Toxic Equivalency Factors (TEFs) for PCBs, PCDDs, PCDFs for Humans and Wildlife. *Environmental Health Perspectives*, 106(12):775-792.

Van Dort, H.M. and D.L. Bedard. 1991. Reductive *ortho* and *meta* Dechlorination of a Polychlorinated Biphenyl Congener by Anaerobic Microorganisms. *Applied Environ. Microbiology*, 57:5:1576-1578.

Wang, X., Y. Ma, W. Yu, and H.J. Geyer. 1997. Two-Compartment Thermodynamic Model for Bioconcentration of Hydrophobic Organic Chemicals by Alga. *Chemosphere*, 35(8):1781-1797.

Wang, J.S. 1998. Accumulation and Depuration of Aqueous and Dietary PCB (Aroclor 1254) by Striped Bass (*Morone saxatilis*). *Bulletin Environmental Contamination Toxicology*, 60:104-111.

WESTON (Roy F. Weston, Inc.) Supplemental Investigation Work Plan, Technical Support Services, General Electric (GE) Housatonic River Project, Pittsfield, Massachusetts. Final Report. Vol. I - Text and Figures & Vol. II - Appendices. Prepared by Roy F. Weston, Inc. West Chester, PA. Prepared for U.S. Army Corps of Engineers, New England District, Concord, MA.

Willman, E.J., J.B. Manchester-Neesvig, and D.E. Armstrong. 1997. Influence of *ortho*-substitution on patterns of PCB accumulation in sediment, plankton, and fish in a freshwater estuary. Environ. Sci. Technol. 31(12):3712-3718.

Wood, L.W., P.O. Keefe and B. Bush. 1997. Similarity analysis of PAH and PCB bioaccumulation patterns in sediment-exposed *Chironomus tentans* larvae. Environ. Toxicol. Chem. 16(2):283-292.

Wu, Q., and J. Wiegel. 1997. Two Anaerobic Polychlorinated Biphenyl-Dehalogenating Enrichments That Exhibit Different *para*-Dechlorination Specificities. *Applied and Environmental Microbiology*, 63:12:4826-4832.

Wu, Q., D.L. Bedard, and J. Wiegel. 1996. Influence of Incubation Temperature on the Microbial Reductive Dechlorination of 2,3,4,6-Tetrachlorobiphenyl in Two Freshwater Sediments. *Applied and Environ. Microbiology*, 62:11:4174-4179.

Wu, Q., D.L. Bedard, and J. Wiegel. 1999. 2,6-Dibromobiphenyl Primes Extensive Dechlorination of Aroclor 1260 in Contaminated Sediment at 8 to 30°C by Stimulating the Growth of Anaerobic PCB-Dehalogenating Microorganisms. *Environ. Sci. Technol.*, 33:595-602.

Wu, Q., D.L. Bedard, and J. Wiegel. 1997a. Effect of Incubation Temperature on the Route of Microbial Reductive Dechlorination of 2,3,4,6-Tetrachlorobiphenyl in Polychlorinated Biphenyl (PCB)-Contaminated and PCB-Free Freshwater Sediments. *Applied and Environmental Microbiology*, 63:7:2836-2843.

Wu, Q., D.L. Bedard, and J. Wiegel. 1997b. Temperature Determines the Pattern of Anaerobic Microbial Dechlorination of Aroclor 1260 Primed by 2,3,4,6-Tetrachlorobiphenyl in Woods

Pond Sediment. *Applied and Environmental Microbiology*, 63:12:4818-4825.

Zaranko, D.T., R.W. Griffiths, and N.K. Kaushik. 1997. Biomagnification of Polychlorinated Biphenyls Through a Riverine Food Web. Environ. Toxicol.Chem., 16(7):1463-1471.

APPENDIX B

HYDROLOGICAL SIMULATION PROGRAM-FORTRAN (HSPF) MODEL

B.1   Hydrological Simulation Program-Fortran (HSPF) Model Description

B.2   HSPF Parameter List for PERLND, IMPLND, and RCHRES Modules

APPENDIX B.1

HYDROLOGICAL SIMULATION PROGRAM-FORTRAN (HSPF) MODEL DESCRIPTION

TABLE OF CONTENTS

Section   **Page**

LIST OF TABLES

Title   **Page**

LIST OF FIGURES

Title   **Page**

APPENDIX B

HYDROLOGICAL SIMULATION PROGRAM-FORTRAN (HSPF) MODEL DESCRIPTION

In the mid-1970s, the U.S. EPA Environmental Research Laboratory in Athens, Georgia, was in the beginning stages of model development and testing efforts that focused on tools and procedures for quantifying nonpoint sources (NPS) of pollution. Initiated by legislative mandates that required assessment of both urban and agricultural NPS contaminants, the laboratory was supporting development and field testing of mathematical models (along with companion data collection programs) to be used to estimate these NPS loadings and, ultimately, to evaluate potential management and control alternatives. However, EPA scientists realized that although these field-scale models could provide loading values, they alone would not be sufficient to evaluate water quality impacts at the larger watershed, or regional scale. Thus, an extensive, comprehensive watershed model development effort was begun to integrate the field-scale models with instream hydraulic and water quality process models within a flexible, modular framework, to allow continuous simulation of complex watersheds with multiple land uses, both point and nonpoint contaminant sources, networked channels and drainage patterns, and lakes and reservoirs. The HSPF model produced by this development effort has been applied throughout North America and numerous countries and climates; it has the joint sponsorship of both the EPA and USGS, and continues to undergo refinement and enhancement of its component simulation capabilities along with user support and code maintenance activities.

Overview

The Hydrological Simulation Program-FORTRAN, known as HSPF, is a mathematical model developed under EPA sponsorship for use on digital computers to simulate hydrologic and water quality processes in natural and man-made water systems. It is an analytical tool that has application in the planning, design, and operation of water resources systems. The model enables the use of probabilistic analysis in the fields of hydrology and water quality management. HSPF uses such information as the time history of rainfall, temperature, evaporation, and parameters related to land use patterns, soil characteristics, and agricultural practices to simulate the processes that occur in a watershed. The initial result of an HSPF simulation is a time history of the quantity and quality of water transported over the land surface and through various soil zones down to the groundwater aquifers. Runoff flow rate, sediment loads, nutrients, pesticides, toxic chemicals, and other water quality constituent concentrations can be predicted. The model uses these results and stream channel information to simulate instream processes. From this information, HSPF produces a time history of water quantity and quality at any point in the watershed.

HSPF is currently one of the most comprehensive and flexible models of watershed hydrology and water quality available. It is one of a small number of available models that can simulate the continuous, dynamic event, or steady-state behavior of both hydrologic/hydraulic and water quality processes in a watershed, with an integrated linkage of surface, soil, and stream processes. The model is also unusual in its ability to represent the hydrologic regimes of a wide variety of streams

and rivers with reasonable accuracy. It has been applied to such diverse climatic regimes as the tropical rain forests of the Caribbean, the arid conditions of Saudi Arabia and the southwestern U.S., the humid eastern U.S. and Europe, and the snow-covered regions of eastern Canada. The potential applications and uses of the model are comparatively large and include the following:

- Flood control planning and operations.

- Hydropower studies.

- River basin and watershed planning.

- Storm drainage analyses.

- Water quality planning and management.

- Point and nonpoint source pollution analyses.

- Soil erosion and sediment transport studies.

- Evaluation of urban and agricultural best management practices.

- Fate, transport, exposure assessment, and control of pesticides, nutrients, and toxic substances.

- Time-series data storage, analysis, and display.

HSPF is designed so that it can be applied to most watersheds using existing meteorologic and hydrologic data; soils and topographic information; and land use, drainage, and system (physical and man-made) characteristics. The inputs required by HSPF are not different from those needed by most other simpler models. The primary difference in data needs is that long, rather than short time-series records are preferred. Typical long time-series records include precipitation, waste discharges, and calibration data such as streamflow and constituent concentrations.

Historical Development

HSPF is an extension and improvement of three previously developed models: 1) The EPA Agricultural Runoff Management Model - ARM (Donigian and Davis, 1978), 2) The EPA Nonpoint Source Runoff Model - NPS (Donigian and Crawford, 1979), and 3) The Hydrologic Simulation Program (HSP), including HSP Quality (Hydrocomp, 1977), a privately developed proprietary program. In the late 1970s EPA recognized that the continuous simulation approach contained in these models would be valuable in solving many complex water resource problems. Thus, a fairly large investment was devoted to developing a highly flexible nonproprietary FORTRAN program containing the capabilities of these three models, plus many extensions.

HSPF incorporates the field-scale ARM and NPS models into a watershed-scale analysis framework that includes the capabilities needed to model fate and transport in one-dimensional stream channels. It is the only comprehensive model of watershed hydrology and water quality that allows the

integrated simulation of land and soil contaminant runoff processes with instream hydraulic and sediment-chemical interactions.

HSPF was first released publicly in 1980, as Release No. 5 (Johanson et al., 1980), by the U.S. EPA Water Quality Modeling Center (now the Center for Exposure Assessment Modeling). Since its initial release, the model has maintained a reputation as perhaps the most useful watershed-scale hydrology/water quality model available within the public domain. The development of HSPF in the late 1970s represented an integration of a variety of EPA-sponsored model development and testing efforts. The basic watershed modeling philosophy and approach embodied in HSP was chosen, a highly modular code design and structure was developed, and all the individual models were redesigned and recoded into FORTRAN to make the resulting package widely usable and available to potential model users. Throughout the 1980s and early 1990s, HSPF underwent a series of code and algorithm enhancements producing a continuing succession of new releases of the code, culminating in the recent release of Version No. 11 (Bicknell et al., 1997). Table 1 lists some of the key enhancements and changes for the various HSPF releases since 1980.

Since 1981, USGS has been developing software to facilitate watershed modeling by providing interactive capabilities for model input development, data storage and data analysis, and model output analysis including hydrologic calibration assistance. The ANNIE, WDM, Scenario Generator (GenScn), and HSPEXP software are USGS products that have greatly advanced and facilitated watershed model applications, not only for HSPF but also for many other USGS models. For example, the WDM (Watershed Data Management) file has effectively replaced the Time Series Store (TSS) file used in the earlier versions of HSPF due to the expanded data analysis and graphical capabilities of the ANNIE software (Flynn et al., 1995), which is designed to interact with WDM files.

Since its initial release in 1980, HSPF applications have been worldwide and number in the hundreds; approximately 50 current active applications continue around the world with the greatest concentration in North America. Numerous studies have been completed or are continuing in the Pacific Northwest, the Washington, DC, metropolitan area, and the Chesapeake Bay region. Table 2 lists a few current HSPF applications, most of which are discussed by Donigian et al. (1995). Today the model serves as the focal point for cooperation and integration of watershed modeling and model support efforts between EPA and USGS. Over the years, development activities and model enhancements, along with these model applications, have continued to improve the model's capabilities and preserve its status as a state-of-the-art tool for watershed analysis.

Overview of HSPF Capabilities and Components

HSPF contains three application modules and five utility modules. The three application modules simulate the hydrologic/hydraulic and water quality components of the watershed. The utility

Table 1

Historical Progression of HSPF Releases

Year	Version	Comments/Enhancements	Document
1980	5	Initial public release	Johanson et al. (1980)
	6	Performance and portability enhancements	
1981	7	GQUAL, SEDTRN, MUTSIN, GENER, DURANL enhancements	Johanson et al. (1981)
1984	8	Special Actions enhancements Initial PC version	Johanson et al. (1984) Application Guide (Donigian et al., 1984)
1988	9	WDM implementation PC version distributed	CEAM publication
1993	10	Sediment-nutrient interactions Mass-Link/Schematic Acid-pH Module	HSPF Rel. 10 Manual (Bicknell et al., 1993)
1996	11	Enhanced special actions Water regulation/accounting Atmospheric deposition HSPF/DSS linkage (COE) Increase operations limit Forest Nitrogen Module	HSPF Rel. 11 Manual (Bicknell et al., 1997)

Table 2

Selected Recent and/or Current HSPF Applications

- Chesapeake Bay Watershed Model of nutrient loadings and management alternatives

- Seattle Metropolitan Area watershed and urban drainage studies

- Metropolitan Washington, DC, urban nonpoint and water quality studies

- U.S. EPA Office of Pesticide Programs assessment of alachlor surface water concentrations

- Sydney Water Board (Australia) assessment of water supply quality and nonpoint pollution

- Maryland Department of the Environment Patuxent River nonpoint source study

- Numerous Florida applications for hydrologic assessments, nutrient loadings and water quality simulation

- Flooding and Water Resource Development studies for Saudi Arabian Ministry of Agriculture

- Upper Grande Ronde (OR) temperature TMDL

- Walnut Creek (IA) MSEA/MASTER surface water exposure assessment

- Minnesota River Nonpoint Source Assessment Project

- Water Management for the Humber River, South Africa

- Long Island Sound Nutrient Study

- Copper Mine Impact Assessment (WI) - EPA/USGS/USACE

modules are used to manipulate and analyze time-series data. Table 3 summarizes the constituents and capabilities of the HSPF modules. A brief description of the three modules follows:

1) PERLND-Simulates runoff and water quality constituents from pervious land areas in the watershed.

2) IMPLND-Simulates impervious land area runoff and water quality.

3) RCHRES-Simulates the movement of runoff water and its associated water quality constituents in stream channels and mixed reservoirs.

PERLND Module

Because PERLND simulates the water quality and quantity processes that occur on pervious land areas, it is the most frequently used part of HSPF. To simulate these processes, PERLND models the movement of water along three paths: overland flow, interflow, and groundwater flow. Each of these three paths experiences differences in time delay and differences in interactions between water and its various dissolved constituents. A variety of storage zones are used to represent the processes that occur on the land surface and in the soil horizons. Snow accumulation and melt are also included in the PERLND module so that the complete range of physical processes affecting the generation of water and associated water quality constituents can be represented. Some of the many capabilities available in the PERLND module include the simulation of:

- Water budget and runoff components.
- Snow accumulation and melt.
- Sediment production and removal.
- Accumulation and washoff of user-defined nonpoint pollutants.
- Nitrogen and phosphorus fate and runoff.
- Pesticide fate and runoff.
- Movement of a tracer chemical.

Figure 1 defines the structure and contents of the PERLND module. The PERLND module features individual compartments (i.e., subroutine groups) for specific modeling capabilities, including: air temperature as a function of elevation (ATEMP), snow accumulation and melting (SNOW), hydrologic water budget (PWATER), sediment production and removal (SEDMNT), soil temperature (PSTEMP), surface runoff water temperature and gas concentrations (PWTGAS), generalized water quality constituents (PQUAL), solute transport (MSTLAY), pesticides (PEST), nitrogen (NITR), phosphorus (PHOS), and conservatives (TRACER).

PWATER is used to calculate the water budget components resulting from precipitation on pervious land areas; as a result, it is the key component of the PERLND module. The basis of the water budget computations contained in HSPF is the Stanford Watershed Model (Crawford and Linsley, 1966). Like the SNOW code, the PWATER code uses both physical and empirical formulations to

Table 3

HSPF Application and Utility Modules

Application Modules		
PERLND	**IMPLND**	**RCHRES**
Snow	Snow	Hydraulics
Water	Water	Conservative
Sediment	Solids	Temperature
Soil temperature	Water Quality*	Sediment
Water Quality*		Nonconservatives
Pesticide		BOD/DO
Nitrogen		Nitrogen
Phosphorus		Phosphorus
Tracer		Carbon/pH
		Plankton
Utility Modules		
COPY	**PLTGEN**	**DISPLAY**
Data transfer	Plot data	Tabulate, summarize
DURANL	**GENER**	**MUSTIN**
Duration	Transform or combine time-series data	Time-series data

* Up to 10 user–specified water quality parameters.
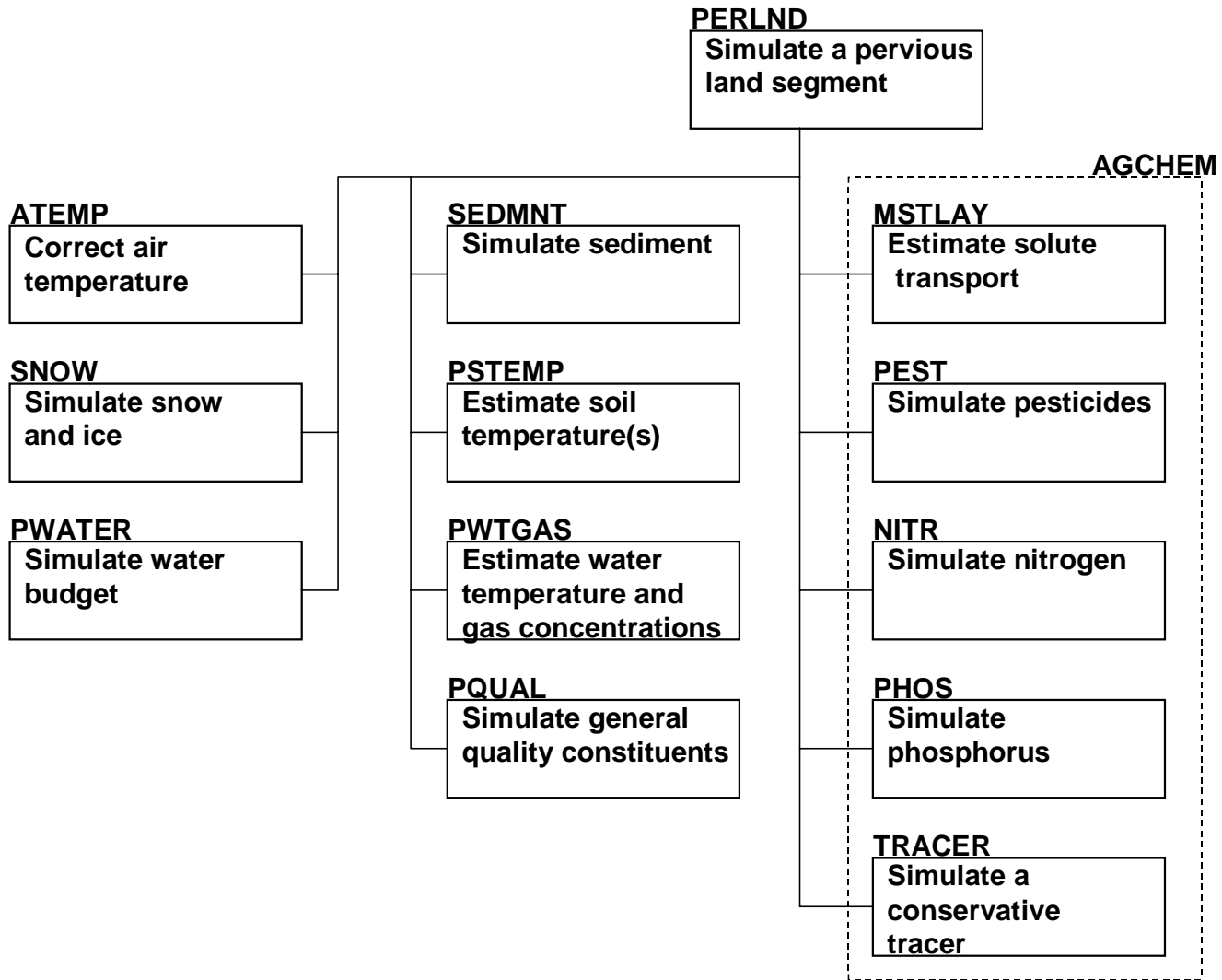
Figure 1 PERLND Structure Chart

model the movement of water through the hydrologic cycle. PWATER considers such processes as evapotranspiration; surface detention; surface runoff; infiltration; shallow subsurface flow (interflow); baseflow; and percolation to deep groundwater. Lateral inflows to surface and shallow subsurface storages can also be modeled.

The equations used in the SEDMNT code to produce and remove sediment are based on the ARM and NPS models, and are modifications of soil and gully erosion equations developed by Negev (1967) and influenced by Meyer and Wischmeier (1969) and Onstad and Foster (1975). Many of the sediment model parameters are derived from the Universal Soil Loss Equation (Wischmeier and Smith, 1978). Removal of sediment by water is simulated as washoff of detached sediment in storage and scour of the soil matrix. Soil detachment is modeled as a function of rainfall, land cover, land management practices, and soil detachment properties. If the modeler so specifies, soil detachment can be incremented by lateral input from an upslope land segment and/or net external additions/removals caused by human activities or wind. Removal of detached sediment and scour of the soil matrix by surface flow are both modeled empirically as a function of surface water storage and surface water outflow.

PWTGAS estimates the water temperature for surface, shallow subsurface (interflow) and groundwater outflows. The temperature of each outflow is considered to be the same as the soil temperature of the layer from which it originates. PWTGAS also computes the dissolved oxygen and carbon dioxide concentrations of overland flow using empirical formulations; concentrations are assumed to be at saturation. PQUAL simulates generalized water quality constituents in the outflows (surface and subsurface) from a pervious land segment using simple relationships with water and/or sediment yield. The behavior of a constituent in surface outflow is considered more complex and dynamic than the behavior in subsurface flow. The code allows quantities in surface outflow to be simulated by one, or both, of two methods. Either (1) a constituent can be modeled using "potency factors" to indicate constituent strength relative to the sediment removal computed by SEDMNT, or (2) storage of a constituent on the land surface can be modeled, considering accumulation and depletion/removal, and a first-order washoff rate of the available constituent can be removed by overland flow, as computed by PWATER. In addition, both formulations can be used for representing the washoff behavior of particulate and dissolved components of an specific pollutant.

The remaining five code compartments in PERLND are used together to model detailed behavior of soil nutrients (i.e., nitrogen and phosphorus) and nonreactive tracer chemicals (e.g., chloride). These five code sections have been referred to as the AGCHEM module because their primary use to date has been for modeling the mass balance and runoff of agricultural chemicals. MSTLAY estimates the storages and fluxes of moisture in the four soil layers—surface, upper, lower, groundwater—that define soil layers used by the remaining four code compartments. MSTLAY is required because the moisture storages and fluxes computed by PWATER must be modified to effectively simulate solute transport through the soil. Estimates of solute flux are computed based on the assumption that the concentration of solute being transported is the same as that for storage; uniform flow through the layers and continuous mixing of solutes is also assumed. Leaching retardation factors are computed to modify the solute fluxes from the top three soil layers based on user-defined model parameters.

PEST simulates pesticide behavior in the soil and runoff from pervious land segments in three forms: dissolved, adsorbed, and crystallized. The PEST code utilizes time-series data generated by other compartments of PERLND (i.e., PWATER, SEDMNT, MSTLAY) to compute transport (runoff and leaching), adsorption/desorption, and degradation. Pesticide transport is modeled as a function of water flow and/or association with transported sediment. Chemicals in solution move to, through, and from storages according to the fractions calculated in MSTLAY. Computations are performed that compute the movement of adsorbed pesticide associated with removal of sediment from the surface layer via scour and washoff. Adsorption/desorption is a function of both chemical and soil layer characteristics; several options for characterizing sorption are offered, including a first-order kinetic approach and the use of two different Freundlich isotherm methods. Degradation from all processes is modeled as a lumped rate in each of the four soil layers.

The NITR code section simulates the transport and soil reactions of nitrate, ammonia, and four forms of organic nitrogen. Nitrogen species are transported by the same methods used for pesticides. Nitrate and dissolved ammonium are transported as a function of water flow; organic nitrogen and adsorbed ammonium are removed from the surface layer storage by association with sediment scour and washoff; nitrate and ammonium in the soil water are transported according to the fractions calculated in MSTLAY; and computations are performed that compute the movement of adsorbed organic nitrogen and ammonium associated with removal of sediment from the topsoil surface layer. First-order kinetics or a Freundlich isotherm can be used to model adsorption/desorption. Nitrogen transformation processes (denitrification, nitrification, plant uptake, immobilization, mineralization, volatilization, plant nitrogen return to organic nitrogen) are modeled using temperature-corrected, first-order kinetics with separate rate constants defined for each soil layer.

PHOS simulates the transport and reaction of phosphate and organic phosphorus using methods parallel to those used for nitrogen species in NITR. Transport mechanisms for phosphate parallel those modeled for ammonium, and those for organic phosphorus parallel organic nitrogen. Like ammonium, phosphate adsorption/desorption can be modeled using either first-order kinetics or a Freundlich isotherm. Phosphorus transformation processes (plant uptake, immobilization, mineralization) are modeled using temperature-corrected, first-order kinetics with separate rate constants defined for each soil layer.

Typically, the TRACER code is applied to chloride (or bromide) to calibrate solute movement through the soil profile. This involves adjustment of leaching retardation factors until good agreement with observed soil chloride concentrations has been obtained. Once appropriate retardation values have been determined, they are used in PEST, NITR, and PHOS to simulate solute transport.

IMPLND Module

IMPLND is used for impervious land surfaces, primarily for urban land categories, where little or no infiltration occurs. However, some land processes do occur, and water, solids, and various pollutants are removed from the land surface by moving laterally downslope to a pervious area, stream channel, or reservoir. IMPLND includes most of the pollutant washoff capabilities of the commonly used urban runoff models, such as the STORM, SWMM, and NPS models. Figure 2 defines   the   structure
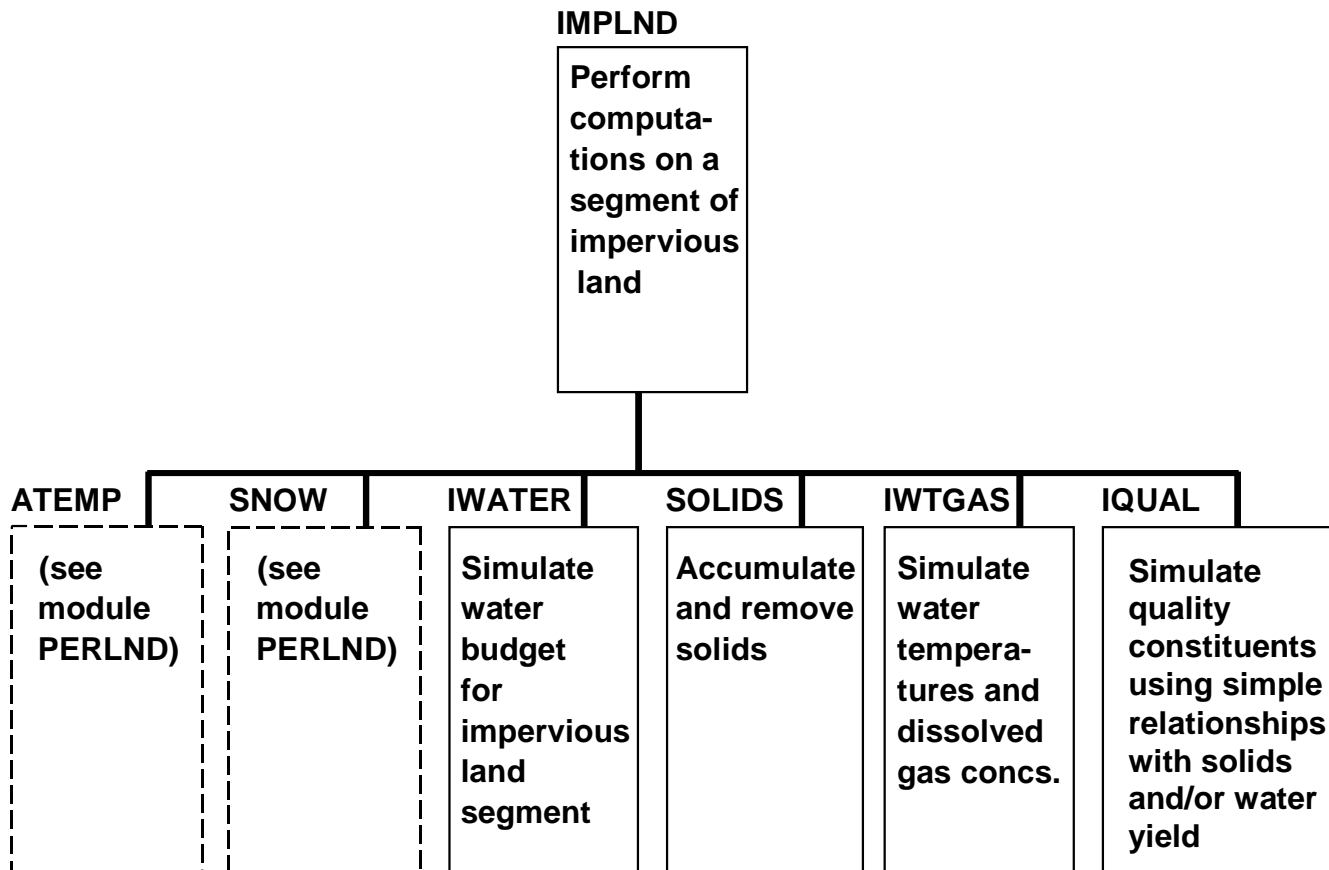
Figure 2 IMPLND Structure Chart

and contents of the IMPLND module. The module shares much of its code with PERLND, but is simplified since infiltration and other interactions with the subsurface cannot occur. The module features individual compartments for modeling air temperature as a function of elevation (ATEMP), snow accumulation and melting (SNOW), hydrologic water budget (IWATER), solids accumulation and removal (SOLIDS), surface runoff water temperature and gas concentrations (IWTGAS), and generalized water quality constituents (IQUAL).

One difference between PERLND and IMPLND process representation is of note. In the SOLIDS code section, IMPLND offers the capability to model the accumulation and removal of urban solids (i.e., solids on impervious areas) by processes that are independent of storm events (e.g., street cleaning, decay, wind deposition or scour). To use this option, the modeler needs to assign monthly or constant rates of solids accumulation and removal, estimate parameter values for impervious solids washoff (analogous to methods in the SEDMNT module of PERLND), and provide 'potency factor' values for constituents associated with the solids removed. Alternatively, the IQUAL module can be used to represent accumulation and removal processes for each constituent individually, analogous to the PQUAL approach.

RCHRES Module

RCHRES is used to route runoff and water quality constituents simulated by PERLND and IMPLND through stream channel networks and reservoirs. The module simulates the processes that occur in a series of open or closed channel reaches or a completely mixed lake. Flow is modeled as unidirectional. A number of processes can be modeled, including the following:

- Hydraulic behavior.

- Heat balance processes that determine water temperature.

- Inorganic sediment deposition, scour, and transport by particle size.

- Chemical partitioning, hydrolysis, volatilization, oxidation, biodegradation, and generalized first-order (e.g., radionuclides) decay, parent chemical/metabolite transformations.

- DO and BOD balances.

- Inorganic nitrogen and phosphorus balances.

- Plankton populations.

- pH, carbon dioxide, total inorganic carbon, and alkalinity.

Figure 3 defines the structure and contents of the RCHRES module. The module features individual compartments for modeling hydraulics (HYDR), constituent advection (ADCALC), conservatives (CONS), water temperature (HTRCH), inorganic sediment (SEDTRN), generalized quality
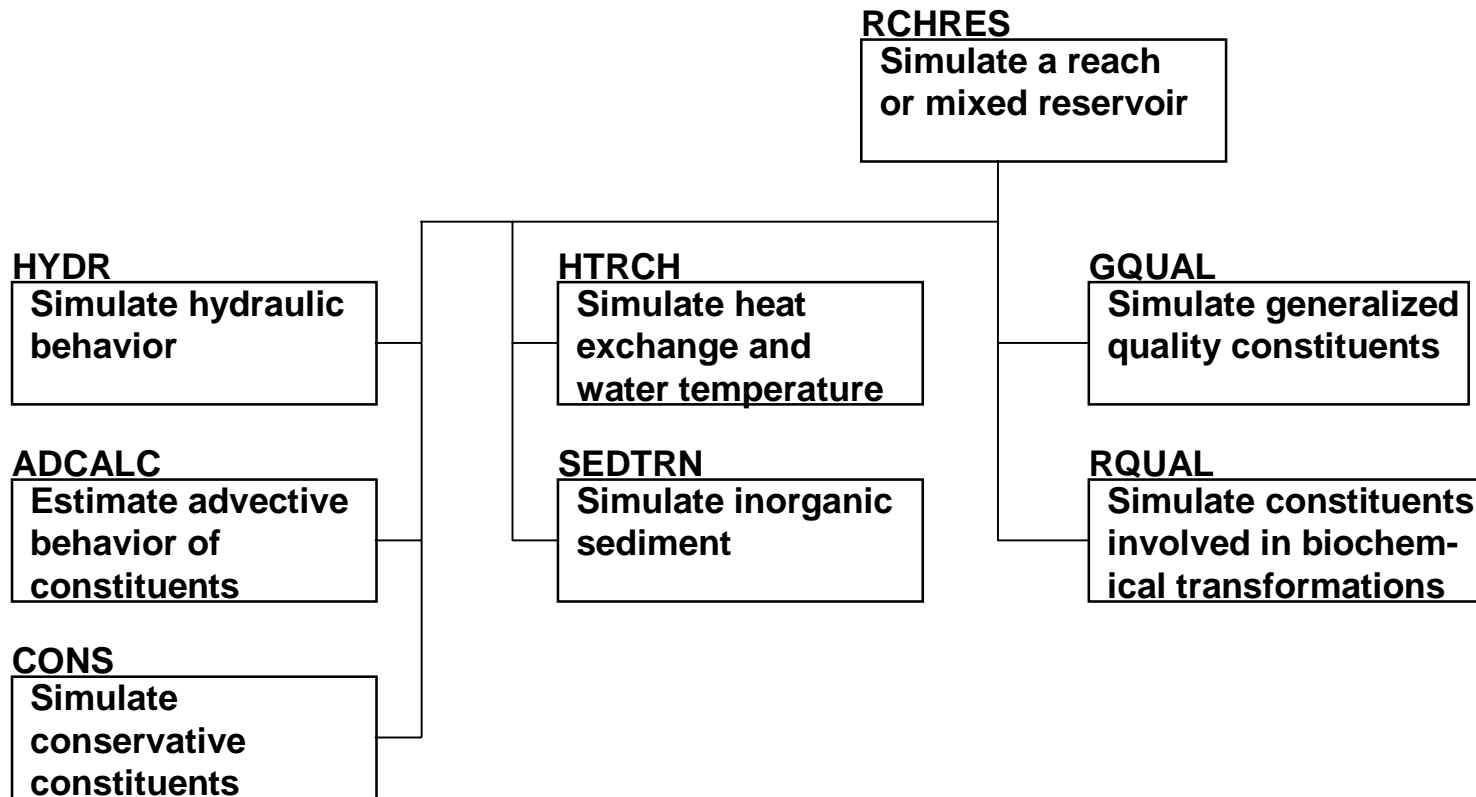
Figure 3 RCHRES Structure Chart

constituents (GQUAL), specific constituents involved in biochemical transformations (RQUAL), and acid mine drainage phenomena (ACIDPH).

HYDR simulates the processes that occur in a single reach of an open channel or a completely mixed lake. Hydraulic behavior is modeled using the kinematic wave assumption. All inflows to a reach are assumed to enter at a single upstream point. The outflow of a reach may be distributed across several targets that might represent normal outflows, diversions, and multiple gates of a reservoir. In HSPF, outflows can be represented by either, or both, of two methods:

1) Outflow can be modeled as a function of reach volume for situations where there is no control of flows, or gate settings are only a function of water level.

2) Outflow can be modeled as a function of time to represent demands for municipal, industrial, or agricultural use. To do so, the modeler must provide a time series of outflow values for the outflow target that is time-dependent and independent of reach volume.

If an outflow demand has both volume-dependent and time-dependent components, the modeler can, and must, specify how the components are combined to define the resulting outflow demand. HSPF allows the modeler to define the resulting demand in one of three manners: (1) as the minimum of the two components, (2) as the maximum of the two components, or (3) as the sum of the two components.

HSPF makes no assumptions regarding the shape of a reach; however, the following assumptions are made:

1) There is a fixed, user-defined relation between water depth, surface area, volume, and discharge. This is specified in a Function Table (FTABLE) defined for each reach by the user.

2) For any outflow demand with a volume-dependent component, the relation between the above variables is usually constant in time; however, predetermined seasonal or daily variations in discharge values can be represented by the user.

These assumptions rule out cases where flow reverses direction (e.g., estuaries) or where one stream reach influences another upstream of it in a time-dependent manner. Momentum is not considered, and the routing technique falls in the class known as "storage routing" or "kinematic wave" methods.

In addition to calculating outflow rates and reach water volumes, HYDR computes the values for additional hydraulic parameters that are used in the other code sections of RCHRES including depth, stage, surface area, average depth, top width, hydraulic radius, bed shear stress and shear velocity.

The approach taken by the SEDTRN code compartment to compute transport of channel sediment is based on the SERATRA model developed by Battelle Laboratories (Onishi and Wise, 1979). Both noncohesive (sand) and cohesive (silt, clay) sediments are simulated in SEDTRN; migration of each sediment fraction between suspension in water and the bed is modeled by balancing deposition and

scour computations. The code allows the modeler to compute the deposition or scour of noncohesive sediment by selecting one of three empirical formulations:

1) A user-defined power function of streamflow velocity.

2) A relationship (Toffaleti method) dependent upon median sand particle diameter, average stream velocity, reach hydraulic radius, reach slope, settling velocity for sand (user-specified), and water temperature.

3) A relationship (Colby method) dependent upon median sand particle diameter, average stream velocity, reach hydraulic radius, fine sediment load concentration, and water temperature.

The simulation of cohesive sediment transport consists of two steps. First, advective transport is calculated; then deposition and scour are calculated based on the calculated bed shear stress. To evaluate deposition, the modeler is required to provide values for settling velocity and critical shear stress for deposition for each fraction (silt, clay) of cohesive sediment that is modeled. To evaluate resuspension, or scour, the modeler must provide values for the erodibility coefficient and critical shear stress for each fraction.

The focus of the GQUAL code development was to allow simulation of agricultural pesticides and other synthetic organic chemicals. Given the diversity of pesticides that might be modeled, the code provides the user with the capability to model any subset of the following generalized processes: advection of dissolved material; decay of dissolved material by hydrolysis, oxidation by free radical oxygen, photolysis, volatilization, biodegradation, and/or generalized first-order decay; production of one modeled constituent as a result of decay of another constituent; advection of adsorbed suspended material; deposition and scour of adsorbed material; and adsorption/desorption between dissolved and sediment-associated phases. Using the GQUAL section in conjunction with the sediment transport code (SEDTRN), adsorbed chemicals may settle or resuspend during each simulation time step, depending on hydrodynamic conditions. Decomposition of adsorbed chemicals may be simulated, both in suspended materials and in the bed, by using a first-order, temperature-corrected decay formulation.

The RQUAL code provides detailed simulation of constituents involved in biochemical transformations. Included are dissolved oxygen, BOD, ammonia, nitrite, nitrate, phosphate, phytoplankton, benthic algae, zooplankton, refractory organics, and pH. The primary dissolved oxygen and biochemical oxygen demand balances are simulated with provisions for decay, settling, benthic sinks and sources, reaeration, and sinks and sources related to plankton. The primary nitrogen balance is modeled as sequential reactions from ammonia through nitrate. Ammonia volatilization, ammonification, denitrification, and ammonium adsorption/desorption interactions with suspended sediment fractions are also considered. Both ammonium and phosphate adsorption/desorption to suspended sediment fractions are modeled using an equilibrium, linear isotherm approach. Both nitrogen and phosphorus species are considered in modeling three types of plankton—phytoplankton, attached algae, and zooplankton. Phytoplankton processes that are modeled include growth, respiration, sinking, zooplankton predation, and death; zooplankton processes include growth, respiration and death; and benthic algae processes modeled are growth,

respiration, and death. Hydrogen ion activity (pH) can be calculated by two independent code sections. The first, named PHCARB, is contained within the RQUAL section and computes pH by considering carbon dioxide, total organic carbon, and alkalinity. In doing so, the code considers the effects on the carbon dioxide-bicarbonate system of carbon dioxide invasion, zooplankton respiration, BOD decay, net growth of algae, and benthic releases.

References

Bicknell, B.R., J.C. Imhoff, J.L. Kittle Jr., A.S. Donigian, Jr. and R.C. Johanson. 1993. Hydrological Simulation Program – FORTRAN. User's Manual for Release 10. EPA/600/R-93-174. U.S. EPA Environmental Research Laboratory, Athens, GA.

Bicknell, B.R., J.C. Imhoff, J.L. Kittle Jr., A.S. Donigian, Jr. and R.C. Johanson. 1997. Hydrological Simulation Program—FORTRAN. User's Manual for Release 11. EPA/600/R-97/080. U.S. EPA Environmental Research Laboratory, Athens, GA.

Crawford, N.H. and R.K. Linsley. 1966. Digital Simulation on Hydrology: Stanford Watershed Model IV. Stanford University Technical Report No. 39, Stanford University, Palo Alto, CA.

Donigian, A.S. Jr. and H.H. Davis. 1978. User's Manual for Agricultural Runoff Management (ARM) Model. EPA-600/3-78-080. U.S. EPA Environmental Research Laboratory, Athens, GA.

Donigian, A.S. Jr. and N.H. Crawford. 1979. User's Manual for the Nonpoint Source (NPS) Model. Unpublished Report. U.S. EPA Environmental Research Laboratory, Athens, GA.

Donigian, A.S. Jr., W.C. Huber, and T.O. Barnwell, Jr. 1995. Models of Nonpoint Source Water Quality in Urban and Nonurban Areas. Chapter 7 In: Nonpoint Pollution and Urban Stormwater Management. V. Novotny (ed). Technomic Publishing Co., Lancaster, PA. pp. 293-346.

Donigian, A.S., Jr., J.C. Imhoff, B.R. Bicknell and J.L. Kittle, Jr. 1984. Application Guide for the Hydrological Simulation Program–FORTRAN EPA 600/3-84-066, Environmental Research Laboratory, U.S. EPA, Athens, GA.

Flynn, K.M., P.R. Hummel, A.M. Lumb, and J.L. Kittle, Jr. 1995. User's Manual for ANNIE, Version 2, A Computer Program for Interactive Hydrologic Data Management, Water-Resources Investigations Report 95-4085, U.S. Geological Survey, Reston, VA. 211 p.

Hydrocomp, Inc. 1977. Hydrocomp Water Quality Operations Manual. Hydrocomp, Inc., Palo Alto, CA.

Johanson, R.C., J.C. Imhoff and H.H. Davis. 1980. User's Manual for the Hydrologic Simulation Program—FORTRAN (HSPF). EPA-600/9-80-105. U.S. EPA Environmental Research Laboratory, Athens, GA.

Johanson, R.C., J.C. Imhoff and H.H. Davis, J.L. Kittle, and A.S. Donigian, Jr. 1981. User's Manual for the Hydrologic Simulation Program - FORTRAN (HSPF): Version No. 7.0. Prepared for U.S. EPA Environmental Research Laboratory, Athens, GA. Prepared by Anderson-Nichols & Co. Inc., Palo Alto, CA.

Johanson, R.C., J.C. Imhoff, J.L. Kittle, Jr. and A.S. Donigian. 1984. Hydrological Simulation Program - FORTRAN (HSPF): Users Manual for Release 8.0, EPA-600/3-84-066, Environmental Research Laboratory, U.S. EPA, Athens, GA. 30613.

Meyer, L.D. and W.H. Wischmeier. 1969. Mathematical Simulation of the Process of Soil Erosion by *Water. Trans. Am. Soc. Agric. Eng.* 12(6):754-758, 762.

Negev, M. 1967. A Sediment Model on a Digital Computer. Department of Civil Engineering, Stanford University. Stanford, CA. Technical Report No. 76. 109 p.

Onishi, Y. and S.E. Wise. 1979. User's Manual for the Instream Sediment-Contaminant Transport Model, SERATRA. Draft Report prepared by Battelle Laboratories, Richland, Washington for U.S. EPA Environmental Research Laboratory, Athens, GA.

Onstad, C.A. and G.R. Foster. 1975. Erosion Modeling on a Watershed. *Trans. Am. Soc Agric. Eng.* 18(2):288-292.

Wischmeier, W.H. and D.D. Smith. 1978. Predicting Rainfall-Erosion Losses: A Guide to Conservation Planning. Agricultural Handbook No. 537. U.S. Department of Agriculture, Agricultural Research Service, Washington, DC. 58 p.

APPENDIX B.2

HSPF PARAMETER LIST FOR PERLND, IMPLND & RCHRES MODULES

HSPF Parameter List for PERLND, IMPLND, & RCHRES Modules

PERLND Parameter List

NAME	DEFINITION	UNITS	TABLE	DATA SOURCE
ATEMP				
AIRTMP	Initial air temperature over the Pervious Land Segment	Deg F	ATEMP-DAT	Site
ELDAT	Difference in elevation between temp gage and the Pervious Land Segment	ft	ATEMP-DAT	Site
PERLND				
AIRTFG	Flag to specify if section ATEMP is active (1) or inactive (0)	N/A	ACTIVITY	Option
IUNITS	Units in input time series--1=English, 2=metric	N/A	GEN-INFO	Option
LSID(5)	Identifier for a Pervious Land Segment	N/A	GEN-INFO	Option
MSTLFG	Flag to specify if section MSTLAY is active (1) or inactive (0)	N/A	ACTIVITY	Option
NBLKS	No. of "blocks" into which the Pervious Land Segment is subdivided	N/A	GEN-INFO	Option
NITRFG	Flag to specify if section NITR is active (1) or inactive (0)	N/A	ACTIVITY	Option
OUNITS	Units in output time series--1=English, 2=metric	N/A	GEN-INFO	Option
PESTFG	Flag to specify if section PEST is active (1) or inactive (0)	N/A	ACTIVITY	Option
PFLAG(12)	Printout level	N/A	PRINT-INFO	Option
PHOSFG	Flag to specify if section PHOS is active (1) or inactive (0)	N/A	ACTIVITY	Option
PIVL	Number of intervals between level 2 printouts	N/A	PRINT-INFO	Option
PQALFG	Flag to specify if section PQUAL is active (1) or inactive (0)	N/A	ACTIVITY	Option
PSTFG	Flag to specify if section PSTEMP is active (1) or inactive (0)	N/A	ACTIVITY	Option
PUNIT(2)	Fortran output unit for English and/or metric units. 0=none for that system.	N/A	GEN-INFO	Option
PWATFG	Flag to specify if section PWATER is active (1) or inactive (0)	N/A	ACTIVITY	Option
PWGFG	Flag to specify if section PWTGAS is active (1) or inactive (0)	N/A	ACTIVITY	Option
PYREND	Calendar month of end of year	N/A	PRINT-INFO	Option

PERLND Parameter List

NAME	DEFINITION	UNITS	TABLE	DATA SOURCE
SEDFG	Flag to specify if section SEDMNT is active (1) or inactive (0)	N/A	ACTIVITY	Option
SNOWFG	Flag to specify if section SNOW is active (1) or inactive (0)	N/A	ACTIVITY	Option
TRACFG	Flag to specify if section TRACER is active (1) or inactive (0)	N/A	ACTIVITY	Option
UUNITS	Units in UCI--1=English, 2=Metric	N/A	GEN-INFO	Option
PQUAL				
ACQOP	Rate of accumulation of QUALOF (overland flow-associated constituent)	lbs/ac.day	QUAL-INPUT	Literature/Site/Calib.
ACQOPM(12)	Monthly accumulation rates of QUALOF (overland flow-associated constituent)	lbs/ac.day	MON-ACCUM	Literature/Site/Calib.
AOQC	Concentration of the constituent in active groundwater outflow (meaningful only if this is a QUALGW (active groundwater-associated constituent))	mg/l	QUAL-INPUT	Site
AOQCM(12)	Monthly conc of QUAL in groundwater if VAQCFG = 3 or 4	mg/l	MON-GRND-CONC	Site/Calib.
AOQCM(12)	Monthly conc of QUAL in groundwater if VAQCFG = 1 or 2	lbs/ft3	MON-GRND-CONC	Site/Calib.
IOQC	Concentration of the constituent in interflow outflow (meaningful only if this is a QUALIF (interflow-associated constituent))	lbs/ft3	QUAL-INPUT	Site/Calib.
IOQCM(12)	Monthly conc of QUAL in interflow if VIQCFG = 1 or 2	lbs/ft3	MON-IFLW-CONC	Site/Calib.
IOQCM(12)	Monthly conc of QUAL in interflow if VIQCFG = 3 or 4	mg/L	MON-IFLW-CONC	Site/Calib.
NQUAL	Total number of quality constituents simulated	N/A	NQUALS	Option
POTFS	Scour potency factor	lbs/ton	QUAL-INPUT	Literature/Site/Calib.
POTFSM(12)	Monthly scour potency factor	lbs/ton	MON-POTFS	Literature/Site/Calib.
POTFW	Washoff potency factor	lbs/ton	QUAL-INPUT	Literature/Site/Calib.
POTFWM(12)	Monthly washoff potency factor	lbs/ton	MON-POTFW	Literature/Site/Calib.
QAGWFG	Flag to specify if constituent is groundwater associated; 1=yes, 0=no	N/A	QUAL-PROPS	Literature/Site
QIFWFG	Flag to specify if constituent is interflow associated; 1=yes, 0=no	N/A	QUAL-PROPS	Literature/Site
QSDFG	Flag to specify if constituent is sediment associated; 1=yes, 0=no	N/A	QUAL-PROPS	Literature/Site
QSOFG	Flag to specify if constituent is directly associated with overland flow; 1=yes, 0=no	N/A	QUAL-PROPS	Literature/Site

PERLND Parameter List

NAME	DEFINITION	UNITS	TABLE	DATA SOURCE
QTYID	String of up to 4 chars identifying units of quality constituent	N/A	QUAL-PROPS	Option
QUALID	String identifying the quality constituent	N/A	QUAL-PROPS	
SQO	Initial storage of QUALOF (overland flow-associated constituent) on the surface of the Pervious Land Segment	lbs/ac	QUAL-INPUT	Literature/Site
SQOLIM	Maximum storage of QUALOF (overland flow-associated constituent)	lbs/ac	QUAL-INPUT	Literature/Site/Calib.
SQOLIM(12)	Monthly limiting storage of QUALOF (overland flow-associated constituent)	lbs/ac	MON-SQOLIM	Literature/Site/Calib.
VAQCFG	If 1, concentration of constituent in groundwater outflow varies monthly; if 2 or 4, daily values are obtained directly from monthly values without interpolation between monthly values; if 3 or 4, the units of input concentrations are mg/L	N/A	QUAL-PROPS	Literature/Site
VIQCFG	If greater than 1, concentration of constituent in interflow outflow varies monthly: if 2 or 4, daily values are obtained directly from monthly values without interpolation between monthly values; if 3 or 4, units of input concentrations are mg/L	N/A	QUAL-PROPS	Literature/Site
VPFSFG	Flag to specify if scour potency factor varies monthly; 1=yes, 0=no	N/A	QUAL-PROPS	Literature/Site
VPFWFG	If 1, washoff potency factor varies monthly; if 2, daily factors are <u>not</u> computed by interpolation between the monthly values; if 0, factor does not vary	N/A	QUAL-PROPS	Literature/Site
VQOFG	Flag to specify if rate of accumulation and limiting storage of constituent varies monthly; 1=yes, 0=no	N/A	QUAL-PROPS	Literature/Site
WSQOP	Rate of surface runoff which will remove 90 percent of stored QUALOF (overland flow-associated constituent) per hour	in/hr	QUAL-INPUT	Literature/Site/Calib.
PSTEMP				
AIRTC	Initial air temperature	deg F	PSTEMP-TEMPS	Site
ASLT	Intercept of the surface layer temperature regression equation	deg F	PSTEMP-PARM2	Literature/Site/Calib.
ASLTM(12)	Monthly values for ASLT	deg F	MON-ASLT	Literature/Site/Calib.

PERLND Parameter List

NAME	DEFINITION	UNITS	TABLE	DATA SOURCE
BSLT	Slope of the surface layer temperature regression equation	deg F	PSTEMP-PARM2	Literature/Site/Calib.
BSLTM(12)	Monthly values for BSLT	deg F	MON-BSLT	Literature/Site/Calib.
LGTMP	Initial lower layer/groundwater layer soil temperature	deg F	PSTEMP-TEMPS	Literature/Site
LGTP1	The smoothing factor for calculating lower layer/groundwater soil temperature if TSOPFG = 0	N/A	PSTEMP-PARM2	Literature/Calib.
LGTP1	The lower layer/groundwater layer soil temperature if TSOPFG = 1	N/A	PSTEMP-PARM2	Literature/Calib.
LGTP1M(12)	Monthly values for LGTP1	see above	MON-LGTP1	Literature/Calib.
LGTP2	Not used if TSOPFG = 1	N/A	PSTEMP-PARM2	Literature/Calib.
LGTP2	The mean departure from air temperature for calculating lower layer/groundwater soil temperature if TSOPFG = 0	deg F	PSTEMP-PARM2	Literature/Calib.
LGTP2M(12)	Monthly values for LGTP2	see above	MON-LGTP2	Literature/Calib.
LGTVFG	Flag to specify if parameters for estimating lower layer temperature vary monthly; 1=yes, 0=no	N/A	PSTEMP-PARM1	Site
SLTMP	Initial surface layer soil temperature	deg F	PSTEMP-TEMPS	Site
SLTVFG	Flag to specify if parameters for estimating surface layer temperature vary monthly; 1=yes, 0=no	N/A	PSTEMP-PARM1	Literature/Site
TSOPFG	Governs the methods used to estimate subsurface soil temperatures - if 0, use mean departure from air temperature with smoothing factors; if 1 upper layer temp is estimated by regression on air temperature and lower/groundwater layers temp supplied by user	N/A	PSTEMP-PARM1	Literature/Site
ULTMP	Initial upper layer soil temperature	deg F	PSTEMP-TEMPS	Site
ULTP1	The smoothing factor in upper layer temperature calculation if TSOPFG = 0	N/A	PSTEMP-PARM2	Literature/Site/Calib.
ULTP1	The intercept in the upper layer soil temperature regression equation if TSOPFG = 1	deg F	PSTEMP-PARM2	Literature/Site/Calib.
ULTP1M(12)	Monthly values for ULTP1	see above	MON-ULTP1	Literature/Site/Calib.
ULTP2	The mean difference between upper layer soil temperature and air temperature if TSOPFG = 0	deg F	PSTEMP-PARM2	Literature/Calib.

HSPF Parameter List for PERLND, IMPLND, & RCHRES MODULES
(Continued)

PERLND Parameter List

NAME	DEFINITION	UNITS	TABLE	DATA SOURCE
ULTP2	The slope in the upper layer soil temperature regression equation if TSOPFG = 1	deg F/F	PSTEMP-PARM2	Literature/Calib.
ULTP2M(12)	Monthly values for ULTP2	see above	MON-ULTP2	Literature/Calib.
ULTVFG	Flag to specify if parameters for estimating upper layer temperature vary monthly; 1=yes, 0=no	N/A	PSTEMP-PARM1	Literature/Site
PWATER				
AGWETP	Fraction of remaining potential E-T which can be satisfied from active groundwater storage if enough is available	N/A	PWAT-PARM3	Literature/Site/Calib.
AGWRC	Basic groundwater recession rate if KVARY is zero and there is no inflow to groundwater (rate of flow today/rate yesterday)	1/day	PWAT-PARM2	Literature/Site/Calib.
AGWS	Active groundwater storage	inches	PWAT-STATE1	Literature/Site/Calib.
BASETP	Fraction of remaining potential E-T which can be satisfied from baseflow if enough is available	N/A	PWAT-PARM3	Literature/Site/Calib.
CEPS	Interception storage	inches	PWAT-STATE1	Site
CEPSC	Interception storage capacity	in	PWAT-PARM4	Literature/Site/Calib.
CEPSCM(12)	Monthly interception storage capacity	in	MON-INTERCEP	Literature/Site/Calib.
CSNOFG	Flag to specify if snow is considered; 1=yes, 0=no	N/A	PWAT-PARM1	Site
DEEPFR	Fraction of groundwater inflow which will enter deep (inactive) groundwater and, thus, be lost from the system	N/A	PWAT-PARM3	Literature/Site/Calib.
FOREST	Fraction of the Pervious Land Segment which is covered by forest which will continue to transpire in winter	N/A	PWAT-PARM2	Site
GWVS	Index to groundwater slope; it is a measure of antecedent active groundwater inflow	inches	PWAT-STATE1	Site/Calib.
IFWS	Interflow storage	inches	PWAT-STATE1	Site/Calib.
INFEXP	Exponent in the infiltration equation	N/A	PWAT-PARM3	Literature/Calib.
INFILD	Ratio between the max and mean infiltration capacities over the Pervious Land Segment	N/A	PWAT-PARM3	Literature/Calib.
INFILT	Index to the infiltration capacity of the soil	in/hr	PWAT-PARM2	Literature/Site/Calib.
INTFW	Interflow inflow parameter	N/A	PWAT-PARM4	Literature/Site/Calib.
INTFWM(12)	Monthly interflow inflow parameters	N/A	MON-INTERFLW	Literature/Site/Calib.

HSPF Parameter List for PERLND, IMPLND, & RCHRES MODULES
(Continued)

PERLND Parameter List

NAME	DEFINITION	UNITS	TABLE	DATA SOURCE
IRC	Interflow recession parm. Under zero inflow, this is the ratio of interflow outflow rate today/rate yesterday	1/day	PWAT-PARM4	Literature/Site/Calib.
IRCM(12)	Monthly interflow recession constants	/day	MON-IRC	Literature/Site/Calib.
KVARY	Parameter which affects the behavior of groundwater recession flow, enabling it to be non-exponential in its decay with time	1/in	PWAT-PARM2	Literature/Site/Calib.
LSUR	Length of the assumed overland flow plane	ft	PWAT-PARM2	Site
LZETP	Lower zone E-T parm; an index to the density of deep-rooted vegetation	N/A	PWAT-PARM4	Literature/Site/Calib.
LZETPM(12)	Monthly lower zone E-T parameter	N/A	MON-LZETPARM	Literature/Site/Calib.
LZS	Lower zone storage	inches	PWAT-STATE1	Site
LZSN	Lower zone nominal storage	in	PWAT-PARM2	Literature/Site/Calib.
NSUR	Manning's n for the assumed overland flow plane	N/A	PWAT-PARM4	Literature/Site
NSURM(12)	Monthly Manning's n values	complex	MON-MANNING	Literature/Site
PETMAX	Air temp below which E-T will arbitrarily be reduced below the value obtained from the input time series	degF	PWAT-PARM3	Literature/Site
PETMIN	Temp below which E-T will be zero regardless of the value in the input time series	degF	PWAT-PARM3	Literature/Site
RTOPFG	Flag to specify if overland flow is routed by HSPX method instead of new method; 1=HSPX method, 0=new method	N/A	PWAT-PARM1	Literature/Site
SLSUR	Slope of the assumed overland flow plane	N/A	PWAT-PARM2	Site
SURS	Surface (overland flow) storage	inches	PWAT-STATE1	Literature/Site
UZFG	Flag to specify if upper zone inflow is computed by HSPX method instead of new method; 1=HSPX method, 0=new method	N/A	PWAT-PARM1	Literature/Site
UZS	Upper zone storage	inches	PWAT-STATE1	Literature/Site
UZSN	Upper zone nominal storage	in	PWAT-PARM4	Literature/Site/Calib.
UZSNM(12)	Monthly upper zone storage	in	MON-UZSN	Literature/Site/Calib.
VCSFG	Flag to specify if interception storage capacity varies monthly; 1=yes, 0=no	N/A	PWAT-PARM1	Site
VIFWFG	Flag to specify if interflow inflow parameter varies monthly; 1=yes, 0=no	N/A	PWAT-PARM1	Site
VIRCFG	Flag to specify if interflow recession constant varies monthly; 1=yes, 0=no	N/A	PWAT-PARM1	Site
VLEFG	Flag to specify if lower zone E-T parameter varies monthly; 1=yes, 0=no	N/A	PWAT-PARM1	Literature/Site

PERLND Parameter List

NAME	DEFINITION	UNITS	TABLE	DATA SOURCE
VNNFG	Flag to specify if Manning's n varies monthly; 1=yes, 0=no	N/A	PWAT-PARM1	Literature/Site
VUZFG	Flag to specify if upper zone nominal storage varies monthly; 1=yes, 0=no	N/A	PWAT-PARM1	Literature/Site
PWTGAS				
ACO2P	Concentration of dissolved CO_2 in active groundwater outflow	mg	PWT-PARM2	Literature/Site
ACO2PM(12)	Monthly groundwater CO_2 concentration	mg	MON-GRNDCO2	Literature/Site
ADOXP	Concentration of dissolved oxygen in active groundwater outflow	mg/l	PWT-PARM2	Literature/Site
ADOXPM(12)	Monthly groundwater DO concentration	mg/l	MON-GRNDDOX	Literature/Site
AOCO2	Initial CO_2 concentration in active groundwater outflow	mg	PWT-GASES	Site
AODOX	Initial DO concentration in active groundwater outflow	mg/l	PWT-GASES	Site
AOTMP	Initial active groundwater outflow temperature	deg F	PWT-TEMPS	Site
ELEV	Elevation of the Pervious Land Segment above sea level	ft	PWT-PARM2	Site
GCVFG	Flag to specify if groundwater CO_2 concentration varies monthly; 1=yes, 0=no	N/A	PWT-PARM1	Site
GDVFG	Flag to specify if groundwater DO concentration varies monthly; 1=yes, 0=no	N/A	PWT-PARM1	Site
ICO2P	Concentration of dissolved CO_2 in interflow outflow	mg	PWT-PARM2	Literature/Site/Calib.
ICO2PM(12)	Monthly interflow CO_2 concentration	mg	MON-IFWCO2	Literature/Site/Calib.
ICVFG	Flag to specify if interflow CO_2 concentration varies monthly; 1=yes, 0=no	N/A	PWT-PARM1	Site
IDOXP	Concentration of dissolved oxygen in interflow outflow	mg/l	PWT-PARM2	Literature/Site/Calib.
IDOXPM(12)	Monthly interflow DO concentration	mg/l	MON-IFWDOX	Literature/Site/Calib.
IDVFG	Flag to specify if interflow DO concentration varies monthly; 1=yes, 0=no	N/A	PWT-PARM1	Site
IOCO2	Initial CO_2 concentration in interflow outflow	mg	PWT-GASES	Site
IODOX	Initial DO concentration in interflow outflow	mg/l	PWT-GASES	Site
IOTMP	Initial interflow outflow temperature	deg F	PWT-TEMPS	Site
SOCO2	Initial CO_2 concentration in surface outflow	mg/l	PWT-GASES	Site
SODOX	Initial DO concentration in surface outflow	mg/l	PWT-GASES	Site
SOTMP	Initial surface outflow temperature	deg F	PWT-TEMPS	Site
SEDMNT				
AFFIX	Fraction by which detached sediment storage decreases each day, as a result of soil compaction	/day	SED-PARM2	Literature/Site/Calib.

HSPF Parameter List for PERLND, IMPLND, & RCHRES MODULES
(Continued)

PERLND Parameter List

NAME	DEFINITION	UNITS	TABLE	DATA SOURCE
COVER	Fraction of land surface which is shielded from erosion by rainfall (not considering snow cover, which can be handled by simulation)	N/A	SED-PARM2	Literature/Site
COVERM(12)	Monthly erosion related cover values	N/A	MON-COVER	Literature/Site
CRVFG	Flag to specify if erosion-related cover varies monthly; 1=yes, 0=no	N/A	SED-PARM1	Site
DETS	Initial storage of detached sediment	tons/ac	SED-STOR	Literature/Site
JGER	Exponent in the matrix soil scour equation (simulates gully erosion, etc)	complex	SED-PARM3	Literature/Site/Calib.
JRER	Exponent in the soil detachment equation	N/A	SED-PARM2	Literature/Site/Calib.
JSER	Exponent in the detached sediment washoff equation	complex	SED-PARM3	Literature/Site/Calib.
KGER	Coefficient in the matrix soil scour equation (simulates gully erosion, etc)	complex	SED-PARM3	Literature/Site/Calib.
KRER	Coefficient in the soil detachment equation	N/A	SED-PARM2	Literature/Site/Calib.
KSER	Coefficient in the detached sediment washoff equation	complex	SED-PARM3	Literature/Site/Calib.
NVSI	Rate at which sediment enters detached storage from the atmosphere; a negative value can be supplied (eg, to simulate removal by human activity or wind)	lb/ac.day	SED-PARM2	Literature/Site
NVSIM(12)	Monthly net vertical sediment input	lb/ac.day	MON-NVSI	Literature/Site
SDOPFG	Flag to specify if removal of sediment from land surface is computed by ARM and NPS method instead of new method; 1=ARM and NPS method, 0=new method	N/A	SED-PARM1	Option
SMPF	"Supporting management practice factor" used to simulate the reduction in erosion achieved by use of erosion control practices	N/A	SED-PARM2	Literature/Site
VSIVFG	Flag to specify if the rate of net vertical sediment input varies monthly; 1=yes, 0=no If 2, vertical sediment input is added to the detached sediment storage only on days when no rainfall occurred during the previous day	N/A	SED-PARM1	Site
SNOW				
CCFACT	Parameter to adapt the snow condensation/convection melt equation to field conditions	N/A	SNOW-PARM2	Literature/Calib.

HSPF Parameter List for PERLND, IMPLND, & RCHRES MODULES
(Continued)

PERLND Parameter List

NAME	DEFINITION	UNITS	TABLE	DATA SOURCE
COVIND	Maximum pack (water equivalent) at which the entire Pervious Land Segment will be covered with snow	in	SNOW-PARM1	Literature/Site
COVINX	Current pack (water equiv) required to obtain complete areal coverage of the Pervious Land Segment	in	SNOW-INIT2	Literature/Site
DULL	Index to the dullness of the pack surface, from which albedo is estimated	N/A	SNOW-INIT1	Literature/Site
ICEFG	Flag to specify if ice formation in snow pack will be simulated; 1=yes, 0=no	N/A	ICE-FLAG	Literature/Site
LAT	Latitude of the Pervious Land Segment	degrees	SNOW-PARM1	Site
MELEV	Mean elevation of the Pervious Land Segment	ft	SNOW-PARM1	Site
MGMELT	Max rate of snowmelt by ground heat	in/day	SNOW-PARM2	Literature/Site/Calib.
MWATER	Max water content of the snow pack, in depth water per depth water equiv	N/A	SNOW-PARM2	Literature/Site/Calib.
Pack-ice	Quantity of ice in the pack (water equiv)	in	SNOW-INIT1	Literature/Site
Pack-snow	Quantity of snow in the pack (water equiv)	in	SNOW-INIT1	Literature/Site
Pack-watr	Quantity of liquid water in the pack	in	SNOW-INIT1	Literature/Site
PAKTMP	Mean temperature of the frozen contents of the pack	degF	SNOW-INIT1	Literature/Site
RDCSN	Density of cold, new snow relative to water	N/A	SNOW-PARM2	Literature/Site
RDENPF	Density of the frozen contents (snow+ice) of the pack, relative to water	N/A	SNOW-INIT1	Literature/Site
SHADE	Fraction of the Pervious Land Segment shaded from solar radiation, e.g. by trees	N/A	SNOW-PARM1	Literature/Site
SKYCLR	Fraction of sky which is clear	N/A	SNOW-INIT2	Literature/Site
SNOEVP	Parameter to adapt the snow evaporation equation to field conditions	N/A	SNOW-PARM2	Literature/Site
SNOWCF	Factor by which recorded snowfall data is multiplied to account for poor snow catch efficiency	N/A	SNOW-PARM1	Literature/Site/Calib.
TSNOW	Air temp below which precip will be snow, under saturated conditions	degF	SNOW-PARM2	Literature/Calib.
XLNMLT	Current remaining possible increment to ice storage in the pack	in	SNOW-INIT2	Literature/Site

HSPF Parameter List for PERLND, IMPLND, & RCHRES MODULES
(Continued)

IMPLND Parameter List

NAME	DEFINITION	UNITS	TABLE	DATA SOURCE
ATEMP				
AIRTMP	Initial air temperature over the ILS	Deg F	ATEMP-DAT	Site
ELDAT	difference in elevation between temp gage and the ILS	ft	ATEMP-DAT	Site
IMPLND				
AIRTFG	Flag to specify if section ATEMP is active (1) or inactive (0)	N/A	ACTIVITY	Option
IQALFG	Flag to specify if section PQUAL is active (1) or inactive (0)	N/A	ACTIVITY	Option
IUNITS	Units in input time series--1=English, 2=Metric	N/A	GEN-INFO	Option
IWATFG	Flag to specify if section IWATER is active (1) or inactive (0)	N/A	ACTIVITY	Option
IWGFG	Flag to specify if section IWTGAS is active (1) or inactive (0)	N/A	ACTIVITY	Option
LSID(5)	Identifier for an ILS	N/A	GEN-INFO	
OUNITS	Units in output time series--1=English, 2=Metric	N/A	GEN-INFO	Option
PFLAG(6)	Printout level	N/A	PRINT-INFO	Option
PIVL	Number of intervals between level 2 printouts	N/A	PRINT-INFO	Option
PUNIT(2)	Fortran output unit for English and/or Metric units. 0=none for that system.	N/A	GEN-INFO	Option
PYREND	Calendar month of end of year	N/A	PRINT-INFO	Option
SLDFG	Flag to specify if section SOLIDS is active (1) or inactive (0)	N/A	ACTIVITY	Option
SNOWFG	Flag to specify if section SNOW is active (1) or inactive (0)	N/A	ACTIVITY	Option/Site
UUNITS	Units in UCI--1=English, 2=Metric	N/A	GEN-INFO	Option
IQUAL				
ACQOP	Rate of accumulation of QUALOF (overland flow-associated constituent)	qty/ac.day	QUAL-INPUT	Literature/Calib.
ACQOPM(12)	Monthly accumulation rates of QUALOF (overland flow-associated constituent)	qty/ac.day	MON-ACCUM	Literature/Calib.
NQUAL	Total number of quality constitutents simulated	N/A	NQUALS	Option
POTFW	Washoff potency factor	qty/ton	QUAL-INPUT	Literature/Site/Calib.

IMPLND Parameter List

NAME	DEFINITION	UNITS	TABLE	DATA SOURCE
POTFWM(12)	Monthly washoff potency factor	qty/ton	MON-POTFW	Literature/Site/Calib.
QSDFG	Flag to specify if constituent is sediment associated; 1=yes, 0=no	N/A	QUAL-PROPS	Literature/Site/Calib.
QSOFG	Flag to specify if constituent is directly associated with overland flow; 1=yes, 0=no	N/A	QUAL-PROPS	Literature/Site
QTYID	String of up to 4 chars identifying units of quality constituent	N/A	QUAL-PROPS	
QUALID	String identifying the quality constituent	N/A	QUAL-PROPS	
SQO	Initial storage of QUALOF (overland flow-associated constituent) on surface	qty/ac	QUAL-INPUT	Literature/Site/Calib.
SQOLIM	Maximum storage of QUALOF (overland flow-associated constituent)	qty/ac	QUAL-INPUT	Literature/Site/Calib.
SQOLIM(12)	Monthly limiting storage of QUALOF (overland flow-associated constituent)	qty/ac	MON-SQOLIM	Literature/Site/Calib.
VPFWFG	Flag to specify if washoff potency factor varies monthly; 1=yes, 0=no	N/A	QUAL-PROPS	Option
VQOFG	Flag to specify if rate of accumulation and limiting storage of constituent varies monthly; 1=yes, 0=no	N/A	QUAL-PROPS	Option
WSQOP	Rate of surface runoff which will remove 90 percent of stored QUALOF (overland flow-associated constituent) per hour	in/hr	QUAL-INPUT	Literature/Calib.
IWATER				
ACCSDM(12)	Monthly solids accumulation rates	tons/ac.day	MON-SACCUM	Literature/Calib.
ACCSDP	Rate at which solids are placed on the land surface	tons/ac.day	SLD-PARM2	Literature/Calib.
CSNOFG	Flag to specify if snow is considered; 1=yes, 0=no	N/A	IWAT-PARM1	Option/Site
JEIM	Exponent in the solids washoff equation	complex	SLD-PARM2	Literature
KEIM	Coefficient in the solids washoff equation	complex	SLD-PARM2	Literature/Calib.
LSUR	Length of the assumed overland flow plane	ft	IWAT-PARM2	Site
NSUR	Manning's n for the overland flow plane	N/A	IWAT-PARM2	Literature/Site
NSURM(12)	Monthly Manning's n values	complex	MON-MANNING	Literature/Site
PETMAX	Air temp below which E-T will arbitrarily be reduced below the value obtained from the input time series	degF	IWAT-PARM3	Literature/Site
PETMIN	Air temp below which E-T will be zero regardless of the value in the input time series	degF	IWAT-PARM3	Literature/Site
REMSDM(12)	Monthly solids unit removal rates	/day	MON-REMOV	Literature/Calib.

HSPF Parameter List for PERLND, IMPLND, & RCHRES MODULES
(Continued)

IMPLND Parameter List

NAME	DEFINITION	UNITS	TABLE	DATA SOURCE
REMSDP	Fraction of solids storage which is removed each day; when there is no runoff, for example, because of street sweeping	/day	SLD-PARM2	Literature/Site
RETS	Retention storage	inches	IWAT-STATE1	Literature/Site
RETSC	Retention (interception) storage capacity of the surface	in	IWAT-PARM2	Literature/Site
RETSCM(12)	Monthly retention storage capacity	in	MON-RETN	Option
RTLIFG	Flag to specify if lateral surface inflow to the ILS is subject to retention storage; 1=yes, 0=no	N/A	IWAT-PARM1	Option
RTOPFG	Flag to specify if overland flow is routed by HSPX method instead of new method; 1=HSPX method, 0=new method	N/A	IWAT-PARM1	Option
SDOPFG	Flag to specify if removal of sediment from land surface is computed by ARM and NPS method instead of new method; 1=ARM and NPS method, 0=new method	N/A	SLD-PARM1	Option
SLDS	Initial storage of solids	tons/ac	SLD-STOR	Literature/Site
SLSUR	Slope of the assumed overland flow plane	N/A	IWAT-PARM2	Site
SURS	Surface (overland flow) storage	inches	IWAT-STATE1	Literature/Site
VASDFG	Flag to specify if accumulation rate of solids varies monthly; 1=yes, 0=no	N/A	SLD-PARM1	Option
VNNFG	Flag to specify if Manning's n varies monthly; 1=yes, 0=no	N/A	IWAT-PARM1	Option
VRSDFG	Flag to specify if unit removal rate of solids varies monthly; 1=yes, 0=no	N/A	SLD-PARM1	Option
VRSFG	Flag to specify if retention storage capacity varies monthly; 1=yes, 0=no	N/A	IWAT-PARM1	Option
IWTGAS				
AWTF	Intercept of surface water temperature regression equation	DegF	IWT-PARM2	Literature/Site/Calib.
AWTFM(12)	Monthly values for AWTF	deg F	MON-AWTF	Literature/Site/Calib.
BWTF	Slope of the surface water temperature regression equation	DegF/F	IWT-PARM2	Literature/Site/Calib.
BWTFM(12)	Monthly values for BWTF	degF/F	MON-BWTF	Literature/Site/Calib.
CSNOFG	Flag to specify if snow is considered; 1=yes, 0=no	N/A	IWT-PARM1	Option
ELEV	Elevation of ILS above sea level	ft	IWT-PARM2	Site
SOCO2	Initial CO_2 content of surface runoff	mg	IWT-INIT	Site

HSPF Parameter List for PERLND, IMPLND, & RCHRES MODULES
(Continued)

IMPLND Parameter List

NAME	DEFINITION	UNITS	TABLE	DATA SOURCE
SODOX	Initial DO content of surface runoff	mg/l	IWT-INIT	Site
SOTMP	Initial temperature of surface runoff	Deg F	IWT-INIT	Site
WTFVFG	Flag to specify if water temperature regression parameters AWTF and BWTF vary monthly; 1=yes, 0=no	N/A	IWT-PARM1	Option
SNOW	Same as Snow list for PERLND Module			

HSPF Parameter List for PERLND, IMPLND, & RCHRES MODULES
(Continued)

RCHRES Parameter List

NAME	DEFINITION	UNITS	TABLE	DATA SOURCE
ADCALC				
CRRAT	Ratio of maximum velocity to mean velocity in RCHRES cross-section under typical flow conditions	N/A	ADCALC-DATA	Literature/Site
VOL	Volume of water in the RCHRES at the start of the simulation (not necessary if section HYDR is active)	ac.ft.	ADCALC-DATA	Site
GQUAL				
ADPM(1-6,1)	Partition coefficients for generalized quality constituent among: 1-suspended sand, 2-suspended silt, 3-suspended clay, 4-bed sand, 5-bed silt, 6-bed clay	l/mg	GQ-KD	Literature/Calib.
ADPM(1-6,2)	Transfer rate between adsorbed and desorbed states for generalized quality constituent. First subscript same as above.	/day	GQ-ADRATE	Literature/Calib.
ADPM(1-6,3)	Temperature correction coefficients for adsorption/ desorption for generalized quality constituent. First subscript same as above.	N/A	GQ-ADTHETA	Literature
ALPH(18)	Base absorption coefficients for 18 wavelengths of light (see HSPF Manual, p. 175) passing through clear water	/cm	GQ-ALPHA	Literature
BIO	Concentration of biomass causing biodegradation of generalized quality constituent.	mg/l	GQ-BIOPM	Literature/Calib.
BIOCON	Second order rate constant for biomass concentration causing biodegradation of generalized quality constituent.	/mg.day	GQ-BIOPM	Literature/Calib.
BIOM(12)	Monthly values of biomass concentration causing biodegradation of generalized quality constituent.	mg/l	MON-BIO	Literature/Calib.
C(3,3)	Matrix of relationship between parent and daughter compounds for a decay process.	N/A	GQ-DAUGHTER	Literature/Site/Calib.
CFGAS	Ratio of volatilization rate for generalized quality constituent to oxygen reaeration rate	N/A	GQ-CFGAS	Literature
CLD	Constant or initial value of cloud cover	tenths	GQ-VALUES	Site

RCHRES Parameter List

NAME	DEFINITION	UNITS	TABLE	DATA SOURCE
CLDFG	Source of cloud cover data: 1 - time series; 2 - constant; 3 - monthly	N/A	GQ-GENDATA	Option
CLDM(12)	Monthly values of cloud cover	tenths	MON-CLOUD	Site
CONCID	Identifier for concentration units of generalized quality constituent.	N/A	GQ-QALDATA	Option
CONV	Conversion factor from QTYID/VOL (where VOL is ft3 or m3) to concentration units specified by CONCID	N/A	GQ-QALDATA	Option
DEL(18)	Increments to base absorption coefficient for 18 wavelengths of light (see HSPF Manual, p. 175) passing through plankton-laden water	l/mg.cm	GQ-DELTA	Literaturer
DQAL	Initial concentration of generalized quality constituent.	concid	GQ-QALDATA	Site
FSTDEC	First order decay rate for generalized quality constituent.	/day	GQ-GENDECAY	Literature/Site/Calib.
GAMM(18)	Increments to base absorbance coefficient for 18 wavelengths of light (see HSPF Manual, p. 175) passing through sediment-laden water	l/mg.cm	GQ-GAMMA	Literature
GQID(5)	Identifier for generalized quality constituent	N/A	GQ-QALDATA	
GQPM2(7)	GQPM2(1-6) are flags indicating whether the generalized quality constituent is a "daughter" product through each of the decay processes. 0 - no; 1 - yes. 1) HDRL - hydrolysis 2) OXID - oxidation by free radical oxygen 3) PHOT - photolysis 4) VOLT - volatilization 5) BIOD - biodegradation 6) GEN - general first order decay GQPM2(7) indicates source of biomass data: 1 - time series; 2 - constant; 3 - monthly	N/A	GQ-FLG2	Literature/Site
KA	Second order acid rate constant for hydrolysis	/M-sec	GQ-HYDPM	Literature
KB	Second order base rate constant for hydrolysis	/M-sec	GQ-HYDPM	Literature
KBED	Decay rate for generalized quality constituent adsorbed to bed sediment	/day	GQ-SEDDECAY	Literature

HSPF Parameter List for PERLND, IMPLND, & RCHRES MODULES
(Continued)

RCHRES Parameter List

NAME	DEFINITION	UNITS	TABLE	DATA SOURCE
KCLD(18)	Light extinction efficiency of cloud cover for 18 wavelengths of light (see HSPF Manual, p. 175)	N/A	GQ-CLDFACT	Literature
KN	First order rate constant of neutral reaction with water	/sec	GQ-HYDPM	Literature
KOX	Second order rate constant for oxidation by free radical oxygen	/M-sec	GQ-ROXPM	Literature
KSUSP	Decay rate for generalized quality constituent adsorbed to suspended sediment	/day	GQ-SEDDECAY	Literature/Site
LAT	Latitude of the RCHRES. Positive for North, negative for South.	degrees	GQ-GENDATA	Site
NGQUAL	Number of generalized quality constituents	N/A	GQ-GENDATA	Option
PHFLAG	Source of pH data (1=time series, 2=constant, 3=monthly values)	N/A	GQ-GENDATA	Option
PHOTPM(1-18)	Molar absorption coefficients for the generalized quality constituent for 18 wavelengths of light. (See HSPF Manual, p. 175.)	/M.cm	GQ-PHOTPM	Literature
PHOTPM(19)	PHOTPM(19) is the quantum yield in air-saturated pure water.	M/E	GQ-PHOTPM	Literature
PHOTPM(20)	PHOTPM(20) is the temperature correction coefficient for photolysis.	N/A	GQ-PHOTPM	Literature
PHVAL	Constant or initial value of pH	pH	GQ-VALUES	Site
PHVALM(12)	Monthly pH	pH	MON-PHVAL	Site
PHY	Constant or initial value of phytoplankton concentration	mg/l	GQ-VALUES	Literature/Site
PHYM(12)	Monthly phytoplankton concentration	mg/l	MON-PHYTO	Literature/Site
PHYTFG	Source of phytoplankton data: 1 - time series; 2 - constant; 3 - monthly	N/A	GQ-GENDATA	Option

RCHRES Parameter List

NAME	DEFINITION	UNITS	TABLE	DATA SOURCE
QALFG(7)	Flags indicating which processes affect a generalized quality constituent. 0 - no; 1 - yes. 1) HDRL - hydrolysis; 2) OXID - oxidation by free radical oxygen; 3) PHOT - photolysis 4) VOLT - volatilization 5) BIOD - biodegradation 6) GEN - first order general decay 7) SDAS - sediment adsorption/desorption	N/A	GQ-QALFG	Literature
QTYID	Identifier for mass units of generalized quality constituent	N/A	GQ-GQALDATA	
ROC	Constant or initial free radical oxygen concentration	mole/l	GQ-VALUES	Site
ROCM(12)	Monthly free radical oxygen concentration	mole/l	MON-ROXYGEN	Site
ROXFG	Source of free radical oxygen concentration data: 1 - time series; 2 - constant; 3 - monthly	N/A	GQ-GENDATA	Option
SDCNC	Constant or initial total suspended sediment concentration	mg/l	GQ-VALUES	Site
SDCNCM(12)	Monthly values of total suspended sediment concentration	mg/l	MON-SEDCONC	Site
SDFG	Source of sediment concentration data: 1 - time series; 2 - constant; 3 - monthly	N/A	GQ-GENDATA	Option
SQAL(6)	Initial concentrations of generalized quality constituent on: 1-suspended sand, 2-suspended silt, 3-suspended clay, 4-bed sand, 5-bed silt, 6-bed clay	concu/mg	GQ-SEDCONC	Site
TEMPFG	Source of water temperature data: 1 - time series; 2 - constant; 3 - monthly	N/A	GQ-GENDATA	Option
TEMPM(12)	Monthly water temperature	degF	MON-WATEMP	Site
THBED	Temperature correction coefficient for decay of generalized quality constituent on bed sediment	N/A	GQ-SEDDECAY	Literature
THBIO	Temperature correction coefficient for biodegradation	N/A	GQ-BIOPM	Literature
THFST	Temperature correction coefficient for first order decay	N/A	GQ-GENDECAY	Literature
THHYD	Temperature correction coefficient for hydrolysis	N/A	GQ-HYDPM	Literature

RCHRES Parameter List

NAME	DEFINITION	UNITS	TABLE	DATA SOURCE
THOX	Temperature correction coefficient for oxidation by free radical oxygen	N/A	GQ-ROXPM	Literature
THSUSP	Temperature correction coefficient for decay of generalized quality constituent on suspended sediment	N/A	GQ-SEDDECAY	Literature
TWAT	Constant or initial water temperature	degF	GQ-VALUES	Site
HTRCH				
AIRTMP	Initial air temperature at the RCHRES	degF	HEAT-INIT	Site
CFSAEX	Correction factor for solar radiation (it includes fraction of RCHRES surface exposed to radiation)	N/A	HEAT-PARM	Literature/Site
ELDAT	Difference in elevation between RCHRES and air temperature gage (positive if RCHRES is higher than the gage)	ft	HEAT-PARM	Site
ELEV	Mean RCHRES elevation	ft	HEAT-PARM	Site
KATRAD	Longwave radiation coefficient	N/A	HEAT-PARM	Literature
KCOND	Conduction-convection heat transport coefficient	N/A	HEAT-PARM	Literature
KEVAP	Evaporation coefficient	N/A	HEAT-PARM	Literature
TW	Initial water temperature in the RCHRES	degF	HEAT-INIT	Site
HYDR				
AUX1FG	Flag to specify if subroutine AUXIL will be called to compute depth, stage, surface area, average depth, and topwidth, and these parameters will be printed out; 1=yes, 0=no	N/A	HYDR-PARM1	Option
AUX2FG	Flag to specify if average velocity and average cross-sectional area will be calculated and printed out; 1=yes, 0=no	N/A	HYDR-PARM1	Option
AUX3FG	Flag to specify if shear velocity and bed shear stress will be calculated; 1=yes, 0=no	N/A	HYDR-PARM1	Option
COLIND(5)	Pair of columns used to evaluate the initial value of F(VOL) component of outflow demand for the exit	N/A	HYDR-INIT	Option/Site
CONVFM(12)	Monthly F(VOL) adjustment factors	N/A	MON-CONVF	Option

HSPF Parameter List for PERLND, IMPLND, & RCHRES MODULES
(Continued)

RCHRES Parameter List

NAME	DEFINITION	UNITS	TABLE	DATA SOURCE
DB50	Median diameter of bed sediment (assumed constant throughout the run)	in	HYDR-PARM2	Literature/Site
DELTH	Drop in water elevation from upstream to downstream extremities of the RCHRES	ft	HYDR-PARM2	Site
FTABNO	If FTBDSN = 0, user's number for F-Table in FTABLES Block, if FTBDSN > 0, WDM table indicator specifying which table within WDM dataset given by FTBDSN contains the F-Table	N/A	HYDR-PARM2	Option
FTBDSN	If greater than zero, WDM table dataset number containing the F-Table; if 0, indicates F-Table is UCI FTABLES Block	N/A	HYDR-PARM2	Option
FUNCT(5)	Determines function used to combine components of an outflow demand -- 1 = MIN(F(VOL),G(T)); 2 = MAX(F(VOL),G(T)); 3 = SUM(F(VOL),G(T))	N/A	HYDR-PARM1	Site
KS	Weighting factor for hydraulic routing	N/A	HYDR-PARM2	Literature/Site
LEN	Length of the RCHRES	miles	HYDR-PARM2	Site
ODFVFG(5)	Determines F(VOL) component of outflow demand -- 0 means outflow demand does not have a volume dependent component; if greater than 0, indicates column number in RCHTAB which contains F(VOL) component; if less than 0, the absolute value indicates the element of array COLIND( ) which defines a pair of columns in RCHTAB which are used to evaluate the F(VOL) component	N/A	HYDR-PARM1	Option/Site
ODGTFG(5)	Determines G(T) component of outflow demand -- 0 means outflow demand does not have such a component; greater than 0 indicates element number of array OUTDGT( ) which contains G(T) component	N/A	HYDR-PARM1	Option/Site
OUTDGT(5)	G(T) component of the initial outflow demand for each exit from the RCHRES	ft3/s	HYDR-INIT	Option/Site
STCOR	Correction to RCHRES depth to calculate stage -- Depth + STCOR = Stage	ft	HYDR-PARM2	Site

RCHRES Parameter List

NAME	DEFINITION	UNITS	TABLE	DATA SOURCE
VCONFG	Flag to specify if F(VOL) outflow demand components are multiplied by a factor which is allowed to vary monthly; 1=yes, 0=no	N/A	HYDR-PARM1	Option/Site
VOL	Initial volume of water in the RCHRES	ac.ft.	HYDR-INIT	Site
NUTRX				
ADNHFG	Flag to specify if NH4 adsorption is simulated; 1=yes, 0=no	N/A	NUT-FLAGS	Option
ADNHPM(3)	Partition coefficients for NH4-N adsorbed to sand, silt,and clay	ml/g	NUT-ADSPARM	Literature/Site/Calib.
ADPOFG	Flag to specify if PO4 adsorption is simulated; 1=yes, 0=no	N/A	NUT-FLAGS	Option/Site
ADPOPM(3)	Partition coefficients for PO4-P adsorbed to sand, silt,and clay	ml/g	NUT-ADSPARM	Literature
AMVFG	Flag to specify if ammonia vaporization is enabled; 1=yes, 0=no	N/A	NUT-FLAGS	Option/Site
ANAER	Concentration of dissolved oxygen below which anaerobic conditions exist	mg/l	NUT-BENPARM	Literature/Site/Calib.
BNH4(3)	Constant bed concentrations of NH4-N adsorbed to sand, silt,and clay	mg/kg	NUT-BEDCONC	Literature/Site/Calib.
BPCNTC	Percentage, by weight, of biomass which is carbon	N/A	CONV-VAL1	Literature/Site
BPO4(3)	Constant bed concentrations of PO4-P adsorbed to sand, silt,and clay	mg/kg	NUT-BEDCONC	Literature/Site/Calib.
BRPO4(1)	Benthal aerobic release of ortho-phosphate	mg/m2.hr	NUT-BENPARM	Literature/Calib.
BRPO4(2)	Benthal anaerobic release of ortho-phosphate	mg/m2.hr	NUT-BENPARM	Literature/Calib.
BRTAM(1)	Benthal aerobic release of total ammonia	mg/m2.hr	NUT-BENPARM	Literature/Calib.
BRTAM(2)	Benthal anaerobic release of total ammonia	mg/m2.hr	NUT-BENPARM	Literature/Calib.
CVBO	Conversion from milligrams biomass to milligrams oxygen	mg/mg	CONV-VAL1	Literature
CVBPC	Conversion from biomass expressed as phosphorus to carbon equivalency	mols/mol	CONV-VAL1	Literature
CVBPN	Conversion from biomass expressed as phosphorus to nitrogen equivalency	mols/mol	CONV-VAL1	Literature
DENFG	Flag to specify if denitrification is enabled; 1=yes, 0=no	N/A	NUT-FLAGS	Literature/Site
DENOXT	Dissolved oxygen concentration threshhold for denitrification	mg/l	NUT-NITDENIT	Literature/Calib.

RCHRES Parameter List

NAME	DEFINITION	UNITS	TABLE	DATA SOURCE
EXPNVG	Exponent in gas layer mass transfer coefficient equation for NH3 volatilization	N/A	NUT-NH3VOLAT	Literature
EXPNVL	Exponent in liquid layer mass transfer coefficient equation for NH3 volatilization	N/A	NUT-NH3VOLAT	Literature
KNO220	Nitrification rate of nitrite at 20 degrees C	/hr	NUT-NITDENIT	Literature/Site/Calib.
KNO320	Denitrification rate at 20 degrees C	/hr	NUT-NITDENIT	Literature/Site/Calib.
KTAM20	Nitrification rate of ammonia at 20 degrees C	/hr	NUT-NITDENIT	Literature/Site/Calib.
NO2	Initial concentration of nitrite (as N)	mg/l	NUT-DINIT	Site
NO2FG	Flag to specify if nitrite is simulated; 1=yes, 0=no	N/A	NUT-FLAGS	Literature/Site
NO3	Initial concentration of nitrate (as N)	mg/l	NUT-DINIT	Site
PHFLG	Source of pH data (1=time series, 2=constant, 3=monthly values)	N/A	NUT-FLAGS	Option
PHVAL	Constant or initial value of pH	pH	NUT-DINIT	Site
PO4	Initial concentration of ortho-phosphorus (as P)	mg/l	NUT-DINIT	Site
PO4FG	Flag to specify if ortho-phosphorus is simulated; 1=yes, 0=no	N/A	NUT-FLAGS	Option
SNH4(3)	Initial concentrations of NH4-N adsorbed to sand, silt, and clay	mg/kg	NUT-ADSINIT	Site
SPO4(3)	Initial concentrations of PO4-P adsorbed to sand, silt, and clay	mg/kg	NUT-ADSINIT	Site
TAM	Initial concentration of total ammonia (as N)	mg/l	NUT-DINIT	Site
TAMFG	Flag to specify if total ammonia is simulated; 1=yes, 0=no	N/A	NUT-FLAGS	Option
TCDEN	Temperature correction coefficient for denitrification	N/A	NUT-NITDENIT	Literature
TCNIT	Temperature correction coefficient for nitrification	N/A	NUT-NITDENIT	Literature
OXRX				
BENOD	Benthal oxygen demand at 20 degrees C (with unlimited DO concentration)	mg/m2.hr	OX-BENPARM	Literature/Site/Calib.
BOD	Biochemical oxygen demand	mg/l	OX-INIT	Site
BRBOD(1)	Benthal release of BOD at high oxygen concentration	mg/m2.hr	OX-BENPARM	Literature/Site/Calib.
BRBOD(2)	Increment to benthal release of BOD under anaerobic conditions	mg/m2.hr	OX-BENPARM	Literature/Site/Calib.

RCHRES Parameter List

NAME	DEFINITION	UNITS	TABLE	DATA SOURCE
CFOREA	Correction factor in lake reaeration equation to account for good or poor circulation characteristics	N/A	OX-CFOREA	Literature/Site
DELTH	Energy drop over length of RCHRES	ft	OX-LEN-DELTH	Site
DOX	Dissolved oxygen	mg/l	OX-INIT	Site
ELEV	RCHRES elevation above sea-level	ft	ELEV	Site
EXPOD	Exponential factor in the dissolved oxygen term of the benthal oxygen demand equation	N/A	OX-BENPARM	Literature/Site
EXPRED	Exponent to depth used in calculation of reaeration coefficient	N/A	OX-REAPARM	Literature/Site
EXPREL	Exponential factor in the dissolved oxygen term of the benthal BOD release equation	N/A	OX-BENPARM	Literature/Site
EXPREV	Exponent to velocity used in calculation of reaeration coefficient	N/A	OX-REAPARM	Literature/Site
KBOD20	Unit BOD decay rate @ 20 degrees C	/hr	OX-GENPARM	Literature/Site/Calib.
KODSET	Rate of BOD settling	ft/hr	OX-GENPARM	Literature/Calib.
LEN	Length of the RCHRES	miles	OX-LEN-DELTH	Site
REAK	Empirical constant for equation used to calculate reaeration coefficient	/hr	OX-REAPARM	Literature/Site
REAKT	Empirical constant in Tsivoglou's equation for reaeration (escape coefficient)	/ft	OX-TSIVOGLOU	Literature/Site
REAMFG	Indicates method used to calculate reaeration coefficient for free-flowing streams: 1) Tsivoglou; 2) Owens, Churchill, or O'Connor-Dobbins method is used depending on velocity and depth of water; 3) coefficient is calculated as a power function of velocity and/or depth -- user inputs exponents for velocity and depth and an empirical constant (REAK)	N/A	OX-FLAGS	Option/Site
SATDO	Dissolved oxygen saturation concentration	mg/l	OX-INIT	Literature/Calib.
SUPSAT	Allowable dissolved oxygen supersaturation (expressed as a multiple of DO saturation concentration)	N/A	OX-GENPARM	Literature/Site/Calib.
TCBEN	Temperature correction coefficient for benthal oxygen demand	N/A	OX-BENPARM	Literature

RCHRES Parameter List

NAME	DEFINITION	UNITS	TABLE	DATA SOURCE
TCBOD	Temperature correction coefficient for BOD decay	N/A	OX-GENPARM	Literature
TCGINV	Temperature correction coefficient for surface gas invasion	N/A	OX-TSIVOGLOU	Literature
TCGINV	Temperature correction coefficient for surface gas invasion	N/A	OX-REAPARM	Literature
TCGINV	Temperature correction coefficient for surface gas invasion	N/A	OX-TCGINV	Literature
PHCARB				
ALKCON	Number of the conservative constituent which is alkalinity	N/A	PH-PARM1	
BRCO2(1)	Benthal aerobic release of CO_2	mg/m2.hr	PH-PARM2	Literature/Site
BRCO2(2)	Benthal anaerobic release of CO_2	mg/m2.hr	PH-PARM2	Literature/Site
CFCINV	Ratio of carbon dioxide invasion rate to oxygen reaeration rate	N/A	PH-PARM2	Literature/Calib.
CO2	Initial value of CO_2 (as carbon) concentration	mg/l	PH-INIT	Site
PH	Initial value of pH	pH	PH-INIT	Site
PHCNT	Maximum number of iterations to pH solution	N/A	PH-PARM1	Option
TIC	Initial total inorganic carbon	mg/l	PH-INIT	Site
PLANK				
ALDH	High algal unit death rate	/hr	PLNK-PARM3	Literature/Site/Calib.
ALDL	Low algal unit death rate	/hr	PLNK-PARM3	Literature/Site/Calib.
ALNPR	Fraction of nitrogen requirements for phytoplankton growth satisfied by nitrate	N/A	PLNK-PARM1	Literature/Calib.
ALR20	Algal unit respiration rate at 20 degrees C	/hr	PLNK-PARM3	Literature/Site/Calib.
AMRFG	Flag to specify if ammonia retardation of nitrogen limited growth is enabled; 1=yes, 0=no	N/A	PLNK-FLAGS	Option/Site
BALFG	Flag to specify if benthic algae are simulated; 1=yes, 0=no	N/A	PLNK-FLAGS	Option/Site

RCHRES Parameter List

NAME	DEFINITION	UNITS	TABLE	DATA SOURCE
BENAL	Benthic algae, as biomass	mg/m2	PLNK-INIT	Site
CFBALG	Ratio of benthic algal to phytoplankton growth rate	N/A	BENAL-PARM	Literature/Calib.
CFBALR	Ratio of benthic algal to phytoplankton respiration rate	N/A	BENAL-PARM	Literature/Calib.
CFSAEX	Factor used to adjust input solar radiation to make it applicable to the RCHRES; for example, to account for shading of the surface by trees or buildings	N/A	SURF-EXPOSED	Site
CLALDH	Chlorophyll "A" concentration above which high algal death rate occurs	ug/l	PHYTO-PARM	Literature/Calib.
CMMLT	Michaelis-Menten constant for light limited growth	ly/min	PLNK-PARM2	Literature
CMMN	Nitrate Michaelis-Menten constant for nitrogen limited growth	mg/l	PLNK-PARM2	Literature
CMMNP	Nitrate Michaelis-Menten constant for phosphorus limited growth	mg/l	PLNK-PARM2	Literature
CMMP	Phosphate Michaelis-Menten constant for phosphorus limited growth	mg/l	PLNK-PARM2	Literature
DECFG	Flag to specify if linkage between carbon dioxide and phytoplankton growth is decoupled; 1=yes, 0=no	N/A	PLNK-FLAGS	Option/Site
EXTB	Base extinction coefficient for light	/ft	PLNK-PARM1	Literature
LITSED	Multiplication factor to total sediment concentration to determine sediment contribution to light extinction	l/mg.ft	PLNK-PARM1	Literature/Site
MALGR	Maximal unit algal growth rate	/hr	PLNK-PARM1	Literature/Site/Calib.
MBAL	Maximum benthic algae density (as biomass)	mg/m2	BENAL-PARM	Literature/Site/Calib.
MXSTAY	Concentration of plankton not subject to advection at very low flow	mg/l	PHYTO-PARM	Literature/Calib.
MZOEAT	Maximum zooplankton unit ingestion rate	mg/hr	ZOO-PARM1	Literature/Site/Calib.
NALDH	Inorganic nitrogen concentration below which high algal death rate occurs (as nitrogen)	mg/l	PLNK-PARM3	Literature/Site
NONREF	Nonrefractory fraction of algae and zooplankton biomass	N/A	PLNK-PARM1	Literature/Calib.
NSFG	Flag to specify if ammonia is included as part of available nitrogen supply in nitrogen limited growth calculations; 1=yes, 0=no	N/A	PLNK-FLAGS	Option/Site
ORC	Dead refractory organic carbon	mg/l	PLNK-INIT	Site

RCHRES Parameter List

NAME	DEFINITION	UNITS	TABLE	DATA SOURCE
OREF	Outflow at which concentration of plankton not subject to advection is midway between SEED and MXSTAY	ft3/s	PHYTO-PARM	Literature/Site
ORN	Dead refractory organic nitrogen	mg/l	PLNK-INIT	Site
ORP	Dead refractory organic phosphorus	mg/l	PLNK-INIT	Site
OXALD	Increment to phytoplankton unit death rate due to anaerobic conditions	/hr	PLNK-PARM3	Literature
OXZD	Increment to unit zooplankton death rate due to anaerobic conditions	/hr	ZOO-PARM1	Literature
PALDH	Inorganic phosphorus concentration below which high algal death rate occurs (as phosphorus)	mg/l	PLNK-PARM3	Literature/Calib.
PHYFG	Flag to specify if phytoplankton is simulated; 1=yes, 0=no	N/A	PLNK-FLAGS	Option/Site
PHYSET	Rate of phytoplankton settling	ft/hr	PHYTO-PARM	Literature/Site/Calib.
PHYTO	Phytoplankton, as biomass	mg/l	PLNK-INIT	Site
RATCLP	Ratio of chlorophyll "A" content of biomass to phosphorus content	N/A	PLNK-PARM1	Literature/Site
REFSET	Rate of settling for dead refractory organics	ft/hr	PHYTO-PARM	Literature/Site/Calib.
SDLTFG	Flag to specify if influence of sediment washload on light extinction is simulated; 1=yes, 0=no	N/A	PLNK-FLAGS	Option/Site
SEED	Minimum concentration of plankton not subject to advection (i.e. at high flow)	mg/l	PHYTO-PARM	Literature/Site/Calib.
TALGRH	Temperature above which algal growth ceases	degF	PLNK-PARM2	Literature
TALGRL	Temperature below which algal growth ceases	degF	PLNK-PARM2	Literature
TALGRM	Temperature below which algal growth is retarded	degF	PLNK-PARM2	Literature
TCZFIL	Temperature correction coefficient for filtering	N/A	ZOO-PARM2	Literature
TCZRES	Temperature correction coefficient for respiration	N/A	ZOO-PARM2	Literature
ZD	Natural zooplankton unit death rate	/hr	ZOO-PARM1	Literature/Calib.
ZEXDEL	Fraction of nonrefractory zooplankton excretion which is immediately decomposed when ingestion rate > MZOEAT	N/A	ZOO-PARM2	Literature/Site
ZFIL20	Zooplankton filtering rate at 20 degrees C	l/mg.hr	ZOO-PARM1	Literature/Site/Calib.
ZFOOD	The quality of zooplankton food	N/A	PLNK-FLAGS	Literature
ZOMASS	Average weight of a zooplankton organism	mg/org	ZOO-PARM2	Literature/Site

RCHRES Parameter List

NAME	DEFINITION	UNITS	TABLE	DATA SOURCE
ZOO	Zooplankton	org/l	PLNK-INIT	Site
ZOOFG	Flag to specify if zooplankton are simulated; 1=yes, 0=no	N/A	PLNK-FLAGS	Option/Site
ZRES20	Zooplankton unit respiration rate at 20 degrees C	/hr	ZOO-PARM1	Literature/Site/Calib.
RCHRES				
ADFG	Flag to specify if section ADCALC active; 1=yes, 0=no	N/A	ACTIVITY	Option
CONSFG	Flag to specify if section CONS active; 1=yes, 0=no	N/A	ACTIVITY	Option
GQALFG	Flag to specify if section GQUAL active; 1=yes, 0=no	N/A	ACTIVITY	Option
HTFG	Flag to specify if section HTRCH active; 1=yes, 0=no	N/A	ACTIVITY	Option
HYDRFG	Flag to specify if section HYDR active; 1=yes, 0=no	N/A	ACTIVITY	Option
IUNITS	Units in input time series--1=English, 2=Metric	N/A	GEN-INFO	Option
LKFG	Indicates whether the RCHRES is a lake (1) or a stream/river (0)	N/A	GEN-INFO	Option/Site
NEXITS	Number of exits from the RCHRES	N/A	GEN-INFO	Option
NUTFG	Flag to specify if section NUTRX active; 1=yes, 0=no	N/A	ACTIVITY	Option
OUNITS	Units in output time series--1=English, 2=Metric	N/A	GEN-INFO	Option
OXFG	Flag to specify if section OXRX active; 1=yes, 0=no	N/A	ACTIVITY	Option
PFLAG(10)	Printout level	N/A	PRINT-INFO	Option
PHFG	Flag to specify if section PHCARB active; 1=yes, 0=no	N/A	ACTIVITY	Option/Site
PIVL	Number of intervals between level 2 printouts	N/A	PRINT-INFO	Option
PLKFG	Flag to specify if section PLANK active; 1=yes, 0=no	N/A	ACTIVITY	Option
PUNIT(2)	Fortran output unit for English and/or Metric units. 0=none for that system.	N/A	GEN-INFO	Option
PYREND	Calendar month of end of year	N/A	PRINT-INFO	Option
RCHID(5)	Identifier for a RCHRES	N/A	GEN-INFO	Option
SEDFG	Flag to specify if section SEDTRN active; 1=yes, 0=no	N/A	ACTIVITY	Option
UUNITS	Units in UCI--1=English, 2=Metric	N/A	GEN-INFO	Option
RQUAL				
BENRFG	Flag to specify if benthal influences to be considered; 1=yes, 0=no	N/A	BENTH-FLAG	Option/Site
SCRMUL	Multiplier to increase benthal releases during scouring	N/A	SCOUR-PARMS	Literature/Site/Calib.

RCHRES Parameter List

NAME	DEFINITION	UNITS	TABLE	DATA SOURCE
SCRVEL	Velocity above which effects of scouring on benthal release rates is considered	ft/sec	SCOUR-PARMS	Literature/Site/Calib.
SEDTRN				
BEDDEP	Initial total depth (thickness) of the bed	ft	BED-INIT	Literature/Site
BEDWID	Width of cross-section over which HSPF will assume bed sediment is deposited regardless of stage, top-width, etc	ft	SED-GENPARM	Site
BEDWRN	Bed depth which, if exceeded (eg, through deposition) will cause a warning message to be printed	ft	SED-GENPARM	Literature/Site
D	Effective diameter of the transported sand particles (Not used. DB50 is used instead)	in	SAND-PM	Literature/Site
D	Effective diameter of silt or clay particles	in	SILT-CLAY-PM	Literature/Site
DB50	Median diameter of bed sediment (assumed constant throughout the run)	in	SED-HYDPARM	Site
DELTH	Drop in water elevation from upstream to downstream extremities of the RCHRES	ft	SED-HYDPARM	Site
EXPSND	Exponent in sandload power function formula	complex	SAND-PM	Literature/Site/Calib.
Fracclay	Initial fraction (by weight) of clay in the bed material	N/A	BED-INIT	Site
Fracsand	Initial fraction (by weight) of sand in the bed material	N/A	BED-INIT	Site
Fracsilt	Initial fraction (by weight) of silt in the bed material	N/A	BED-INIT	Site
KSAND	Coefficient in sandload power function formula	complex	SAND-PM	Literature/Site/Calib.
LEN	Length of the RCHRES	miles	SED-HYDPARM	Site
M	Erodibility coefficient of the sediment	lb/ft2.d	SILT-CLAY-PM	Literature/Calib.
POR	Porosity of the bed (volume voids/total volume)	N/A	SED-GENPARM	Site
RHO	Density of sand particles	gm/cm3	SAND-PM	Literature/Site
RHO	Density of silt or clay particles	gm/cm3	SILT-CLAY-PM	Literature/Site

HSPF Parameter List for PERLND, IMPLND, & RCHRES MODULES
(Continued)

RCHRES Parameter List

NAME	DEFINITION	UNITS	TABLE	DATA SOURCE
SANDFG	Indicates the method for sandload simulation: 1 = Toffaleti method; 2 = Colby method; 3 = user-specified power function method	N/A	SANDFG	Option
SSED(3)	Initial concentrations in suspension of sand, silt, and clay	mg/l	SSED-INIT	Site
TAUCD	Critical bed shear stress for deposition	lb/ft2	SILT-CLAY-PM	Literature/Calib.
TAUCS	Critical bed shear stress for scour	lb/ft2	SILT-CLAY-PM	Literature/Calib.
W	Fall velocity of transported sand particles in still water	in/sec	SAND-PM	Literature/Site
W	Fall velocity of silt or clay particles in still water	in/sec	SILT-CLAY-PM	Literature/Site

APPENDIX C

ENVIRONMENTAL FLUID DYNAMICS CODE (EFDC) MODEL

C.1   Hydrodynamic Theoretical and Technical Aspects

C.2   EFDC Parameter List

C.3   EFDC Technical Memorandum: Theoretical and Computational Aspects of Sediment Transport in the EFDC Model (Tetra Tech, Inc., 2000)

1

APPENDIX C.1

3
4

THE ENVIRONMENTAL FLUID DYNAMICS CODE (EFDC): HYDRODYNAMIC THEORETICAL AND TECHNICAL ASPECTS

5

TABLE OF CONTENTS

Appendix C.1

Environmental Fluid Dynamics Code (EFDC):
Hydrodynamic Theoretical and Technical Aspects

MODEL DESCRIPTION

Introduction

The environmental fluid dynamics code (EFDC) is a general-purpose modeling package for simulating three-dimensional (3-D) flow, transport, and biogeochemical processes in surface water systems including: rivers, lakes, estuaries, reservoirs, wetlands, and near-shore to shelf-scale coastal regions. The EFDC model was originally developed at the Virginia Institute of Marine Science for estuarine and coastal applications and is considered public domain software. In addition to hydrodynamic and salinity and temperature transport simulation capabilities, EFDC is capable of simulating cohesive and noncohesive sediment transport, near-field and far-field discharge dilution from multiple sources, eutrophication processes, the transport and fate of toxic contaminants in the water and sediment phases, and the transport and fate of various life stages of fish and shellfish. Special enhancements to the hydrodynamic portion of the code, including vegetation resistance, drying and wetting, hydraulic structure representation, wave-current boundary layer interaction, and wave-induced currents, allow refined modeling of wetland and marsh systems, controlled-flow systems, and near-shore wave-induced currents and sediment transport. The EFDC code has been extensively tested and documented and used in more than 20 modeling studies. The code is currently used by university, government, and engineering and environmental consulting organizations. The following sections summarize the major features and capabilities of the EFDC modeling package that will be used in the Housatonic River modeling project.

Hydrodynamics

The physics of the EFDC model and many aspects of the computational scheme are equivalent to the widely used Blumberg-Mellor model (Blumberg and Mellor, 1987) and the U.S. Army Corps of Engineers CH3D or Chesapeake Bay model (Johnson et al., 1993). The EFDC model solves the vertically hydrostatic, free-surface, turbulent-averaged equations of motions for a variable-density fluid. Dynamically coupled transport equations for turbulent kinetic energy, turbulent length scale, salinity, and temperature are also solved. The two turbulence parameter transport equations implement the Mellor-Yamada level 2.5 turbulence closure scheme (Mellor and Yamada, 1982; Galperin et al., 1988). The EFDC model uses a stretched or sigma vertical coordinate and cartesian or curvilinear, orthogonal horizontal coordinates.

The numerical scheme used in EFDC to solve the equations of motion uses second-order accurate spatial finite differencing on a staggered or C grid. The model's time integration uses a second-order accurate three time-level, finite difference scheme with a internal-external mode splitting procedure to separate the internal shear or baroclinic mode from the external free-surface gravity wave or barotropic mode. The external mode solution is semi-implicit, and simultaneously computes the two-dimensional surface elevation field by a preconditioned

1 conjugate gradient procedure. The external solution is completed by the calculation of the depth-
2 averaged barotropic velocities using the new surface elevation field. The model's semi-implicit
3 external solution allows large time steps that are constrained only by the stability criteria of the
4 explicit central difference or high-order upwind advection scheme (Smolarkiewicz and Margolin,
5 1993) used for the nonlinear accelerations. Horizontal boundary conditions for the external
6 mode solution include options for simultaneously specifying the surface elevation only, the
7 characteristic of an incoming wave (Bennett and McIntosh, 1982), free radiation of an outgoing
8 wave (Bennett, 1976; Blumberg and Kantha, 1985), or the normal volumetric flux on arbitrary
9 portions of the boundary. The EFDC model's internal momentum equation solution, at the same
10 time step as the external, is implicit with respect to vertical diffusion. The internal solution of
11 the momentum equations is in terms of the vertical profile of shear stress and velocity shear,
12 which results in the simplest and most accurate form of the baroclinic pressure gradients and
13 eliminates the over-determined character of alternate internal mode formulations. Time splitting
14 inherent in the three time-level scheme is controlled by periodic insertion of a second-order
15 accurate two-time level trapezoidal step. The EFDC model is also readily configured as a
16 two-dimensional model in either the horizontal or vertical planes.

17 The EFDC model implements a second-order accurate in space and time, mass conservation
18 fractional-step solution scheme for the Eulerian transport equations for salinity, temperature,
19 suspended sediment, water quality constituents, and toxic contaminants. The transport equations
20 are temporally integrated at the same time step or twice the time step of the momentum equation
21 solution (Smolarkiewicz and Margolin, 1993). The advective step of the transport solution uses
22 either the central difference scheme used in the Blumberg-Mellor model or a hierarchy of
23 positive definite upwind difference schemes. The highest accuracy upwind scheme, second-
24 order accurate in space and time, is based on a flux-corrected transport version of
25 Smolarkiewicz's multidimensional positive definite advection transport algorithm
26 (Smolarkiewicz and Clark, 1986; Smolarkiewicz and Grabowski, 1990), which is monotonic and
27 minimizes numerical diffusion. The horizontal diffusion step, if required, is explicit in time,
28 while the vertical diffusion step is implicit. Horizontal boundary conditions include time
29 variable material inflow concentrations, upwinded outflow, and a damping relaxation
30 specification of climatological boundary concentration. For the temperature transport equation,
31 the NOAA Geophysical Fluid Dynamics Laboratory's atmospheric heat exchange model (Rosati
32 and Miyakoda, 1988) is implemented.

33 **Sediment Transport**

34 The EFDC code is capable of simulating the transport and fate of multiple size classes of
35 cohesive and noncohesive suspended sediment, including bed deposition and resuspension.
36 Water column transport is based on the same high-order advection-diffusion scheme used for
37 salinity and temperature. A number of options are included for the specification of settling
38 velocities. For the transport of multiple size classes of cohesive sediment, an optional
39 flocculation model (Burban et al., 1989 and 1990) can be activated. Sediment mass conservative
40 deposited bed formulations are included for both cohesive and noncohesive sediment. The
41 deposited bed may be represented by a single layer or multiple layers. The multiple-bed layer
42 option provides a time-since-deposition versus vertical position in the bed relationship to be
43 established. Water column-sediment bed interface elevation changes can be optionally

1 incorporated into the hydrodynamic continuity equation. An optional, one-dimensional in the
2 vertical, bed-consolidation calculation can be performed for cohesive beds.

Toxic Contaminant Transport and Fate

4 The EFDC code includes two internal submodels for simulating the transport and fate of toxic
5 contaminants. A simple, single-contaminant submodel can be activated from the master input
6 file. The simple model accounts for water and suspended sediment phase transport with
7 equilibrium partitioning and a lumped first-order reaction. Contaminant mass per unit area in the
8 sediment bed is also simulated. The second, more complex submodel simulates the transport and
9 fate of an arbitrary number of reacting contaminants in the water and sediment phases of both the
10 water column and sediment bed. In this mode, the contaminant transport and fate simulation is
11 functionally similar to the WASP5 TOXIC model (Ambrose et al., 1993) with the added
12 flexibility of simulating an arbitrary number of contaminants, and the improved accuracy of
13 more complex three-dimensional physical transport fields in a highly accurate numerical-
14 transport scheme. Water-sediment phase interaction may be represented by equilibrium or
15 nonlinear sorption processes. In this mode, the multilayer sediment bed formulation is active,
16 with sediment bed water volume and dissolved contaminant mass balances activated to allow
17 contaminants to reenter the water column by both sediment resuspension, pore water expulsion
18 due to consolidation, and diffusion from the pore water into the water column. The complex
19 contaminant model activates a subroutine describing reaction processes with appropriate reaction
20 parameters provided by a toxic reaction processes input file.

Wetland, Marsh, and Tidal Flat Simulation Extension

22 The EFDC model provides a number of enhancements for the simulation of flow and transport in
23 wetlands, marshes, and tidal flats. The code allows for drying and wetting in shallow areas by a
24 mass-conservative scheme. This capability will be used to simulate periodic overbank flood
25 flow onto the floodplain of the Housatonic River. The drying and wetting formulation is coupled
26 to the mass transport equations in a manner that prevents negative concentrations of dissolved
27 and suspended materials. A number of alternatives are in place in the model to simulate general
28 discharge control structures such as weirs, spillways, culverts, and water surface elevation-
29 activated pumps. The effect of submerged and emergent plants is incorporated into the
30 turbulence-closure model and flow-resistance formulation. Plant density and geometric
31 characteristics of individual and composite plants are required as input for the vegetation-
32 resistance formulation. A simple soil moisture model, allowing rainfall infiltration and soil
33 water loss due to evapotranspiration under dry conditions, is implemented.

34 To represent narrow channels and canals in wetland, marsh, and tidal flat systems, a subgrid
35 scale channel model is implemented. The subgrid channel model allows a network of
36 one-dimensional (1-D) in the horizontal channels to be dynamically coupled to the
37 two-dimensional (2-D) in the horizontal grid representing the wetland, marsh, or tidal flat
38 system. Volume and mass exchanges between 2-D wetland cells and the 1-D channels are
39 accounted for. The channels may continue to flow when the 2-D wetland cells become dry.
40 Although not explicitly designed for application to riverine floodplains, the subgrid scale channel
41 capability of EFDC will be tested as a feasible strategy to couple coarse cartesian floodplain grid
42 cells with the narrow Housatonic River channel.

1 **Near-shore Wave-Induced Currents and Sediment Transport Extensions**

2 The EFDC code includes a number of extensions for simulation of near-shore wave-induced
3 current and noncohesive sediment transport. The extensions include a wave-current boundary
4 layer formulation similar to that of Grant and Madsen (1986); modifications of the
5 hydrodynamic model's momentum equations to represent wave period-averaged Eulerian mean
6 quantities; the inclusion of 3-D wave-induced radiation or Reynold's stresses in the momentum
7 equations; and modifications of the velocity fields in the transport equations to include advective
8 transport by the wave-induced Stoke's drift. High-frequency surface wave fields are provided by
9 an external wave refraction-diffraction model or by an internal mild slope equation submodel
10 similar to that of Madsen and Larsen (1987). The internal refraction-diffraction computation is
11 executed on a refined horizontal grid coincident with the main model's horizontal grid.

12 **User Interface**

13 The EFDC modeling package's user interface is based on text input file templates. This choice
14 was selected in the interest of maintaining model portability across a range of computing
15 platforms and readily allows the model user to modify input files using most text-editing
16 software. The text interface also allows modification of model files on remote computing
17 systems and in heterogeneous network environments. All input files have standard templates
18 available with the EFDC code and in the digital version of the user's manual. The file templates
19 include extensive built-in documentation and explanation of numerical input data quantities.
20 Actual numerical input data are inserted into the text template in a flexible free format as
21 internally specified in the file templates. Extensive checking of input files is implemented in the
22 code and diagnostic on-screen messages indicate the location and nature of input file errors. All
23 input files involving dimensional data have unit conversion specifications for the MKS unit
24 system used internally in the model.

25 **Preprocessing Software**

26 The EFDC modeling package includes a grid-generating preprocessor code, GEFDC, which is
27 used to construct the horizontal model grid, interpolate bathymetry, and initial fields such as
28 water surface elevation and salinity, to the grids. EFDC input files specifying the grid geometry
29 and initial fields are generated by the preprocessor. The preprocessor is capable of generating
30 Cartesian and curvilinear-orthogonal grids using a number of grid-generation schemes (Mobley
31 and Stewart, 1980; Ryskin and Leal, 1983; Kang and Leal, 1992).

32 **Model Configuration**

33 The EFDC code exists in only one generic version. A model application is specified entirely by
34 information in the input files. To minimize memory requirements for specific applications, an
35 executable file for the application is created by setting appropriate model variable array sizes in
36 the model's parameter file and compiling the source code. The EFDC model may be configured
37 to execute all or a portion of a model application in reduced-spatial-dimension mode, including
38 2-D depth or width-averaged and 1-D cross section averaged. The number of layers used in the
39 3-D mode or 2-D width-averaged mode is readily changed by one line of model input. Model
40 grid sections specified as 2-D width averaged are allowed to have depth-varying widths to

provide representations equivalent to those of 2-D width-averaged estuarine and reservoir models such as CE- QUAL-W2 (Cole and Buchak, 1994).

Run Time Diagnostics

The EFDC modeling package includes extensive built-in run time diagnostics that may be activated in the master input file by the model user. Representative diagnostics include records of maximum CFL numbers, times and locations of negative depths, a variety of volume and mass balance checks, and global mass and energy balances. An on-screen print of model variables in a specified cell can be activated during modeling execution. A number of log files are generated during model execution that allow additional diagnostics of run time problems encountered in setting up a new application.

Model Output Options

A wide variety of model output options are available. These options include specification of output files for horizontal plane and vertical plane transect plotting of vector and scalar field at specified time; the generation of time series of model variables at selected locations and time intervals; grab sample simulation at specified times and locations; and the specification of least-squares analysis of selected model variables at a defined location over a specified interval. A general 3-D output option allows output of all major model variables in a compressed form at specified times. A restart file is generated at user-specified intervals during model execution.

Postprocessing, Graphics, and Visualization

The generic model output files may be readily processed by a number of third-party graphics and visualization software packages, often without need for intermediate processing (Rennie and Hamrick, 1992). The availability of the source code to the user allows the code to be modified for specific output options. Graphics and visualization software successfully used with EFDC output include APE, AVS, IDL, Mathematica, MatLab, NCAR Graphics, PV-Wave, Techplot, SiteView, Spyglass Transform and Slicer, and Voxelview. The model developer currently uses Spyglass and Voxelview and a number of special image enhancement postprocessor applications are available for these products.

Documentation

Extensive documentation of the EFDC model is available. Theoretical and computational aspects of the model are described for hydrodynamics (Hamrick, 1992a), sediment transport (Tetra Tech, 2000), and toxic contaminants (Tetra Tech, 1999). The model user's manual (Hamrick, 1996) provides details on use of the GEFDC preprocessor and setup of the EFDC input files. Input file templates are also included. A number of papers (Hamrick, 1992b; Hamrick, 1994; Moustafa and Hamrick, 1994; Hamrick and Wu, 1997; and Wu et al., 1997) describe model applications and capabilities.

Computer Requirements

The EFDC modeling system is written in FORTRAN 77. The few nonstandard VAX FORTRAN language extensions in the code are supported by a wide variety of ANSI standard

FORTRAN 77 compilers. The generic or universal source code has been compiled and executed on most UNIX workstations (DEC Alpha, Hewlett-Packard, IBM RISC6000, Silicon Graphics, Sun and Sparc compatibles), Cray and Convex supercomputers, and PC compatibles and Macintosh personal computers. Absoft, Lahey, and Microsoft compilers are supported on PC compatibles, while Absoft, Language Systems, and Motorola compilers are supported on Macintosh and compatible systems.

Availability

The EFDC source code, file templates, preprocessing and postprocessing software, and user's manual are available from the code's principal developer, John M. Hamrick (email: ham@visi.net). An earlier version of the code is available from the Virginia Institute of Marine Science in the HEM3D (Hydrodynamic-Eutrophication Model: 3D) modeling package.

References

Ambrose, R.B., T.A. Wool, and J.L. Martin, 1993: The water quality analysis and simulation program, WASP5: Part A, model documentation version 5.1. U.S. EPA, Athens Environmental Research Laboratory, 210 pp.

Bennett, A. F., 1976: Open boundary conditions for dispersive waves. *J. Atmos. Sci.,* 32, 176-182.

Bennett, A.F., and P.C. McIntosh, 1982: Open ocean modeling as an inverse problem: tidal theory. *J. Phys. Ocean.,* 12, 1004-1018.

Blumberg, A.F., and L.H. Kantha, 1985: Open boundary condition for circulation models. *J. Hydr. Engr.,* 111, 237-255.

Blumberg, A.F., and G.L. Mellor, 1987: A description of a three-dimensional coastal ocean circulation model. In: Three-Dimensional Coastal Ocean Models, Coastal and Estuarine Science, Vol. 4. (Heaps, N. S., ed.) American Geophysical Union, pp. 1-19.

Burban, P.Y., W. Lick, and J. Lick, 1989: The flocculation of fine-grained sediments in estuarine waters. *J. Geophys.* Res., 94, 8323-8330.

Burban, P.Y., Y. J. Xu, J. McNeil, and W. Lick, 1990: Settling speeds of flocs in fresh and seawater. *J. Geophys. Res.,* 95, 18,213-18,220.

Cole, T.M., and E.M. Buchak, 1994: CE-QUAL-W2: A two-dimensional laterally averaged, hydrodynamic and water quality model, Version 2.0. U. S. Army Corps of Engineers, Waterway Experiment Station, Vicksburg, MS, Report ITL-93-7.

Galperin, B., L.H. Kantha, S. Hassid, and A. Rosati, 1988: A quasi-equilibrium turbulent energy model for geophysical flows. *J. Atmos. Sci.,* 45, 55-62.

Grant, W.D., and O.S. Madsen, 1986: The continental-shelf bottom boundary layer. In: Annual Review of Fluid Mechanics, (Van Dyke, M. et al., eds.) Annual Review, Inc., pp. 365-306.

1   Hamrick, J.M., 1992a: A Three-Dimensional Environmental Fluid Dynamics Computer Code:
2   Theoretical and Computational Aspects. The College of William and Mary, Virginia Institute
3   of Marine Science. Special Report 317, 63 pp.

4   Hamrick, J.M., 1992b: Estuarine environmental impact assessment using a three-dimensional
5   circulation and transport model. Estuarine and Coastal Modeling, Proceedings of the 2nd
6   International Conference, M. L. Spaulding et al., Eds., American Society of Civil Engineers,
7   New York, 292-303.

8   Hamrick, J.M., 1994: Linking hydrodynamic and biogeochemical transport models for estuarine
9   and coastal waters. Estuarine and Coastal Modeling, Proceedings of the 3nd International
10   Conference, M. L. Spaulding et al., Eds., American Society of Civil Engineers, New York,
11   591-608.

12   Hamrick, J.M., 1996: A User's Manual for the Environmental Fluid Dynamics Computer Code
13   (EFDC). The College of William and Mary, Virginia Institute of Marine Science, Special
14   Report 331, 234 pp.

15   Hamrick, J.M., and T.S. Wu, 1997: Computational design and optimization of the
16   EFDC/HEM3D surface water hydrodynamic and eutrophication models. Chapter 16 In: Next
17   Generation Environmental Models and Computational Methods, G. Delic and M.F. Wheeler,
18   Eds., Society of Industrial and Applied Mathematics, Philadelphia.

19   Johnson, B.H., K.W. Kim, R.E. Heath, B.B. Hsieh, and H.L. Butler, 1993: Validation of
20   three-dimensional hydrodynamic model of Chesapeake Bay. *J. Hyd. Engrg.,* 119, 2-20.

21   Kang, I.S., and L.G. Leal, 1992: Orthogonal grid generation in a 2D domain via the boundary
22   integral technique. *J. Comp. Phys.,* 102, 78-87.

23   Madsen, P.A., and J. Larsen, 1987: An efficient finite-difference approach to the mild-slope
24   equation. Coastal Engr., 11, 329-351.

25   Mellor, G.L., and T. Yamada, 1982: Development of a turbulence closure model for geophysical
26   fluid problems. Rev. Geophys. Space Phys., 20, 851-875.

27   Mobley, C.D., and R.J. Stewart, 1980: On the numerical generation of boundary-fitted
28   orthogonal Curvilinear coordinate systems. *J. Comp. Phys.,* 34, 124-135.

29   Moustafa, M.Z., and J.M. Hamrick, 1994: Modeling circulation and salinity transport in the
30   Indian River Lagoon. Estuarine and Coastal Modeling, Proceedings of the 3nd International
31   Conference, M. L. Spaulding et al., Eds., American Society of Civil Engineers, New York,
32   381-395.

33   Rennie, S., and J.M. Hamrick, 1992: Techniques for visualization of estuarine and coastal flow
34   fields. Estuarine and Coastal Modeling, Proceedings of the 2nd International Conference, M.
35   L. Spaulding et al., Eds., American Society of Civil Engineers, New York, 48-55.

1   Rosati, A.K., and K. Miyakoda, 1988: A general circulation model for upper ocean simulation.
2   *J. Phys. Ocean.,* 18, 1601-1626.

3   Ryskin, G. and L.G. Leal, 1983: Orthogonal mapping. *J. Comp. Phys.,* 50, 71-100.

4   Smolarkiewicz, P.K., and T.L. Clark, 1986: The multidimensional positive definite advection
5   transport algorithm: further development and applications. *J. Comp. Phys.,* 67, 396-438.

6   Smolarkiewicz, P.K., and W.W. Grabowski, 1990: The multidimensional positive definite
7   advection transport algorithm: nonoscillatory option. *J. Comp. Phys.,* 86, 355-375.

8   Smolarkiewicz, P.K., and L.G. Margolin, 1993: On forward-in-time differencing for fluids:
9   extension to a curvilinear framework. Mon. Weather Rev., 121, 1847-1859.

10   Tetra Tech, Inc., 2000: A theoretical description of sediment transport formulations used in the
11   EFDC model. Tech. Memo TT-EFDC-00-1, Tetra Tech, Inc., Fairfax, VA.

12   Tetra Tech, Inc., 1999: A theoretical description of toxic contaminant transport formulations
13   used in the EFDC model. Tech. Memo TT-EFDC-99-2, Tetra Tech, Inc., Fairfax, VA.

14   Wu, T.S., J.M. Hamrick, S.C. McCutcheon, and R.B. Ambrose, 1997. Benchmarking the
15   EFDC/HEM3D surface water hydrodynamic and eutrophication models. Next Generation
16   Environmental Models and Computational Methods, G. Delic and M.F. Wheeler, Eds.,
17   Society of Industrial and Applied Mathematics, Philadelphia.

1 # APPENDIX C.2

2

3 # EFDC PARAMETER LIST

4

Housatonic River EFDC Model Parameters

	Definition/Description	Units	Data Source
Volumetric Source/Sinks			
Upstream Boundary Conditions			
QSER	Volumetric inflow time series for East and West Branches of the Housatonic River	(m^3/s)	HSPF
CSER(,,1)	Salinity Time Series (not used)	(ppt)	NA
CSER(,,2)	Temperature Time Series	(°C)	HSPF
Cohesive Seds (CSER)	Cohesive Time Series (One for each class)	(g/m^3)	HSPF
NonCohesive Seds (CSER)	NonCohesive Series	(g/m^3)	HSPF
Toxics (CSER)	Toxic Time Series	(g/m^3)	Derived
Point Source Tributary			
QSER	Volumetric inflow time series for each tributary	(m^3/s)	HSPF
CSER(,,1)	Salinity Time Series (not used)	(ppt)	NA
CSER(,,2)	Temperature Time Series	(°C)	HSPF
Cohesive Seds (CSER)	Cohesive Time Series (One for each class)	(g/m^3)	HSPF
NonCohesive Seds (CSER)	NonCohesive Series	(g/m^3)	HSPF
Toxics (CSER)	Toxic Time Series	(g/m^3)	HSPF
External Point Source Loadings			
QSER	Volumetric inflow time series for each tributary	(m^3/s)	Site
CSER(,,1)	Salinity Time Series (not used)	(ppt)	NA
CSER(,,2)	Temperature Time Series	(°C)	Site
Cohesive Seds (CSER)	Cohesive Time Series (One for each class)	(g/m^3)	Site
NonCohesive Seds (CSER)	NonCohesive Series	(g/m^3)	Site
Toxics (CSER)	Toxic Time Series	(g/m^3)	Site
Non-Point Source (Distributed)			
QSER	Volumetric inflow time series for each tributary	(m^3/s)	HSPF
CSER(,,1)	Salinity Time Series (not used)	(ppt)	NA
CSER(,,2)	Temperature Time Series	(°C)	HSPF
Cohesive Seds (CSER)	Cohesive Time Series (One for each class)	(g/m^3)	HSPF
NonCohesive Seds (CSER)	NonCohesive Series	(g/m^3)	HSPF
Toxics (CSER)	Toxic Time Series	(g/m^3)	HSPF
Constant Source/Sinks	(Not used for the Housatonic)		
Flow/Temp/Toxic/Seds	A contant value for each parameter for the entire simulation		NA
Setup/Settings/Assumptions			
NTOX	# of toxic contaminants		Lit/Site
NSED	# of cohesive sediment size classes		Lit/Site
NSND	# of non-cohesive sediment size classes		Lit/Site
Cohesive Settings	Needed nsed times		
SDEN	Sediment specific volume	(m^3/g)	Site
SSG	Sediment specific gravity		Lit/Site
WSEDO	Constant or reference sediment settling velocity	(m/s)	Lit/Site
SEDSN	Normalizing sediment concentration	(g/m^3)	Lit/Site
TAUD	Boundary stress below which deposition takes place	(m^2/s^2)	Lit/Site
IWRSP	0 - Use specified resuspension rate and critical stresses		Lit/Site
	>1 - Use bed properties dependent (computed) resuspension rate and critical stresses		
WRSPO	Reference surface erosion rate	$(g/m^2\text{-}s)$	Lit/Site
TAUR	Boundary stress above which surface erosion occurs	(m^2/s^2)	Lit/Site
TAUN	Normalizing stress	(m^2/s^2)	Lit/Site
TEXP	Exponent for surface erosion		Lit/Site
NonCohesive Settings	Needed nsnd times		
SDEN	Sediment spec volume (ie 1/2.65e6 m**3/gm)	(m^3/g)	Lit/Site
SSG	Sediment specific gravity		Lit/Site
SNDDIA	Representative diameter of sediment class	(m)	Lit/Site
WSNDO	Constant or reference sediment settling velocity	(m/s)	Lit/Site
SNDN	Maximum mass/Total volume in bed	(g/m^3)	3
TAUD	Dune break point stress	(m^2/s^2)	Lit/Site
ISNDEQ:	>1 Calculate above bed reference nonchohesive sediment equilibrium concentration		Lit/Site
	1 - Garcia and Parker, 2 - Smith and McLean, 3 - van Rijn		
TAUR	Critical Shields stress (water density normalized)	(m^2/s^2)	Lit/Site
TAUN	Normalizing stress	(m^2/s^2)	Lit/Site
TEXP	Critical Shields parameter		Lit/Site

	Definition/Description	Units	Data Source
Volumetric Source/Sinks			
Toxic Settings	Needed for each nsed and nsnd		
NTOXC	Toxic contaminant number ID.		
ITXPARW	Flag to enable solids dependent partitioning in the water column		Lit/Site
TOXPARW	Water column partitioning coefficient between each toxic and sediment class	(l/mg)	Lit/Site
CONPARW	Exponent in Water column solids dependent partitioning		Lit/Site
ITXPARB	Flag to enable solids dependent partitioning in the bed		Lit/Site
TOXPARB	Sediment bed partitioning coefficient between each toxic and sediment class	(l/mg)	Lit/Site
CONPARB	Exponent in sediment solids dependent partitioning		Lit/Site
RKTOXW	First order water column decay rate for toxic variable	(s^{-1})	Lit/Site
TKTOXW	Reference temperature for 1st order water column toxic decay	(°C)	Lit/Site
RKTOXB	First order sediment bed decay rate for toxic variable	(s^{-1})	Lit/Site
TKTOXB	Reference temperature for 1st order sediment bed toxic decay	(°C)	Lit/Site
VOLTOX	Water surface volitilization rate multiplier		Lit/Site
RMOLTX	Molecular weight for determining volatilization rate		Lit/Site
RKTOXP	Reference photolysis decay rate	(s^{-1})	Lit/Site
SKTOXP	Reference solar radiation for photolysis	$(watts/m^2)$	Lit/Site
DIFTOX	Diffusion coefficient for toxicant in sediment bed pore water	(m^2/s)	Lit/Site
NonCohesive/Cohesive Sediment Options			
ISEDINT	0 - Constant initial conditions for Water and Bed		Lit/Site
	1 - Spatially variable Water column initial conditions		
	2 - Spatially variable Bed initial conditions		
	3 - Spatially variable Water column and Bed initial conditions		
ISEDBINT	0 - Spatially varying bed initial conditions in mass/area		Lit/Site
	1 - Spatially varying bed initial conditions in mass fraction of total sediment mass.		
ISEDWC	0 - Cohesive sed wc/bed exchange based on bottom layer conditions		Lit/Site
	1 - Cohesive sed wc/bed exchange based on wave/current/sediment boundary layers embedded in bottom layer		
ISMUD	1 - Include cohesive fluid mud viscous effects		Lit/Site
ISNDWC	0 - Noncohesive sediment wc/bed exchange based on bottom layer conditions		Lit/Site
	1 - Noncohesive sediment wc/bed exchange based on wave/current/sediment boundary layers embedded in bottom layer.		
ISEDVW	0 - Constant or simple concentration dependent cohesive sediment settling velocity		Lit/Site
	>0 Computed: 1 - Huang and Metha, 2 - Shresta and Orlob, 3 - Ziegler and Nesbit		
ISNDVW	0 - Use constant specified nonchoesive sed settling velocities or calculate for class diameter if specified value is negative.		Lit/Site
	>1 - Follow Option 0 procedure but apply hindered settling correction.		
KB	Maximum number of bed layers (excluding active layer)		Lit/Site/Calib
ISEDAL	1 - Activate stationary cohesive mud active layer		Lit/Site
ISNDAL	1 - Activate non-cohesive armoring layer active layer		Lit/Site
Bed Mechanics			
IBMECH	0 - Time invariant constant bed mechanical properites		Lit/Site
	1 - Simple consolidation calculation with constant coefficients		
	2 - Simple consolidation with variable coefficients internally computed		
	3 - Complex consolidation with variable coefficients internally computed		
IMORPH	0 - Constant bed morphology		Lit/Site
	1 - Active bed morphology: no water entrain/expulsion effects		
	2 - Active bed morphology: with water entrain/expulsion effects		
HBEDMAX	Top bed layer thickness at which new layer is added or if kbt(i,j) = kb, new layer added and lowest two layers combined	(m)	Lit/Site
BEDPORC	Constant bed porosity for IBMECH=0 or NSED=0		Lit/Site
SEDMDMX	Maximum fluid mud cohesive sediment concentration	(mg/l)	Lit/Site
SEDMDMN	Minimum fluid mud cohesive sediment concentration	(mg/l)	Lit/Site
SEDVDRD	Void ratio of depositing cohesive sediment		Lit/Site
SEDVDRM	Minimum cohesive sediment bed void ratio (IBMECH > 0)		Lit/Site
SEDVDRT	Bed consolodation rate constant (IBMECH = 1,2)	(s^{-1})	Lit/Site
Initial Conditions			
Bed Conditions			
SNDBO	Constant initial nonchoesive sediment in bed per unit area (nsnd times)	(g/m^2)	Site
SEDBO	Constant initial cohesive sediment in bed per unit area (nsed times)	(g/m^2)	Site
BEDLINIT	Bed layer thickness	(m)	Site
BEDBINIT	Bed layer bulk density	(g/m^3)	Site
BEDDINIT	Bed layer dry density, porosity or void ratio		Site
ITXINT	Toxic flag for spatially constant/variable water col and bed initial cond		Lit/Site
ITXBDUT	Flag for constant initial bed toxic total or sorbed mass toxic/mass sediment		Site
TOXINTB	Initial bed sediment toxic concentration	(mg/kg)	Site

	Housatonic River EFDC Model Parameters		
	Definition/Description	**Units**	**Data Source**
Volumetric Source/Sinks			
Water Column			
TEMINIT	Temperature	(°C)	Site
SNDO	Constant initial noncohesive sediment conc in water column (nsnd times)	(g/m^3)	Site
SEDO	Constant initial cohesive sediment conc in water column (nsed times)	(g/m^3)	Site
TOXINTW	Initial water column total concentration for nth toxic	ug/l	Site
Physical Domain/Grid	These parameters dictated by scale and channel/floodplain geometry		
CORIOLIS	Constant coriolis parameter in 1/sec		Lit
KC	Number of vertical layers		Site & Calib
IC	Number of cells in i direction		Site & Calib
JC	Number of cells in j direction		Site & Calib
LC	Number of active cells in horizontal + 2		Site & Calib
LVC	Number of variable size horizontal cells		Site & Calib
NDM	Number of domains for horizontal domain decomposition		Site & Calib
LDW	Number of water cells per domain		Site & Calib
XX	Dimesionless layer thicknesss		Site & Calib
DX	Cartesian cell length in x or i direction	(m)	Site & Calib
DY	Cartesion cell length in y or j direction	(m)	Site & Calib
CDLONx	Longitudinal coordinates for cartesian grids		Site
CDLATx	Latitude coordinates for cartesian grids		Site
HDRY	Depth at which cell or flow face becomes dry	(m)	Lit & Site
HWET	Depth at which cell or flow face becomes wet	(m)	Lit & Site
ZBRADJ	Log boundary layer constant or variable roughness height adjustment	(m)	Lit & Site
ZBRCVRT	Log boundary layer variable roughness height conversion		Lit & Site
HMIN	Minimum depth of inputs depths	(m)	Lit & Site
DZC(KC)	Layer thickness ratio		Site & Calib
SubGrid/Channel Modifier			
ISCHAN	1 - Activate subgrid channel model		
IS1DCHAN	1 - Activate 1D channel geometry/grid		
Hydrodyamic Options			
AHO	Horizontal momentum and mass diffusivity	(m^2/s)	Lit/Site
AHD	Dimesionless horizontal momentum diffusivity		Lit/Site
AVO	Molecular kinematic viscosity	(m^2/s)	Lit
ABO	Molecular diffusivity	(m^2/s)	Lit
AVMN	Minimum kinematic eddy viscosity	(m^2/s)	Lit
ABMN	Minimum eddy diffusivity	(m^2/s)	Lit
VKC	Von Karman's Constant		Lit
CTURB1	Turbulence closure constant A1		Lit
CTURB2	Turbulence closure constant B1		Lit
CTE1	Turbulent constant E1		Lit
CTE2	Turbulent constant E2		Lit
CTE3	Turbulent constant E3		Lit
QQMIN	Minimum turbulent intensity squared	(q^2)	Lit
QQLMIN	Minimum turbulent intensity squared time length-scale (l^2)	(M^2)	Lit
DMLMIN	Dimensionless length -scale		Lit
ZBRADJ	Const or variable roughness height adjustment in meters	(m)	Site/Calib
	Vegitative resistance function		Site/Calib
Atmospheric Forcing Functions			
WINDS	Wind Speed	(m/s)	Site
WINDD	Wind Direction (blowing toward)	(degrees)	Site
TDRY	Temperature (Dry Bulb)	(°C)	Site
TWET	Temperature (Wet Bulb)	(°C)	Site
RAIN	Rainfall	(m/s)	Site
EVAP	Evaporation	(m/s)	Site
SOLSWR	Solar Radiation	(J/s/m^2)	Site

1 **APPENDIX C.3**
2
3 **EFDC TECHNICAL MEMORANDUM: THEORETICAL AND**
4 **COMPUTATIONAL ASPECTS OF SEDIMENT TRANSPORT IN THE**
5 **EFDC MODEL**

6

2nd DRAFT

EFDC Technical Memorandum

Theoretical and Computational Aspects of Sediment Transport in the EFDC Model

Prepared for:

US Environmental Protection Agency, Office of Science and Technology
401 M Street SW
Washington, DC 20460

Prepared by:

Tetra Tech, Inc.
10306 Eaton Place
Suite 340
Fairfax, Virginia 22030

August 2000

Table of Contents

1.   Introduction

This report summarizes theoretical and computational aspects of the sediment transport formulations used in the EFDC model. Theoretical and computational aspects for the basic EFDC hydrodynamic and generic transport model components are presented in Hamrick (1992). Theoretical and computational aspects of the EFDC water quality-eutrophication model component are presented in Park et al. (1995). The paper by Hamrick and Wu (1997) also summarized computational aspects of the hydrodynamic, generic transport and water quality-eutrophication components of the EFDC model. This report is organized as follows. Chapter 2 summarizes the hydrodynamic and generic transport formulations used in EFDC. Chapter 3 summarizes the solution of the transport equation for suspended cohesive and noncohesive sediment. A discussion of near bed turbulence closure approximations relevant to sediment transport processes is presented in Chapter 4. Chapters 5 and 6 summarize noncohesive and cohesive sediment settling, deposition and resuspension process representations used the sediment transport model component.   The representation of the sediment bed and it geomechanical properties are presented in Chapter 7. This report will be subsequently revised to incorporate documentation of the EFDC model's sorptive contaminant transport and fate formulations as well as additional enhancements to the sediment transport formulations which are currently being tested.

2.   Summary of Hydrodynamic and Generic Transport Formulations

The EFDC model's hydrodynamic component is based on the three-dimensional hydrostatic equations formulated in curvilinear-orthogonal horizontal coordinates and a sigma or stretched vertical coordinate. The momentum equations are:

$$\partial_t\left(m_x m_y Hu\right) + \partial_x\left(m_y Huu\right) + \partial_y\left(m_x Hvu\right) + \partial_z\left(m_x m_y wu\right) - f_e m_x m_y Hv$$

$$= -m_y H\partial_x\left(p + p_{atm} + \phi\right) + m_y\left(\partial_x z_b^* + z\partial_x H\right)\partial_z p + \partial_z\left(m_x m_y \frac{A_v}{H}\partial_z u\right)$$

$$+ \partial_x\left(\frac{m_y}{m_x} HA_H\partial_x u\right) + \partial_y\left(\frac{m_x}{m_y} HA_H\partial_y u\right) - m_x m_y c_p D_p\left(u^2 + v^2\right)^{1/2} u \tag{2.1}$$

$$\partial_t\left(m_x m_y H v\right) + \partial_x\left(m_y H u v\right) + \partial_y\left(m_x H v v\right) + \partial_z\left(m_x m_y w v\right) + f_e m_x m_y H u$$

$$= -m_x H \partial_y\left(p + p_{atm} + \phi\right) + m_x\left(\partial_y z_b^* + z\partial_y H\right)\partial_z p + \partial_z\left(m_x m_y \frac{A_v}{H}\partial_z v\right) \qquad (2.2)$$

$$+ \partial_x\left(\frac{m_y}{m_x} H A_H \partial_x v\right) + \partial_y\left(\frac{m_x}{m_y} H A_H \partial_y v\right) - m_x m_y c_p D_p\left(u^2 + v^2\right)^{1/2} v$$

$$m_x m_y f_e = m_x m_y f - u\partial_y m_x + v\partial_x m_y \qquad (2.3)$$

$$\left(\tau_{xz}, \tau_{yz}\right) = A_v H^{-1}\partial_z(u, v) \qquad (2.4)$$

where u and u are the horizontal velocity components in the dimensionless curvilinear-orthogonal horizontal coordinates x and y, respectively. The scale factors of the horizontal coordinates are m_x and m_y. The vertical velocity in the stretched vertical coordinate z is w. The physical vertical coordinates of the free surface and bottom bed are z_s* and z_b* respectively. The total water column depth is H, and ϕ is the free surface potential which is equal to gz_s*. The effective Coriolis acceleration f_e incorporates the curvature acceleration terms, with the Coriolis parameter, f, according to (2.3). The Q terms in (2.1) and (2.2) represent optional horizontal momentum diffusion terms. The vertical turbulent viscosity A_v relates the shear stresses to the vertical shear of the horizontal velocity components by (4.4). The kinematic atmospheric pressure, referenced to water density, is p_{atm}, while the excess hydrostatic pressure in the water column is given by:

$$\partial_z p = -gHb = -gH(\rho - \rho_o)\rho_o^{-1} \qquad (2.5)$$

where ρ and ρ_o are the actual and reference water densities and b is the buoyancy. The horizontal turbulent stress on the last lines of (2.1) and (2.2), with A_H being the horizontal turbulent viscosity, are typically retained when the advective acceleration are represented by central differences. The last terms in (2.1) and (2.2) represent vegetation resistance where c_p is a resistance coefficient and D_p is the dimensionless projected vegetation area normal to the flow per unit horizontal area.

The three-dimensional continuity equation in the stretched vertical and curvilinear-orthogonal horizontal coordinate system is:

$$\partial_t\left(m_x m_y H\right) + \partial_x\left(m_y H u\right) + \partial_y\left(m_x H v\right) + \partial_z\left(m_x m_y w\right) = Q_H \qquad (2.6)$$

with Q_H representing volume sources and sinks including rainfall, evaporation, infiltration and lateral inflows and outflows having negligible momentum fluxes. When the sediment transport

model component operates in a geomorphologic mode, Q_H also includes the volume flux of sediment and water between the sediment bed and the water column. Integration of (2.6) over the water column gives

$$\partial_t\left(m_x m_y H\right) + \partial_x\left(m_y H\bar{u}\right) + \partial_y\left(m_x H\bar{v}\right) = \bar{Q}_H \qquad (2.7)$$

the barotropic or external mode continuity equation where the over bars indicate depth averaged quantities. Subtracting (2.7) form (2.6) gives

$$\partial_x\left(m_y H(u-\bar{u})\right) + \partial_y\left(m_x H(v-\bar{v})\right) + \partial_z\left(m_x m_y w\right) = Q_H - \bar{Q}_H \qquad (2.8)$$

the internal mode continuity equation.

The generic transport equation for a dissolved or suspended material having a mass per unit volume concentration C, is

$$\partial_t\left(m_x m_y HC\right) + \partial_x\left(m_y HuC\right) + \partial_y\left(m_x HvC\right) + \partial_z\left(m_x m_y wC\right) - \partial_z\left(m_x m_y w_{sc}C\right)$$
$$= \partial_x\left(\frac{m_y}{m_x} HK_H\partial_x C\right) + \partial_y\left(\frac{m_x}{m_y} HK_H\partial_y v\right) + \partial_z\left(m_x m_y \frac{K_v}{H}\partial_z C\right) + Q_c \qquad (2.9)$$

where K_v and K_H are the vertical and horizontal turbulent diffusion coefficients, respectively, w_{sc} is a positive settling velocity went C represents a suspended material, and Q_c represents external sources and sinks and reactive internal sources and sinks.

The solution of the momentum equations, (2.1) and (2.2) and the transport equation (2.9), requires the specification of the vertical turbulent viscosity, A_v, and diffusivity, K_v. To provide the vertical turbulent viscosity and diffusivity, the second moment turbulence closure model developed by Mellor and Yamada (1982) and modified by Galperin *et al* (1988) and Blumberg *et al* (1988) is used. The MY model relates the vertical turbulent viscosity and diffusivity to the turbulent intensity, q, a turbulent length scale, l, and a turbulent intensity and length scaled based Richardson number, R_q, by:

$$A_v = f_A \, ql$$

$$f_A = \frac{A_o\left(1 + R_1^{-1} R_q\right)}{\left(1 + R_2^{-1} R_q\right)\left(1 + R_3^{-1} R_q\right)}$$

$$A_o = A_1\left(1 - 3C_1 - \frac{6A_1}{B_1}\right) = \frac{1}{B_1^{1/3}}$$

$$R_1^{-1} = 3A_2 \, \frac{\left(B_2 - 3A_2\right)\left(1 - \dfrac{6A_1}{B_1}\right) - 3C_1\left(B_2 + 6A_1\right)}{\left(1 - 3C_1 - \dfrac{6A_1}{B_1}\right)}$$

$$R_2^{-1} = 9A_1 A_2 \tag{2.10}$$

$$R_3^{-1} = 3A_2\left(6A_1 + B_2\right)$$

$$K_v = f_K \, ql$$

$$f_K = \frac{K_o}{\left(1 + R_3^{-1} R_q\right)}$$

$$K_o = A_2\left(1 - \frac{6A_1}{B_1}\right) \tag{2.11}$$

$$R_q = -\frac{gH \partial_z b}{q^2} \frac{l^2}{H^2} \tag{2.12}$$

where the so-called stability functions, f_A and f_K, account for reduced and enhanced vertical mixing or transport in stable and unstable vertically density stratified environments, respectively. Mellor and Yamada (1982) specify the constants A_1, B_1, C_1, A_2, and B_2 as 0.92, 16.6, 0.08, 0.74, and 10.1, respectively.

The turbulent intensity and the turbulent length scale are determined by a pair of transport equations:

$$\partial_t\left(m_x m_y H q^2\right) + \partial_x\left(m_y H u q^2\right) + \partial_y\left(m_x H v q^2\right) + \partial_z\left(m_x m_y w q^2\right)$$

$$= \partial_z\left(m_x m_y \frac{A_q}{H} \partial_z q^2\right) - 2 m_x m_y \frac{H q^3}{B_1 l}$$

$$+ 2 m_x m_y \left(\frac{A_v}{H}\left(\left(\partial_z u\right)^2 + \left(\partial_z v\right)^2\right) + h_p c_p D_p\left(u^2 + v^2\right)^{3/2} + g K_v \partial_z b\right) + Q_q \tag{2.13}$$

$$\P_t\left(m_x m_y H q^2 l\right) + \P_x\left(m_y H u q^2 l\right) + \P_y\left(m_x H v q^2 l\right) + \P_z\left(m_x m_y w q^2 l\right)$$

$$= \P_z\left(m_x m_y \frac{A_q}{H} \P_z\left(q^2 l\right)\right) - m_x m_y \frac{H q^3}{B_1}\left(1 + E_2\left(\frac{l}{\mathbf{k} H z}\right)^2 + E_3\left(\frac{l}{\mathbf{k} H(1-z)}\right)^2\right)$$

$$+ m_x m_y E_1 l\left(\frac{A_v}{H}\left((\P_z u)^2 + (\P_z v)^2\right) + g K_v \P_z b + \mathbf{h}_p c_p D_p\left(u^2 + v^2\right)^{3/2}\right) + Q_l$$

(2.14)

where $(E_1, E_2, E_3) = (1.8, 1.33, 0.25)$. The third on the last line of each equation represents net turbulent energy production by vegetation drag where $\mathbf{h}_p$ is a production efficiency factor have a value less than one. The terms Q_q and Q_l may represent additional source-sink terms such as subgrid scale horizontal turbulent diffusion. The vertical diffusivity, A_q, is set to $0.2ql$ as recommended by Mellor and Yamada (1982) For stable stratification, Galperin *et al* (1988) suggest limiting the length scale such that the square root of R_q is less than 0.52. When horizontal turbulent viscosity and diffusivity are included in the momentum and transport equations, they are determined independently using Smagorinsky's (1963) subgrid scale closure formulation.

Vertical boundary conditions for the solution of the momentum equations are based on the specification of the kinematic shear stresses, equation (2.4), at the bed and the free surface. At the free surface, the x and y components of the stress are specified by the water surface wind stress

$$(\mathbf{t}_{xz}, \mathbf{t}_{yz}) = (\mathbf{t}_{sx}, \mathbf{t}_{sy}) = c_s \sqrt{U_w^2 + V_w^2}\,(U_w, V_w)$$

(2.15)

where U_w and V_w are the x and y components of the wind velocity at 10 meters above the water surface. The wind stress coefficient is given by:

$$c_s = 0.001 \frac{\mathbf{r}_a}{\mathbf{r}_w}\left(0.8 + 0.065\sqrt{U_w^2 + V_w^2}\right)$$

(2.16)

for the wind velocity components in meters per second, with $\mathbf{r}_a$ and $\mathbf{r}_w$ denoting air and water densities respectively. At the bed, the stress components are presumed to be related to the near bed or bottom layer velocity components by the quadratic resistance formulation

$$(\mathbf{t}_{xz}, \mathbf{t}_{yz}) = (\mathbf{t}_{bx}, \mathbf{t}_{by}) = c_b \sqrt{u_1^2 + v_1^2}\,(u_1, v_1)$$

(2.17)

where the 1 subscript denotes bottom layer values. Under the assumption that the near bottom velocity profile is logarithmic at any instant of time, the bottom stress coefficient is given by

$$c_b = \left(\frac{\mathbf{k}}{\ln(\Delta_1 / 2 z_o)}\right)^2$$

(2.18)

where $\mathbf{k}$, is the von Karman constant, $\mathbf{D}$ is the dimensionless thickness of the bottom layer, and $z_o = z_o*/H$ is the dimensionless roughness height. Vertical boundary conditions for the turbulent kinetic energy and length scale equations are:

$$q^2 = B_1^{2/3}|\mathbf{t}_s| \quad : \quad z = 1 \tag{2.19}$$

$$q^2 = B_1^{2/3}|\mathbf{t}_b| \quad : \quad z = 0 \tag{2.20}$$

$$l = 0 \quad : \quad z = 0,1 \tag{2.21}$$

where the absolute values indicate the magnitude of the enclosed vector quantity. Equations (2.17) and (2.18) can become inappropriate under a number of conditions associated with either or both high near bottom sediment concentrations and high frequency surface wave activity. The quantification of sediment and wave effects on the bottom stress is discussed in Chapter 4.

3.   Solution of the Sediment Transport Equation

The EFDC model uses a high order upwind difference solution scheme for the advective terms in the transport equation. Although the scheme is designed to minimize numerical diffusion, a small amount of horizontal diffusion remains inherent in the scheme. Due the small inherent numerical diffusion, the physical horizontal diffusion terms in (2.9) are omitted as to give:

$$\P_t\left(m_x m_y H S_j\right) + \P_x\left(m_y H u S_j\right) + \P_y\left(m_x H v S_j\right) + \P_z\left(m_x m_y w S_j\right)$$

$$-\P_z\left(m_x m_y w_{sj} S_j\right) = \P_z\left(m_x m_y \frac{K_V}{H} \P_z S_j\right) + Q_{sj}^E + Q_{sj}^I \tag{3.1}$$

where S_j represents the concentration of the jth sediment class and the source-sink term has been split into an external part, which would include point and nonpoint source loads, and internal part which could include reactive decay of organic sediments or the exchange of mass between sediment classes if floc formation and destruction were simulated. Vertical boundary conditions for (3.1) are:

$$-\frac{K_V}{H} \P_z S_j - w_s S = J_{jo} : z \approx 0$$

$$-\frac{K_V}{H} \P_z S_j - w_{sj} S_j = 0 : z = 1 \tag{3.2}$$

where J_o is the net water column-bed exchange flux defined as positive into the water column.

The numerical solution of (3.1) utilizes a fractional step procedure. The first step advances the concentration due to advection and external sources and sinks having corresponding volume fluxes by

$$H^{n+1}S^* = H^nS^n + \frac{q}{m_xm_y}\left(Q_{sj}^E\right)^{n+1/2}$$

$$-\frac{q}{m_xm_y}\left(\P_x\left(m_y(Hu)^{n+1/2}S^n\right) + \P_y\left(m_x(Hv)^{n+1/2}S^n\right) + \P_z\left(m_xm_yw^{n+1/2}S^n\right)\right)$$

(3.3)

where n and $n+1$ denote the old and new time levels and $*$ denotes the intermediate fractional step results. The portion of the source and sink term, associated with volumetric sources and sinks is included in the advective step for consistency with the continuity constraint. This term, as well as the advective field (u,v,w), is defined as intermediate in time between the old and new time levels consistent with continuity. Note that the sediment class subscripts have be dropped for clarity. The advection set uses the antidiffusive MPDATA scheme (Smolarkiewicz and Clark, 1986) with optional flux corrected transport (Smolarkiewicz and Grabowski, 1990).

The second fractional settling step is given by

$$S^{**} = S^* + \frac{q}{H^{n+1}}\,\P_z\left(w_sS^{**}\right)$$

(3.4)

which is solved by a fully implicit upwind difference scheme with an optional antidiffusion correction across internal water column layer interfaces. For the bottom bed adjacent layer, (3.4) is written as:

$$S_1^{**} = S_1^* + \frac{q}{\Delta_1 H^{n+1}}\left(w_sS^{**}\right)_2 - \frac{q}{\Delta_z H^{n+1}}\left(w_sS^{**}\right)_1$$

(3.5)

The water column-bed flux (3.2) can be written as

$$-\frac{K_V}{H}\,\P_zS_j - w_sS = J_o = w_rS_r - P_dw_sS$$

(3.6)

where the product, w_rS_r symbolically represents the resuspension flux and P_d the probability of deposition which is less than or equal to one. Since the remaining step will represent diffusion, for solution efficiency, the diffusive flux at the bed in (3.6) is set to zero in the settling and subsequent diffusion set. Equation (3.5) then becomes

$$\left(1 + \frac{qP_dw_s}{\Delta_z H^{n+1}}\right)S_1^{**} = S_1^* + \frac{q}{\Delta_1 H^{n+1}}\left(w_sS^{**}\right)_2 + \frac{q}{\Delta_z H^{n+1}}\,w_rS_r$$

(3.7)

In the actual EFDC code, if the net bed flux, J_o is positive, it is limited such that only the current top layer of the bed can be completely resuspended in single time step. The remaining fractional step is an implicit diffusion step

$$S^{n+1} = S^{**} + q\P_z\left(\left(\frac{K_V}{H^2}\right)^{n+1}\P_zS^{n+1}\right)$$

(3.8)

with zero diffusive fluxes at the bed and water surface.

4.   Near Bed Turbulence Closure

The proper formulation of hydrodynamic and sediment boundary layer parameterization appropriate for representing the bottom stress and the water column-bed exchange of sediment under conditions including high frequency surface waves and high near bed suspended sediment gradients should be based upon the near bed turbulent kinetic energy balance. The near bed balance assumes an equilibrium between production of turbulence by shear stresses, vegetation drag, and unstable density stratification, the suppression of turbulence by stable stratification, and the dissipation. The turbulent kinetic energy equation (2.13) reduces to

$$\frac{A_v}{H}\left((\partial_z u)^2 + (\partial_z v)^2\right) + h_p c_p D_p \left(u^2 + v^2\right)^{3/2} + gK_v \partial_z b = \frac{Hq^3}{B_l l} \tag{4.1}$$

Multiplying (4.1) by A_v/H and using (2.4) gives

$$\left(t_{xz}^2 + t_{yz}^2\right) + h_p c_p D_p \frac{A_v}{H}\left(u^2 + v^2\right)^{3/2} + gK_v \frac{A_v}{H}\partial_z b = \frac{A_v}{H}\frac{Hq^3}{B_l l} \tag{4.2}$$

In the absence of vegetation and stratification, evaluation of (4.2) at the bed, using (2.10) gives

$$\left(t_{xz}^2 + t_{yz}^2\right)_b = |t_b|^2 = \frac{1}{B_1^{1/3}} q \frac{l}{H} \frac{Hq^3}{B_l l} = \frac{q^4}{B_1^{4/3}} \tag{4.3}$$

recovering the boundary condition (2.20).

For the general case, the definition of A_v is introduced into (4.2) to give

$$q^4 - B_1\left(gH\frac{l}{H}\frac{K_v}{H}\partial_z b + h_p c_p D_p \frac{l}{H}\left(u^2 + v^2\right)^{3/2}\right)q - \frac{B_1}{f_A}\left(t_{xz}^2 + t_{yz}^2\right) = 0 \tag{4.4}$$

Near the bed for three-dimensional model applications and over the depth for two-dimensional applications, the turbulent length scale can be specified by the algebraic relationship

$$\frac{l}{H} = kz(1 - z)^l \tag{4.5}$$

If high frequency surface waves are present, the shear stress can be decomposed into current and wave components

$$t_{xz} = t_c \cos y_c + t_w \cos y_w \tag{4.6}$$
$$t_{yz} = t_c \sin y_c + t_w \sin y_w$$

where t_c and t_w are the current and wave shear stress magnitudes. Evaluating the stress term in (4.4) gives

$$\left(t_{xz}^2 + t_{yz}^2\right) = t_c^2 + t_w^2 + 2\left(\cos y_c \cos y_w + \sin y_c \sin y_w\right)t_c t_w \tag{4.7}$$

Assuming the wave shear stress to be periodic

$$t_w = t_{wm} \sin(wt) \tag{4.8}$$

$$y_w = y_{wm} \text{sgn}(\sin(wt))$$

the mean square stress average over the wave period is given by

$$\left\langle t_{xz}^2 + t_{yz}^2 \right\rangle = t_c^2 + \frac{1}{2} t_{wm}^2 + \frac{4}{p} t_c t_{wm} \cos(y_c - y_{wm}) \tag{4.9}$$

For wave periods much smaller than the time step of the numerical integration, (4.4) is well approximated using (4.9) as

$$q^4 - B_1\left(gH\frac{l}{H}\frac{K_v}{H}\,\mathbb{1}_z b + h_p c_p D_p \frac{l}{H}\left(u^2 + v^2\right)^{3/2}\right)q \tag{4.10}$$

$$-\frac{B_1}{f_A}\left(t_c^2 + \frac{1}{2} t_{wm}^2 + \frac{4}{p} t_c t_{wm} \cos(y_c - y_{wm})\right) = 0$$

The buoyancy gradient near the bed is primarily due to gradients in suspended sediment concentration with the effect of sediment on density given by

$$r = \left(\frac{e}{1+e}\right)r_w + \left(\frac{1}{1+e}\right)r_s = \left(\frac{e}{1+e}\right)r_w + S \tag{4.11}$$

where e is the void ratio of the sediment water mixture and S is the mass concentration of sediment. The buoyancy can be expressed in terms of the sediment concentration using

$$b = \frac{r - r_w}{r_w} = \left(\frac{r_s - r_w}{r_w r_s}\right)S = aS \tag{4.12}$$

with (4.10) becoming

$$q^4 - B_1\left(agH\frac{l}{H}\frac{K_v}{H}\,\mathbb{1}_z S + h_p c_p D_p \frac{l}{H}\left(u^2 + v^2\right)^{3/2}\right)q$$

$$-\frac{B_1}{f_A}\left(t_c^2 + \frac{1}{2} t_{wm}^2 + \frac{4}{p} t_c t_{wm} \cos(y_c - y_{wm})\right) = 0 \tag{4.13}$$

Equation (4.13) provides an algebraic equation for specifying the turbulent intensity q at any level in the hydrodynamic and sediment boundary layers. Since the boundary layer parameter are recalculated at each time step of the hydrodynamic model integration, the solution of (4.13) can be approximated by

$$\left(q^4\right)^{n+1} = B_1\left(\alpha g H \frac{l}{H} \frac{K_v}{H} \P_z S q + h_p c_p D_p \frac{l}{H}\left(u^2 + v^2\right)^{3/2} q\right)^n$$

$$+ \frac{B_1}{f_A}\left(t_c^2 + \frac{1}{2}t_{wm}^2 + \frac{4}{p}t_c t_{wm}\cos(y_c - y_{wm})\right)^n \tag{4.14}$$

where $n+1$ and n denote the new and old time levels, respectively. Since the vertical gradient of the sediment concentration is generally negative, there is low possibility of the right side of (4.13) also being negative. In such and event, the turbulent intensity is set to a small value on the order of 1E-4 meters/second.

5. Noncohesive Sediment Settling, Deposition and Resuspension

Noncohesive inorganic sediments settle as discrete particles, with hindered settling and multiphase interactions becoming important in regions of high sediment concentration near the bed. At low concentrations, the settling velocity for the jth noncohesive sediment class corresponds to the settling velocity of a discrete particle:

$$W_{sj} = W_{soj} \tag{5.1}$$

Useful expressions for the discrete particle settling velocity which depends on the sediment density, effective grian diameter, and fluid kinematic viscosity, provide by van Rijn (1984b) are:

$$\frac{W_{soj}}{\sqrt{g' d_j}} = \begin{cases} \dfrac{R_{dj}}{18} & : \quad d \le 100\,\mu m \\[2ex] \dfrac{10}{R_{dj}}\left(\sqrt{1 + 0.01 R_{dj}^2} - 1\right) & : \quad 100\,\mu m < d_j \le 1000\,\mu m \\[2ex] 1.1 & : \quad d_j > 1000\,\mu m \end{cases} \tag{5.2}$$

where

$$g' = g\left(\frac{r_{sj}}{r_w} - 1\right) \tag{5.3}$$

is the reduced gravitational acceleration and

$$R_{dj} = \frac{d_j \sqrt{g' d_j}}{n} \tag{5.4}$$

is a the sediment grain densimetric Reynolds number.

At higher concentrations and hindering settling conditions, the settling velocity is less than the discrete velocity and can be expressed in the form

$$w_{sj} = \left(1 - \sum_{i}^{I} \frac{S_i}{\boldsymbol{r}_{si}}\right)^n w_{soj} \qquad (5.5)$$

where $\boldsymbol{r}_s$ is the sediment particle density with values of n ranging from 2 (Cao et al, 1996) to 4 (Van Rijn, 1984). The expression (5.2) is approximated to within 5 per cent by

$$w_{sj} = \left(1 - n\sum_{i}^{I} \frac{S_i}{\boldsymbol{r}_{si}}\right) w_{soj} \qquad (5.6)$$

for total sediment concentrations up to 200,000 mg/liter. For total sediment concentrations less than 25,000 mg/liter, neglect of the hindered settling correction results in less than a 5 per cent error in the settling velocity, which is well within the range of uncertainty in parameters used to estimate the discrete particle settling velocity.

Noncohesive sediment is transported as bed load and suspended load. The initiation of both modes of transport begins with erosion or resuspension of sediment from the bed when the bed stress, $\boldsymbol{t}_b$, exceeds a critical stress referred to as the Shield's stress, $\boldsymbol{t}_{cs}$. The Shield's stress depends upon the density and diameter of the sediment particles and the kinematic viscosity of the fluid and can be expressed in empirical dimensionless relationships of the form:

$$\boldsymbol{q}_{csj} = \frac{\boldsymbol{t}_{csj}}{g' d_j} = \frac{u_{*csj}^2}{g' d_j} = f\left(R_{dj}\right) \qquad (5.7)$$

Useful numerical expressions of the relationship (5.5), provided by van Rijn (1984b), are:

$$\boldsymbol{q}_{csj} = \begin{cases} 0.24\left(R_{dj}^{2/3}\right)^{-1} & : & R_{dj}^{2/3} < 4 \\ 0.14\left(R_{dj}^{2/3}\right)^{-0.64} & : & 4 \le R_{dj}^{2/3} < 10 \\ 0.04\left(R_{dj}^{2/3}\right)^{-0.1} & : & 10 \le R_{dj}^{2/3} < 20 \\ 0.013\left(R_{dj}^{2/3}\right)^{0.29} & : & 20 \le R_{dj}^{2/3} < 150 \\ 0.055 & : & R_{dj}^{2/3} \ge 150 \end{cases} \qquad (5.8)$$

A number of approaches have been used to distinguish wheather a particular sediment size class is transported as bed load or suspended load under specific local flow conditions characherized by the bed stress or bed shear velocity:

$$u_* = \sqrt{\boldsymbol{t}_b} \qquad (5.9)$$

The approach proposed by van Rijn (1984a) is adopted in the EFDC model and is as follows. When the bed velocity is less than the critical shear velocity

$$u_{*csj} = \sqrt{\boldsymbol{t}_{csj}} = \sqrt{g' d_j \boldsymbol{q}_{csj}} \qquad (5.10)$$

no erosion or resuspension takes place and there is no bed load transport. Sediment in suspension under this condition will deposit to the bed as will be subsequently discussed. When the bed shear velocity exceeds the critial shear velocity but remains less than the settling velocity,

$$u_{*csj} < u_* < W_{soj} \qquad (5.11)$$

sediment will be eroded from the bed and transported as bed load. Sediment in suspension under this condition will deposit to the bed. When the bed shear velocity exceeds both the critical shear velocity and the settling velocity, bed load transport ceases and the eroded or resuspended sediment will be transported as suspended load. These various transport modes are further illustrated by reference to Figure 1, which shows dimensional forms of the settling velocity relationship (5.2) and the critical Shield's shear velocity (5.10), determined using (5.8) for sediment with a specific gravity of 2.65. For grain diameters less than approximately 1.3E-4 m (130 um) the settling velocity is less than the critical shear velocity and sediment resuspend from the bed when the bed shear velocity exceeds the critical shear velocity will be transported entirely as suspended load. For grain diameters greater than 1.3E-4 m, eroded sediment be transported by bed load in the region corresponding to (5.11) and then as suspended load when the bed shear velocity exceeds the settling velocity.

In the EFDC model, the preceding set of rules are used to deterimne the mode of transport of multiple size classes of noncohesive sediment. Bed load transport is determined using a general bed load transport rate formula:

$$\frac{q_B}{r_s d \sqrt{g'd}} = \Phi(\boldsymbol{q}, \boldsymbol{q}_{cs}) \qquad (5.12)$$

where q_B is the bed load transport rate (mass per unit time per unit width) in the direction of the near bottom horizontal flow velocity vector. The function $\boldsymbol{F}$ depends on the Shield's parameter

$$\boldsymbol{q} = \frac{\boldsymbol{t}_b}{g' d_j} = \frac{u_*^2}{g' d_j} \qquad (5.13)$$

and the critical Shield's parameter defined by (5.7) and (5.8). A number of bed load transport formulas explicity incorprate the settling velocity. However, since both the critical Shield's parameter and the settling velocity are unique functions of the sediment grain densimetric Reynolds number, the settling velocity can also be expressed as a funtion of the critical Shield's parameter with (5.12) remaining an appropriate representation.

A number of bed load formulations developed for riverine prediction (Ackers and White, 1973; Laursen, 1958; Yang, 1973; Yang and Molinas, 1982) do not readily conform to (1) and were not incorporated as options in the EFDC model. Two widely used bed load formulations wihch do conform to (5.12) are the Meyer-Peter and Muller (1948) and Bagnold (1956) formulas and their derivatives (Raudkivi, 1967; Neilson, 1992; Reid and Frostick, 1994) which have the general form

$$\Phi(\boldsymbol{q}, \boldsymbol{q}_{cs}) = \boldsymbol{f}(\boldsymbol{q} - \boldsymbol{q}_{cs})^a \left(\sqrt{\boldsymbol{q}} - \boldsymbol{g} \sqrt{\boldsymbol{q}_{cs}} \right)^b \tag{5.14}$$

where

$$\boldsymbol{f} = \boldsymbol{f}(\boldsymbol{q}_{cs}) \quad or \quad \boldsymbol{f}(R_d) \tag{5.15}$$

The Meyer-Peter and Muller formulations are typified by

$$\Phi = \boldsymbol{f}(\boldsymbol{q} - \boldsymbol{q}_{cs})^{3/2} \tag{5.16}$$

while Bagnold formulations are typified by

$$\Phi = \boldsymbol{f}(\boldsymbol{q} - \boldsymbol{q}_{cs}) \left(\sqrt{\boldsymbol{q}} - \boldsymbol{g} \sqrt{\boldsymbol{q}_{cs}} \right) \tag{5.17}$$

with Bagnold's original formula having $\boldsymbol{g}$ equal to zero. The Meyer-Peter and Muller formulation has been extended to heterogeneous beds by Suzuki et al. (1998), while Bagnold's formula has been similarly extended by van Niekerk et al. (1992). The bed load formulation by van Rijn (1984a) having the form

$$\Phi = \boldsymbol{f}(\boldsymbol{q} - \boldsymbol{q}_{cs})^{2.1}$$
$$\boldsymbol{f} = \frac{0.053}{R_d^{1/5} \boldsymbol{q}_{cs}^{2.1}} \tag{5.18}$$

has been incorporated int the CH3D-SED model and modified for heterogeneous beds by Spasojevic and Holly (1994). Equation (5.18) can be implemented in the EFDC model with an appropriately specified $\boldsymbol{f}$. A modified formulation of the Einstein bed load function (Einstein, 1950) which confoms to (5.12) and (5.14) has been presented by Rahmeyer (1999) and will be later incorporated into the EFDC model.

The procedure for coupling bed load transport with the sediment bed in the EFDC model is as follows. First, the magnitude of the bed load mass flux per unit width is calculated according to (5.12) at horizontal model cell centers, denoted by the subscript c. The cell center flux is then transformed into cell center vector components using

$$q_{bcx} = \frac{u}{\sqrt{u^2 + v^2}} q_{bc}$$
$$q_{bcy} = \frac{v}{\sqrt{u^2 + v^2}} q_{bc} \tag{5.19}$$

where u and v are the cell center horizontal velocities near the bed. Cell face mass fluxes are determined by down wind projection of the cell center fluxes

$$q_{bfx} = (q_{bcx})_{upwind}$$

$$q_{bfy} = (q_{bcy})_{upwind} \qquad (5.20)$$

where the subscript *upwind* denotes the cell center upwind of the *x* normal and *y* normal cell faces. The net removal or accumulation rate of sediment material from the deposited bed underlying a water cell is then given by:

$$m_x m_y J_b = (m_y F_{bfx})_e - (m_y F_{bfx})_w + (m_x F_{bfy})_n - (m_x F_{bfy})_s \qquad (5.21)$$

where J_b is the net removal rate (gm/m*m-sec) from the bed, m_x and m_y are *x* and *y* dimensions of the cell, and the compass direction subscripts define the four cell faces. The implementation of (5.19) through (5.21) in the EFDC code includes logic to limit the out fluxes (5.20) over a time step, such that the time integrated mass flux from the bed does not exceed bed sediment available for erosion or resuspension.

Under conditions when the bed shear velocity exceeds the settling velocity and critical Shield's shear velocity, noncohesive sediment will be resuspended and transported as suspended load. When the bed shear velocity falls below both settling velocity and the critical Shield's shear velocity, suspended sediment will deposit to the bed. A consistent formulation of these processes can be developed using the concept of a near bed equilibrium sediment concentration. Under steady, uniform flow and sediment loading conditions, an equilibrium distribution of sediment in the water column tends to be established, with the resuspension and deposition fluxes canceling each other. Using a number of simplifying assumptions, the equilibrium sediment concentration distribution in the water column can be expressed analytically in terms of the near bed reference or equilibrium concentration, the settling velocity and the vertical turbulent diffusivity. For unsteady or spatially varying flow conditions, the water column sediment concentration distribution varies in space and time in response to sediment load variations, changes in hydrodynamic transport, and associated nonzero fluxes across the water column-sediment bed interface. An increase or decrease in the bed stress and the intensity of vertical turbulent mixing will result in net erosion or deposition, respectively, at a particular location or time.

To illustrate how an appropriate suspended noncohesive sediment bed flux boundary condition can be established, consider the approximation to the sediment transport equation (3.1) for nearly uniform horizontal conditions

$$\partial_t (HS) = \partial_z \left(\frac{K_v}{H} \partial_z S + w_s S \right) \qquad (5.22)$$

Integrating (5.22) over the depth of the bottom hydrodynamic model layer gives

$$\partial_t (\Delta H \bar{S}) = J_0 - J_\Delta \qquad (5.23)$$

where the over bar denotes the mean over the dimensionless layer thickness, **D**. Subtracting (5.23) from (5.22) gives

$$\P_t(HS') = \P_z\left(\frac{K_v}{H}\,\P_z S + w_s S\right) - \left(\frac{J_0 - J_\Delta}{\Delta}\right) \tag{5.24}$$

Assuming that the rate of change of the deviation of the sediment concentration from the mean is small

$$\P_t(HS') << \P_t(H\bar{S}) \tag{5.25}$$

allows (5.24) to be approximated by

$$\P_z\left(\frac{K_v}{H}\,\P_z S + w_s S\right) = \left(\frac{J_0 - J_\Delta}{\Delta}\right) \tag{5.26}$$

Integrating (5.26) once gives

$$\frac{K_v}{H}\,\P_z S + w_s S = (J_0 - J_\Delta)\frac{z}{\Delta} - J_0 \tag{5.27}$$

Very near the bed, (5.27) can be approximated by

$$\frac{K_v}{H}\,\P_z S + w_s S = -J_0 \tag{5.28}$$

Neglecting stratification effects and using the results of Chapter 4, the near bed diffusivity is approximately

$$\frac{K_v}{H} = K_o\, q\frac{l}{H} \cong u_* \boldsymbol{k} z \tag{5.29}$$

Introducing (5.29) into (5.28) gives

$$\P_z S + \frac{R}{z} S = -\frac{R}{z}\frac{J_o}{w_s} \tag{5.30}$$

where

$$R = \frac{w_s}{u_* \boldsymbol{k}} \tag{5.31}$$

is the Rouse parameter. The solution of (5.30) is

$$S = -\frac{J_o}{w_s} + \frac{C}{z^R} \tag{5.32}$$

The constant of integration is evaluated using

$$S = S_{eq} \quad : \quad z = z_{eq} \quad and \quad J_o = 0 \tag{5.33}$$

which sets the near bed sediment concentration to an equilibrium value, defined just above the bed under no net flux condition. Using (5.33), equation (5.32) becomes

$$S = \left(\frac{z_{eq}}{z}\right)^R S_{eq} - \frac{J_o}{w_s} \tag{5.34}$$

For nonequilibrium conditions, the net flux is given by evaluating (5.34) at the equilibrium level

$$J_o = w_s \left(S_{eq} - S_{ne}\right) \tag{5.35}$$

where S_{ne} is the actual concentration at the reference equilibrium level. Equation (5.35) clearly indicates that when the near bed sediment concentration is less than the equilibrium value a net flux from the bed into the water column occurs. Likewise when the concentration exceeds equilibrium, a net flux to the bed occurs.

For the relationship (5.35) to be useful in a numerical model, the bed flux must be expressed in terms of the model layer mean concentration. For a three-dimensional application, (5.34) can be integrated over the bottom model layer to give

$$J_o = w_s \left(\overline{S}_{eq} - \overline{S}\right) \tag{5.36}$$

where

$$\overline{S}_{eq} = \frac{\ln\left(\Delta z_{eq}^{-1}\right)}{\left(\Delta z_{eq}^{-1} - 1\right)} S_{eq} : R = 1$$

$$\overline{S}_{eq} = \frac{\left(\left(\Delta z_{eq}^{-1}\right)^{1-R} - 1\right)}{(1 - R)\left(\Delta z_{eq}^{-1} - 1\right)} S_{eq} : R \neq 1 \tag{5.37}$$

defines an equivalent layer mean equilibrium concentration in terms of the near bed equilibrium concentration.   The   corresponding   quantities   in   the   numerical   solution   bottom   boundary condition (3.6) are

$$w_r S_r = w_s \overline{S}_{eq} \tag{5.38}$$

$$P_d w_s = w_s$$

If the dimensionless equilibrium elevation, z_{eq} exceeds the dimensionless layer thickness, (5.19) can be modified to

$$\bar{S}_{eq} = \frac{\ln\left(M\Delta z_{eq}^{-1}\right)}{\left(M\Delta z_{eq}^{-1} - 1\right)} S_{eq} : R = 1$$

$$\bar{S}_{eq} = \frac{\left(\left(M\Delta z_{eq}^{-1}\right)^{1-R} - 1\right)}{(1 - R)\left(M\Delta z_{eq}^{-1} - 1\right)} S_{eq} : R \neq 1 \tag{5.39}$$

where the over bars in (5.36) and (5.38) implying an average of the first M layers above the bed.

For two-dimensional, depth averaged model application, a number of additional considerations are necessary. For depth average modeling, the equivalent of (5.27) is

$$\frac{K_v}{H} \, \P_z S + w_s S = -J_o (1 - z) \tag{5.40}$$

Neglecting stratification effects and using the results of Chapter 4, the diffusivity is

$$\frac{K_v}{H} = K_o q \frac{l}{H} \cong u_* k z (1 - z)^l \tag{5.41}$$

Introducing (5.41) into (5.40) gives

$$\P_z S + \frac{R}{z(1 - z)^l} S = -\frac{R(1 - z)^{l-1}}{z} \frac{J_o}{w_s} \tag{5.42}$$

A close form solution of (5.42) is possible for λ equal to zero. Although the resulting diffusivity is not as reasonable as the choice of λ equal to one, the resulting vertical distribution of sediment is much more sensitive to the near bed diffusivity distribution than the distribution in the upper portions of the water column. For λ equal to zero, the solution of (5.42) is

$$S = -\left(1 - \frac{Rz}{(1 + R)}\right) \frac{J_o}{w_s} + \frac{C}{z^R} \tag{5.43}$$

Evaluating the constant of integration using (5.43) gives

$$S = \left(\frac{z_{eq}}{z}\right)^R S_{eq} - \left(1 - \frac{Rz}{(1 + R)}\right) \frac{J_o}{w_s} \tag{5.44}$$

For nonequilibrium conditions, the net flux is given by evaluating (5.44) at the equilibrium level

$$J_o = w_s \left(\frac{(1 + R)}{1 + R(1 - z_{eq})}\right) (S_{eq} - S_{ne}) \tag{5.45}$$

where S_{ne} is the actual concentration at the reference equilibrium level. Since z_{eq} is on the order of the sediment grain diameter divided by the depth of the water column, (5.45) is essentially

equivalent (5.35). To obtain an expression for the bed flux in terms of the depth average sediment concentration, (5.44) is integrated over the depth to give

$$J_o = w_s \left(\frac{2(1+R)}{2 + R(1 - z_{eq})} \right) (\overline{S}_{eq} - \overline{S}) \qquad (5.46)$$

where

$$\overline{S}_{eq} = \frac{\ln(z_{eq}^{-1})}{(z_{eq}^{-1} - 1)} S_{eq} : R = 1$$

$$\overline{S}_{eq} = \frac{(z_{eq}^{R-1} - 1)}{(1 - R)(z_{eq}^{-1} - 1)} S_{eq} : R \neq 1 \qquad (5.47)$$

The corresponding quantities in the numerical solution bottom boundary condition (3.6) are

$$w_r S_r = w_s \left(\frac{2(1+R)}{2 + R(1 - z_{eq})} \right) \overline{S}_{eq}$$

$$P_d w_s = \left(\frac{2(1+R)}{2 + R(1 - z_{eq})} \right) w_s \qquad (5.48)$$

When multiple sediment size classes are simulated, the equilibrium concentrations given by (5.37), (5.39), and (5.47) are adjusted by multiplying by their respective sediment volume fractions in the surface layer of the bed.

The specification of the water column-bed flux of noncohesive sediment has been reduced to specification of the near bed equilibrium concentration and its corresponding reference distance above the bed. Garcia and Parker (1991) evaluated seven relationships, derived by combinations of analysis and experiment correlation, for determining the near bed equilibrium concentration as well as proposing a new relationship. All of the relationships essential specify the equilibrium concentration in terms of hydrodynamic and sediment physical parameters

$$S_{eq} = S_{eq}(d, \boldsymbol{r}_s, \boldsymbol{r}_w, w_s, u_*, \boldsymbol{n}) \qquad (5.49)$$

including the sediment particle diameter, the sediment and water densities, the sediment settling velocity, the bed shear velocity, and the kinematic molecular viscosity of water. Garcia and Parker concluded that the representations of Smith and McLean (1977) and Van Rijn (1984b) as well as their own proposed representation perform acceptably when tested against experimental and field observations.

Smith and McLean's formula for the equilibrium concentration is

$$S_{eq} = r_s \frac{0.65 g_o T}{1 + g_o T} \tag{5.50}$$

where g_o is a constant equal to 2.4E-3 and T is given by

$$T = \frac{t_b - t_{cs}}{t_{cs}} = \frac{u_*^2 - u_{*cs}^2}{u_{*cs}^2} \tag{5.51}$$

where t_b is the bed stress and t_{cs} is the critical Shields stress. The use of Smith and McLean's formulation requires that the critical Shields stress be specified for each sediment size class. Van Rijn's formula is

$$S_{eq} = 0.015 \, r_s \frac{d}{z_{eq}^*} \, T^{3/2} R_d^{-1/5} \tag{5.52}$$

where z_{eq}^* ($= H z_{eq}$) is the dimensional reference height and R_d is a sediment grain Reynolds number. When Van Rijn's formula is select for use in EFDC, the critical Shields stress in internally calculated using relationships from Van Rijn (1984b). Van Rijn suggested setting the dimensional reference height to three grain diameters. In the EFDC model, the user specifies the reference height as a multiple of the largest noncohesive sediment size class diameter.

Garcia and Parker's general formula for multiple sediment size classes is

$$S_{jeq} = r_s \frac{A(I Z_j)^5}{\left(1 + 3.33 \, A (I Z)^5\right)} \tag{5.53}$$

$$Z_j = \frac{u_*}{w_{sj}} R_{dj}^{3/5} F_H \tag{5.54}$$

$$F_H = \left(\frac{d_j}{d_{50}}\right)^{1/5} \tag{5.55}$$

$$I = 1 + \frac{s_f}{s_{fo}} (I_o - 1) \tag{5.56}$$

where A is a constant equal to 1.3E-7, d_{50} is the median grain diameter based on all sediment classes, I is a straining factor, F_H is a hiding factor and s_f is the standard deviation of the sedimentological phi scale of sediment size distribution. Garcia and Parker's formulation is unique in that it can account for armoring effects when multiple sediment classes are simulated. For simulation of a single noncohesive size class, the straining factor and the hiding factor are set to one. The EFDC model has the option to simulate armoring with Garcia and Parker's formulation. For armoring simulation, the current surface layer of the sediment bed is restricted to a thickness equal to the dimensional reference height.

6. Cohesive Sediment Settling, Deposition and Resuspension

The settling of cohesive inorganic sediment and organic particulate material is an extremely complex process. Inherent in the process of gravitational settling is the process of flocculation, where individual cohesive sediment particles and particulate organic particles aggregate to form larger groupings or flocs having settling characteristics significantly different from those of the component particles (Burban et al., 1989,1990; Gibbs, 1985; Mehta et al., 1989). Floc formation is dependent upon the type and concentration of the suspended material, the ionic characteristics of the environment, and the fluid shear and turbulence intensity of the flow environment. Progress has been made in first principles mathematical modeling of floc formation or aggregation, and disaggregation by intense flow shear (Lick and Lick, 1988; Tsai, et al., 1987). However, the computational intensity of such approaches precludes direct simulation of flocculation in operational cohesive sediment transport models for the immediate future.

An alternative approach, which has met with reasonable success, is the parameterization of the settling velocity of flocs in terms of cohesive and organic material fundamental particle size, d; concentration, S; and flow characteristics such as vertical shear of the horizontal velocity, du/dz, shear stress, A_vdu/dz, or turbulence intensity in the water column or near the sediment bed, q. This has allowed semi-empirical expressions having the functional form

$$W_{se} = W_{se}\left(d, S, \frac{du}{dz}, q \right) \tag{6.1}$$

to be developed to represent the effective settling velocity. A widely used empirical expression, first incorporated into a numerical by Ariathurai and Krone (1976), relates the effective settling velocity to the sediment concentration:

$$w_s = w_{so}\left(\frac{S}{S_o} \right)^a \tag{6.2}$$

with the o superscript denoting reference values. Depending upon the reference concentration and the value of α, this equation predicts either increasing or decreasing settling velocity as the sediment concentration increases. Equation (6.2) with user defined base settling velocity, concentration and exponent is an option in the EFDC model. Hwang and Metha (1989) proposed

$$w_s = \frac{aS^n}{\left(S^2 + b^2 \right)^m} \tag{6.3}$$

based on observations of settling at six sites in Lake Okeechobee. This equation has a general parabolic shape with the settling velocity decreasing with decreasing concentration at low concentrations and decreasing with increasing concentration at high concentration. A least squares for the paramters, a, m, and n, in (6.3) was shown to agree well with observational data. Equation (6.3) does not hav a dependence on flow characteristics, but is based on data from an energetic field condition having both currents and high frequency surface waves. A generalized form of (6.3) can be selected as an option in the EFDC model.

Ziegler and Nisbet, (1994, 1995) proposed a formulation to express the effective settling as a function of the floc diameter, d_f

$$w_s = ad_f^b \tag{6.4}$$

with the floc diameter given by:

$$d_f = \left(\frac{a_f}{S \sqrt{t_{xz}^2 + t_{xz}^2}} \right)^{1/2} \tag{6.5}$$

where S is the sediment concentration, α_f is an experimentally determined constant and τ_{xz} and τ_{yz} are the x and y components of the turbulent shear stresses at a given position in the water column. Other quantities in (6.4) have been experimentally determined to fit the relationships:

$$a = B_1 \left(S \sqrt{t_{xz}^2 + t_{xz}^2} \right)^{-0.85} \tag{6.6}$$

$$b = -0.8 - 0.5 \log \left(S \sqrt{t_{xz}^2 + t_{xz}^2} - B_2 \right) \tag{6.7}$$

where B_1 and B_2 are experimental constants. This formulation is also an option in the EFDC model.

A final settling option in EFDC is based on that proposed by Shrestha and Orlob (1996). The formulation in EFDC has the form

$$w_s = S^a \exp(-4.21 + 0.147G) \tag{6.8}$$
$$a = 0.11 + 0.039G$$

where

$$G = \sqrt{\left(\P_z u \right)^2 + \left(\P_z v \right)^2} \tag{6.9}$$

is the magnitude of the vertical shear of the horizontal velocity. It is noted that all of these formulations are based on specific dimensional units for input parameters and predicted settling velocities and that appropriate unit conversion are made internally in their implementation in the EFDC model.

Water column-sediment bed exchange of cohesive sediments and organic solids is controlled by the near bed flow environment and the geomechanics of the deposited bed. Net deposition to the bed occurs as the flow-induced bed surface stress decreases. The most widely used expression for the depositional flux is:

$$J_o^d = \begin{cases} -w_s S_d \left(\dfrac{t_{cd} - t_b}{t_{cd}} \right) = -w_s T_d S_d & : \quad t_b \le t_{cd} \\[2em] 0 & : \quad t_b \ge t_{cd} \end{cases}$$

<div align="right">(6.10)</div>

where t_b is the stress exerted by the flow on the bed, t_{cd} is a critical stress for deposition which depends on sediment material and floc physiochemical properties (Mehta et al., 1989) and S_d is the near bed depositing sediment concentration. The critical deposition stress is generally determined from laboratory or in situ field observations and values ranging form 0.06 to 1.1 N/m**2 have been reported in the literature. Given this wide range of reported values, in the absence of site specific data the depositional stress and is generally treated as a calibration parameter. The depositional stress is an input parameter in the EFDC model.

Since the near bed depositing sediment concentration in (6.10) is not directly calculated, the procedures of Chapter 5 can be applied to relate the the near bed depositional concentration to the bottom layer or depth averge concentration. Using (5.14) the near bed concentration during times of deposition can be determined in terms of the bottom layer concentration for three-dimensional model applications. Inserting (6.10) into (5.14) and evaluating the constant at a near bed depositional level gives

$$S = \left(T_d + (1 - T_d) \frac{z_d^R}{z^R} \right) S_d$$

<div align="right">(6.11)</div>

Integrating (6.11) over the bottom layer gives

$$S_d = \left(T_d + \frac{\ln(\Delta z_d^{-1})}{(\Delta z_d^{-1} - 1)} (1 - T_d) \right)^{-1} \bar{S} : R = 1$$

$$S_d = \left(T_d + \frac{\left((\Delta z_{eq}^{-1})^{1-R} - 1 \right)}{(1 - R)(\Delta z_d^{-1} - 1)} (1 - T_d) \right)^{-1} \bar{S} : R \ne 1$$

<div align="right">(6.12)</div>

The corresponding quantities in the numerical solution bottom boundary condition (3.6) are

$$P_d W_s = \left(T_d + \frac{\ln(\Delta z_d^{-1})}{(\Delta z_d^{-1} - 1)} (1 - T_d) \right)^{-1} w_s : R = 1$$

$$P_d W_s = \left(T_d + \frac{\left((\Delta z_{eq}^{-1})^{1-R} - 1 \right)}{(1 - R)(\Delta z_d^{-1} - 1)} (1 - T_d) \right)^{-1} w_s : R \ne 1$$

<div align="right">(6.13)</div>

For depth averaged model application, (6.10) is combined with (5.25) and the constant of integration is evaluated at a near bed depositional level to give

$$S = \left(1 - \frac{Rz}{(1+R)}\right)T_d S_d + \left(1 - \left(1 - \frac{Rz_d}{(1+R)}\right)T_d\right)S_d \frac{z_d^R}{z^R} \tag{6.14}$$

Integrating (6.14) over the depth gives

$$S_d = \left(\left(\frac{2 + R(1 - z_d)}{2(1+R)}\right)T_d + \frac{\ln(z_d^{-1})}{(z_d^{-1} - 1)}\left(1 - \left(\frac{1 + R(1 - z_d)}{(1+R)}\right)T_d\right)\right)^{-1}\overline{S} : R = 1$$

$$S_d = \left(\left(\frac{2 + R(1 - z_d)}{2(1+R)}\right)T_d + \frac{(z_d^{R-1} - 1)}{(1-R)(z_d^{-1} - 1)}\left(1 - \left(1 - \frac{Rz_d}{(1+R)}\right)T_d\right)\right)^{-1}\overline{S} : R \neq 1 \tag{6.15}$$

The corresponding quantities in the numerical solution bottom boundary condition (3.6) are

$$P_d w_s = \left(\left(\frac{2 + R(1 - z_d)}{2(1+R)}\right)T_d + \frac{\ln(z_d^{-1})}{(z_d^{-1} - 1)}\left(1 - \left(\frac{1 + R(1 - z_d)}{(1+R)}\right)T_d\right)\right)^{-1} w_s : R = 1$$

$$P_d w_s = \left(\left(\frac{2 + R(1 - z_d)}{2(1+R)}\right)T_d + \frac{(z_d^{R-1} - 1)}{(1-R)(z_d^{-1} - 1)}\left(1 - \left(1 - \frac{Rz_d}{(1+R)}\right)T_d\right)\right)^{-1} w_s : R \neq 1 \tag{6.16}$$

It is noted that the assumptions used to arrive at the relationships, (6.12) and (6.15) are more teneous for cohesive sediment than the similar relationships for noncohesive sediment. The settling velocity for cohesive sediment is highly concentration dependent and the use of a constant settling velocity to arrive at (6.12) and (6.15) is questionable. The specification of an appropriate reference level for cohesive sediment is difficult. One possibility is to relate the reference level to the floc diameter using (6.5). An alternative is to set the reference level to a laminar sublayer thickness

$$z_d = \frac{\boldsymbol{n}(S)}{Hu_*} \tag{6.17}$$

where $\boldsymbol{n}(S)$ is a sediment concentration dependent kinematic viscosity and the water depth is include to nondimensionlize the reference level. A number of investigators, including Mehta and Jiang (1990) have presented experimental results indicating that at high sediment concentrations, cohesive sediment-water mixtures behave as high viscosity fluids. Mehta and Jain's results indicate that a sediment concentration of 10,000 mg/L results in a viscosity ten time that of pure water and that the viscosity increases bgrithmically with increasing mixture density. Use of the relationships (6.12) and (6.16) is optional in the EFDC model. When they are used, the reference height is set using (6.17) with the viscosity determined using Mehta and Jain's experimental relationship between viscosity and sediment concentration. To more fully address the deposition prediction problem, a nested sediment, current and wave boundary layer model based on the near bed closure presented in Chapter 4 is under development.

Cohesive bed erosion occurs in two distinct modes, mass erosion and surface erosion. Mass erosion occurs rapidly when the bed stress exerted by the flow exceeds the depth varying shear strength, t_s, of the bed at a depth, H_{me}, below the bed surface. Surface erosion occurs gradually when the flow-exerted bed stress is less than the bed shear strength near the surface but greater than a critical erosion or resuspension stress, t_{ce}, which is dependent on the shear strength and density of the bed. A typical scenario under conditions of accelerating flow and increasing bed stress would involve first the occurrence of gradual surface erosion, followed by a rapid interval of mass erosion, followed by another interval of surface erosion. Alternately, if the bed is well consolidated with a sufficiently high shear strength profile, only gradual surface erosion would occur. Transport into the water column by mass or bulk erosion can be expressed in the form

$$ J_o^r = w_r S_r = \frac{m_{me}(t_s \leq t_b)}{T_{me}} \tag{6.18} $$

where J_o is the erosion flux, the product $w_r S_r$ represents the numerical boundary condition (3.6), m_{me} is the dry sediment mass per unit area of the bed having a shear strength, t_s, less than the flow-induced bed stress, t_b, and T_{me} is a somewhat arbitrary time scale for the bulk mass transfer. The time scale can be taken as the numerical model integration time step (Shrestha and Orlob, 1996). Observations by Hwang and Mehta (1989) have indicated that the maximum rate of mass erosion is on the order of 0.6 gm/s-m**2 which provides an means of estimating the transfer time scale in (4.10). The shear strenght of the cohesive sediment bed is generally agreed to be a linear function of the bed bulk density (Metha et al., 1982; Villaret and Paulic, 1986; Hwang and Mehta, 1989)

$$ t_s = a_s r_b + b_s \tag{6.19} $$

For the shear strength in N/m**2 and the bulk density in gm/cm**3, Hwang and Mehta (1989) give a_s and b_s values of 9.808 and -9.934 for bulk density greater than 1.065 gm/cm**3. The EFDC model currently implements Hwang and Mehta's relationship, but can be readily modified to incorporated other functional relationships.

Surface erosion is generally represented by relationships of the form

$$ J_o^r = w_r S_r = \frac{dm_e}{dt}\left(\frac{t_b - t_{ce}}{t_{ce}}\right)^a \quad : \quad t_b \geq t_{ce} \tag{6.20} $$

or

$$ J_o^r = w_r S_r = \frac{dm_e}{dt}\exp\left(-b\left(\frac{t_b - t_{ce}}{t_{ce}}\right)^g\right) \quad : \quad t_b \geq t_{ce} \tag{6.21} $$

where dm_e/dt is the surface erosion rate per unit surface area of the bed and t_{ce} is the critical stress for surface erosion or resuspension. The critical erosion rate and stress and the parameters a, b, and g are generally determined from laboratory or in situ field experimental observations.

Equation (6.20) is more appropriate for consolidated beds, while (6.21) is appropriate for soft partially consolidated beds. The base erosion rate and the critical stress for erosion depend upon the type of sediment, the bed water content, total salt content, ionic species in the water, pH and temperature (Mehta, *et al.*, 1989) and can be measured in laboratory and sea bed flumes.

The critical erosion stress is related to but generally less than the shear strength of the bed, which in turn depends upon the sediment type and the state of consolidation of the bed. Experimentally determined relationships between the critical surface erosion stress and the dry density of the bed of the form

$$\boldsymbol{t}_{ce} = c\boldsymbol{r}_s^d \tag{6.22}$$

have been presented (Mehta, et al., 1989). Hwang and Mehta (1989) proposed the relationship

$$\boldsymbol{t}_{ce} = a\left(\boldsymbol{r}_b - \boldsymbol{r}_l\right)^b + c \tag{6.23}$$

between the critical surface erosion stress and the bed bulk density with *a, b, c,* and $\boldsymbol{r}$ equal to 0.883, 0.2, 0.05, and 1.065, respectively for the stress in N/m**2 and the bulk density in gm/cm**3. Considering the relationship between dry and bulk density

$$\boldsymbol{r}_d = \boldsymbol{r}_s \frac{\left(\boldsymbol{r}_b - \boldsymbol{r}_w\right)}{\left(\boldsymbol{r}_s - \boldsymbol{r}_w\right)} \tag{6.24}$$

equations (6.22) and (6.23) are consistent. The EFDC model allow for a user defined constant crital stress for surface erosion or the use of (6.23). Alternate predictive expression can be readily incorporated into the model.

Surface erosion rates ranging from 0.005 to 0.1 gm/s-m**2 have been reported in the literature, and it is generally accepted that the surface erosion rate decreases with increasing bulk density. Based on experimental observations, Hwang and Mehta (1989) proposed the relationship

$$\log_{10}\left(\frac{dm_e}{dt}\right) = 0.23 \exp\left(\frac{0.198}{\boldsymbol{r}_b - 1.0023}\right) \tag{6.25}$$

for the erosion rate in mg/hr-cm**2 and the bulk density in gm/cm**3. The EFDC model allow for a user defined constant surface erosion rate or predicts the rate using (6.25). Alternate predictive expression can be readily incorporated into the model. The use of bulk density functions to predict bed strength and erosion rates in turn requires the prediction of time and depth in bed variations in bulk density which is related to the water and sediment density and the bed void ratio by

$$\boldsymbol{r}_b = \left(\frac{e}{1+e}\right)\boldsymbol{r}_w + \left(\frac{1}{1+e}\right)\boldsymbol{r}_s \tag{6.26}$$

Selection of the bulk density dependent formulations in the EFDC model requires implmentation of a bed consolidation simulation to predict the bed void ratio as discussed in the following chapter.

7. Sediment Bed Geomechanical Processes

This chapter describes the representation of the sediment bed in the EFDC model. To make the information presented self contained, the derivation of mass balance equations and comparison with formulations used in other models is also presented.

Consider a sediment bed represented by discrete layers of thickness B_k, which may be time varying. The conservation of sediment and water mass per unit horizontal area in layer k is given by:

$$\partial_t\left(\frac{r_s B_k}{1+e_k}\right) = J_{s:k-} - J_{s:k+} - d(k,k_b)J_{sb} \tag{7.1}$$

$$\partial_t\left(\frac{r_w e_k B_k}{1+e_k}\right) = J_{w:k-} - J_{w:k+} - d(k,k_b)\frac{r_w}{r_s}\left(e_k \max(J_{sb},0)+ e_b \min(J_{sb},0)\right) \tag{7.2}$$

where e is the void ratio, r_s and r_w are the sediment and water density and J_s and J_w are the sediment and water mass fluxes with $k-$ and $k+$ defining the bottom and top boundaries, respectively of layer k. The mass fluxes are defined as positive in the vertical direction and exclude fluxes associated with sediment depostion and erosion. The last term in equation (7.1) represents erosion and deposition of sediment at the top of the upper most bed layer, $k=k_b$, where

$$d(k,k_b)= \begin{array}{l} 1: k= k_b \\ 0: k\neq k_b \end{array} \tag{7.3}$$

Consitent with this partitioning of flux,

$$J_{s:k+} = 0: k\neq k_b \tag{7.4}$$

The last term in (7.2) represents the corresponding entrainment of bed water into the water column during sediment erosion and entrainment of water column water into the bed during deposition. The water flux, $J_{w:k+}$, at the top of the upper most layer, k_b, is not necessarily zero, since it can include ambient seepage and pore water explusion due to bed consolidation.

Assuming sediment and water to be incompressible, (7.1) and (7.2) can be written as:

$$\partial_t\left(\frac{B_k}{1+e_k}\right) = \frac{1}{r_s}(J_{s:k-} - J_{s:k+})- d(k,k_b)\frac{J_{sb}}{r_s} \tag{7.5}$$

$$\P_t\left(\frac{e_k B_k}{1+e_k}\right) = q_{w:k-} - q_{w:k+} - \d(k, k_b)\left(e_k \max\left(\frac{J_{sb}}{r_s}, 0\right) + e_b \min\left(\frac{J_{sb}}{r_s}, 0\right)\right) \tag{7.6}$$

where the water specfic discharges

$$J_{w:k-} = r_w q_{w:k-} \tag{7.7}$$
$$J_{w:k+} = r_w q_{w:k-}$$

have been introduced into (7.6). Four approaches for the solution of the mass conservation equations (7.5) and (7.6) have been previously utilized. The solution approaches, hereafter referred to as solution levels, increase in complexity and physical realism and will be briefly summarized.

The first level or simplest approach assumes specified time-constant layer thicknesses and void ratios with the left sides of (7.5) and (7.6) being identically zero. Sediment mass flux at all layer interfaces are then identical to the net flux from the bed to the water column.

$$J_{s:k-} = J_{sb} : k = 1, k_b$$
$$J_{s:k+} = \begin{array}{l} 0 : k = k_b \\ J_{sb} : k \neq k_b \end{array} \tag{7.8}$$

Bed representations at this level, as exemplified by the RECOVERY model (Boyer, et al., 1994), typically omit the water mass conservation equations. However, it is noted that the water mass conservation is ill posed unless either q_{1-}, the specific discharge at the bottom of the deepest layer or q_{kb+}, the specific discharge at the top of the water column adjacent layer, is specified. If q_{1-} is set to zero, q_{ka+} is then required to exactly cancel the entrainment terms is (7.6).

The second level of bed mass conservation representation assumes specified time invariant layer thicknesses. The mass conservation equations (7.5) and (7.6) become

$$B_k \P_t\left(\frac{1}{1+e_k}\right) = \frac{1}{r_s}(J_{s:k-} - J_{s:k+}) - \d(k, k_b)\frac{J_{sb}}{r_s} \tag{7.9}$$

$$B_k \P_t\left(\frac{e_k}{1+e_k}\right) = q_{w:k-} - q_{w:k+} - \d(k, k_b)\left(e_k \max\left(\frac{J_{sb}}{r_s}, 0\right) + e_b \min\left(\frac{J_{sb}}{r_s}, 0\right)\right) \tag{7.10}$$

This system of 2 x k_b equations includes k_b unknow void ratios, k_b unknow internal sediment fluxes, and k_{b+1} unknow specific discharges and is under determined unless additional information is specified. The constant bed layer thickness option in the WASP5 model (Ambrose, et al., 1993) uses specifed burial velocities to define the internal sediment fluxes

$$J_{s:k-} = -w_{b:k-}S_k$$

$$J_{s:k+} = -w_{b:k+}S_{k+1}$$

$$w_{b:k+} = w_{b:k+1-}$$

(7.11)

$$S_k = \frac{r_s}{1 + e_k}$$

(7.12)

where w_b is the burial velocity and S is the sediment concentration (mass per unit total volume). Use of the burial velocity eliminates the indetermincy in (7.9) and allowing its solution for the void ratio. In the event that the sediment concentration in the upper most layer becomes negative, the layer is eliminated and the underlying layer become water column adjacent. The left side of the water mass conservation equations (7.10) is now know and the equation is more appropriately written as

$$q_{w:k-} - q_{w:k+} = B_k \P_t\left(\frac{e_k}{1+e_k}\right) + d(k,k_b)\left(e_k \max\left(\frac{J_{sb}}{r_s},0\right) + e_b \min\left(\frac{J_{sb}}{r_s},0\right)\right)$$

(7.13)

The determination of the specific discharges using (7.13) can be viewed is either under determined or physically inconsistent. As shown for the first level approach, the solution of (7.13) is ill posed unless either q_{1-}, the specific discharge at the bottom of the deepest layer or q_{kb+}, the specific discharge at the top of the upper most layer is independently specified. If q_{1-} is specified and the internal specific discharges are determined from (7.13), q_{ka+} is then required to partially cancel the entrainment terms in (7.13). As will be subsequently shown, the specific discharges can be dynamically determined using Darcy's law. However, the specific discharges determined using Darcy's law and the known void ratios are not guaranteed to satisfy (7.13) the level two formulation is dynamically inconsistent with respect to water mass conservation in the sediment bed. The constant bed layer thickness option in the WASP5 ignores this problem entirely by not considering the water mass balance and hence neglecting pore water advection of dissolved contaminants.

The third level of bed mass conservation representation assumes specified time invariant layer void ratios. The mass conservation equations (7.5) and (7.6) become

$$\left(\frac{1}{1+e_k}\right)\P_t B_k = \frac{1}{r_s}(J_{s:k-} - J_{s:k+}) - d(k,k_b)\frac{J_{sb}}{r_s}$$

(7.14)

$$\left(\frac{e_k}{1+e_k}\right)\P_t B_k = q_{w:k-} - q_{w:k+} - d(k,k_b)\left(e_k \max\left(\frac{J_{sb}}{r_s},0\right) + e_b \min\left(\frac{J_{sb}}{r_s},0\right)\right)$$

(7.15)

This system of equations exhibits the same under determined nature as (7.9) and (7.10). Specification of internal sediment fluxes or burial velocities allows (7.14) to be solved for the layer thicknesses. Solution of (7.15) for the specific discharges then requires the specification either q_{1-}, the specific discharge at the bottom of the deepest layer or q_{kb+}, the specific discharge at the top of the upper most layer. The variable bed layer thickness option in the WASP5 model

(Ambrose, et al., 1993) exemplifies the third level of bed representation. Specifically, the thickness of the water column adjacent layer is allowed to vary in time, while the thicknesses of the underlying layers remain constant. A periodic time variation is specified for the bottom sediment flux in the upper most layer

$$J_{s:kb-} = 0 \quad : \quad t_o \leq t \leq t_o + (N-1)\Delta t$$

$$J_{s:kb-} = \int_{t_o}^{t_o+N\Delta t} J_{sb}dt \quad : \quad t_o + (N-1)\Delta t \leq t \leq t_o + N\Delta t \qquad (7.16)$$

where $\mathbf{D}t$ is the standard water time step and $N\mathbf{D}t$ is the sediment compaction time. This results in the thickness of the upper most layer periodically returning to its initial value at time intervals of $N\mathbf{D}t$ unless the thickness becomes negative due to net resuspension. In that event, the underlying layer becomes the water column adjacent layer. The water mass conservation (7.15) for all but the upper most layer becomes

$$q_{k+} = q_{k-} = q_{1-} \quad : \quad k \neq k_b \qquad (7.17)$$

indicating that all internal specific discharges are equal a specified specific discharge at the bottom of layer 1. Given the solution for the time variation of the water column adjacent thickness and bottom specific discharge, (7.15) can be solved for the specific discharge at the top of the layer. The constant porosity bed option in EFDC is also a level three approach. In EFDC, the internal sediment fluxes are set to zero and the change in thickness of the water column adjacent layer is determined directly using (7.14) while the underlying layers have time invariant thicknesses. As a result, the internal water specific discharges are set to zero and the water entrainment and expulsion in the water column adjacent layer are determined directly from (7.15). The EFDC model is configured to have a user specified maximum number of sediment bed layer. A the start of a simulation, the number of layers containing sediment at a specific horizontal location is specified. Under continued deposition, a new water column layer is created when the thickness of the current layer exceeds a user specified value. If the current water column adjacent layer's index is equal to the maximam number of layers, the bottom two layers are combined and the remaining layers renumbered before addition of the new layer. Under continued resuspension, the layer underlying the current water column adjacent layer becomes the new adjacent layer when all sediment is resuspended form the current layer.

The fourth level of bed representation accounts for bed consolidation by allowing the layer void ratios and thicknesses to vary in time. The simplest and most elegant formulations at this level utilize a Lagrangian approach for sediment mass conservation. The Lagrangian approach requires that the sediment mass per unit horizontal area in all layers, except the upper most, be time invariant and without loss of generality, the internal sediment fluxes can be set to zero. Consistent with these requirements (7.5) becomes

$$\P_t\left(\frac{B_k}{1+\boldsymbol{e}_k}\right) = -\boldsymbol{d}(k,k_b)\frac{J_{sb}}{\boldsymbol{r}_s} \qquad (7.18)$$

Expanding the left side of the water conservation equation (7.6), and using (7.18) gives

$$\left(\frac{B_k}{1+e_k}\right)\partial_t e_k = q_{w:k-} - q_{w:k+} + d(k,k_b)(e_k - e_b)\min\left(\frac{J_{sb}}{r_s},0\right) \tag{7.19}$$

The Lagrangian approach for sediment mass conservation also requires that the number of bed layers vary in time. Under conditions of continued deposition, a new water column adjacent layer would be added when either the thickness, void ratio or mass per unit area of the current water column adjacent layer reaches a predefined value. Under conditions of continued resuspension, the bed layer immediately under the current water column adjacent layer would become the new water column adjacent layer when the entire sediment mass of the current layer has been resuspended.

At the fourth and most realistic level of bed representation, three approaches can be used to represent bed consolidation. Two of the approaches are semi-empirical with the first assuming that the void ratio of a layer decreases with time. A typical relationship which is used for the simple consolidation option in the EFDC model is

$$e = e_m + (e_o - e_m)\exp(-a(t - t_o)) \tag{7.20}$$

where e_o is the void ratio at the mean time of deposition, t_o, e_m is the ultimate minimum void ratio corresponding to complete consolidation, and a is an empirical or experimental constant. Use of (7.20) in the EFDC model involves specifying the depositional void ratio, the ultimate void ratios and the rate constants. The ultimate void ratio can be specified as a function depth below the water column-bed interface. The actual calculation involves using the initial void ratios to determine the deposition time t_o, after which (7.20) is used to update the void ratios as the simulation progresses. After equation (7.20) is used to calculate the new time level void ratios, equation (7.18) provides the new layer thicknesses. The water conservation equations (7.19) can then be solved using

$$q_{w:k+} = q_{w:k-} - \left(\frac{B_k}{1+e_k}\right)\partial_t e_k + d(k,k_b)(e_k - e_b)\min\left(\frac{J_{sb}}{r_s},0\right) \tag{7.21}$$

to determine the water specific discharges, provided that the specific discharge q_{1-}, at the bottom of layer 1 is specified. When this option is specified in the EFDC model, the specific discharge at bottom of the bottom sediment layer is set to zero. Layers are added and deleted in the manner previously described for EFDC's constant porosity option. The SED2D-WES model (Letter et al., 1998) utilizes a similar approach based on a specified time variation of bulk density

$$r_b = \frac{r_s + e r_w}{1 + e} = r_{bm} + (r_{bo} - r_{bm})\exp(-a(t - t_o)) \tag{7.22}$$

which in turn defines the variation in void ratio.

The second semi-empirical approach assumes that the vertical distribution of the bed bulk density or equivalently the, void ratio at any time is given by a self-similar function of vertical position, bed thickness and fixed surface and bottom bulk densities or void ratios. Functionally this equivalent to

$$e = V(z, B_T, e_{kb}, e_1) \tag{7.23}$$

where V represents the function, z is a vertical coordinate measured upward from the bottom of the lowest layer, and B_T is the total thickness of the bed. This approach is used in the original HSTM model (Hayter and Mehta, 1983), the new HSCTM model (Hayter et al., 1998) and is an option in the CE-QUAL-ICM/TOXI model (Dortch, et al., 1998). The determination of the new time level layer thicknesses and void ratios requires an iterative solution of equations (7.18) and (7.23). The solution is completed using (7.21) to determine the water specific discharges.

The third and most realistic approach is to dynamically simulate the consolidation of the bed. In the Lagrangian formulation, (7.18) is directly solved for the equivalent sediment thickness

$$\Delta_k = \frac{B_k}{1 + e_k} \tag{7.24}$$

and the water conservation equation (7.19) is integrated to determine the void ratio.

$$\Delta_k \partial_t e_k = q_{w:k-} - q_{w:k+} + d(k, k_b)(e_k - e_b) \min\left(\frac{J_{sb}}{r_s}, 0 \right) \tag{7.25}$$

The specific discharges in (7.25) are determined using the Darcy equation

$$q = -\frac{K}{g r_w} \partial_z u \tag{7.26}$$

where K is the hydraulic conductivity and u is the excess pore pressure defined as the difference between the total pore pressure u_t, and the hydrostatic pressure u_h.

$$u = u_t - u_h \tag{7.27}$$

The total pore pressure is defined as the difference between the total stress s and effective stress s_e.

$$u_t = s - s_e \tag{7.28}$$

The total stress and hydrostatic pressure are given by

$$s = p_b + g \int_z^{z_b} \left(\left(\frac{e}{1+e} \right) r_w + \left(\frac{1}{1+e} \right) r_s \right) dz \tag{7.29}$$

$$u_h = p_b + g r_w (z_b - z) \tag{7.30}$$

where p_b is the water column pressure at the bed z_b. Solving for the excess pore pressure using (7.27) through (7.30) gives

$$u = g\mathbf{r}_w\left(\frac{\mathbf{r}_s}{\mathbf{r}_w}-1\right)\int_z^{z_b}\left(\frac{1}{1+\mathbf{e}}\right)dz - \mathbf{s}_e \tag{7.31}$$

The specific discharge (7.26), can alternately be expressed in terms of the effective stress

$$q = \frac{K}{g\mathbf{r}_w}\,\P_z\mathbf{s}_e - \left(\frac{\mathbf{r}_s}{\mathbf{r}_w}-1\right)K\P_z\left(\int_z^{z_b}\left(\frac{1}{1+\mathbf{e}}\right)dz\right) \tag{7.32}$$

or the void ratio

$$q = \frac{K}{g\mathbf{r}_w}\left(\frac{d\mathbf{s}_e}{d\mathbf{e}}\right)\P_z\mathbf{e} - \left(\frac{\mathbf{r}_s}{\mathbf{r}_w}-1\right)K\P_z\left(\int_z^{z_b}\left(\frac{1}{1+\mathbf{e}}\right)dz\right) \tag{7.33}$$

where $d\mathbf{e}/d\mathbf{s}_e$ is a coefficient of compressibility.

For consistency with the Lagrangian representation of sediment mass conservation, a new vertical coordinate $\mathbf{z}$, defined by

$$\frac{d\mathbf{z}}{dz} = \frac{1}{1+\mathbf{e}} \tag{7.34}$$

is introduced. The discrete form of (7.34) is

$$\mathbf{z}_{k+} - \mathbf{z}_{k-} = \frac{z_{k+} - z_{k-}}{1+\mathbf{e}_k} = \frac{B_k}{1+\mathbf{e}_k} = \Delta_k \tag{7.35}$$

where D is the equivalent sediment thickness previously defined by (7.24). Introducing (7.34) into (7.26), (7.32), and (7.33) gives

$$q = -\frac{K}{g\mathbf{r}_w(1+\mathbf{e})}\,\P_z u \tag{7.36}$$

$$q = \frac{K}{g\mathbf{r}_w(1+\mathbf{e})}\,\P_z\mathbf{s}_e + \left(\frac{\mathbf{r}_s}{\mathbf{r}_w}-1\right)\frac{K}{(1+\mathbf{e})} \tag{7.37}$$

$$q = \mathbf{l}\left(\frac{K}{1+\mathbf{e}}\right)\P_z\mathbf{e} + \left(\frac{\mathbf{r}_s}{\mathbf{r}_w}-1\right)\left(\frac{K}{1+\mathbf{e}}\right) \tag{7.38}$$

where

$$\mathbf{l} = \frac{1}{g\mathbf{r}_w}\frac{d\mathbf{s}_e}{d\mathbf{e}} \tag{7.39}$$

is a compressibility length.

Three formulations for the solution the consolidation problem can be utilized. The void ratio-excess pore pressure formulation, used in the EFDC model, evaluates the specific discharges at the current time level n, using (7.36) and explicitly integrates (7.25)

$$e_k^{n+1} = e_k^n + \frac{q}{\Delta_k^n}\left(q_{w:k-} - q_{w:k+} + d(k,k_b)(e_k - e_b)\min\left(\frac{J_{sb}}{r_s},0\right)\right)^n \qquad (7.40)$$

where q is the time step, to give the new time level void ratios. The layer thicknesses are then determined by explicit integration of (7.18).

$$\left(\frac{B}{1+e}\right)_k^{n+1} = \left(\frac{B}{1+e}\right)_k^n - qd(k,k_b)\frac{J_{sb}}{r_s}$$

$$\Delta_k^{n+1} = \Delta_k^n - qd(k,k_b)\frac{J_{sb}}{r_s} \qquad (7.41)$$

Constitutive equations required for consolidation prediction generally express the effective stress and hydraulic conductivity as functions of the void ratio. Thus the new time level void ratio is used to determine new time level values of the effective stress and hydraulic conductivity. The new time level excess pore pressures is then given by

$$u = gr_w\left(\frac{r_s}{r_w} - 1\right)(z_b - z) - s_e \qquad (7.42)$$

the transformed equivalent of (7.31). The primary advantage of the void ratio-excess pore pressure formulation is the simplicity of its boundary conditions

$$u = u_b : z = z_b \qquad (7.43)$$

$$u = u_o : z = 0$$
$$or$$
$$q = q_o : z = 0 \qquad (7.44)$$

The water column-sediment bed interface boundary condition generally sets u_b to zero if the surface water flow is hydrostatic but can incorporate wave induced pore pressures. The bottom boundary conditions allows either the specification of pressure or specific discharge. The primary disadvantage of this formulation is the stability or positivity criterion imposed on the time step

$$q \leq \frac{\Delta_k^n e_k^n}{\left(q_{w:k+} - q_{w:k-} + d(k,k_b)(e_b - e_k)\min\left(\frac{J_{sb}}{r_s},0\right)\right)^n} \qquad (7.40)$$

$$q \le \frac{\Delta_k^n}{d(k,k_b)\max\left(\frac{J_{sb}}{r_s},0\right)} \tag{7.41}$$

In practice, these criteria are readily satisfied if the consolidation time step is identical to the time step of the hydrodynamic model. In the event that these criteria are not met using the hydrodynamic time step, the bed consolidation is sub-cycled using an integer number of time steps, meeting (7.40) and (7.41), per each hydrodynamic time step.

Alternately, the consolidation problem can be directly formulated in terms of the effective stress or void ratio. Combining (7.25) and (7.37) using (7.39) gives the effective stress formulation

$$\Delta_k \P_t e_k = \left\{ \mathbf{1}\left(\frac{K}{1+e}\right) \P_z e + \left(\frac{r_s}{r_w}-1\right)\left(\frac{K}{1+e}\right) \right\}_{k-}$$

$$-\left\{ \mathbf{1}\left(\frac{K}{1+e}\right) \P_z e + \left(\frac{r_s}{r_w}-1\right)\left(\frac{K}{1+e}\right) \right\}_{k+} + d(k,k_b)(e_k - e_b)\min\left(\frac{J_{sb}}{r_s},0\right) \tag{7.42}$$

The continuum equivalent is

$$\frac{1}{\mathbf{1}} \P_t s_{e:k} = -\P_z\left(\frac{K}{(1+e)} \P_z s_e + g(r_s - r_w)\frac{K}{(1+e)}\right)$$

$$+ g r_w d(z_b)(e_k - e_b)\min\left(\frac{J_{sb}}{r_s},0\right) \tag{7.43}$$

which is parabolic since λ is negative. Combining (7.25) and (7.38) using (7.39) gives the void ration formulation

$$\Delta_k \P_t e_k = \left\{ \mathbf{1}\left(\frac{K}{1+e}\right) \P_z e + \left(\frac{r_s}{r_w}-1\right)\left(\frac{K}{1+e}\right) \right\}_{k-}$$

$$-\left\{ \mathbf{1}\left(\frac{K}{1+e}\right) \P_z e + \left(\frac{r_s}{r_w}-1\right)\left(\frac{K}{1+e}\right) \right\}_{k+} + d(k,k_b)(e_k - e_b)\min\left(\frac{J_{sb}}{r_s},0\right) \tag{7.44}$$

The continuum equivalent is

$$\P_t e_k = -\P_z\left(\mathbf{1}\left(\frac{K}{1+e}\right) \P_z e + \left(\frac{r_s}{r_w}-1\right)\left(\frac{K}{1+e}\right)\right) + d(z_b)(e_k - e_b)\min\left(\frac{J_{sb}}{r_s},0\right) \tag{7.45}$$

Equation (7.45) is the discrete form of the finite strain consolidation equation first derived by Gibson et al. (1967). Equation (7.45) was used by Cargill (1985) in the formulation of a model for dredge material consolidation and by Le Normant (1998) to represent bed consolidation in a three-dimensional cohesive sediment transport model.

The classic linear consolidation equation (Middleton and Wilcock, 1994) omits the second term associated with self weight in (7.45) and introduces a constant consolidation coefficient

$$C_c = -(1+e)\frac{\partial s_e}{\partial e}\frac{K}{g\rho_w} \qquad (7.46)$$

reducing (7.45) to

$$\partial_t e = C_c \partial_{zz} e \qquad (7.47)$$

Equation (7.47) has separable solutions of the form

$$e = f_n(z)\exp\left(-\lambda_n\frac{C_c}{B^2}t\right)$$
$$\partial_{zz}f_n + \lambda_n f_n = 0 \qquad (7.48)$$
$$z = \frac{z}{B}$$

which provides some justification for empirical relationship (7.20).

The solution of the finite strain consolidation problem in any of its three forms requires constitutive relationships

$$s_e = s_e(e) \qquad (7.49)$$

$$K = K(e) \qquad (7.50)$$

Bear (1979) notes that curve fitting of experimental data typically results in relationships of the form

$$e - e_o = -a_v(s_e - s_{eo}) \qquad (7.51)$$

$$e - e_o = -C_c \ln\left(\frac{s_e}{s_{eo}}\right) \qquad (7.52)$$

for noncohesive and coheasive soils respectively, where a_v is the coefficient of compressibility and C_c is the compression index. Graphical presentation of experimental forms of (7.49) and (7.50) are presented in Cargill (1985) and Palermo et al., (1998) which are generally consistent with (7.52) and suggest

$$e - e_o \propto \ln\left(\frac{K}{K_o}\right) \qquad (7.53)$$

as a candidate relationship between the void ratio and hydraulic conductivity for cohesive sediment beds. Similarly, a linear relationship

$$e - e_o \propto K - K_o \qquad (7.54)$$

would likely suffice for noncohesive sediment beds.

8. References

Ackers, P., and W. R. White, 1973: Sediment transport: New approaches and analysis. *J. Hyd. Div. ASCE*, **99**, 2041-2060.

Ariathurai, R., and R. B. Krone, 1976: Finite element model for cohesive sediment transport. *J. Hyd. Div. ASCE*, **102**, 323-338.

Ambrose, R. B., T. A. Wool, and J. L. Martin, 1993: The water quality analysis and simulation program, WASP5: Part A, model documentation version 5.1. U. S. EPA, Athens Environmental Research Laboratory, 210 pp.

Bear, J., 1879: *Hydraulics of groundwater*, McGraw-Hill, New York.

Bagnold, R. A., 1956: The flow of cohesionless grains in fluids. *Phil. Trans. Roy. Soc. Lond.,* Series A, Vol **249**, No. 964, 235-297.

Blumberg, A. F., B. Galperin, and D. J. O'Connor, 1992: Modeling vertical structure of open-channel flow. *J. Hydr. Engr.*, **118**, 1119-1134.

Boyer, J. M., S. C. Chapra, C. E. Ruiz, and M. S. Dortch, 1994: RECOVERY, a mathematical model to predict the temporal response of surface water to contaminated sediment. Tech. Rpt. W-94-4, U. S. Army Engineer Waterways Experiment Station, Vicksburg, MS, 61 pp.

Burban, P. Y., W. Lick, and J. Lick, 1989: The flocculation of fine-grained sediments in estuarine waters. *J. Geophys. Res.*, **94**, 8323-8330.

Burban, P. Y., Y. J. Xu, J. McNeil, and W. Lick, 1990: Settling speeds of flocs in fresh and seawater. *J. Geophys. Res.*, **95**, 18,213-18,220.

Cargill, K. W., 1985: Mathematical model of the consolidation and desiccation processes in dredge material. U.S. Army Corps of Engineers, Waterways Experiment Station, Technical Report D-85-4.

Dortch, M., C. Ruiz, T. Gerald, and R. Hall, 1998: Three-dimensional contaminant transport/fate model. *Estuarine and Coastal Modeling, Proceedings of the 5nd International Conference*, M. L. Spaulding and A. F. Blumberg, Eds., American Society of Civil Engineers, New York, 75-89.

Einstein, H. A., 1950: The bed load function for sediment transport in open channel flows. *U.S. Dept. Agric. Tech. Bull.*, 1026.

Galperin, B., L. H. Kantha, S. Hassid, and A. Rosati, 1988: A quasi-equilibrium turbulent energy model for geophysical flows. *J. Atmos. Sci.,* **45**, 55-62.

Garcia, M., and G. Parker, 1991: Entrainment of bed sediment into suspension. *J. Hyd. Engrg.*, **117**, 414-435.

Gibbs, R. J., 1985: Estuarine Flocs: their size, settling velocity and density. *J. Geophys. Res.*, **90**, 3249-3251.

Gibson, R. E., G. L. England, and M. J. L. Hussey, 1967: The theory of one-dimensional consolidation of saturated clays. *Geotechnique*, **17**, 261-273.

Hamrick, J. M., 1992: A three-dimensional environmental fluid dynamics computer code: Theoretical and computational aspects. The College of William and Mary, Virginia Institute of Marine Science, Special Report 317, 63 pp.

Hamrick, J. M., and T. S. Wu, 1997: Computational design and optimization of the EFDC/HEM3D surface water hydrodynamic and eutrophication models. *Next Generation Environmental Models* and *Computational Methods.* G. Delich and M. F. Wheeler, Eds., Society of Industrial and Applied Mathematics, Philadelphia, 143-156.

Hayter, E. J., and A. J. Mehta, 1983: Modeling fine sediment transport in estuaries. Report EPA-600/3-83-045, U.S. Environmental Protection Agency. Athens, GA>

Hayter, E.J., M. Bergs, R. Gu, S. McCutcheon, S. J. Smith, and H. J. Whiteley, 1998: HSCTM-2D, a finite element model for depth-averaged hydrodynamics, sediment and contaminant transport. Technical Report, U. S. EPA Environmental Research Laboratory, Athens, GA.

Hwang, K.-N, and A. J. Mehta, 1989: Fine sediment erodibility in Lake Okeechobee. Coastal and Oeanographic Enginnering Dept., University of Florida, Report UFL/COEL-89/019, Gainsville, FL.

Laursen, E., 1958: The total sediment load of streams *J. Hyd. Div. ASCE*, **84**, 1-36.

Letter, J. V., L. C. Roig, B. P. Donnell, Wa. A. Thomas, W. H. McAnally, and S. A. Adamec, 1998: A user's manual for SED2D-WES, a generalized computer program for two-dimensional, vertically averaged sediment transport. Version 4.3 Beta Draft Instructional Report, U. S. Army Corps of Engrs., Wtrwy. Exper. Sta., Vicksburg, MS.

Le Normant, C., E. Peltier, and C. Teisson, 1998: Three dimensional modelling of cohesive sediment in estuaries. in Physics of Estuaries and Coastal Seas, (J. Dronkers and M. Scheffers, Eds.), Balkema, Rotterdam, pp 65-71.

Lick, W., and J. Lick, 1988: Aggregation and disaggregation of fine-grained lake sediments. *J Great Lakes Res.*, **14**, 514-523.

Mehta, A. J., E. J. Hayter, W. R. Parker, R. B. Krone, A. M. Teeter, 1989: Cohesive sediment transport. I: Process description. *J. Hyd. Engrg.*, **115**, 1076-1093.

Mehta, A. J., T. M. Parchure, J. G. Dixit, and R. Ariathurai, 1982: Resuspension potential of deposited cohesive sediment beds, in *Estuarine Comparisons*, V. S. Kennedy, Ed., Academic Press, New York, 348-362.

Mehta, A. J., and F. Jiang, 1990: Some field observations on bottom mud motion due to waves. Coastal and Oeanographic Enginnering Dept., University of Florida, Gainsville, FL.

Mellor, G. L., and T. Yamada, 1982: Development of a turbulence closure model for geophysical fluid problems. *Rev. Geophys. Space Phys.*, **20**, 851-875.

Meyer-Peter, E. and R. Muller, 1948: Formulas for bed-load transport. Proc. Int. Assoc. Hydr. Struct. Res., Report of Second Meeting, Stockholm, 39-64.

Middleton, G. V., and P. R. Wilcock, 1994: Mechanics in the Earth and Environmental Sciences. Cambridge University Press, Cambridge, UK.

Nielsen, P., 1992: *Coastal bottom boundary layers and sediment transport*, World Scientific, Singapore.

Park, K., A. Y. Kuo, J. Shen, and J. M. Hamrick, 1995: A three-dimensional hydrodynamic-eutrophication model (HEM3D): description of water quality and sediment processes submodels. The College of William and Mary, Virginia Institute of Marine Science. Special Report 327, 113 pp.

Rahmeyer, W. J., 1999: Lecture notes for CEE5560/6560: Sedimentation Engineering, Dept. of Civil and Environmental Engineering, Utah State University, Logan, Utah.

Raukivi, A. J., 1990: *Loose boundary hydraulics*. 3rd Ed. Pergamon, New York, NY.

Ried, I., and L. E. Frostick, 1994: Fluvial sediment transport and deposition. in *Sediment Transport and Depositional Processes*, K. Pye, ed., Blackwell, Oxford, UK, 89-155.

Shrestha, P. A., and G. T. Orlob, 1996: Multiphase distribution of cohesive sediments and heavy metals in estuarine systems. *J. Environ. Engrg.*, **122**, 730-740.

Smagorinsky, J., 1963: General circulation experiments with the primative equations, Part I: the basic experiment. *Mon. Wea. Rev.*, **91**, 99-152.

Smith, J. D., and S. R. McLean , 1977: Spatially averaged flow over a wavy bed. *J. Geophys. Res.*, **82**, 1735-1746.

Smolarkiewicz, P. K., and T. L. Clark, 1986: The multidimensional positive definite advection transport algorithm: further development and applications. *J. Comp. Phys.*, **67**, 396-438.

Smolarkiewicz, P. K., and W. W. Grabowski, 1990: The multidimensional positive definite advection transport algorithm: nonoscillatory option. *J. Comp. Phys.*, **86**, 355-375.

Spasojevic, M., and F. M. Holly, 1994: Three-dimensional numerical simulation of mobile-bed hydrodynamics. Contract Report HL-94-2, US Army Engineer Waterways Experiment Station, Vicksburg, MS.

Stark, T. D., 1996: Program documentation and users guide: PSDDF primary consolidation, secondary compression, and desiccation of dredge fill. Instructional Report EL-96-xx, US Army Engineer Waterways Experiment Station, Vicksburg, MS.

Suzuki, K., H. Yamamoto, and A. Kadota, 1998: Mechanism of bed load fluctuations of sand-gravel mixture in a steep slope channel, Proc. of the 11th congress of APD IAHR, Yogyakarta, pp.679-688.

Tsai, C. H., S. Iacobellis, and W. Lick, 1987: Floccualtion fo fine-grained lake sediments due to a uniform shear stress. *J Great Lakes Res.*, **13**, 135-146.

van Niekerk, A., K. R. Vogel, R. L Slingerland, and J. S. Bridge, 1992: Routing of heterogeneous sedimetns over movable bed: Model development. *J. Hyd. Engrg.*, **118**, 246-262.

Van Rijin, L. C., 1984a: Sediment transport, Part I: Bed load transport. *J. Hyd. Engrg.*, **110**, 1431-1455.

Van Rijin, L. C., 1984b: Sediment transport, Part II: Suspended load transport. *J. Hyd. Engrg.*, **110**, 1613-1641.

Villaret, C., and M. Paulic, 1986: Experiments on the erosion of deposited and placed cohesive sediments in an annular flume and a rocking flume. Coastal and Oeanographic Enginnering Dept., University of Florida, Report UFL/COEL-86/007, Gainsville, FL.

Ziegler, C. K., and B. Nesbit, 1994: Fine-grained sediment transport in Pawtuxet River, Rhode Island. *J. Hyd. Engrg.*, **120**, 561-576.

Ziegler, C. K., and B. Nesbit, 1995: Long-term simulation of fine-grained sediment transport in large reservoir. *J. Hyd. Engrg.*, **121**, 773-781.

Yang, C. T., 1973: Incipient motion and sediment transport. *J. Hyd. Div. ASCE*, **99**, 1679-1704.

Yang, C. T., 1984: Unit stream power equation for gravel. *J. Hyd. Engrg.*, **110**, 1783-1797.

Yang, C. T., and A. Molinas, 1982: Sediment transport and unit streams power function. *J. Hyd. Div. ASCE*, **108**, 774-793.

9. Figures
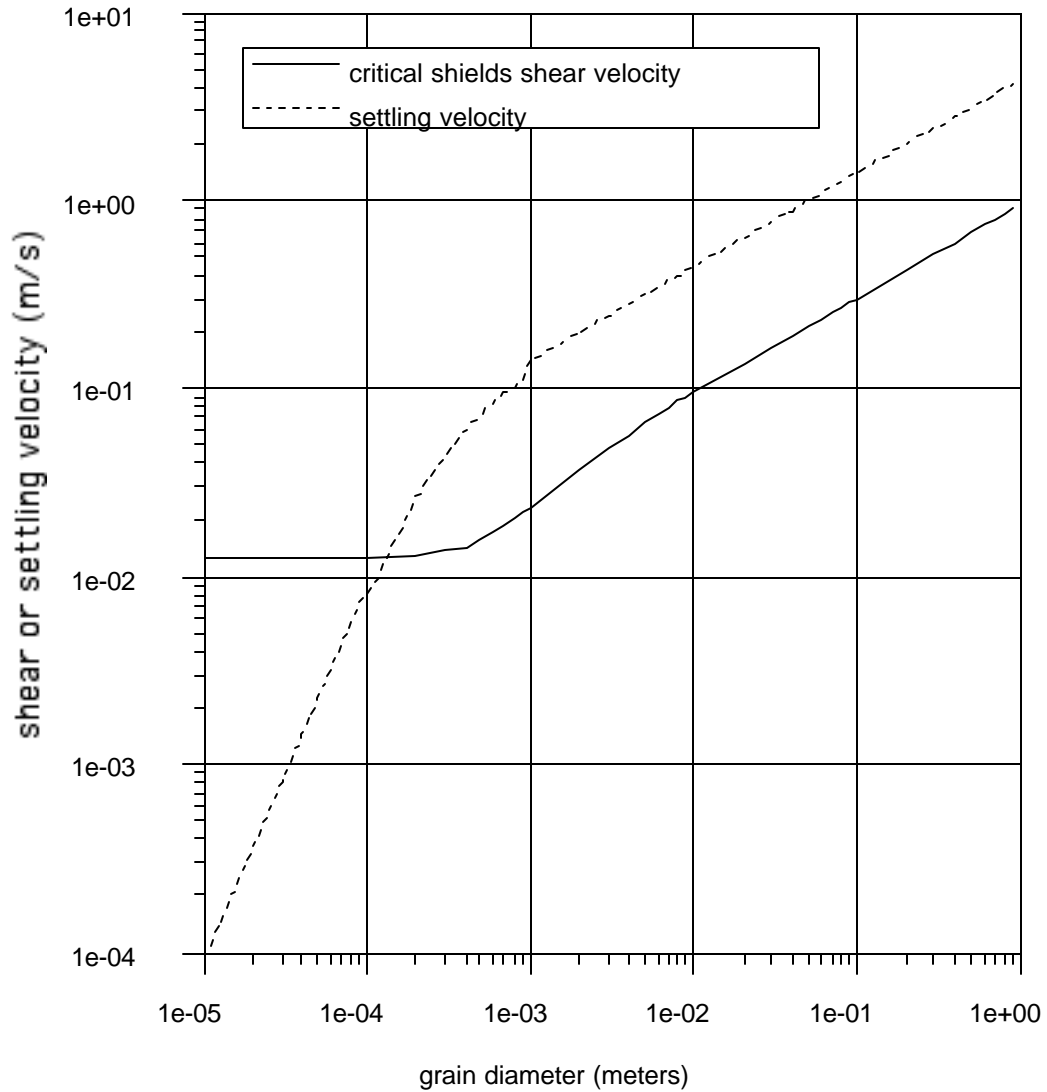
Figure 1. Critical Shield's shear velocity and settling velocity as a function of sediment grain size.

APPENDIX D

AQUATOX MODEL

D.1 AQUATOX Model Description

D.2 AQUATOX Parameter List

APPENDIX D.1

AQUATOX MODEL DESCRIPTION

TABLE OF CONTENTS

Section	Page

APPENDIX D

AQUATOX MODEL DESCRIPTION

INTRODUCTION

AQUATOX is a general ecological risk assessment model that represents the combined environmental fate and effects of conventional pollutants, such as nutrients, and sediments and toxic chemicals in aquatic ecosystems. This model considers several trophic levels, including attached and planktonic algae and submerged aquatic vegetation, invertebrates, and forage, bottom-feeding, and piscivorous (game) fish. This model also represents associated organic toxicants (Figure 1). AQUATOX can be implemented as a simple model (indeed, it has been used to simulate an abiotic flask) or as a truly complex food-web model. Often it is desirable to model a food web rather than a food chain, for example, to examine the possibility of less tolerant organisms being replaced by more tolerant organisms as environmental perturbations occur. "Food web models provide a means for validation because they mechanistically describe the bioaccumulation process and ascribe causality to observed relationships between biota and sediment or water" (Connolly and Glaser, 1998).

AQUATOX has been implemented for streams, small rivers, ponds, lakes, and reservoirs. This model is intended to be used to evaluate the bioaccumulation of organic contaminants and the effects of various stressors including potentially toxic organic chemicals, nutrients, organic wastes, sediments, and temperature. The stressors may be considered individually or together.

The fate portion of this model, which is applicable especially to organic toxicants, includes: partitioning among organisms, suspended and sedimented detritus, suspended and sedimented inorganic sediments, and water; volatilization; hydrolysis; photolysis; ionization; and microbial degradation. The effects portion of the model includes chronic and acute toxicity to the various organisms modeled and indirect effects such as release of grazing and predation pressure, increase in detritus and recycling of nutrients from killed organisms, dissolved oxygen sag due to increased decomposition, and loss of food base for animals.

AQUATOX represents the aquatic ecosystem by simulating the changing concentrations (in mg/L or g/m^3) of organisms, nutrients, chemicals, and sediments in a unit volume of water (**Figure 1**). As such, AQUATOX differs from population models, which represent the changes in numbers of individuals. As O'Neill et al. (1986) stated, ecosystem models and population models are complementary; one cannot take the place of the other. Population models excel at modeling individual species at risk and modeling fishing pressure and other age/size-specific aspects; but recycling of nutrients, the combined fate and effects of toxic chemicals, and other interdependencies in the aquatic ecosystem are important aspects that AQUATOX represents and that cannot be addressed by a population model.

Figure 1. Conceptual Model of Ecosystem Represented by AQUATOX
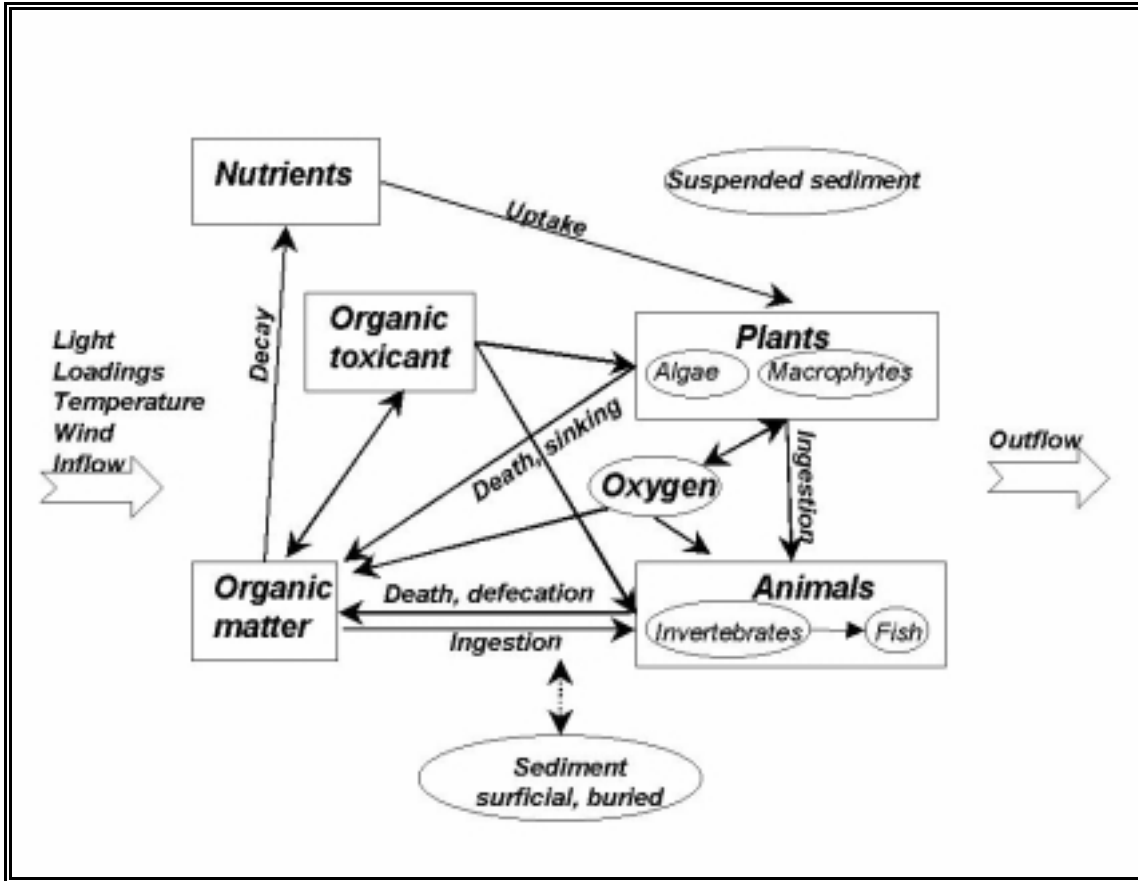
Any ecosystem model consists of multiple components requiring input data. These are the abiotic and biotic **state variables** or compartments being simulated (**Figure 2**). In AQUATOX, the biotic state variables may represent trophic levels, guilds, and/or species. This model can represent a food web with both detrital- and algal-based trophic linkages. Closely related are **driving variables**, such as temperature, light, and nutrient loadings, which force the system to behave in certain ways. In AQUATOX, state variables and driving variables are treated similarly in the code. This provides flexibility because external loadings of state variables, such as phytoplankton carried into a reach from upstream, may function as driving variables; and driving variables, such as pH and temperature, could be treated as dynamic state variables in a future implementation. Constant, dynamic, and multiplicative loadings can be specified for atmospheric, point and nonpoint sources. Loadings of pollutants can be turned off to obtain a **control** simulation for comparison with the **perturbed** simulation.

Figure 2 Compartments (State Variables) in AQUATOX

Phosphate	**Ammonia**	**Nitrate and Nitrate**	**Carbon Dioxide**	**Oxygen**

Filamentous Algae and Duckweed *Toxicant*	**Phytoplankton** *Toxicant*	**Periphyton** *Toxicant*	**Rooted Macrophyte** *Toxicant*
Zoobenthos Gatherer/Filterer midges, sphaerids, oligochaetes *Toxicant*	**Zoobenthos Grazer/Shredder** mayflies, snails *Toxicant*	**Herbivorous Zooplankton** cladocerans *Toxicant*	**Predatory Invertebrate** dragonflies, crayfish *Toxicant*
Bottom Fish carp/goldfish brown bullhead, white suckers *Toxicant*	**Forage Fish** shiner, pumpkinseed *Toxicant*	**Piscivore** yellow perch *Toxicant*	**Multi-Aged Piscivore** bass *Toxicant*
Dissolved Organic Matter *Toxicant*	**Dissolved Organic Toxicants (up to 20)**		**Suspended Detritus** *Toxicant*

Sediment Detritus *Toxicant*	**Suspended and Sedimented Cohesive Inorganics** *Toxicant*	**Dissolved and Colloidal Pore Water Toxicants**	**Suspended and Sedimented Noncohesive Inorganics** *Toxicant*	**Noncohesive Inorganic Bedload** *Toxicant*

00M-0320 USEPA GE.ppt

AQUATOX is written in object-oriented Pascal using the Delphi programming system for Windows[TM]. An object is a unit of computer code that can be duplicated, and the object's parameters and procedures can be inherited by higher-level objects. For example, the plant object, including variables such as the *PMax* (maximum photosynthesis rate) and process functions such as photosynthesis, is inherited by the algal object; that is, enhanced by plant-specific variables and functions and duplicated for several kinds of algae. It can also be inherited and modified slightly for macrophytes. This modularity forms the basis for the flexibility of the model, including the ability to add and delete given state variables interactively.

AQUATOX uses **differential equations** to represent changing values of state variables, normally with a reporting time step of one day. These equations require starting values or **initial conditions** for the beginning of the simulation. If the first day of a simulation is changed, then the initial conditions may need to be changed. A simulation can begin with any date and may be for any length of time from a few days, corresponding to a microcosm experiment, to decades.

The **process equations** contain another class of input variables: the **parameters** or coefficients that allow the user to specify key process characteristics. For example, the maximum consumption rate is a critical parameter characterizing various consumers. AQUATOX is a mechanistic model with many parameters; however, default values are available so that the modeler has to be concerned only with those parameters necessary for a specific risk analysis, such as characterization of a new chemical. In the pages that follow, differential equations for the state variables will be followed by process equations and parameter definitions.

Usually the reporting time step is one day, but numerical instability is avoided by allowing the step size of the integration to vary to achieve a predetermined accuracy in the solution; this is a numerical approach, and the step size is not directly related to the temporal scale of the ecosystem simulation. AQUATOX uses a fourth- and fifth-order Runge-Kutta integration routine with adaptive step size to solve the differential equations (Press et al., 1986). The routine uses the fifth-order solution to determine the error associated with the fourth-order solution; it decreases the step size (often to 15 minutes or less) when rapid changes occur and increases the step size when there are slow changes, such as in winter. However, the step size is constrained to a maximum of one day so that short-term pollutant loadings are always detected.

BACKGROUND

AQUATOX is the latest in a series of models, starting with the aquatic ecosystem model CLEAN (Park et al., 1974) and subsequently improved in consultation with numerous researchers at various European hydrobiological laboratories, resulting in the CLEANER series (Park et al., 1975, 1979; Park, 1978; Scavia and Park, 1976; Park, Collins, et al., 1980) and LAKETRACE (Collins and Park, 1989). The MACROPHYTE model, developed for the U.S. Army Corps of Engineers (Collins et al., 1985), provided additional capability for representing submersed aquatic vegetation. Another series started with the toxic fate model PEST, developed to complement CLEANER (Park, Connolly, et al., 1980, 1982), and continued with the TOXTRACE model (Park, 1984) and the spreadsheet equilibrium fugacity PART model.

AQUATOX combined algorithms from these models with ecotoxicological constructs, and additional code was written as required for a truly integrative fate and effects model (Park, 1990, 1993). AQUATOX was then restructured and linked to Microsoft Windows™ interfaces to provide greater flexibility, capacity for additional compartments, and user friendliness. AQUATOX has also been improved with the addition of constructs for chronic effects and uncertainty analysis, making this model a powerful tool for probabilistic risk assessment. AQUATOX has been validated, documented, and released by the U.S. Environmental Protection Agency (2000a, 2000b, 2000c).

Recently, AQUATOX was enhanced by doubling the number of biotic state variables so that each guild or taxonomic group could be represented by tolerant and intolerant species. Elimination of organic chemicals by organisms was also split into depuration and biotransformation. For the Housatonic River project, AQUATOX was expanded to simulate 20 chemicals simultaneously, with transformations from one to another, and to model as many as 15 age classes of one game fish and two size classes for all other fish species. AQUATOX was also made spatially explicit to model linked river tributaries, reaches, and backwater areas.

SPATIAL REPRESENTATION

AQUATOX can link several segments into one larger system. Segments can be joined in two ways. The first is a unidirectional linkage, referred to as a "cascade" link. In this case, water flows in only one direction, and there is no feedback from the lower segment to the upper segment. Segments that are linked together in this manner are solved separately from one another. The upstream segment outflow is treated as a loading into the downstream segment, along with any dissolved or particulate matter within that outflow.

The second way in which two segments can be linked is called a "feedback" link. In this case, water can flow in both directions over a segment boundary or there can be a circular link between segments. Diffusion of dissolved and suspended state variables also occurs between segments (see Equation **(5)**). Segments that are linked together as feedback segments are solved simultaneously as one large system of interacting state variables.

Simulations can include a mixture of cascade and feedback links. Only one group of segments can be linked with feedback links. However, cascade links can lead into and out of this feedback system. AQUATOX first solves all cascade segments upstream of the feedback system. Then, the feedback system of segments is solved. Finally, AQUATOX solves all segments that remain downstream of the feedback segments.

In the linked version of AQUATOX, stratification does not occur dynamically based on system characteristics. Instead, two segments can be characterized as epilimnion and hypolimnion by the user and they must also be linked together with a feedback link. These segments will then act as though they are stratified and linked throughout the simulation.

Bathymetric Approximations

The depth distribution of a water body is important because it determines the areas and volumes subject to mixing and light penetration. Within AQUATOX, a user is given a choice of employing general bathymetric relationships to represent the morphometry of an ecosystem. When simulating a river, a user often will not find the bathymetric equations to be relevant and so will choose not to employ them. One possible exception would be an impoundment within a riverine system.

When the user chooses to employ bathymetric equations, the shapes of ponds, lakes, and reservoirs are represented by idealized geometrical approximations, following the topological treatment of Junge (1966; see also Straškraba and Gnauck, 1985).

When a user chooses not to employ bathymetric equations, AQUATOX assumes that a segment is essentially represented by a given surface area. All the water and sediment below the given area make up the model segment. Because of this, a few simple equations are implied:

$$ZMean = \frac{Volume}{SurfaceArea} \tag{1}$$

where:
$ZMean$ = mean depth (m);
$Volume$ = volume of water (m^3); and
$SurfaceArea$ = surface area of system (m^2).

Also, when bathymetry is not used, the euphotic zone is defined as follows:

$$FracLittoral = \frac{ZEuphotic}{ZMean} \tag{2}$$

where:

FracLittoral	=	fraction of site area that is within the euphotic zone (unitless);
ZEuphotic	=	depth of the euphotic zone, where primary production exceeds respiration, usually calculated as a function of extinction (m); and
ZMean	=	mean depth (m).

Washout and Wash-in

Transport out of the system, or washout, is an important loss term for nutrients, floating organisms, and dissolved toxicants in reservoirs and streams. Although it is considered separately for several state variables, the process is a general function of discharge:

$$Washout = \frac{Discharge}{Volume} \cdot State \qquad (3)$$

where:

Washout	=	loss due to being carried downstream ($g/m^3 \cdot d$), and
State	=	concentration of dissolved or floating state variable (g/m^3).

In a linked system, "wash-in" can occur, which is the transport of state variables into the current segment from an upstream segment due to moving water. When two segments are joined with a cascade link, the washout of the upper segment is saved for each day and used as a loading into the lower segment. When two segments are linked with a feedback link, wash-in is calculated as follows:

$$Washin = \sum\nolimits_{inlinks} (Washout_{upstream} \cdot FracWashThisLink \cdot \frac{UpStreamVolume}{Volume}) \qquad (4)$$

where:

Washin	=	gain from all upstream segments ($g/m^3 \cdot d$);
inlinks	=	all upstream segments linked directly to this one;
Washout$_{upstream}$	=	washout of this variable from one upstream segment (g/m^3);
FracWashThisLink	=	fraction of total discharge from that segment that goes to this segment;
UpStreamVolume	=	volume of the upstream segment (m^3); and
Volume	=	volume of this segment (m^3).

Stratification and Mixing

Thermal stratification is handled in the simplest form consistent with the goals of forecasting the effects of nutrients and toxicants. Reservoirs and lakes are considered in the model to have two vertical zones: epilimnion and hypolimnion; the metalimnion zone that separates these is ignored. Instead, the thermocline, or plane of maximum temperature change, is taken as the separator; this is also known as the mixing depth (Hanna, 1990).

In a linked-mode run, stratification is defined as a condition of the system by defining one segment as the epilimnion and another linked segment as the hypolimnion. The dynamics of the system are then controlled by user input data for flow and diffusion over the thermocline. When a system is linked, diffusion between the epilimnion and hypolimnion is treated the same as diffusion between any two segments:

$$Diffusion = \frac{\frac{DispCoeff \cdot Area}{Length} \cdot (OtherSegConc - ThisConc)}{Volume} \qquad (5)$$

where:

Diffusion	=	diffusion between two segments ($g/m^3 \cdot d$);
DispCoeff	=	dispersion coefficient (m^2 /d);
Area	=	area of interface between two segments (m^2);
Length	=	characteristic length of interface (m);
OtherSegConc	=	concentration of given compartment in other segment (g/m^3);
ThisConc	=	concentration of given compartment in this segment (g/m^3); and
Volume	=	volume of given segment (m^3).

BIOTA

The biota consist of two main groups, plants and animals; each is represented by a set of process-level equations. In turn, plants are differentiated into algae and macrophytes, represented by slight variations in the differential equations. Algae may be either phytoplankton or periphyton. Phytoplankton are subject to sinking and washout, whereas periphyton are subject to substrate limitation and scour by currents. These are treated as process-level differences in the equations.

Animals are subdivided into invertebrates and fish; the invertebrates may be pelagic invertebrates, benthic insects, or other benthic invertebrates. These groups are represented by different parameter values and by variations in the equations. Insects are subject to emergence, but benthic invertebrates are not. Fish can be represented by two size classes, usually young-of-the-year and adults, which are connected by promotion; and one fish species can be represented by up to 15 age classes.

Algae

The change in algal biomass—expressed as g/m^3 for phytoplankton, and as g/m^2 for periphyton—is a function of the loading (especially phytoplankton from upstream), photosynthesis, respiration, excretion or photorespiration, nonpredatory mortality, grazing or predatory mortality, and washout; as noted above, phytoplankton also are subject to sinking. If the system is stratified, turbulent diffusion also affects the biomass of phytoplankton:

$$\frac{dBiomass}{dt} = Loading + Photosynthesis - Respiration - Excretion - Mortality$$
$$- Predation \pm Sinking - Washout + Washin - Floodloss \pm TurbDiff \qquad (6)$$

where:

dBiomass/dt	=	change in biomass of algae with respect to time $(g/m^3 \cdot d)$;
Loading	=	loading of algal group $(g/m^3 \cdot d)$;
Photosynthesis	=	rate of photosynthesis $(g/m^3 \cdot d)$;
Respiration	=	respiratory loss $(g/m^3 \cdot d)$;
Excretion	=	excretion or photorespiration $(g/m^3 \cdot d)$;
Mortality	=	nonpredatory mortality $(g/m^3 \cdot d)$;
Predation	=	herbivory $(g/m^3 \cdot d)$;
Washout	=	loss due to being carried downstream $(g/m^3 \cdot d)$;
Washin	=	addition from upstream $(g/m^3 \cdot d)$;
Floodloss	=	loss overbank during flood event $(g/m^3 \cdot d)$;
Sinking	=	loss or gain due to sinking between layers and sedimentation to bottom $(g/m^3 \cdot d)$; and
TurbDiff	=	turbulent diffusion $(g/m^3 \cdot d)$.

Figure 3 is an example of changes in the processes that contribute to changes in the predicted biomass in a eutrophic lake.

Figure 3
Predicted Algal Process Rates
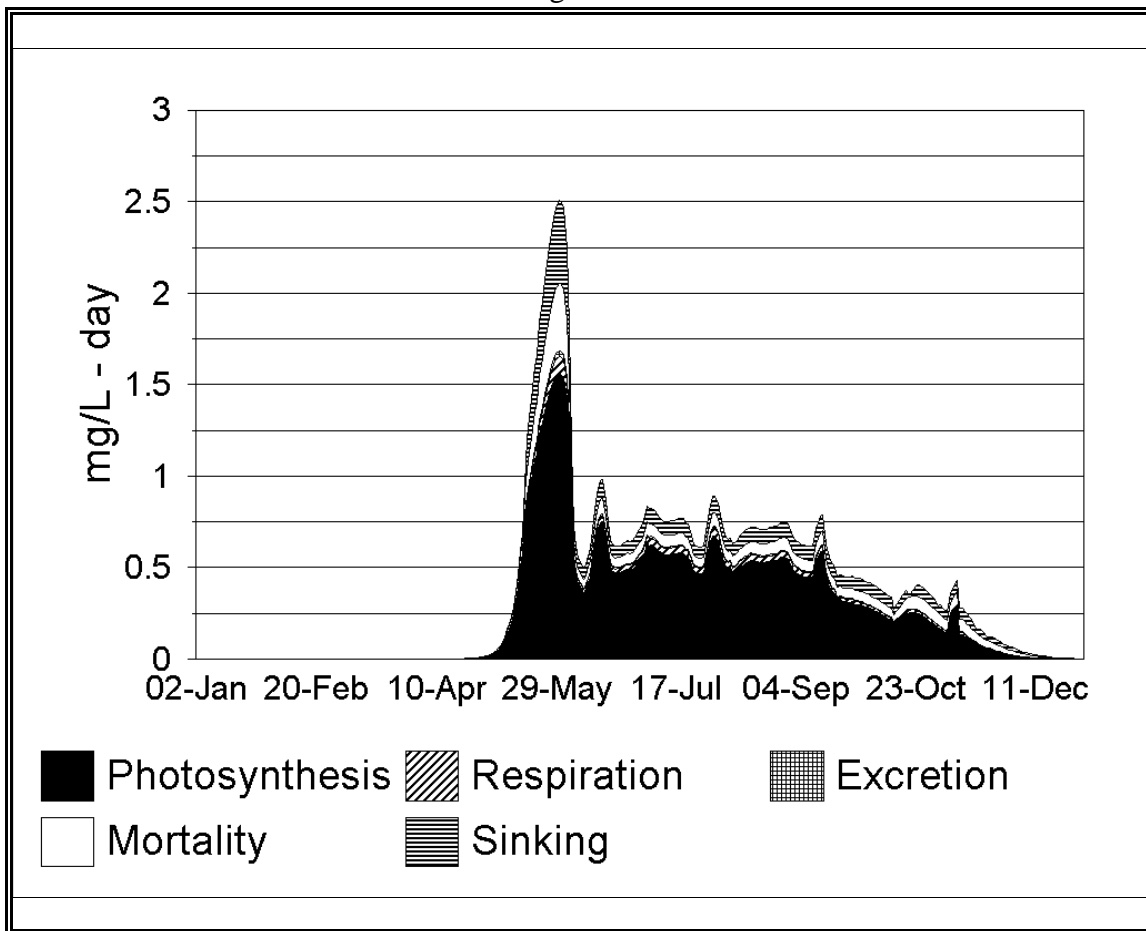
Phytoplankton are subject to downstream drift. In streams, and in lakes and reservoirs with low retention times, this may be a significant factor in reducing or even precluding phytoplankton

populations (Le Cren and Lowe-McConnell, 1980). Periphyton (and macrophytes, as discussed in the next section) also may be subject to entrainment and transport as they outgrow their substrate and as discharge increases (McIntire, 1968, 1973). Because periphyton are limited by the area of substrate available, as the biomass approaches the carrying capacity of the substrate, AQUATOX predicts that increasing quantities are dislodged and available for transport.

Macrophytes

Submerged aquatic vegetation, or macrophytes, can be an important component of shallow aquatic ecosystems. It is not unusual for the majority of the biomass in an ecosystem to be in the form of macrophytes during the growing season. Seasonal macrophyte growth, death, and decomposition can affect nutrient cycling, and detritus and oxygen concentrations; macrophytes can also sequester contaminants. By forming dense cover, they can modify habitat and provide protection from predation for invertebrates and smaller fish (Howick et al., 1993); this function is represented in AQUATOX. Macrophytes also provide direct and indirect food sources for many species of waterfowl, including ducks and coots (Jupp and Spence, 1977b).

AQUATOX represents macrophytes as occupying the littoral zone, that area of the bottom surface that occurs within the euphotic zone. Similar to periphyton, the compartment has units of g/m^2. In nature, macrophytes can be greatly reduced if phytoplankton blooms or higher levels of detritus increase the turbidity of the water (Jupp and Spence, 1977a). Because the depth of the euphotic zone is computed as a function of the extinction coefficient, the area predicted to be occupied by macrophytes can increase or decrease depending on the clarity of the water. Periphyton are epiphytic in the presence of macrophytes; by growing on the leaves, they contribute to the light extinction for the macrophytes (Sand-Jensen, 1977). Extinction due to periphyton biomass is computed in AQUATOX. The macrophyte equations are based on submodels developed for the International Biological Program (Titus et al., 1972; Park et al., 1974) and CLEANER models (Park, Collins, et al., 1980) and for the Corps of Engineers CE-QUAL-R1 model (Collins et al., 1985).

Animals

Zooplankton, benthic invertebrates, benthic insects, and fish are modeled, with only slight differences in formulations, with a generalized animal submodel that is parameterized to represent different groups:

$$
\begin{aligned}
\frac{dBiomass}{dt} &= Load + Consumption - Defecation - Respiration \\
&\quad - Excretion - Death - Predation - GameteLoss + Washin \\
&\quad - Washout - Floodloss \pm Migration - Promotion + Recruit
\end{aligned}
\tag{7}
$$

where:
dBiomass/dt	=	change in biomass of animal with respect to time ($g/m^3 \cdot d$);
Load	=	biomass loading, usually from upstream ($g/m^3 \cdot d$);
Consumption	=	consumption of food ($g/m^3 \cdot d$);
Defecation	=	defecation of unassimilated food ($g/m^3 \cdot d$);

Respiration	=	respiration $(g/m^3 \cdot d)$;
Excretion	=	excretion $(g/m^3 \cdot d)$;
Death	=	nonpredatory mortality $(g/m^3 \cdot d)$;
Predation	=	predatory mortality $(g/m^3 \cdot d)$;
GameteLoss	=	loss of gametes during spawning $(g/m^3 \cdot d)$;
Washout	=	loss due to being carried downstream by washout and drift $(g/m^3 \cdot d)$;
Washin	=	addition from upstream $(g/m^3 \cdot d)$;
Floodloss	=	loss overbank during flood event $(g/m^3 \cdot d)$;
Migration	=	loss (or gain) due to vertical migration $(g/m^3 \cdot d)$;
Promotion	=	promotion to next size class or emergence $(g/m^3 \cdot d)$; and
Recruit	=	recruitment from previous size class $(g/m^3 \cdot d)$.

The change in biomass (**Figure 4**) is a function of a number of processes (**Figure 5**) that are subject to environmental factors, including biotic interactions. Similar to the way algae are treated, parameters for different species of invertebrates and fish are loaded and available for editing by means of the entry screens.

Figure 4
Change in Animal Biomass in Stream
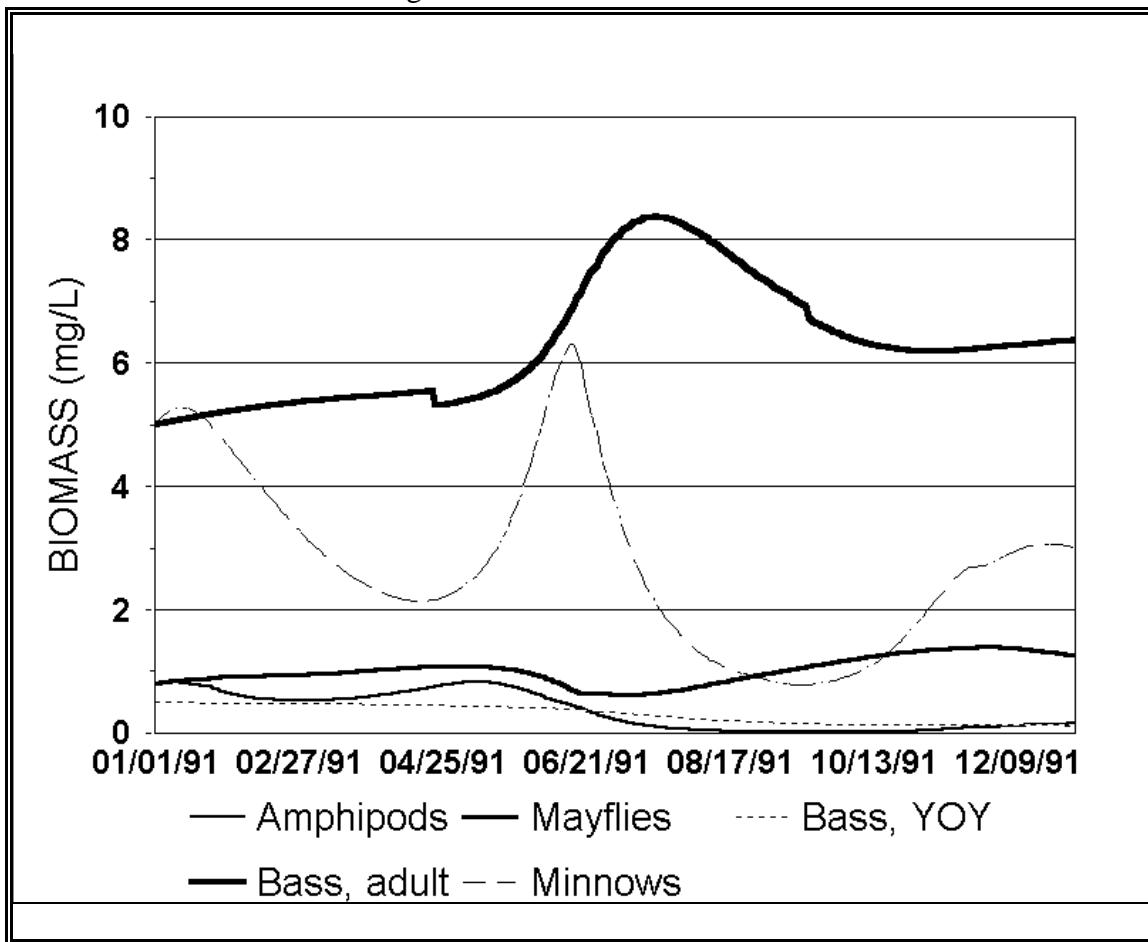
Figure 5
Mayfly Processes
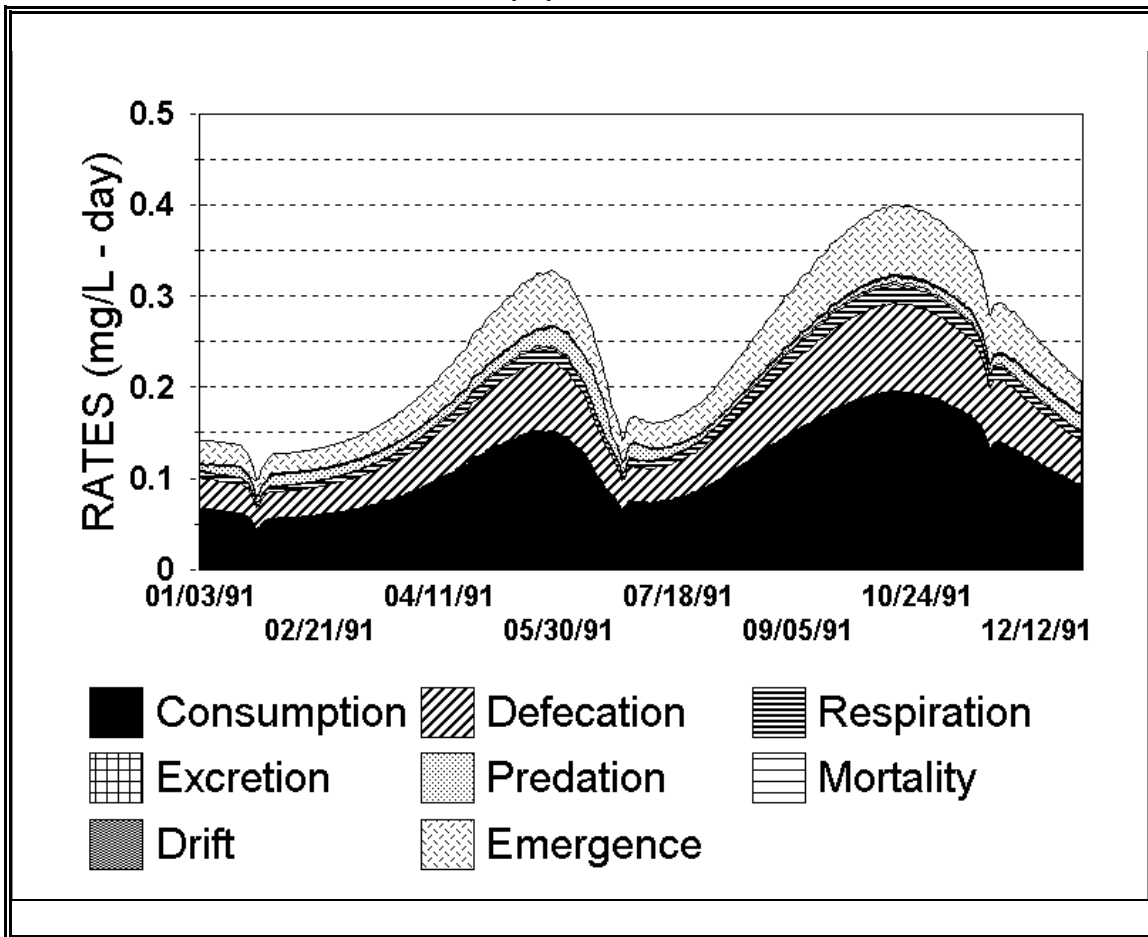
Many animals adjust their search or filtration rate in accordance with the concentration of prey; therefore, a saturation-kinetic term is used (Park et al., 1974; Scavia and Park, 1976; Park, Collins, et al., 1980):

$$SatFeeding = \frac{Preference_{prey,\,pred} \cdot Food}{\Sigma_{prey}(Preference_{prey,\,pred} \cdot Food) + FHalfSat_{pred}} \tag{8}$$

where:

$Sat\ Feeding$	=	maximum feeding factor based on food availability (unitless);
$Preference_{prey,\,pred}$	=	preference of predator for prey (unitless);
$Food$	=	available food (g/m^3); and
$FhalfSat_{pred}$	=	half-saturation constant for feeding by a predator (g/m^3).

The food actually available to a predator may be reduced in two ways:

$$Food = (Biomass_{prey} - BMin_{pred}) \cdot Refuge \tag{9}$$

where:

$Biomass_{prey}$ = concentration of organism (g/m^3 d*)*;
$BMin_{pred}$ = minimum prey biomass needed to begin feeding (g/m^3); and
Refuge   = reduction factor for prey hiding in macrophytes (unitless).

Search or filtration may virtually cease below a minimum prey biomass (*BMin*) to conserve energy, so that a minimum food level is incorporated (Parsons et al., 1969; Steele, 1974; Park et al., 1974; Scavia and Park, 1976; Scavia et al., 1976; Steele and Mullin, 1977).

Macrophytes can provide refuge from predation (Howick et al., 1993); this is represented by a factor related to the macrophyte biomass:

$$Refuge = 1 - \frac{Biomass_{Macro}}{Biomass_{Macro} + HalfSat} \qquad (10)$$

where:

HalfSat   = half-saturation constant (20 g/m^3); and
$Biomass_{Macro}$ = biomass of macrophyte (g/m^3).

AQUATOX is a food-web model with multiple potential food sources. Passive size-selective filtering and active raptorial selection occur among aquatic organisms. Relative preferences are represented in AQUATOX by a matrix of preference parameters first proposed by O'Neill (1969) and used in several aquatic models (Bloomfield et al., 1973; Park et al., 1974; Canale et al., 1976; Scavia et al., 1976). Higher values indicate increased preference by a given predator for a particular prey compared to the preferences for all possible prey. In other words, the availability of the prey is weighted by the preference factor.

The preference factors are normalized so that if a potential food source is not modeled or is below the *BMin* value, the other preference factors are modified accordingly, representing adaptive preferences:

$$Preference_{prey,pred} = \frac{Pref_{prey,pred}}{SumPref} \qquad (11)$$

where:

$Preference_{prey,pred}$ = normalized preference of given predator for given prey (unitless);
$Pref_{prey, pred}$ = initial preference value from the animal parameter screen (unitless); and
SumPref   = sum of preference values for all food sources that are present above the minimum biomass level for feeding during a particular time step (unitless).

Similarly, different prey types have different potentials for assimilation by different predators. The fraction of ingested prey that is egested as feces or discarded (and which is treated as a source of

detritus by the model) is indicated by a matrix of egestion coefficients with the same structure as the preference matrix.

Downstream transport is an important loss term for invertebrates. Zooplankton are subject to transport downstream similar to phytoplankton. Likewise, many zoobenthic invertebrates exhibit nocturnal drift. Both processes are represented in AQUATOX.

When presented with anoxic conditions, most animals will attempt to migrate to an adjacent area with more favorable conditions. The current version of AQUATOX, following the example of CLEANER (Park, Collins, et al., 1980), assumes that zooplankton and fish will exhibit avoidance behavior by migrating vertically from an anoxic hypolimnion to the epilimnion. The construct calculates the absolute mass of the given group of organisms in the hypolimnion, then divides by the volume of the epilimnion to obtain the biomass being added to the epilimnion.

Although AQUATOX is an ecosystem model, promotion to the next size class is important in representing the emergence of aquatic insects, and therefore loss of biomass from the system, and in predicting bioaccumulation of hydrophobic organic compounds in larger fish. The model assumes that promotion is determined by the rate of growth. Growth is considered to be the sum of consumption and the loss terms other than mortality and migration; a fraction of the growth goes into promotion to the next size class (cf. Park, Collins, et al., 1980). Insect emergence can be an important factor in the dynamics of an aquatic ecosystem. Often there is synchrony in the emergence; in AQUATOX this is assumed to be cued to temperature or specified by the user.

REMINERALIZATION

Detritus

The term "detritus" is used to include all non-living organic material and associated decomposers (bacteria and fungi); as such, it includes both particulate and dissolved material in the sense of Wetzel (1975), but it also includes the microflora and is analogous to "biodetritus" of Odum and de la Cruz (1963). Detritus can be modeled as dissolved, suspended, sedimented, and buried detritus (**Figure 6**). Buried detritus is considered to be taken out of active participation in the functioning of the ecosystem. In general, the mass of dissolved organic material is about 10 times that of suspended particulate matter in lakes and streams (Saunders, 1980); however, the proportions are modeled dynamically.

Figure 6
Detrital Compartments in AQUATOX
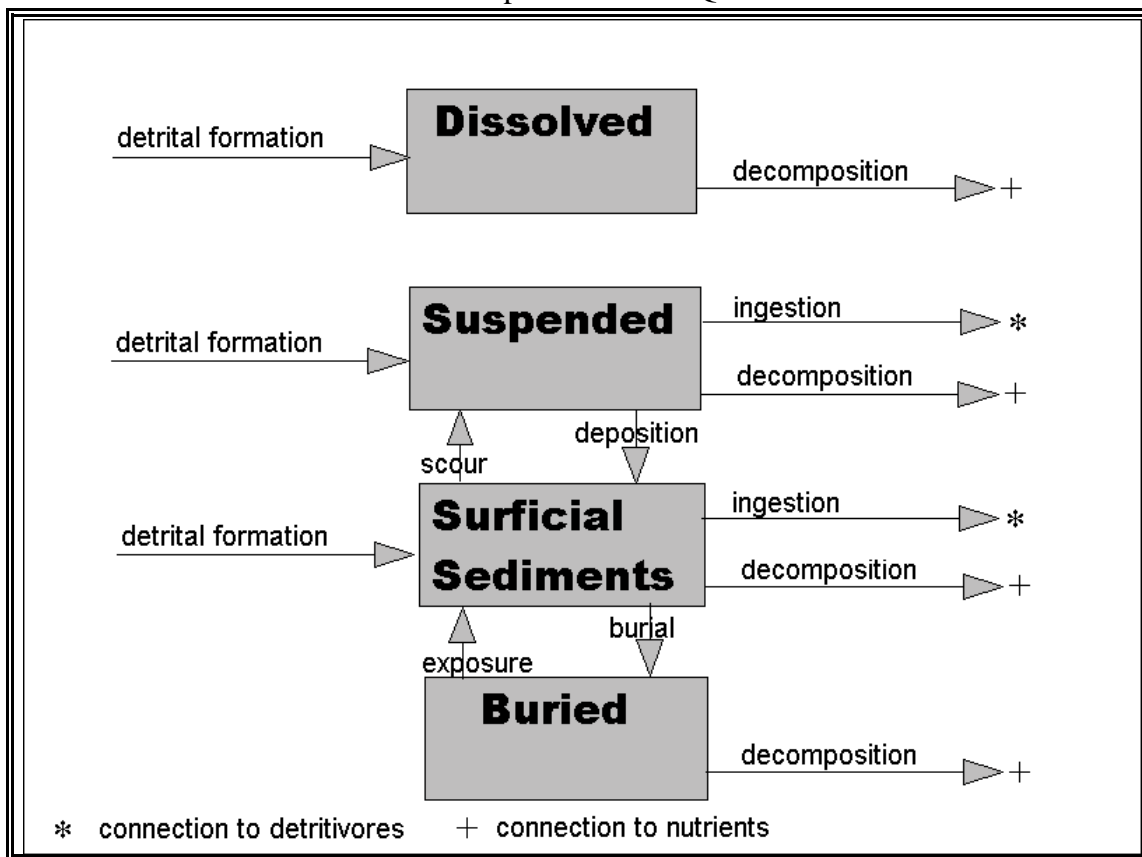
Note: Dissolved Detritus is in Water Column and Pore Water

Decomposition is the process by which detritus is broken down by bacteria and fungi, yielding constituent nutrients, including nitrogen, phosphorus, and inorganic carbon. Therefore, it is a critical process in modeling nutrient recycling. In AQUATOX, following a concept first advanced by Park et al. (1974), the process is modeled as a first-order equation with multiplicative limitations for suboptimal environmental conditions. The model accounts for both decreased and increased degradation rates under anaerobic conditions. Detritus will always decompose more slowly under anaerobic conditions; but some organic chemicals, such as some halogenated compounds (Hill and McCarty, 1967), will degrade more rapidly.

Biomass of bacteria is not explicitly modeled in AQUATOX. In some models (for example, EXAMS, Burns et al., 1982), decomposition is represented by a second-order equation using an empirical estimate of bacteria biomass. However, using bacterial biomass as a site constant constrains the model, potentially forcing the rate. Decomposers were modeled explicitly as a part of the CLEAN model (Clesceri et al., 1977). However, if conditions are favorable, decomposers can double in 20 minutes; this can result in stiff equations, adding significantly to the computational time. Ordinarily, decomposers will grow rapidly as long as conditions are favorable. The only time the biomass of decomposers might need to be considered explicitly is when a new organic chemical

is introduced and the microbial assemblage requires time to become adapted to using it as a substrate.

SEDIMENTS

Inorganic sediments are important to the functioning of natural and perturbed ecosystems for several reasons. When suspended, they increase light extinction and decrease photosynthesis. When sedimented, they can temporarily or permanently remove toxicants from the active ecosystem through deep burial. Rapid sedimentation can adversely affect periphyton and some zoobenthos. Scour can also adversely affect periphyton and zoobenthos.

AQUATOX models up to 10 bottom layers of sediment. Within each sediment layer, the state variables consist of inorganic solids, pore water, dissolved organic matter in pore water, and sedimented detritus. Each of these state variables can also have up to 20 organic toxicant concentrations associated with it. The AQUATOX sediment transport component is summarized in **Figure 7**.

For backwards compatibility, the AQUATOX model can be run without the sediment transport model included. In this case, the state variable that represents the active layer of sedimented detritus remains in the model, but there are no other state variables that represent the sediment of the system.

Figure 7. Components of the AQUATOX Sediment Transport Model and Units
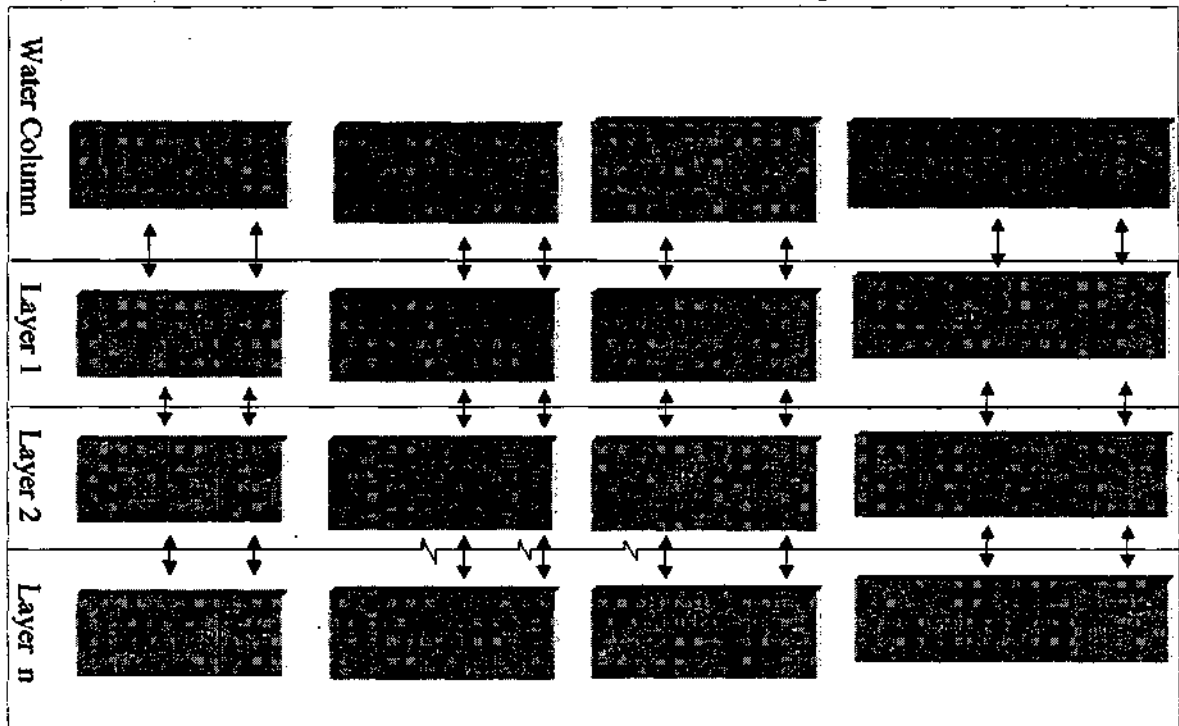
The Sediment Transport Model

Within AQUATOX, inorganic sediments are represented as three distinct state variables as defined below:

Cohesives: particle size smaller than 63 microns
Non-Cohesives: particle size from 63 to 250 microns
Non-Cohesives2: particle size greater than 250 microns

For each inorganic compartment, the sediment transport model accepts daily input parameters for interactions between the top sediment layer and the water column. These interactions are input as daily scour and daily deposition for each inorganic sediment type in units of grams per day. The model also requires deposition and erosion velocities for cohesive inorganic sediments. These inputs are then used to calculate the deposition and erosion of organic matter within the system.

AQUATOX assumes that the density of each sediment layer will remain constant throughout a simulation. Because of this, the volume and thickness of the top bed layer will vary in response to deposition and erosion.

When the top layer has reached a maximum thickness, it is broken into two layers. Other layers in the system are moved down one layer without disturbing their concentrations or thicknesses. This allows the model to maintain a contaminant-concentration gradient within the sediment layers during depositional regimes. Similarly, when the top layer has eroded to a minimum size, the layer beneath it is joined with the active layer to form a new top layer. In this case, lower layers are moved up one level, without changing their concentrations, densities, or thicknesses. More details about these processes can be found in **Sediment Interactions**, below.

At the bottom of the system, a hardpan barrier is assumed. The model, therefore, has no interaction beneath its lowest layer. If enough erosion takes place so that this hardpan barrier is exposed, no further erosion will be possible. Deposition can, however, rebuild the sediment layer system. This hardpan bottom prevents the artificial inclusion of "clean" sediment and organic matter into the simulation during erosional events. Because it is a barrier and not a boundary, it prevents loss of toxicant to the system under depositional regimes.

AQUATOX writes output data for a fixed number of sediment layers. When, due to deposition, a layer is buried below the fixed number of sediment layers, AQUATOX keeps track of that layer, but does not write daily output. When, due to erosion, there are fewer than the fixed number of sediment layers, AQUATOX writes zeros for all layers below the hardpan barrier.

Pore water moves up and down through the sediment system when layers move upward and downward in the system. Substances dissolved in pore water also move through the system as a result of diffusion.

Suspended Inorganic Sediments

As mentioned above, inorganic sediments are broken into three sets of state variables based on particle size. Each of these three inorganic sediment types is found in the water column as well as in each modeled sediment layer.

For inorganic sediments suspended in the water column, the derivative is as follows:

$$\frac{\mathrm{d}SuspSediment}{\mathrm{d}t} = Loading + Scour - Deposition$$
$$- Washout + Washin - Floodloss$$

(12)

where:

d*SuspSediment*/d*t*	=	change in concentration of suspended sediment (g/m^3·d);
Loading	=	inflow loadings (excluding upstream segments) (g/m^3·d);
Scour	=	scour from the active sediment layer (g/m^3·d);
Deposition	=	deposition to the active sediment layer (g/m^3·d);
Washout	=	loss due to being carried downstream (g/m^3·d);
Washin	=	loadings from upstream segments (g/m^3·d); and
FloodLoss	=	loss to the floodplain during a flood event (g/m^3·d).

For each of the three categories of suspended sediment, deposition to and scour from the active layer are input to AQUATOX as a daily time series in units of g/d. These inputs are converted into units of g/m^3·d by dividing by the volume of the segment.

Inorganics in the Sediment Bed

Inorganic sediments are found in each sediment layer that is modeled. The derivative for the active (top) layer is:

$$\frac{\mathrm{d}BottomSediment}{\mathrm{d}t} = Deposition - Scour + Bedload - Bedloss$$

(13)

where:

d*BottomSediment*/d*t*	=	change in concentration of sediment in this bed layer (g/m^2·d);
Deposition	=	deposition from the water column (g/m^2·d);
Scour	=	movement to the water column (g/m^2·d);
Bedload	=	bedload from all upstream segments (g/m^2·d); only relevant for the active layer of sediment; and
Bedloss	=	loss due to bedload to all downstream segments (g/m^2·d); only relevant for the active layer of sediment.

Deposition and scour are input into the model in units of g/d. These inputs are divided by the area of the system to get units of g/m^2·d.

Bedload is input as a loading in g/d for each link between two segments. This process is only relevant for the top layer of sediment modeled. The total bedload for a particular segment can be calculated by summing the loadings over all incoming links.

$$BedLoad = \sum \frac{BedLoad_{Upstreamlink}}{AvgArea} \qquad (14)$$

where:

$BedLoad$ = total bedload from all upstream segments (g/m^2·d);
$BedLoad_{Upstreamlink}$ = bedload over one of the upstream links (g/d); and
$AvgArea$ = average area of the segment (m^2).

Similarly, total bed loss is the sum of the loadings over all outgoing links:

$$BedLoss = \sum \frac{BedLoss_{Downstreamlink}}{AvgArea} \qquad (15)$$

where:
$BedLoss$ = total bedloss to all downstream segments (g/m^2·d);
$BedLoss_{Downstreamlink}$ = bedload over one of the downstream links (g/d); and
$AvgArea$ = average area of the segment (m^2).

The derivative presented is relevant only for the active layer. Inorganic sediments below the active layer do move up and down through the system as a result of exposure or deposition. However, these sediments move as a part of their entire intact layer when the active layer has reached its maximum or minimum level.

When the top layer reaches a minimum thickness, the layer below the active layer is added to the active layer to form one new layer. The inorganic sediments within these two layers do undergo mixing, represented by weighted averages of properties and constituents.

Detritus in the Sediment Bed

State variables tracking sedimented detritus are also included in each layer of sediment that is simulated. Like inorganic sediments, buried detritus below the active layer only moves up and down in the system when its layer moves up and down intact. Therefore, detritus found below the active layer has a very simple derivative:

$$\frac{\mathrm{d}BuriedDetritus}{\mathrm{d}t} = - Decomp \qquad (16)$$

where:
    d*BuriedDetritus*/dt   =   change in concentration of sediment on bottom (g/m^2·d); and
    Decomp   =   microbial decomposition in (g/m^2·d).

Pore Waters in the Sediment Bed

Pore waters are also tracked in the sediment beds. Pore waters below the top layer only move when the enclosing layer moves up or down. The derivative for pore waters in the top layer is:

$$\frac{\mathrm{d}PoreWater}{\mathrm{d}t} = Gain_{Up} - Loss_{Up} \tag{17}$$

where:
    d*PoreWater*/dt   =   change in volume of pore water in the sediment bed normalized per unit area (m^3/m^2·d);
    Gain$_{Up}$ =   gain of pore water from the water column above (m^3/m^2·d); and
    Loss$_{Up}$ =   loss of pore water to the water column above (m^3/m^2·d).

In the active layer, pore waters are assumed to move into the water column when scour occurs. To keep the density constant, the same fraction of pore water must be released as the fraction of sediment that has been scoured:

$$Loss_{Up} = \frac{\sum SedScour}{\sum SedMass} \cdot PoreWater \tag{18}$$

where:
    Loss$_{Up}$ =   loss of pore water to the water column above (m^3/m^2·d);
    SedScour   =   scour of all sediment to the water column above, (g/d);
    SedMass   =   mass of all sediment in the active layer, (g); and
    PoreWater   =   volume of pore water in the sediment bed normalized to unit area (m^3/m^2).

Pore waters are also squeezed into the water column when the active layer reaches a maximum thickness and is split into two layers. The bottom of these two new layers is assumed to be compressed and pore water is released as a result. More details about this process can be found in **Sediment Interactions** below.

Pore waters are taken from the water column when deposition occurs. This process is also required to maintain the constant density of the top sediment layer. To keep the density constant, the same fraction of pore water must be deposited as the fraction of sediment that has been deposited:

$$Gain_{Up} = \frac{\sum SedDeposition}{\sum SedMass} \cdot PoreWater \tag{19}$$

where:

$Gain_{Up}$	=	gain of pore water from the water column above $(m^3/m^2 \cdot d)$;
$SedDeposition$	=	deposition of all sediment to the water column above, (g/d);
$SedMass$	=	mass of all sediment in the active layer, (g); and
$PoreWater$	=	volume of pore water in the sediment bed normalized to unit area (m^3/m^2).

Dissolved Organic Matter within Pore Waters

Another state variable tracked within the sediment bed is dissolved organic matter within pore waters of the respective layers. Like other dissolved detritus compartments, these variables use units of mg/L. However, it is important to note that these are liters of pore water and not liters in the water column.

$$\frac{\mathrm{d}DOM_{PoreWater}}{\mathrm{d}t} = GainDOM_{Up} - LossDOM_{Up} + Diff_{Down} - Diff_{Up} - Decomp \qquad (20)$$

where:

$\mathrm{d}DOM_{PoreWater}/\mathrm{d}t$	=	change in concentration of DOM in pore water in the sediment bed normalized per unit area $(mg/L_{pw} \cdot d)$;
$GainDOM_{Up}$	=	active layer only: gain of DOM due to pore water gain from the water column $(mg/L_{pw} \cdot d)$;
$LossDOM_{Up}$	=	active layer only: loss of DOM due to pore water loss to the water column $(mg/L_{pw} \cdot d)$;
$Diff_{Down}$	=	diffusion over the lower boundary $(mg/L_{pw} \cdot d)$;
$Diff_{Up}$	=	diffusion over upper boundary $(mg/L_{pw} \cdot d)$; and
$Decomp$	=	microbial decomposition $(mg/L_{pw} \cdot d)$.

The increase of DOM due to pore water gain from the water column is simply the volume of water that is moving from the water column above multiplied by the DOM concentration in the water column. However, the concentration then needs to be normalized for the volume of pore water in the current segment:

$$GainDOM_{up} = (Conc_{DOM\ n-1})(GainPW_{up})\frac{AvgArea \cdot 1E3}{PoreWaterVol} \qquad (21)$$

where:

$GainDOM_{Up}$	=	gain of DOM due to pore water gain from the layer above $(mg/L_{pw} \cdot d)$;
$Conc_{DOM-1}$	=	concentration of DOM in above layer $(mg/L_{upper\ water})$;
$GainPW_{up}$	=	gain of pore water from above $(m^3_{upper\ water}/m^2 \cdot d)$;
$AvgArea$	=	average area of the segment (m^2);
$1E3$	=	units conversion (L/m^3); and
$PoreWaterVol$	=	pore water volume (L).

The loss of DOM in pore water to the water column is a simpler equation because no unit conversions are necessary:

$$LossDOM_{up} = Conc_{DOM\,n}\ \frac{LossPW_{up}}{PoreWaterConc} \tag{22}$$

where:

$LossDOM_{Up}$	=	loss of DOM due to pore water movement to the layer above (mg/L_{pw}·d);
$Conc_{DOM\,n}$	=	concentration of DOM in this layer (mg/L_{pw});
$LossPW_{up}$	=	loss of pore water to above layer (m^3_{pw}/m^2·d); and
$PoreWaterConc$	=	pore water concentration (m^3_{pw}/m^2).

Because diffusion and decomposition of DOM in pore water occur throughout the system, this derivative is relevant for the whole system. DOM in pore water also moves up and down through a system when its layer moves intact due to erosion or deposition.

Sediment Interactions

The mass of the top sediment layer increases and decreases as a result of deposition and scour. Therefore, the volume and thickness of the top sediment layer also increases and decreases. When the thickness of the top sediment layer reaches its maximum, as defined by the user, the upper bed is split into two layers. The top of these two layers maintains the same density it had before the layer was split up. It is assigned the initial condition depth of the active layer.

The lower level is assumed to be compressed to the same density as the level below it. This compression results in pore water being squeezed into the water column. The volume that is lost as a result of this compression can be solved as follows:

$$VolumeLost = Volume_{new2} - Volume_{new2} \cdot \frac{Density_{active}}{Density_{lower}} \tag{23}$$

where:

$VolumeLost$	=	volume of active layer lost due to compaction (m^3);
$Volume_{new2}$	=	volume of the new second layer before compression (m^3);
$Density_{active}$	=	density of the active layer (g/m^3); and
$Density_{lower}$	=	density of the lower below the active layer (g/m^3).

This equation also provides the quantity of pore water squeezed into the water column because the compression of the active layer is entirely the result of pore water being squeezed out. If there is only one layer in the system when the splitting of the active layer takes place, $Density_{lower}$ is assumed to be the initial condition density of the second layer in the system.

The volume of a sediment layer is defined as follows:

$$BedVol_n = \frac{\sum SedMass}{BedDensity} \qquad\qquad (24)$$

where:

    $BedVol_n$ = volume of bed at layer n (m^3);
    $SedMass$ = mass of sediment type (g); and
    $BedDensity$ = density of bed (g/m^3).

The porosity of a sediment layer is defined as:

$$FracWater_n = 1 - \sum_{Sedtypes} (Conc_{sed} / Density_{sed}) \qquad\qquad (25)$$

where:

    $FracWater_n$ = porosity of the sediment layer (fraction);
    $Sedtypes$ = all organic and inorganic sediments;
    $Conc_{sed}$ = concentration of the sediment (g/m^3); and
    $Density_{sed}$ = density of the sediment (g/m^3).

When the thickness of the top sediment layer reaches a minimum, as defined by the user, the two top layers combine into one new active layer. The density of this new layer is the weighted average of the two existing layers. This allows the layers to be combined while requiring no additional pore-water interactions.

The bottom of the system is a hardpan barrier. When this bottom is exposed, no further erosion can take place. When deposition occurs on this hardpan bottom, it is rebuilt with the density of the layer that existed previously. If enough deposition occurs so that two layers are created, the new second layer is compressed to the density of the original second layer.

If a system starts with exposed hardpan as an initial condition, the user must still specify the density of the top layer to be used when the top layer is created. If the user specifies a density for the second layer, this will be used when enough deposition occurs so that two layers are created.

TOXIC ORGANIC CHEMICALS

The chemical fate module of AQUATOX predicts the partitioning of a compound between water, sediment, and biota, and estimates the rate of degradation of the compound. Photolysis, hydrolysis, microbial degradation, and volatilization are modeled in AQUATOX. The latter two processes are especially applicable to PCBs and are discussed in greater detail below.

Microbial degradation is modeled by entering a maximum biodegradation rate for a particular organic toxicant, which is subsequently reduced to account for suboptimal temperature, pH, and dissolved oxygen. Photolysis is modeled by using a light-screening factor (Schwarzenbach et al.,

1993) and the near-surface, direct photolysis first-order rate constant for each pollutant. The light screening factor is a function of both the diffuse attenuation coefficient near the surface and the average diffuse attenuation coefficient for the whole water column. For those organic chemicals that undergo hydrolysis, neutral, acid-, and base-catalyzed reaction rates are entered into AQUATOX as applicable. Volatilization is modeled using a stagnant two-film model, with the air and water transfer velocities approximated by empirical equations based on reaeration of oxygen (Schwarzenbach et al., 1993).

The mass balance equations are presented below. The change in mass of toxicant in the water includes explicit representations of degradation pathways, mobilization of the toxicant from sediment to water as a result of decomposition of the sediment detritus compartment, sorption to and desorption from the detrital sediment compartments, uptake by algae and macrophytes, uptake across the gills of animals, depuration by organisms, advective transport and diffusion between segments, transfer to and from pore water, net loss to the floodplain, and turbulent diffusion between epilimnion and hypolimnion:

$$
\begin{aligned}
\frac{\mathrm{d}Toxicant_{Water}}{\mathrm{d}t} = {} & Loading + \sum\nolimits_{Detr} (Decomposition_{Detr} \cdot PPB_{Detr} \cdot 1\mathrm{E}-6) \\
& + \sum Desorption_{DetrTox} + \sum\nolimits_{Org} (K2 \cdot PPB_{Org} \cdot 1\mathrm{E}-6) \\
& - \sum Sorption_{DetrTox} - \sum GillUptake_{Pred} - MacroUptake \\
& - \sum AlgalUptake_{Alga} - Hydrolysis - Photolysis - MicrobialDegrdn \\
& - Volatilization - Discharge + TurbDiff + Inflow \\
& + MicrobTrans \pm Diffusion - Floodloss \pm PoreWaterTransfer
\end{aligned}
\tag{26}
$$

The equations for the toxicant associated with sedimented detritus compartments are rather involved:

$$
\begin{aligned}
\frac{\mathrm{d}Toxicant_{SedDetritus}}{\mathrm{d}t} = {} & Sorption - Desorption \\
& + \sum\nolimits_{Pred} \sum\nolimits_{Prey} \left(Def2Detr \cdot DefecationTox_{Pred,\ Prey}\right) \\
& - (Resuspension + Decomposition) \cdot PPB_{SedDetritus} \cdot 1\mathrm{E}-6 \\
& - \sum\nolimits_{Pred} Ingestion_{Pred,\ SedDetritus}) \cdot PPB_{SedDetritus} \cdot 1\mathrm{E}-6 \\
& + Sedimentation \cdot PPB_{SuspDetritus} \cdot 1\mathrm{E}-6 \\
& + \sum (Sed2Detr \cdot Sink_{Phyto} \cdot PPB_{Phyto} \cdot 1\mathrm{E}-6) \\
& - Hydrolysis - MicrobialDegrdn \\
& \mp MicrobTrans - Burial + Expose
\end{aligned}
\tag{27}
$$

Similarly, for the toxicant associated with suspended particulate and dissolved detritus, the equations are:

$$\frac{\mathrm{d}Toxicant_{DissolvedDetr}}{\mathrm{d}t} = Loading + Sorption - Desorption + \sum ExcrToxToDiss_{Org}$$
$$+ \sum\nolimits_{Org}(Mort2Detr \cdot Mortality_{Org} \cdot PPB_{Org} \cdot 1E-6)$$
$$- (Washout + Decomposition) \cdot PPB_{DissolvedDetr} \cdot 1E-6 \qquad (28)$$
$$+ Inflow + MicrobTrans \pm Diffusion$$
$$\pm PoreWaterTransfer - FloodLoss$$
$$- Hydrolysis - Photolysis - MicrobialDegrdn + TurbDiff$$

$$\frac{\mathrm{d}Toxicant_{SuspDetr}}{\mathrm{d}t} = Loading + Sorption - Desorption + \sum\nolimits_{Pred}(Def2Sed \cdot Def_{Pred})$$
$$+ \sum\nolimits_{Org}((Mort2Detr \cdot Mortality_{Org} + GameteLoss_{Org})$$
$$\cdot PPB_{Org} \cdot 1E-6) - (Sedimentation + Washout + Decomp$$
$$+ \sum\nolimits_{Pred} Ingestion_{Pred, SuspendedDetr}) \cdot PPB_{SuspendedDetr} \cdot 1E-6 \qquad (29)$$
$$+ Resuspension \cdot PPB_{SedimentedDetr} \cdot 1E-6 - SedToHyp + SedFrEpi$$
$$+ MicrobTrans + Inflow \pm Diffusion - FloodLoss$$
$$- Hydrolysis - Photolysis - MicrobialDegrdn + TurbDiff$$

Algae are represented as:

$$\frac{\mathrm{d}Toxicant_{Alga}}{\mathrm{d}t} = Loading + AlgalUptake - Depuration + TurbDiff$$
$$+ (- Excretion - Washout - \sum\nolimits_{Pred} Predation_{Pred, Alga} - Mortality \qquad (30)$$
$$- Sink + SinkToHypo - SinkFrEpi) \cdot PPB_{Alga} \cdot 1E-6$$
$$\pm Diffusion \pm Biotransformation + Inflow - Floodloss$$

Macrophytes are represented similarly, but they move only if they are floating macrophytes. Otherwise, they are stationary:

$$\frac{\mathrm{d}Toxicant_{Macrophyte}}{\mathrm{d}t} = Loading + MacroUptake - Depuration - (Excretion$$
$$+ \sum\nolimits_{Pred} Predation_{Pred, Macro} + Mortality + Washout) \qquad (31)$$
$$\cdot PPB_{Macro} \cdot 1E-6 \pm Biotransformation + Inflow - Floodloss$$

The toxicant associated with animals is represented by a kinetic equation because of the various routes of exposure and transfer:

$$\frac{\mathrm{d}Tox_{Animal}}{\mathrm{d}t} = Loading + GillUptake + \sum\nolimits_{Prey} DietUptake + TurbDiff$$
$$- (Depuration + \sum\nolimits_{Pred} Predation_{Pred,\,Animal} + Mortality + Spawn \qquad (32)$$
$$\pm\ Promotion + Drift + Migration + EmergeInsect) \cdot PPB_{Animal} \cdot 1\,\mathrm{E}-6$$
$$\pm\ Diffusion - Floodloss$$

where:

PPB_{Alga}	=	concentration of toxicant in given alga (μg/kg);
$Toxicant_{SedDetr}$	=	mass of toxicant associated with the sediment detritus compartments in unit volume of water (μg/L);
$Toxicant_{SuspDetr}$	=	mass of toxicant associated with the suspended detritus compartments in unit volume of water (μg/L);
$Toxicant_{DissDetr}$	=	mass of toxicant associated with the dissolved organic compartments in unit volume of water (μg/L);
$Toxicant_{Alga}$	=	mass of toxicant associated with given alga in unit volume of water (μg/L);
$Toxicant_{Macrophyte}$	=	mass of toxicant associated with given macrophyte in unit volume of water(μg/L);
$Toxicant_{Animal}$	=	mass of toxicant associated with given animal in unit volume of water (μg/L);
$PPB_{SedDetr}$	=	concentration of toxicant in sediment detritus (μg/kg);
$PPB_{SuspDetr}$	=	concentration of toxicant in suspended detritus (μg/kg);
$PPB_{DissDetr}$	=	concentration of toxicant in dissolved organics (μg/kg);
$Toxicant_{Water}$	=	toxicant in dissolved phase in unit volume of water (μg/L);
$PPB_{Macrophyte}$	=	concentration of toxicant in given macrophyte (μg/kg);
PPB_{Animal}	=	concentration of toxicant in given animal (μg/kg);
1 E -6	=	units conversion (kg/mg);
$Loading$	=	loading of toxicant from external sources (μg/L·d);
$TurbDiff$	=	depth-averaged turbulent diffusion between epilimnion and hypolimnion (μg/L·d);
$Inflow$	=	flow of toxicant from upstream linked segments (μg/L·d);
$MicrobTrans$	=	microbial transformation of another toxicant type to this toxicant type (μg/L·d);
$Diffusion$	=	diffusion over segment boundaries. If the toxicant is in a dissolved phase and if the sediment bed model is included, this term includes diffusion to or from the active layer (μg/L·d);
$Biotransformation$	=	biotransformation to or from this toxicant within an organism (μg/L·d);
$Floodloss$	=	loss to the floodplain during a flood event (μg/L·d);
$PoreWaterTransfer$	=	transfer to or from pore water in the active layer during deposition or erosion (μg/L·d);
$Hydrolysis$	=	rate of loss due to hydrolysis (μg/L·d);
$Photolysis$	=	rate of loss due to direct photolysis (μg/L·d);

MicrobialDegrdn	=	rate of loss due to microbial degradation (μg/L·d);
Volatilization	=	rate of loss due to volatilization (μg/L·d);
Discharge	=	rate of loss of toxicant due to discharge downstream (μg/L·d);
Burial	=	rate of loss due to deep burial (μg/L·d);
Expose	=	rate of exposure due to resuspension of overlying sediments (μg/L·d);
Decomposition	=	rate of decomposition of given detritus (mg/L·d);
Depuration	=	elimination rate for toxicant due to clearance (μg/L·d);
Sorption	=	rate of sorption to given compartment (μg/L·d);
Desorption	=	rate of desorption from given compartment (μg/L·d);
DefecationTox$_{Pred, Prey}$	=	rate of transfer of toxicant due to defecation of given prey by given predator (μg/L·d);
Def2Detr	=	fraction of defecation that goes to given compartment;
Resuspension	=	rate of resuspension of given sediment detritus (mg/L·d);
Sedimentation	=	rate of sedimentation of given suspended detritus (mg/L·d);
Sed2Detr	=	fraction of sinking phytoplankton that goes to given detrital compartment;
Sink	=	loss rate of phytoplankton to bottom sediments (mg/L·d);
Death	=	nonpredatory mortality of given organism (mg/L·d);
Mort2Detr	=	fraction of dead organism that is labile (unitless);
GameteLoss	=	loss rate for gametes (g/m^3·d);
Washout or *Drift*	=	rate of loss of given suspended detritus or organism due to being carried downstream (mg/L·d);
SedToHyp	=	rate of settling loss to hypolimnion from epilimnion (mg/L·d);
SedFrEpi	=	rate of gain to hypolimnion from settling out of epilimnion (mg/L·d);
Ingestion$_{Pred, Prey}$	=	rate of ingestion of given food or prey by given predator (mg/L·d);
Predation$_{Pred, Prey}$	=	predatory mortality by given predator on given prey (mg/L·d);
ExcToxToDiss$_{Org}$	=	toxicant excretion from plants to dissolved organics (mg/L·d);
Excretion	=	excretion rate for given organism (g/m^3·d);
SinkToHypo	=	rate of transfer of phytoplankton to hypolimnion (mg/L·d);
SinkFrEpi	=	loss rate of phytoplankton to hypolimnion (mg/L·d);
AlgalUptake	=	rate of sorption by algae (μg/L·d);
MacroUptake	=	rate of sorption by macrophytes (μg/L·d);
GillUptake	=	rate of absorption of toxicant by the gills (μg/L·d);
DietUptake$_{Prey}$	=	rate of dietary absorption of toxicant associated with given prey (μg/L·d);
Promotion	=	promotion from one age class to the next (mg/L·d);
Migration	=	rate of migration (g/m^3·d); and
EmergeInsect	=	insect emergence (mg/L·d).

The derivatives for toxicants in the sediment transport component of AQUATOX are described below.

$$\frac{\mathrm{d}Toxicant_{Porewater}}{\mathrm{d}t} = GainTox_{up} - LossTox_{up}$$

$$\pm DiffUp \pm DiffDown$$
$$+ \sum\nolimits_{Detr\ n} (Decomposition_{Detr\ n} \cdot PPB_{Detr\ n} \cdot 1\mathrm{E}{-6})$$
$$+ \sum Desorption_{DetrTox\ n} + \sum\nolimits_{Org\ n} (K2 \cdot PPB_{Org\ n} \cdot 1\mathrm{E}{-6})$$
$$- \sum Sorption_{DetrTox\ n} - \sum GillUptake_{Pred\ n}$$
$$- MicrobialDegrdn + MicrobTransfIn$$

$$\tag{33}$$

$$\frac{\mathrm{d}Toxicant_{SuspSediment}}{\mathrm{d}t} = Scour/Volume \cdot PPB_{ActiveLayer} \cdot 1\mathrm{E}{-6}$$

$$- Deposition/Volume \cdot PPB_{SuspSediment} \cdot 1\mathrm{E}{-6}$$
$$- (Washout - Floodloss) \cdot PPB_{SuspSediment} \cdot 1\mathrm{E}{-6}$$
$$+ WashinTox - MicrobialDegrdn + MicrobTransfIn$$

$$\tag{34}$$

$$\frac{\mathrm{d}Toxicant_{BottomSediment}}{\mathrm{d}t} = Deposition/AvgArea \cdot PPB_{UpperLayer} \cdot 1\mathrm{E}{-3}$$

$$- Scour/AvgArea \cdot PPB_{ThisLayer} \cdot 1\mathrm{E}{-3}$$
$$+ ToxBedLoad - ToxBedLoss - MicrobialDegrdn + MicrobTransfIn$$

$$\tag{35}$$

$$\frac{\mathrm{d}Toxicant_{BuriedDetritus}}{\mathrm{d}t} = - Decomposition \cdot PPB_{ThisLayer} \cdot 1\mathrm{E}{-3}$$

$$- MicrobialDegrdn + MicrobTransfIn + Sorption - Desorption$$

$$\tag{36}$$

$$\frac{dToxicant_{DOM\ Porewater}}{dt} = GainTox_{up} - LossTox_{up}$$

$$\pm\ DiffUp\ \cdot\ PPB_{DOM\ init\ layer}\ \cdot\ 1E-6$$
$$\pm\ DiffDown\ \cdot\ PPB_{DOM\ init\ layer}\ \cdot\ 1E-6 \tag{37}$$
$$+\ Sorption\ -\ Desorption$$
$$-\ MicrobialDegrdn\ +\ MicrobTransfIn$$
$$-\ Decomposition\ \cdot\ PPB_{DissLabileDetr\ pore\ water}\ \cdot\ 1E-6\ (if\ labile)$$

where:

$Toxicant_{SuspSediment}$	=	toxicant within suspended sediments (μg/L);
$Scour/Volume$	=	scour from the active sediment layer normalized to unit volume (g/m^3·d);
$Deposition/Volume$	=	deposition to the active sediment layer normalized to unit volume (g/m^3·d);
$PPB_{SuspSediment}$	=	concentration of toxicant in suspended sediment (μg/kg);
$PPB_{ActiveLayer}$	=	concentration of toxicant in this state variable in the top layer of sediment (μg/kg);
1 E -6	=	units conversion (kg/mg);
$Washout$	=	loss due to being carried downstream (g/m^3·d);
$FloodLoss$	=	loss to the floodplain during a flood event (g/m^3·d);
$WashinTox$	=	toxicant loadings from upstream segments (g/m^3·d);
$MicrobialDegrdn$	=	rate of loss due to microbial degradation (μg/L·d);
$MicrobTransfIn$	=	rate of gain due to microbial transformation of another chemical to this chemical type (μg/L·d);
$Scour/AvgArea$	=	scour from this sediment layer normalized to unit area (g/m^2·d);
$Deposition/AvgArea$	=	deposition to this sediment layer normalized to unit area (g/m^2·d);
$PPB_{ThisLayer}$	=	concentration of toxicant in this state variable in this layer of sediment (μg/kg);
$PPB_{UpperLayer}$	=	concentration of toxicant in this state variable in the layer above this layer of sediment (μg/kg);
$PPB_{init\ layer}$	=	concentration of toxicant in the given state variable in the layer where diffusive movement originates (μg/kg);
1 E -3	=	units conversion (kg/g);
$Exposure$	=	movement up from lower sediment layer (g/m^2·d);
$Burial$	=	movement down to lower sediment layer (g/m^2·d);
$ToxBedLoad$	=	toxicant bedload from upstream segments (μg/L·d);
$ToxBedLoss$	=	toxicant bedloss to downstream segments (μg/L·d) ;
$Deposition_{Detr}$	=	deposition of detritus to this layer from the above layer (g/m^2);
$Scour_{Detr}$	=	scour of detritus from this layer to the above layer (g/m^2);
$Decomposition$	=	rate of decomposition of given detritus, relevant to labile detritus only (mg/L·d);
$Sorption$	=	rate of sorption to given compartment (μg/L·d);
$Desorption$	=	rate of desorption from given compartment (μg/L·d);
$GainTox_{up}$	=	gain of toxicant from above layer due to pore water transport (μg/L·d); and
$LossTox_{up}$	=	loss of toxicant to below layer due to pore water transport (μg/L·d).

The wash-in of toxicants in carriers from upstream segments is calculated by summing the total toxins in carriers that wash over each of the upstream segment links.

$$WashinTox_{Thisvar} = \sum Washout_{Upstreamlink} \cdot PPB_{Upstreamvar} \cdot 1E-6 \qquad (38)$$

where:

$WashinTox_{Thisvar}$ = total toxicant in this state variable that is washed into this segment from all upstream links ($\mu g/L \cdot d$);

$Washout_{Upstreamlink}$ = washout of this state variable from this particular upstream segment ($g/m^3 \cdot d$);

$PPB_{Upstreamvar}$ = toxicant in this state variable in the upstream segment ($\mu g/kg$); and

$1E-6$ = units conversion (kg/mg).

Equations for the movement of toxins due to pore water transport are the same whether the toxin is directly dissolved in the pore water or is carried by DOM in pore water. These equations are basically the same as the equations for the transport of DOM in pore water described earlier. As a reminder, these equations are relevant only for the active layer of the sediment system. Pore water below the active layer moves only as a result of diffusion or when a layer moves up or down one layer intact as a result of an erosional or depositional regime.

$$GainTox_{up} = (Conc_{Tox\ n-1})\ (GainPW_{up})\ \frac{AvgArea \cdot 1E3}{PoreWaterVol} \qquad (39)$$

where:

$GainTox_{Up}$ = gain of toxicant due to pore water gain from the layer above ($mg/L_{pw} \cdot d$);

$Conc_{Tox-1}$ = concentration of toxicant in above layer ($mg/L_{upper\ water}$);

$GainPW_{up}$ = gain of pore water from above ($m^3_{upper\ water}/m^2 \cdot d$);

$AvgArea$ = average area of the segment (m^2);

$1E3$ = units conversion (L/m^3);

$PoreWaterVol$ = pore water volume (L);

and

$$LossTox_{up} = Conc_{Tox\ n}\ \frac{LossPW_{up}}{PoreWaterConc} \qquad (40)$$

where:

$LossTox_{Up}$ = loss of toxicant due to pore water movement to the layer above ($mg/L_{pw} \cdot d$);

$Conc_{Tox\ n}$ = concentration of toxicant in this layer (mg/L_{pw});

$LossPW_{up}$ = loss of pore water to above layer ($m^3_{pw}/m^2 \cdot d$); and

$PoreWaterConc$ = pore water concentration (m^3_{pw}/m^2).

Microbial Degradation

Not only can microorganisms decompose the detrital organic material in ecosystems, they also can degrade xenobiotic organic compounds such as fuels, solvents, pesticides, and PCBs to obtain energy. In AQUATOX, this process of biodegradation of pollutants, whether they are dissolved in the water column or adsorbed to organic detritus in the water column or sediments, is modeled using the same equations as for decomposition of detritus, substituting the pollutant and its degradation parameters for detritus:

$$MicrobialDegrdn = KMDegrdn_{Phase} \cdot DOCorrection \cdot TCorr \cdot pHCorr \cdot Toxicant_{Phase} \tag{41}$$

where:

$MicrobialDegrdn$	=	loss due to microbial degradation ($g/m^3 \cdot d$);
$KMDegrdn_{phase}$	=	maximum degradation rate, either in water column or sediments (day^{-1});
$DOCorrection$	=	effect of anaerobic conditions (unitless);
$TCorr$	=	effect of suboptimal temperature (unitless);
$pHCorr$	=	effect of suboptimal pH (unitless); and
$Toxicant_{phase}$	=	concentration of organic toxicant in water column or sediments (g/m^3).

Volatilization

Volatilization is modeled using the "stagnant boundary theory," or two-film model, in which a pollutant molecule must diffuse across both a stagnant water layer and a stagnant air layer to volatilize out of a waterbody (Whitman, 1923; Liss and Slater, 1974). Diffusion rates of pollutants in these stagnant boundary layers can be related to the known diffusion rates of chemicals such as oxygen and water vapor. The thickness of the stagnant boundary layers must also be taken into account to estimate the volatile flux of a chemical out of (or into) the waterbody.

The time required for a pollutant to diffuse through the stagnant water layer in a waterbody is based on the well-established equations for the reaeration of oxygen, corrected for the difference in diffusivity as indicated by the respective molecular weights (Thomann and Mueller, 1987, p. 533). The diffusivity through the water film is greatly affected by the degree of ionization (Schwarzenbach et al., 1993, p. 243), and the depth-averaged reaeration coefficient is multiplied by the thickness of the well-mixed zone:

$$KLiq = KReaer \cdot Thick \cdot \left(\frac{MolWtO2}{MolWt} \right)^{0.25} \cdot \frac{1}{Nondissoc} \tag{42}$$

where:

$KLiq$	=	water-side transfer velocity (m/d);
$KReaer$	=	depth-averaged reaeration coefficient for oxygen (L/d);

Thick	=	thickness of well-mixed layer (m);
MolWtO2	=	molecular weight of oxygen (g/mol, =32);
MolWt	=	molecular weight of pollutant (g/mol); and
Nondissoc	=	nondissociated fraction (unitless).

Reaeration is a function of the depth-averaged mass transfer coefficient *KReaer*, corrected for ambient temperature, multiplied by the difference between the dissolved oxygen level and the saturation level (cf. Bowie et al., 1985):

$$\textit{Reaeration} = \textit{KReaer} \cdot (\textit{O2Sat} - \textit{Oxygen}) \tag{43}$$

where:

Reaeration	=	mass transfer of oxygen (g/m^3·d);
KReaer	=	depth-averaged reaeration coefficient (L/d);
Temperature	=	ambient water temperature (°C);
O2Sat	=	saturation concentration of oxygen (g/m^3); and
Oxygen	=	concentration of oxygen (g/m^3).

In standing water, *KReaer* is computed as a minimum transfer velocity plus the effect of wind on the transfer velocity (Schwarzenbach et al., 1993) divided by the thickness of the mixed layer to obtain a depth-averaged coefficient.

In streams, reaeration is a function of current velocity and water depth (**Figure 8**) following the approach of Covar (1976, see Bowie et al., 1985) and used in WASP (Ambrose et al., 1991). The decision rules for which equation to use are taken from the WASP5 code (Ambrose et al., 1993).

Figure 8
Reaeration in Streams
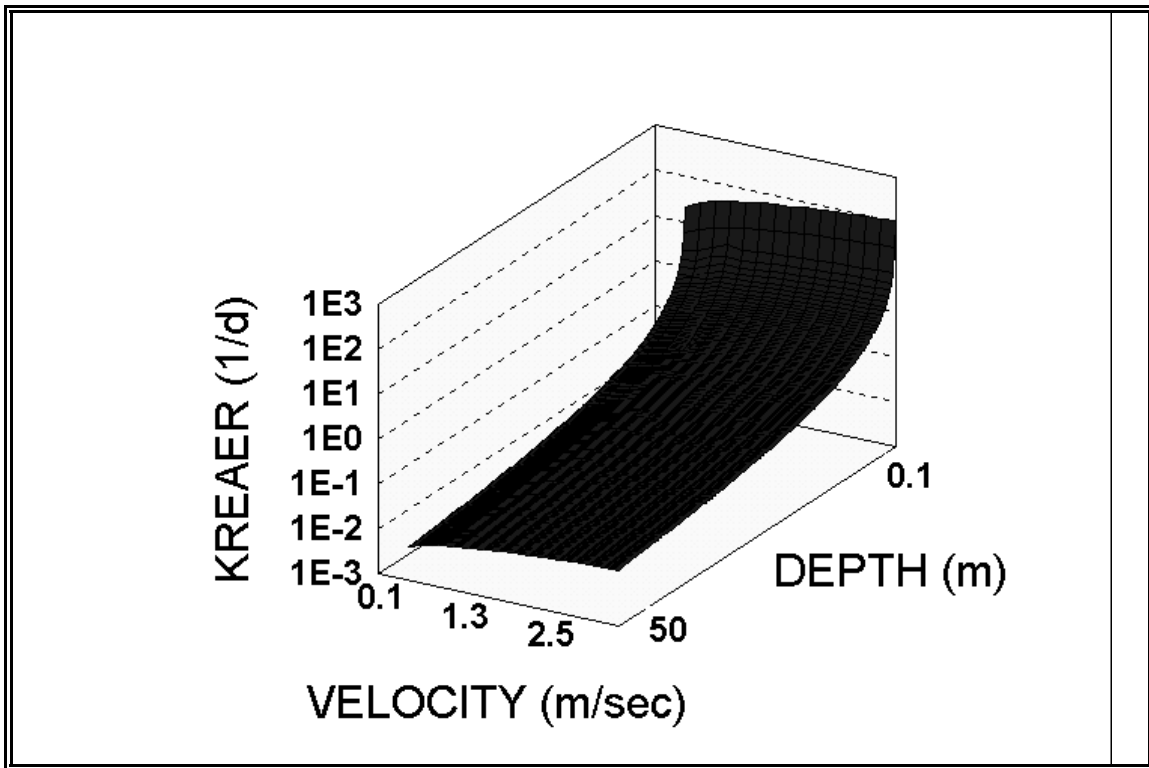
If reaeration due to wind exceeds that due to current velocity, the equation for standing water is used; reaeration is set to 0 if there is ice cover.

To estimate the air-side transfer velocity of a pollutant, the following empirical equation, based on the evaporation of water, corrected for the difference in diffusivity of water vapor compared to the toxicant (Thomann and Mueller, 1987, p. 534), is used:

$$KGas = 168 \cdot \left(\frac{MolWtH2O}{MolWt} \right)^{0.25} \cdot Wind \tag{44}$$

where:
$\quad$ *KGas* $\quad\quad$ = $\quad$ air-side transfer velocity (m/d);
$\quad$ *Wind* $\quad\quad$ = $\quad$ wind speed ten meters above the water surface (m/s); and
$\quad$ *MolWtH2O* $\quad$ = $\quad$ molecular weight of water (g/mol, =18).

The total resistance to the mass transfer of the pollutant through both the stagnant boundary layers can be expressed as the sum of the resistances—the reciprocals of the air- and water-phase mass transfer coefficients (Schwarzenbach et al., 1993), modified for the effects of ionization:

$$\frac{1}{KOVol} = \frac{1}{KLiq} + \frac{1}{KGas \cdot HenryLaw \cdot Nondissoc} \tag{45}$$

where:

  KOVol   =   total mass transfer coefficient through both stagnant boundary layers (m/d);

$$HenryLaw = \frac{Henry}{R \cdot TKelvin} \qquad (46)$$

and where:

  HenryLaw =   Henry's Law constant (unitless);
  Henry   =   Henry's Law constant (atm m^3 mol^{-1});
  R   =   gas constant (=8.206E-5 atm m^3 (mol K)$^{-1}$); and
  TKelvin   =   temperature in $^\circ$K.

The Henry's law constant is applicable only to the fraction that is nondissociated because the ionized species will not be present in the gas phase (Schwarzenbach et al., 1993, p. 179).

The atmospheric exchange of the pollutant can be expressed as the depth-averaged total mass transfer coefficient times the difference between the concentration of the chemical and the saturation concentration:

$$Volatilization = \frac{KOVol}{Thick} \cdot \left(ToxSat - Toxicant_{water}\right) \qquad (47)$$

where:

  Volatilization   =   interchange with atmosphere (μg/L·d);
  Thick   =   depth of water or thickness of surface layer (m);
  ToxSat   =   saturation concentration of pollutant (μg/L); and
  Toxicant$_{water}$ =   concentration of pollutant in water (μg/L).

The saturation concentration depends on the concentration of the pollutant in the air, ignoring temperature effects (Thomann and Mueller, 1987, p. 532), but adjusting for ionization and units:

$$ToxSat = \frac{Toxicant_{air}}{HenryLaw \cdot Nondissoc} \cdot 1000 \qquad (48)$$

where:

  Toxicant$_{air}$ =   gas-phase concentration of the pollutant (g/m^3); and
  Nondissoc   =   nondissociated fraction (unitless).

Often the pollutant can be assumed to have a negligible concentration in the air and *ToxSat* is zero. However, this general construct can represent the transferral of volatile pollutants into water bodies. Because ionized species do not volatilize, the saturation level increases if ionization is occurring.

The nondimensional Henry's law constant, which relates the concentration of a compound in the air phase to its concentration in the water phase, strongly affects the air-phase resistance. Depending on the value of the Henry's law constant, the water phase, the air phase, or both may control volatilization.

Partition Coefficients

Although AQUATOX is a kinetic model, steady-state partition coefficients for organic pollutants are computed to place constraints on competitive uptake and loss processes, speeding up computations. They can be supplied by the user or estimated from empirical regression equations and the octanol-water partition coefficient for the contaminant.

Natural organic matter is the primary sorbent for neutral organic pollutants. Hydrophobic chemicals partition primarily in nonpolar organic matter (Abbott et al., 1995). Most detritus is relatively nonpolar; its partition coefficient is a function of the octanol-water partition coefficient (N = 34, r^2 = 0.93; Schwarzenbach et al. 1993):

$$KOM_{Detr} = 1.38 \cdot KOW^{0.82} \qquad (49)$$

where:
KOM_{Detr} = detritus-water partition coefficient (L/kg); and
KOW = octanol-water partition coefficient (unitless).

O'Connor and Connolly (1980); (see also Ambrose et al., 1991) found that the sediment partition coefficient is the inverse of the mass of suspended sediment. Di Toro (1985) developed a construct to represent the relationship. This may be an artifact due to complexation with dissolved and colloidal organics (Schnoor, 1996); therefore, the partition coefficient is not corrected for mass of sediment.

Association of hydrophobic compounds with colloidal and dissolved organic matter (DOM) reduces bioavailability; such contaminants are unavailable for uptake by organisms (Stange and Swackhamer, 1994; Gilek et al., 1996). Therefore, it is important that complexation of organic chemicals with DOM be modeled. Analysis of data from a study using naturally occurring fulvic acids (Uhle et al., 1999) exhibits a relationship between these two parameters (**Figure 9**; N = 3, r^2 = 0.76). Although additional points would be preferable, the relationship is consistent with other lines of evidence (see below); therefore, it is used as the default estimator to represent complexation with DOM in AQUATOX:

$$KOM_{DOM} = 190 \cdot KOW^{0.38} \cdot 0.526 \qquad (50)$$

where:
KOM_{DOM} = partition coefficient for dissolved organic matter (L/kg);
0.526 = factor to convert from organic carbon to organic matter.

Comparing the results of using these coefficients, we see that they are consistent with the relative importance of the forms of detritus in binding organic chemicals (**Figure 9**). Binding capacity of particulate detritus is greater than dissolved organic matter in Great Lakes waters (Stange and Swackhamer, 1994; Gilek et al., 1996). In a study using Baltic Sea water, less than 7% of the mass of PCBs was associated with dissolved organic matter and most of the mass was associated with algae (Björk and Gilek, 1999). Analysis of PCB data from the Hudson River indicated that partitioning to dissolved organic matter was a significant component for Cl_1 and Cl_2 PCBs, but not for more chlorinated congeners; however, a three-component model may still be advisable to avoid overestimating bioavailability (Butcher et al., 1998).

Figure 9
Partitioning to Dissolved and Particulate Organic Matter
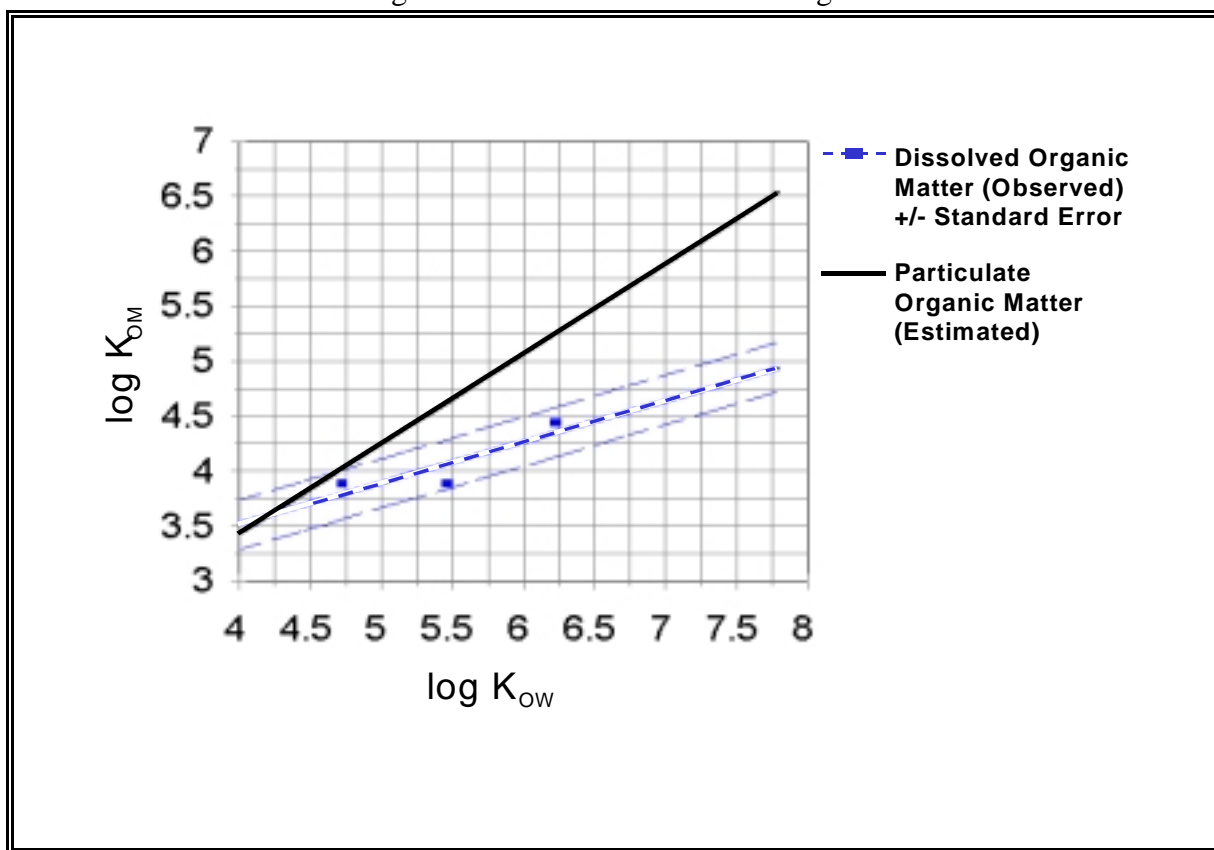
Older data and modeling efforts failed to distinguish between hydrophobic compounds that were truly dissolved and those that were complexed with DOM. For example, the PCB water concentrations for Lake Ontario, reported by Oliver and Niimi (1988) and used by many subsequent researchers, included both dissolved and DOC-complexed PCBs (a fact which they recognized). In their steady-state model of PCBs in the Great Lakes, Thomann and Mueller (1983) defined "dissolved" as that which is not particulate (passing a 0.45-micron filter). In their Hudson River PCB model, Thomann et al. (1991) again used an operational definition of dissolved PCBs. AQUATOX models truly dissolved and complexed compounds separately, but offers the analyst the

option of calculating apparent partitioning factors using either definition of "dissolved," facilitating comparison with observed data.

Bioaccumulation of PCBs in algae depends on solubility; hydrophobicity and molecular configuration of the compound, growth rate, surface area and type, and content and type of lipid in the algae (Stange and Swackhamer, 1994). Phytoplankton biomass may double or triple in one day and periphyton turnover may be so rapid that some PCBs will not reach equilibrium (Hill and Napolitano, 1997); therefore, one should use the term "bioaccumulation factor" (BAF) rather than "bioconcentration factor," which implies equilibrium (Stange and Swackhamer, 1994). Algal lipids have a much stronger affinity for hydrophobic compounds than does octanol, so that the algal $BAF_{lipid} > K_{OW}$ (Stange and Swackhamer, 1994; Koelmans et al., 1995; Sijm et al., 1998).

For phytoplankton, the approximation to estimate the dry-weight bioaccumulation factor ($r^2 = 0.87$), computed from Swackhamer and Skoglund's (1993) study of approximately 52 PCB congeners, is:

$$\log(BAF_{Alga}) = 0.41 + 0.91 \cdot \log K_{OW} \tag{51}$$

where:
BAF_{Alga} =   partition coefficient between algae and water (L/kg).

For macrophytes, an empirical relationship reported by Gobas et al. (1991) for nine chemicals with $logK_{OW}$s of 4 to 8.3 ($r^2 = 0.97$) is used:

$$\log(BAF_{Macro}) = 0.98 \cdot \log K_{OW} - 2.24 \tag{52}$$

Periphyton bioconcentration factors are an order of magnitude less than those for phytoplankton (Wang et al., 1999), and this relationship is used to estimate the partition coefficients in AQUATOX (**Figure 10**).

Figure 10
Partitioning to Various Types of Plants
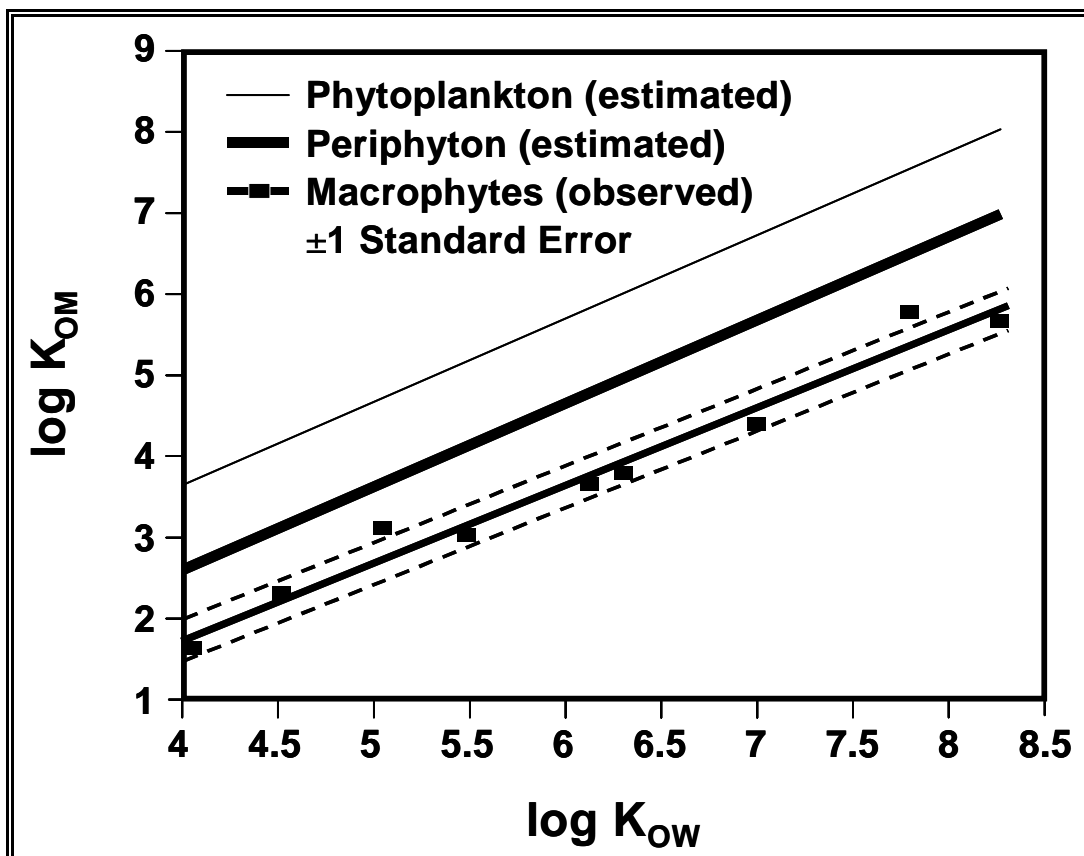
For the invertebrate partition coefficient, if the user does not supply a value, the following empirical equation is used, based on seven chemicals with log K_{OW}s ranging from 3.3 to 6.2 and bioaccumulation factors for *Daphnia pulex* (r^2 = 0.85; Southworth et al., 1978; see also Lyman et al., 1982), converted to dry weight :

$$\log(KB_{Invertebrate}) = (0.7520 \cdot \log K_{OW} - 0.4362) \cdot WetToDry \tag{53}$$

where:
$KB_{Invertebrate}$	=	partition coefficient between invertebrates and water (L/kg); and
$WetToDry$	=	wet to dry conversion factor (unitless, default = 5).

Fish take longer to reach equilibrium with the surrounding water; therefore, a nonequilibrium bioconcentration factor is used. For each pollutant, a whole-fish bioconcentration factor is based on the lipid content of the fish extended to hydrophilic chemicals (McCarty et al., 1992), with provision for ionization:

$$KB_{Fish} = 1 + Lipid \cdot WetToDry \cdot K_{OW} \tag{54}$$

where:
KB_{Fish} =   partition coefficient between whole fish and water (L/kg);
Lipid   =   fraction of fish that is lipid (g lipid/g fish); and
WetToDry   =   wet to dry conversion factor (unitless, default = 5).

Lipid content of fish can be fixed by the modeler or can be varied depending on the potential for growth as predicted by the bioenergetics equations; the initial lipid values for each species are given. The bioconcentration factor is adjusted for the time to reach equilibrium as a function of the clearance or elimination rate and the time of exposure (Hawker and Connell, 1985; Connell and Hawker, 1988; **Figure 11**):

$$BCF_{Fish} = KB_{Fish} \cdot \left(1 - e^{(-Elimination \cdot TElapsed)}\right) \tag{55}$$

where:
BCF_{Fish} =   quasi-equilibrium bioconcentration factor for fish (L/kg);
TElapsed   =   time elapsed since fish was first exposed (d); and
Elimination   =   combined clearance and biotransformation.

The concentration in each carrier is given by:

$$PPB_i = \frac{ToxState_i}{CarrierState_i} \cdot 1E6 \tag{56}$$

where:
PPB_i =   concentration of chemical in carrier *i* (μg/kg);
$ToxState_i$ =   mass of chemical in carrier *i* (ug/L);
CarrierState   =   biomass of carrier (mg/L); and
1E6   =   conversion factor (mg/kg).

Figure 11
Bioconcentration Factor for Fish as a Function of Time and Log K_{ow}
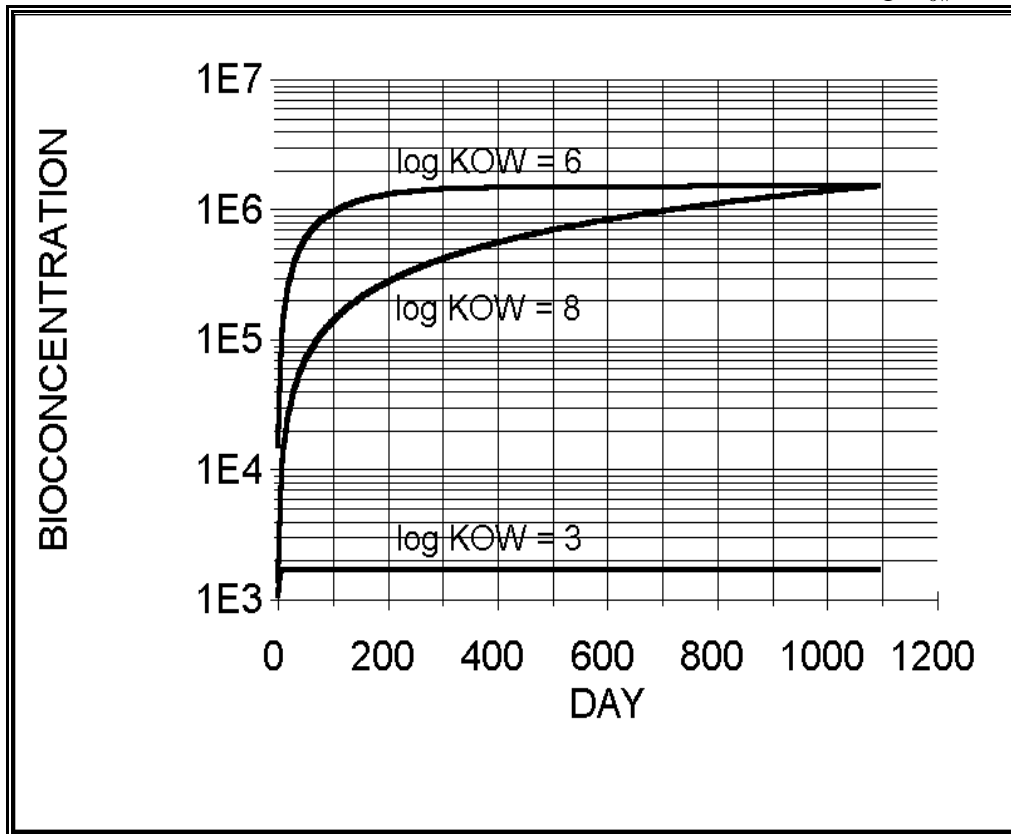
Nonequilibrium Kinetics

Often there is an absence of equilibrium due to growth or insufficient exposure time, metabolic biotransformation, dietary exposure, and nonlinear relationships for very large and/or superhydrophobic compounds (Bertelsen et al., 1998). Although it is important to have a knowledge of equilibrium partitioning because it is an indication of the condition toward which systems tend (Bertelsen et al., 1998), it is often impossible to determine steady-state potential due to changes in bioavailability and physiology (Landrum, 1998). For example, PCBs may not be at steady state even in large systems such as Lake Ontario that have been polluted over a long period of time. In fact, PCBs in Lake Ontario exhibit a 25-fold disequilibrium (Cook and Burkhard, 1998).

Sorption and Desorption to Sedimented Detritus

Partitioning to sediments appears to involve rapid sorption to particle surfaces, followed by slow movement into, and out of, organic matter and porous aggregates (Karickhoff and Morris, 1985). Therefore, attainment of equilibrium may be slow. This applies to suspended detritus compartments as well. Because of the need to represent sorption and desorption separately in detritus, kinetic formulations are used (Thomann and Mueller, 1987):

$$Sorption = k1_{Detr} \cdot Toxicant_{Water} \cdot Diff1_{Carrier} \cdot Org2C \cdot Detr \cdot 1E-6 \qquad (57)$$

$$Desorption = k2_{Detr} \cdot Diff2_{Carrier} \cdot Toxicant_{Detr} \qquad (58)$$

where:

$Sorption$	=	rate of sorption to given detritus compartment (μg/L·d);
$k1_{Detr}$	=	sorption rate constant (L/kg·d);
$Toxicant_{Water}$	=	concentration of toxicant in water (μg/L);
$Diff1_{Carrier}$	=	factor to normalize rate constant for given carrier (detritus compartment in this case) based on all competing uptake rates (unitless);
$Diff2_{Carrier}$	=	factor to normalize loss rates (unitless);
$Org2C$	=	conversion factor for organic matter to carbon (= 0.526 g C/g organic matter);
$Detr$	=	mass of each of the detritus compartments per unit volume (mg/L);
1e -6	=	units conversion (kg/mg);
$Desorption$	=	rate of desorption from given sediment detritus compartment (μg/L·d);
$k2_{Detr}$	=	desorption rate constant (day⁻¹); and
$Toxicant_{Detr}$	=	mass of toxicant in each of the detritus compartments (μg/L).

Because there are several processes competing for the dissolved toxicant, the rate constants for these processes are normalized to preserve mass balance. The *Diff1* factor is computed for each direct uptake process, including sorption to detritus and algae, uptake by macrophytes, and uptake across animals' gills:

$$RateDiff1_{Carrier} = Gradient1_{Carrier} \cdot k1 \qquad (59)$$

$$Gradient1_{Carrier} = \frac{Toxicant_{Water} \cdot kp_{Carrier} - PPB_{Carrier}}{Toxicant_{Water} \cdot kp_{Carrier}} \qquad (60)$$

$$Diff1_{Carrier} = \frac{RateDiff_{Carrier}}{\sum RateDiff_{Carrier}} \qquad (61)$$

$k2_{Detr}$ = desorption rate constant (day^{-1}); and

where:

$RateDiff1_{Carrier}$ = maximum rate constant for uptake given the concentration gradient (L/kg·d);

$Gradient1_{Carrier}$ = gradient between potential and actual concentrations of toxicant in each carrier (unitless);

$kp_{Carrier}$ = partition coefficient or bioconcentration factor for each carrier (L/kg); and

$PPB_{Carrier}$ = concentration of toxicant in each carrier (μg/kg).

Likewise, the loss rate constants are normalized; the equations parallel those for uptake, with the gradient being reversed:

$$RateDiff2_{Carrier} = Gradient2_{Carrier} \cdot k2 \tag{62}$$

$$Gradient2_{Carrier} = \frac{PPB_{Carrier} - (PPB_{Water} \cdot kp_{Carrier})}{PPB_{Carrier}} \tag{63}$$

$$Diff2_{Carrier} = \frac{RateDiff2_{Carrier}}{\sum RateDiff2_{Carrier}} \tag{64}$$

where:

$RateDiff2_{Carrier}$ = maximum rate constant for loss given the concentration gradient (L/kg·d); and

$Gradient2_{Carrier}$ = gradient between actual and potential concentrations of toxicant in each carrier (unitless).

Desorption of the slow compartment is the reciprocal of the reaction time, which Karickhoff and Morris (1985) found to be a linear function of the partition coefficient over three orders of magnitude ($r^2 = 0.87$):

$$\frac{1}{k2} \approx 0.03 \cdot 24 \cdot KPSed \tag{65}$$

So $k2$ is taken to be:

$$k2 = \frac{1.39}{KPSed} \tag{66}$$

where:
> $KPSed$ =   detritus-water partition coefficient (L/kg); and
> 24   =   conversion from hours to days.

The slow compartment may be involved in 40 to 90% of the desorption so, as a simplification, fast desorption of the labile compartment is ignored. The sorption rate constant $k1$ is set to 1200 L/kg·d, representing the very fast sorption of most chemicals. Alternative formulations recognizing both fast and slow sorption and desorption are still being evaluated.

Bioconcentration in Macrophytes and Algae

Macrophytes—As Gobas et al. (1991) have shown, submerged aquatic macrophytes take up and release organic chemicals over a measurable period of time at rates related to the octanol-water partition coefficient. Uptake and elimination are modeled assuming that the chemical is transported through both aqueous and lipid phases in the plant, with rate constants using empirical equations fit to observed data (Gobas et al., 1991), modified to account for ionization effects (**Figure 12**, **Figure 13**):

$$MacroUptake \ = \ k1 \ \cdot \ Diff1_{Plant} \ \cdot \ Toxicant_{Water} \ \cdot \ StVar_{Plant} \ \cdot \ 1E-6 \qquad (67)$$

$$Depuration_{Plant} \ = \ k2 \ \cdot \ Toxicant_{Plant} \ \cdot \ Diff2_{Plant} \qquad (68)$$

$$k1 \ = \ \frac{1}{0.0020 \ + \ \dfrac{500}{KOW \ \cdot \ Nondissoc}} \qquad (69)$$

$$k2 \ = \ \frac{1}{1.58 \ + \ 0.000015 \ \cdot \ KOW \ \cdot \ Nondissoc} \qquad (70)$$

where:
> $MacroUptake$ =   uptake of toxicant by plant (μg/L·d);
> $Depuration_{Plant}$ =   clearance of toxicant from plant (μg/L·d);
> $StVar_{Plant}$ =   biomass of given plant (mg/L);
> 1 E -6   =   units conversion (kg/mg);
> $Toxicant_{Plant}$ =   mass of toxicant in plant (μg/L);
> $k1$ =   sorption rate constant (L/kg·d);
> $k2$ =   elimination rate constant (1/d);
> $Diff1_{Plant}$ =   factor to normalize uptake rates (unitless);
> $Diff2_{Plant}$ =   factor to normalize loss rates (unitless);
> KOW =   octanol-water partition coefficient (unitless); and

Nondissoc = fraction of un-ionized toxicant (unitless).

Figure 12
Uptake Rate Constant for Macrophytes
(after Gobas et al., 1991)
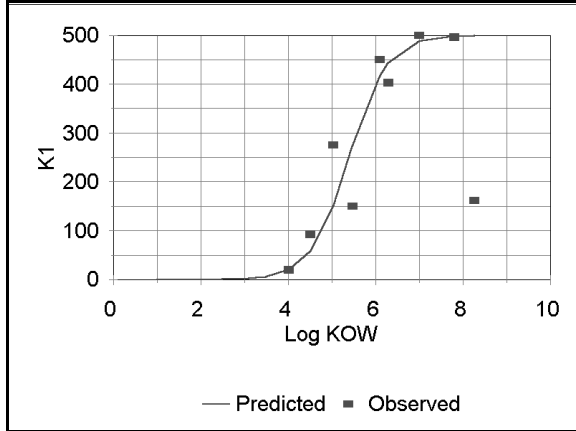
Figure 13
Elimination Rate Constant for Macrophytes
(after Gobas et al., 1991)
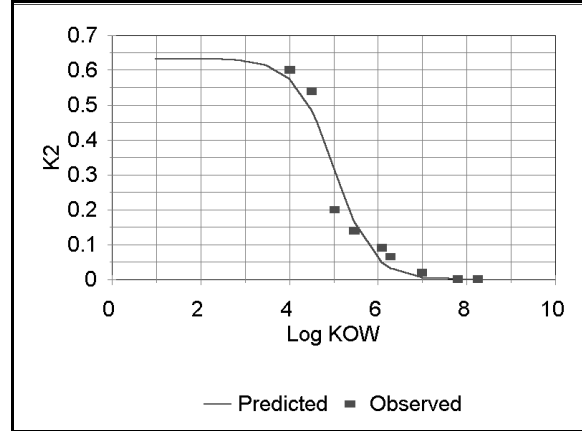
Algae—There is probably a two-step algal bioaccumulation mechanism for hydrophobic compounds, with rapid surface sorption of 40-90% of the compound within 24 hours and then a small, steady increase with transfer to interior lipids for the duration of the exposure (Swackhamer and Skoglund, 1991). Uptake increases with increase in the relative surface area of algae (Wang et al., 1997). Therefore, the smaller the organism the larger the uptake rate constant (Sijm et al., 1998). However, in small phytoplankton, such as the nannoplankton that dominate the Great Lakes, a high surface to volume ratio can increase sorption, but high growth rates can limit internal contaminant concentrations (Swackhamer and Skoglund, 1993). The combination of lipid content, surface area, and growth rate results in species differences in bioaccumulation factors among algae (Wood et al., 1997). Uptake of toxicants is a function of the uptake rate constant and the concentration of toxicant truly dissolved in the water, and is constrained by competitive uptake by other compartments:

$$AlgalUptake = k1 \cdot Michaelis \cdot Diff1 \cdot ToxState \cdot Carrier \cdot 1E-6 \qquad (71)$$

where:

AlgalUptake	=	rate of sorption by algae (μg/L·d);
k1	=	uptake rate constant (L/kg·d), see **(72)**;
Michaelis	=	Michaelis-Menten construct for nonlinear uptake (unitless), see **(73)**;
Diff1	=	factor to normalize uptake rates (unitless), see **(59)**;
ToxState	=	concentration of dissolved toxicant (μg/L);
Carrier	=	biomass of algal compartment (mg/L); and
1E-6	=	conversion factor (kg/mg).

The kinetics of partitioning of toxicants to algae is based on studies on PCB congeners in The Netherlands by Koelmans, Sijm, and colleagues and at the University of Minnesota by Skoglund and Swackhamer. Both groups found uptake to be very rapid. Sijm et al. (1998) presented data on several congeners that were used in this study to develop the following relationship for phytoplankton (**Figure 14**):

$$kl = \frac{1}{1.8 \text{E}-6 + 1/(K_{OW} \cdot \textit{Nondissoc})} \tag{72}$$

Because size-dependent passive transport is indicated (Sijm et al., 1998) and the bioaccumulation factor for periphyton has been found to be an order of magnitude less than that for phytoplankton (Wang et al.,1999), uptake by periphyton is set at 10% of that for phytoplankton.

To represent saturation kinetics, *Michaelis* is computed as:

$$\textit{Michaelis} = \frac{BCF_{Algae} \cdot \textit{ToxState} - PPB_{Algae}}{BCF_{Algae} \cdot \textit{ToxState}} \tag{73}$$

where:
BCF_{Algae} = steady-state bioconcentration factor for algae (L/kg); and
PPB_{Algae} = concentration of toxicant in algae (mg/kg).

Depuration is modeled as a linear function; it does not include loss due to excretion of photosynthate with associated toxicant, which is modeled separately.

$$\textit{Depuration} = k2 \cdot \textit{State} \tag{74}$$

where:
Depuration = elimination of toxicant (μg/L·d);
State = concentration of toxicant associated with alga (μg/L); and
k2 = elimination rate constant (day^{-1}).

Based in part on Skoglund et al. (1996), but ignoring surface sorption and recognizing that growth dilution is explicit in AQUATOX, the elimination rate constant (**Figure 15**) is computed as:

$$k2 = \frac{kl}{K_{OW}} \tag{75}$$

Aside from obvious structural differences, algae may have very high lipid content (20% for *Chlorella* sp. according to Jørgensen et al., 1979) and macrophytes have a very low lipid content (0.2% in *Myriophyllum spicatum* as observed by Gobas et al., 1991), which affect both uptake and elimination of toxicants. The uptake rate for macrophytes is much less than for phytoplankton, but in a shallow-water system, such as parts of the Housatonic River, very high macrophyte biomass may constitute a large seasonal sink for PCBs.

Figure 14
Algal Sorption Rate Constant as a Function of
Octanol-Water Partition Coefficient
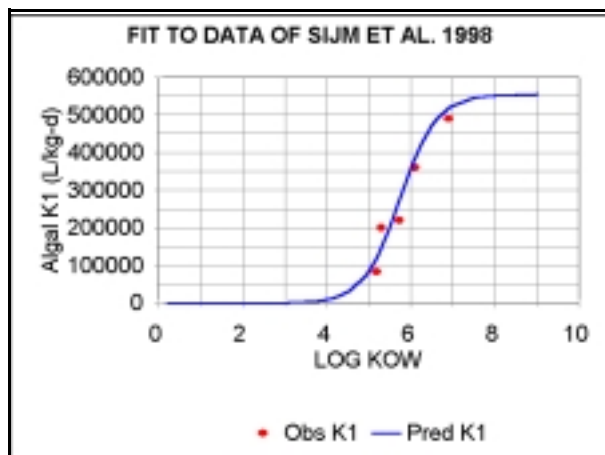
Figure 15
Rate of Elimination by Algae as a Function of
Octanol-Water Partition Coefficient
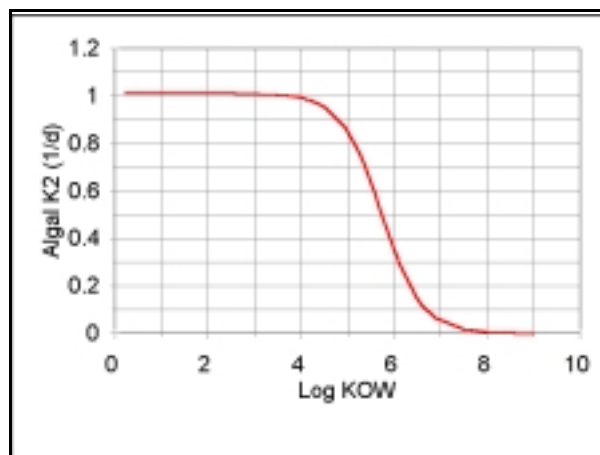
Bioaccumulation in Animals

Animals can absorb toxic organic chemicals directly from the water through their gills and from contaminated food through their guts. Direct sorption onto the body is ignored as a simplifying assumption in this version of the model. Reduction of body burdens of organic chemicals is accomplished through excretion and biotransformation, which are often considered together as empirically determined elimination rates. "Growth dilution" occurs when growth of the organism is faster than accumulation of the toxicant. Gobas (1993) includes fecal egestion, but in AQUATOX egestion is merely the amount ingested but not assimilated; it is accounted for indirectly in *DietUptake*. However, fecal loss is important as an input to the detrital toxicant pool, and it is considered below in that context. Inclusion of mortality and promotion terms is necessary for mass balance, but emphasizes the fact that average concentrations are being modeled for any particular compartment.

Gill Sorption—Active transport through the gills is an important route of exposure (Macek et al., 1977). This is the route that has been measured so often in bioconcentration experiments with fish. As the organism respires, water is passed over the outer surface of the gill and blood is moved past the inner surface. The exchange of toxicant through the gill membrane is assumed to be facilitated by the same mechanism as the uptake of oxygen, following the approach of Fagerström and Åsell (1973, 1975), Weininger (1978), and Thomann and Mueller (1987; see also Thomann, 1989). Therefore, the uptake rate for each animal can be calculated as a function of respiration (Leung, 1978; Park, Connolly, et al., 1980):

$$KUptake \ = \ \frac{WEffTox \ \cdot \ Respiration \ \cdot \ O2Biomass}{Oxygen \ \cdot \ WEffO2} \tag{76}$$

$$GillUptake = KUptake \cdot Toxicant_{Water} \cdot Diff1_{Carrier} \qquad\qquad \textbf{(77)}$$

where:

GillUptake	=	uptake of toxicant by gills (μg/L·d);
KUptake	=	uptake rate (day^{-1});
Toxicant$_{Water}$	=	concentration of toxicant in water (μg/L);
Diff1$_{Carrier}$	=	factor to normalize rate constant for given carrier (animal compartment in this case) based on all competing uptake rates (unitless), see **(59)**;
WEffTox	=	withdrawal efficiency for toxicant by gills (unitless), see **(78)**;
Respiration	=	respiration rate (mg biomass/L·d);
O2Biomass	=	ratio of oxygen to organic matter (mg oxygen/mg biomass; generally 0.575);
Oxygen	=	concentration of dissolved oxygen (mg oxygen/L); and
WEffO2	=	withdrawal efficiency for oxygen (unitless, generally 0.62).

The oxygen uptake efficiency *WEffO2* is assigned a constant value of 0.62 based on observations of McKim et al. (1985). The toxicant uptake efficiency, *WEffTox*, can be expected to have a sigmoidal relationship to the log K_{ow} based on aqueous and lipid transport (Spacie and Hamelink, 1982). This is represented by a piece-wise fit (**Figure 16**) to the data of McKim et al. (1985) using 750-g fish, corrected for ionization:

$$\text{If } \log K_{OW} < 1.5 \text{ then}$$
$$WEffTox = 0.1$$

$$\text{If } 1.5 \leq \log K_{OW} > 3.0 \text{ then}$$
$$WEffTox = 0.1 + Nondissoc \cdot (0.3 \cdot LogKOW - 0.45)$$

$$\text{If } 3.0 \leq \log K_{OW} \leq 6.0 \text{ then}$$
$$WEffTox = 0.1 + Nondissoc \cdot 0.45 \qquad\qquad \textbf{(78)}$$

$$\text{If } 6.0 < \log K_{OW} < 8.0 \text{ then}$$
$$WEffTox = 0.1 + Nondissoc \cdot (0.45 - 0.23 \cdot (LogKOW - 6.0))$$

$$\text{If } \log K_{OW} \geq 8.0 \text{ then}$$
$$WEffTox = 0.1$$

where:

LogKOW	=	log octanol-water partition coefficient (unitless); and
Nondissoc	=	fraction of toxicant that is un-ionized (unitless).

This same algorithm is used for invertebrates. Thomann (1989) has proposed a similar construct for these same data and a slightly different construct for small organisms, but the scatter in the data does not seem to justify using two different constructs.

Figure 16
Piece-Wise Fit to Observed Toxicant Uptake Data;
Modified from McKim et al., 1985
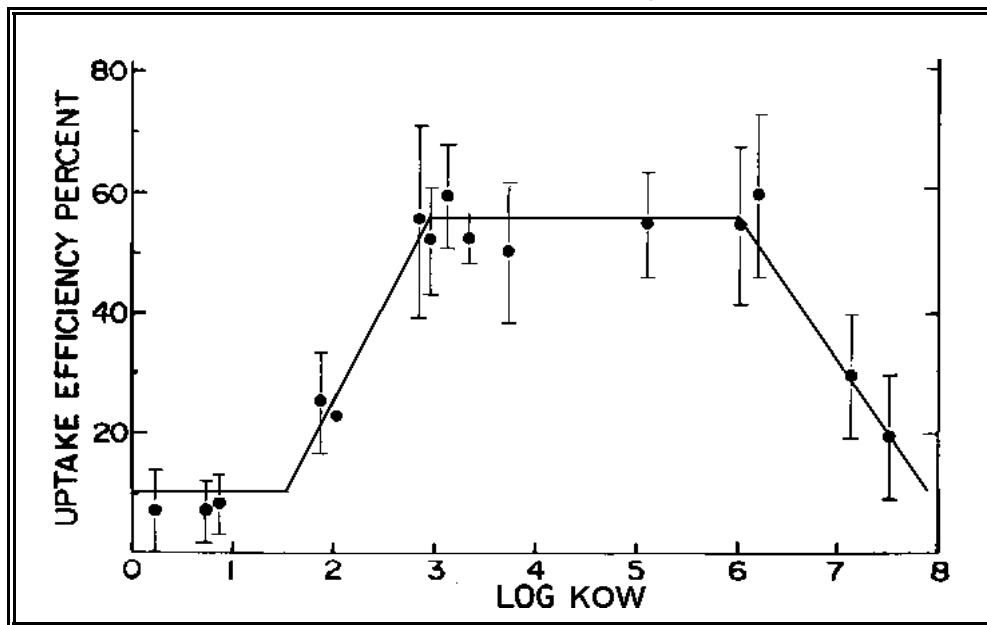
Dietary Uptake—Hydrophobic chemicals usually bioaccumulate primarily through absorption from contaminated food. Persistent, highly hydrophobic chemicals demonstrate biomagnification or increasing concentrations as they are passed up the food chain from one trophic level to another; therefore, dietary exposure can be quite important (Gobas et al., 1993). Uptake from contaminated prey can be computed as (Thomann and Mueller, 1987; Gobas, 1993):

$$DietUptake_{Prey} = KD_{Prey} \cdot PPB_{Prey} \cdot 1E-6 \tag{79}$$

$$KD_{Prey} = GutEffTox \cdot Ingestion_{Prey} \tag{80}$$

where:

$DietUptake_{Prey}$	=	uptake of toxicant from given prey (μg toxicant/L·d);
KD_{Prey}	=	dietary uptake rate for given prey (mg prey/L·d);
PPB_{Prey}	=	concentration of toxicant in given prey (μg toxicant/kg prey);
1 E-6	=	units conversion (kg/mg);
$GutEffTox$	=	efficiency of sorption of toxicant from gut (unitless); and

$Ingestion_{Prey}$ = ingestion of given prey (mg prey/L·d).

Data published by Gobas et al. (1993) suggest that there is no trend in efficiency for chemicals with log K_{OW} between 4.5 and 7.5 (**Figure 17**); this is to be expected because the digestive system has evolved to assimilate a wide variety of organic molecules. Nichols et al. (1998) demonstrated that uptake is more efficient in larger fish; this could be a function of higher quality food. Invertebrates generally exhibit lower efficiencies; Landrum and Robbins (1990) showed that values ranged from 0.42 to 0.24 for chemicals with log K_{OW}s from 4.4 to 6.7. It appears that assimilation of lipophilic chemicals follows the assimilation of lipids (van Veld, 1990). Therefore, AQUATOX uses the same assimilation efficiency for contaminant as for food, similar to the approach taken in a bioaccumulation model for PCBs in the Upper Hudson River (QEA, 1999):

$$GutEffTox = 1 - Egest \tag{81}$$

where:
 $Egest$ = portion of ingested food not assimilated (unitless).

Figure 17
Efficiency of Uptake, Data from Gobas et al., 1993
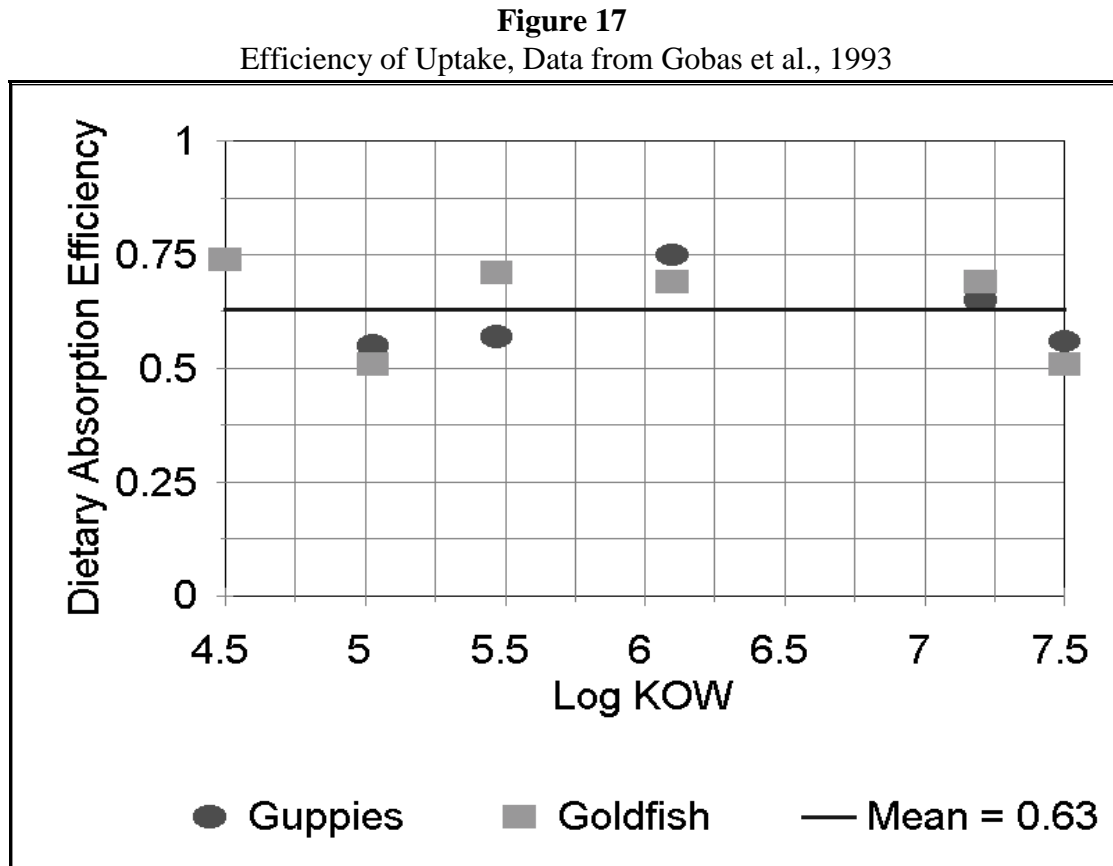
Elimination—Elimination or clearance includes both excretion (depuration) and biotransformation of a contaminant by organisms. Biotransformation may cause underestimation of elimination

(McCarty et al., 1992). An overall elimination rate constant, based on a fit to laboratory data, is estimated for both invertebrates and fish. The user may enter both a biotransformation rate constant and a depuration rate constant based on observed data or may accept the estimate for a given organism and contaminant.

The estimation procedure is based on a slope related to log K_{OW} and an intercept that is a direct function of respiration, assuming an allometric relationship between respiration and the weight of the animal (Thomann, 1989), and an inverse function of the lipid content:

$$\text{Log } k2 = -0.536 \cdot \log K_{OW} + 0.116 \cdot \frac{WetWt^{-0.2}}{LipidFrac} \tag{82}$$

where:
$k2$ = elimination rate constant (day^{-1}); and
KOW = octanol-water partition coefficient (unitless);
$WetWt$ = mean wet weight of organism (g);
$LipidFrac$ = fraction of lipid in organism (g lipid/g organism, dry weight);

This function is used in AQUATOX to estimate the elimination rate constant for both invertebrates and fish (**Figure 18**).

For any given time period, the clearance rate is:

$$Depuration_{Animal} = k2 \cdot Toxicant_{Animal} \tag{83}$$

where:
$Depuration_{Animal}$ = clearance rate (μg/L·d); and
$Toxicant_{Animal}$ = mass of toxicant in given animal (μg/L).

Biotransformation is modeled as:

$$Biotransformation = Toxicant_{Organism} \cdot BioRateConst \tag{84}$$

where:
$Biotransformation$ = rate of conversion of chemical by organism (μg/L·d); and
$BioRateConst$ = biotransformation rate constant (day^{-1}).

Linkages to Detrital Compartments

Toxicants are transferred from organismal to detrital compartments through defecation and mortality. The amount transferred due to defecation is the unassimilated portion of the toxicant that is ingested:

$$DefecationTox = \sum (KEgest_{Pred, Prey} \cdot PPB_{Prey} \cdot 1E-6) \tag{85}$$

Figure 18
Depuration Rate Constants for Zooplankton (Daphnia), 10-g Fish, and Amphipods (Diporeia)
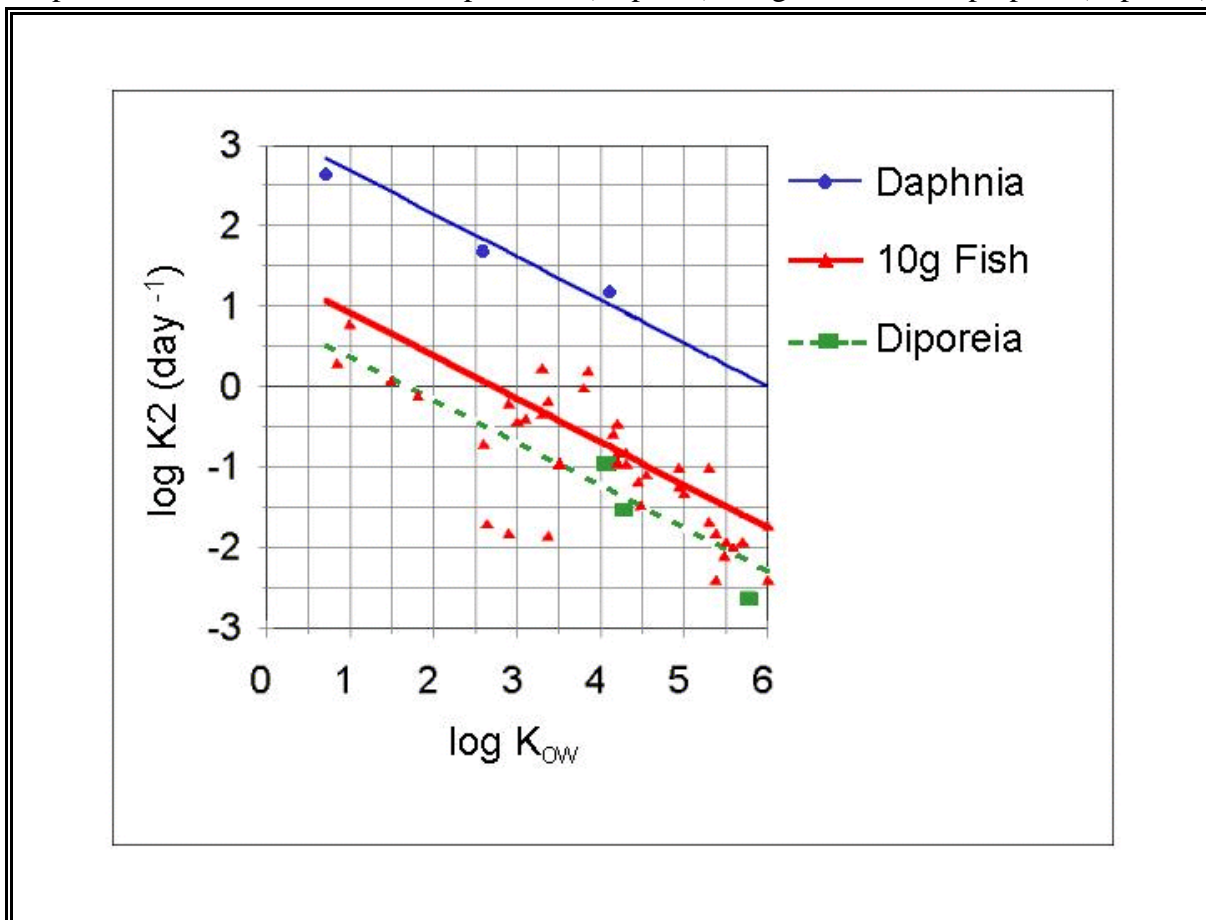
$$KEgest_{Pred, Prey} = (1 - GutEffTox) \cdot Ingestion_{Pred, Prey} \qquad (86)$$

where:

$DefecationTox$	=	rate of transfer of toxicant due to defecation (μg/L·d);
$KEgest_{Pred, Prey}$	=	fecal egestion rate for given prey by given predator (mg prey/L·d);
PPB_{Prey}	=	concentration of toxicant in given prey (μg/kg);
1 E-6	=	units conversion (kg/mg);
$GutEffTox$	=	efficiency of sorption of toxicant from gut (unitless); and
$Ingestion_{Pred, Prey}$	=	rate of ingestion of given prey by given predator (mg/L·d).

The amount of toxicant transferred due to mortality may be large; it is a function of the concentrations of toxicant in the dying organisms and the mortality rates:

$$MortTox = \sum (Mortality_{Org} \cdot PPB_{Org} \cdot 1E-6) \qquad (87)$$

where:

MortTox	=	rate of transfer of toxicant due to mortality (μg/L·d);
Mortality$_{Org}$	=	rate of mortality of given organism (mg/L·d);
PPB$_{Org}$	=	concentration of toxicant in given organism (μg/kg); and
1 E-6	=	units conversion (kg/mg).

ECOTOXICOLOGY

Toxicity can be modeled if desired; however, we do not anticipate modeling PCB toxicity in the Housatonic River project. When modeled, toxicity is based on the internal concentration of the toxicant in the specified organism. Many compounds, especially those with higher octanol-water partition coefficients, take appreciable time to accumulate in tissue. Therefore, length of exposure is critical in determining toxicity and is modeled following Mancini (1983); (see also Crommentuijn et al., 1994). The fraction killed by a given internal concentration of toxicant is estimated using the cumulative form of the Weibull distribution (Christensen and Nyholm, 1984; Mackay et al., 1992).

Organisms usually have adverse reactions to toxicants at levels significantly below those that cause death; in fact, the acute to chronic ratio is commonly used to quantify this relationship. Default application factors, which are the inverse of the acute to chronic ratio, are employed in the model to estimate chronic effect parameters. These can be supplied by the user or the default of 0.10 reported by McCarty et al. (1992) can be used.

Similar to acute toxicity, chronic toxicity is based on internal concentrations of a toxicant. The simplifying assumption is that chronic effects form a continuum with acute effects and that the difference is merely one of degree (McCarty et al., 1992). Because AQUATOX simulates biomass, no distinction is made between reduction in a process in an individual and the fraction of the population exhibiting that response. The commonly measured reduction in photosynthesis is a good example: the data indicate only that a given reduction takes place at a given concentration, not whether all individuals are affected. This approach permits efficient computation of chronic effect factors in conjunction with computation of acute effects.

REFERENCES

Abbott, J.D., S.W. Hinton, and D.L. Borton. 1995. Pilot Scale Validation of the RIVER/FISH Bioaccumulation Modeling Program for Nonpolar Hydrophobic Organic Compounds Using the Model Compounds 2,3,7,8-TCDD and 2,3,7,8-TCDF. *Environmental Toxicology and Chemistry*, 14(11):1999-2012.

Ambrose, R.B., Jr., T.A Wool, and J.L. Martin. 1993. *The Water Quality Analysis Simulation Program WASP5. Version 5.00.* U.S. Environmental Protection Agency, Environmental Research Laboratory, Athens, Georgia.

Ambrose, R.B., Jr., T.A. Wool, J.L. Martin, J.P. Connolly, and R.W. Schanz. 1991. *WASP4, A Hydrodynamic and Water Quality Model—Model Theory, User's Manual, and Programmer's Guide.* U.S. Environmental Protection Agency, Environmental Research Laboratory, Athens, Georgia.

Bertelsen, S.L., A.D. Hoffman, C.A. Gallinat, C.M. Elonen, and J.W. Nichols. 1998. Evaluation of Log K_{OW} and Tissue Lipid Content as Predictors of Chemical Partitioning to Fish Tissues. *Environmental Toxicology and Chemistry*, 17(8):1447-1455.

Bloomfield, J.A., R.A. Park, D. Scavia, and C.S. Zahorcak. 1973. Aquatic Modeling in the EDFB, US-IBP in E.J. Middlebrooks, D.H. Falkenborg, and T.W. Maloney, Eds., *Modeling the Eutrophication Process,* Ann Arbor, Michigan: Ann Arbor Science Publishers.

Bowie, G.L., W.B. Mills, D.B. Porcella, C.L. Campbell, J.R. Pagenkopf, G.L. Rupp, K.M. Johnson, P.W.H. Chan and S.A. Gherini. 1985. *Rates, Constants, and Kinetics Formulations in Surface Water Quality Modeling (Ed. 2).* U.S. Environmental Protection Agency, Athens, Georgia. EPA-600/3-85-040.

Björk, M., and M Gilek. 1999. Efficiencies of Polychlorinated Biphenyl Assimilation from Water and Algal Food by the Blue Mussel (*Mytilus edulis*). *Environmental Toxicology and Chemistry*, 18(4):765-771.

Burns, L.A., D.M. Cline, and R.R. Lassiter. 1982. *Exposure Analysis Modeling System (EXAMS): User Manual and System Documentation*. U.S. Environmental Protection Agency, Athens, Georgia. EPA-600/3-82-023.

Butcher, J.B., E.A. Garvey, and V.J. Bierman, Jr. 1998. Equilibrium Partitioning of PCB Congeners in the Water Column: Field Measurements from the Hudson River. *Chemosphere*, 36(15):3149-3166.

Canale, R.P., L.M. Depalma, and A.H. Vogel. 1976. A Plankton-Based Food Web Model for Lake Michigan, *in* R.P. Canale (ed.) *Modeling Biochemical Processes in Aquatic Ecosystems.* Ann Arbor Science Publishers, Ann Arbor, Michigan, pp. 33-74.

Christensen, E.R., and N. Nyholm. 1984. Ecotoxicological Assays with Algae: Weibull Dose-Response Curves. *Environ. Sci. Technol.,* 18(9):713-718.

Clesceri L.S., R.A. Park, and J.A. Bloomfield. 1977. A General Model of Microbial Growth and Decomposition in Aquatic Ecosystems. *Applied and Environmental Microbiology* 33(5):1047-1058.

Collins, C.D., and R.A. Park. 1989. Chapter 15, Primary Productivity. In *Mathematical Submodels in Water Quality Systems* , S.E. Jørgensen and M.J. Gromiec, eds. Amsterdam: Elsevier, pp. 299-330.

Collins, C.D., R.A. Park, and C.W. Boylen. 1985. *A Mathematical Model of Submersed Aquatic Plants*. Miscell. Paper A-85-2, U.S. Army Engineers Waterways Experiment Station, Vicksburg, Mississippi.

Connell, D.W., and D.W. Hawker. 1988. Use of Polynomial Expressions to Describe the Bioconcentraton of Hydrophobic Chemicals by Fish. *Ecotoxicology and Environmental Safety* 16:242-257.

Connolly, J.P., and D. Glaser. 1998. Use of Food Web Models to Evaluate Bioaccumulation. *National Sediment Bioaccumulation Conference Proceedings*. U.S. Environmental Protection Agency Office of Water EPA 823-R-98-002, p.4-5-4-17.

Cook, P.M., and L.P. Burkhard. 1998. Development of Bioaccumulation Factors for Protection of Fish and Wildlife in the Great Lakes. *National Sediment Bioaccumulation Conference Proceedings*. U.S. Environmental Protection Agency Office of Water EPA 823-R-98-002, p. 3-19-3-27.

Covar, A.P. 1976. Selecting the Proper Reaeration Coefficient for Use in Water Quality Models. Presented at US EPA Conference on Environmental Simulation and Modeling, April 19-22, Cincinnati, Ohio.

Crommentuijn, T., C.J.A.M. Doodeman, A. Doornekamp, J.J.C. van der Pol, J.J.M. Bedaux, and C.A.M. van Gestel. 1994. Lethal Body Concentrations and Accumulation Patterns Determine Time-Dependent Toxicity of Cadmium in Soil Arthropods. *Environmental Toxicity and Chemistry* 13(11):1781-1789.

Di Toro, D.M. 1985. A Particle Interaction Model of Reversible Organic Chemical Sorption. *Chemosphere*, 14(10):1503-1538.

Fagerström, T., and B. Åsell. 1973. Methyl Mercury Accumulation in an Aquatic Food Chain, A Model and Some Implications for Reesearch Planning. *Ambio*, 2(5):164-171.

Fagerström, T., R. Kurtén ,and B. Åsell. 1975. Statistical Parameters as Criteria in Model Evaluation: Kinetics of Mercury Accumulation in Pike *Esox lucius*. *Oikos* 26:109-116.

Gilek, M., M. Björk, D. Broman, N. Kautsky, and C. Näf. 1996. Enhanced Accumulation of PCB Congeners by Baltic Sea Blue Mussels, *Mytilus edulis*, with Increased Algae Enrichment. *Environmental Toxicology and Chemistry*, 15(9):1597-1605.

Gobas, F.A.P.C. 1993. A Model for Predicting the Bioaccumulation Hydrophobic Organic Chemicals in Aquatic Food-Webs: Application to Lake Ontario. *Ecological Modelling*, 69:1-17.

Gobas, F.A.P.C., E.J. McNeil, L. Lovett-Doust, and G.D. Haffner. 1991. Bioconcentration of Chlorinated Aromatic Hydrocarbons in Aquatic Macrophytes (*Myriophyllum spicatum*). *Environmental Science & Technology*, 25:924-929.

Gobas, F.A.P.C., Xin Zhang, and Ralph Wells. 1993. Gastrointestinal Magnification: The Mechanism of Biomagnification and Food Chain Accumulation of Organic Chemicals. *Environmental Science & Technology*, 27:2855-2863.

Hanna, M. 1990. Evaluation of Models Predicting Mixing Depth. *Can. J. Fish. Aquat. Sci.*, 47:940-947.

Hawker, D.W. and D.W. Connell. 1985. Prediction of Bioconcentration Factors Under Non-Equilibrium Conditions. *Chemosphere* 14(11/12):1835-1843.

Hill, I.R., and P.L. McCarty. 1967. Anaerobic Degradation of Selected Chlorinated Pesticides. *Jour. Water Poll. Control Fed.* 39:1259.

Hill, W.R., and Napolitano, G.E. 1997. PCB Congener Accumulation by Periphyton, Herbivores, and Omnivores. *Archives Environmental Contamination Toxicology*, 32:449-455.

Howick, G.L., F. deNoyelles, S.L. Dewey, L. Mason, and D. Baker. 1993. The Feasibility of Stocking Largemouth Bass in 0.04-ha Mesocosms Used for Pesticide Research. *Environmental Toxicology and Chemistry*, 12:1883-1893.

Jørgensen, S.E., H.F. Mejer, M. Friis, L.A. Jørgensen, and J. Hendriksen (Eds.). 1979. *Handbook of Environmental Data and Ecological Parameters*. Copenhagen: International Society of Ecological Modelling.

Junge, C.O. 1966. Depth distributions for quadratic surfaces and other configurations. In: Hrbáček, J. (Ed.): *Hydrobiological Studies. Vol. 1*, Academia, Prague, pp. 257-265.

Jupp, B.P., and D.H.N. Spence. 1977a. Limitations on Macrophytes in a Eutrophic Lake, Loch Leven I. Effects of Phytoplankton. *Journal Ecology*, 65:175-186.

Jupp, B.P., and D.H.N. Spence. 1977b. Limitations on Macrophytes in a Eutrophic Lake, Loch Leven II. Wave Action, Sediments, and Waterfowl Grazing. *Journal Ecology*, 65:431-446.

Karickhoff, S.W., and K.R. Morris. 1985. Sorption Dynamics of Hydrophobic Pollutants in Sediment Suspensions. *Environmental Toxicology and Chemistry*, 4:469-479.

Koelmans, A.A., S.F.M. Anzion, and L. Lijklema. 1995. Dynamics of Organic Micropollutant Biosorption to Cyanobacteria and Detritus. *Environmental Science & Technology*, 29(4):933-940.

Landrum, P. 1998. Kinetic models for assessing bioaccumulation. National Sediment Bioaccumulation Conference Proceedings. U.S. Environmental Protection Agency Office of Water EPA 823-R-98-002, P. 1-47-1-50.

Landrum, P.F., J. A. Robbins. 1990. Bioavailability of Sediment-Associated Contaminants to Benthis Invertebrates. In R. Baudo, J.P. Giesy, and H. Muntau (eds) *Sediments: Chemistry and Toxicity of In-Place Pollutants*, Ann Arbor: Lewis Publishers, pp. 237-263.

Le Cren, E.P., and R.H. Lowe-McConnell (Eds.). 1980. *The Functioning of Freshwater Ecosystems*. Cambridge: Cambridge University Press, 588 pp.

Leung, D.K. 1978. *Modeling the Bioaccumulation of Pesticides in Fish*. Report N. 5, Center for Ecological Modeling, Rensselaer Polytechnic Institute, Troy, N.Y.

Liss, P.S., and P.G. Slater. 1974. Flux of Gases Across the Air-Sea Interface. *Nature*, 247:181-184.

Lyman, W.J., W.F. Reehl, and D.H. Rosenblatt. 1982. *Handbook of Chemical Property Estimation Methods*. McGraw-Hill, New York.

Macek, K.J., M.E. Barrows, R.F. Frasny, and B.H. Sleight III. 1977. Bioconcentration of ^{14}C-Pesticides by Bluegill Sunfish During Continuous Aqueous Exposure. In *Structure-Activity Correlations in Studies of Toxicity and Bioconcentration with Aquatic Organisms*, G.D. Veith and D. Konasewick, eds.

Mackay, D., H. Puig, and L.S. McCarty. 1992. An Equation Describing the Time Course and Variability in Uptake and Toxicity of Narcotic Chemicals to Fish. *Environmental Tixcology and Chemistry*, 11:941-951.

Mancini, J.L. 1983. A Method for Calculating Effects on Aquatic Organisms of Time Varying Concentrations. *Water Res*. 10:1355-1362.

McCarty, L.S., G.W. Ozburn, A.D. Smith, and D.G. Dixon. 1992. Toxicokinetic Modeling of Mixtures of Organic Chemicals. *Environmental Toxicology and Chemistry*, 11:1037-1047.

McKim, J.M., P.K. Schneider, and G. Veith. 1985. Absorption dynamics of organic chemical transport across trout gills as related to octanol-water partition coefficient. *Toxicol. Appl. Pharmacol.* 77: 1-10.

McIntire, C.D. 1968. Structural Characteristics of Benthic Algal Communities in Laboratory Streams. *Ecology* 49(3):520-537.

McIntire, C.D. 1973. Periphyton Dynamics in Laboratory Streams: a Simulation Model and Its Implications. *Ecological Monographs* 43(3):399-419.

Nichols, J. W., K. M. Jensen, J. E. Tietge, and R. D. Johnson. 1998. Physiologically Based Toxicokinetic Model for Maternal Transfer of 2,3,7,,8-Tetrachlorodibenzo-*p*-Dioxin in Brook Trout (*Salvelinus fontinalis*). *Environmental Toxicology and Chemistry*, 17(12):2422-2434.

O'Connor, D.J., and J.P. Connolly. 1980. The Effect of Concentration of Adsorbing Solids on the Partition Coefficient. *Water Research*, 14:1517-1523.

Odum, E.P., and A.A. de la Cruz. 1963. Detritus as a Major Component of Ecosystems. *Amer. Inst. Biol. Sci. Bull.*, 13:39-40.

Oliver, B.G., and A.J. Niimi. 1988. Trophodynamic Analysis of Polychlorinated Biphenyl Congeners and Other Chlorinated Hydrocarbons in the Lake Ontario Ecosystem. *Environ. Sci. Technol.*, 22(4):388-397.

O'Neill, R.V. 1969. Indirect Estimation of Energy Fluxes in Animal Food Webs. *Jour. Theoret. Biol.*, 22:284-290.

O'Neill, R.V., D.L. DeAngelis, J.B. Waide, and T.F.H. Allen. 1986. *A Hierarchical Concept of the Ecosystem*. Princeton University Press, Princeton, NJ.

Park, R.A. 1978. *A Model for Simulating Lake Ecosystems*. Center for Ecological Modeling Report No. 3, Rensselaer Polytechnic Institute, Troy, New York, 19 pp.

Park, R.A. 1984. TOXTRACE: A Model to Simulate the Fate and Transport of Toxic Chemicals in Terrestrial and Aquatic Environments. *Acqua e Aria,* No. 6, p. 599-607 (in Italian).

Park, R.A. 1990. *AQUATOX, a Modular Toxic Effects Model for Aquatic Ecosystems*. Final Report, EPA-026-87; U.S. Environmental Protection Agency, Corvallis, Oregon.

Park, R.A., 1993. *AQUATOX, a Modular Toxic Effects Model for Aquatic Ecosystems Version 3.5.* Abt Associates Inc., Bethesda, Maryland, 28 pp.

Park, R.A., C.D. Collins, C.I. Connolly, J.R. Albanese, and B.B. MacLeod. 1980. *Documentation of the Aquatic Ecosystem Model MS.CLEANER, A Final Report for Grant No. R80504701*, U.S. Environmental Protection Agency, Environmental Research Laboratory, Athens, Georgia. 112 pp.

Park, R.A., C.D. Collins, D.K. Leung, C.W. Boylen, J.R. Albanese, P. deCaprariis, and H. Forstner. 1979. The Aquatic Ecosystem Model MS.CLEANER. In *State-of- the-Art in Ecological Modeling*, edited by S.E. Jorgensen, 579-602. International Society for Ecological Modelling, Denmark.

Park, R.A., C.I. Connolly, J.R. Albanese, L.S. Clesceri, G.W. Heitzman, H.H. Herbrandson, B.H. Indyke, J.R. Loehe, S. Ross, D.D. Sharma, and W.W. Shuster. 1980. *Modeling Transport and Behavior of Pesticides and Other Toxic Organic Materials in Aquatic Environments.* Center for Ecological Modeling Report No. 7. Rensselaer Polytechnic Institute, Troy, New York. 163 pp.

Park, R.A., C.I. Connolly, J.R. Albanese, L.S. Clesceri, G.W. Heitzman, H.H. Herbrandson, B.H. Indyke, J.R. Loehe, S. Ross, D.D. Sharma, and W.W. Shuster. 1982. *Modeling the Fate of Toxic Organic Materials in Aquatic Environments*. U.S. Environmental Protection Agency Rept. EPA-6OO/S3-82-028, Athens, Georgia.

Park, R.A., R.V. O'Neill, J.A. Bloomfield, H.H. Shugart, Jr., R.S. Booth, J.F. Koonce, M.S. Adams, L.S. Clesceri, E.M. Colon, E.H. Dettman, R.A. Goldstein, J.A. Hoopes, D.D. Huff, S. Katz, J.F. Kitchell, R.C. Kohberger, E.J. LaRow, D.C, McNaught, J.L. Peterson, D. Scavia, J.E. Titus, P.R. Weiler, J.W. Wilkinson, and C.S. Zahorcak. 1974. A Generalized Model for Simulating Lake Ecosystems. *Simulation*, 23(2):30-50. Reprinted in *Benchmark Papers in Ecology*.

Park, R.A., D. Scavia, and N.L. Clesceri. 1975. CLEANER, The Lake George Model. In *Ecological Modeling in a Management Context*. Resources for the Future, Inc., Washington, D.C.

Parsons, T.R., R.J. LeBresseur, J.D. Fulton, and O.D. Kennedy. 1969. Production Studies in the Strait of Georgia II. Secondary Production Under the Fraser River Plume, February to May, 1967. *Jour. Exp. Mar. Biol. Ecol.* 3:39-50.

Press, W.H., B.P. Flannery, S.A. Teukolsky, and W.T. Vetterling. 1986. *Numerical Recipes: The Art of Scientific Computing*. Cambridge University Press, Cambridge, U.K. 818 pp.

QEA (Quantitative Environmental Analysis, LLC). 1999. *PCBs in the Upper Hudson River*. Prepared for General Electric, Albany NY. May 1999.

Sand-Jensen, K. 1977. Effects of Epiphytes on Eelgrass (*Zostera marina* L.) in Danish Coastal Waters. *Marine Technology Society Journal* 17:15-21.

Saunders, G.W. 1980. 7. Organic Matter and Decomposers. In E.P. Le Cren and R.H. Lowe-McConnell (Eds.), *The Functioning of Freshwater Ecosystems*. Cambridge: Cambridge University Press, pp. 341-392.

Scavia, D., B.J. Eadie, and A. Robertson. 1976. *An Ecological Model for Lake Ontario—Model Formulation, Calibration, and Preliminary Evaluation.* Tech. Report ERL 371-GLERL 12, National Oceanic and Atmospheric Administration, Boulder, Colorado.

Scavia, D., and R.A. Park. 1976. Documentation of Selected Constructs and Parameter Values in the Aquatic Model CLEANER. *Ecological Modelling* 2(1):33-58.

Schnoor, J.L. 1996. *Environmental Modeling: Fate and Transport of Pollutants in Water, Air, and Soil.* New York: John Wiley & Sons, 682 pp.

Schwarzenbach, R.P., P.M. Gschwend, and D.M. Imboden. 1993. *Environmental Organic Chemistry*. Wiley and Sons, Inc., New York.

Sijm, D.T.H.M., K.W. Broersen, D.F de Roode, and P. Mayer. 1998. Bioconcentration Kinetics of Hydrophobic Chemicals in Different Densities of *Chlorella 0pyrenoidosa*. *Environmental Toxicology and Chemistry* 17:9:1695-1704.

Skoglund, R.S., K. Stange, and D.L. Swackhamer. 1996. A Kinetics Model for Predicting the Accumulation of PCBs in Phytoplankton. *Environmental Science and Technology* 30:7:2113-2120.

Southworth, G.R., J.J. Beauchamp, and P.K. Schmieder. 1978. Bioaccumulation Potential of Polycyclic Aromatic Hydrocarbons in *Daphnia pulex*. *Water Res.*, 12:973-977.

Spacie, A., and J.L. Hamelink. 1982. Alternative Models for Describing the Bioconcentration of Organics in Fish. *Environmental Toxicology and Chemistry*, 1:309-320.

Stange, K., and D.L. Swackhamer. 1994. Factors Affecting Phytoplankton Species-Specific Differences in Accumulation of 40 Polychlorinated Biphenyls (PCBs). *Environmental Toxicology and Chemistry*, 13(11):1849-1860.

Steele, J.H. 1974. *The Structure of Marine Ecosystems*. Harvard University Press, Cambridge, Massachusetts, 128 pp.

Steele, J.H., and M.M. Mullin. 1977. Zooplankton Dynamics. In E.D. Goldberg, I.N. McCave, J.J. O'Brien, and J.H. Steele (Eds.), *The Sea Vol. 6: Marine Modeling*, New York: Wiley-Interscience, p. 857.

Straškraba, M. and A.H. Gnauck. 1985. *Freshwater Ecosystems: Modelling and Simulation*. Developments in Environmental Modelling, 8. Elsevier Science Publishers, Amsterdam, The Netherlands. 309 pp.

Swackhamer, D.L., and R.S. Skoglund. 1993. Bioaccumulation of PCBs by Algae: Kinetics versus Equilibrium. *Environmental Toxicology & Chemistry*, 12:831-838.

Swackhamer, D.L., and R.S. Skoglund. 1991. The Role of Phytoplankton in the Partitioning of Hydrophobic Organic Contaminants in Water. In Baker, R.A., ed., *Organic Substances and Sediments in Water Vol. 2 C Processes and Analytical*, Lewis: Chelsea MI, pp. 91-105.

Thomann, R.V., and J.A. Mueller. 1987. *Principles of Surface Water Quality Modeling and Control*, Harper Collins: new York N.Y., 644 pp.

Thomann, R.V. 1989. Bioaccumulation Model of Organic Chemical Distribution in Aquatic Food Chains. *Environmental Science & Technology*, 23:699-707.

Thomann, R.V. and J.A. Mueller. 1983. Chapter 16 Steady-State Modeling of Toxic Chemicals—Theory and Application of PCBs in The Great Lakes and Saginaw Bay. In D. Mackay, S. Paterson, S.J. Eisenreich, and M.S. Simmons (eds.), Physical Behavior of PCBs in the Great Lakes, Ann Arbor, MI: Ann Arbor Science, pp. 283-309.

Thomann, R.V., J.A. Mueller, R.P. Winfield, and C.-R. Huang. 1991. Model of Fate and Accumulation of PCB Homologues in Hudson Estuary. *Jour. Environ. Engineering*, 117(2):161-178.

Titus, J.E., M.S. Adams, P.R. Weiler, R.V. O'Neill, H.H. Shugart, Jr., and J.B. Mankin. 1972. *Production Model for* Myriophyllum spicatum *L.* Memo Rept. 72-19, U.S. International Biological Program Eastern Deciduous Forest Biome, University of Wisconsin, Madison, 17 pp.

Uhle, M.E., Y-P. Chin, G.R. Aiken, and D.M. McKnight. 1999. Binding of Polychlorinated Biphenyls to Aquatic Humic Substances: The Role of Substrate and Sorbate Properties on Partitioning. *Environ. Sc. Technol.*, 33:2715-2718.

U.S. Environmental Protection Agency. 2000a. *AQUATOX for Windows: A Modular Fate and Effects Model for Aquatic Ecosystems–Volume 1: User's Manual.* EPA-823-R-00-006.

U.S. Environmental Protection Agency. 2000b. *AQUATOX for Windows: A Modular Fate and Effects Model for Aquatic Ecosystems–Volume 2: Technical Documentation.* EPA-823-R-00-007.

U.S. Environmental Protection Agency. 2000c. *AQUATOX for Windows: A Modular Fate and Effects Model for Aquatic Ecosystems–Volume 3: Model Validation Reports.* EPA-823-R-00-008.

Van Veld, P.A. 1990. Absorption and metabolism of dietary xenobiotics by the intestines of fish. *Rev. Aquat. Sci 2*:185-203.

Wang, H., J.A. Kostel, A.L. St. Amand, and K.A. Gray. 1999. 2. The Response of a Laboratory Stream System to PCB Exposure: Study of Periphytic and Sediment Accumulation Patterns. *Water Res.*, 33(18):3749-3761.

Wang, X., Y. Ma, W. Yu, and H.J. Geyer. 1997. Two-Compartment Thermodynamic Model for Bioconcentration of Hydrophobic Organic Chemicals by Alga. *Chemosphere*, 35(8):1781-1797.

Weininger, D. 1978. *Accumulation of PCBs by Lake Trout in Lake Michigan.* Ph.D. Dissertation, University of Wisconsin, Madison, 232 pp.

Wetzel, R.G. 1975. *Limnology*, W.B. Saunders, Philadelphia, 743 pp.

Whitman, W.G. 1923. The two-film theory of gas absorption. *Chem. Metal. Eng.* 29:146-148.

Wood, L.W., P. O.Keefe, and B. Bush. 1997. Similarity Analysis of PAH and PCB Bioaccumulation Patterns in Sediment-Exposed *Chironomus tentans* Larvae. *Environmental Toxicology and Chemistry*, 16(2):283-292.

APPENDIX D.2

AQUATOX PARAMETER LIST

AQUATOX Parameter List

Internal to AQUATOX	Tech Doc Reference	Description	Units	Data Source
ChemicalRecord	**Chemical Underlying Data**	*For each Chemical Simulated, the following parameters are required*		
ChemName	N / A	Chemical's Name. Used for Reference only.	N / A	
CASRegNo	N / A	CAS Registry Number. Used for Reference only.	N / A	
MolWt	MolWt	molecular weight of pollutant	(g/mol)	lit
Solubility	N / A	Not utilized as a parameter by the code.	(ppm)	
Henry	Henry	Henry's law constant	(atm m^3 mol^{-1})	lit & est
pka	pKa	acid dissociation constant	negative log	NA
VPress	N / A	Not utilized as a parameter by the code.	mm Hg	
LogP	LogKow	log octanol-water partition coefficient	(unitless)	lit
En	En	Arrhenius activation energy	(cal/mol)	default
KMDegrdn	MicrobialDegrdn	rate of loss due to microbial degradation	(µg/L d)	site calib
KMDegrAnaerobic	KAnaerobic	decomposition rate at 0 g/m3 oxygen	(1/d)	site & calib
KUnCat	KUncat	the measured first-order reaction rate at pH 7	(1/d)	NA
KAcid	KAcidExp	pseudo-first-order acid-catalyzed rate constant for a given pH	(1/d)	NA
KBase	KBaseExp	pseudo-first-order rate constant for a given pH	(1/d)	NA
PhotolysisRate	KPhot	direct photolysis first-order rate constant	(1/d)	NA
OxRateConst	N / A	Not utilized as a parameter by the code.	(L/ mol d)	
KPSed	KPSed	detritus-water partition coefficient	(L/kg)	site & lit calc
Weibull_Shape	Shape	parameter expressing variability in toxic response	(unitless)	lit
ChemIsBase		if the compound is a base	(True/False)	NA
SiteRecord	**Site Underlying Data**	*For each Segment Simulated, the following parameters are required*		
SiteName	N / A	Site's Name. Used for Reference only.	N / A	
ECoeffWater	ExtinctH2O	light extinction of wavelength 312.5 nm in pure water	(1/m)	lit
SiteLength	Length	maximum effective length for wave setup, not used for Housatonic	(m)	
Volume	Volume	initial volume of site	(m^3)	EFDC
Area	Area	surface area of site (usually constant)	(m^2)	EFDC
ZMean	ZMean	mean depth	(m)	EFDC
ZMax	ZMax	maximum depth	(m)	EFDC
TempMean	TempMean	mean annual temperature	(°C)	site
TempRange	TempRange	annual temperature range	(°C)	site
Latitude	Latitude	latitude	(°, decimal)	site
LightMean	LightMean	mean annual light intensity	(ly/d)	site
LightRange	LightRange	annual range in light intensity	(ly/d)	site
AlkCaCO3	N / A	Not utilized as a parameter by the code.	mg/L	
HardCaCO3	N / A	Not utilized as a parameter by the code.	mg CaCO$_3$ / L	
SO4Conc	N / A	Not utilized as a parameter by the code.	mg/L	
TotalDissSolids	N / A	Not utilized as a parameter by the code.	mg/L	
StreamType	Stream Type	concrete channel, dredged channel, natural channel, not used for Housatonic	Choice from List	
Channel_Slope	Slope	slope of channel, not used for Housatonic	(m/m)	
Max_Chan_Depth	Max_Chan_Depth	depth at which flooding occurs , not used for Housatonic	(m)	
SedDepth	SedDepth	maximum sediment depth , not used for Housatonic	(m)	

Appendix D.2

AQUATOX Parameter List

Internal to AQUATOX	Tech Doc Reference	Description	Units	Data Source
LimnoWallArea	LimnoWallArea	area of limnocorral walls; only relevant to limnocorral	(m^2)	NA
MeanEvap	MeanEvap	mean annual evaporation, not used for Housatonic	inches / year	
UseEnteredManning		do not determine Manning coefficient from streamtype, not used for Housatonic	(true/false)	
EnteredManning	Manning	manually entered Manning coefficient, not used for Housatonic	s / m$^{1/3}$	
ReminRecord	**Remineralization Data**	*For each simulation, the following parameters are required*		
DecayMax	DecayMax	maximum decomposition rate for detritus	(g/g·d)	lit
Q10	NA	Not utilized as a parameter by the code.	(unitless)	NA
TOpt	TOpt	optimum temperature	(°C)	lit
TMax	TMax	maximum temperature tolerated	(°C)	lit
TRef	NA	Not utilized as a parameter by the code.	(°C)	NA
pHMin	pHMin	minimum pH below which limitation on biodegradation rate occurs.	pH	lit
pHMax	pHMax	maximum pH above which limitation on biodegradation rate occurs.	pH	lit
Org2Phosphate	Org2Phosphate	ratio of phosphate to organic matter (unitless)	(unitless)	lit
Org2Ammonia	Org2Ammonia	ratio of ammonia to organic matter	(unitless)	lit
O2Biomass	O2Biomass	ratio of oxygen to organic matter	(unitless)	lit
O2N	O2N	ratio of oxygen to nitrogen	(unitless)	lit
KSed	KSed	intrinsic settling rate	(m/d)	EFDC
PSedRelease	N / A	Not utilized as a parameter by the code.	(g/m^2·d)	NA
NSedRelease	N / A	Not utilized as a parameter by the code.	(g/m^2·d)	NA
ZooRecord	**Animal Underlying Data**	*For each animal in the simulation, the following parameters are required*		
AnimalName	N / A	Animal's Name. Used for Reference only.	N / A	
FHalfSat	FHalfSat	half-saturation constant for feeding by a predator	(g/m^3)	calib
CMax	CMax	maximum feeding rate for predator	(g/g·d)	lit calc
BMin	BMin	minimum prey biomass needed to begin feeding	(g/m^3)	calib
Q10	Q10	slope or rate of change per 10°C temperature change	(unitless)	lit
TOpt	TOpt	optimum temperature	(°C)	lit
TMax	TMax	maximum temperature tolerated	(°C)	lit
TRef	TRef	adaptation temperature below which there is no acclimation	(°C)	lit
EndogResp	EndogResp	basal respiration rate at 0° C for given predator	(1/day)	lit calc
KResp	KResp	proportion assimilated energy lost to specific dynamic action	(unitless)	lit
KExcr	KExcr	proportionality constant for excretion:respiration	(unitless)	lit
PctGamete	PctGamete	fraction of adult predator biomass that is in gametes	(unitless)	lit & site
GMort	GMort	gamete mortality	(1/d)	site calib
KMort	KMort	intrinsic mortality rate	(g/g·d)	site calib
KCap	KCap	carrying capacity	(mg/L)	lit & site
MeanWeight	WetWt	mean wet weight of organism	(g)	site
FishFracLipid	LipidFrac	fraction of lipid in organism	(g lipid/g organism)	site & calc
LifeSpan	LifeSpan	mean lifespan in days	days	site
Animal_Type	Animal Type	Animal Type (Fish, Pelagic Invert, Benthic Invert, Benthic Insect)	Choice from List	
AveDrift	Dislodge	fraction of biomass subject to drift per day	fraction / day	lit
AutoSpawn		Should AQUATOX calculate Spawn Dates	(true/false)	prob. false

Appendix D.2

AQUATOX Parameter List

Internal to AQUATOX	Tech Doc Reference	Description	Units	Data Source
SpawnDate1..3		Automatically Entered Spawn Dates	(date)	site
UnlimitedSpawning		Allow fish to spawn unlimited times each year	(true/false)	site
SpawnLimit		Number of spawns allowed for this species this year	(integer)	site
UseAllom_C		Use Allometric Consumption Equation	(true/false)	TRUE
CA		Allometric Consumption Parameter	(real number)	lit
CB		Allometric Consumption Parameter	(real number)	lit
UseAllom_R		Use Allometric Consumption Respiration	(true/false)	TRUE
RA		Allometric Respiration Parameter	(real number)	lit
RB		Allometric Respiration Parameter	(real number)	lit
UseSet1		Use "Set 1" of Allometric Respiration Parameters	(true/false)	lit
RQ		Allometric Respiration Parameter	(real number)	lit
RK1		Allometric Respiration Parameter	(real number)	lit
PlantRecord	**Plant Underlying Data**	*For each Plant in the Simulation, the following parameters are required*		
PlantName		Plant's Name. Used for Reference only.	N / A	
PlantType	Plant Type	Plant Type: (Phytoplankton, Periphyton, Macrophytes)	Choice from List	
LightSat	LightSat	light saturation level for photosynthesis	(ly/d)	lit & calib
KPO4	KP	half-saturation constant for phosphorus	(gP/m^3)	lit & calib
KN	KN	half-saturation constant for nitrogen	(gN/m^3)	lit & calib
KCarbon	KCO2	half-saturation constant for carbon	(gC/m^3)	lit & calib
Q10	Q10	slope or rate of change per 10°C temperature change	(unitless)	lit
TOpt	TOpt	optimum temperature	(°C)	lit
TMax	TMax	maximum temperature tolerated	(°C)	lit
TRef	TRef	adaptation temperature below which there is no acclimation	(°C)	lit
PMax	PMax	maximum photosynthetic rate	(1/d)	lit
KResp	KResp	coefficient of proportionality btwn. excretion and photosynthesis at optimal light levels	(unitless)	lit
KMort	KMort	intrinsic mortality rate	(g/g·d)	calib
EMort	EMort	exponential factor for suboptimal conditions	(unitless)	calib
KSed	KSed	intrinsic settling rate	(m/d)	lit
ESed	ESed	exponential settling coefficient	(unitless)	lit
UptakePO4	Uptake $_{Phosphorus}$	fraction of photosynthate that is nutrient	(unitless)	lit
UptakeN	Uptake $_{Nitrogen}$	fraction of photosynthate that is nutrient	(unitless)	lit
ECoeffPhyto	EcoeffPhyto	attenuation coefficient for given alga	$(1/m-g/m^3)$	lit
CarryCapac	KCap	carrying capacity of periphyton	(g/m^2)	site
Red_Still_Water	RedStillWater	reduction in photosynthesis in absence of current	(unitless)	lit
Macrophyte_Type	Macrophyte Type	Type of macrophyte (benthic, rooted floating, free-floating)	Choice from List	site
TAnimalToxRecord	**Animal Toxicity Parameters**	*For each Chemical Simulated, the following parameters are required for each animal in the model*		
LC50	LC50	external concentration of toxicant at which 50% of population is killed *	(µg/L)	site & lit
LC50_exp_time	ObsTElapsed	exposure time in toxicity determination *	(h)	site & lit
K2	K2	elimination rate constant	(1/d)	calc & calib
Bio_rate_const : Double;	Biotransformation Rate		(1/d)	lit & calib
EC50_growth	EC50Growth	external concentration of toxicant at which there is a 50% reduction in growth *	(µg/L)	site & lit

Appendix D.2

AQUATOX Parameter List

Internal to AQUATOX	Tech Doc Reference	Description	Units	Data Source
Growth_exp_time	ObsTElapsed	exposure time in toxicity determination *	(h)	site & lit
EC50_repro	EC50Repro	external concentration of toxicant at which there is a 50% reduction in reproduction *	(µg/L)	site & lit
Repro_exp_time	ObsTElapsed	exposure time in toxicity determination *	(h)	site & lit
Ave_wet_wt	WetWt	mean wet weight of organism	(g)	site
Lipid_frac	LipidFrac	fraction of lipid in organism	(g lipid/g organism)	site & calc
Drift_Thresh	Drift Threshold	concentration at which drift is initiated *	(µg/L)	lit & calib
		* prob. not used for Housatonic		
TPlantToxRecord	**Plant Toxicity Parameters**	*For each Chemical Simulated, the following parameters are required for each plant in the model*		
EC50_photo	EC50Photo	external concentration of toxicant at which there is 50% reduction in photosynthesis *	(µg/L)	lit
EC50_exp_time	ObsTElapsed	exposure time in toxicity determination *	(h)	lit
K2	K2	elimination rate constant	(1/d)	lit & calib
Bio_rate_const	Biotransformation Rate		(1/d)	lit & calib
LC50	LC50	external concentration of toxicant at which 50% of population is killed *	(µg/L)	lit & site
LC50_exp_time	ObsTElapsed	exposure time in toxicity determination *	(h)	lit & site
Lipid_frac	LipidFrac	fraction of lipid in organism	(g lipid/g organism)	lit & site
		* prob. not used for Housatonic		
TBioTransRecord	**Biotransformation Params.**	*For each type of Biotransformation to be simulated, the following parameters are required*		
BTType	Category of Biotransformation	AerobicMicrobial, AnaerobicMicrobial, Algae, BenthInsect, OtherBenthos, Fish, UserSpecifie	Choice from List	lit & calib
UserSpec	User Specified Species	If this type of biotransf. occurs in user specified species, that species chosen here	Choice from List	lit & calib
Percent	Biotransformation to	Of total biotransformation within this category, the % transformed to various chemicals	Set of Percentages	lit & calib
TChemical	**Chemical**	*For each Chemical to be simulated, the following are required*		
InitialCond	Initial Condition	Initial Condition of the state variable	µg/L	site
Loadings	Inflow Loadings	Daily loading as a result of the inflow of water (excluding modeled upstream reaches)	µg/L	HSPF
Alt_Loadings[Pointsource]	Point Source Loadings	Daily loading from point sources	(g/d)	HSPF
Alt_Loadings[Direct Precip]	Direct Precipitation Loadings	Daily loading from direct precipitation	(g/m^2·d)	site
Alt_Loadings[NonPointsource]	Non-Point Source Loadings	Daily loading from non-point sources	(g/d)	HSPF
Tox_Air	Gas-phase concentration	will prob. ignore for Housatonic	(g/m^3)	site & lit
TRemineralize	**Nutrient**	*For each Nutrient to be simulated, including O$_2$ and CO$_2$, the following are required*		
InitialCond	Initial Condition	Initial Condition of the state variable	mg/L	site
Loadings	Inflow Loadings	Daily loading as a result of the inflow of water (excluding modeled upstream reaches)	mg/L	HSPF
Alt_Loadings[Pointsource]	Point Source Loadings	Daily loading from point sources	(g/d)	HSPF
Alt_Loadings[Direct Precip]	Direct Precipitation Loadings	Daily loading from direct precipitation; will prob. ignore for Housatonic	(g/m^2·d)	site
Alt_Loadings[NonPointsource]	Non-Point Source Loadings	Daily loading from non-point sources	(g/d)	HSPF
TSedDetr	**Sed. Detritus Parameters**	*For Sedimented POM the following parameters are required*		
InitialCond	Initial Condition	Initial Condition of the state variable	(g/m^2)	site
TToxicant.InitialCond	Toxicant Exposure	Initial Toxicant Exposure of the state variable, for each chemical simulated	µg/kg	site
TDetritus	**Susp & Dissolved Detritus**	*For the Suspended and Dissolved Detritus compartments, the following parameters are required*		
InitialCond	Initial Condition	Initial Cond. of susp. & diss. detritus, as organic matter, organic carbon, or BOD	mg/L	site

Appendix D.2

AQUATOX Parameter List

Internal to AQUATOX	Tech Doc Reference	Description	Units	Data Source
Percent_Part_IC	Percent Particulate $_{Init\ Cond}$	Percent of Initial Condition that is particulate as opposed to dissolved detritus	percentage	site
Loadings	Inflow Loadings	Daily loading as a result of the inflow of water (excluding modeled upstream reaches)	mg/L	HSPF
Percent_Part	Percent Particulate $_{Inflow}$	Daily parameter; % of loading that is particulate as opposed to dissolved detritus	percentage	site
Alt_Loadings[Pointsource]	Point Source Loadings	Daily loading from point sources	(g/d)	HSPF
Percent_Part_PS	Percent Particulate $_{PointSrc}$	Daily parameter; % of loading that is particulate as opposed to dissolved detritus	percentage	site
Alt_Loadings[NonPointsource]	Non-Point Source Loadings	Daily loading from non-point sources	(g/d)	HSPF
Percent_Part_NPS	Percent Particulate $_{NonPointSrc}$	Daily parameter; % of loading that is particulate as opposed to dissolved detritus	percentage	site
TToxicant.InitialCond	Toxicant Exposure	Initial Toxicant concentration of the state variable	µg/kg	site
TToxicant.Loads	Tox Exposure of Inflow Load	Daily parameter; Tox. concentration of each type of inflowing detritus, for each chemical	µg/kg	site
TBuried Detritus	**Buried Detritus**	***For Each Layer of Buried Detritus, the following parameters are required***		
InitialCond	Initial Condition	Initial Condition of the state variable	(g/m^2)	site
TToxicant.InitialCond	Toxicant Exposure	Initial Toxicant concentration of the state variable, for each chemical simulated	µg/kg	site
TPlant	**Plant Parameters**	***For each plant type simulated, the following parameters are required***		
InitialCond	Initial Condition	Initial Condition of the state variable	mg/L	site
Loadings	Inflow Loadings	Daily loading as a result of the inflow of water (excluding modeled upstream reaches)	mg/L	site
TToxicant.InitialCond	Toxicant Exposure	Initial Toxicant concentration of the state variable	µg/kg	site
TToxicant.Loads	Tox Exposure of Inflow Load	Daily parameter; Tox. concentration of the Inflow Loadings, for each chemical	µg/kg	site
TAnimal	**Animal Parameters**	***For each animal type simulated, the following parameters are required***		
InitialCond	Initial Condition	Initial Condition of the state variable	mg/L	site
Loadings	Inflow Loadings	Daily loading as a result of the inflow of water (excluding modeled upstream reaches)	mg/L	site
TToxicant.InitialCond	Toxicant Exposure	Initial Toxicant concentration of the state variable	µg/kg	site
TToxicant.Loads	Tox Exposure of Inflow Load	Daily parameter; Tox. concentration of the Inflow Loadings, for each chemical simulated	µg/kg	site
TrophIntArray.Pref	Pref$_{prey,\ pred}$	for each prey-type ingested, a preference value within the matrix of preference parameters	(unitless)	lit
TrophIntArray.ECoeff	EgestCoeff	for each prey-type ingested, the fraction of ingested prey that is egested	(unitless)	lit
TVolume	**Volume Parameters**	***For each segment simulated, the following water flow parameters are required***		
InitialCond	Initial Condition	Initial Condition of the state variable	(m^3)	site
InflowLoad	Inflow of Water	Inflow of water, excluding upstream linked segments	(m^3/d)	EFDC
DischargeLoad	Discharge of Water	Discharge of water, excluding downstream linked segments	(m^3/d)	EFDC
FlowToFlood	FlowToFlood	Daily parameter; water flow into the floodplain during flood events	(m^3/d)	EFDC
FlowFromFlood	FlowFromFlood	Daily parameter; water flow out of the floodplain during flood events	(m^3/d)	EFDC
Site Characteristics	**Site Characteristics**	***For each segment simulated, the following characteristics parameters are required***		
Temperature	Temperature	Daily parameter; temperature of the segment; ***Optional***, can use annual mean	(°C)	site
Wind	Wind	Daily parameter; wind velocity 10 m above the water; ***Optional***, default time series avail.	(m/s)	site
Light	Light	Daily parameter; avg. light intensity at segment top; ***Optional***, can use annual Mean and Range	(ly/d)	site
Photoperiod	Photoperiod	Fraction of day with daylight; ***Optional***, can be calculated from latitude	(hr/d)	calc.
pH	pH	Daily parameter; pH of the segment.	(pH)	site

Appendix D.2

AQUATOX Parameter List

Internal to AQUATOX	Tech Doc Reference	Description	Units	Data Source
Physical Geometry	**Physical Geometry**	*For each segment simulated, the following physical geometry parameters are required for each day*		
Thickness	Segment Thickness	Thickness of the segment	m	EFDC
XSection	Cross Section Area	Cross sectional area of the segment	(m^2)	EFDC
Surface Area	Surface Area	Surface area of the segment	(m^2)	EFDC
TSegmentLink	**Segment Link Parameters**	*For each Link between two Segments, the following parameters are required*		
LinkType	Link Type	Is this a "Cascade Link" or a "Feedback Link"	Choice from List	site
FromID, ToID	Link Location	Describes which segments are linked together	Choice from List	site
Length	Length	Characteristic Length	(m)	site
XSectionData	Cross Section Loadings	Cross Sectional Area for each day of simulation	(m^2)	EFDC
DiffusionData	Diffusion Loadings	Daily Dispersion Coefficient	(m^2/d)	EFDC
WaterFlowData	Water Flow Loadings	Daily water flow through the linkage	(m^3/d)	EFDC
TSedimentData	**Sediment Data Parameters**	*For each AQUATOX segment, for each sediment modeled, the following parameters are required each day*		
Loading	External Loading	external load of this suspended sediment type (not from upstream link)	(g/d)	HSPF
BedLoad	BedLoad	bed load of cohesive and noncohesive sediments	(g/d)	EFDC
Deposition	Deposition	net deposition of cohesive and noncohesive sediments	(g/d)	EFDC
Resuspension	Resuspension	net resuspension of cohesive and noncohesive sediments	(g/d)	EFDC
LErodVel	Erosion Velocity	erosional velocity for cohesive sediments	(m/d)	EFDC
LDepVel	Deposition Velocity	depositional velocity for cohesive sediments	(m/d)	EFDC
TStates (sed. parmameters)	**Sediment Model Parameters**	*For each AQUATOX segment, the following parameters are required*		
MaxUpperThick	MaxThick	maximum thickness of the active layer	(m)	site & lit
BioturbThick	Bioturbation Depth	depth at which bioturbation takes place, also the minimum thickness for this layer	(m)	site & lit
TBuriedSedimentData	**Sediment Layer Parameters**	*For each Sediment Layer modeled in each segment, the following parameters are required*		
BedDepthIC	Thickness	initial condition thickness of the sediment layer	(m)	site
CharLength	Characteristic Length	characteristic length of the interface with above water or above sediment layer	(m)	site
UpperDispCoeff	Dispersion Coefficient	dispersion coefficient for interface with above water or above sediment layer	(m^2/d)	site & lit
InitCond	Initial Conditions	initial conditions for each type of sediment modeled (organic and inorganic)	(g/m^2)	site
Tox InitCond	Toxicant Init. Conditions	initial conditions for toxicant concentration in each type of sediment modeled	µg/kg	site
TPoreWater	**Pore Water Parameters**	*For each Sediment Layer modeled in each segment, the following pore water parameters are required*		
PoreWaterIC	Initial condition	initial quantity of pore water in the sediment layer	(m^2/m^3)	site
TDOMPoreWater	DOM Init. Condition	initial quantity of DOM in the pore water	(g/m^3)	site
Tox InitCond	Toxicant Init. Conditions	initial conditions for toxicant concentration in above pore water compartments	µg/kg	site
TSediment	**Density Parameters**	*For each type of sediment modeled, (organic and inorganic)*		
Densities[ ]	Density	the density of this sediment within the sediment bed	g/m3	site & lit

APPENDIX E

HOUSATONIC WATERSHED MODEL SEGMENTATION DATA

Table E-1 Housatonic Watershed Model Segment Areas, Elevations, and Slopes

Model Segment	Area (SqMeters)	Area (Acres)	Area (SqMi)	Mean Elev (ft MSL)	Min Elev (ft MSL)	Max Elev (ft MSL)	% Slope
100	44726788.00	11051.84	17.27	549.18	340	670	3.497
110	26884080.00	6642.97	10.38	541.96	438	658	3.210
120	25783914.00	6371.12	9.95	498.19	437	609	2.586
130	34575248.00	8543.43	13.35	468.35	341	609	3.234
140	11161694.00	2758.02	4.31	453.01	332	639	5.021
200	6901047.50	1705.23	2.66	330.22	301	396	2.722
500	33995160.00	8400.09	13.13	444.22	332	792	5.551
510	16852558.00	4164.21	6.51	453.13	332	731	6.148
520	7781181.00	1922.70	3.00	343.48	301	396	1.478
530	30894690.00	7633.97	11.93	417.52	301	695	4.454
540	57948796.00	14318.95	22.37	403.76	301	670	4.551
550	5740871.50	1418.55	2.22	311.94	301	335	1.139
560	24843770.00	6138.81	9.59	463.78	301	609	5.466
570	13782092.00	3405.51	5.32	398.79	298	628	5.096
580	14682229.00	3627.93	5.67	506.31	299	609	5.794
700	28794370.00	7114.99	11.12	554.15	285	670	3.533
710	39295964.00	9709.90	15.17	478.32	271	670	6.194
720	61699364.00	15245.70	23.82	426.71	271	609	5.946
730	20433102.00	5048.95	7.89	509.67	271	620	4.836
740	38815892.00	9591.28	14.99	348.14	245	579	6.098
750	43776644.00	10817.06	16.90	335.04	242	548	4.449
1000	6681014.00	1650.86	2.58	355.60	301	518	3.315
1010	8691319.00	2147.60	3.36	429.52	301	609	4.725
2000	12231857.00	3022.45	4.72	326.71	301	547	2.280
3000	1090165.50	269.38	0.42	304.52	301	319	0.458
4000	4930748.50	1218.37	1.90	312.84	301	365	0.899
5000	4640704.50	1146.70	1.79	315.77	300	396	2.058
5010	9831492.00	2429.33	3.80	331.41	297	518	3.365
5020	2160328.00	533.81	0.83	304.98	297	335	0.980
5030	11561755.00	2856.87	4.46	364.62	295	579	4.272
6000	6210942.50	1534.70	2.40	439.26	295	579	6.354
7000	5660859.00	1398.78	2.19	337.70	280	548	3.153
7010	30744666.00	7596.90	11.87	353.35	271	640	3.256
7020	5090772.50	1257.91	1.97	324.27	271	487	4.994
7030	2110320.25	521.45	0.81	291.42	271	481	3.523
7040	15292321.00	3778.68	5.90	301.57	245	487	3.377
7050	11091684.00	2740.72	4.28	284.71	216	487	5.342
8000	2090317.25	516.51	0.81	288.69	211	518	9.052
9000	1590241.38	392.94	0.61	236.55	210	366	4.198

Table E-2 AVSWAT Land Use Categories for Housatonic Watershed Model Areas in Acres

MODEL SEGMENT	URBAN	AGRICULTURE	FOREST DECIDUOUS	FOREST EVERGREEN	FOREST MIXED	WATER	WETLANDS FORESTED	TOTAL
100	182.9	1104.7	4633.8	4475.6	0.0	79.1	516.5	10992.5
110	388.0	370.7	1801.6	3776.2	0.0	212.5	93.9	6643.0
120	96.4	790.8	1722.5	2557.8	12.4	93.9	1082.4	6356.3
130	1077.5	598.1	3991.2	1198.6	519.0	215.0	884.7	8484.1
140	585.7	113.7	1794.2	217.5	0.0	0.0	0.0	2711.1
200	929.2	118.6	435.0	222.4	0.0	0.0	0.0	1705.2
500	931.7	1811.5	5199.7	234.8	0.0	217.5	4.9	8400.1
510	215.0	412.7	3373.4	0.0	0.0	0.0	145.8	4146.9
520	973.7	153.2	333.6	103.8	0.0	254.5	49.4	1868.3
530	1438.3	832.8	4174.1	274.3	304.0	565.9	0.0	7589.5
540	2585.0	2389.8	6289.6	2199.5	74.1	249.6	494.3	14281.9
550	1144.2	0.0	222.4	12.4	0.0	0.0	0.0	1379.0
560	444.8	491.8	2802.5	2362.6	0.0	9.9	0.0	6111.6
570	459.7	42.0	1873.3	509.1	304.0	0.0	180.4	3368.4
580	7.4	66.7	2335.4	1028.1	0.0	42.0	34.6	3514.2
700	42.0	106.3	3536.5	2854.4	0.0	69.2	506.6	7115.0
710	929.2	96.4	4315.0	4011.0	0.0	358.3	0.0	9709.9
720	168.1	1564.4	6096.8	6304.4	0.0	44.5	1013.2	15191.3
730	12.4	0.0	1902.9	3133.7	0.0	0.0	0.0	5049.0
740	380.6	1070.1	2792.6	4297.7	0.0	34.6	1000.9	9576.4
750	2115.5	1757.1	3336.3	1910.3	640.1	442.4	489.3	10691.0
1000	852.6	24.7	397.9	375.6	0.0	0.0	0.0	1650.9
1010	741.4	98.9	1038.0	200.2	0.0	0.0	0.0	2078.4
2000	1801.6	350.9	252.1	494.3	0.0	0.0	81.6	2980.4
3000	266.9	0.0	0.0	0.0	0.0	2.5	0.0	269.4
4000	1077.5	0.0	128.5	0.0	0.0	12.4	0.0	1218.4
5000	489.3	84.0	543.7	29.7	0.0	0.0	0.0	1146.7
5010	785.9	825.4	224.9	568.4	0.0	0.0	9.9	2414.5
5020	116.2	22.2	9.9	336.1	0.0	0.0	49.4	533.8
5030	689.5	170.5	1005.8	692.0	0.0	0.0	187.8	2745.7
6000	61.8	135.9	813.1	385.5	0.0	79.1	32.1	1507.5
7000	553.6	222.4	0.0	603.0	0.0	0.0	0.0	1379.0
7010	2328.0	1853.5	1692.9	1529.8	0.0	173.0	0.0	7577.1
7020	182.9	301.5	0.0	721.6	0.0	0.0	51.9	1257.9
7030	49.4	232.3	2.5	190.3	0.0	0.0	47.0	521.5
7040	1028.1	815.5	153.2	1297.5	138.4	0.0	274.3	3707.0
7050	558.5	128.5	563.5	1472.9	0.0	0.0	0.0	2723.4
8000	158.2	74.1	247.1	0.0	0.0	37.1	0.0	516.5
9000	106.3	177.9	106.3	0.0	0.0	2.5	0.0	392.9
TOTAL	26954.9	19409.9	70141.6	50580.9	1991.9	3195.4	7231.1	179505.9
% of Total	15.0%	10.8%	39.1%	28.2%	1.1%	1.8%	4.0%	

Table E-3 Housatonic Watershed Model Reach Characteristics for HSPF

Reach	Downstream Reach	Length (meters)	% Slope	Length (miles)	Diff in elev (ft)
100	140	12132.04	1.95	7.54	774.31
110	130	6627.46	0.72	4.12	157.49
120	130	3809.48	0.32	2.37	39.37
130	140	8898.95	1.07	5.53	312.17
140	1000	1690.08	0.30	1.05	16.40
200	2000	1922.94	0.10	1.19	6.31
500	520	10645.53	0.83	6.61	288.72
510	520	4013.05	0.82	2.49	108.27
520	550	5746.02	0.56	3.57	104.99
530	550	5458.13	1.08	3.39	193.57
540	5000	10424.80	0.58	6.48	196.86
550	5000	4580.25	0.10	2.84	15.03
560	5010	6020.31	1.56	3.74	308.41
570	5020	5116.65	1.36	3.18	227.79
580	5030	2988.10	5.02	1.86	492.44
700	7010	9028.25	3.17	5.61	938.37
710	7020	8565.47	1.77	5.32	498.72
720	7030	14225.70	1.08	8.84	501.98
730	7040	5437.42	3.84	3.38	684.82
740	7050	11856.28	0.32	7.36	124.68
750	7050	12066.35	0.74	7.49	292.00
1000	1010	2372.97	1.39	1.47	108.28
1010	2000	1624.39	0.10	1.01	5.33
2000	3000	2597.25	0.10	1.61	8.52
3000	4000	948.60	0.10	0.59	3.11
4000	5000	2272.96	0.10	1.41	7.46
5000	5010	2131.53	0.05	1.32	3.28
5010	5020	5304.57	0.08	3.29	13.12
5020	5030	1482.96	0.20	0.92	9.84
5030	6000	1890.09	0.26	1.17	16.40
6000	7000	1390.06	0.07	0.86	3.28
7000	7010	2731.58	0.59	1.70	52.49
7010	7020	5518.80	0.26	3.43	47.89
7020	7030	2714.42	0.10	1.69	8.91
7030	7040	1690.08	0.10	1.05	5.55
7040	7050	6911.79	0.43	4.29	98.43
7050	8000	5870.29	0.56	3.65	108.28
8000	9000	1407.21	0.36	0.87	16.40
9000		1215.78	0.25	0.76	9.84

APPENDIX F

TIMELINE SUMMARY OF AVAILABLE MODEL APPLICATION DATA FOR THE HOUSATONIC RIVER ABOVE CANAAN, CT

Table F-1

Summary of Housatonic River Flow Data Above Canaan, CT

	General Location	Sample Type	REF / SOURCE	1979	1980	1981	1982	1983	1984	1985	1986	1987	1988	1989	1990	1991	1992	1993	1994	1995	1996	1997	1998	1999	2000
Flow	Great Barrington, MA	Flow	USGS																						
	Coltsville, MA	Flow	USGS																						

Note: Colored gages are within the study area

Explanation of Sample Types

Flow - Discharge measurement
St-30min - Stage taken at 30 minute increments
T-30min - Temperature taken at 30 minute increments
Comp. - Composite sample of biota
Indiv. - Individual sample of biota
F - Fillet sample of biota

WB - Whole Body sample of biota
TSS - Total Suspended Solids concentration
PSD - Particle Size Distribution of sediment sample
BD - Bulk Density (net weight) of sediment samples
CS - Core Sediment sample
SS - Surficial Sediment sample

GSvsC - Grain Size vs PCB Concentration
BOD_5- Biological Oxygen Demand 5 day
WC - Water Column sample
Hazardous - Various Hazardous Constituents other than PCBs
DO - Dissolved Oxygen concentration
GrbS - Grab Sample

$T\&UNH_3$- Total and Unionized Ammonia concentrations
NO_3 - Nitrate concentration in water-column sample
Oil&Grease - Oil and Grease concentration
Tmp - Temperature measurement taken at daily increments
Nutr - Nutrients

	General Location	Sample Type	REF / SOURCE	1979	1980	1981	1982	1983	1984	1985	1986	1987	1988	1989	1990	1991	1992	1993	1994	1995	1996	1997	1998	1999	2000
Snow Depth	HARTFORD	Daily	NCDC																						
	ALBANY	Daily	NCDC																						
	WORCESTER	Daily	NCDC																						
	WEST OTIS	Daily	NCDC																						
	BERLIN 5 S	Daily	NCDC																						
	PLAINFIELD 2	Daily	NCDC																						
	BECKET 2 SW	Daily	NCDC																						
	LANESBORO	Daily	NCDC																						
	STOCKBRIDGE	Daily	NCDC																						
	LENOX DALE	Daily	NCDC																						
	CHESTER2	Daily	NCDC																						
	CUMMINGTON HILL	Daily	NCDC																						
	GREAT BARRINGTON	Daily	NCDC																						
	DALTON	Daily	NCDC																						
	WORTHINGTON	Daily	NCDC																						
	COPAKE	Daily	NCDC																						

Note: Colored sites are within or close to the study area

Summary of Housatonic River Stage/Temp Data Above Canaan, CT

	General Location	Sample Type	REF / SOURCE	1979	1980	1981	1982	1983	1984	1985	1986	1987	1988	1989	1990	1991	1992	1993	1994	1995	1996	1997	1998	1999	2000
Stage/ Temp	Woods Pond Dam	St-30min T-30min	GE/QEA GE/QEA																			— —			
	Woods Pond Headwaters	St-30min T-30min	GE/QEA GE/QEA																			— —			
	Rising Pond Dam	St-30min T-30min	GE/QEA GE/QEA																			— —			
	PSA Stations	SW/Events	Weston/USEPA																					—	

Explanation of Sample Types

Flow - Discharge measurement
St-30min - Stage taken at 30 minute increments
T-30min - Temperature taken at 30 minute increments
Comp. - Composite sample of biota
Indiv. - Individual sample of biota
F - Fillet sample of biota

WB - Whole Body sample of biota
TSS - Total Suspended Solids concentration
PSD - Particle Size Distribution of sediment sample
BD - Bulk Density (net weight) of sediment samples
CS - Core Sediment sample
SS - Surficial Sediment sample

GSvsC - Grain Size vs PCB Concentration
BOD$_5$- Biological Oxygen Demand 5 day
WC - Water Column sample
Hazardous - Various Hazardous Constituents other than PCBs
DO - Dissolved Oxygen concentration
GrbS - Grab Sample

T&UNH$_3$- Total and Unionized Ammonia concentrations
NO$_3$ - Nitrate concentration in water-column sample
Oil&Grease - Oil and Grease concentration
Tmp - Temperature measurement taken at daily increments
Nutr - Nutrients

Table F-3

Summary of Housatonic River Sediment Data Above Canaan, CT

	General Location	Sample Type	REF / SOURCE	1979	1980	1981	1982	1983	1984	1985	1986	1987	1988	1989	1990	1991	1992	1993	1994	1995	1996	1997	1998	1999	2000
Sed.	Coltsville, MA	PSD	USGS/CAES																						
		TSS	GE,BBL[2]																						
		TSS	USEPA																						
	Pittsfield, MA	PSD	USGS/CAES																						
		PSD,TSS	GE,BBL[2]																						
	(PSA Stations)	PSD,TSS	Weston/USEPA																						
	Great Barrington, MA	PSD,BD	LMS																						
		TSS	LMS																						
		PSD,TSS	Stewart																						
		TSS	GE,BBL[2]																						
		TSS	USGS/CTDEP																						
		PSD,TSS	USGS[1]																						
	Ashley Falls, MA	PSD,BD	LMS																						
		TSS	LMS																						
		PSD,TSS	Stewart																						
		TSS	USGS/CTDEP																						
		TSS	USGS[3]																						
		TSS	GE																						
	Canaan, CT	PSD,BD	LMS																						
		TSS	LMS																						
		TSS	USGS/CTDEP																						
		TSS	USGS[4]																						

Explanation of Sample Types

Flow - Discharge measurement	WB - Whole Body sample of biota	GSvsC - Grain Size vs PCB Concentration	T&UNH$_3$- Total and Unionized Ammonia concentrations
St-30min - Stage taken at 30 minute increments	TSS - Total Suspended Solids concentration	BOD$_5$- Biological Oxygen Demand 5 day	NO$_3$ - Nitrate concentration in water-column sample
T-30min - Temperature taken at 30 minute increments	PSD - Particle Size Distribution of sediment sample	WC - Water Column sample	Oil&Grease - Oil and Grease concentration
Comp. - Composite sample of biota	BD - Bulk Density (net weight) of sediment samples	Hazardous - Various Hazardous Constituents other than PCBs	Tmp - Temperature measurement taken at daily increments
Indiv. - Individual sample of biota	CS - Core Sediment sample	DO - Dissolved Oxygen concentration	Nutr - Nutrients
F - Fillet sample of biota	SS - Surficial Sediment sample	GrbS - Grab Sample	

Table F-4

Summary of Housatonic River PCB Data Above Canaan, CT

General Location	Sample Type	REF / SOURCE	1979	1980	1981	1982	1983	1984	1985	1986	1987	1988	1989	1990	1991	1992	1993	1994	1995	1996	1997	1998	1999	2000

PCBs

Coltsville, MA
- CS — Stewart
- CS,GrbS — USGS/CAES
- WC — GE,BBL[2]
- WC — USEPA

Pittsfield, MA
- CS — Stewart
- CS,GrbS — USGS/CAES
- CS,GrbS — GE,BBL[2]
- WC — GE,BBL[2]
- WC — Weston/USEPA

Great Barrington, MA
- CS,WC — Stewart
- CS,GrbS — USGS/CAES
- WC — LMS
- CS,GrbS — LMS
- WC — USGS/CTDEP
- CS — GE,BBL[2]
- WC — GE,BBL[2]

Ashley Falls, MA
- CS,WC — Stewart
- CS,GrbS — USGS/CAES
- WC — LMS
- CS,GrbS — LMS
- WC — USGS/CTDEP
- CS — GE,BBL[2]

Canaan, CT
- CS,GrbS — USGS/CAES
- WC — LMS
- CS,GrbS — LMS
- WC — USGS/CTDEP
- CS — GE,BBL[2]

Explanation of Sample Types

Flow - Discharge measurement
St-30min - Stage taken at 30 minute increments
T-30min - Temperature taken at 30 minute increments
Comp. - Composite sample of biota
Indiv. - Individual sample of biota
F - Fillet sample of biota

WB - Whole Body sample of biota
TSS - Total Suspended Solids concentration
PSD - Particle Size Distribution of sediment sample
BD - Bulk Density (net weight) of sediment samples
CS - Core Sediment sample
SS - Surficial Sediment sample

GSvsC - Grain Size vs PCB Concentration
BOD$_5$ - Biological Oxygen Demand 5 day
WC - Water Column sample
Hazardous - Various Hazardous Constituents other than PCBs
DO - Dissolved Oxygen concentration
GrbS - Grab Sample

T&UNH$_3$ - Total and Unionized Ammonia concentrations
NO$_3$ - Nitrate concentration in water-column sample
Oil&Grease - Oil and Grease concentration
Tmp - Temperature measurement taken at daily increments
Nutr - Nutrients

Table F-5

Summary of Housatonic River Biota Data Above Canaan, CT

	General Location	Sample Type	REF / SOURCE	1979–2000 data timeline
Biota	GE - MA/CT border	Comp.	Stewart	(data: 1980, 1982)
	Burlington Hatchery	Indiv.	ANS	(data: 1987, 1989)
	Woods Pond Dam	Indiv.	BBL[1]	(data: 1990, 1994)
	Rising Pond Dam	Indiv. / F,WB,Comp. / F,WB,Comp.	BBL[1] / USEPA / GE	(data: 1990, 1998)
	GE Plant Site	Comp.	BBL[1]	(data: 1997–1998)
	Upper E. Br. - Dalton	F,WB,Comp.	USEPA	(data: 1998–1999)
	Three Mile Pond	F,WB,Comp.	USEPA	(data: 1998)
	Goodrich Pond	F,WB,Comp. / F,WB	USEPA / GE	(data: 1998)
	W. Br. Confluence - WWTP	F,WB,Comp. / F,WB,Comp.	USEPA / GE	(data: 1998)
	WWTP - Woods Pond Headwaters	F,WB,Comp. / F,WB,Comp.	USEPA / GE	(data: 1998–1999)
	Woods Pond and Backwaters	F,WB,Comp. / F,WB,Comp.	USEPA / GE	(data: 1998–2000)

Explanation of Sample Types

Flow - Discharge measurement
St-30min - Stage taken at 30 minute increments
T-30min - Temperature taken at 30 minute increments
Comp. - Composite sample of biota
Indiv. - Individual sample of biota
F - Fillet sample of biota

WB - Whole Body sample of biota
TSS - Total Suspended Solids concentration
PSD - Particle Size Distribution of sediment sample
BD - Bulk Density (net weight) of sediment samples
CS - Core Sediment sample
SS - Surficial Sediment sample

GSvsC - Grain Size vs PCB Concentration
BOD_5 - Biological Oxygen Demand 5 day
WC - Water Column sample
Hazardous - Various Hazardous Constituents other than PCBs
DO - Dissolved Oxygen concentration
GrbS - Grab Sample

$T\&UNH_3$ - Total and Unionized Ammonia concentrations
NO_3 - Nitrate concentration in water-column sample
Oil&Grease - Oil and Grease concentration
Tmp - Temperature measurement taken at daily increments
Nutr - Nutrients

Table F-6

Summary of Housatonic River TOC Data Above Canaan, CT

	General Location	Sample Type	REF / SOURCE	Data Period (1979–2000)
TOC	Coltsville, MA	CS,GrbS	USGS/CAES	1979–1980
		CS,GrbS	USEPA	1998–1999
	Pittsfield, MA	CS,GrbS	GE,BBL[2]	1994–1996
		WC,CS	Weston/USEPA	1998
		CS,GrbS	USGS/CAES	1979–1980; 1998
	Great Barrington, MA	CS,GrbS	LMS	1992
		SS,CS	USGS/CAES	1979–1980
	Ashley Falls, MA	CS,GrbS	LMS	1992
		CS,GrbS	USGS/CAES	1979–1980
		CS	GE,BBL[2]	1998
	Canaan, CT	CS,GrbS	LMS	1992
		WC	USGS	1979–1987
		CS,GrbS	USGS/CAES	1979–1980
		CS	GE,BBL[2]	1998

Explanation of Sample Types

Flow - Discharge measurement
St-30min - Stage taken at 30 minute increments
T-30min - Temperature taken at 30 minute increments
Comp. - Composite sample of biota
Indiv. - Individual sample of biota
F - Fillet sample of biota

WB - Whole Body sample of biota
TSS - Total Suspended Solids concentration
PSD - Particle Size Distribution of sediment sample
BD - Bulk Density (net weight) of sediment samples
CS - Core Sediment sample
SS - Surficial Sediment sample

GSvsC - Grain Size vs PCB Concentration
BOD$_5$ - Biological Oxygen Demand 5 day
WC - Water Column sample
Hazardous - Various Hazardous Constituents other than PCBs
DO - Dissolved Oxygen concentration
GrbS - Grab Sample

T&UNH$_3$ - Total and Unionized Ammonia concentrations
NO$_3$ - Nitrate concentration in water-column sample
Oil&Grease - Oil and Grease concentration
Tmp - Temperature measurement taken at daily increments
Nutr - Nutrients

Table F-7

Summary of Housatonic River Other Data Above Canaan, CT

	General Location	Sample Type	REF / SOURCE	1979-2000 timeline
Other	Pittsfield, MA	Hazardous	GE,BBL[2]	(1990; 1994; 1998)
		DO, pH	BBL[2]	(1993)
		T&UNH₃,NO₃	BBL[2]	(1993)
	(PSA Stations)	Oil&Grease	BBL[2]	(1994)
		Nutr,BOD₅	Weston/USEPA	(1998)
	Great Barrington, MA	Tmp,DO	USGS[1]	(1979-1981)
		Hazardous	GE,BBL[2]	(1998)
	Ashley Falls, MA	Tmp,DO	USGS[3]	(1986-1987)
		Tmp,DO,Nutr	USGS[3]	(1994-1995)
		Hazardous	GE,BBL[2]	(1998)
	Canaan, CT	Tmp,DO	USGS[4]	(1979-1985)
		Hazardous	GE,BBL[2]	(1998)

Timeline column headers: 1979, 1980, 1981, 1982, 1983, 1984, 1985, 1986, 1987, 1988, 1989, 1990, 1991, 1992, 1993, 1994, 1995, 1996, 1997, 1998, 1999, 2000 (each subdivided Jan, May, Aug, Dec)

Explanation of Sample Types

Flow - Discharge measurement
St-30min - Stage taken at 30 minute increments
T-30min - Temperature taken at 30 minute increments
Comp. - Composite sample of biota
Indiv. - Individual sample of biota
F - Fillet sample of biota

WB - Whole Body sample of biota
TSS - Total Suspended Solids concentration
PSD - Particle Size Distribution of sediment sample
BD - Bulk Density (net weight) of sediment samples
CS - Core Sediment sample
SS - Surficial Sediment sample

GSvsC - Grain Size vs PCB Concentration
BOD₅ - Biological Oxygen Demand 5 day
WC - Water Column sample
Hazardous - Various Hazardous Constituents other than PCBs
DO - Dissolved Oxygen concentration
GrbS - Grab Sample

T&UNH₃- Total and Unionized Ammonia concentrations
NO₃ - Nitrate concentration in water-column sample
Oil&Grease - Oil and Grease concentration
Tmp - Temperature measurement taken at daily increments
Nutr - Nutrients

Table F-8

Summary of Housatonic Meteorological Data

	General Location	Sample Type	REF / SOURCE	Data Period (1979–2000)
Air Temp	PITTSFIELD GE FACILITY	15-minute	GE	1993–1998
	PITTSFIELD GE FACILITY	Hourly	GE	1993–1998
	HARTFORD	Hourly	NRCC	1996–2000
	ALBANY	Hourly	NRCC	1979–2000
	KNIGHTVILLE	Hourly	BASINS	1979–1996
	WEST OTIS	Daily	NRCC	1979–2000
	BERLIN 5 S	Daily	NRCC	1979–2000
	PLAINFIELD	Daily	NRCC	1979–2000
	BECKET	Daily	Earthinfo	1979–1981
	LANESBORO	Daily	Earthinfo	1979–1995
	STOCKBRIDGE	Daily	Earthinfo	1979–1984
	BORDEN BROOK RSVR	Daily	Earthinfo	1979–1995
	CHESTER2	Daily	Earthinfo	1979–1988
	CUMMINGTON HILL	Daily	Earthinfo	1979–1995
	GREAT BARRINGTON AP	Daily	Earthinfo	1979–2000
	NORTH ADAMS	Daily	Earthinfo	1986–1988
	WORTHINGTON	Daily	Earthinfo	1994–1995
	COPAKE	Daily	Earthinfo	1988–1995

Note: Colored gages intend to be used for watershed simulation

MK01\O:\20123001.096\MFD_ApFtbl.xlsMet

10/13/00

Reference/Source List for Timeline Data Tables (REF/SOURCE)

USGS[1] Ɓ U.S. Geological Survey

Surface-water station on the Housatonic River near Great Barrington, Mass. (01197500).

USGS[2] Ɓ U.S. Geological Survey

Surface-water station on the Housatonic River at Coltsville, Mass. (01197000).

QEA Ɓ Quantitative Environmental Analysis

Quantitative Environmental Analysis. 1998. Technical Memorandum - Spring 1997 High Flow Monitoring & Summer 1997 Bathymetric Sediment Bed Mapping Survey. Prepared to present data collected by BB&L and HydroQual.

Stewart Ɓ Stewart Laboratories, Inc

Stewart Ɓ Stewart Laboratories, Inc. 1982. Housatonic River Study 1980 and 1982 Investigations. Prepared for General Electric Company.

ANS Ɓ Academy of Natural Sciences

 General Electric Company 1999. Preliminary Draft of Biota Database Summary. Prepared for discussion purposes only.

BBL[1] - Blasland, Bouck and Lee

General Electric Company 1999. Preliminary Draft of Biota Database Summary. Prepared for discussion purposes only.

USEPA Ɓ U.S. Environmental Protection Agency.

General Electric Company 1999. Preliminary Draft of 1998 Biota Database Summary. Prepared for discussion purposes only.

GE Ɓ General Electric Company

General Electric Company 1999. Preliminary Draft of 1998 Biota Database Summary. Prepared for discussion purposes only.

LMS - Lawler, Matusky and Skelly Engineers

General Electric Company. 1994. Housatonic River Connecticut Cooperative Agreement Ɓ Task IV.B: PCB Fate and Transport Model: Additional Monitoring and Model Verification. Prepared by Lawler, Matusky and Skelly Engineers.

BBL[2] - Blasland, Bouck and Lee

General Electric Company. 1996. Supplemental Phase II/RCRA Facility Investigation Report for Housatonic River and Silver Lake. Vol. II.: with Figures and Tables. Prepared by Blasland, Bouck and Lee.

Weston Ɓ Roy F. Weston, Inc.

Roy F. Weston, Inc. 1999. Microsoft Access Database Ɓ Data Mart. Preliminary Summary of available data.

USGS/CAES Ɓ CAES, CDEP, and USGS

Frink, C. R., K. P. Kulp, C. G. Fredette. 1981. PCBs in Housatonic River Sediments: Determination, Distribution and Transport. Draft. Prepared by CAES, CDEP, and USGS.

USGS/CTDEP Ɓ USGS and CT Department of Environmental Protection

Kulp, K.P. 1991. Concentration and Transport of Polychlorinated Biphenyls in the Housatonic River Between Great Barrington, Massachusetts, and Kent, Connecticut, 1984-1988, 1991. Prepared by USGS and CT Department of Environmental Protection.

USGS[3] Ɓ U.S. Geological Survey

Surface-water station on the Housatonic near Ashley Falls, Mass. (001198125).

USGS[4] Ɓ U.S. Geological Survey

Surface-water station on the Housatonic River near Canaan, Conn. (01198550).

USGS – U.S. Geological Survey

General Electric Company 1999. Preliminary Draft of 1998 Sediment Database Summary. Prepared for discussion purposes only.

CAES Ɓ Connecticut Agricultural Experiment Station

General Electric Company 1999. Preliminary Draft of 1998 Sediment Database Summary. Prepared for discussion purposes only.

APPENDIX G

GLOSSARY OF TERMS

APPENDIX G
GLOSSARY OF TERMS

Abiotic   Nonliving, pertaining to physical-chemical factors only.

Absorption   The process of taking up matter or energy by a substance.

Activated sludge   A secondary wastewater treatment process that removes organic matter by mixing air and recycled sludge bacteria with sewage to promote decomposition.

Acute toxicity   A chemical stimulus severe enough to rapidly induce an effect; in aquatic toxicity tests, an effect observed within 96 hours or less is considered acute. When referring to aquatic toxicology or human health, an acute effect is not always measured in terms of lethality.

Adsorption   The process by which atoms, molecules, or ions are taken up from soil, water solution, or soil atmosphere and retained on surfaces of solids by chemical or physical bonding.

Advection   Bulk transport of the mass of discrete chemical or biological constituents by fluid flow within a receiving water. Advection describes the mass transport due to the velocity, or flow, of the waterbody.

Aerobic   Environmental conditions characterized by the presence of oxygen; used to describe biological or chemical processes that occur in the presence of oxygen.

Aggradation   Process by which stream beds, flood plains, and the bottoms of other water bodies are raised in elevation by the deposition of material eroded and transported from other areas.

Algae   Any organisms of a group of chiefly aquatic nonvascular plants; most algae have chlorophyll as the primary pigment for carbon fixation. As primary producers, algae serve as the base of the aquatic food web, providing food for zooplankton and fish resources. An overabundance of algae in natural waters is known as eutrophication.

Algal bloom   Rapidly occurring growth and accumulation of algae within a body of water, usually resulting from excessive nutrient loading and/or sluggish circulation regime with a long residence time. Persistent and frequent blooms can result in low oxygen conditions.

Algal growth   Increase in algal biomass. Algal growth is related to temperature, available light, and the available abundance of inorganic nutrients (N,P,Si). Algal species groups (e.g., diatoms, greens, etc.) are typically characterized by different maximum growth rates.

Algal respiration	Process of endogenous respiration of algae in which organic carbon is oxidized to carbon dioxide.
Algal settling	Loss of phytoplankton cells from the water column by physical sedimentation of the cell particles. Algal biomass lost from the water column is then incorporated as sediment organic matter and undergoes bacterial and biochemical reactions releasing nutrients and consuming dissolved oxygen.
Allochthonous	Material derived from outside a habitat or environment under consideration.
Alluvium	Sand, clay, and other earth materials gradually deposited by streams along riverbeds and floodplains.
Ambient conditions	Natural levels or conditions of environmental factors such as temperature.
Ambient water quality	Natural concentration of water quality constituents prior to mixing of either point or nonpoint source load of contaminants. Reference ambient concentration is used to indicate the concentration of a chemical that will not cause adverse impact to human health.
Ammonia	Inorganic form of nitrogen; product of hydrolysis of organic nitrogen and denitrification. Ammonia is preferentially used by phytoplankton over nitrate for uptake of inorganic nitrogen.
Ammonia toxicity	Under specific conditions of temperature and pH, the un-ionized component of ammonia can be toxic to aquatic life. The un-ionized component of ammonia increases with pH and temperature.
Amphibian	Any of a class of vertebrate animals most of which have both aquatic larval and terrestrial adult stages.
Anaerobic	Environmental condition characterized by zero oxygen levels. Describes biological and chemical processes that occur in the absence of oxygen.
Analytical model	Exact mathematical solution of the differential equation formulation of the transport, diffusion, and reactive terms of a water quality model. Analytical solutions of models are often used to check the magnitude of the system response computed using numerical model approximations.
Anoxic	Aquatic environmental conditions containing zero or little dissolved oxygen. See also Anaerobic.
Anthropogenic	Pertains to the [environmental] influence of human activities.

Aphotic	Characterized by a lack of light; below the level of light penetration in water.
Aquatic ecosystem	Complex of biotic and abiotic components of natural waters. The aquatic ecosystem is an ecological unit that includes the physical characteristics (such as flow or velocity and depth); the biological community of the water column and benthos; and the chemical characteristics such as dissolved solids, dissolved oxygen, and nutrients. Both living and nonliving components of the aquatic ecosystem interact and influence the properties and status of each other component.
Assimilation	Uptake of food and/or contaminant through the gut.
Assimilative capacity	The amount of contaminant load (expressed as mass per unit time) that can be discharged to a specific stream or river without exceeding water quality standards or criteria. Assimilative capacity is used to define the ability of a waterbody to naturally absorb and use waste matter and organic materials without impairing water quality or harming aquatic life.
Attached algae	Photosynthetic organisms that remain stationary by attachment to (usually) hard rocky substrate. Attached algae, usually present in shallow hard-bottom environments, can significantly influence nutrient uptake and diurnal oxygen variability. See Periphyton.
Autochthonous	Material derived from within a habitat, such as through plant growth.
Autotroph	Organisms that derive cell carbon from carbon dioxide. The conversion of carbon dioxide to organic cell tissue is a reductive process that requires a net input of energy. The energy needed for cell synthesis is provided by either light or chemical oxidation. Autotrophs that use light (phototrophs) include photosynthetic algae and bacteria. Autotrophs that use chemical energy (chemotroph) include nitrifying bacteria.
Average annual runoff	The average value of annual runoff volume calculated for a selected period of record, at a specified location, such as a dam or stream gage.
Background levels	Background levels represent the chemical, physical, and biological conditions that would result from natural geomorphological processes such as weathering or dissolution.
Backwater	A temporary or permanent water body out of the main river or stream channel and at the edge of the flood plain, most often caused by an obstruction or constriction in the main channel or waterbody.

Bacterial decomposition	Breakdown by oxidation or decay of organic matter by heterotrophic bacteria. Bacteria use the organic carbon in organic matter as the energy source for cell synthesis.
Bankfull	A discharge or flow rate within a river which just fills the channel, and when exceeded, will inundate adjacent lands.
Base flow	That part of the stream discharge that is not attributable to direct runoff from precipitation or melting snow; it is usually sustained by ground-water discharge to the stream.
Bedload	Sediment particles, composed mostly of coarse materials, that are moving on or near the bottom due to flow within the stream or river.
Benthic ammonia flux	The decay of organic matter within the sediments of a natural water body results in the release of ammonia nitrogen from the interstitial water to the overlying water column. Benthic release, or regeneration, of ammonia is an essential component of the nitrogen cycle.
Benthic drift	Downstream transport of invertebrates, especially insect larvae.
Benthic photosynthesis	Synthesis of cellular carbon by algae attached to the bottom of a natural water system. Benthic photosynthesis typically is limited to shallow waters because of the availability of light at the bottom.
Benthic	Refers to material, especially sediment, at the bottom of an aquatic ecosystem. It can also be used to describe the organisms that live on or in the bottom of a waterbody.
Benthos	Those organisms that live in or on the bottom of a body of water.
Bioaccumulation	The uptake of contaminants, such as PCBs, from all sources including direct sorption to the body, transport across gill membranes, and through ingestion of prey and sediments. See Bioconcentration and Biomagnification.
Biochemical Oxygen Demand (BOD)	The amount of oxygen per unit volume of water required to bacterially or chemically oxidize the oxidizable matter in water. Biochemical oxygen demand measurements are usually conducted over specific time intervals (5, 10, 20, 30 days). The term BOD generally refers to the standard 5-day BOD test.
Bioconcentration	The direct uptake of contaminants from the dissolved phase through direct sorption to the body and through transport across gill membranes. See Bioaccumulation and Biomagnification.
Biodegradable	Able to be broken down into simple inorganic substances by the action of decomposers (bacteria and fungi).

Bioenergetics	Processes leading to growth and expenditure of energy by organisms.
Biomagnification	The step-by-step concentration of chemicals in successive levels of a food chain or food web. See Bioaccumulation and Bioconcentration.
Biomass	The amount or weight of a species or group of biological organisms within a specific volume or area of an ecosystem.
Biota	The fauna and flora of a habitat or region.
Biotransformation	The process by which compounds are changed by decomposers and by higher organisms. One example is dechlorination of PCBs.
Bioturbation	Disturbance of surficial sediments through burrowing of invertebrates, amphibians, and reptiles, and feeding and nest-building of fish.
Bottom feeders	Fish that feed on sediments and benthic organisms.
Boundary conditions	Values or functions representing the state of a system at its boundary limits, either in space or time.
Calibration	Testing and tuning of a model to a set of field data not used in the development of the model; also includes minimization of deviations between measured field conditions and output of a model by selecting appropriate model coefficients.
Carbonaceous	Pertaining to or containing carbon derived from plant and animal residues.
Channel improvement	The improvement of the flow characteristics of a channel by clearing, excavation, realignment, lining, or other means in order to increase its capacity. Sometimes used to connote channel stabilization.
Channel stabilization	Erosion prevention and stabilization of velocity distribution in a channel using jetties, drops, revetments, vegetation, and other measures.
Channel	A natural stream that conveys water; a ditch or channel excavated for the flow of water.
Chitin	Composition of the exoskeleton of an arthropod.
Chloride	An ion of chlorine in solution, bearing a single negative charge.
Chlorination	Combination with chlorine or a chlorine compound.
Chlorophyll	A group of green photosynthetic pigments that occur primarily in the chloroplast of plant cells. The amount of chlorophyll-a, a specific pigment, is frequently used as a measure of algal biomass in natural waters.

Chronic toxicity	Toxicity impact that becomes evident only after a relatively long period of time, often one-tenth of the life span or more. Chronic effects could include reduced growth, reduced reproduction, or death.
Coliform bacteria	A group of bacteria that normally live within the intestines of warm-blooded animals, including humans. Coliform bacteria are used as an indicator of the presence of sewage in natural waters.
Combined Sewer Overflow (CSO)	A combined sewer carries both wastewater and stormwater runoff. CSO discharges to receiving water can result in contamination problems that may prevent the attainment of water quality standards.
Complete mixing	The modeling assumption that no significant difference in concentration of an ecosystem constituent or pollutant exists either across the transect or along the length of the waterbody or a portion of the waterbody.
Concentration	Amount of a substance or material in a given unit volume of water or mass of sediment or organisms. Usually measured in milligrams per liter (mg/L) or parts per million (ppm).
Congener	One of the 209 different PCB molecular configurations. A congener may have between 1 and 10 chlorine atoms, which may be located at various positions on the PCB molecule.
Congener-specific analysis	A form of chemical analysis that distinctly identifies and quantifies individual PCB congeners. It allows scientists to see distinct PCB patterns or signatures in the environment. These can identify the PCB source material, the likely source areas, and the degree and type of subsequent alteration.
Conservative substance	Substance that does not undergo any chemical or biological transformation or degradation in a given ecosystem.
Consumer	An organism that eats a plant or another animal.
Contamination	Act of polluting or making impure; any indication of chemical, sediment, or biological impurities.
Conventional pollutants	As specified under the Clean Water Act, conventional contaminants include suspended solids, coliform bacteria, BOD, pH, oil, and grease.
Core sampling	Sampling of sediment or soil by pushing a hollow tube into the river bottom and removing a core. The cylindrical core sample is then sliced and the various slices analyzed. High-Resolution Sampling requires slicing the core into many thin slices (approximately 1 to 1.5-inches thick). Low-Resolution Sampling requires slicing the core into fewer slices (approximately 9-inches thick).

Criteria	Water quality criteria (WQC) comprise numeric and narrative criteria. Numeric criteria are scientifically derived ambient concentrations developed by EPA or States for various pollutants of concern to protect human health and aquatic life. Narrative criteria are statements that describe the desired water quality goal.
Cross-sectional area	Wet area of a waterbody normal, or perpendicular, to the longitudinal component of the flow.
Crustacea	A Class (large grouping) of the Phylum Arthropoda, including crayfish and water fleas, that bear a horny shell.
Decay	Gradual decrease in the amount of a substance in a system due to various sink processes including chemical and biological transformation, dissipation to other environmental media, or deposition into storage areas.
Dechlorination	The process of removing chlorine atoms from a PCB molecule while leaving the main molecular structure intact. In most instances, dechlorination of a PCB molecule simply yields a different PCB molecule.
Decomposers	Bacteria and fungi that break down organic detritus.
Decomposition	Metabolic breakdown of organic materials by bacteria and fungi, releasing energy and simple organics and inorganic compounds. See also Respiration.
Deep percolation	The drainage of soil water downward by gravity below the maximum effective depth of the root zone toward storage in subsurface strata.
Degradation	The sum of natural processes which cause a decrease in PCB mass by either dechlorination or outright destruction of PCB molecules.
Denitrification	Under anaerobic or low-oxygen conditions, denitrifying bacteria synthesize cellular material by reducing nitrate to ammonia and nitrogen gas.
Depuration	Excretion of contaminant by an organism.
Designated use	Uses specified in water quality standards for each waterbody or segment regardless of actual attainment.
Desorption	The process by which chemicals are detached and released from solid surfaces. The opposite of adsorption.
Detritus	Organic material resulting from the death or disintegration (such as sloughing of macrophyte leaves) of organisms; usually with associated decomposers.

Diagenesis	Any alteration of sediments, especially though compaction and decomposition.
Diatom	Algae of the Phylum Chrysophyta, commonly unicellular with a siliceous case.
Dilution	Addition of less-concentrated liquid (water) that results in a decrease in the original concentration.
Discharge	The volume of water that passes a given point within a given period of time. It is an all-inclusive outflow term, describing a variety of flows such as from a pipe to a stream, or from a stream to a lake or ocean.
Discharge Monitoring Report (DMR)	Report of effluent characteristics submitted by a municipal or industrial facility that has been granted an NPDES discharge permit.
Discharge permits (NPDES)	A permit issued by EPA or a State regulatory agency that sets specific limits on the type and amount of pollutants that a municipality or industry can discharge to a receiving water; it also includes a compliance schedule for achieving those limits. It is called the NPDES permit because the permit process was established under the National Pollutant Discharge Elimination System, under provisions of the Federal Clean Water Act.
Disequilibrium	Not in equilibrium.
Dispersion	The spreading of chemical or biological constituents, including pollutants, in various directions from a point source at varying velocities depending on the differential instream flow characteristics.
Dissolved Oxygen (DO)	The amount of oxygen that is dissolved in water. It also refers to a measure of the amount of oxygen available for biochemical activity in a water body and as indicator of the quality of that water.
Dissolved oxygen sag	Longitudinal variation of dissolved oxygen representing the oxygen depletion and recovery following a waste load discharge into a receiving water.
Diurnal	Actions or processes having a period or cycle of one day, particularly the daylight-night cycle.
Domestic wastewater	Also called sanitary wastewater, consists of wastewater discharged from residences and from commercial, institutional, and similar facilities.
Drainage basin	Land area enclosed by a topographic divide from which direct surface runoff from precipitation normally drains by gravity into a receiving water. Also referred to as watershed, river basin, or hydrologic unit.

Dye study	Use of conservative substances to assess the physical behavior of a natural system to a given stimulus.
Dynamic equilibrium	A state of relative balance between processes having opposite effects.
Dynamic model	A mathematical formulation describing the physical behavior of a system or a process and its temporal variability.
Dynamic simulation	Modeling of the behavior of physical, chemical, and/or biological phenomena and their variation over time.
Ecology	The study of the interrelationships of organisms with and within their environment.
Ecosystem	An interactive system that includes the organisms of a natural community association together with their abiotic physical, chemical, and geochemical environment.
Effluent	Municipal sewage or industrial liquid waste (untreated, partially treated, or completely treated) that flows out of a treatment plant, septic system, or pipe.
Egestion	Defecation.
Elimination	Loss of contaminant by organism, including biotransformation and depuration.
Emergent vegetation	Aquatic plants, usually rooted, which have portions above water for part of their life cycle.
Environment	The sum total of all the external conditions that act on an organism.
Epilimnion	The well-mixed surficial layer of a waterbody; above the hypolimnion.
Epiphyte	A plant growing on another plant; more generally, any organism attached and growing on a plant.
Equilibrium	A steady state in a dynamic system, with outflow balancing inflow.
Erosion	Wearing away and removal of materials of the earth's crust by natural means. Examples include Streambank and Streambed (scouring of material and cutting of channel banks and beds), Sheet (removal of a thin layer by runoff waters), Rill (forming numerous small channels), Gully (widening and deepening of small channels).
Estuary	Brackish water areas influenced by the tides where a river meets the sea.
Euphotic	Pertaining to the upper layers of water through which sufficient light penetrates to permit growth of plants.

Eutrophic	Aquatic systems with high nutrient input and high plant growth.
Eutrophication model	Mathematical formulation that describes the advection; dispersion; and biological, chemical, and geochemical reactions that influence the growth and accumulation of algae in aquatic ecosystems. Models of eutrophication typically include one or more species groups of algae; inorganic and organic nutrients (N,P); organic carbon; and dissolved oxygen.
Eutrophication	Enrichment of an aquatic ecosystem with nutrients (nitrates, phosphates) that accelerate biological productivity (growth of algae and aquatic weeds) and an undesirable accumulation of algal biomass.
Evapotranspiration	A collective term that describes water movement back to the atmosphere as a result of evaporation from soil surfaces and surface water bodies and by plant transpiration.
Extinction coefficient	Measure for the reduction (absorption) of light intensity within a water column.
Factor of safety	Coefficient used to account for uncertainties in representing, simulating, or designing a system.
Fate of pollutants	Physical, chemical, and biological transformation in the nature and changes of the amount of a pollutant in an environmental system. Transformation processes are pollutant specific. However, they have comparable kinetics so that different formulations for each pollutant are not required.
Fauna	The animals of a habitat or region.
Fecal coliform bacteria	Bacteria that are present in the intestines or feces of warm-blooded animals. They are often used as indicators of the sanitary quality of water.
Fecundity	The capacity to produce offspring. Usually the number of eggs per female that hatch and become larvae.
Filamentous algae	Algae with long, thread-like growth form.
First-order kinetics	Describes a reaction in which the rate of transformation of a pollutant is proportional to the amount of that pollutant in the environmental system.
Flocculation	The process by which suspended colloidal or very fine particles are assembled into larger masses or floccules that eventually settle out of suspension.

Floodplain	That part of a river valley that is covered in periods of high (flood) water.
Flora	Plants of a habitat or region.
Fluvial	Pertaining to a stream.
Flux	Movement and transport of mass of any water quality constituent over a given period of time. Units of mass flux are mass per unit time.
Food chain	Animals linked by linear predator-prey relationships with plants or detritus at the base.
Food web	Similar to food chain, but implies cross connections.
Forage fish	Fish eaten by other fish.
Forcing functions	External empirical formulation used to provide model input describing a number of processes or conditions. Typical forcing functions include model inputs such as precipitation, temperature, point and tributary sources, solar radiation, and waste loads and flow.
Fugacity	Escaping tendency of a chemical from one state to another.
Gaging station	Particular site on a stream, canal, lake, or reservoir where systematic observations of height or discharge are obtained.
Geochemical	Refers to chemical reactions related to earth materials such as soil, rocks, and water.
Gradient	The rate of decrease (or increase) of one quantity with respect to another; for example, the rate of decrease of temperature with depth in a lake.
Groundwater	All subsurface water that fills the pores, voids, fractures, and other spaces between soil particles and in rock strata in the saturated zone of geologic formations.
Habitat	The environment in which a population of plants or animals occurs.
Half-saturation constant	Nutrient concentration at which the growth rate is half the maximum rate. Half-saturation constants define the nutrient uptake characteristics of different plant species.
Heterotrophs	Organisms that must obtain their food from living or dead organisms.
Homolog	A grouping of PCB congeners based on the number of chlorine atoms present on the molecule. There are 10 homolog groups corresponding to the range of chlorine atoms possible.

Humic	Pertaining to the partial decomposition of leaves and other plant material.
Hydrodynamic model	Mathematical formulation used in describing circulation, transport, and deposition processes in receiving water.
Hydrodynamics	The study of the movement of water within a waterbody, such as a river, lake, estuary, or coastal ocean environment.
Hydrograph	A graphic plot of changes in the flow of water or in the elevation of water level plotted against time.
Hydrologic cycle	The circuit of water movement from the atmosphere to the earth and return to the atmosphere through various stages or processes, such as precipitation, interception, runoff, infiltration, storage, evaporation, and transpiration.
Hydrology	The science dealing with the properties, distribution, and flow of water on or in the Earth.
Hydrolysis	Reactions that occur between chemicals and water molecules resulting in the cleaving of a molecular bond and the formation of new bonds with components of the water molecule.
Hypolimnion	The lower layer of a stratified water body, below the well-mixed zone.
Impervious	The characteristic of being incapable of penetration by water. Impervious areas refer to roads, parking lots, rooftops, and other land surface types that inhibit infiltration of precipitation and rapidly convey the resulting runoff to a waterbody.
In situ (in place)	In situ measurements consist of measurement of components or processes in a full-scale system or the field rather than in a laboratory.
Infiltration	The downward entry of water into the Earth's surface. Infiltration usually refers to water movement into a soil or rock surface, while the terms hydraulic conductivity, percolation, and permeability usually relate to water movement within a soil or rock layer.
Infiltration capacity	The maximum rate at which infiltration can occur under specific soil moisture conditions.
Influent	Any liquid that flows into a water body, treatment plant, or other facility; the opposite of effluent.
Initial conditions	A state of a system prior to an introduction of an induced stimulus. Describes conditions at the startup of system simulations.

Initial mixing zone	Region immediately downstream of an outfall where effluent dilution processes occur. Because of the combined effects of the effluent buoyancy, ambient stratification, and current, the prediction of initial dilution can be involved.
Inorganic	Pertaining to matter that is neither living nor immediately derived from living matter, such as sand, silt, and clay.
Interflow	The lateral subsurface movement of a significant amount of water through the soil above the regional water table as discharge to a waterbody.
Interstitial water	Water contained in the interstices, which are the pore spaces or voids in soils and rocks.
Invertebrate	Animals lacking a backbone.
Kinetic processes	Description of the dynamic rate and mode of change in the transformation or degradation of a substance in an ecosystem.
Labile	Substances that are quickly degraded, in contrast to refractory; also referring to fast adsorption.
Light saturation	Optimal light level for algal and macrophyte photosynthesis and growth.
Limiting factor	An environmental factor that limits the growth of an organism; the factor that is closest to the physiological limits of tolerance of that organism.
Limnetic zone	The open water zone of a lake or pond from the surface to the depth of effective light penetration.
Limnology	The scientific study of the biological, chemical, geographical, and physical features of fresh waters, usually lakes and ponds.
Lipids	Structural components of the cell that are fatty or waxy.
Littoral zone	The shoreward zone of a water body in which the light penetrates to the bottom, thus usually supporting rooted aquatic plants.
Load allocation (LA)	The portion of a receiving water's total maximum daily load that is attributed either to one of its existing or future nonpoint sources of pollution or to natural background sources.
Loading, load, loading rate	The total amount of material (pollutants) entering the system from one or multiple sources; measured as a rate in weight per unit time.

Longitudinal dispersion	The spreading of chemical or biological constituents, including pollutants, downstream from a point source at varying velocities due to the differential instream flow characteristics.
Low-flow (7Q10)	Low-flow (7Q10) is the 7-day average low flow occurring once in 10 years; this probability-based statistic is used in determining stream design flow conditions and for evaluating the water quality impact of effluent discharge limits.
Macrofauna	Animals visible to the naked eye.
Macrophyte	Large, vascular aquatic plants, usually rooted.
Mass balance	An equation that accounts for the flux of mass going into a defined area and the flux of mass leaving the defined area. The flux in must equal the flux out.
Mathematical model	A system of mathematical expressions that describe the spatial and temporal distribution of flow and/or water quality constituents resulting from fluid transport and one or more individual processes and interactions within some prototype aquatic ecosystem.
Metabolism	Processes that make energy available in an organism.
Mineralization	The transformation of organic matter into an inorganic compound.
Mixing characteristics	Refers to the tendency for natural waters to blend; i.e. for dissolved and particulate substances to disperse into adjacent waters.
Monte Carlo simulation	A stochastic modeling technique that involves the random selection of sets of input data for use in repetitive model runs. Probability distributions of receiving water quality concentrations are generated as the output of a Monte Carlo simulation.
N/P ratio	The ratio of nitrogen to phosphorus in an aquatic system. The ratio is used as an indicator of the nutrient limiting conditions for algal growth.
Natural waters	Waterbodies (e.g., ponds, rivers, streams) within a physical system that have developed without human intervention, in which natural processes continue to take place.
Nitrate (NO_3) and nitrite (NO_2)	Oxidized nitrogen species; important nutrients for aquatic plants.
Nitrification	The oxidation of ammonium salts to nitrites (via *Nitrosomonas* bacteria) and the further oxidation of nitrite to nitrate (via *Nitrobacter* bacteria).

Nitrifier organisms	Bacterial organisms that mediate the biochemical oxidative processes of nitrification.
Nitrobacter	Type of bacteria responsible for the conversion of nitrite to nitrate.
Nitrogenous BOD (NBOD)	Refers to the oxygen demand associated with the oxidation of nitrate.
Nitrosomonas	Type of bacteria responsible for the oxidation of ammonia to the intermediate product nitrite.
Nonconservative substance	Substances that undergo chemical or biological transformation in a given environment.
Nonpoint source	Pollution that is not released through pipes but rather originates from multiple sources over a relatively large area. Nonpoint sources can be divided into source activities related to either land or water use including failing septic tanks, improper animal-keeping practices, forest practices, and urban and rural runoff.
Numerical model	Models that approximate a solution of governing partial differential equations which describe a natural process. The approximation uses a numerical discretization of the space and time components of the system or process.
Nutrient limitation	Deficit of nutrient (e.g., nitrogen and phosphorus) required by microorganisms in order to metabolize organic substrates.
Nutrient	A primary element necessary for the growth of living organisms. Carbon dioxide, nitrogen, and phosphorus, for example, are required nutrients for phytoplankton growth.
Offal	Waste parts of an animal, in contrast to fillets in a fish.
Omnivorous	Feeding on a variety of organisms and organic detritus.
One-dimensional model (1-D)	A mathematical model defined along one spatial coordinate of a natural water system. Typically 1-D models are used to describe the longitudinal variation of water quality constituents along the downstream direction of a stream or river. In writing the model, it is assumed that the cross-channel (lateral) and vertical variability is relatively homogenous and can, therefore, be averaged over those spatial coordinates.
Organic matter	Living organisms and material obtained from living organisms Commonly determined as the amount of organic material contained in a soil or water sample.
Organic nitrogen	Form of nitrogen bound to an organic compound.

Orthophosphate   Form of phosphate available for biological metabolism without further breakdown.

Outfall point   Point on a waterbody where water flows from a conduit, tributary stream, or storm drain.

Overland flow   The quantity of water that moves across the land surface. Contributions to overland flow are from runoff and from the surfacing of subsurface flows before they reach a receiving stream or a defined drainage channel.

Overturn   The complete circulation or mixing of the upper and lower waters of a lake when temperatures (and densities) are similar.

Oxidation   The chemical union of oxygen with metals or organic compounds accompanied by a removal of hydrogen or another atom. It is an important factor for soil formation and permits the release of energy from cellular fuels.

Oxygen demand   Measure of the dissolved oxygen used by a system (microorganisms) in the oxidation of organic matter. See also Biochemical Oxygen Demand.

Oxygen depletion   Deficit of dissolved oxygen in a water system due to oxidation of organic matter.

Oxygen saturation   Natural or artificial reaeration or oxygenation of a water system (water sample) to bring the level of dissolved oxygen to saturation. Oxygen saturation is greatly influenced by temperature and other water characteristics.

Parameter   A variable that must be given a specific value in a simulation. In mathematical models, parameters usually refer to characteristics of the system, such as reaction rates, decay constants, or partition coefficients.

Parameterize   To provide parameter values for a simulation.

Partition coefficients   Chemicals in solution are partitioned into dissolved and particulate adsorbed phases based on their corresponding partition coefficients, assuming equilibrium.

Peak runoff   The highest value of the stage or discharge attained by a flood or storm event, also referred to as flood peak or peak discharge.

Pelagic zone   Open water with no association with the bottom.

Pelagic   Living in the water column.

Percolation	The movement of water through soil or rock, usually from shallow soil or aquifer surfaces to deeper zones.
Periphyton	Algae attached to the bottom or to macrophytes.
Permeability	The capacity of soil, sediment, or porous rock to transmit water, usually in the vertical direction.
Pharmacokinetics	Transport and fate of chemicals within the body.
Photic zone	The region of aquatic environments in which the intensity of light is sufficient for photosynthesis.
Photoperiod	The seasonally varying period of daylight.
Photosynthesis	The biochemical synthesis of carbohydrate-based organic compounds from water and carbon dioxide using light energy in the presence of chlorophyll. Photosynthesis occurs in all plants, including aquatic organisms such as algae and macrophytes. Photosynthesis also occurs in primitive bacteria such as blue-green algae.
Phyla	The largest grouping of related organisms; examples include arthropods and molluscs.
Phytoplankton	A group of generally unicellular microscopic plants characterized by passive drifting within the water column. See Algae.
Piscivore	Fish eater; examples include game fish and hawks.
Plankton	Group of generally microscopic plants and animals passively floating, drifting, or swimming weakly. Plankton include the phytoplankton (plants) and zooplankton (animals).
Point source	Pollutant loads discharged at a specific location from pipes, outfalls, and conveyance channels from either municipal wastewater treatment plants or industrial waste treatment facilities. Point sources can also include pollutant loads contributed by tributaries to the main receiving water stream or river.
Pollutant	A contaminant in a concentration or amount that adversely alters the physical, chemical, or biological properties of a natural environment. The term includes pathogens, toxic metals, carcinogens, oxygen demanding substances, or other harmful substances.
Pond	A body of standing water smaller than a lake, often artificially formed.
Population	A group of organisms of the same species.

Porewater exchange	Exchange of water contained within the sediment with the overlying river water. This exchange occurs through diffusion, bioturbation, and movement of groundwater through the sediment.
Postaudit	A subsequent examination and verification of model predictive performance following implementation of an environmental control program.
Predator	An organism, usually an animal, that kills and consumes another organism.
Pretreatment	The treatment of wastewater to remove or reduce contaminants prior to discharge into another treatment system or a receiving water.
Prey	An organism killed and at least partially consumed by a predator.
Primary productivity	A measure of the rate at which new organic matter is formed and accumulated through photosynthesis and chemosynthesis activity of producer organisms (chiefly, green plants). The rate of primary production is estimated by measuring the amount of oxygen released (oxygen method) or the amount of carbon assimilated by the plant (carbon method).
Priority pollutant	Substances listed by the EPA under the Federal Clean Water Act as harmful substances and having priority for regulatory controls. The list includes metals (13), inorganic compounds (2), and a broad range of naturally occurring or artificial organic compounds (111).
Producer	An organism that can synthesize organic matter using inorganic materials and an external energy source (light or chemical).
Production	The amount of organic material produced by biological activity.
Productivity	The rate of production of organic matter. It may be primary, by plants, or secondary, by consumers.
Publicly Owned Treatment Work (POTW)	Municipal wastewater treatment plant owned and operated by a public governmental entity such as a town or city.
Raw sewage	Untreated municipal sewage.
Reaction rate coefficient	A factor in formulas describing the rate of transformation of a substance in an environmental medium characterized by a set of physical, chemical, and biological conditions such as temperature and dissolved oxygen level.
Reaeration	The net flux of oxygen occurring from the atmosphere to a body of water.

Receiving waters	Creeks, streams, rivers, lakes, estuaries, groundwater formations, or other bodies of water into which surface water and/or treated or untreated waste are discharged, either naturally or in man-made systems.
Recharge	Downward movement of water through soil to groundwater derived from precipitation on the overlying land surface.
Recurrence interval	Average amount of time between events of a given magnitude. For example, for a recurrence interval of 100 years, there is a 1% chance that a 100-year flood will occur in any given year.
Refractory organics	A broad category of detritus and chemicals that resist chemical or bacterial decomposition.
Refractory	Slowly degraded, in contrast to labile.
Relief	Variations or differences in elevation or height of land forms on the Earth's surface.
Remote sensing	A method for determining the characteristics of a landscape or community from afar.
Reserve capacity	Pollutant loading rate set aside in determining stream waste load allocation accounting for uncertainty and future growth.
Residence time	Length of time that a pollutant remains within a section of a stream or river. The residence time is determined by the streamflow and the volume of the river reach or the average stream velocity and the length of the river reach.
Respiration	Breathing; the oxidative breakdown of cellular material to release energy. During respiration, oxygen is consumed and carbon dioxide is released.
Riparian	Pertaining to the banks of a river, stream, or other body of water as well as to plant and animal communities along such bodies of water.
Risk assessment	The qualitative and quantitative evaluation performed in an effort to define the risk posed to human health and/or the environment by the presence or potential presence and/or use of specified pollutants.
Riverine	Pertaining to areas on or near the banks of rivers.
Rough fish	A non-sport fish, usually omnivorous in food habits.
Roughness coefficient	A factor in velocity and discharge formulas representing the effects of channel roughness on energy losses in flowing water. Manning's "n" is a commonly used roughness coefficient.

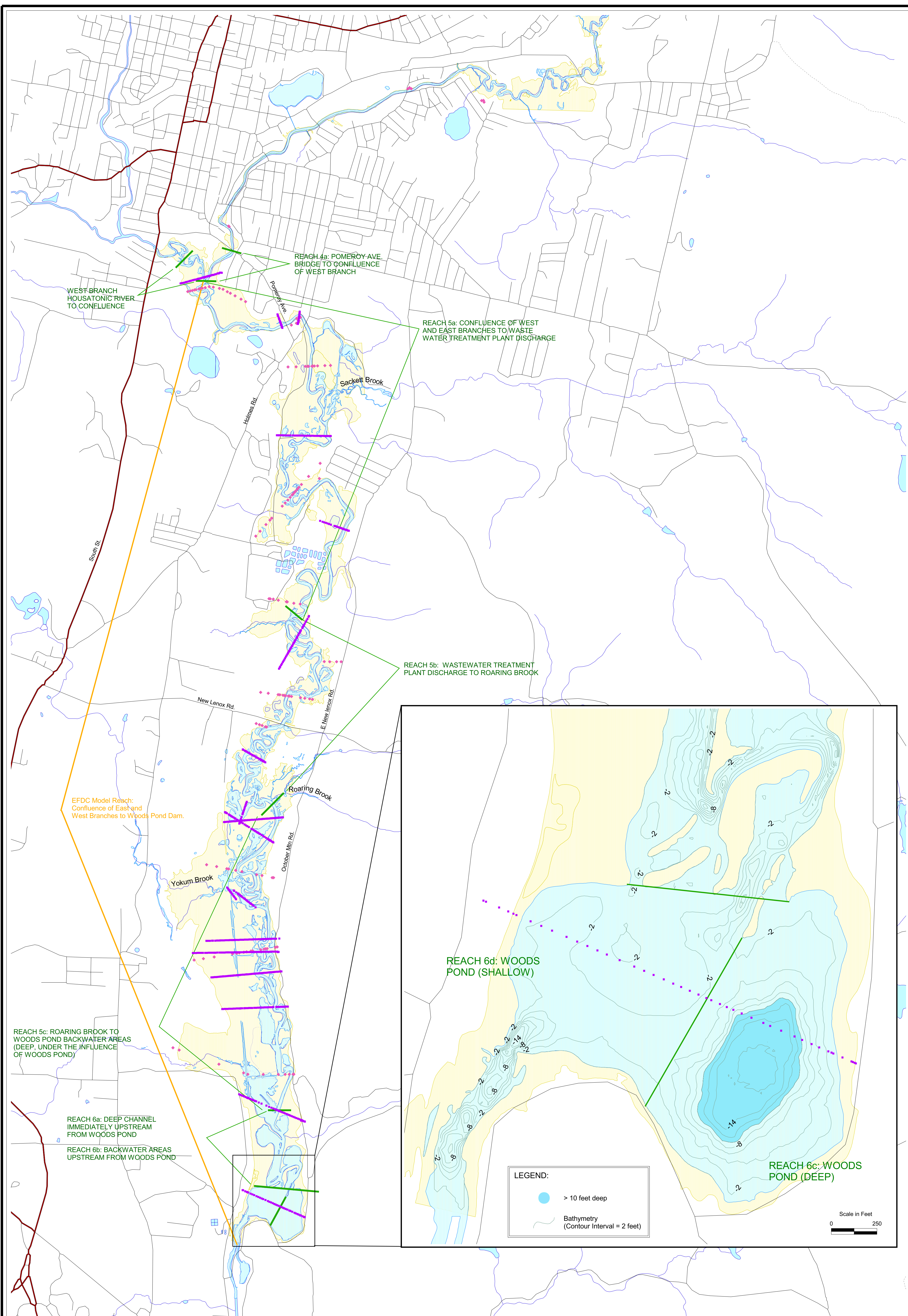|	
Routing	Derivation of an outflow hydrograph of a stream from known values of upstream flow, using the wave velocity and/or storage equation; technique used to compute the effect of channel storage and translation on the shape and movement of a flood wave through a river reach.
Runoff	Precipitation, snow melt, or irrigation water that appears in uncontrolled surface streams or rivers.
Scour	The abrading action of flowing water; the erosion of a channel or streambed and abrasion of periphyton and macrophytes, especially during flood events.
Secchi depth	A measure of the light penetration into the water column, influenced by turbidity due to suspended sediments, phytoplankton, and dissolved organic matter.
Sediment load	Total sediment, including bedload, being moved by flowing water in a stream at a specified cross section.
Sediment Oxygen Demand (SOD)	The solids discharged to a receiving water are partly organics, and upon settling to the bottom, they decompose anaerobically as well as aerobically, depending on conditions. The oxygen consumed in aerobic decomposition represents another dissolved oxygen sink for the waterbody.
Sedimentation	Deposition of waterborne sediment; also refers to the infilling of bottom substrate in a waterbody by sediment (siltation).
Sediment	Particulate organic and inorganic matter that is transported and accumulates in waterbodies.
Seepage	The relatively slow trickling of water or other liquid from a source.
Shoal	A shallow place in a body of water.
Siltation	The deposition of silt-sized and clay-sized (smaller than sand-sized) particles.
Simulation	Refers to the use of mathematical models to approximate the observed behavior of a natural system in response to a specific known set of input and forcing conditions. Models that have been validated, or verified, are then used to predict the response of a natural system to changes in the input or forcing conditions.
Soil erosion	The processes by which soil is removed from one place by forces such as wind, water, waves, glaciers, and construction activity and eventually deposited at some new place.

Sorption	The adherence of ions or molecules in a gas or liquid to the surface of a solid particle with which they are in contact. The removal of an ion or molecule from solution by adsorption and absorption. The term is often used when the exact nature of the mechanism is not known.
Spatial segmentation	A numerical discretization of the spatial component of a system into one or more dimensions; forms the basis for application of numerical simulation models.
Stabilization pond	Large earthen basins that are used for the treatment of wastewater by natural processes involving the use of both algae and bacteria.
Stage	Height of a water surface above some established reference point at a given location.
State variable	A compartment that is being represented with a numerical model.
Steady-state model	Mathematical model of fate and transport that uses constant values of input variables to predict constant values of receiving water quality concentrations.
Stoichiometric ratio	Mass-balance-based ratio for nutrients and organic carbon (e.g., nitrogen-to-carbon ratio) in organisms and detritus.
STORET	U.S. Environmental Protection Agency (EPA) national water quality database for STORage and RETrieval (STORET). Mainframe water quality database that includes physical, chemical, and biological data measured in waterbodies throughout the United States.
Storm runoff	Rainfall that does not evaporate or infiltrate the ground because of impervious land surfaces or a soil infiltration rate lower than rainfall intensity, but instead flows onto adjacent land or waterbodies or is routed into a drain or sewer system.
Stratification (of water body)	Formation of water layers, each with specific physical, chemical, and biological characteristics. As the density of water decreases due to surface heating, a stable situation develops with lighter water overlaying heavier and denser water.
Streamflow	Discharge that occurs in a natural channel. Although the term "discharge" can be applied to the flow of a canal, the word "streamflow" uniquely describes the discharge in a surface stream course. The term streamflow is more general than "runoff" as streamflow may be applied to discharge whether or not it is affected by diversion or regulation.
Substrate	The layer on which organisms grow, often synonymous with surface; also, a substance attached by an enzyme.

Succession	The replacement of one biotic assemblage with another through time.
Surface waters	Water that flows in streams, rivers, natural lakes, and wetlands; in reservoirs or impoundments constructed by humans; and in estuaries.
Suspended solids or Load	Organic and inorganic particles (sediment) suspended in and carried by a fluid (water). The suspension is governed by the upward components of turbulence, currents, or colloidal suspension.
Temperature coefficient	Rate of increase in an activity or process over a 10 degree Celsius increase in temperature.
Thalweg	The lowest point, or elevation, in the channel bed taken within a cross-section perpendicular to the direction of flow.
Three-dimensional model (3-D)	Mathematical model defined along three spatial coordinates where the water quality constituents are considered to vary over the three spatial coordinates of length, width, and depth.
Tolerance	An organism's capacity to endure or adapt to unfavorable conditions.
Topography	Representation of natural and artificial physical features of the landscape.
Total coliform bacteria	A particular group of bacteria that are used as indicators of possible sewage pollution. They are characterized as aerobic or facultative anaerobic, gram-negative, nonspore-forming, rod-shaded bacteria which ferment lactose with gas formation within 48 hours at 35 degrees Celsius. See also Fecal coliform bacteria.
Total Kjeldahl Nitrogen (TKN)	The total of organic and ammonia nitrogen in a sample, determined by the Kjeldahl method.
Toxic substances	Those chemical substances, such as pesticides, plastics, heavy metals, detergent, solvent, or any other material that are poisonous, carcinogenic, or otherwise directly harmful to human health and the environment.
Transect sampling	Sequential river water sampling at several stations providing instantaneous "snapshots" of water column parameters.
Transport	Conveyance of solutes and particulates in flow systems.
Transport of pollutants (in water)	Transport of pollutants in water involves two main process: (1) advection, resulting from the flow of water, and (2) diffusion, or transport due to turbulence in the water.
Travel time	Time period required by a particle to cross a transport route such as a watershed, river system, or stream reach.

Tributary	A stream that contributes its water to another stream or body of water. A lower order stream compared to a receiving waterbody. "Tributary to" indicates the largest stream into which the reported stream or tributary flows.
Trickling filter	A wastewater treatment process consisting of a bed of highly permeable medium to which microorganisms are attached and through which wastewater is percolated or trickled.
Trophic level	All organisms that secure their food at a common step in the food chain.
Turbidity	Measure of the amount of suspended material in water.
Turbulence	A type of flow in which any particle may move in any direction with respect to any other particle and in a regular or fixed path. Turbulent water is agitated by cross currents and eddies. Turbulent velocity is that velocity above which turbulent flow will always exist and below which the flow may be either turbulent or laminar.
Turbulent flow	A flow characterized by irregular, random-velocity fluctuations.
Two-dimensional model (2-D)	Mathematical model defined along two spatial coordinates where the water quality constituents are considered averaged over the third remaining spatial coordinate. Examples of 2-D models include descriptions of the variability of water quality properties along: (a) the length and width of a river that incorporates vertical averaging or (b) length and depth of a river that incorporates lateral averaging across the width of the waterbody.
Ultimate Biochemical Oxygen Demand (UBOD or BOD_U)	Long-term oxygen demand required to completely stabilize organic carbon in wastewater or natural waters.
Unsaturated zone	The subsurface zone between the water table (zone of saturation) and the land surface where some of the spaces between the soil particles are filled with air. Also called vadose zone.
Unstratified	Indicates a vertically uniform or well-mixed condition in a waterbody. See also Stratification.
Verification (of a model)	Subsequent testing of a precalibrated model to additional field data usually under different external conditions to further examine model validity (also called validation).
Volatilization	Process by which chemical compounds are vaporized (evaporated) at given temperature and pressure conditions by gas transfer reactions. Volatile compounds have a tendency to partition into the gas phase.

Wastewater treatment	Chemical, biological, and mechanical procedures applied to an industrial or municipal discharge or to any other sources of contaminated water in order to remove, reduce, or neutralize contaminants.
Wastewater	Usually refers to effluent from a sewage treatment plant. See also Domestic wastewater.
Water quality standard (WQS)	A law or regulation that consists of the beneficial designated use or uses of a waterbody, the numeric and narrative water quality criteria that are necessary to protect the use or uses of that particular waterbody, and an antidegradation statement.
Water quality	The biological, chemical, and physical conditions of a water body. It is a measure of a water body to support beneficial uses.
Water table	The upper limit of that part of the ground that is saturated with groundwater.
Watershed	All lands enclosed by a continuous hydrologic drainage divide and lying upslope from a specified point on a stream; also, an entire drainage basin.
Wetland	Area that is regularly wet or flooded and has a water table that stands at or above the land surface for at least part of the year, such as a bog, pond, fen, estuary, or marsh.
Wind mixing	Refers to a physical process occurring when wind over a free water surface influences the atmospheric reaeration rate.
Zero-order kinetics	Describes the rate of transformation or degradation of a substance; the reaction rate of change is independent of the concentrations in solution.
Zooplankton	Very small animals (protozoans, crustaceans, fish embryos, insect larvae) that live in a waterbody and are moved passively by water currents and wave action.

REACH 4a: POMEROY AVE.
BRIDGE TO CONFLUENCE
OF WEST BRANCH

WEST BRANCH
HOUSATONIC RIVER
TO CONFLUENCE

REACH 5a: CONFLUENCE OF WEST
AND EAST BRANCHES TO WASTE
WATER TREATMENT PLANT DISCHARGE

Pomeroy Ave.

Sackett Brook

Holmes Rd.

South St.

REACH 5b: WASTEWATER TREATMENT
PLANT DISCHARGE TO ROARING BROOK

New Lenox Rd.

E. New Lenox Rd.

EFDC Model Reach:
Confluence of East and
West Branches to Woods Pond Dam.

Roaring Brook

October Mtn Rd.

Yokum Brook

REACH 5c: ROARING BROOK TO
WOODS POND BACKWATER AREAS
(DEEP, UNDER THE INFLUENCE
OF WOODS POND)

REACH 6a: DEEP CHANNEL
IMMEDIATELY UPSTREAM
FROM WOODS POND

REACH 6b: BACKWATER AREAS
UPSTREAM FROM WOODS POND

REACH 6d: WOODS
POND (SHALLOW)

REACH 6c: WOODS
POND (DEEP)

LEGEND:

> 10 feet deep

Bathymetry
(Contour Interval = 2 feet)

Scale in Feet
0   250

LEGEND:

GE Transects

Corp of Engineers Transects

Modeling Transects

Roads

Hydrology

Floodplain

Source:

GE Survey Data - letter dated 16 September 1998
from GE (Andrew T. Silfer) to EPA (Susan Svirsky)

USACE Modeling Transect Survey Data
collected fall 1998

N

Scale in Feet
1500   0   1500   3000   4500

Housatonic River Project
Pittsfield, Massachusetts

PLATE NO. 1
PRIMARY STUDY AREA